New Jersey Institute of Technology

Digital Commons @ NJIT

Dissertations   Electronic Theses and Dissertations

Spring 8-31-1985

Ternary ion exchange in fixed beds : equilibrium and dynamics

David W. H. Roth
New Jersey Institute of Technology

Recommended Citation

TERNARY ION EXCHANGE IN FIXED BEDS

- EQUILIBRIUM AND DYNAMICS -

by
David W. H. Roth, Jr.

Dissertation submitted to the Faculty of the Graduate School
of the New Jersey Institute of Technology in partial fulfillment
of the requirements for the degree of
Doctor of Engineering Science
1985

APPROVAL SHEET

Title of Thesis: Ternary Ion Exchange in Fixed Beds
                          - Equilibrium and Dynamics -

Name of Candidate: David W. H. Roth, Jr.
                          Doctor of Engineering Science, 1984

Thesis and Abstract Approved: _____ _____
                          Ching-Rong Huang   Date
                          Professor, Chemical Engineering
                          Department of Chemical Engineering
                           and Chemistry

                          _____ _____
                                                              Date

                          _____ _____
                                                              Date

                          _____ _____
                                                              Date

                          _____ _____
                                                              Date

CURRICULUM VITAE

Name: David W. H. Roth, Jr.

Degree and date to be conferred: Doctor of Engineering Science, 1985

Secondary education: Allentown High School, 1947

Collegiate institutions attended: Degree   Date of Degree

   Lafayette College   B.S. Ch.E.   1951

   New Jersey Institute of Technology   M.S. Ch.E.   1961

Major: Chemical Engineering

Positions held: Allied Corporation

                                    1980-Present - Director, Office of
                                                Science & Technology
                                    1979-1980   - Director, Consolidated
                                                 Metal Products
                                    1978-1979   - Director, Engineering
                                                 Sciences Department
                                    1976-1978   - Director, Engineering
                                                 Technology Center
                                    1972-1976   - Director, Corporate
                                                 Engineering
                                    1971-1972   - Venture Director,
                                                 Fibers Division
                                    1969-1971   - Director, Fibers Division
                                               Engineering

ABSTRACT

Title of Thesis: Ternary Ion Exchange in Fixed Beds
                          - Equilibrium and Dynamics -

David W. H. Roth, Jr., Doctor of Engineering Science, 1985

Thesis directed by: Professor Ching-Rong Huang

A model was developed to simulate ion exchange within fixed beds for ternary systems. Models of the fluid phase material balance, phase equilibria, and diffusion of ions through the film and within the resin phase incorporated the latest advances in ion exchange theory. The separate model elements were combined after testing into an overall general model. Non-linear regression support programs were developed to estimate equilibrium parameters and resin phase diffusion coefficients.

A computer program was developed to estimate axial dispersion coefficients from experimental data. General correlations derived from literature sources were tested, and axial dispersion terms were included in the electrolyte phase material balance equations.

The rational thermodynamic equilibrium constant, utilizing resin phase activity coefficients based on the 3 suffix Redlich-Kister equation and the Bromley equation for electrolyte phase activity coefficients, was selected. The Wilson and NRTL equations were tested but were not as good. This model was used to correlate published data on 13 binary systems and to predict ternary compositions for comparison to published data on 4 ternary systems. Average root mean square of % normalized difference was about 3% on the binary systems and 4-12% on data predicted for the ternary systems.

The Nernst-Planck equation was used to model resin phase diffusion. An integrated form of the Nernst-Hartley equation, based on the Bromley

equation, was developed and tested to predict the effect of concentration on electrolyte phase diffusion coefficients. These coefficients were used in a pseudo electric field model which was developed and tested to approximate the electric field effect on diffusion of ions in the film.

The overall ternary system model resulted in four coupled non-linear second order parabolic partial differential equations, with appropriate boundary conditions. The equations were reduced to a set of algebraic equations by finite difference approximations and solved by the implicit Crank-Nicholson method. Non-linear terms were quasilinearized. The resulting five diagonal coefficient matrix describing the fluid phase, coupled with the 7 diagonal coefficient matrices describing the resin phase, were inverted with algorithms developed in this work. An iterative procedure resolved all non-linear terms at each time step. Comparison of concentration histories generated by the model with experimental results obtained by previous researchers showed that the ternary model could be used in practice to optimize process design applications with a bed in a condition of partial presaturation, and for favorable or unfavorable ion exchange.

Resin phase activity coefficients developed in correlation of the equilibrium data were used to test chemical potential as a driving force in the systems simulated. Indication that use of chemical potential would obviate the need for ion pair specific diffusion coefficients in the Nernst-Planck model, or the use of ion pair corrector coefficients (Stefan-Maxwell), is shown by comparison of results on seven binary systems. Implications for industrial application and directions for further research are discussed.

ACKNOWLEDGEMENTS

TABLE OF CONTENTS

LIST OF FIGURES

LIST OF TABLES

LIST OF ILLUSTRATIONS

Illustrations

CHAPTER I

INTRODUCTION, BACKGROUND, AND REVIEW OF LITERATURE

A. Introduction

"But now it should be entirely in the realm of possibility to develop computer programs to handle general (ion exchange) entry conditions...and that the time is not far off when ion exchange adsorption separations can be designed in the same way as distillation separations are today." These words, printed in CEP of October 1977, by Dr. Friedrich Helfferich, who is a world leader in the science of ionic separations, clearly summarize the objectives of this work. The computer based simulation model developed in this work has moved Dr. Helfferich's predictions in that direction, since the purpose of this research was to advance the science of the engineering of ion exchange systems.

Specifically, the objective was to develop a simulation model for ternary systems which would embody most of the currently proven factors applying to prediction of phase equilibria, and to the prediction of the dynamics of ion exchange in fixed beds. The goal was to utilize as many parameters as could be derived from reliable published correlations and to minimize the amount of experimentation required to supply the requisite data for unknown parameter estimation. The simulation objective, therefore, could not be complete until computer based regression analysis support programs, specific to estimation of typical ion exchange parameters, were included as a codevelopment of the dynamic model.

1. <u>General Overview</u>

The use of ion exchange as a unit process in chemical operations dates back more than half a century and, for a large number of commercial ion exchange installations made during that period, the major utility was to produce deionized water for process or boiler feed water makeup. The most important class of ion exchange resins are the gel type beads formed by polymerization of styrene and crosslinked to varying degrees by addition of divinyl benzene. The cation exchange types commonly in use have (1) strongly acidic functionality resulting from sulfonic acid groups attached to the polymer, or (2) weakly acidic functionality due to carboxylic acid groups being part of the polymer structure. Bifunctionality, which may yield a particular cation selectivity relationship, may be obtained by combining in one resin both functionalities.

The anion exchange types of resins in common use involve (1) quaterary ammonium functional groups to yield strongly basic types, and (2) polyamine functional groups to yield weakly basic anion characteristics.

Resin types can be created having both anionic and cationic functionality and, for example, are used in the production of high quality deionized water. Macroreticular (macroporous) resins have been developed with the same functional groups described above. These resins have large discrete pores for use in recovery of high molecular weight

species, or in nonaqueous applications, and where resin toughness and resistance to breakdown is required.

In recent years, interest in recovery of heavy metals in hydrometallurgical applications or in waste water cleanup has led to the development of resin with high selectivity towards these ionic species. These are resins containing functional groups, such as iminodiacetic acid, which have the ability to chelate the desired species and can be designed to be highly selective for say Cu^{++} in Cu^{++}/Fe^{+++} mixtures (leach dump solutions) at a given pH. Elution with strong acid at low pH is then possible in order to recover the copper for subsequent electro-winning.

The number of commercial applications for ion exchange operations has grown rapidly since the 1950s, and the following tabulation represents just a sampling of applications other than water demineralization:

a)   Isolation and recovery of metals (hydrometallurgy or waste treatment.

b)   Isolation and recovery of high molecular weight organic acids or bases.

c)   Separation and purification of amino acids.

d)   Separation of rare earths.

e)   Purification of sugars.

f)   Uranium recovery.

g)   Antibiotic recovery.

h)   Catalysis such as inversion of sugar.

i) Recovery of actinides.

j) Catalysis of organic reactions in non-aqueous solutions.

2. Objectives

2.1 General Objectives

The objective of this work, as stated, was to
create a simulation model for the exchange of three
counterions between an aqueous electrolyte solution and
a monofunctional ion exchange resin performed within a
fixed bed. The type of ion exchange resin upon which
the model was premised was the gel type having either
cationic or anionic functional groups. Most
investigators seeking to develop mechanisms and models
for ion exchange equilibria and dynamics have
standardized on the cation exchange resin Dowex 50W X8
for their experiments. The extensive data available on
Dowex 50W X8 was used in this work for parameter
estimation and model verification. Dowex 50W X8 is a
strongly acidic cation exchange resin produced by Dow
Chemical Company with about 8% divinyl benzene cross
linkages.

Models dealing with the exchange of two ionic
species in such resins are available based upon varying
degrees of simplifying assumptions. However, in many of
the above-listed applications the selective exchange of
two ionic species is performed in the presence of a
third ionic species, and in many instances this ion is

H^+. General models for fixed bed ion exchange involving ternary systems do not exist, except for cases involving major simplifying assumptions (22, 78).

The most definitive publication to date dealing with all aspects of ion exchange (including ionic separations by membranes) is the book, Ion Exchange, by Friedrich Helfferich, McGraw Hill, New York, 1962. The book is out of print but an authorized facsimile was produced in 1978 by University Microfilms International, Ann Arbor, Michigan, USA. Dr. Helfferich continues to be a world leader in the science of ionic separation and, in a complete quotation from the CEP issue of October 1977 stated, "I have so often seen it in practice that, when it comes to sizing or designing a (ion exchange) column, just about anything that goes beyond the equilibrium capacity is left to a strange mixture of experience, intuition, folklore, and black magic. But I believe a change here is imminent, and my confidence is based on two factors. One is the advent of multicomponent theory, which inherently is much nearer to many of the practical problems, more ions being involved than just two. The second is the availability of faster and cheaper computers. What the man in practice usually needs is to calculate a process where an ion exchange bed is run to breakthrough and then is incompletely regenerated. The solutions

tabulated and easily looked up in Perry's Handbook are largely or exclusively for calculation of behavior of a bed of uniform initial composition and receiving a constant feed, and they are only of limited use. But now it should be entirely in the realm of possibility to develop computer programs to handle general entry conditions. I believe that this will happen shortly and that such programs will be used to a much greater extent than we have been accustomed to, and that the time is not far off when ion exchange adsorption separations can be designed in the same way as distillation separations are today."

2.2 Approach

The "generalized approach" used in this research project to develop a fixed bed ion exchange model for binary and ternary systems is shown in Figure 1-1. In this instance, the goal is to optimize, scale up, and design controllable ion exchange processes. In many instances, industrial applications of ion exchange can prove to be more economic than other separation process. The model development methodology depicted, including experimentation to generate equilibrium data and dynamic information plus model verification techniques, are general to any process modeling effort. A more detailed "road map" of modeling effort specifically related to ion exchange processes is

Figure 1-1

ION EXCHANGE PROCESS OPTIMIZATION

BINARY AND TERNARY SYSTEMS

Installation and
profitable operation

Ion Exchange
Process Application

assumptions
scientific principles

Mathematical Model
with unknown parameters

scale-up and
control

Computer based Numerical
Approximations

test
model

Analytical Solutions
simplified cases

model validation
and/or map areas for further experiments

test for stability
and convergence

Experimental Data ion
exchange equilibria

Thermodynamic Model
with unknown parameters

Parameter Estimation
through regression
analysis

thermodynamic
parameter input

Computer based Numerical
Model - simulation of
complex cases

model validation
and/or map areas for further experiments

Experimental Data
ion exchange dynamics

Parameter Estimation
through regression
analysis

model support for
regression analysis

model utilization
in simulations

model
validation

Parameter Estimation
through trial & error
curve fitting w/model

Plant Design and
Optimization

model validation
and/or map areas for further experiments

outlined in section C of Chapter VIII, Summary, in Figure 8-1. The reader is invited to read section C of Chapter VIII following Chapter I, since this dissertation is prepared so that each subsequent chapter deals with a major element of the overall model on a stand-alone basis. The model development approach shown in Figure 8-1 provides the unifying framework for all of the elements as they are combined in an ion exchange process modeling and design optimization procedure.

2.3 Specific objective

The objective of this research work was to advance the engineering of ion exchange systems. Specifically, the goal was to create a general computer based simulation model which would describe ion exchange in fixed beds for ternary systems. The model was to be based on the best currently held theories related to phase equilibria, ionic transport through the film phase, and ionic transport within gel type ion exchange resins. Development of support programs which would perform non-linear regression analytic estimation of phase equilibria parameters and resin phase diffusion coefficients from experimental data was a necessary companion research objective. All other information required to design and optimize fixed bed ion exchange processes was to be derived from reliable published correlations. These include (1) film coefficients in

packed beds, (2) ionic species diffusion coefficients in aqueous solutions, (3) ionic species activity coefficients in aqueous solutions, and (4) axial dispersion coefficients in packed beds.

2.4 Experimental Data Utilized

In order to test the model components, and ultimately the overall simulation model, suitable experimental data had to be found which described both ion exchange equilibria and fixed bed dynamics in binary and ternary systems. The following three major sources of data were utilized in this work:

(1) K. L. Erickson - "Fixed Bed Ion Exchange with Differing Ionic Mobilities and Nonlinear Equilibria." PhD dissertation, University of Texas, 1977.

System NH_3 - Ethylene Diamine in H_2O.
Column operation using Dowex 50w X8 resin at 25° and 1.0 normal Cl^- solutions.

Conditions

Two favorable (Ethylene Diamine (ETDA) for NH_3) exchanges at two flow rates, 1.85 cm/sec and 0.94 cm/sec superficial velocity. Reynolds No. 20 and 40.

One unfavorable (NH_3 for ETDA) exchange at 1.85 cm/sec superficial velocity. Reynolds No. 40.

<u>Equilibrium Data</u> at 25° C for 1.0 normal and

0.1 normal Cl^{-} solutions. (15 and 12 data

points respectively.)

(2)   O. O. Omatete - "Column Dynamics of Ternary Ion

Exchange." PhD dissertation, University of

California at Berkeley, 1971.

System Ag^{+}, Na^{+}, H^{+} in H_2O.

Column operation using Dowex 50w X8 resin at

$25^{\circ}C$ and NO_3^{-} solutions of 0.05 and

1.5 normality.

<u>Conditions</u>

<u>Binary runs</u> for <u>favorable</u> exchange of all ion

pairs at 2 normalities (6 runs).

<u>0.05 normal</u>, superficial velocity -

0.18-0.2 cm/sec; Reynolds No. 4.-4.4.

<u>1.5 normal</u>, superficial velocity - 0.08

cm/sec; Reynolds No. 1.9.

<u>Ternary runs</u> for <u>favorable</u> exchange

1.   Resin in H^{+} form.

Feed comp. $X_{Ag}=0.25$, $X_{Na}=0.24$, $X_{H}=0.51$

(equivalent fraction) at 0.0533 normality

of NO_3^{-} ion.

Superficial velocity = 0.097 cm/sec,

Reynolds No. 1.94.

2.   Resin in H^{+} form.

Feed comp. $X_{Ag}=0.35$, $X_{Na}=0.24$, $X_{H}=0.41$

(equivalent fraction) at 1.51 normality of NO_3^- ion.

Superficial velocity = 0.0346 cm/sec,

Reynolds No. 0.70.

Ternary run for unfavorable exchange

1. Resin in Na^+ form.

    Feed comp. $X_{Ag}=0.187$, $X_{Na}=0.133$, $X_H=0.68$ (equivalent fraction) at 1.5 normality of NO_3 ion.

    Superficial velocity = 0.046 cm/sec,

    Reynolds No. 0.92.

Equilibrium Data at 25°C for all binary pairs at NO_3 solutions of 0.1 & 1.5 normality (16 total points for all 6 sets).

Ternary Equilibrium data for 0.1 normal & 1.5 normal at 25°C (2 points + 3 material balance points generated in this research project from the three rate runs).

(3) R. K. Bajpai, A. K. Gupta, M. Gopalo Rao, "Single Particle Studies of Binary and Ternary Cation Exchange Kinetics," AIChE Journal, September 1974 (Vol. 20, No. 5), pp. 989-995 plus Supplementary Material, rev., Dept. of Chem. Eng., Indian Inst. Tech., Kanpur, 17 pp. and "Binary and Ternary Ion Exchange Equilibria Sodium-Cesium-Manganese-Dowex 50w-X8 and Cesium-Manganese-Strontium-Dowex 50w-X8

Systems," _Journal of Physical Chemistry_, (Vol. 77,
No. 10) 1973, reprint.

Systems Sr^{++}, Mn^{++}, Cs^{+} in H_2O & Mn^{++},
Cs^{+}, Na^{+} in aqueous solutions of Cl^{-} anion.

Single particle "batch operation" using Dowex 50W
X8 resin at $23^{\circ}C$ in 0.1 normal Cl^{-} solutions.

Binary runs; concentration vs. time curves
were generated for the systems SrMn, MnSr,
MnCs, SrCs, MnNa, NaMn, & NaCs, where the bar
refers to the species in the resin.
Superficial velocity - 25 cm/sec, Reynolds No.
700.

Ternary runs;

22 runs of various resin and electrolyte
compositions. Conditions were similar to
the binary runs. Since only one species
in three could be radioactively tagged,
only one concentration vs. time curve
could be generated; whereas for ternary
modeling, two curves or concentration
traces are desirable.

Equilibrium Data

Experiments were performed using tagged ionic
species for all binary pairs, and various
ternary compositions for the ternary systems
Sr^{++}, Mn^{++}, Cs^{+} & Mn^{++}, Cs^{+}, Na^{+}.

(16 points for the first ternary system and 15

points for the second ternary system.)

The quality of the experimental procedures and

attention to detail was judged to be very good for the

Erickson column experiments on NH_3-EDTA, as was the

work of Bajpai, Gupta, & Rao on single particle

techniques. There have been questions raised on the

general extendability of single particle experiments to

full column operation, but the investigators carried out

the experimentation carefully, and reproducibility on

the equilibrium experiments was ± 2%. Omatete's

experimental work appeared to be less carefully

controlled, and certainly did not yield a sufficient

number of data points to satisfy the equilibrium

correlation requirements.

B. Background

    1. Equilibria

        1.1 Equilibrium Relationships

           A multitude of conventions are used to relate the

concentration of an ionic species in the electrolyte

phase with its concentration in the resin phase. The

concentration units used in the various conventions can

involve molar, molal, mole fraction, or equivalent

fraction for both phases, or different units for each

phase in all combinations. Helfferich (36) discusses

these conventions in his outstanding book on ion

exchange. The exchanging ions have an electric charge opposite in sign to the charge of the fixed functional groups in the resin and are called <u>counterions</u>. The ionic species in the electrolyte having an electric charge of similar sign to the resin phase charge are called <u>coions</u>. A favorable exchange involves replacement of ions in the resin phase with ions from the electrolyte phase which are preferred by the ion exchange resin. The opposite is an unfavorable exchange.

The simplest equilibrium convention utilized is the <u>distribution coefficient</u> which implies a linear relationship:

$$\lambda_i = \frac{\overline{x}_i}{x^*_{i_{int}}} \qquad (1\text{-}1)$$

where: $\overline{x}_i$ = equivalent fraction of species i species i in the resin

$x^*_{i_{int}}$ = equivalent fraction of species i in the electrolyte in equilibrium with the resin.

Other concentration units could be used. Rao and his coworkers (93) used this relationship but corrected for the non-linearity actually experienced in most ion exchange equilibrium relationships by using the expressions:

$$\lambda_i = a + b \cdot \overline{x}_1 + c \cdot \overline{x}_1^2 \qquad (1\text{-}2)$$

$$\circ \qquad \lambda_2 = \frac{(1-\bar{x}_1)}{(1-x_{1_{int}}^{*})} \qquad (1\text{-}3)$$

Ternary systems were correlated by Rao and his coworkers based on pseudo equivalent fractions, i.e., excluding the concentration of the ion not involved in the binary distribution coefficient being calculated.

A more frequently used convention is the separation factor involving any of the concentration units described above, and is given in equivalent fraction units as:

$$\circ \qquad \alpha' = \frac{(\bar{x}_1 \cdot x_{2_{int}}^{*})}{(\bar{x}_2 \cdot x_{1_{int}}^{*})} \qquad (1\text{-}4)$$

where ion 1 is the favored species. This is similar to the K factor used in distillation and contains no provisions for non-ideality in either phase. Omatete (78) used this representation for ternary systems with the convention:

$$\circ \qquad x_{j_{int}}^{*} = \left[\frac{\alpha_j^{ref} \cdot \bar{x}_j}{\sum\limits_{\substack{k=1 \\ k \neq ref}}^{n} \alpha_k^{ref} \cdot \bar{x}_k} \right] \quad \text{for } j=1,\ 2,\ 3 \qquad (1\text{-}5)$$

The various mass action forms appear as is shown for equivalent fraction units:

$$\circ \qquad \bar{K}_2^1 = \left(\frac{\bar{x}_1}{x_{1_{int}}^{*}} \right)^{|z_2|} \cdot \left(\frac{x_{2_{int}}^{*}}{\bar{x}_2} \right)^{|z_1|} \qquad (1\text{-}6)$$

where z_i = charge on ionic species i.

These forms can be altered by substitution of activity, $a_{i_{int}}^*$ for the electrolyte phase and finally, with the substitution of activity $\bar{a}_i$ for the resin phase, appear as <u>thermodynamic equilibrium</u> constants:

o $\qquad t\bar{K}_2^1 = \left(\dfrac{\bar{a}_1}{a_{1_{int}}^*}\right)^{|z_2|} \cdot \left(\dfrac{a_{2_{int}}^*}{\bar{a}_2}\right)^{|z_1|}$ (1-7)

The molal form appears as

o $\qquad t\bar{K}_2^1 = \left(\dfrac{\bar{m}_1 \cdot \bar{\gamma}_1}{m_1^* \cdot \gamma_{1_{int}}^*}\right)^{|z_2|} \cdot \left(\dfrac{m_{2_{int}}^* \cdot \gamma_2^*}{\bar{m}_2 \cdot \bar{\gamma}_2}\right)^{|z_1|}$ (1-8)

If the standard and reference states are chosen so they are the same in the electrolyte and resin pore solution, then $t\bar{K}_2^1 = 1$, and selectivity shown by the relationship is vested in the activity coefficients. The <u>rational form</u>,

o $\qquad {}_t^n\bar{K}_2^1 = \left(\dfrac{\bar{x}_1 \cdot \bar{\gamma}_1}{m_1^* \cdot \gamma_{1_{int}}^*}\right)^{|z_2|} \cdot \left(\dfrac{m_{2_{int}}^* \cdot \gamma_2^*}{\bar{x}_2 \cdot \bar{\gamma}_2}\right)^{|z_1|}$ (1-9)

is often used and in this case the standard and reference states of the resin phase and the electrolyte phase are quite different. The selectivity shown by the relationship is vested in the equilibrium constant, ${}_t^n\bar{K}_2^1$, with the activity coefficients providing "trim

up" to correct extreme non-linearity conditions.

Both thermodynamic forms are based on the simplification assumptions that electrolyte and solvent sorption and desorption are negligibly small. They are normally used to describe binary systems, since multicomponent models for activity coefficients in either phase have not been extensively explored.

1.2 Electrolyte Phase Activity Coefficients

Electrolyte phase activity coefficients of individual ions in aqueous solutions of mixed salts are required in the thermodynamic equilibrium relationships. The familiar Debye-Huckel relationship which predicts activity coefficients for single ions and mean activity coefficients for pure salts dissolved in water is based on the long range electrostatic interaction of charged particles. It holds only for dilute solutions in which short range (van der Waals) interactions are minimal. At higher concentrations these forces become significant, and second or third terms which are functions of the solution ionic strength, I, are added to the Debye-Huckel equation to account for ion-ion short range interactions. These equations constitute the extended forms of the Debye-Huckel equation, one of which is given by Robinson and Stokes (103) for single ions as follows:

$$o \qquad \ell n \gamma_i = - \left[\frac{A \cdot z_i^2 \cdot \sqrt{I}}{(1+B \cdot a_i) \cdot \sqrt{I}} \right] + b_i \cdot I \qquad (1-10)$$

in which the a_i and b_i parameters are given by Truesdell and Jones (128).

The relationship of activity coefficients of salts in mixed electrolytes has been studied by Guggenheim and Turgeon (31), Meissner and Kusik (67), and Pitzer (86), Edwards, Newman and Prausnitz (24) and others. The treatment introduced by Guggenheim involved the normal Debye-Huckel long range interaction effect plus a summation term which related the short range interactions of specific cation-anion pairs. An ion pair parameter was used in combination with the molal concentration of the specific ion (cation or anion) to represent the magnitude of the interaction. Bromley (9) and Meissner and Kusik (67, 68) extended the predictive ability of such models to concentrations as high as 6 molal by introduction of additional terms, but yet requiring only one pair corrector constant for each salt present. Bromley (9), with later evaluation and testing by Zemaitis (139), correlated a large number of extended coefficients for various salts. Based on a variation of the Guggenheim model, Bromley (9) derived an activity coefficient model for single ions in mixed electrolytes with applicability up to the 6 molal range.

Measurement of the activity of a single ionic species is not possible, so the criteria of predictive capability of a model is limited to the mean activity coefficient of a given salt in mixed electrolytes. Several of these methods for prediction of activity coefficients for salts in multicomponent aqueous solutions were evaluated by Sangster and Lenzi (111). The overall efficacy of prediction of single ion activity coefficients from tabulated Debye-Huckel extension parameters in mixed salts up to 6 molal concentrations can best be judged by the results of simulations in which these parameters are important. The success of the use of the Bromley type relationship has been aptly demonstrated by the predictive capability of the systems developed and tested by Zemaitis (139) while at Chem Systems, Inc. to predict complex ionic phase equilibria. Some of this work (25) was done under sponsorship of the AIChE Design Institute for Physical Property Data (DIPPR).

1.3 Resin Phase Activity Coefficients

Models for resin phase activity coefficients have not been studied extensively for multicomponent systems. For binary systems, Rao and David (88) used the observation that the activity coefficients of species in the resin phase are lower but proportional to the activity coefficients of the species in electrolyte solutions having the same ionic strength as the solution

in the resin phase. This correlation was successful in predicting the binary data with a ± 10% maximum error; however, it is noted that ionic strength in the resin may exceed 13, well beyond the electrolyte phase activity coefficient correlation capability. The method has not had wide acceptance. Although several predictive binary models have been proposed by various investigators (40), these models as yet only give qualitative information. The resin phase activity coefficients must be correlated from experimental data with thermodynamically consistent representations. One such early model was developed by Kielland (53) and put on a more sound theoretical footing by Barrer (5). The model is in fact a one suffix Redlich-Kister type equation, and led to trial of multisuffix Redlich-Kister equations in this work. Salmon (110) has investigated a statistical thermodynamic approach for correlation of multivalent anion exchange equilibria in binary systems with some success.

The most significant work on correlation of resin phase activity coefficients in multicomponent systems was performed by Smith and Woodburn (116) on the system $NO_3^--Cl^--SO_4^=$ on Dowex 50W X8/Na^+. The Wilson equation (98) is used in correlation of activity coefficients in liquid systems based on assumptions of non-randomness of local compositions to express the excess Gibbs free

energy relationships. The equation has two adjustable parameters per binary system. Smith and Woodburn showed that the Wilson equation, utilizing fitted binary system coefficients, could predict ternary system equilibrium concentrations for the system investigated with a standard deviation of % normalized difference of 4.3%. This model, along with the 3 suffix Redlich-Kister and NRTL equations, were evaluated in this work.

2. Film Mass Transfer Coefficients

2.1 Film Coefficient Correlations for Packed Beds

Many investigators have studied the mass transfer from fluids to particles in fixed beds. Carberry (11) generated a boundary layer model of the form

$$j_{b.1.} = \frac{k_L \cdot \varepsilon}{v_a} \cdot Sc^{\frac{2}{3}} = b \cdot Re^{-\frac{1}{2}} \qquad (1-11)$$

where:

$$b = 1.15$$
$$v_a = \text{superficial velocity}$$
$$\varepsilon = \text{bed void fraction}$$
$$Re = \text{Reynolds No. based on } \frac{v_a}{\varepsilon}$$
$$Sc = \text{Schmidt No.}$$

Data from numerous experimental studies for gases and liquids was correlated well by this relationship down to Reynolds No. of 1.0. Wilson and Geankoplis (138) showed for transfer from benzoic acid spheres to water or propylene glycol that Re' raised to the $-2/3$ power

correlated the data well (Re' based on superficial

velocity). Work by Snowdon and Turner (131) on

correlation of film coefficients for mass transfer to

ion exchange resins in fluidized beds found a

Carberry-type relationship fit the experimental data

well. Comparison of the two equations showed:

Carberry correlation for fixed beds

$$\circ \quad Sh = \frac{k_L \cdot D}{d} = 1.15 \cdot \left[\frac{Re'}{\epsilon} \right]^{\frac{1}{2}} \cdot Sc^{\frac{1}{3}} \tag{1-12}$$

where Re' is based on superficial velocity

Snowdon & Turner correlation for fluid beds

$$\circ \quad Sh = \frac{k_L \cdot D}{d} = 0.81 \cdot \frac{Re'^{\frac{1}{2}}}{\epsilon} \cdot Sc^{\frac{1}{3}} \tag{1-13}$$

where for fluid beds the coefficient b = 0.81 and   is

raised to the first power.

P. N. Rowe (109) also evaluated particle to liquid mass

transfer in fluidized beds based on work done by Nelson

and Galloway (73) at low Reynolds No.,∿1-10 . Koloini

and his coworkers (54, 55) studied mass transfer in

liquid fluidized beds at low Reynolds No. (∿1) and found

the following correlation,

$$\circ \quad Sh = \frac{k_L \cdot D}{d} = 1.10 \cdot \frac{Re'}{\epsilon} \cdot Sc^{\frac{1}{3}} \tag{1-14}$$

represented data for ion exchange in dilute solutions of

HCl and benzoic acid, as contrasted to the Snowdon and

Turner correlation which fit the data well in the region

of 5<Re<100.

2.2 Effects of Electric Field in the Film

Helfferich (43) describes the effect of exchange of ions having differing mobilities as they pass through the film surrounding an ion exchange resin. Since the conditions of electroneutrality and no electric current must exist in the film, the coion distributes itself in the film in such a manner as to counterbalance the electric field gradient in the film. The interdiffusivity relationship is described by the Nernst-Planck equation, which is given as:

$$J_i = -D_i \cdot (\nabla c_i + z_i \cdot c_i \cdot \frac{F}{RT} \cdot \nabla \Phi) \qquad (1-15)$$

where:

F	= Faraday's constant
Φ	= electric potential
c_i	= concentration
D_i	= diffusion coefficient
z_i	= charge on particle
J_i	= molar flux
T	= temperature
R	= gas constant

The usual assumption is to assume a quasi-stationary state for the coion in the film which presumes any coion dynamics have occurred prior to the quasi-stationary state condition. In addition to Helfferich, Snowdon and Turner (131) have evaluated the effect for exchange of

Na^+ and H^+ on Zeo-Karb 225 in dilute Cl^-

solutions. Their measurements agree with the

Nernst-Planck model. They assumed a stagnant film

thickness based on the Reynolds No. and an effective

diffusion coefficient determined by the Nernst-Planck

model interdiffusivity constraints. Van Brocklin and

David (132) extended the Nernst-Planck concept to a

calculable ratio, R_i, of effective film coefficient

with electric field effects to the film coefficient

calculated from packed bed correlations, such as

Carberry's. They investigated three models, (1) a Film

Model similar to Turner and Snowdon, (2) a Penetration

Theory Model, and (3) a Boundary Layer Model. Tables of

R_i values were calculated for various diffusivity

ratios of ions being exchanged and for a variety of

electrolyte concentrations at the film boundaries. No

experimental verification was offered. Van Brocklin and

David (133), in a later work, used data developed by

other investigators (single particle studies with

radioactively tagged ionic species) to test the various

models. The data were insufficiently accurate to select

the best mass transfer model, although the direction and

magnitude of correction given by the models gave better

agreement with the data than did uncorrected film

coefficients. Pan and David (83) computed the effect of

R_i model on the design of a moving packed bed ion

exchange process. No experimental data was available for comparison but, in unfavorable exchange, more than 50% underdesign could be experienced if the electric field effect was neglected. Kataoka and Yoshida (50) developed rigorous equations to describe homovalent exchange of ions through a film under the influence of an electric field. A factor,β , similar to the R_i factor, related the film coefficient corrected for electric field effects to the film coefficient without the effects. Experimental effluent concentration histories (ECH) were obtained for the favorable and unfavorable exchange of Na^+-H^+ on DIAION SK1B resin in fixed beds. Chloride solution normality of 0.005 was maintained in order to operate in a film diffusion controlling regime. In order to simplify the mathematics, resistance to mass transport in the resin was assumed to be negligible. The electric field model gave the best representation of the ECH curves, particularly during unfavorable exchange when the least favored ion has the highest mobility. For favorable exchange, particularly when the most favored ion has the lowest mobility, use of the uncorrected diffusion coefficient for the slower ion can be used to approximate column behavior within an error of 30%.

3. Diffusion in the Resin Phase and Various Representations in Fixed Bed Operations

Early representations of rate laws governing diffusion

in the resin phase had more to do with the ability of the resulting equations to be solved analytically then with actual physical process phenomena. Thomas (127) in 1944 represented ion exchange rates in the resin as two opposing second order reactions. Other "rate law" formats were solved by Amundson (3) in 1949 and Vermeulen and Hiester (134) in 1952. Vermeulen and Hiester (136) also treated the dynamics of ion exchange involving uniform partial presaturation of a column utilizing dominant film theory. Dominant film theory is based on the assumption that resistance to ionic transport from the electrolyte phase to the resin phase is controlled by diffusion through a stagnant film around the particle in external diffusion control, or through a hypothetical thickness of resin constituting a "film" in internal diffusion control.

Rosen (107) in 1951 made the first analytical solution of a fixed bed ion exchange process using Fick's Law for diffusion in the resin phase, coupled with ionic diffusion through an adjacent electrolyte film. The major simplifying assumptions were that axial diffusion in the fluid phase was negligible and that the equilibrium isotherm was linear. The analytical solution contained an infinite integral which converged slowly during computation. This was a milestone effort, however, since the solutions represented benchmarks against which later investigators could test numerical solutions. In 1954 Rosen (108) derived a general solution

for solid diffusion in fixed beds by use of a partial
integrodifferential equation.

Dranoff and Lapidus (22) performed the solution of
ternary ion exchange in a fixed bed in 1957. They assumed
(1) mass action type equilibria for monovalent systems, (2)
Thomas type reaction rate laws, (3) no axial diffusion in the
fluid phase, and (4) that an asymptotic solution method could
be applied based on achievement of a stable concentration
configuration in the column (i.e., infinite column). The
method of characteristics was used to transform the partial
differential equations into ordinary differential equations,
and solutions were obtained by numerical approximation.
Typical results for column operation were generated for the
system Ag^+-Na^+-H^+ on Dowex 50 using literature values
for parameters. No experimental comparison was made, since
the parameters had been derived in batch experiments. Tien
and Thodos (126) in 1959, assuming Fick's Law for diffusion
in the resin phase, essentially added the effects of a
non-linear Freundlich type equilibria isotherm relationship
to the case treated analytically by Rosen. Numerical methods
were used to solve the resulting integrodifferential
equation. Masamune and Smith (63, 64) in 1965 investigated
the case of adsorption into a porous media from a gas stream
using the following model features: (1) film resistance, (2)
Fick's Law diffusion in the pores, and (3) a reversible first
order adsorption rate equation with linear equilibria.

Additionally, asymptotic conditions were assumed with no axial diffusion term in the gas phase. The resulting analytical solution contained an infinite integral which was evaluated numerically.

In 1965 Cooney and Lightfoot (18) proved the existence of asymptotic solutions to constant pattern operation of fixed bed separations, including the case involving non-linear equilibria with axial dispersion and finite mass transfer resistance. Following this, Hall, Eagleton, Acrivos, and Vermeulen (34) in 1966 studied constant pattern behavior in fixed beds based on both pore and solid diffusion mechanisms within the porous particle. The axial dispersion term was assumed to be negligible, non-linear equilibrium of the Langmuir type was assumed, and numerical solutions were obtained for a wide range of dimensionless variables. These solutions merged smoothly into the analytic solutions for linear equilibrium cases. Rhee and Amundson (101) in 1971 extended the asymptotic type of nonequilibrium exchange to include an axial dispersion term in the fluid phase by applying shock layer theory. The mass transfer to the solid phase was based on ionic diffusion through a fictitious "solid film" utilizing an effective film coefficient; however non-linear equilibria of the Langmuir type was assumed in one example. Transient behavior of the column operation was studied by numerical solution of the basic partial differential equations and the profiles compared to those

given by asymptotic shock theory solution. The concentration profile shape and location in the column coincided with that predicted by shock theory as steady state conditions were approached in the "infinite" column. This approach led ultimately to the more general case developed by Bradley and Sweed (8) for multicomponent systems in 1975. All of these asymptotic approaches are, in effect, equilibrium cases since transient behavior cannot be portrayed. However, in systems where constant concentration patterns are attained, they give good representation of profile shape and location in the column of each specie's concentration plateau with minimum calculation effort.

4. Nernst-Planck Representation of Diffusion in the Resin Phase

4.1 Concentration Driving Force

Helfferich and Plesset in 1958 proposed application of the Nernst-Planck equation (42) to describe the interdiffusivity relationship between counterions in binary exchange. By assuming (1) no coion intrusion into the resin, (2) a condition of electroneutrality at all points in the resin, and (3) that no electric currents are present, the following equation results:

$$\circ \qquad \bar{D}_{12_{eff}} = \left[\frac{\bar{D}_1 \cdot \bar{D}_2 \cdot (\bar{x}_1 \cdot |z_1| + \bar{x}_2 \cdot |z_2|)}{\sum\limits_{i=1}^{2} \bar{x}_i \cdot |z_i| \cdot \bar{D}_i} \right] \qquad (1\text{-}16)$$

Hering and Bliss (46) measured the diffusion rates of various ions in Dowex 50W resins having varying degrees

of crosslinking. The batch type experiments were run under conditions which would minimize film resistance effects (high stirrer speed and high (0.2 - 1.0 normal) solution strength). The Nernst-Planck model was compared to Fick's Law for its ability to represent the experimental data. Hering and Bliss state that there was no observable better fit of the data by the Nernst-Planck model; however, the Nernst-Planck model was theoretically superior in that the same ionic species "self diffusion" coefficients fit both favorable and unfavorable exchange of a given ion pair. Utilizing Fick's Law, different coefficient values are required to fit each exchange direction. The Nernst-Planck "self diffusion" coefficient for a given ionic species was different, however, depending on the nature of the counterion species for which it was being exchanged.

Rao and David (87) investigated the efficacy of the Nernst-Planck model vs. Fick's Law in single particle studies on the system Cu^{++}-Na^{+} on Dowex 50W X8 resin. Their model included the effect of film resistance (without electric field), and the Nernst-Planck model fit the data reasonably well in the regions where the film diffusion resistance was clearly not a factor; whereas the Fick's Law model did not.

Kuo and David (56) in 1963 showed with single particle studies on the system Ba^{++}-Na^{+} on

Dowex 50W X8 that a numerical model, which included coupled film resistance with Nernst-Planck representation of resin phase diffusion, simulated the experimental curves well.

Morig and Rao (89) in 1965, using a similar procedure for the system Sr^{++}-Na^{+} on Dowex 50W X8 resin, found that single "self diffusion" coefficients for each ionic species would not fit both the favorable and unfavorable exchange curves satisfactorily. However, they had used the Helfferich-Plesset (42) model which was based on isotopic exchange (i.e., no selectivity) and did not include film resistance, so the discrepancy is not surprising.

Turner, Church, Johnson and Snowdon (129) in 1965 measured the interdiffusion coefficients for the exchange of H^{+} and Na^{+} ions on Zeo-Karb 225-8%, using batch experiments. Progress of the exchange was monitored by solution conductivity. They found good agreement of the Nernst-Planck equation, based on the Helfferich-Plesset model (42) with the experimental data. More recently, as indicated in section A, part 2 of this chapter, the experimental work of Bajpai, Gupta and Rao was cited. Their batch model included a film resistance to mass transport as well as the Nernst-Planck model for ion exchange in binary and ternary systems. They derived the flux equations for

ternary ion exchange based on the Nernst-Planck

equations, and these are given in Chapter V of this

work. In a later paper, Rao and his coworkers (94)

derived the ternary system flux equations from

principles of irreversible thermodynamics. The

resulting final equations are identical since they

assumed conditions of ideal solution in the resin phase,

i.e., $\overline{\mu}_i^C = RT\ln(\overline{c}_i)$. In general, the results for the

binary simulations showed that the Nernst-Planck model

was effective in representing the concentration

histories for a variety of ions tested. The agreement

with the ternary system data was just fair, so only

qualitative conclusions could be drawn. The Fick's Law

model was not used in the comparisons, since the

investigators felt that the superiority of the

Nernst-Planck model had been adequately demonstrated by

others. However, in a later study Gupta and Rao (95)

used isotopic exchange techniques, in which tagged

Mn^{++} ion was exchanged in the presence of

Ba^{++}, Sr^{++}, Cs^{+}, and Na^{+} ions, and found that

the effective diffusivity of Mn^{++} changed as a

function of the concentration of Mn^{++} ion in the

resin. Their explanation was that as the water takeup

of the resin increased as a function of ionic

composition, the effective diffusivity of the exchanging

isotopes increased as well. As will be developed in

this work, use of activity driving force versus concentration driving force should minimize the dependency of effective ionic diffusivity on the resin water content, since the equilibrium resin water content is a function of system excess free energy.

Kataoka, Yoshida, and Ozasa (52) in 1977 conducted experiments in shallow beds on the system Na^+-H^+/OH^- and Na^+-Ce^{+++}/NO_3^- on various resins with differing degrees of crosslinking. Because of the neutralization reaction, the R-H/NaOH system has an infinite equilibrium constant. Their Nernst-Planck based model did not consider axial diffusion in the electrolyte phase, nor was film mass transport resistance considered. The agreement of the simulated results with the experimental curves was excellent.

The work of Erickson (26) is outlined in part section A, part 2 of this chapter, as is the work of Omatete (78). Since their data was utilized along with that of Rao and his coworkers, the detailed analysis of their work is contained in the body of this dissertation.

4.2 Chemical Potential Driving Force

Helfferich (45) derived the Nernst-Planck relationship in which chemical potential, $\bar{\mu}_i^c$, is used as the driving force versus concentration. Barrer and Rees (6) derived the effective diffusion coefficient for exchange of Ca^{++} and Sr^{++} ions in chabazite type ion

exchangers using irreversible thermodynamics. They
showed that when the cross-phenomenoligical coefficients
are set equal to zero, the equation reduces to the
Helfferich form for diffusion in membranes. The
additional terms to be added to the Nernst-Planck
equation for a binary system are:

$$
o \quad \frac{\bar{D}_1 \cdot \bar{D}_2}{\sum\limits_{1=1}^{2} \bar{x}_i \cdot |z_i| \cdot \bar{D}_i} \cdot \bar{x}_1 \cdot \bar{x}_2 \cdot \frac{\partial \ell n \left[\frac{\bar{\gamma}_1^{|z_2|}}{\bar{\gamma}_2^{|z_1|}} \right]_{molar}}{\partial \bar{x}_1} \qquad (1\text{-}17)
$$

The derivation for this term is given in Chapter V,
along with the derivation in this work of the
Nernst-Planck ternary system model in terms of chemical
potential utilizing the activity coefficients of ionic
species 1, 2, and 3. In order to use this extended
Nernst-Planck model, the molar activity coefficients
must be known as a function of resin phase composition
throughout the binary or ternary system phase diagram.
No literature was found dealing with the use of this
model to simulate the dynamics of ion exchange.

5. Other Model Considerations Not Included in this Work

    5.1 Resin phase mass transfer in ion exchange accompanied by
         a substantial change in resin volume was studied by
         Kataoka and Yoshida (49). Four factors come into
         consideration: (1) the diffusion length changes, (2)
         specific ion diffusion coefficient values change, (3)
         the fixed ionic groups in the resin move, and (4) the

activity gradient is altered. The investigators ignored the fourth effect since they did not have an activity driving force model. The expansion or shrinkage of the particular resin must be measured as a function of the concentration of one of the ions, $\bar{x}_i$, and the volume ratio fitted to a polynomial in $\bar{x}_i$. The equations are given which represent the standard Nernst-Planck continuity equation plus a term for resin volume change as a function of composition. Systems exhibiting up to 40% volume change such as $Ba^{++}-Na^{+}$ and $Ba^{++}-H^{+}$ exchange on DIAION SK1B X8 resin were measured for exchange kinetics using single particle tracer techniques. The revised Nernst-Planck model fit the experimental concentration history curves significantly better than the Nernst-Planck model without volume correction.

5.2 Effects of Sorbent Shrinking and Swelling on Fixed-Bed Sorption Operations

Marra and Cooney (17) studied this effect and found that due to effects related to resin shrinkage or swelling as discussed above, the physical bed volume may change by up to 40%. Experimental relationships must be developed for resin diameter change and bed void volume change as a function of composition in the resin. Using the simplifying assumptions of no axial dispersion in the fluid phase, and a "film model" for mass transport

in the resin, the fluid phase continuity equation was developed and solved numerically. The experimentally measured column behavior for the physical adsorption of NaCl into a solute free bed is predicted accurately by the dynamic model.

5.3 Prediction of Effects of Coion Intrusion and Formation of a Stable Complex with the Displaced Counterion

Chmutov, Kalinachev, and Semenovskaya (15) have developed a model in which the Nernst-Planck includes coion diffusion into the resin under conditions of electric neutrality, and the displaced ion, say Ni^{++} for Na^{+}, forms a stable $NiCl_2$ complex. This leads to the movement of a sharp Ni^{++}-Na^{+} boundary which moves toward the resin core, in a shrinking core model manner. The model fit the experimental data and, since coion intrusion is a factor, the exchange rate increased as solution concentration was increased.

5.4 Intraparticle Ion Exchange Accompanied by Instantaneous Irreversible Reaction

Kataoka, Yoshida, and Ozasa (51) have investigated ion exchange within a resin particle in which the ion exchanged reacts immediately and irreversibly with electrolyte phase coion which has intruded into the ion exchange resin. In this case the diffusion of the coion must be considered, along with the usual considerations of electroneutrality and no electric current. In

experiments involving H^+ form of resin exchanging with Na^+ in the presence of OH^-, water forms to give a stable reaction product. Similarly, CH_3COO^- forms of resin exchanging with HCl formed a stable reaction product in acetic acid. This model fit the experimental data better than the Nernst-Planck model which assumed no coion intrusion. Of course, this somewhat special circumstance of condition limits the models widespread application, but builds on the validity of the Nernst-Planck model and conditions of utility.

5.5 Prediction of Resin Phase Diffusion When Accompanied by Irreversible Exchange and Finite Rates of Reaction

Rao, Gupta, Williams, and Aguwa (96) found that chelating resins coordinate metals irreversibly at a given electrolyte pH, and that, in many cases, the rate of reaction is a significant factor in the exchange process. Using Levenspiel's (60) shrinking core model they successfully simulated exchange of Pb and Cd on Dowex A-1.

5.6 Use of Multi-Suffix Diffusion Coefficients in the Nernst-Planck Model

Graham and Dranoff (30) have applied the Stefan-Maxwell equations to ion exchange involving binary systems. The resulting equations are given in Chapter V. By use of these equations with the Nernst-Planck model the authors satisfactorily fit the

experimental concentration history curves for Na^+

displacing Cs^+ and H^+ displacing Na^+ on

Dowex 50W X8 resin. The "effective" Nernst-Planck

diffusion coefficients are each determined as functions

of three parameters, as shown in Chapter V.

C. Other Relevant Literature

1. Literature Search Methodology

The author was assisted in compiling an extensive

bibliography on ion exchange and related phenomena by

technical information specialists at Allied Corporation.

Working with these specialists, a search strategy based on

key word and reference-to-reference traceback techniques was

worked out to obtain the most pertinent information. Allied

searches on-line via the DIALOG INFORMATION SERVICES on the

following data bases:

Chemical Abstracts 1967-date

Compendex 1970-date (the machine-readable version of the

Engineering Index)

Abstracts of relevant article were provided to the

investigator based on key word search. Circled abstracts

were then obtained from the Allied collection or via outside

resources provided by the Allied library. References from

the full article many times lead to other relevant articles,

also provided by the library.

CHAPTER II

MULTICOMPONENT ION EXCHANGE EQUILIBRIA

A. General Background

1. Ion Exchange Equilibrium Conventions

The simulation of fixed bed ion exchange operations requires knowledge of the equilibrium relationship between ionic species contained in the electrolyte phase and those contained in the ion exchange resin. Helfferich (36) has reviewed extensively the many ion exchange equilibria representations, primarily for binary systems. The equilibrium conventions given by Helfferich are as follows:

for the following general binary exchange,

$$z_b A + z_a \overline{B} \; \overset{\longrightarrow}{\longleftarrow} \; z_b \overline{A} + z_a B \qquad (2\text{-}1)$$
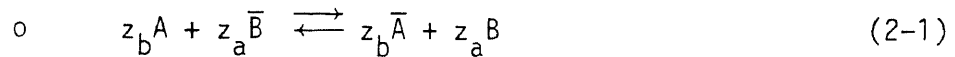
in which

z_i = absolute charge of ith species[1]

A = favored counterion; bar represents the resin phase

a) separation factor

$$\alpha_b^a \equiv \frac{\overline{m}_a m_b}{\overline{m}_b m_a} = \frac{\overline{C}_a C_b}{\overline{C}_b C_a} = \frac{\overline{x}_a x_b}{\overline{x}_b x_a} \qquad (2\text{-}2)$$

$$\qquad\qquad \text{molal} \qquad \text{molar} \qquad \text{ionic equivalent fraction}$$

[1] Although charge on an ionic species is not always the valence of the species (ex., NH_4^+), henceforth in this treatise the commonly used and misapplied term valence will be used as "shorthand" for charge on the defined species.

39

b) <u>mass action forms</u>

o $K_b^a = \dfrac{\bar{m}_a^{|z_b|} \cdot m_b^{|z_a|}}{\bar{m}_b^{|z_a|} \cdot m_a^{|z_b|}}$ molal selectivity coefficient   (2-3)

o $K_b^{a'} = \dfrac{\bar{C}_a^{|z_b|} \cdot C_b^{|z_a|}}{\bar{C}_b^{|z_a|} \cdot C_a^{|z_b|}}$ molar selectivity coefficient   (2-4)

(2-5)

o $nK_b^a = \dfrac{\bar{x}_a^{|z_b|} \cdot x_b^{|z_a|}}{\bar{x}_b^{|z_a|} \cdot x_a^{|z_b|}}$ equivalent ionic fraction or rational selectivity coefficient

c) <u>corrected mass action forms</u>

The example given is for the molal selectivity coefficient, but the format applies to all three of the above coefficients:

o $Ka_b^a = \dfrac{\bar{m}_a^{|z_b|} \cdot a_b^{|z_a|}}{\bar{m}_b^{|z_a|} \cdot a_a^{|z_b|}} = K_b^a \cdot \dfrac{\gamma_b^{|z_a|}}{\gamma_a^{|z_b|}}$ (2-6)

where γ_i = molal activity coefficient of species i in the electrolyte phase

d) <u>thermodynamic equilibrium constant</u>

<u>molal form</u>

o $tK_b^a = \dfrac{\bar{a}_a^{|z_b|} \cdot a_b^{|z_a|}}{\bar{a}_b^{|z_a|} \cdot a_a^{|z_b|}} = \left(\dfrac{\bar{m}_a \bar{\gamma}_a}{m_a \gamma_a}\right)^{|z_b|} \cdot \left(\dfrac{m_b \gamma_b}{\bar{m}_b \bar{\gamma}_b}\right)^{|z_a|}$ (2-7)

where

$$\Delta G^O = -R \cdot T \cdot \ln(tK_b^a) \tag{2-8}$$

and the molal scale is used for both the resin and electrolyte phases.

Referring to the diagram below:

Illustration 2.1
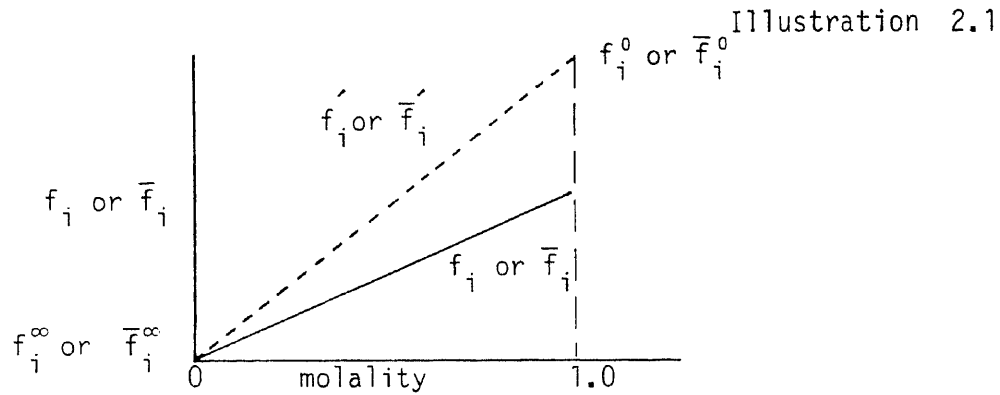
Infinite Dilution Standard State Relationships

f_i represents the fugacity of component i, with the bar signifying the resin phase, and f_i^O is the infinite dilution standard state reference fugacity.

The infinite dilution standard state reference fugacity is determined by the intersection of the tangent to the f_i or $\overline{f}_i$ curve, as m_i or $\overline{m}_i$ approaches zero concentration, with the ordinate of molality = 1. For the resin phase, this concentration would represent a fictitious "pore" fluid.

Then:

$$\gamma_i = \frac{f_i}{f_i'} = \frac{f_i}{m_i f_i^O} \tag{2-9}$$

and

$$\overline{\gamma}_i = \frac{\overline{f}_i}{\overline{f}_i'} = \frac{\overline{f}_i}{\overline{m}_i \overline{f}_i^O} \tag{2-10}$$

So as $\quad m_i$ or $\overline{m}_i \rightarrow 0$ concentration

then $\quad f_i^\infty = f_i'^\infty$ and $\overline{f}_i^\infty = \overline{f}_i'^\infty$

resulting in $\quad \gamma_i = 1 \quad$ and $\quad \overline{\gamma}_i = 1$

The activities, a_i and $\overline{a}_i$ are zero for values m_i and

$\overline{m}_i$ equal to zero concentrations, since f_i^∞ and $\overline{f}_i^\infty$ are

also zero. If the standard and reference states for the

electrolyte and the resin phase are chosen so that they are

the same, then:

$$\circ \qquad {}_t K_b^a = \left(\frac{\overline{f}_a}{f_a}\right)^{|z_b|} \cdot \left(\frac{f_b}{\overline{f}_b}\right)^{|z_a|} = 1 \qquad\qquad (2\text{-}11)$$

since $\overline{f}_a = f_a$ and $\overline{f}_b = f_b$

Therefore with this convention, the ion exchange

selectivity is vested in the activity coefficients $\overline{\gamma}_i$ and γ_i

Rational form

$$\circ \qquad {}_t^n K_b^a = \left(\frac{\overline{a}_a^n}{a_a}\right)^{|z_b|} \cdot \left(\frac{a_b}{\overline{a}_b^n}\right)^{|z_a|} \qquad\qquad (2\text{-}12)$$

$$= \left(\frac{\overline{x}_a \overline{\gamma}_a^n}{m_a \gamma_a}\right)^{|z_b|} \cdot \left(\frac{m_b \gamma_b}{\overline{x}_b \overline{\gamma}_b^n}\right)^{|z_a|}$$

where $\overline{x}_i$ is the ionic equivalent fraction of species i in

the exchanger phase, and the resin is treated as a solid

solution of the swollen resinates AR and BR. Both the

standard and reference states of AR and BR are taken to be

the respective monoionic forms of the ion exchanger in equilibrium with water. Referring to the diagram which follows:

Illustration 2.2
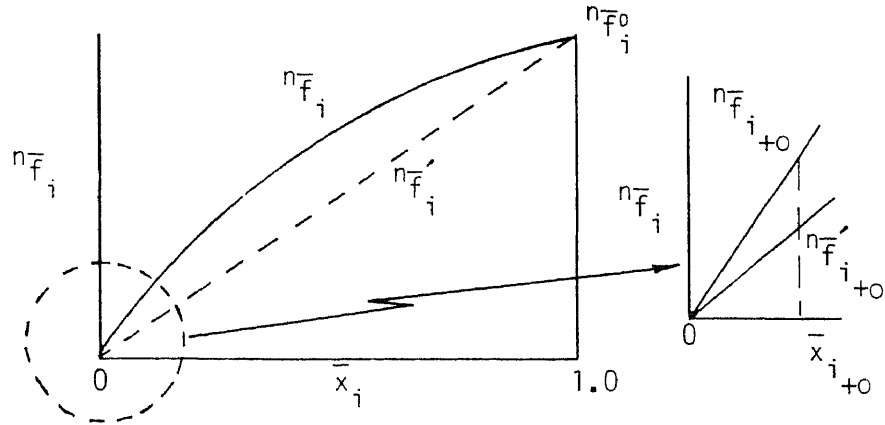
Standard State Relationships for Resin Phase

here $^{n}\bar{\gamma}_i = \dfrac{^{n}\bar{f}_i}{^{n}\bar{f}_i'} = \dfrac{^{n}\bar{f}_i}{\bar{x}_i \, ^{n}\bar{f}_i^0}$ (2-13)

and $^{n}\bar{a}_i = \bar{x}_i \, ^{n}\bar{\gamma}_i = \dfrac{^{n}\bar{f}_i}{^{n}\bar{f}_i^0}$ (2-14)

Values of activity coefficients at the limits are:

o at $\bar{x}_i = 1.0$, $^{n}\bar{f}_i = ^{n}\bar{f}_i^0$, so $^{n}\bar{\gamma}_i = 1.0$ and $^{n}\bar{a}_i = 1.0$

o at $\bar{x}_i \to 0$, slope $K = \dfrac{(^{n}\bar{f}_{i_{+0}} - 0)}{(\bar{x}_{i_{+0}} - 0)} = \dfrac{^{n}\bar{f}_{i_{+0}}}{\bar{x}_{i_{+0}}}$ (2-15)

and $^{n}\bar{f}_{i_{+0}}^0 = ^{n}\bar{f}_i^0 \, \bar{x}_{i_{+0}}$

(2-16)

so $^{n}\bar{\gamma}_{i_{+0}} = \dfrac{^{n}\bar{f}_{i_{+0}}}{^{n}\bar{f}_i'} = \dfrac{K \bar{x}_{i_{+0}}}{^{n}\bar{f}_i^0 \, \bar{x}_{i_{+0}}} = \dfrac{K}{^{n}\bar{f}_i^0}$

i.e. $\quad {}^n\overline{\gamma}_{i_0} = \dfrac{K}{{}^n\overline{f}^0_i} \quad$ and $\quad {}^n\overline{a}_{i_0} = 0 \quad$ as $\quad \overline{x}_i \to 0$

The rational form of the thermodynamic equilibrium constant is then given as:

$$O \qquad {}^n_t K^a_b = \left[\dfrac{{}^n\overline{f}^0_a}{f^0_a} \right]^{|z_b|} \cdot \left[\dfrac{f^0_b}{{}^n\overline{f}^0_b} \right]^{|z_a|} \qquad (2\text{-}17)$$

Since the standard and reference states of the electrolyte and resin phases are different, the ion exchanger selectivity is vested in the equilibrium constant. The activity coefficients mainly trim up compositional variations.

Complete definition of the Thermodynamic Equilibrium Relationship

The above expressions for the thermodynamic equilibrium constant were based on the assumption that electrolyte and solvent sorption and desorption were small and could be neglected.

The full expression (39) is:

$$O$$

$$_t K^a_b = \left[\dfrac{\overline{m}_a\overline{\gamma}_a}{m_a\gamma_a} \right]^{|z_b|} \cdot \left[\dfrac{m_b\gamma_b}{\overline{m}_b\overline{\gamma}_b} \right]^{|z_a|} \cdot \left[\dfrac{\overline{a}_w}{a_w} \right]^h \cdot \left[\dfrac{\overline{a}_{ay}}{a_{ay}} \right]^g \cdot \left[\dfrac{a_{by}}{\overline{a}_{by}} \right]^f \qquad (2\text{-}18)$$

where:

   w is solvent, ay is salt AY, and by is salt BY, with h,g, & f representing Δ moles of each species between the solvent and exchanger phase.

Chain Rule Relationship

The thermodynamic equilibrium constants, both the molal and the rational form, satisfy the Gibbs free energy equilibrium constraints in that the activity relationship of each species, in both phases (resin and electrolyte), are related by a constant at a given temperature. This leads to the chain rule convention in which:

$$o \qquad K_{ij} = \frac{K_{ik}^{(|z_j|/|z_k|)}}{K_{jk}^{(|z_i|/|z_k|)}} \qquad \text{for species i,j, and k} \quad (2\text{-}19)$$

in which the equilibrium constants K_{ij} can be all $_t K_j^i$ molal forms, or all $_t^n K_j^i$, rational forms, and z_i represents valence of species i.

2. ## Ion Exchange Equilibrium Models

2.1 ## Pressure and Temperature Considerations

In terms of the swelling pressure of the resin and the partial molar volume of each species, the electric double layer or Donnan potential created by electrolyte sorption is defined by Helfferich (35) as:

$$o \qquad E_{DON} = \frac{1}{z_i F} \cdot \left(RT \ell n \left(\frac{a_i}{\bar{a}_i} \right) - \pi v_i \right) \qquad (2\text{-}20)$$

where:

F = Faraday's constant

π = swelling pressure

v_i = partial molar volume of species i

For binary exchange this leads to (38):

$$RT\ln\left[\left(\frac{\bar{a}_a}{a_a}\right)^{|z_b|} \cdot \left(\frac{a_b}{\bar{a}_b}\right)^{|z_a|}\right] = \pi(|z_a|\nu_b - |z_b|\nu_a) \qquad (2\text{-}21)$$

This equation and (2-18) lead to the following expression when the water and coion effects are included (39):

$$\ln tK_b^a = \frac{\pi}{RT}\left[|z_a|\nu_b - |z_b|\nu_a - h\nu_w - g\nu_{ay} + f\nu_{by}\right] \qquad (2\text{-}22)$$

which shows the effect of swelling pressure and partial molar volume on the thermodynamic molal equilibrium constant. Barrer and Rees (6) point out that in a binary exchange of ions in zeolites, the Gibbs-Duhem relationship is:

$$\qquad (2\text{-}23)$$

$$\bar{n}_a\partial\ln\bar{a}_a + \bar{n}_b\partial\ln\bar{a}_b + \bar{n}_w\partial\ln\bar{a}_w + \bar{n}_{sites}\partial\ln\bar{a}_{sites} = -\frac{\partial(\pi\nu)_T}{RT}$$

where

n_i = moles of species i

subscripts w referring to water, sites referring to charges in the resin

ν = resin volume, cc

π = osmotic or swelling pressure, bars

Barrer and Rees (6) did not include coion sorption since in zeolites this tendency is very small.

Barrer and Rees point out that in zeolites, $\bar{n}_{sites}$ is constant and water change during ion exchange is small and can be said to be constant. For univalent exchange,

$$dn_a = -d\bar{n}_b, \text{ so:} \tag{2-24}$$

$$0 \quad \bar{n}_a \cdot \frac{\partial \ln \bar{a}_a}{\partial \bar{n}_a} - \bar{n}_b \cdot \frac{\partial \ln \bar{a}_b}{\partial \bar{n}_b} = - \left[\bar{n}_w \cdot \frac{\partial \ln \bar{a}_w}{\partial \bar{n}_a} \right.$$

$$\left. + \bar{n}_{sites} \cdot \frac{\partial \ln \bar{a}_{sites}}{\partial \bar{n}_a} + \frac{1}{RT} \cdot \frac{\partial (\pi v)_T}{\partial \bar{n}_a} \right]$$

In order for

$$\frac{\partial \ln \bar{a}_a}{\partial \ln \bar{n}_a} = \frac{\partial \ln \bar{a}_b}{\partial \ln \bar{n}_b} \tag{2-25}$$

the right side of equation (2-23) must be zero. This assumption is implicit in most ion exchange models, even for gel exchangers where osmotic pressure and volume changes may be significant during the exchange, and indeed, equation (2-22) shows that if the thermodynamic equilibrium constant is to remain constant throughout a complete exchange of one species for another, then the volume and pressure changes must be relatively small.

Helfferich (37) points out that in the free energy expression:

$$\Delta G = \Delta H - T \Delta S \tag{2-26}$$

that the enthalpy term, ΔH, is usually small. Most of the free energy changes in ion exchange are due to entropic effects, primarily mixing effects but to some extent due to configurational changes in the resin matrix and the adding or losing of solvation shells by the ionic species. The temperature dependence of ion exchange is similar to that

describing chemical reactions, so:

$$\circ \quad \left(\frac{d\ln {}_t^n K_b^a}{dT}\right)_P = \frac{\Delta H^o}{RT^2} \qquad (2\text{-}27)$$

where ΔH^o = standard enthalpy of reaction

As Helfferich [37] points out, normal ΔH^o values for ion exchange are only on the order of 2 kcal/mole, so ion exchange equilibria is not affected greatly by temperature changes.

A number of models for ion exchange equilibrium are discussed by Helfferich [41].

2.2 Resin Phase Activity Coefficient Models

The development of a model which can represent the activity coefficients of ionic species in an ion exchange resin depends on the assumptions made in developing the Gibbs-Duhem equation. As Soldatov [119] points out, the Gibbs-Duhem equation for the resin phase has the general form:

$$\sum_{i=1}^{\ell} \bar{n}_i d\bar{\mu}_i = 0 \qquad (2\text{-}28)$$

This of course assumes, as discussed above, that the pressure volume effects are negligible, and all references found in this work have included that assumption as inherent in their various model derivations for equilibrium in ion exchanges.

Soldatov [119] made one very good observation

pertaining to ion exchange thermodynamics, and that has to do with the use of mole fractions or equivalent fractions as surrogates for molal or molar concentrations in the Gibbs-Duhem equation. In systems where the total numbers of moles is a constant, i.e., physical systems with no reactions, the Gibbs-Duhem for a binary system would be:

$$\bar{c}_1 d\ell n \bar{a}_1 + \bar{c}_2 d\ell n \bar{a}_2 = 0 \tag{2-29}$$

or $\quad \bar{c}_1 (d\ell n\bar{\gamma}_1 + d\ell n\bar{c}_1) + \bar{c}_2 (d\ell n\bar{\gamma}_2 + d\ell n\bar{c}_2) = 0 \tag{2-30}$

then $\quad \bar{c}_1 d\ell n\bar{\gamma}_1 + \bar{c}_2 d\ell n\bar{\gamma}_2 = 0 \tag{2-31}$

since $\quad \bar{c}_1 + \bar{c}_2 = \bar{c}_{total}$, $d(\bar{c}_1 + \bar{c}_2) = 0 \tag{3-32}$

Soldatov's equation for ion exchange was given as:

$$o \quad \sum_{i=1}^{\ell} \bar{c}_i d\ell n\bar{\gamma}_i + d\bar{c}_{total} = 0 \tag{2-33}$$

where in heterovalent binary exchange, $d\bar{c}_{total} \neq 0$ but is equal to $- \left(\dfrac{|z_1|}{|z_2|} \right) \cdot d\bar{c}_1$, since:

$$o \quad \bar{c}_{total} = \left(\frac{Q_r}{|z_2|} \right) + \left(1 - \left(\frac{|z_1|}{|z_2|} \right) \right) \cdot \bar{c}_1 \tag{2-34}$$

where Q_r = equivalent sites in ion exchanger

In homovalent systems for which z_1 equals z_2, the total

moles, $\bar{c}_{total}$, equals $\left(\dfrac{Q_r}{|z_2|} \right)$ and the term, $d\bar{c}_{total}$ equals zero. However, in heterovalent systems such as the system $Sr^{++} - Cs^{+}$, $d\bar{c}_{total}$ is equal to $-2d\bar{c}_1$ and also

is equal to $d\bar{c}_2$ (since $d\bar{c}_1 = -\left(\dfrac{|z_2|}{|z_1|}\right)\cdot d\bar{c}_2$), and is not

zero. Most investigators of ion exchange equilibria models either limit the model to homovalent exchange, or ignore the discrepancy. The residual values $d\bar{c}_{total}$ get "buried" in the equilibrium constant or "absorbed" by the activity coefficient correlation--as was the case in this research. As will be discussed later, this works out very well in correlating binary heterovalent system equilibrium relationships, but may be responsible for the just fair ability of the correlation methods to predict ternary equilibrium concentrations from binary system parameters in such circumstances.

Two resin phase activity coefficient models will be discussed here since they led to the approach taken in this work. These are:

a. Kielland's Equation

Kielland's equation (53) for zeolites for homovalent exchange, neglecting water and electrolyte sorption as discussed, and assuming constant temperature and pressure:

$$B + \overline{AZ} \;\overset{\rightarrow}{\leftarrow}\; \overline{BZ} + A \tag{2-35}$$

The relationship of excess free energy to activity coefficients for a binary system is:

$$\ln{}^n\bar{\gamma}_1 = \frac{\Delta^n\bar{G}^{ex}}{RT} - \bar{x}_2\left[\frac{\partial\left(\dfrac{\Delta^n\bar{G}^{ex}}{RT}\right)}{\partial\bar{x}_2}\right]_{T,P} \tag{2-36}$$

In many regular systems $(\Delta^n \bar{S}^{ex} = 0)$ the representation:

$$\frac{\Delta^n \bar{H}^{ex}}{RT} = A\bar{x}_1 \bar{x}_2 \qquad (2\text{-}37)$$

gives a reasonable representation of $\Delta^n \bar{G}^{ex}$. This is Kielland's approach and he defined:

$$\bar{x}_i = \frac{\bar{n}_{iz}}{(\bar{n}_{az} \cdot \bar{n}_{bz})} \qquad (2\text{-}38)$$

where $\bar{n}_{iz}$ are moles/volume of component iz

By use of equation (2-36) and (2-37) he arrived at the truncated Redlich-Kister form of:

$$\ln {}^n\bar{\gamma}_1 = A\bar{x}_2^2 \quad \text{and} \quad \ln {}^n\bar{\gamma}_2 = A\bar{x}_1^2 \qquad (2\text{-}39,40)$$

to correlate resin phase activity coefficients in the resin phase. This approach was put on a more sound theoretical footing by Barrer (5).

b. Smith and Woodburn Model

Smith and Woodburn (116) were concerned with multicomponent ion exchange equilibria, and developed an approach to model the anionic exchange of NO_3^-, Cl^-, $SO_4^=$ with Rohm and Haas Amberlite 400 resin. Although Danes and Danes (19) had investigated approaches where the excess free energy of mixing in polyionic systems was expressed as a polynomial, (Redlich-Kister type representations), Smith and Woodburn felt that this confined the relationship to regular solutions, and binary constants could not readily be utilized to predict multicomponent system activity coefficients. They noted that some features

of the ion exchange system lent themselves to the
approach used by Wilson (98) in development of his
equation based on non-randomness of local mole
fractions in liquid mixtures for athermal solutions.
As discussed above, ion exchange systems exhibit low
heats of mixing and analogy can be made to non-random
clustering of ion species in the exchanger phase. The
Wilson equation in general form is:

$$\ln \gamma_i = 1 - \ln \sum_{j=1}^{n} X_j G_{ji} - \sum_{j=1}^{n} \frac{X_j G_{ij}}{\sum_{k=1}^{n} G_{kj} X_k} \qquad (2-41)$$

where

$$G_{ji} = \rho_{ji} \exp(-\tau_{ji}) \qquad (2-42)$$

and

$$\tau_{ji} = \frac{(g_{ji} - g_{ii})}{RT} \qquad (2-43)$$

where

$$g_{ji} = g_{ij}, \quad so \quad \tau_{jj} = \tau_{ii} = 0 \qquad (2-44)$$

and

$$\rho_{ij} = \frac{\nu_i}{\nu_j}, \text{ molar volume ratio} \qquad (2-45)$$

The Wilson equation was used by Smith and Woodburn to
describe the resin phase interactions involved in the
ternary system NO_3^-, Cl^-, $SO_4^=$, based on predictions
made from the binary pair correlations. Smith and
Woodburn based the electrolyte phase ionic species
activity coefficients on the extended Debye-Huckel
equation given by Robinson and Stokes (103);

$$o \qquad \ln\gamma^{*}_{i_{int}} = \frac{-Az_i^2\sqrt{I}}{(1+Ba_i\sqrt{I})} + b_i I \qquad (2\text{-}46)$$

where I = ionic strength

and used the Truesdell and Jones (128) parameters for

a_i and b_i. The binary pair data was regressed

using the least square of normalized error criteria

and they represented the system with the rational

thermodynamic equilibrium treatment, $^n_t K^a_b$ given in

equation (2-12) above.

The combinatorial rules are straight forward for

multicomponent mixtures utilizing binary pair G_{ij}

fitted parameters, and is not subject to possible

ambiguity, as is the combining of polynomial

expressions derived for binary pairs into ternary

representations. The results of the application of

this model to predict the ternary compositions versus

actual experimental results was quite good, with a

standard deviation of ±4.26%.

One complication in considering the

$NO_3^-, Cl^-, SO_4^=$ system is that:

$$Na^+ + SO_4^= \rightleftharpoons NaSO_4^- \qquad (2\text{-}47)$$
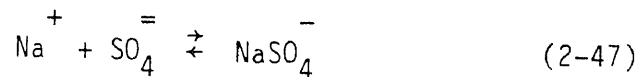
where:

$$K_{dist} = \frac{a^{*}_{NaSO_4^-}}{a^{*}_{Na^+} \cdot a^{*}_{SO_4^=}} = 5.248 \qquad (2\text{-}48)$$

and was considered as an additional reaction in the

electrolyte phase. Since total $SO_4^=$ in the resin

phase was assayed, it was not possible to determine the amount of $SO_4^=$ due to the $SO_4^=$ source or the $NaSO_4^-$ source without a Na^+ analysis. In any event, a ternary system was modeled, not a quaternary system, and the simplest approach was to treat $NaSO_4^=$ as a non-exchanged species.

Smith and Woodburn used the chain rule:

$$o \qquad {}_t^n K_2^1 = \frac{{}_t^n K_3^{1^{(|z_2|/|z_3|)}}}{{}_t^n K_3^{2^{(|z_1|/|z_3|)}}} \qquad (2-49)$$

to determine the value of ${}_t^n K_{SO_4}^{Cl}$ from the regression values of ${}_t^n K_{Cl}^{NO_3}$ and ${}_t^n K_{SO_4}^{NO_3}$ for comparison to the fitted value of ${}_t^n K_{SO_4}^{Cl}$ and found excellent agreement.

They felt this was an indication of data consistency.

3. Tabulation of Thermodynamic Models

Table 2-1 shows a compilation of various thermodynamic representations used by other investigators in modeling either the equilibria or the dynamics of ion exchange. Dranoff and Lapidus (21, 22), Rao and his coworkers (91, 92, 93), and Omatete (78, 79, 80) are the only investigators cited here who modeled dynamic ternary exchange, and therefore required ternary equilibrium representation; however, others such as Smith and Woodburn (116), Soldatov and Bychkova (121, 122, 123), and Pieroni and Dranoff (85) have investigated ternary equilibria representation with a variety of approaches.

Table 2-1

ION EXCHANGE EQUILIBRIA - VARIOUS INVESTIGATORS

Investigator(s)	System	Equilibrium Convention	Activity Coefficients	
			Electrolyte	Resin Phase
Binary				
(1) David & Kuo (56) for equilibrium fit	Ba^{++}-Na^+	Mass action- Rational Selectivity	ideal	ideal
(2) David & Rao (88) for equilibrium fit	Cu^{++}-Na^+	Mass action- Molal Selectivity	literature Harned & Owen (33)	see below*

*used version of Harned's Rule:

$$\frac{\overline{\gamma_1}}{\overline{\gamma_2}} \sim \frac{\gamma_1}{\gamma_2}$$

i.e., activity coefficients in resin are proportional to to activity coefficients in the electrolyte

Investigator(s)	System	Equilibrium Convention	Electrolyte	Resin Phase
(3) Erickson (26) for dynamic simulation	Ethylene^{++} diamine^{++}-NH_4^+	total empirical equation (see Chapter VII)		
(4) Kataoka & Yoshida (49) for dynamic simulation	Na^+H^+	Mass action- Molal Selectivity	ideal	ideal
(5) Pan (84) for dynamic simulation	Na^+H^+	Mass action- Rational Selectivity	ideal	ideal
(6) Selke & Bliss (113) for dynamic simulation	$Cu^{++}H^+$ $Cu^{++}Mg^+$	Mass action- Rational Selectivity	ideal	ideal

Table 2-1 (continued)

Investigator(s)	System	Equilibrium Convention	Activity Coefficients	
			Electrolyte	Resin Phase

Ternary

Investigator(s)	System	Equilibrium Convention	Electrolyte	Resin Phase
(1) Smith & Woodburn (116) for equilibrium fit	$NO_3^- - Cl^- - SO_4^=$	Mass action- Rational Thermodynamic	extended Debye-Huckel, Stokes & Robinson (Truesdell & Jones)	Wilson Equation
(2) Soldatov & Bychkova (121, 122, 123) for equilibrium fit	$K^+ - NH_4 - H^+$ $Na^+ - NH_4 - H^+$ $Ba^{++} - Cu^{++} - Co^{++}$	Mass action- Modified Rational	Harned's Rule	Activity Coefficients interpolated from plots for binary pairs

$$\frac{A}{KB} = \left(\frac{\bar{x}_{NH_4}\bar{x}_K}{\bar{x}_H^2}\right) \cdot \left(\frac{x_H^{*2}}{x_{NH_4}^* x_K^*}\right)$$

where $\frac{A}{KB} = 2.5 + 9.3\bar{x}_H + 0.2\bar{x}_K - 1.6\bar{x}_H\bar{x}_K + 28.0\bar{x}_H^2\bar{x}_K$

for system $K^+ - NH_4^+ - H^+$

Investigator(s)	System	Equilibrium Convention	Electrolyte	Resin Phase
(3) Bajpai, Gupta, Rao (91) for equilibrium fit	$Sr^{++} - Mn^{++} - Cs^+$ $Mn^{++} - Cs^+ - Na^+$ $Ba^{++} - Sr^{++} - Na^+$	Mass action- Modified Rational Thermodynamic (mol. frac. both phases)	ideal	see equations (a) and (b) below

(a) $z_j \ln \bar{\gamma}_i = -\bar{x}_j \ln K_{a_j}^i + \int_{\bar{x}_i}^1 \ln K_{a_j}^i d\bar{x}_i$

(b) $z_j \ln \bar{\gamma}_j = +\bar{x}_i \ln K_{a_j}^i - \int_0^{\bar{x}_i} \ln K_{a_j}^i d\bar{x}_i$

$\ln K_j^i = \int_0^1 \ln K_{a_j}^i d\bar{x}_i$

Table 2-1 (continued)

Investigator(s)	System	Equilibrium Convention	Activity Coefficients	
			Electrolyte	Resin Phase

(3) Bajpai, Gupta, Rao (91)
   for equilibrium fit (cont.)

and for ternary

$$\bar{\gamma}_i = \sum_{\substack{k = 1 \\ k \neq i}}^{n} \left(\frac{\bar{x}_k}{\sum_{\substack{j = 1 \\ j \neq i}}^{n} \bar{x}_j} \right) \bar{\gamma}_i \Bigg|_{ik}$$

(4) Bajpai, Gupta, Rao (93)   above   Distribution Coefficient   ideal   see equations
   for ternary dynamic   (a), (b) and
   simulation   (c) below

(a) $\lambda_i = \dfrac{\bar{x}_i}{x^*_i \big|_{int}}$, i = 1,2,3 in eqv. fractions

binary

$$\lambda_1 = a + b\bar{x}_1 + c\bar{x}_1^2$$

$$\lambda_2 = \frac{(1-\bar{x}_1)}{(1-x^*_1 \big|_{int})}$$

for ternary, where selectivity is 1,2,3

(b) $\left(\dfrac{x^*_1}{(x^*_1 + x^*_2)} \right) \lambda_1 \Bigg|_{1-2} = \left(\dfrac{\bar{x}_1}{(\bar{x}_1 + \bar{x}_2)} \right) = \bar{x}_1 \Bigg|_{1-2}$

(c) $\left(\dfrac{x^*_1}{(x^*_1 + x^*_3)} \right) \lambda_1 \Bigg|_{1-3} = \left(\dfrac{\bar{x}_1}{(\bar{x}_1 + \bar{x}_3)} \right) = \bar{x}_1 \Bigg|_{1-3}$

Table 2-1 (continued)

Investigator(s)	System	Equilibrium Convention	Activity Coefficients Electrolyte	Resin Phase
(5) Omatete (78) for ternary dynamic simulation	Ag^+-Na^+-H^+	Separation Factor	ideal	ideal
(6) Pieroni & Dranoff (85) for equilibrium fit	Cu^{++}-Na^+-H^+	Mass action-Rational Selectivity	ideal	ideal

$$\alpha_{ij} = \frac{(\bar{x}_i x^*_{j_{int}})}{(x^*_{i_{int}} \bar{x}_j)}$$

ternary system   (ref. is also equated to n)

$$\bar{x}^*_j = \frac{\alpha^j_{ref} x_{j_{int}}}{\sum\limits_{k=1}^{n} \alpha^k_{ref} x_{k_{int}}} \quad \text{or} \quad x^*_{j_{int}} = \frac{\alpha^{ref}_j \bar{x}_j}{\sum\limits_{k=1}^{n} \alpha^{ref}_k \bar{x}_k}$$

binary system

$$\bar{x}^*_i = \frac{(\alpha_{ij} x_{i_{int}})}{(x_{i_{int}} \cdot (\alpha_{ij}-1) + 1)}$$

binary system

$$X_a = x_a \quad \text{in equivalent fractions}$$

$$\bar{X}_a = \bar{x}_a$$

ternary system - use of pseudo binary

$$X_a = \frac{c_a}{(c_a + c_b)} \quad ; \quad \bar{X}_a = \frac{\bar{q}_a}{(\bar{q}_a + \bar{q}_b)}$$

$$K^{Na}_H = \frac{(\bar{x}_{Na} x_H)}{(\bar{x}_H x_{Na})}$$

Table 2-1 (continued)

Investigator(s)	System	Equilibrium Convention	Activity Coefficients	
			Electrolyte	Resin Phase

(6) Pieroni & Dranoff (85)
    for equilibrium fit (cont.)

$$K_H^{Cu} = \left(\frac{\bar{x}_{Cu} x_H^2}{\bar{x}_H^2 x_{Cu}}\right) \cdot \left(\frac{(c_H + c_{Cu})}{(\bar{q}_H + \bar{q}_{Cu})}\right)$$

$$K_{Na}^{Cu} = \left(\frac{\bar{x}_{Cu} x_{Na}^2}{\bar{x}_{Na}^2 x_{Cu}}\right) \cdot \left(\frac{(c_{Na} + c_{Cu})}{(\bar{q}_{Na} + \bar{q}_{Cu})}\right)$$

B. **Equilibria Models Tested - This Report**

1. **General**

Review of the literature and background provided by other investigators led to the conclusions that ternary equilibrium correlating relationships for this work should be based on:

a. **The Rational Thermodynamic Selectivity** relationship as demonstrated by Smith and Woodburn (116), since equivalent or mole fraction of each species in the resin phase could be directly calculated as opposed to using pseudo binary relationships. This was particularly important, since with the proposed solution method for ternary dynamic modeling the quasilinearization procedure required clear definition of the partials

$$\frac{\partial x^*_{i_{int}}}{\partial \bar{x}_j} \quad (i = 1,2) \text{ for } (j = 1,2) \tag{2-50}$$

In addition, if the activity coefficients of species in the resin phase could be expressed as functions of $\bar{x}_i$, then the activity driving force could be investigated as an alternative to concentration driving force.

Use of the **Rational Thermodynamic Selectivity** allowed application of the chain rule for calculating one ${}^n_t K^i_j$ in terms of ${}^n_t K^i_k$ and ${}^n_t K^j_k$ as described in equation (2-19), and provided a basis for consistency between three binary pairs without ambiguity.

Finally, as discussed for heterovalent systems, some "burying" of the residual $d\bar{c}_{total}$ term has to be absorbed by

the activity coefficients. Putting most of the selectivity effects into the equilibrium constant would relieve the function of the activity correlation method chosen to that of primarily representing the excess free energy relationships related to mixing and resin configurational changes.

b. Use of generalized correlations such as the Redlich-Kister three suffix equation, the Wilson equation, and the NRTL equation to relate the excess properties of the resin phase to the concentration of ionic species. Each of these correlations has combinatorial rules for the parameters so that constants derived for the three binary pairs can be combined to yield prediction of ternary system behavior. It would have been desirable to:

o   be able to predict the equilibrium constant of the least favored binary pair by application of the chain rule using values of the equilibrium constants for the two most favored binary pairs;

o   be able to predict ternary system behavior directly from the binary pair equilibrium constants and activity coefficient correlation parameters utilizing the mixing conventions of the method.

This would minimize the requirement to obtain experimentally many ternary data points and, in the case of the Redlich-Kister equation, obviate the need to fit parameters for ternary systems. If the predictions for ternary systems could be shown to be dependable, then preliminary computer mapping of ternary

regions of maximum interest could be accomplished from the binary parameters--with experimentation on ternary systems limited in scope to check these regions.

c. Use of a correlation package for activity coefficient prediction in the electrolyte phase for single ions in binary and ternary systems. The predictive method would have the ability to:

o   predict single ion activities in multicomponent mixtures containing other cationic and anionic species;

o   provide a reliable range of accuracy up to about 6 molal concentration of electrolyte salts;

o   have extended Debye Huckel relationships for which constants were available for many ubiquitous salts.

The Bromley (9) equation was selected as the prediction method for the electrolyte phase, and is discussed in Chapter III.

2. Derivation of Equilibrium Relationships

2.1 Equilibrium Equations

Derivation of the binary equilibrium relationships for the three binary pairs in a ternary system is straightforward, given the Helfferich conventions. From this point on, the shorthand symbol for the rational thermodynamic equilibrium constant will be given as $\bar{K}_{ij}$ in this report; and $^{n}\bar{\gamma}_{i}$ will be given as $\bar{\gamma}_{i}$.

$$
\text{o} \qquad \bar{K}_{ij} = \left(\frac{\bar{a}_i}{a_i}\right)^{|z_j|} \cdot \left(\frac{a_j}{\bar{a}_j}\right)^{|z_i|} \tag{2-51}
$$

$$= \left(\frac{\bar{x}_i \bar{\gamma}_i}{m^*_{i_{int}} \gamma_i} \right)^{|z_j|} \cdot \left(\frac{m^*_{j_{int}} \gamma_j}{\bar{x}_j \bar{\gamma}_j} \right)^{|z_i|} \qquad \text{(2-51 continued}$$

for ij of 12,13,23

where:

$\bar{x}_i$ or $_j$	=	mole or equivalent fraction in the resin phase of species i or j
$\bar{\gamma}_i$ or $_j$	=	activity coefficient of species i or j in the resin phase as a function of mole or equivalent fraction
$m^*_{i_{int}}$ or $_{j_{int}}$	=	molality of species i or j in the electrolyte in equilibrium with the resin
γ_i or $_j$	=	activity coefficient of species i or j in the electrolyte phase

Since solutions were dilute in this work,

c^*_i or $_j$	=	molarity of species (instead of molality)

Equation (2-51) was transformed so that mole fraction or equivalent fraction could be used in the electrolyte phase as well as the resin phase to simplify representation. Equivalent fraction in the electrolyte phase is given as:

$$\circ \qquad x^*_{i_{int}} = \left(\frac{|z_i| c^*_{i_{int}}}{\text{norm}} \right) \qquad \text{(2-52)}$$

where norm = normality of coions in the electrolyte phase.

Substitution of equation (2-52) in equation (2-51) gives:

o   (2-53)

$$\bar{K}_{ij} = \left[\frac{\bar{x}_i\bar{\gamma}_i}{x^*_{i_{int}}\gamma_i}\right]^{|z_j|} \cdot \left[\frac{x^*_{j_{int}}\gamma_j}{\bar{x}_j\bar{\gamma}_j}\right]^{|z_i|} \cdot norm^{(|z_i|-|z_j|)} \cdot \left(\frac{|z_i|^{|z_j|}}{|z_j|^{|z_i|}}\right)$$

for ij of 12,13,23

keeping in mind that γ_i or γ_j are <u>still functions</u> of

$m^*_{i_{int}}$ (or $c^*_{i_{int}}$), not $x^*_{i_{int}}$, as given by the Bromley equation.

Equation (2-53) shows that if mole or equivalent fractions are used for electrolyte phase compositions, then in heterovalent systems the normality of the electrolyte has a strong influence on the ion exchanger selectivity.

2.2 Resin Phase Activity Coefficient Relationships

a. The generalized form of the Wilson equation was given above in the Smith and Woodburn discussion.

b. The NRTL equation or non-random, two liquid model developed by Renon and Prausnitz (98) is given by those investigators as:

(2-54)

$$o \quad \ln\gamma_i = \frac{\sum\limits_{j=1}^{n} \tau_{ji}G_{ji}X_j}{\sum\limits_{k=1}^{n} G_{ki}X_k} + \sum\limits_{j=1}^{n} \frac{X_jG_{ij}}{\sum\limits_{k=1}^{n} G_{kj}X_k} \times \left[\tau_{ij} - \frac{\sum\limits_{\ell}^{n} X_\ell\tau_{\ell j}G_{\ell j}}{\sum\limits_{k=1}^{n} G_{kj}X_k}\right]$$

where

$$\tau_{ji} = \frac{(g_{ji} - g_{ii})}{RT} \qquad (2\text{-}55)$$

$$G_{ji} = \exp(-\alpha_{ji}\tau_{ji}) \qquad (2\text{-}56)$$

and

$$g_{ji} = g_{ij} \text{ , so } \tau_{jj} = \tau_{ii} = 0 \qquad (2\text{-}57)$$

$$\alpha_{ji} = \alpha_{ij} \qquad (2\text{-}58)$$

c. The three suffix Redlich-Kister equation is given by Smith (117) as:

$$\ell n\gamma_r = \sum_{i=1}^{n} B_{ri}X_i(X_r - X_i)^{-1}\{X_r(1 - X_r + X_i) - X_i\} \qquad (2\text{-}59)$$

$$- \sum_{\substack{i \neq j \\ i \neq r}}^{n} B_{ij}X_iX_j(X_i - X_j)^0 + \sum_{i=1}^{n} C_{ri}X_i(X_r - X_i)^0$$

$$x\{2X_r(1 - X_r + X_i) - X_i\} - 2\sum_{\substack{i \neq j \\ i \neq r}}^{n} C_{ij}X_iX_j(X_i - X_j)^1$$

$$+ \sum_{i=1}^{n} D_{ri}X_i(X_r - X_i)^1 \{3X_r(1 - X_r + X_i) - X_i\}$$

$$-3\sum_{\substack{i \neq j \\ i \neq r}}^{n} D_{ij}X_iX_j(X_i - X_j)^2$$

where B_{rr}, C_{rr}, D_{rr} terms are zero $\qquad (2\text{-}60)$

and $\quad B_{12} = B_{21}$

$$C_{12} = -C_{21}$$

$$D_{12} = D_{21}$$

if a fourth suffix is included

$$E_{12} = -E_{21}$$

The constants for ternary systems are also given in this literature source, but the relationships are not

listed. Later in this chapter the discussion will include reference to regression fits of data from ternary systems made early in this research which included a fourth suffix term, E, and the three ternary constants. Along with the equilibrium constants, this required fitting 17 parameters to the experimental data. Since there were only 30 or so data points, the "principle of parsimony" was being encroached upon, and Occam's razor prevailed. This principle of the "simplest explanation which explains phenomena is probably the correct one" (paraphrased) led to working with only a three suffix expression without ternary constants.

2.3 Mole Fractions versus Equivalent Fraction

All of the systems involving heterovalent exchange were tested utilizing both mole fraction and equivalent fraction concentration to determine which system would give better prediction of ternary system behavior. One difference of convention which was introduced during the equilibrium phase of the project was that for equivalent fractions, the valence ratio adjustment term $\left(\dfrac{|z_i|^{|z_j|}}{|z_j|^{|z_i|}} \right)$ collected into the equilibrium constant, (see equation 2-53), so

$$\text{o} \quad \bar{K}_{ij_{eq.fr.}} = \bar{K}'_{ij_{eq.fr.}} \cdot \left(\frac{|z_j|^{|z_i|}}{|z_i|^{|z_j|}} \right) \tag{2-61}$$

Since valence i for the heterovalent systems investigated
was 2 with $j = 1$,

$$\bar{K}_{ij_{eq.fr.}} = \frac{1}{2}\bar{K}'_{ij_{eq.fr.}} \qquad (2\text{-}62)$$

During the regression of the heterovalent systems, when the
binary system parameters were used to predict ternary
system equilibrium data points, the equivalent fraction
convention had a slight edge in standard deviation over use
of mole fractions, as will be discussed later. It also was
felt that it would be an advantage to use the equivalent
fraction concentration units, since the dynamic models were
designed to utilize equivalent fraction units. The
combining of the valence relationship into the equilibrium
constant caused no harm, in that in heterovalent systems
the additional factor canceled with the chain rule
convention. Using the system $Mr^{++}\text{-}Cs^{+}\text{-}Na^{+}$:

$$\sqrt[1]{2}\bar{K}^{Mn}_{Cs} = \frac{\sqrt[1]{2}\bar{K}^{Mn}_{Na}{}^{(1/1)}}{\bar{K}^{Cs}_{Na}{}^{(2/1)}} \qquad (2\text{-}63)$$

or with $Sr^{++}\text{-}Mn^{++}\text{-}Cs^{+}$

$$\bar{K}^{Sr}_{Mn} = \frac{(\frac{1}{2}\bar{K}^{Sr}_{Cs})^{(2/1)}}{(\frac{1}{2}\bar{K}^{Mn}_{Cs})^{(2/1)}} \qquad (2\text{-}64)$$

In comparison of equilibrium constants between the two
systems, one other major difference was apparent. In
heterovalent ion exchange the total number of moles in the

resin phase is a variable, whereas the number of

equivalents is a constant. Mole fraction is defined as:

$$\overline{mf}_1 = \frac{\overline{c}_1}{(\overline{c}_1+\overline{c}_2)} \qquad (2\text{-}65)$$

whereas equivalent fraction is given by

$$\overline{eq.fr.} = \left(\frac{\overline{c}_1 \,|z_1|}{Q_r}\right) , \qquad (2\text{-}66)$$

Q_r = resin equivalent monoionic sites/volume of resin.

The relationship between mole fraction and equivalent

fraction can be shown to be:

$$\overline{mf}_1 = \frac{\left(\dfrac{Q_r\overline{eqf}_1}{|z_1|}\right)}{\left(\dfrac{Q_r\overline{eqf}_1}{|z_1|} + \dfrac{Q_r\overline{eqf}_2}{|z_2|}\right)} \qquad (2\text{-}67)$$

$$= \frac{\overline{eqf}_1}{\left[\{1-(|z_1|/|z_2|)\}\overline{eqf}_1+(|z_1|/|z_2|)\right]}$$

for a 2-1 heterovalent system, this relationship reduces to:

$$\overline{mf}_1 = \frac{\overline{eqf}_1}{(2-\overline{eqf}_1)} \qquad (2\text{-}68)$$

In comparing the ratio of $\overline{K}_{12_{eqf.}}$ to $\overline{K}_{12_{m.f.}}$, keep in mind that

in a 2-1 system the concentration ratios appear as:

$$\circ \qquad R\frac{\overline{eqf}}{\overline{mf}} = \left(\frac{\dfrac{\overline{eqf}_1}{\overline{eqf}_2{}^2}}{\dfrac{\overline{mf}_1}{\overline{mf}_2{}^2}}\right) , \text{ and} \qquad (2\text{-}69)$$

after the substitution of equation (2-68) in equation (2-69)

the following ratio results:

$$R\frac{\overline{eqf}}{\underline{mf}} = \frac{4}{(2-\overline{eqf}_1)} \quad \cdot \qquad (2\text{-}70)$$

Since the entire range of concentration values must be examined

(from 0 to 1.0) in evaluating the operative ratio, $R\frac{\overline{eqf}\cdot}{m.f.}$, equal to

$\dfrac{\overline{K}_{12\frac{}{eqf\cdot}}}{\overline{K}_{12\frac{}{m.f.}}}$, expression (2-70) is integrated to yield:

$$R\frac{\overline{eqf}}{\underline{mf}}\bigg|_{ave} = \frac{\displaystyle\int_0^1 \frac{4}{(2-\overline{eqf}_1)}\, d\,\overline{eqf}_1}{\displaystyle\int_0^1 d\,\overline{eqf}_1} \qquad (2\text{-}71)$$

$$= -4\ln(2-\overline{eqf}_1)\bigg|_0^1$$

$$= 4\ln 2 = 2.773$$

Due to the effect of the change in total moles occurring within

the resin during heterovalent exchange it could be expected

that $\overline{K}_{12\frac{}{eqf\cdot}}$ would be about 2.8 times greater than $\overline{K}_{12\frac{}{m.f.}}$. Since

the valence ratio adjustment (equation (2-62)) had been

incorporated into $\overline{K}_{12\frac{}{eqf\cdot}}$, the observed ratio should have been

about 1.4.

A relationship similar to equation (2-71) can be derived

for 1-2 systems such as NO_3-$SO_4^=$. It can be shown that:

$$R\frac{\overline{eqf}}{\underline{mf}} = \frac{(1+\overline{eqf}_1)}{4} \qquad (2\text{-}72)$$

which upon integration yields:

$$o \qquad R\frac{\overline{eqf}}{\overline{mf}} = \frac{1}{4} \cdot \left[1 + \frac{\overline{eqf}_1{}^2}{2} \right] \Bigg|_0^1 = 0.375 \qquad (2\text{-}73)$$

Actual comparison of the ratio, $R\frac{\overline{eqf.}}{m.f._{ave}}$ shown in Table 2-4

gives the average for the three cationic heterovalent systems as

1.5475, with the difference from 1.4 of about 10% being absorbed

into the activity coefficient ratio, $\left.\overline{\gamma}_1\!\Big/\overline{\gamma}_2{}^2\right|_{eqf.}$ vs. $\left.\overline{\gamma}_1\!\Big/\overline{\gamma}_2{}^2\right|_{m.f.}$.

In the anionic exchange, the average ratio is 0.2915 vs. 0.375,

with an almost 30% difference being absorbed by the activity

coefficient ratios.

C. Experimental Data for Ternary Systems

    1. General

          Experimental data was available for five systems, and

regression analysis of the binary pair data was utilized to

generate equilibrium constants and the resin phase activity

coefficient parameters based on the Redlich-Kister, Wilson, and

NRTL equations (the Omatete (78) system of Ag^+-Na^+-H^+ was

only fitted with Redlich-Kister). These parameters were used to

simulate the ternary data points and the results compared to the

actual points, with standard deviations computed for each system

and correlation method.

    2.   The systems investigated are shown in Table 2-2. The

ternary system experimental data was accompanied with the

experimental binary system data given either in tabular or

graphical format.

Table 2-2

TERNARY EQUILIBRIUM DATA SOURCES

Investigator(s)	System	Experimental Method	No. of Ternary Data Points
Omatete (78)	Ag^+-Na^+-H^+/NO_3 on Dowex 50W X8 0.1 normal solution at 23°C.	Column displacement technique. Ag^+ by Volhard titration, (±0.2%) H^+ by titration with NaOH (±0.2%), Na^+ by flamespectroscopy, (±7%). spectroscopy, (±7%).	2 points + 3 by material balance on rate runs - this project
Rao et al (91)	Sr^{++}, Mn^{++}, Cs^+/Cl^- on Dowex 50W X8.	Radioactive tracer technique. Reproducibility was ±2%.	16 points
	Mn^{++}, Cs^+, Na^+/Cl^- on Dowex 50W X8 0.1 normal solution at 23°C.		15 points
Smith & Woodburn (116)	NO_3-Cl^--SO_4/Na^+ on Rohm & Haas Amberlite IRA 400 0.2 normal solution at 25 ±3°C.	Column displacement technique Cl^- by potentiometric titration with $AgNO_3$ solution (±1%), SO_4 gravimetrically (±2%) NO_3 by difference.	16 points with 2 additional replication runs.
Soldatov & Bychkova (121)	NH_4-Na^+-H^+/Cl^- on Dowex 50B X12 0.1 normal solution at 25°C.	Equilibrium method not stated, but believed to be Column displacement. H^+ by alkalimetry, NH_4 by formaldehyde method.	45 points distributed along NH_4 ion isotherms of 0.05, 0.10, 0.20, 0.30, 0.40, 0.50, 0.60, 0.70 in the electrolyte phase.

D. Correlation Model - Ion Exchange Equilibrium

1. General Background

A powerful general purpose non-linear regression program based on a variation of the Gauss-Newton method was developed by Dr. A. K. S. Murthy at Allied Corporation, and a general description is given in Appendix B. In fitting the equilibrium constants and activity coefficient parameters for the species in the resin phase, obviously one equlibrium relationship is required per binary pair, and the number of equilibrium equations required for the ternary systems is three.

The equilibrium relationship for, say the 1-2 pair, is divided into terms containing the known parameters, and terms constituting the unknown side contain the parameters to be fitted:

$$\circ \qquad Y(1)_{calc} = \overline{K}_{12\overline{eqf}} \cdot \left(\frac{\gamma_2^{|z_1|}}{\gamma_1^{|z_2|}} \right) \qquad (2\text{-}74)$$

where:

$$\overline{\gamma}_1 = func \ (B_{12}, \ C_{12}, \ D_{12})$$
$$\overline{\gamma}_2 = func \ (B_{11}, \ C_{12}, \ D_{12})$$

Redlich-Kister
Constant

and

$$B_{12}, \ C_{12}, \ D_{12} \ are \ func \ (\overline{x}_1, \ \overline{x}_2)$$

and the terms containing the known parameters are:

$$\circ \qquad Y(1)_{exp} = \left(\frac{\overline{x}_1}{x^*_{1_{int}}\gamma_1} \right) \cdot \left(\frac{x^*_{2_{int}}\gamma_2}{\overline{x}_2} \right) \cdot norm^{(|z_1|-|z_2|)} \qquad (2\text{-}75)$$

where $\overline{x}_1$, $\overline{x}_2$, $x^*_{1_{int}}$, and $x^*_{2_{int}}$ correspond to data points and, γ_1 plus γ_2 are calculated using the

Bromley equation for the electrolyte phase activity

coefficients.

The $Y(1)_{exp}$ terms represent the experimental knowns.

The regression program then finds the numerical derivatives of

$Y(1)_{calc}$ with respect to each parameter, i.e.:

$$\frac{\partial Y(1)_{calc}}{\partial \bar{K}_{12_{eqf}}} , \frac{\partial Y(1)_{calc}}{\partial B_{12}} , \frac{\partial Y(1)_{calc}}{\partial C_{12}} , \frac{\partial Y(1)_{calc}}{\partial D_{12}} \qquad (2\text{-}76)$$

and using the weighted objective function:

$$(2\text{-}77)$$

$$wgt_i \cdot \left[\frac{(Y_{exp} - Y_{calc})}{Y_{exp}} \right]^2 \qquad \begin{array}{l} \text{for i=1 to number of} \\ \text{dependent variables} \end{array}$$

searches for global minima for all data points in each set. If

some parameters are used to describe the calculation of

variables in other data sets, then these sets are also included

in the global minima search for that parameter. When

convergence criteria have been met in terms of residual error

for all parameters, the regression program prints out values for

each fitted parameter along with standard deviation and cross

correlation coefficients.

2. Ion Exchange Equilibrium Regression Program, RIONFT, for Ternary

Systems

The general purpose ion exchange correlation program

developed as part of this research was called RIONFT (Resin

phase Ion exchange FiTting program). Dr. A. K. S. Murthy's

generalized regression program (Appendix B) is the heart of a

program developed specifically for fitting resin phase ion
exchange parameters to experimental binary and ternary
equilibrium data. It step-wise performs 26 sequential
correlation combinations to arrive at a best portrayal of the
three binary systems and the ternary points. Using the
Redlich-Kister equation for resin phase activity coefficients
(parameters B_{ij}, C_{ij}, D_{ij}) as an example, these steps are:

o **Binary pair 1-2**

    1   fits $\overline{Ke}_{12}$ and B_{12}

    2   fits $\overline{Ke}_{12}$ and B_{12}, C_{12} using initial estimates
       for $\overline{Ke}_{12}$ and B_{12} from 1

    3   fits $\overline{Ke}_{12}$, B_{12}, C_{12} and D_{12} using initial
       estimates for $\overline{Ke}_{12}$, B_{12} and C_{12} from 2

o **Binary pair 1-3**

    4-6   performs same steps for $\overline{Ke}_{13}$, B_{13}, C_{13} and D_{13}
       as were carried out in steps 1-3

o **Binary pair 2-3**

    7-9   performs same steps for $\overline{Ke}_{23}$, B_{23}, C_{23} and D_{23}
       as were carried out in steps 1-3

o **Binary pair 2-3**

    10   uses $\overline{Ke}_{23}$ computed by the chain rule using the
       $\overline{Ke}_{12}$ and $\overline{Ke}_{13}$ fitted in steps 2 and 5, and fits
       B_{23} and C_{23}

    11   uses $\overline{Ke}_{23}$ computed by the chain rule using the
       $\overline{Ke}_{12}$ and $\overline{Ke}_{13}$ fitted in steps 3 and 6, and fits
       B_{23}, C_{23}, and D_{23}

o   <u>Binary pair 1-3</u>

    12   uses chain rule for $\overline{Ke}_{13}$ using $\overline{Ke}_{12}$ and $\overline{Ke}_{23}$

        from fits 2 and 8 and correlates B_{13} and C_{13}

    13   uses chain rule for $\overline{Ke}_{13}$ using $\overline{Ke}_{12}$ and $\overline{Ke}_{23}$

        from fits 3 and 9 and correlates B_{13}, C_{13} and D_{13}

o   <u>Binary pair 1-2</u>

    14   uses chain rule for $\overline{Ke}_{12}$ using $\overline{Ke}_{13}$ and $\overline{Ke}_{23}$

        from fits 5 and 8 and correlates B_{12} and C_{12}

    15   uses chain rule for $\overline{Ke}_{12}$ using $\overline{Ke}_{13}$ and $\overline{Ke}_{23}$

        from fits 6 and 9 and correlates B_{12}, C_{12} and D_{12}

o   <u>Ternary data for system 1,2,3</u>

    16   correlates the parameters to best fit the ternary data

        only using the $\overline{Ke}_{12}$ from 3, the $\overline{Ke}_{13}$ from 6 and

        $\overline{Ke}_{23}$ derived from those using the chain rule to fit

        B_{ij}, C_{ij}, and D_{ij},

                ($i = 1,2,3$ for $j = 1,2,3$, $i = j$).

        Provision is made to switch $\overline{Ke}_{13}$ to be calculated

        from $\overline{Ke}_{12}$ and $\overline{Ke}_{23}$ derived from 3 and 9

    17   using parameters fitted in 2, 5, and 10, calculates

        ternary resin phase compositions using those

        parameters and computes standard deviation of the

        calculated points from the experimental data points

    18   repeats 17 using parameters fitted in 3, 6, and 11

    19   repeats 17 using parameters fitted in 2, 8, and 12

    20   repeats 17 using parameters fitted in 3, 9, and 13

    21   repeats 17 using parameters fitted in 5, 8, and 14

    22   repeats 17 using parameters fitted in 6, 9, and 15

o   <u>Binary sets fit together</u>

23   all three binary sets then are submitted by the

program for simultaneous fitting of $\overline{Ke}_{12}$, B_{12},

C_{12}, D_{12}, Ke_{13}, B_{13}, C_{13}, D_{13}, B_{23},

C_{23} and D_{23} with $\overline{Ke}_{23}$ = f ($\overline{Ke}_{12}$ and $\overline{Ke}_{13}$)

24   same as 24 but $\overline{Ke}_{13}$ = f ($\overline{Ke}_{12}$, $\overline{Ke}_{23}$)

o   <u>Total data sets fit, 3 binaries and ternary data</u>

25   similar to 23 except ternary data set is included

26   similar to 24 except ternary data set is included

The optional correlation methods for fitting the resin

phase activity coefficients are the one, two or three parameter

Redlich-Kister equation, the Wilson equation with ρ_{ij}= 1.0 (or

set to some other value) to fit τ_{ij}, or ρ_{ij} can be fit as well.

The NRTL equation with α_{ij} = 0.3 (or set to some other value) to

fit τ_{ij}, or α_{ij} can be fit as well.

One additional feature was built into RIONFT in order to

regress the data of Smith and Woodburn involving the stable

intermediate, $NaSO_4^-$. The program has a subroutine which

computes the equilibrium concentration of <u>one</u> of the stable

complexes formed by <u>one</u> of the three ionic species, providing

the stability constant is available for that complexation

reaction. The use of this type of relationship is questionable

in a ternary system, since it assumes that the complex is either

(1) not involved in the ion exchange process or (2) has the same

ion exchange equilibrium relationship as the uncomplexed ion.

It most likely is involved in the ion exchange process, and the

complexity now introduced is that a quaternary non-stoiciometric exchange process is involved, with the attendant experimental complications of measuring the amount of counterion in the exchanger due to the uncomplexed __and__ the complexed form. As will be discussed below, the Smith Woodburn ternary system of $NO_3^- - Cl^- - SO_4^=$ was equally well fit to experimental data without considering the complexation reaction to yield $NaSO_4^-$.

3. Features of RIONFT

The operational features of the ion exchange equilibrium regression program, RIONFT, for ternary systems is given in Appendix C.

E. Correlation Results - Ternary and Binary Systems

1. Comparison of Correlation Models

The results of data regression on four ternary systems utilizing RIONFT is given in Table 2-3. If the judgment of method used were made solely on the predicted ternary results, the Wilson equation would be preferred; however, in terms of total ability to correlate binary pairs (with $\overline{K}_{ij}$ being a function of $\overline{K}_{ik}$ and $\overline{K}_{jk}$) and predict ternary systems, the Redlich-Kister three suffix equation was selected. The Omatete (78) Ag^+, Na^+, H^+ system was not included in this comparison because of the paucity of data.

2. Ternary Phase Diagrams

Utilizing the Redlich-Kister model for the prediction of resin phase activity coefficients, resin compositions were

Table 2-3

Ternary Ion Exchange Equilibrium Data Regression

- Based on Ionic Equivalent Fraction -

Resin Phase Activity Coefficient Model

Redlich-Kister - three suffix

Wilson - $\rho_{ij} = \dfrac{\text{molar volume } i}{\text{molar volume } j} = 1.0$

NRTL - $\alpha_{ij} = 0.3$

Standard Deviation - % Normalized Difference

System	Pair 1-2	Pair 1-3	Pair 2-3	Ternary Calculated from Binary Parameters
1. Mn^{++}-Cs^+-Na^+				
R-K	1.70	8.8	3.8	11.6
Wilson	6.9	17.7	5.1	12.6
NRTL	7.5	18.5	5.2	13.2
2. Sr^{++}-Mn^{++}-Cs^+				
R-K	1.4	2.0	1.7	11.8
Wilson	1.4	1.7	7.2	10.5
NRTL	1.5	2.9	5.5	10.9
3. NH_4^+-Na^+-H^+				
R-K	1.1	1.05	7.8	4.6
Wilson	1.05	3.3	9.5	3.7
NRTL	1.1	3.3	9.4	3.7
4. NO_3^--Cl^--SO_4				
R-K	1.34	1.44	3.4	4.1
Wilson				
Roth	1.9	1.8	3.3	2.7
Smith & Woodburn	3.5	5.8	2.7	4.3
NRTL	2.3	3.0	3.3	5.9

calculated at regular electrolyte composition isotherms and plotted on triangular coordinate graphs. Figures 2-1 through 2-6 show the calculated position for the ternary resin compositions at the intersections of isotherms, and the experimental data points are superimposed. Two graphs are included for the Omatete data at normalities of 0.10 and 1.5 solution concentrations.

3. Binary Phase Diagrams

The Erickson (26) $ETDA^{++}-NH_4^+$ system is shown on Figure 2-7 for two normalities, 0.1 and 1 solution concentrations. The percent normalized standard deviations are 5.5 and 1.3% respectively, based on a two suffix Redlich-Kister equation. A plot of the activity coefficients is shown on Figures 2-8 showing that the system exhibits positive deviation and is almost symmetrical.

Omatete's (78) systems of Ag^+-H^+, Ag^+-Na^+, and Na^+-H^+ are shown on Figures 2-9, 2-10, and 2-11 for 0.1 and 0.5 normal Cl^- solutions. In the Na^+-H^+ system, Turner and Snowdon's (129, 130) data which was required to fill out the lower region is also plotted on Figures 2-11.

4. Discussion and Conclusions

Smith and Woodburn's (116) model for prediction of ternary ion exchange equilibria utilizing the Wilson equation has been extended to include the Redlich-Kister and NRTL activity coefficient models. The three models have been tested against the original system investigated by Smith and Woodburn, plus

Ternary Equilibrium Diagram
Resin Phase, Equivalent Fraction

Figure 2-1

$Mn^{++} - Cs^{+} - Na^{+}$

Dowex 50W – x8 Resin

Cl^{-} 0.1 Normal, 23°C

⊙ Experimental Points
– Resin Phase

Calculated Solution Phase
Isotherms

⎯⎯ Mn^{++}

––– Cs^{+} equivalent fraction

····· Na^{+}

Mn^{++} in solution

Cs^{+} in solution

Ternary Equilibrium Diagram
Resin Phase, Equivalent Fraction

$Sr^{++} - Mn^{++} - Cs^{+}$

Dowex 50W — x8 Resin

$\underline{\underline{Cl^{-} \quad 0.1 \text{ Normal}, 23°C}}$

⊙ Experimental Points
— Resin Phase

Calculated Solution Phase
Isotherms

—— Sr^{++}

— — — Mn^{++} equivalent
fraction

····· Cs^{+}

Sr^{++} in solution
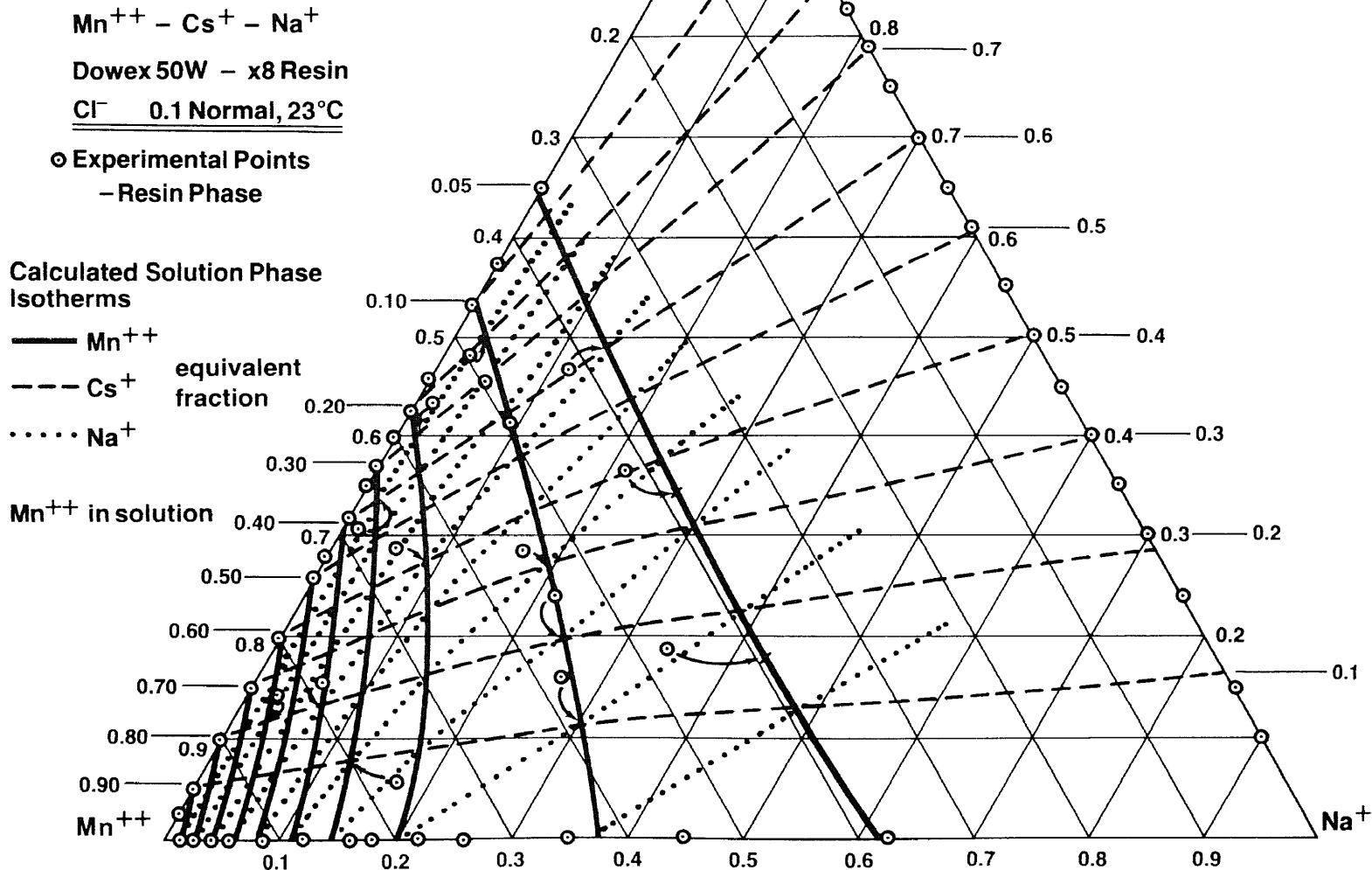
Mn^{++} in solution
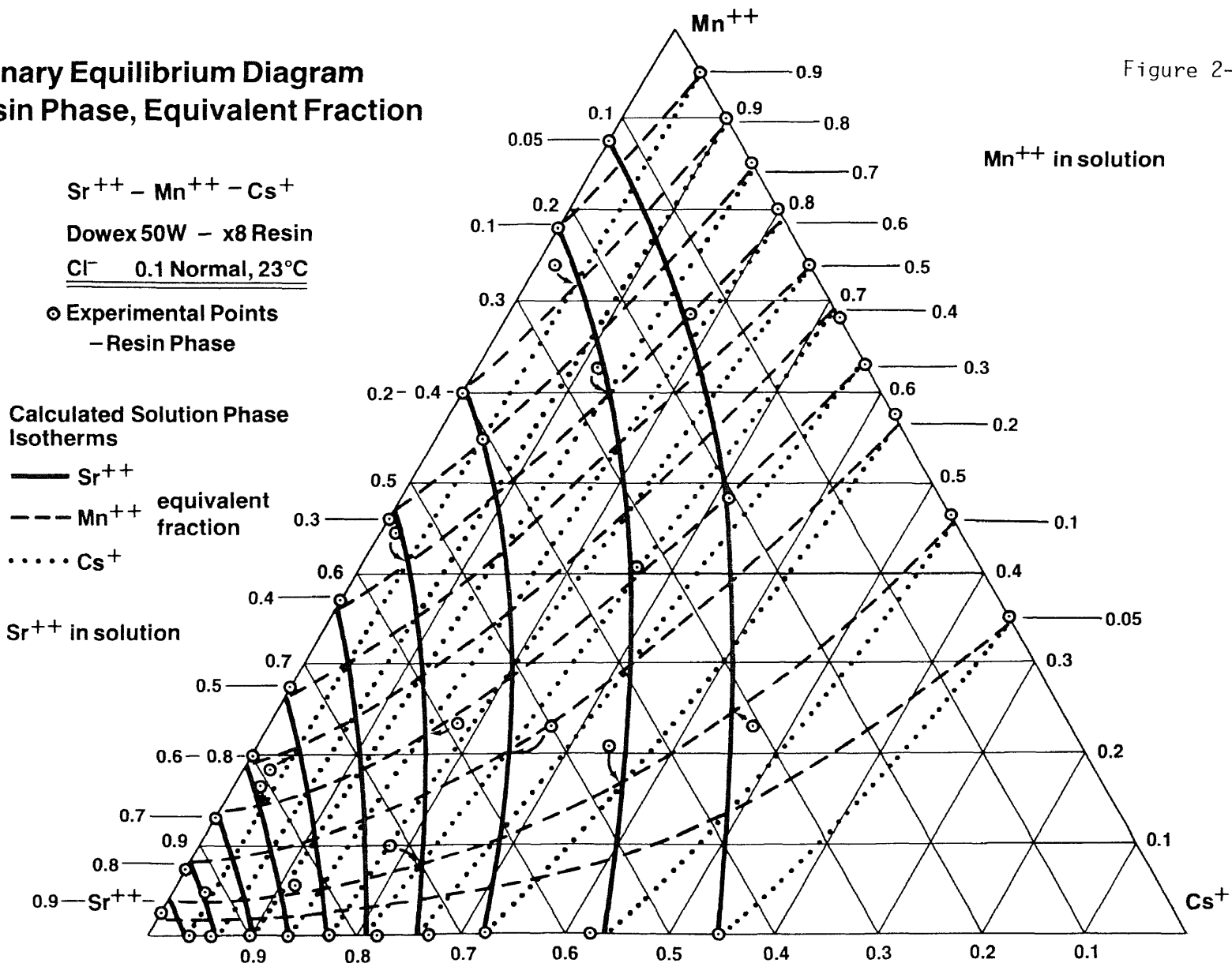
Figure 2-2

Ternary Equilibrium Diagram
Resin Phase, Equivalent Fraction

Figure 2-3

NH_4^+ in solution

$NH_4^+ - Na^+ - H^+$

Dowex 50W − 12x Resin

Cl^- ion   0.1 Normal, 25°C

⊙ Experimental Points
  − Resin Phase

Calculated Solution Phase
Isotherms

━━━ NH_4^+

− − − Na^+ equivalent
        fraction

· · · · · H^+

Na^+ in solution

Na^+

NH_4^+
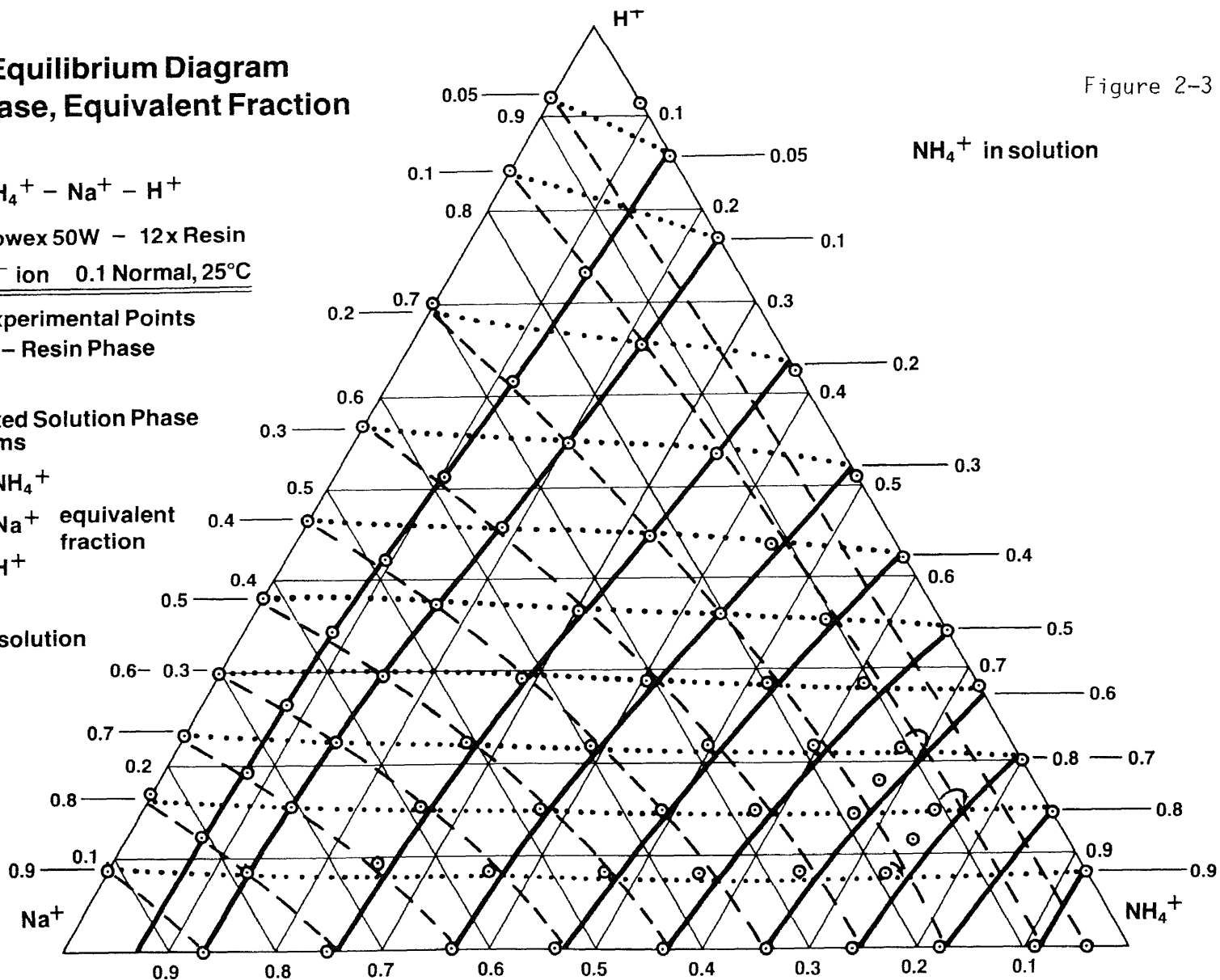
Ternary Equilibrium Diagram
Resin Phase, Equivalent Fraction

Figure 2-4

$NO_3^- - Cl^- - SO_4$

Amberlite 400

Na^+ 0.2 Normal, 25°C

○ Experimental Points

— Resin Phase

Calculated Solution Phase
Isotherms

——— NO_3^-

— — — Cl^- equivalent
fraction

• • • • • SO_4

Cl^- in solution

NO_3^-

NO_3^- in solution

Cl^-

$SO_4^=$
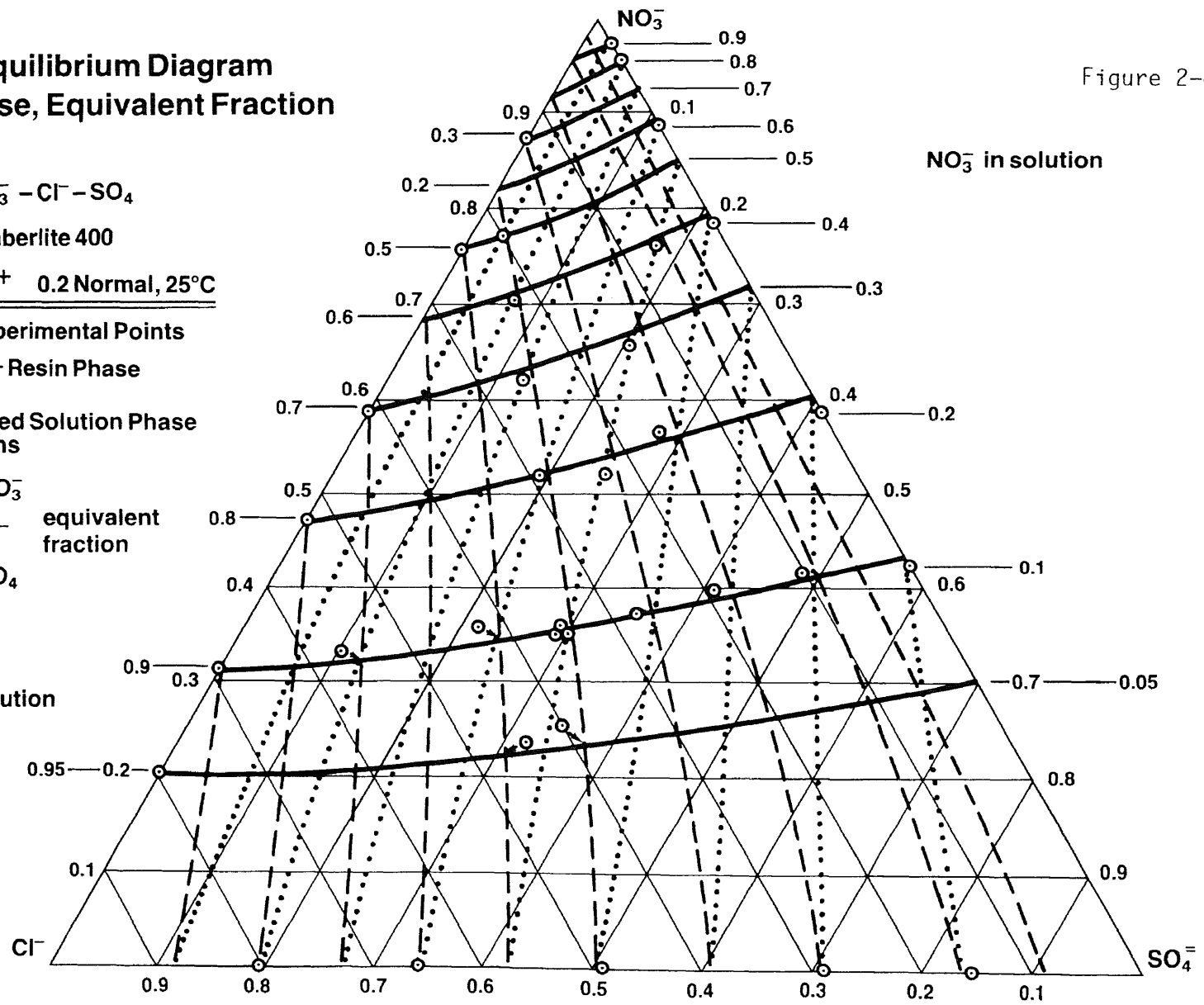
Ternary Equilibrium Diagram
Resin Phase, Equivalent Fraction

Figure 2–5

$Ag^+ - Na^+ - H^+/NO_3^-$

Dowex 50W – x8 Resin

0.10 Normal, 25°C

⊙ Experimental Points
– Resin Phase

Calculated Solution Phase
Isotherms

· · · · · Ag^+

—— Na^+ equivalent fraction

– – – H^+

Ag^+ in solution

Na^+ in solution

Na^+ in solution

Ternary Equilibrium Diagram
Resin Phase, Equivalent Fraction

Figure 2-6

$Ag^+ - Na^+ - H^+/NO_3^-$

Dowex 50W − x8 Resin

1.5 Normal, 25°C

⊙ Experimental Points
− Resin Phase

Calculated Solution Phase
Isotherms

····· Ag^+

——— Na^+ equivalent
            fraction

−−− H^+

Ag^+ in solution

Na^+

Na^+ in solution

Ag^+

H^+

Figure 2-7

System Ethylene Diamine/NH_3 - Dowex 50W x 8 Resin
Temp. 25°C

Equivalent Fraction Diamine in Resin $\overline{X}_A$

X_A

Equivalent Fraction Diamine in Solution

Experimental Data*

o 1 Normal Cl^-

△ 0.1 Normal$^-$

$K_{ETDA^{++}NH_4^{+}} = 16.1206$

Redlich-Kister Constants

B = 0.34626
C = –0.02223

Bromley Constants

$B_{ETDACl} \cong 0.09$
$B_{NH_4Cl} = 0.02$

Standard Deviation	1 Normal	0.1 Normal
	1.3%	5.5%
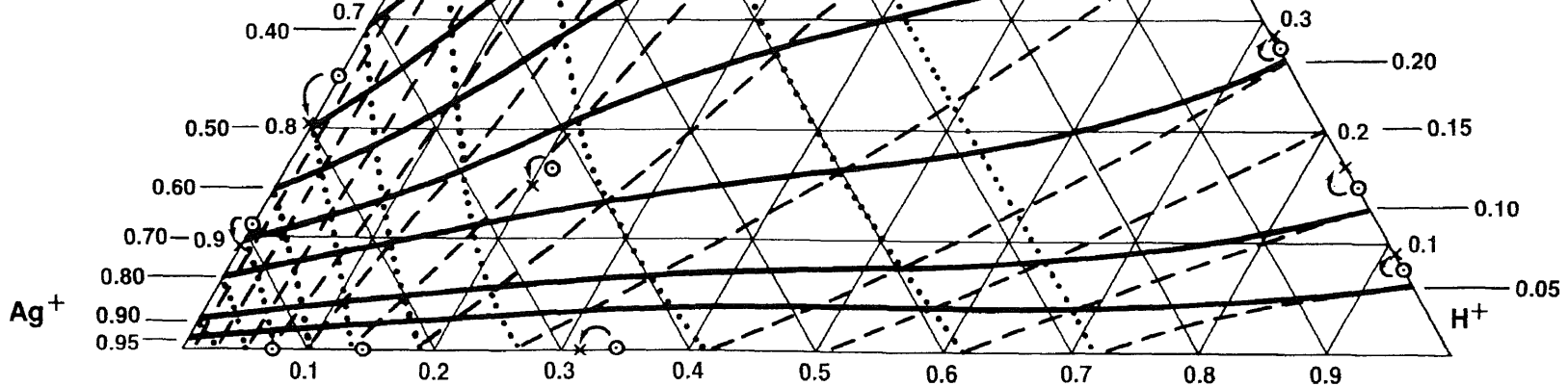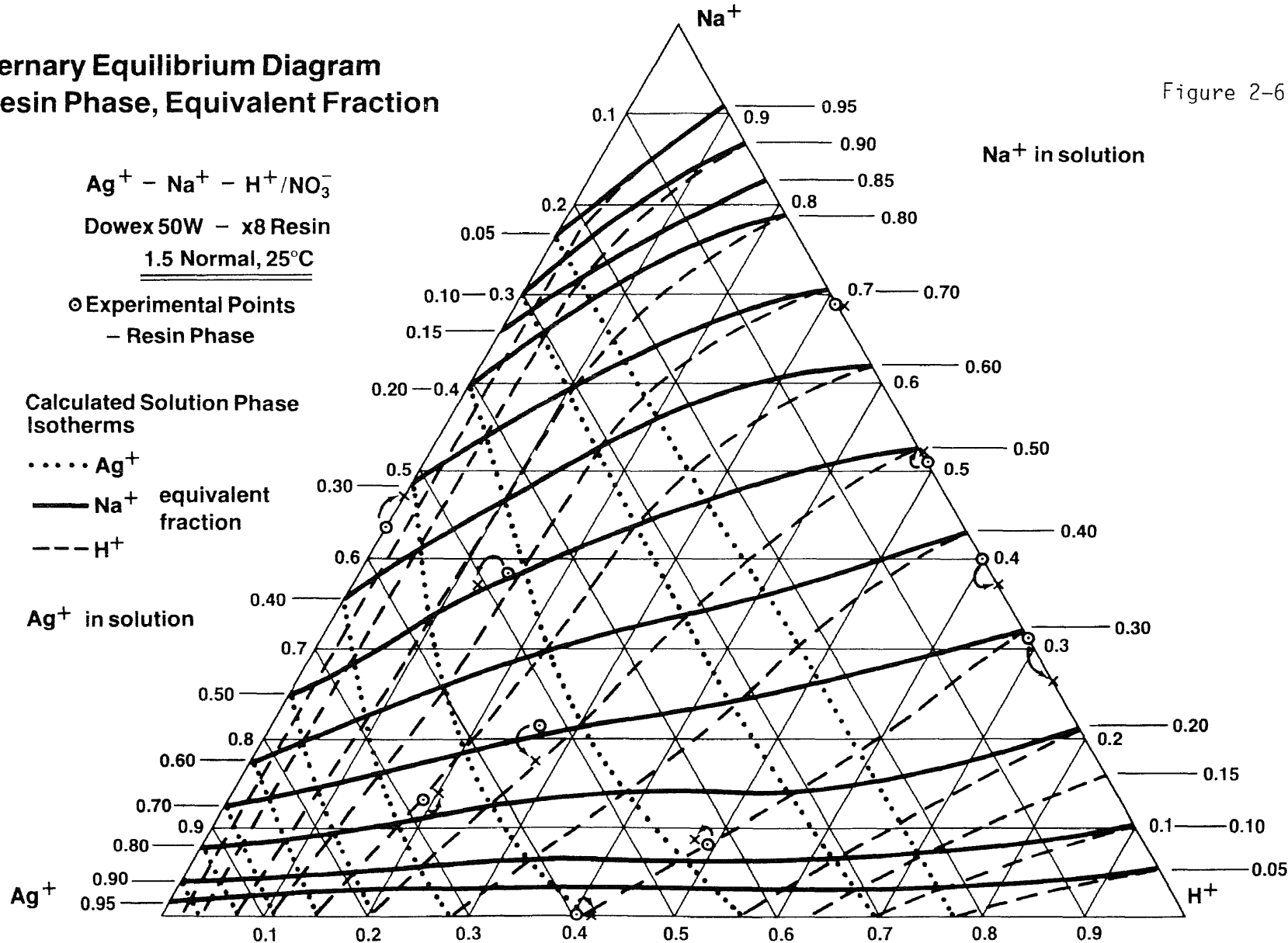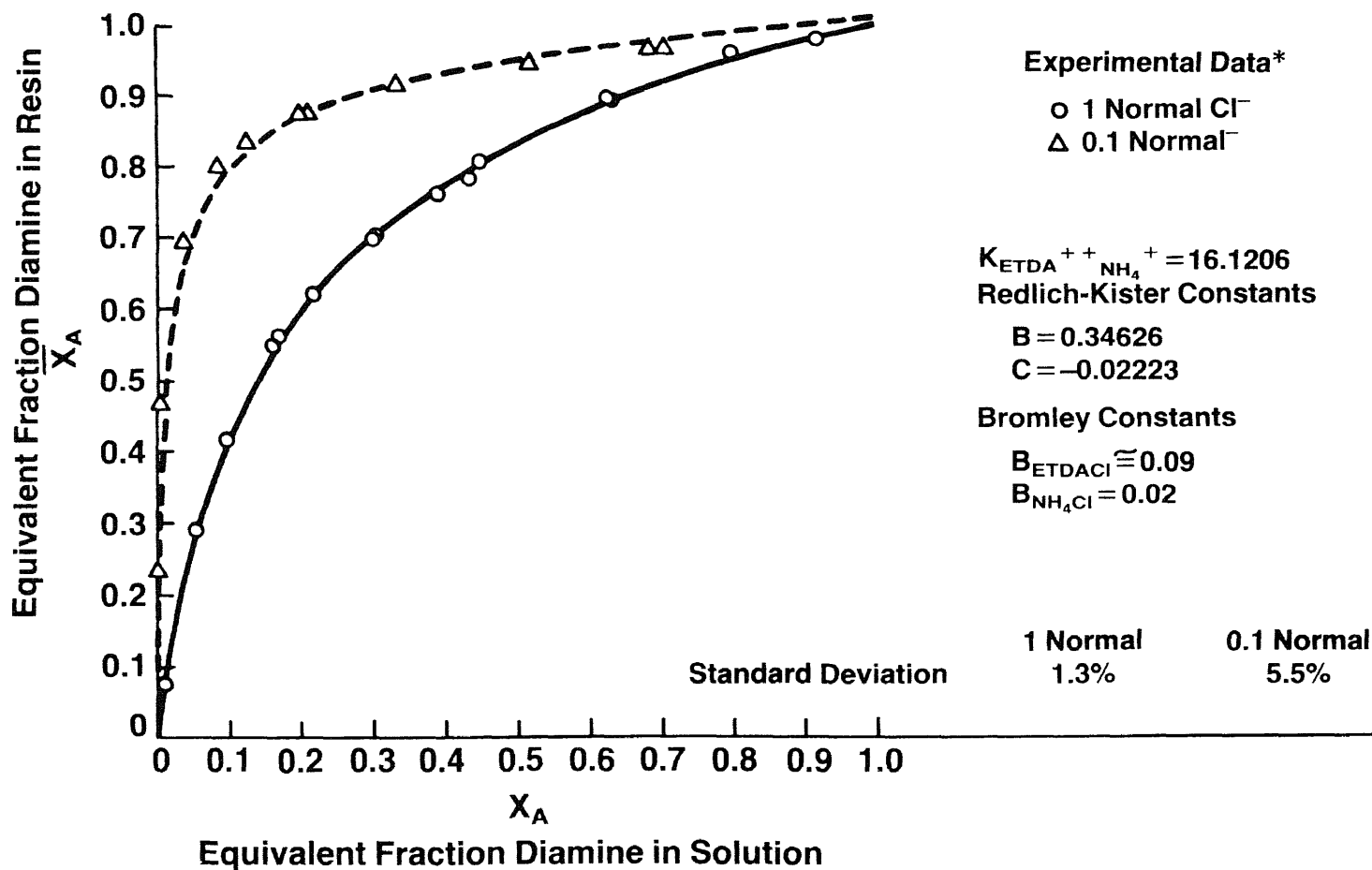
*K.L. Erickson
"Fixed Bed Exchange with Differing Ionic Mobilities
and Non-linear Equilibria" U. Texas, 1977

Figure 2-8

System Ethylene Diamine/NH_3 - Dowex 50W x 8 Resin $-Cl^-$
Resin Phase Activity Coefficients

Redlich-Kister Constants

B = 0.346256
C = -0.02223

1 - Diamine
2 - Ammonia

Y-axis: Resin Phase Activity Coefficients

X-axis: Equivalent Fraction Diamine in Resin
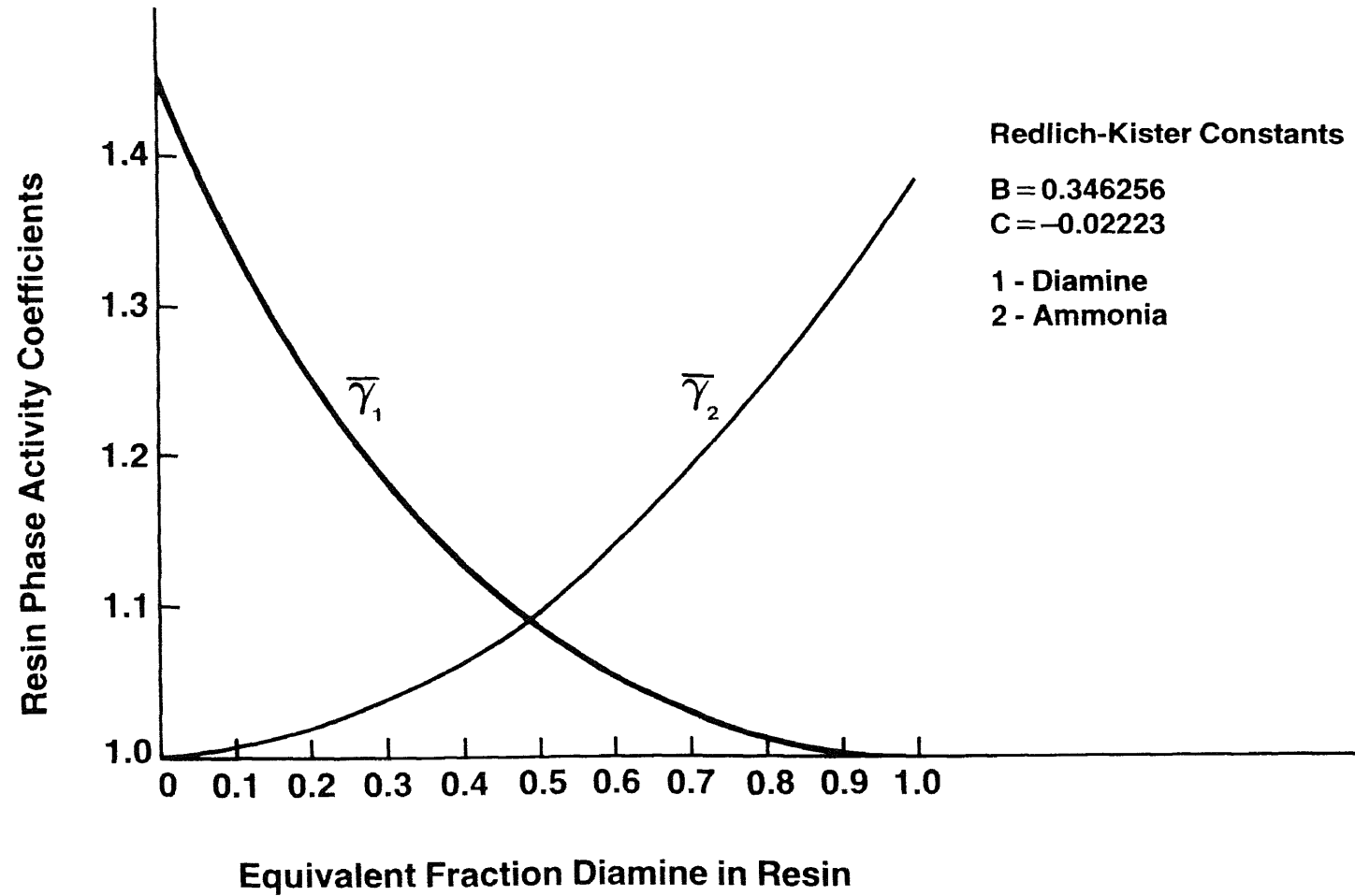
System $Ag^+/H^+/NO_3/$Dowex 50W x 8 Resin
Temp. 25°C

Figure 2-9

Data

O. Omatete "Dynamics of
Ternary Ion Exchange"
 O 0.1 Normal
 □ 1.5 Normal

Calculated
0.1 Normal – – – –
1.5 Normal ———

$K_{Ag^+H^+} = 8.8761$

Redlich-Kister Constants
$B = -0.7257$
$C = 0.8998$
$D = -0.9350$

Bromley Constants
$B_{AgNO_3} = -0.0828$
$B_{HNO_3} = 0.0776$

Equivalent Fraction Ag^+ in Resin
$\overline{X}_{Ag}^+$

X_{Ag}^+
Equivalent Fraction Ag^+ in Solution
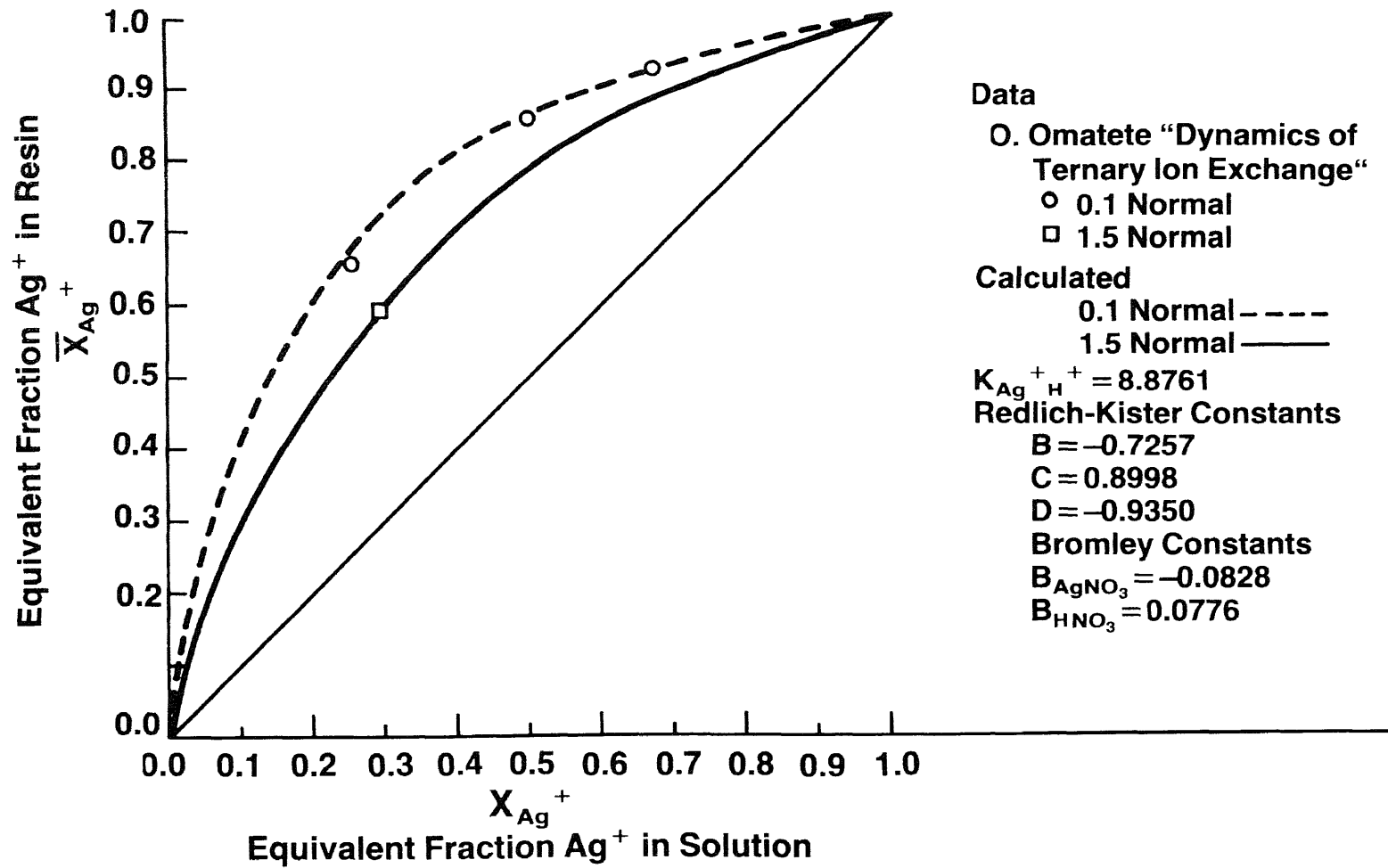
System Ag$^+$/Na$^+$/NO$_3^-$/Dowex 50W x 8 Resin
Temp. 25°C

Figure 2-10

Data

O. Omatete "Dynamics of Ternary Ion Exchange"
- o 0.1 Normal
- □ 1.5 Normal

Calculated

- 0.1 Normal ———
- 1.5 Normal – – – –

$K_{Ag^+ Na^+} = 5.924$

Redlich-Kister Constants
- B = –1.000
- C = 1.2472
- D = –0.8957

Bromley Constants
- $B_{AgNO_3} = -0.0828$
- $B_{NaNO_3} = -0.0128$

Equivalent Fraction Ag$^+$ in Resin — $\overline{X}_{Ag}^+$

X$_{Ag}^+$

Equivalent Fraction Ag$^+$ in Solution
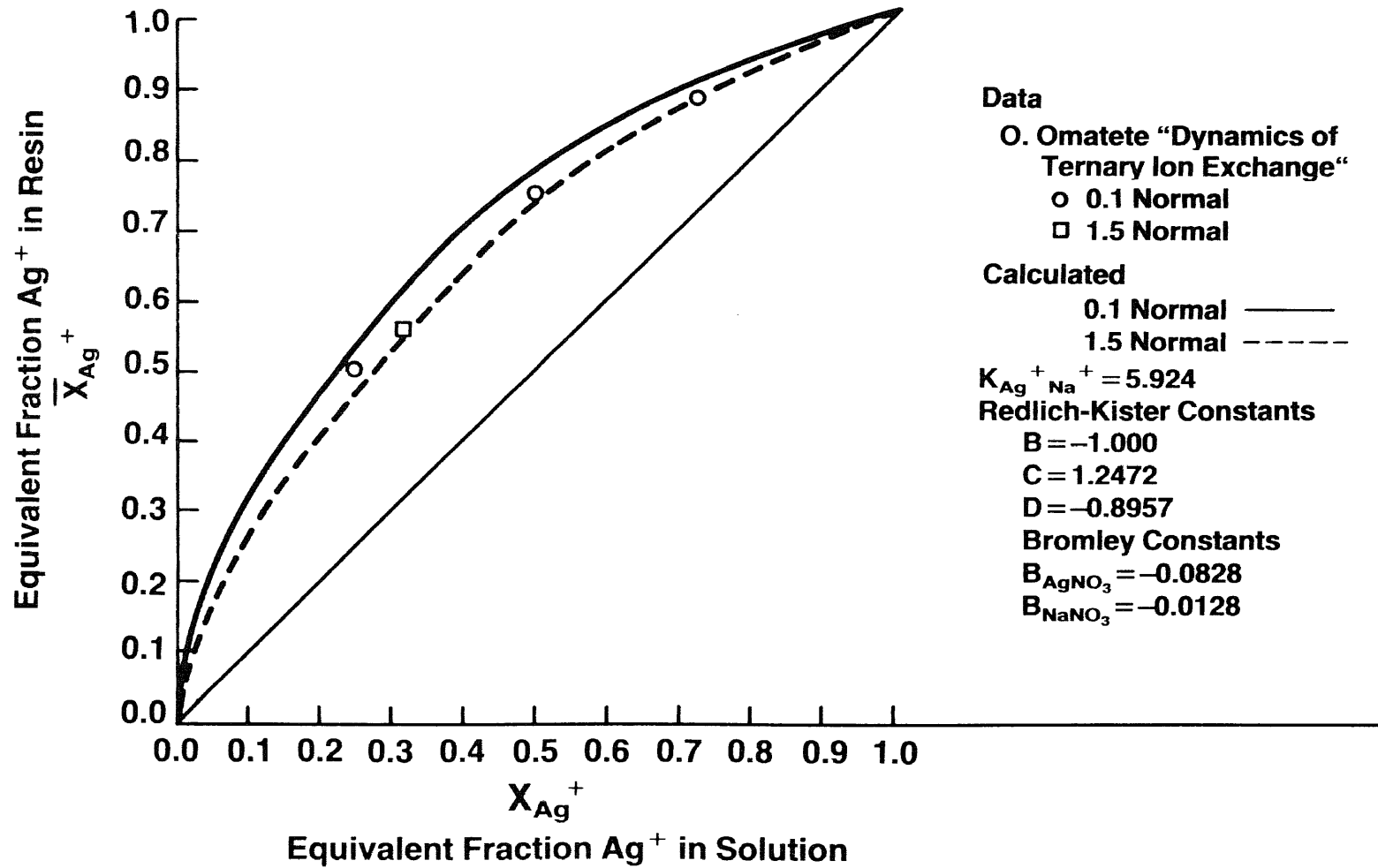
Figure 2-11

System Na$^+$/H$^+$/NO$_3^-$/Dowex 50W x 8 Resin
Temp. 25°C

Equivalent Fraction Na$^+$ in Resin $\overline{X}_{Na}^+$

X$_{Na}^+$
Equivalent Fraction Na$^+$ in Solution

Data
  O. Omatete "Dynamics of
    Ternary Ion Exchange"
    o 0.1 Normal
    □ 1.5 Normal

Turner, et al.
  System Cl$^-$/ZEO-Karb 8x
  x 0.1 Normal
Averaged Omatete/Turner
  + 0.1 Normal

    0.05 N Same as 0.1N
    0.10 N ———
    1.5 N — — —
K$_{Na^+ H^+}$ = 1.49827
Redlich-Kister Constants, Bromley Constants
    B = −0.15021   B$_{NaNO_3}$ = −0.0128
    C = −0.15682   B$_{HNO_3}$ = 0.0776
    D = −0.08917
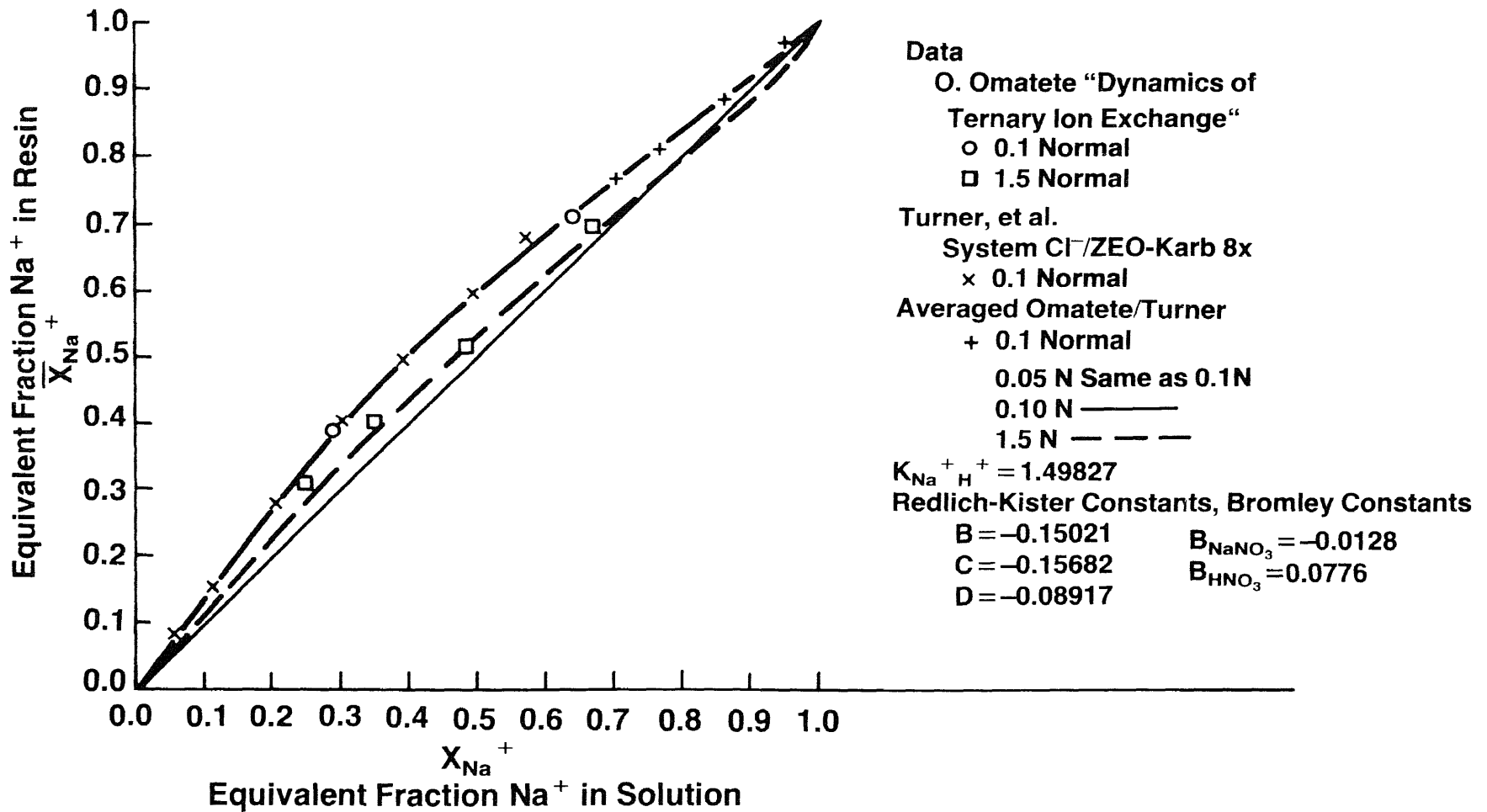
three other systems. The results are encouraging and suggest that the Redlich-Kister model gives better overall results. The fact that the activity coefficient, whether correlated with mole fractions or equivalent fraction concentration units, must "correct" for the changing number of moles in the ion exchanger during heterovalent exchange, i.e., $\overline{dc}_{total}$, accounts for the poorer results obtained with heterovalent cationic exchange as compared to homovalent cationic exchange. The extra suffix term, or "knob," on the Redlich-Kister equation allows for more non-linear compensation than the two "suffix" Wilson and NRTL equations. In terms of extending the system to more than three ionic species, if such data were available, the Wilson equation would be more straightforward in its general application to multicomponent systems.

It should be noted that runs were made on the two heterovalent cationic systems in which ρ_{ij} in the Wilson equation and α_{ij} in the NRTL equation were also fit with the regression model. The results were improved on some binary systems, and made worse in others, with a general degradation in the ability to predict ternary data points. In addition, physically absurd values of parameters such as ρ_{ij} were obtained. Since ρ_{ij} represents the molar volume ratios of the two solvated ions, some order of magnitude check against literature observations would have been encouraging. In any event, the values of $\rho_{ij} = 1.0$ and $\alpha_{ij} = 0.3$ gave overall best results for the Wilson and NRTL equations respectively.

Mole fraction and equivalent fraction concentration units were utilized in fitting the heterovalent ternary systems (obviously in the homovalent systems mol. fr. = equiv. fr.). Table 2-4 shows that overall, the equivalent fraction units yielded somewhat better results than the mole fraction system based on standard deviation of normalized difference. The same Table, 2-4, shows the mole fraction based equilibrium constants for the three binary pairs and the Redlich-Kister parameters for those systems.

The use of a four suffix Redlich-Kister equation (E_{ij} term) plus three ternary constants was evaluated initially as perhaps a more powerful activity coefficient model for both binary and ternary systems. In the case of the binary systems, experimental data for each binary pair was fit with five parameters (including $\overline{K}_{ij}$). Since in some instances the number of data points may have been between 8 and 10, this was clearly a case of "overkill." In fact, in the binary systems, more of the equilibrium selectivity for a given pair became vested in the activity coefficients than in the equilibrium constant. Although the fits were slightly improved over the three suffix system, attempts to correlate the activity coefficients for a third pair based on the chain rule deriving $\overline{K}_{ij}$ as a function of $\overline{K}_{ik}$ and $\overline{K}_{jk}$ led to poor results. This was so because the values of $\overline{K}_{ik}$ and $\overline{K}_{jk}$ were beginning to lose their identities as equilibrium constants when they should have represented the strongest correlatable parameter in the equilibrium

Table 2-4

Comparison of Mole Fraction vs. Equivalent Fraction

- Resin Phase Equilibria Correlation -

Heterovalent Exchange

Redlich-Kister three suffix equation
utilized for resin phase activity coefficients

System	Equilibrium Constant $\overline{K}_{ij}$	Redlich-Kister Coefficients			Standard Deviation % Normalized Difference	
		B_{ij}	C_{ij}	D_{ij}		
1. $Sr^{++}Mn^{++}Cs^+$						
$Sr^{++}Mn^{++}$						
m.f.	7.3112	0.0420	0.0707	-0.0679	1.41	
eq.f.	7.3111	0.0420	0.0707	-0.0679	1.41	
$Sr^{++}Cs^+$						
m.f.	2.8994	-0.8050	0.1689	-0.1325	2.8	ternary
eq.f.	4.4890	-0.4994	0.0170	-0.1270	2.02	m.f. 11.2
						eq.f. 11.8
$Mn^{++}Cs^+$						
m.f.	1.0723	-0.8029	0.1253	0.2425	4.85	
eq.f.	1.6602	-0.4552	-0.2965	0.3943	1.73	

Table 2-4,cont.

System	Equilibrium Constant $\bar{K}_{ij}$	Redlich-Kister Coefficients			Standard Deviation % Normalized Difference	
		B_{ij}	C_{ij}	D_{ij}		
2. $\frac{Mn^{++}Cs^+Na^+}{Mn^{++}Cs^+}$						
m.f.	1.0723	-0.8029	0.1253	0.2425	4.85	
eq.f.	1.6602	-0.4552	-0.2965	0.3943	1.73	
$Mn^{++}Na^+$						ternary
m.f.	3.0236	0.5847	-0.3281	0.0259	2.11	m.f. 12.3
eq.f.	4.6746	0.4677	0.4031	-0.5137	8.8	eq.f. 11.6
Cs^+Na^+						
m.f.	1.6792	-0.0869	0.1471	-0.0181	3.8	
eq.f.	1.6792	-0.0869	0.1471	-0.0182	3.8	
3. $\frac{NO_3^-Cl^-SO_4^{-2}}{NO_3^-Cl^-}$						
m.f.	3.9506	-0.4276	0.1805	-0.1719	1.34	
eq.f.	3.9506	-0.4276	0.1805	-0.1719	1.34	
$NO_3^-SO_4^{-2}$						ternary
m.f.	131.0740	-1.2959	-0.1781	-0.2944	0.91	m.f. N.A.
eq.f.	38.2100	-1.2306	0.2030	-0.2314	1.44	eq.f. 4.1
$Cl^-SO_4^{-2}$						
m.f.	8.3990	-0.8172	-0.1312	-0.2340	2.62	
eq.f.	2.4483	-0.5527	-0.1076	-0.1154	3.45	

relationship. The standard deviations for ternary systems predicted from the binaries correlated with the four suffix Redlich-Kister equation were generally poorer than obtained with the three suffix model.

Fitting the ternary data with a four suffix Redlich-Kister model including three ternary system constants, or 17 independent parameters, for 15 ternary data points (30 independent variables) showed no important improvement over use of the three suffix model without the ternary system constants. In any case, a requirement for ternary system constants would have negated any possibility of predicting ternary equilibrium system behavior from the binary correlation constants. The four suffix Redlich-Kister model and the ternary system constants were ruled out in subsequent correlation studies in this research.

It was concluded that the three suffix Redlich-Kister equation for resin phase activity coefficients based on equivalent fraction concentration units, and coupled with the Bromley equation to predict electrolyte phase activity coefficients, generally gave excellent fits of binary systems, even in heterovalent exchange, and gave fair representation of predicted ternary equilibrium points. This system for representation of binary and ternary equilibria was selected for use in the dynamic ion exchange model.

F. Relationship of Activity Coefficients Utilized in Deriving Diffusion Coefficients - Activity Driving Force

1. Binary Systems

1.1 Background

The dynamics of ions exchanging within an ion exchange resin is discussed in Chapter V. As in all mass transport processes, the rate of transfer of a molecular or ionic species through a given media is governed by a factor which is proportional to the ease with which the species moves through the media (diffusion coefficient), and the chemical potential gradient of the species in the media (driving force). In the case of ion exchange it is the electrochemical potential gradient that is operational, since the movement of charged ions or molecules is influenced by electrical gradients as well as chemical concentration gradients. In Chapter V, the molar flux for binary ion exchange is given as:

$$\bar{N}_1 = -\bar{D}_{11}' \cdot \nabla \bar{c}_1 \quad \text{Or} \quad \bar{N}_1 = -\bar{D}_{12_{eff}} \cdot \nabla \bar{c}_1 \qquad \text{from equation (5-12)}$$
$$\text{and} \qquad (5\text{-}13)$$

where: from equation (5-14)

$$\bar{D}_{12_{eff}} = \frac{\bar{D}_1 \bar{D}_2}{\sum\limits_{i=1}^{2} \bar{c}_i z_i^2 \bar{D}_i} \cdot \left[\bar{c}_1 z_1^2 + \bar{c}_2 z_2^2 + z_2 \bar{c}_1 \bar{c}_2 \cdot \frac{\partial \ell n \left[\frac{\bar{\gamma}_1^{-|z_2|}}{\bar{\gamma}_2^{-|z_1|}} \right]}{\partial \bar{c}_1} \right]_{molar}$$

Manipulation of variables during subsequent derivations and computations can be performed more readily if the diffusional flux relationship is expressed in equivalent fractions by recognizing that:

$$\bar{x}_i = \frac{|z_i| \cdot \bar{c}_i}{Q_r} \tag{5-16}$$

so that in equivalent fractions equation (5-23) becomes:

$$\bar{J}_1 = - \bar{D}_{12_{eff}} \cdot \nabla \bar{x}_1 \cdot Q_r \tag{5-24}$$

The expression for effective diffusivity becomes:

o $\qquad\qquad$ (5-21)

$$\bar{D}_{12_{eff}} = \frac{\bar{D}_1 \bar{D}_2}{\sum\limits_{i=1}^{2} \bar{x}_i |z_i| \bar{D}_i} \cdot \left[\bar{x}_1 |z_1| + \bar{x}_2 |z_2| + \bar{x}_1 \bar{x}_2 \cdot \frac{\partial \ln \left(\frac{\bar{\gamma}_1^{|z_2|}}{\bar{\gamma}_2^{|z_1|}} \right)}{\partial \bar{x}_1} \right]_{molar}$$

The current chapter on equilibrium involves methods for correlating binary and ternary ion exchange systems with models involving equivalent fraction, or alternatively mole fraction, of each species in the ion exchange resin. These models are consistent in that the standard states chosen allow prediction of the equilibrium relationships, $x_{i_{int}}^{*}$, for use in the flux equation (5-23) so long as the correct concentration units are employed. As an example, if the system of interest was correlated in mole fraction resin phase concentration units then, in employing the equivalent flux equation (5-60) at the boundary condition,

$$\left(A \frac{\partial \bar{x}_i}{\partial \rho} \Big|_{\rho=1} = k_{L_{i_{eff}}} \cdot (x_{i_{bulk}} - x_{i_{int}}^{*}) \right) , \text{ the equivalent}$$

fraction concentration, $\bar{x}_i \Big|_{\rho=1}$, must be converted to mole fraction, $\bar{x}_{i_{m.f.}} \Big|_{\rho=1}$, in order to obtain the electrolyte

phase equilibrium value, $x^*_{i_{int}}$ by use of equation (2-53).

1.2 Change of Standard States for Activity Driving Force

- Conversion of Molar to Equivalent Fraction Concentrations

Equation (5-21) describes the effective diffusivity for interchange of ionic species 1 and 2 in the resin. If the system can be considered to be ideal, then the term

$$\frac{\partial \ell n \left[\dfrac{\bar{\gamma}_1^{|z_2|}}{\bar{\gamma}_2^{|z_1|}} \right]_{molar}}{\partial \bar{x}_1}$$ is zero, and the equation can be used

directly in terms of resin phase equivalent fraction concentration units. If the chemical potential, $\bar{\mu}_i^c$, is to be used as the driving force then, in deriving the effective diffusivity for interchange of species 1 and 2, the activity

coefficient terms in the factor $\dfrac{\partial \ell n \left[\dfrac{\bar{\gamma}_1^{|z_2|}}{\bar{\gamma}_2^{|z_1|}} \right]_{molar}}{\partial \bar{x}_1}$ must be

computed from a model relating molar activity coefficients to molar concentration units in the resin. The models discussed in this chapter have been correlated in mole fraction or equivalent fraction concentration units, and a conversion in standard states to reflect molar concentration units must be made in order to utilize the molar flux equation correctly for non-ideal systems.

As derived in Appendix A, it was shown that the activity coefficients based on equivalent fraction concentration units

are identical to those based on molar concentration units.
The limiting values are:

$$\bar{x}_1 \longrightarrow 1.0 \ , \ \bar{\gamma}_1 \longrightarrow 1.0 \ , \ \text{and} \ \bar{a}_1 \longrightarrow 1.0 \qquad (2\text{-}78)$$

$$\bar{x}_1 \longrightarrow 0.0 \ , \ \bar{\gamma}_1 \longrightarrow \frac{K}{n_{\bar{f}_1^0}} \ , \ \text{and} \ \bar{a}_1 \longrightarrow 0.0 \qquad (2\text{-}79)$$

With molar concentration units, the limiting values are:

$$\bar{c}_1 \longrightarrow \bar{c}_T = \frac{Q_r}{|z_1|} \ , \ \bar{\gamma}_1 \longrightarrow 1.0 \ , \ \text{and} \ \bar{a}_1 \longrightarrow \frac{Q_r}{|z_1|} \qquad (2\text{-}80)$$

$$\bar{c}_1 \longrightarrow 0.0 \ , \qquad \bar{\gamma}_1 \longrightarrow \frac{K}{n_{\bar{f}_1^0}} \ , \ \text{and} \ \bar{a}_1 \longrightarrow 0.0 \qquad (2\text{-}81)$$

Models of activity coefficients based on molar versus
equivalent fraction concentration units can be illustrated
by using a truncated Redlich-Kister equation. In molar
units the expression for $\bar{\gamma}_{1_{molar}}$ would be;

$$\ell n \bar{\gamma}_{1_{molar}} = A \cdot \bar{c}_2^{\ 2} \qquad (2\text{-}82)$$

If equivalent fraction units are used,

$$\ell n \bar{\gamma}_1 = A \cdot \bar{x}_2^{\ 2} \qquad (2\text{-}83)$$

and since $\bar{x}_2 = \dfrac{\bar{c}_2 \cdot |z_2|}{Q_r}$, and $\bar{\gamma}_{1_{molar}} = \bar{\gamma}_1$

$$A \cdot \bar{c}_2^{\ 2} = A' \cdot \bar{c}_2^{\ 2} \cdot \left(\frac{|z_2|}{Q_r} \right)^2 \ , \ \text{so} \ A = A' \cdot \left(\frac{|z_2|}{Q_r} \right)^2 \qquad (2\text{-}84)$$

and the systems are made congruent by the term $\left(\dfrac{|z_2|}{Q_r} \right)^2$.
Consequently, in utilizing the non-ideal version of the
equation for effective diffusion coefficients, (5-14),

activing coefficients correlated in equivalent fraction
concentration units can be used directly, or:

$$\frac{\partial \ln \left(\overline{\gamma}_1^{-|z_2|} \Big/ \overline{\gamma}_2^{-|z_1|} \right)_{molar}}{\partial \overline{x}_1} = \frac{\partial \ln \left(\overline{\gamma}_1^{-|z_2|} \Big/ \overline{\gamma}_2^{-|z_1|} \right)_{eq.fr.}}{\partial \overline{x}_1} \qquad (2\text{-}85)$$

1.3 Change of Standard States for Activity Driving Force
- Conversion of Molar to Mole Fraction Concentrations

The change of standard states involved with conversion
of activity coefficients correlated in molar concentration
terms to activity coefficients correlated in mole fraction
terms is more complicated. The values of activity
coefficients correlated in mole fractions, $(\overline{\gamma}_{i_{m.f.}})$ are
not equal to the values for activity coefficients correlated
in molar or equivalent fraction concentration units
$(\overline{\gamma}_{i_{molar}}$ or $\overline{\gamma}_i)$, as is shown in Appendix A.

As indicated in Appendix A, the limiting values of
activity coefficients correlated in mole fraction
concentration units is as follows:

$$\overline{x}_1 \xrightarrow[m.f.]{} 1.0 \; , \; \overline{\gamma}_1 \xrightarrow[m.f.]{} 1.0 \; , \; \text{and} \; \overline{a}_1 \xrightarrow[m.f.]{} 1.0 \qquad (2\text{-}86)$$

$$\overline{x}_1 \xrightarrow[m.f.]{} 0.0 \; , \; \overline{\gamma}_1 \xrightarrow[m.f.]{} \left(\frac{K'}{n \overline{f}_1^0} \cdot \frac{Q_r}{|z_2|} \right) \; , \; \text{and} \; \overline{a}_1 \xrightarrow[m.f.]{} 0.0 \qquad (2\text{-}87)$$

and for molar concentration units,

$$\overline{c}_1 \xrightarrow{} \overline{c}_T = \left| \frac{Q_r}{z_1} \right| \; , \; \overline{\gamma}_1 \xrightarrow[molar]{} 1.0 \; , \; \text{and} \; \overline{a}_1 \xrightarrow[molar]{} \left| \frac{Q_r}{z_1} \right| \qquad (2\text{-}88)$$

$$\qquad\qquad (2\text{-}89)$$

$$\overline{c}_1 \xrightarrow{} 0.0 \qquad , \; \overline{\gamma}_1 \xrightarrow[molar]{} \left(\frac{K'}{n \overline{f}_1^0} \cdot \frac{|z_1|}{Q_r} \right) \; , \; \text{and} \; \overline{a}_1 \xrightarrow[molar]{} 0.0$$

The relationship between activity coefficients based on molar versus mole fraction concentration units is given in equation (A-18) as:

$$\circ \quad {}^{n}\overline{\gamma}_{1_{molar}} = {}^{n}\overline{\gamma}_{1_{m.f.}} \cdot \left[\frac{1}{\{(1-VR)\cdot\overline{x}_1 + VR\}} \right] \quad (2\text{-}90)$$

noting that $\overline{x}_1$ is the equivalent fraction

The following procedure is followed to make the standard state correction. The equilibrium relationship in molar concentration units for components 1 and 2 is:

$$\circ \quad\quad\quad\quad\quad\quad\quad (2\text{-}91)$$

$$\overline{K}_{12_{molar}} = \left(\frac{\overline{a}_1^{|z_2|}}{\overline{a}_2^{|z_1|}} \right) \cdot \left(\frac{(x^*_{2_{int}} \cdot \gamma_2)^{|z_1|}}{(x^*_{1_{int}} \cdot \gamma_1)^{|z_2|}} \right) \cdot norm^{(|z_1|-|z_2|)} \cdot \left(\frac{|z_1|^{|z_2|}}{|z_2|^{|z_1|}} \right)$$

where the bracket over the K_{elec} portion spans:

$$K_{elec}$$

or simplifying:

$$\circ \quad\quad \overline{K}_{12_{molar}} = \left(\frac{\overline{a}_1^{|z_2|}}{\overline{a}_2^{|z_1|}} \right) \cdot K_{elec} \quad\quad (2\text{-}92)$$

where:

$$\overline{a}_{i_{molar}} = \overline{c}_i \cdot \overline{\gamma}_{i_{molar}} \quad\quad (2\text{-}93)$$

The equilibrium relationship in mole fraction concentration units for components 1 and 2 is:

$$\circ \quad\quad \overline{K}_{12_{m.f.}} = \left(\frac{\overline{a}_1^{|z_2|}}{\overline{a}_2^{|z_1|}} \right) \cdot K_{elec} \quad\quad (2\text{-}94)$$

where:

$$\bar{a}_{i_{m.f.}} = \bar{x}_{i_{m.f.}} \cdot \bar{\gamma}_{i_{m.f.}} \qquad (2\text{-}95)$$

The molar activity coefficient relationship can be given as:

$$(2\text{-}96)$$

$$\frac{\partial \ell n \left[\frac{\bar{\gamma}_1^{|z_2|}}{\bar{\gamma}_2^{|z_1|}}\right]_{molar}}{\partial \bar{x}_1} = \frac{\partial \ell n \left[\frac{\bar{\gamma}_1^{|z_2|}}{\bar{\gamma}_2^{|z_1|}}\right]_{mf}}{\partial \bar{x}_1} + \frac{\partial \ell n \left[\frac{\left[\frac{\bar{\gamma}_1^{|z_2|}}{\bar{\gamma}_2^{|z_1|}}\right]_{molar}}{\left[\frac{\bar{\gamma}_1^{|z_2|}}{\bar{\gamma}_2^{|z_1|}}\right]_{mf}}\right]}{\partial \bar{x}_1}$$

Combining equations (2-92) and (2-94) yields:

$$\frac{\bar{K}_{12_{molar}}}{\bar{K}_{12_{mf}}} = \frac{\left[\frac{\bar{a}_1^{|z_2|}}{\bar{a}_2^{|z_1|}}\right]_{molar}}{\left[\frac{\bar{a}_1^{|z_2|}}{\bar{a}_2^{|z_1|}}\right]_{mf}} \qquad (2\text{-}97)$$

and in view of equations (2-93) and (2-95), equation (2-97) can be expanded to give the relationship:

$$(2\text{-}98)$$

$$\frac{\left[\frac{\bar{\gamma}_1^{|z_2|}}{\bar{\gamma}_2^{|z_1|}}\right]_{molar}}{\left[\frac{\bar{\gamma}_1^{|z_2|}}{\bar{\gamma}_2^{|z_1|}}\right]_{mf}} = \frac{\bar{K}_{12_{molar}}}{\bar{K}_{12_{mf}}} \cdot \left[\frac{\bar{x}_{1_{mf}}^{|z_2|}}{\bar{x}_{2_{mf}}^{|z_1|}}\right] \cdot \left[\frac{\bar{c}_2^{|z_1|}}{\bar{c}_1^{|z_2|}}\right]$$

The ratio expressed by the following relationship,

o
$$R = \frac{\left(\dfrac{\bar{x}_1^{|z_2|}}{\bar{x}_2^{|z_1|}}\right)_{mf}}{\left(\dfrac{\bar{c}_1^{|z_2|}}{\bar{c}_2^{|z_1|}}\right)}$$
(2-99)

can be transformed to an expression based on equivalent fraction concentration units by use of the relationships:

$$\bar{x}_{1_{mf}} = \frac{\bar{c}_1}{\left(\left[\dfrac{Q_r}{|z_2|}\right] + (1-VR)\cdot\bar{c}_1\right)}$$
(2-100)

and:

$$\bar{x}_{2_{mf}} = \frac{\bar{c}_2}{\left(\left[\dfrac{Q_r}{|z_1|}\right] + (1-\dfrac{1}{VR})\cdot\bar{c}_2\right)}$$
(2-101)

where $VR = \dfrac{|z_1|}{|z_2|}$

The expression for R becomes:

o
$$R = C\cdot\left(\frac{\left[(1-VR)\cdot\bar{x}_1 + VR\right]^{|z_1|}}{\left[(1-VR)\cdot\bar{x}_1 + VR\right]^{|z_2|}}\right)$$
(2-102)

where:

$$C = \left(\frac{|z_1|}{Q_r}\right)^{|z_2|} \cdot \left(\frac{Q_r}{|z_2|}\right)^{|z_1|} \cdot \left(\frac{1}{VR}\right)^{|z_1|}$$

In view of equations (2-96) and (2-98), and (2-102), the following relationship obtains:

o $\qquad$ (2-103)

$$\frac{\partial \ell n\left[\dfrac{\overline{\gamma}_1^{|z_2|}}{\overline{\gamma}_2^{|z_1|}}\right]_{molar}}{\partial \overline{x}_1} = \frac{\partial \ell n\left[\dfrac{\overline{\gamma}_1^{|z_2|}}{\overline{\gamma}_2^{|z_1|}}\right]_{mf}}{\partial \overline{x}_1} + \frac{\partial \ell n\left[\dfrac{\overline{K}_{12\,molar}}{\overline{K}_{12\,mf}}\right]}{\partial \overline{x}_1} + \frac{\partial \ell n(C)}{\partial \overline{x}_1}$$

$$- \frac{\partial \ell n\left[\left[(1-VR)\cdot\overline{x}_1 + VR\right]^{|z_2|}\right]}{\partial \overline{x}_1} + \frac{\partial \ell n\left[\left[(1-VR)\cdot\overline{x}_1 + VR\right]^{|z_1|}\right]}{\partial \overline{x}_1}$$

By carrying out the differentiation of the last two terms in equation (2-103), the final conversion equation is obtained,:

o $\qquad$ (2-104)

$$\frac{\partial \ell n\left[\dfrac{\overline{\gamma}_1^{|z_2|}}{\overline{\gamma}_2^{|z_1|}}\right]_{molar}}{\partial \overline{x}_1} = \frac{\partial \ell n\left[\dfrac{\overline{\gamma}_1^{|z_2|}}{\overline{\gamma}_2^{|z_1|}}\right]_{mf}}{\partial \overline{x}_1} - \left[\frac{(|z_1|-|z_2|)\cdot(VR-1)}{\left[(1-VR)\cdot\overline{x}_1 + VR\right]}\right]$$

The substitution of the right side of equation (2-104) in (5-21) corrects the activity coefficient relationship from molar units to mole fraction units. Obviously, if $|z_1|=|z_2|$ the second right hand term is zero, and the activity coefficient relationship is the same whether molar, mole fraction or equivalent fraction concentration units are utilized.

Since it would be more conveniuent to take the partial

of $\ln\left[\dfrac{\bar{\gamma}_1^{|z_2|}}{\bar{\gamma}_2^{|z_1|}}\right]$ with respect to mole fraction concentration

units rather than equivalent fraction concentration units, the following can be arranged:

$$\frac{\partial(\quad)}{\partial \bar{x}_1} = \frac{\partial(\quad)}{\partial \bar{x}_{1_{mf}}} \cdot \frac{\partial \bar{x}_{1_{mf}}}{\partial \bar{c}_1} \cdot \frac{\partial \bar{c}_1}{\partial \bar{x}_1} \qquad (2\text{-}105)$$

and since,

$$\bar{x}_1 = \frac{\bar{c}_1 \cdot |z_1|}{Q_r} \quad , \quad \frac{\partial \bar{c}_1}{\partial \bar{x}_1} = \frac{Q_r}{z_1} \qquad (2\text{-}106)$$

plus equation (2-100) can be arranged to give,

$$\bar{c}_1 = \left[\frac{\bar{x}_{1_{mf}} \cdot Q_r}{(|z_2|) \cdot \left[1 + \bar{x}_{1_{mf}} \cdot (VR-1)\right]}\right] \qquad (2\text{-}107)$$

then,

$$\frac{\partial \bar{c}_1}{\partial \bar{x}_{1_{mf}}} = \frac{Q_r}{|z_2|} \cdot \left[\frac{1}{\left[1 + \bar{x}_{1_{mf}} \cdot (VR-1)\right]^2}\right] \qquad (2\text{-}108)$$

and finally,

$$\frac{\partial(\quad)}{\partial \bar{x}_1} = \frac{\partial(\quad)}{\partial \bar{x}_{1_{mf}}} \cdot \left[\frac{\left[1 + \bar{x}_{1_{mf}} (VR-1)\right]^2}{VR}\right] \qquad (2\text{-}109)$$

The resulting transformation from molar activity coefficients to mole fraction activity coefficients is then;

$$
\circ \qquad \frac{\partial \ln \left[\overline{\gamma}_1^{|z_2|} \Big/ \overline{\gamma}_2^{|z_1|} \right]_{molar}}{\partial \overline{x}_1} = \frac{\partial \ln \left[\overline{\gamma}_1^{|z_2|} \Big/ \overline{\gamma}_2^{|z_1|} \right]_{m.f.}}{\partial \overline{x}_{1_{mf}}} \cdot \left[\frac{\{1+\overline{x}_{1_{mf}} \cdot (VR-1)\}^2}{VR} \right] \qquad (2\text{-}110)
$$

$$
- \left[\frac{(|z_1|-|z_2|)(VR-1)}{\{(1-VR)\overline{x}_1 + VR\}} \right]
$$

It is obvious from the above that computations involving determination of the effective diffusion coefficients in non-ideal systems are greatly simplified if the activity coefficients have been correlated in equivalent fraction units.

2. Ternary Systems

The use of chemical potential as a driving force, if of value in describing binary systems, must be extended to ternary dynamic models if the concept is to be proved efficacious in this research. Again, the effective diffusion coefficients derived from equations (5-27) and (5-28) involve the terms,

$$
\circ \qquad \left[\frac{\partial \ln \overline{\gamma}_3}{\partial \overline{x}_3} \right]_{\substack{molar \\ k/j}} \qquad and \qquad \left[\frac{\partial \ln \overline{\gamma}_{k/j}}{\partial \overline{x}_{k/j}} \right]_{\substack{molar \\ j/k \text{ and } 3}} \qquad (2\text{-}111)
$$

in which the molar activity coefficients are employed. Since all of the ternary dynamic batch simulation runs were made with activity coefficients derived in equivalent fraction concentrations, there was no activity coefficient standard state correction required to satisfy equations (2-111) expressions. Equations (5-27) and (5-28) were solved by direct utilization of the equivalent fraction activity coefficients.

CHAPTER III

ELECTROLYTE PHASE - ACTIVITY COEFFICIENTS OF IONIC SPECIES

& EFFECT ON DIFFUSION COEFFICIENTS

A. Activity Coefficients - Electrolyte Phase

1. General

The various methods for describing ion exchange equilibria the thermodynamic equilibrium constant, whether it be based on molalities or equivalent fractions (see chapter on Equilibrium), require knowledge of the activity coefficients of ionic species in the electrolyte. Most investigators have dealt with binary systems, and have either assumed ideality, or invoked Harned's Rule for the electrolyte phase. Harned's Rule (105) states that at constant ionic strength, I, the ratio of activity coefficients in an electrolyte mixture is constant, and equal to the ratio for the pure electrolyte solutions of the various ionic species at the same ionic strength.

$$\circ \quad Log\ \gamma_1 = Log\ \gamma_{1(o)} - \alpha_1 \cdot m_{2_{bulk}} \quad\quad (3\text{-}1)$$

where:

γ_1 = activity coefficient of ionic species 1 in a mixture of 1 and 2

$\gamma_{1(o)}$ = activity coefficient of ionic species 1 in a solution containing only species 1 at a total solution molality = m_{bulk}

m_2 = molality of species 2 in mixture

likewise:

$$\circ \quad Log\ \gamma_2 = Log\ \gamma_{2(o)} - \alpha_2 \cdot m_{1_{bulk}} \quad\quad (3\text{-}2)$$

108

Presumably this treatment could be extended to ternary systems, but the literature search for this project did not find any reference to such extension of Harned's Rule.

In any event, during exchange of ions of differing valences, the ionic strength, I, of the electrolyte phase will change. For example, during the exchange of a valence 1 cation species for a cation species having a valence of 2, at 1 normal electrolyte solution strength and with anion valence of 1:

$$
\circ \qquad I = \frac{1}{2} \cdot norm \cdot \left(\sum_{i=1}^{n} x_{i_{bulk}} \cdot |z_i| + |z_{anion}| \right) \qquad (3\text{-}3)
$$

where:

$$I \quad = \quad \text{ionic strength}$$

$$x_{i_{bulk}} \quad = \quad \text{equivalent fraction of cation}$$

$$z_i \quad = \quad \text{valence of ion}$$

$$norm \quad = \quad \text{solution normality}$$

for example:

$$
\text{if } x_{i_{bulk}} \quad = 1 \text{ for } z_i = 1
$$
$$
I \qquad\qquad = \frac{1}{2} \cdot (1 + 1) = 1
$$

$$
\text{if } x_{i_{bulk}} \quad = 1 \text{ for } z_i = 2
$$
$$
I \qquad\qquad = \frac{1}{2} \cdot (2 + 1) = 1.5
$$

So conditions for application of Harned's Rule during multivalent exchange will not hold. Reference is made to Robinson and Stokes (105) who state that Harned's Rule is valid for systems such as $HCl\text{-}BaCl_2$ provided the total ionic strength is kept constant, as contrasted to constant molality.

2. Treatment of Electrolyte Activity Coefficients - This Research

Smith and Woodburn (116), in their treatment of ternary equilibrium for the system $SO_4^=$, NO_3^-, & Cl^- used activity coefficients for the electrolyte phase based on the extended Debye-Huckel equation given by Robinson and Stokes (103), and interaction parameters by Truesdell and Jones (128). For this work, the Bromley version of the extended Debye-Huckel equation (9) was selected. Bromley has published (9) values of his short range interaction parameters, B, for 175 salts in aqueous solution. Parameter B can also be estimated by combining contributions of individual cations (36) with those of individual anions (40). The predictive range of the Bromley equation extends to 6 molal concentration, and is available in a form which permits the approximation of the activity coefficients of individual ionic species in mixtures of both cations and anions. The tables in Appendix C are for runs made in this research project to test this correlation against data for a variety of salts (total of 17) with molality ranging from 0.1 to 6.0, as given in Robinson and Stokes (106). The averaged root mean square of % relative difference, actual to predicted, was 2.7% for the combined total of all 17 salts.

3. The L.A. Bromley equation is:

For salt in aqueous solution, where $\gamma_\pm$ is the molal activity coefficient for the salt at a given solution ionic strength,

$$\text{Log } \gamma_\pm^o = \left[\frac{-0.511 \cdot |z_+z_-| \cdot I^{\frac{1}{2}}}{(1 + I^{\frac{1}{2}})} \right] + \left[\frac{(0.06+0.60 \cdot B_{12}) \cdot (|z_+z_-|) \cdot I}{\left[1 + \frac{1.5 \cdot I}{(|z_+z_-|)} \right]^2} \right] + B_{12} \cdot I \tag{3-4}$$

where:

$$I \quad = \text{ionic strength}$$

$$= \frac{1}{2} \cdot \sum_{i=1}^{n} m_i \cdot z_i^2 \qquad (3-5)$$

$m_i \quad$ = molality of species i

$z_i \quad$ = valence of species i

i $\quad$ = 1,3,5---represents cations

i $\quad$ = 2,4,6---represents anions

$B_{12} \quad$ = experimental correlation constant for salt 12

Single Ionic Species

$$(3-6)$$

Since:

$$\circ \quad \text{Log } \gamma_{12} \equiv \left(\frac{|z_2|}{(|z_1|+|z_2|)} \right) \cdot \text{Log } \gamma_1 + \left(\frac{|z_1|}{(|z_1|+|z_2|)} \right) \cdot \text{Log } \gamma_2$$

it was shown that:

$$\circ \quad \text{Log}_1 = \left(\frac{-0.511 \cdot z_1^2 \cdot I^{\frac{1}{2}}}{(1 + I^{\frac{1}{2}})} \right) + F_1 \qquad (3-7)$$

where for anions 2,4,--; molalities are $m_2, m_4, --m_n$

and, $\qquad (3-7)$

$$F_1 = \bar{B}_{12} \cdot \bar{z}_{12}^2 \cdot m_2 + \bar{B}_{14} \cdot \bar{z}_{14}^2 \cdot m_4 + ---\bar{B}_{1n} \cdot \bar{z}_{1n}^2 \cdot m_n$$

plus,

$$\bar{z}_{12} \equiv \frac{(|z_1|+|z_2|)}{2} \quad , \bar{z}_{14} \equiv \frac{(|z_1|+|z_4|)}{2} \quad (3-9)$$

so, $\qquad (3-10)$

$$\bar{B}_{12} \approx \left(\frac{(0.06+0.60 \cdot B_{12}) \cdot (|z_1 \cdot z_2|)}{\left[1 + \frac{1.5 \cdot I}{(|z_1 \cdot z_2|)} \right]^2} \right) + B_{12}$$

with $\bar{B}_{14}$ described analogously to $\bar{B}_{12}$

B. Diffusion Coefficients - Electrolyte Phase

1. General

Development of a pseudo electric field model for ionic

diffusion through the boundary separating the electrolyte

solution and the ion exchange is covered in Chapter IV. However,

most other investigators have utilized ionic diffusion

coefficients given in the literature as limiting values (infinite

dilution of the electrolyte). This work includes correction to

the limiting diffusivities of ionic species by utilizing the

Nernst-Hartley equation (104) in an integrated form.

2. Nernst-Hartley Equation

The Nernst-Hartley equation (104) for dilute solutions is

given as:

$$ \text{o} \qquad D_\pm = D_{o_\pm} \cdot (1 + c \cdot \frac{d \ \ell n \ \nu_\pm}{dc}) \qquad\qquad (3\text{-}11) $$

Two correction versions were tested, the differential form

as given, and an integrated form, both utilizing the Bromley

equation to provide the relationship between concentration of

ionic species and its activity coefficient. The derivations are

given in Appendix D.

3. Treatment of Electrolyte Diffusion Coefficients - This Research

The integrated version of the Nernst-Hartley equation was

chosen since, in many electrolytes, the activity coefficient

first decreases, then increases with concentration. The

differential form would hold during the initial decrease, but

would not represent the relationship during and after the

reversal point. The results for both methods tested on data for

17 salts, as given in Robinson & Stokes (106), are included in Appendix C.

The ability of the two models to predict the experimental values of diffusivities is given as:

Diffusion Coefficients - Nernst-Hartley Correction

	Averaged Root Mean Square of % Relative Difference
differential	26.6%
integral	13.2%

The integral version was adopted for inclusion in this modeling effort.

CHAPTER IV

TREATMENT OF ELECTROLYTE PHASE FILM COEFFICIENTS

A. General Background

1. Diffusion Coefficients of Ionic Species in the Film

Most investigators of ion exchange in binary systems
calculate the ionic flux through the film surrounding the resin
by using the infinite dilution diffusion coefficient of a single
counterion, or the average of both ionic species. As was
discussed in Chapter III, the diffusion coefficients of ionic
species vary considerably with increasing electrolyte
concentration. This chapter deals with development of a model for
diffusion of up to three ionic species through the boundary layer
separating the bulk fluid from the resin outer surface. The resin
surface is assumed to be in equilibrium with the boundary layer
fluid in contact with it. In all cases in this research,
diffusion coefficients of ionic species are corrected from their
values at infinite dilution to estimated values at the average
film concentration for the species in the film, based on an
integrated form of the Nernst-Hartley equation as described in
Chapter III.

2. Film Coefficient Correlations for Packed Beds

Film coefficients for diffusion through the boundary layer
surrounding resin beads are adequately computed by equations of
the form:

$$o \qquad j = k_L \cdot \frac{\varepsilon \cdot Sc^{\frac{2}{3}}}{v_s} = A \cdot Re^n \qquad \text{(Lightfoot (62))} \qquad (4\text{-}1)$$

Pan and David (83) and this investigation found Carberry's relationship (11) satisfactory for Re' >1 based on superficial velocity, or Re $\gtrsim$ 3 based on actual velocity, $\frac{v_s}{\epsilon}$.

Carberry's equation for fixed beds is given as:

$$o \qquad k_L = 1.15 \cdot \frac{Re'^{\frac{1}{2}} \cdot Sc^{\frac{1}{3}} \cdot D_{eff}}{\epsilon^{\frac{1}{2}} \cdot dp} \qquad (4\text{-}2)$$

where:

v_s = superficial velocity, cm/sec

ϵ = bed voidage

ρ = density, grams/cc

μ = viscosity, grams/cm/sec

D_{eff} = effective diffusivity, cm^2/sec

dp = particle diameter, cm

$$Re = \frac{v_s \rho dp}{\mu \, \epsilon} \qquad (4\text{-}3)$$

$$Re' = \frac{v_s \rho dp}{\mu} \qquad (4\text{-}4)$$

$$Sc = \frac{\mu}{\rho \, D_{eff}} \qquad (4\text{-}5)$$

k_L = film coefficient, cm/sec

For ion exchange in fluidized beds, Turner & Snowdon (131) found the coefficient should be about 0.81 vs. 1.15 used by Carberry for packed beds. For Re' < 1, the correlation by Koloini and is coworkers (54,55) was found satisfactory in this investigation.

$$o \qquad k_L = 1.1 \cdot \frac{Re' \cdot Sc^{\frac{1}{3}} \cdot D_{eff}}{dp} \qquad (4\text{-}6)$$

Plots of the Carberry and Koloini & Zumer correlations intercept at Re=1.0, and choice of preferred correlation would be made at that Re number.

Postulating a "film" of some thickness across which ionic species migrate as a function of concentration driving force, then

$$o \qquad k_L = \frac{D_{eff}}{\delta_{eff}} \qquad (4\text{-}7)$$

where δ_{eff} = effective "thickness", in cm, as in Boundary Layer theory
so:

$$\delta_{eff} = \frac{dp \cdot \epsilon^{\frac{1}{2}}}{(1.15 \cdot Re^{\frac{1}{2}} \cdot Sc^{\frac{1}{3}})} \qquad (4\text{-}8)$$

A problem which other investigators have researched has been to determine an effective diffusion coefficient that can be used to compute a film coefficient which properly simulates ion exchange when the film represents the major resistance to mass transfer.

3. Nernst-Planck Models for Ionic Migration in the Film - Other Investigators

3.1 Description of Nernst-Planck Model

Investigators such as Turner & Snowdon (131), Van Brocklin & David (132), Pan & David (83), and Kataoka & Yoshida (50) have examined the effect of the concentration gradient of the coion in the "stagnant film" during binary ion exchange--caused by the electric field generated in the film to satisfy (1) condition of electroneutrality and (2) that no electric current flow through the film as a result of diffusion of counterions. As will be shown, this effect

causes the effective diffusion coefficient of a species to vary across a "film," although the flux of that species does not vary across the film at any time (t). The mathematical treatment of the physics of ionic movement through electrolytes by W. Nernst and M. Planck resulted in a relation known as the Nernst-Planck equation (42), which for dilute solutions is given as:

$$\text{o} \qquad N_i = - D_i \cdot \left[\nabla c_i + \left(\frac{c_i z_i F \nabla \phi}{RT} \right) \right] \qquad (4\text{-}9)$$

Equations for Film with Electric Field - Nernst-Planck Relationship

Assumptions

o   Film has thickness δ_{eff} as described above

o   All velocity components in the film are zero

o   Fluid beyond the film is well mixed at composition c_i bulk

o   Mass transfer is in the radial direction of the resin "sphere." Since the film dimension is small compared to the resin radius, the film can be treated as a slab with thickness δ_{eff}, and surface and volume based on $r_{eff} = r_0 + \delta_{eff}$ where r_0 is the resin radius. (4-10)

o   No accumulation in film

Molar flux in film is then given as:

$$\text{o} \qquad N_i^* = - D_i \cdot \left[\frac{\partial c_i^*}{\partial y} + \frac{c_i^* \cdot z_i \cdot F \frac{\partial \phi^*}{\partial y}}{RT} \right] \qquad (4\text{-}11)$$

$$i = 1, 2, a(\text{coion})$$

where:

N_i^* = molar flux of species in film, moles/cm²/sec

D_i^* = diffusivity of species at film concentration, cm²/sec

c_i^* = concentration of species in the film, molarity, moles/liter

z_i = valence of species

F = Faraday constant

ϕ^* = electric field in film, volts

y = film thickness dimension, cm

x = column length dimension, cm

L = column length, cm

The assumption of electro neutrality requires:

$$\sum_{i=1}^{2} |z_i| c_i^* = |z_a| c_a^* \qquad (a \text{ is coion}) \qquad (4\text{-}12)$$

The assumption of no electric current flow, and postulating a quasi-stationary state for the coion, or $N_a^* = 0$, results in:

$$o \qquad \frac{\partial c_a^*}{\partial y} = -\left(\frac{z_a c_a^* F}{RT}\right) \cdot \frac{\partial \phi^*}{\partial y} \qquad (4\text{-}13)$$

and it follows from equation (4-12) that:

$$\sum_{i=1}^{2} |z_i| \cdot \frac{\partial c_i^*}{\partial y} = +|z_a| \cdot \frac{\partial c_a^*}{\partial y} \qquad (4\text{-}14)$$

No accumulation in film, i.e., flux of each species, is constant through film, resulting in:

$$\frac{\partial N_i^*}{\partial y} = 0 \text{ at } (x,t) \qquad i=1,2,a \qquad (4\text{-}15)$$

Initial Condition:

$$c_i^*(x) = c_{i_{bulk}}(x, t_0) \qquad \begin{cases} t=0 \\ 0 \leq x \leq L \end{cases} \qquad (4\text{-}16)$$

Boundary Condition:

$$c_i^*\left[(r_0 + \delta_{eff}), x, t\right] = c_{i_{bulk}}(x, t) \qquad \begin{cases} t \geq 0 \\ 0 \leq x \leq L \end{cases} \qquad (4\text{-}17)$$

Equilibrium Relationship

$$c_{i_{int}}^*(r_0, x, t) = f(\overline{c}_{i_{int}}, x, t) \qquad \begin{cases} t \geq 0 \\ 0 \leq x \leq L \end{cases} \qquad (4\text{-}18)$$

$\overline{c}_{i_{int}}$ = molar concentration of species in resin in equilibrium with $c_{i_{int}}^*$ in film.

These equations have been integrated by various investigators, and the results of three of these investigators will be discussed in detail.

3.2. Model of Kataoka and Yoshida (50)

Kataoka & Yoshida for equal valence exchange of two species, developed the following equations:

$$\circ \quad N_1^* = \left[\frac{6 \cdot k_L^0 \cdot \beta}{dp}\right] \cdot (c_{1_{bulk}} - c_{1_{int}}^*) \qquad (4\text{-}19)$$

where species 1 is migrating to the resin,

and:

$$\beta = \frac{k_L}{k_L^0} = \frac{\text{film coeff.-electric field}}{\text{film coeff. w/o electric field}} - D_1^* \qquad (4\text{-}20)$$

D_1^*= diffusion coefficient of species 1, cm^2/sec

Equilibrium is based on a mass action type relationship:

$$\overline{K}_{12} = \left(\frac{\overline{x_1}_{int} \cdot x^*_{2\,int}}{x^*_{1\,int} \cdot \overline{x_2}_{int}} \right) \qquad (4\text{-}21)$$

where equivalent fraction is defined as:

$$x_i = \left(\frac{c_i \cdot |z_i|}{c_a \cdot |z_a|} \right) \qquad (4\text{-}22)$$

and:

subscript int is the interface between resin/film

superscript bar is the resin phase

superscript star is the electrolyte film phase

Substitution and subsequent integration across the film yielded;

$$o \qquad \left(\frac{x^*_{1\,int} + \alpha x^*_{2\,int}}{\left[(1-\alpha) \cdot x^*_{1\,int} + \alpha \right]} \right)^{\frac{1}{M}} \cdot (x^*_{1\,int} + x^*_{2\,int}) = 1 \qquad (4\text{-}23)$$

where:

$$\alpha = \frac{D^*_2}{D^*_1} \qquad (4\text{-}24)$$

$$M = \frac{|z_1|}{|z_a|} \qquad ; \text{ a is coion} \qquad (4\text{-}25)$$

$$(4\text{-}26)$$

and:

$$o \qquad De' = \frac{D^*_{eff}}{D^*_1} = \left(\frac{\alpha \cdot (M+1) \cdot (x^*_{2\,int} + x^*_{1\,int} - 1)}{(1-\alpha) \cdot (x_{1\,bulk} - x_{1\,int})} \right)$$

where in equation (4-19):

$$o \qquad \beta = De' \qquad (4\text{-}27)$$

Later in the chapter this treatment will be compared against a pseudo electric field treatment derived in this

research project for the extreme case of unfavorable exchange with $\overline{K}_{12} < 1$ and $\alpha < 1$, specifically for the exchange of H^+ ion for Ag^+ ion on Dowex 50W -X8 resin.

Kataoka and Yoshida point out that in favorable exchange, i.e., $\overline{K}_{12} > 1$, and with $\alpha > 1$, as in most industrially important cases, the breakthrough curve based on k_L calculated using the diffusion coefficient of the slower ion gives rise to errors of less than 30% in prediction of breakthrough curve, breakthrough time, and column utilization.

3.3 Model of Van Brocklin and David (132)

Van Brocklin & David for multivalent exchange of two species, developed the following equations.

The following factor was defined:

$$\circ \quad R_i = \frac{\dfrac{N_i^{*'}}{s}}{\dfrac{N_i^{*}}{s}} = \frac{k_L'}{k_L} \quad , \text{for } i=1,2 \tag{4-28}$$

where:

$$s = \text{area, cm}^2$$

or,

$$R_i = \frac{\text{Nernst-Planck model}}{\text{Fick's Law model}} \tag{4-29}$$

so,

$$\circ \quad R_i = \left\{ \frac{\left[\dfrac{\partial c_i^{*}}{\partial \eta} + z_i c_i^{*} \cdot \dfrac{F}{RT} \cdot \dfrac{\partial \phi^{*}}{\partial \eta}\right]_{\eta=0}}{\left(\dfrac{\partial c_i^{*}}{\partial \eta}\right)_{\eta=0}} \right\} \tag{4-30}$$

where:

$$z_i = \text{valence}$$

$$c_i^* = \text{concentration in film, moles/liter}$$

and η is a transformation for 3 models

- film: $\qquad \eta = \dfrac{y}{\delta_{eff}}$ $\qquad\qquad$ (4-31)

- penetration theory:

$$\eta = \left(\frac{y}{2\sqrt{D_n^* \cdot t}} \right) \qquad\qquad (4\text{-}32)$$

- boundary layer theory

$$\eta = \left(\frac{y \sqrt{\beta(x)}}{\left[9 D_n^* \cdot \int_0^x \sqrt{\beta(x)} \, dx \right]^{\frac{1}{3}}} \right) \qquad\qquad (4\text{-}33)$$

where:

$y \qquad = \text{distance into film, cm}$

$x \qquad = \text{distance along exchange surface, cm}$

$\delta_{eff} = \text{effective film thickness, cm}$

$D_n^* \quad = \text{constant, normally equal to one of the}$
$\qquad\quad\ \text{diffusion coefficients, } cm^2/sec$

$\beta(x) = \text{velocity gradient at interface, } 1/sec$

$t \qquad = \text{"residence time"}$

The film model was solved analytically by integration across the film. The other two models were solved by numerical methods on a computer--and use of the model involves table look up based on D_i^*/D_j^* and film boundary

concentrations to obtain the R_i factor. This model was used in carrying out ion exchange computations for a moving bed column (Pan & David (83)). Figures (4-1) through (4-6) from their work are shown depicting the effect on coion and counterion concentration, as well as electric field gradient, ϕ^*, for the various models. Pan & David (83) computed the height of a moving bed ion exchange column based on the Fick's Law model in the film and compared that to the height of a bed calculated with electric field effects, (H/H_e). They conclude that "only for H^+ ion-multivalent ion exchange systems in dilute solution do highly unfavorable equilibrium and large effects of R_i correction occur simultaneously." Normally these types of ion exchanges have no practical application, so it can be anticipated that for most simulations the R_i correction factor will be small.

Pan and David (83) continue, "In practical ion exchange applications, this exchange operation is rather unusual. For exchanges with highly unfavorable equilibrium, but without H^+, the effect is expected to be small because of the small diffusivity ratio of the exchanging ion pair."

3.4 Model of Turner and Snowden (131)

Turner & Snowdon integrated the basic Nernst-Planck film equations for two species interchanging, using the usual assumption of the coion in a quasistationary condition. Fluid bed experiments on resin with H^+ and Na^+ ions exchanging was the basis for a correlation which, though specific to this system, show agreement with the N.P. model.

Figure 4-1

Calculated R_1 Factors

$Cu^{++} - Na^+$ Exchange
$Z_2 = -Z_3 = 1$
$Z_1 = 1$
$D_{Cu} = D_1 = 1$
$D_{Na} = D_2 = 1.87$
$X_1^\circ = 1.0$

Film

Boundary Layer

Penetration

R_1

$X_1^* = \dfrac{Z_1 C_1^*}{Z_3 C_3^*}$
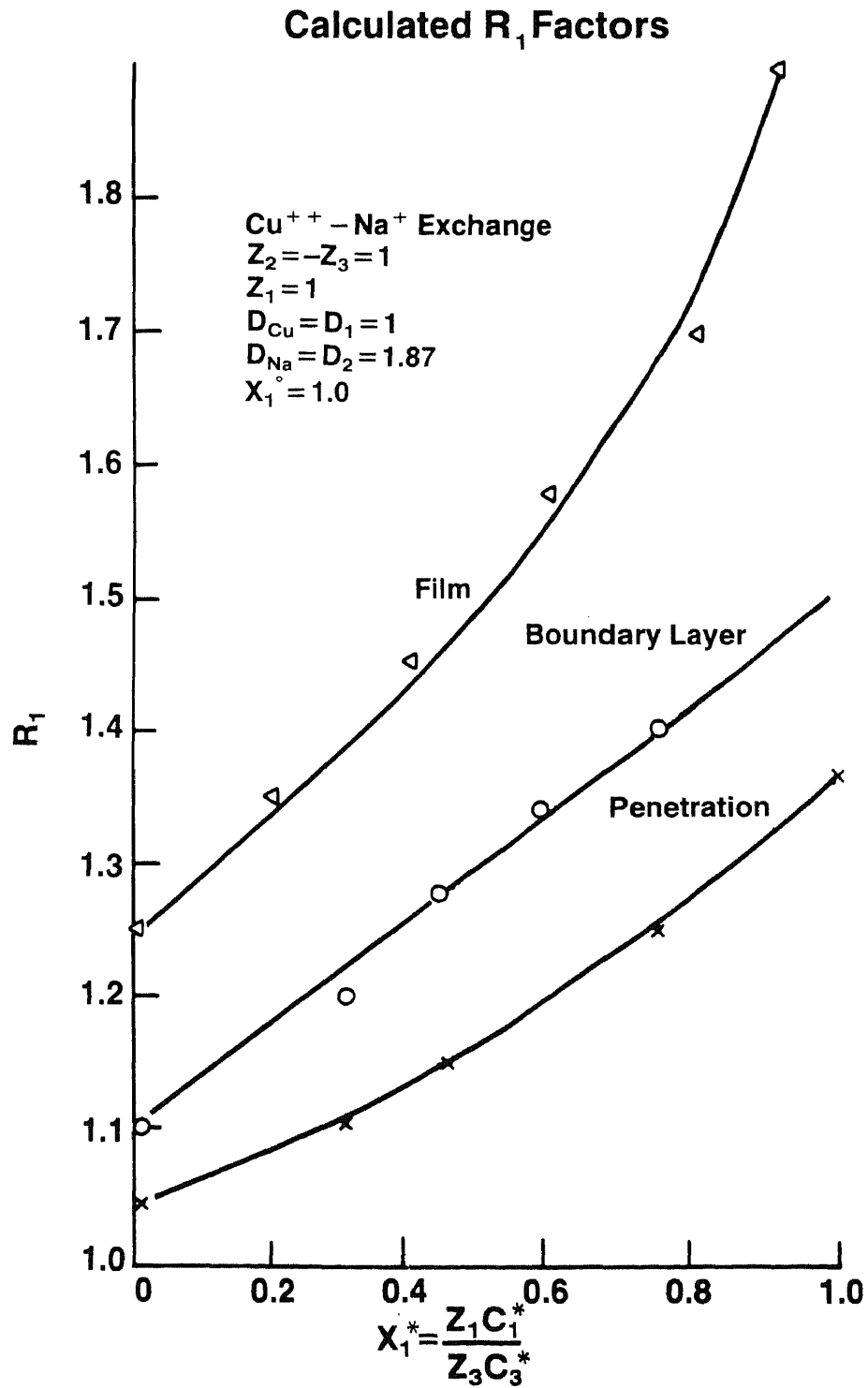
Van Brocklin & Davis

Figure 4-2

Moving Ion Exchange Bed Height Correction Factor - Nernst Planck Effect vs. No Correction

H_e - N.P. in Resin & Film
H_c - N.P. in Resin - Ordinary Film Diffusion
H_b - Ordinary Diffusion in Resin & Film
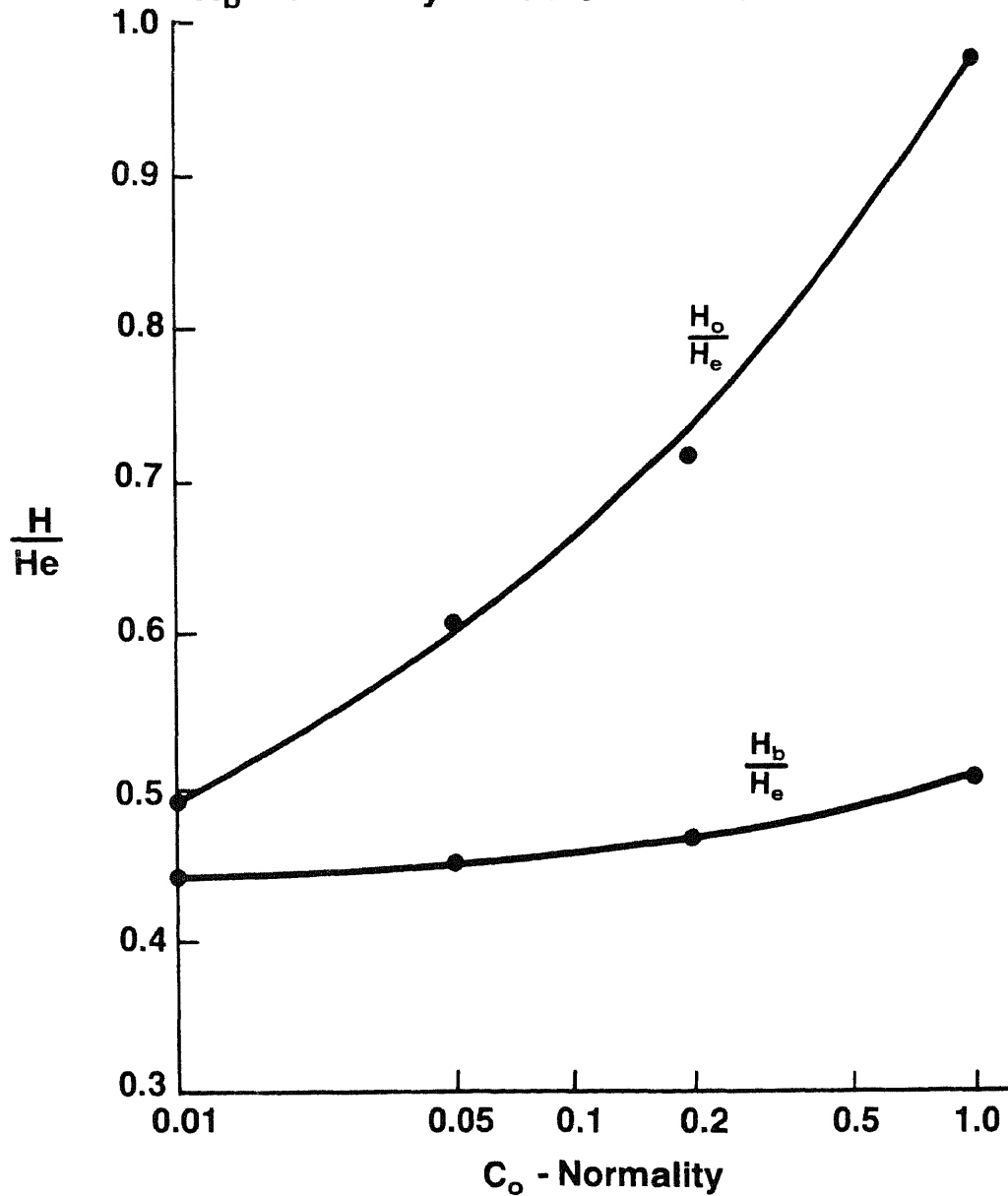
$\dfrac{H}{He}$ (y-axis)

$\dfrac{H_o}{H_e}$

$\dfrac{H_b}{H_e}$

C_o - Normality

Pan & David

Figure 4-3

Calculated Concentration Profiles - Boundary Layer Model
Na^+-H^+ Exchange

Resin Surface   **Bulk Fluid**

−Charge

+Charge

Cl^-

Na^+

$\dfrac{\phi F}{2RT}$

H^+

η_N Normalized B.L. Parameter
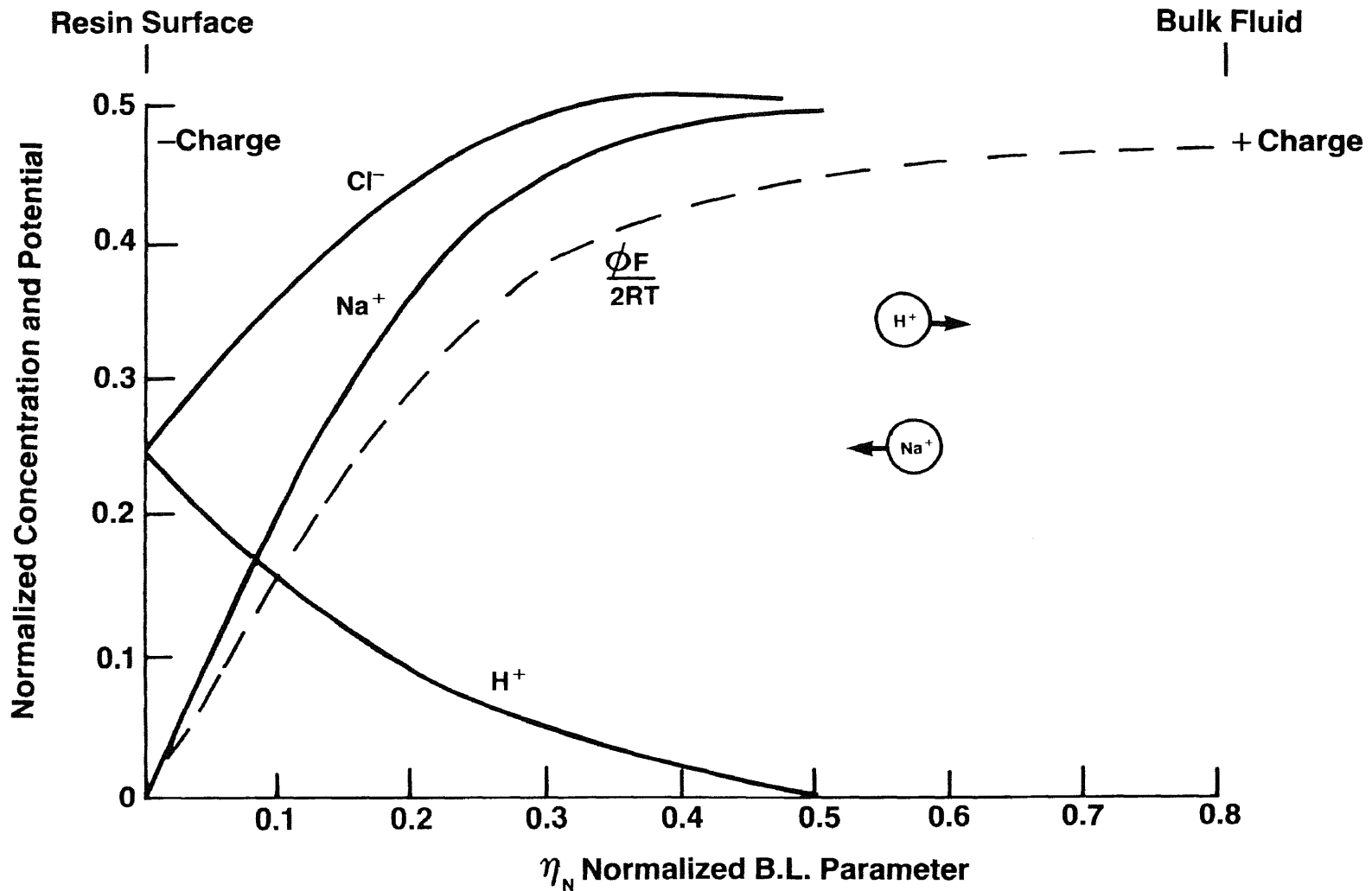
Van Brocklin & David

Figure 4-4

Calculated Concentration Profiles - Boundary Layer Model
Na^+-H^+ Exchange

Resin Surface

Bulk Fluid

+ Charge

−Charge

Cl^-

$\dfrac{\phi F}{2RT}$

H^+

Na^+

H^+

Na^+

η_N-Normalized B.L. Parameter

Van Brocklin & David

127

Figure 4-5

Calculated Concentration Profiles
Film Model
Na^+–H^+ Exchange

Resin Surface **Bulk Fluid**

–Charge + Charge

$\eta = y/\delta$ **Film Thickness**
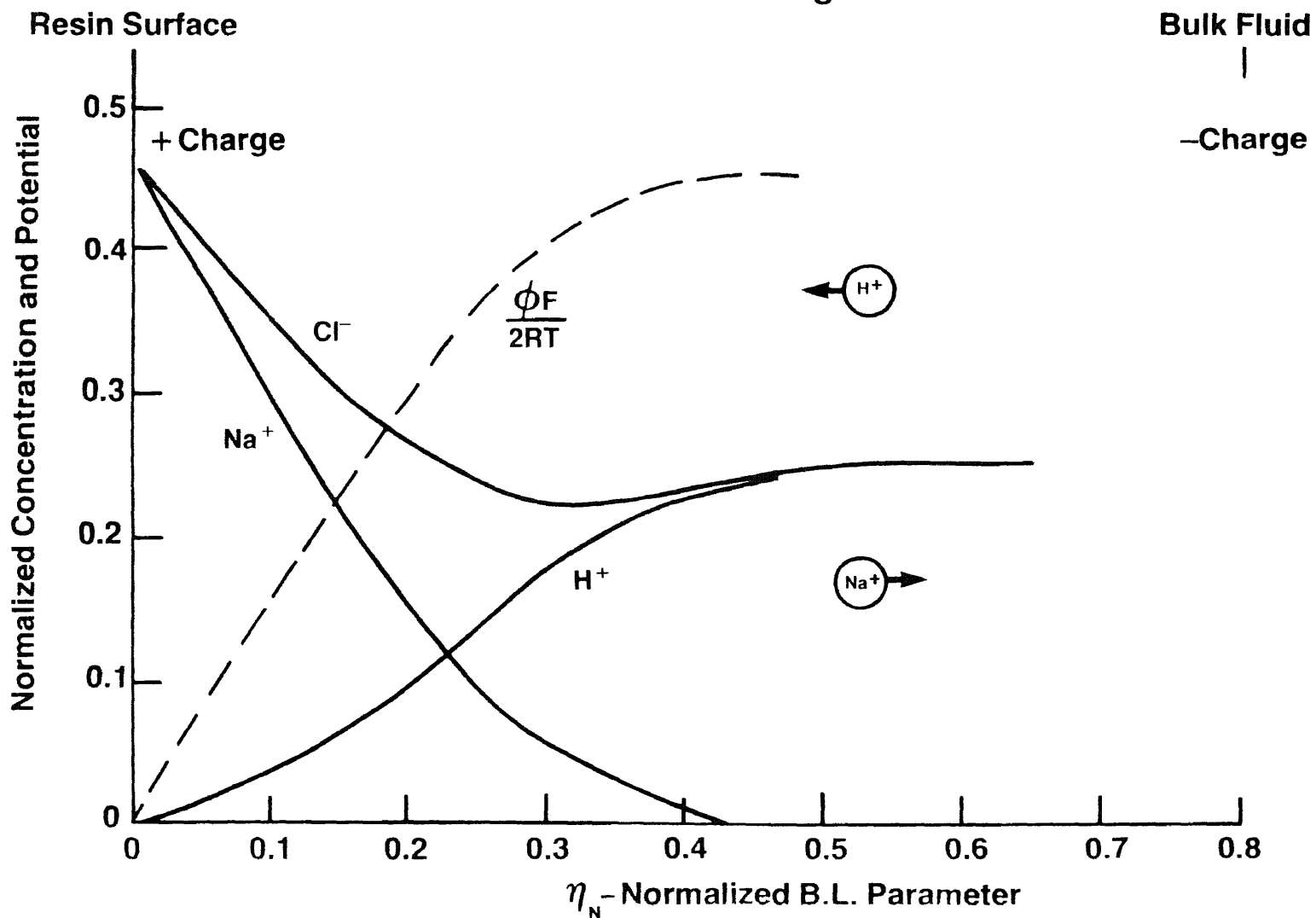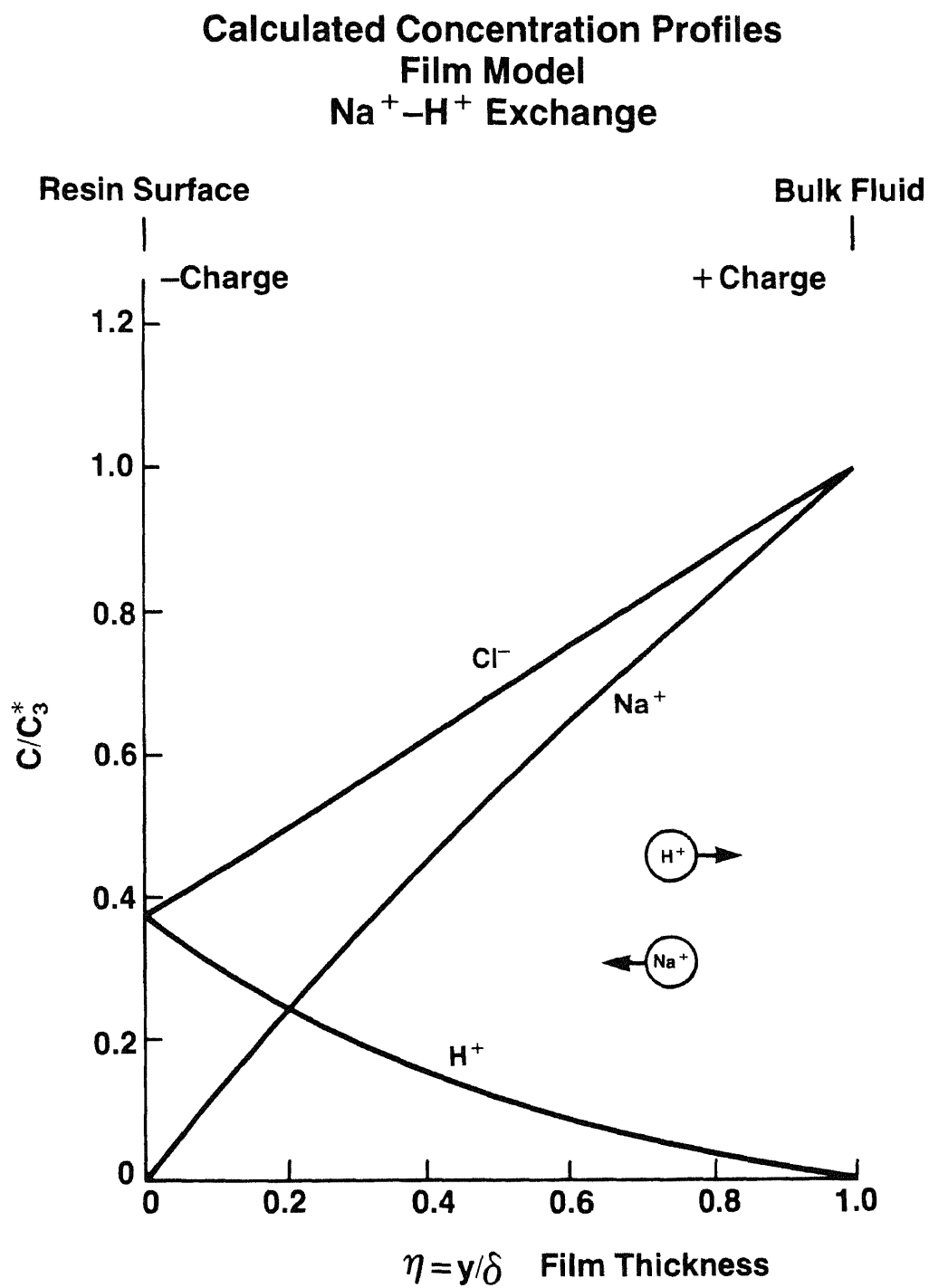
Van Brocklin & David

Figure 4-6

Calculated Concentration Profiles
Film Model
H^+–Na^+ Exchange

Resin Surface   **Bulk Fluid**

+ Charge   –Charge

Cl^-

Na^+

H^+

H^+

Na^+

C/C_3^*

1.4
1.2
1.0
0.8
0.6
0.4
0.2
0

0   0.2   0.4   0.6   0.8   1.0

$\eta = y/\delta$ Film Thickness
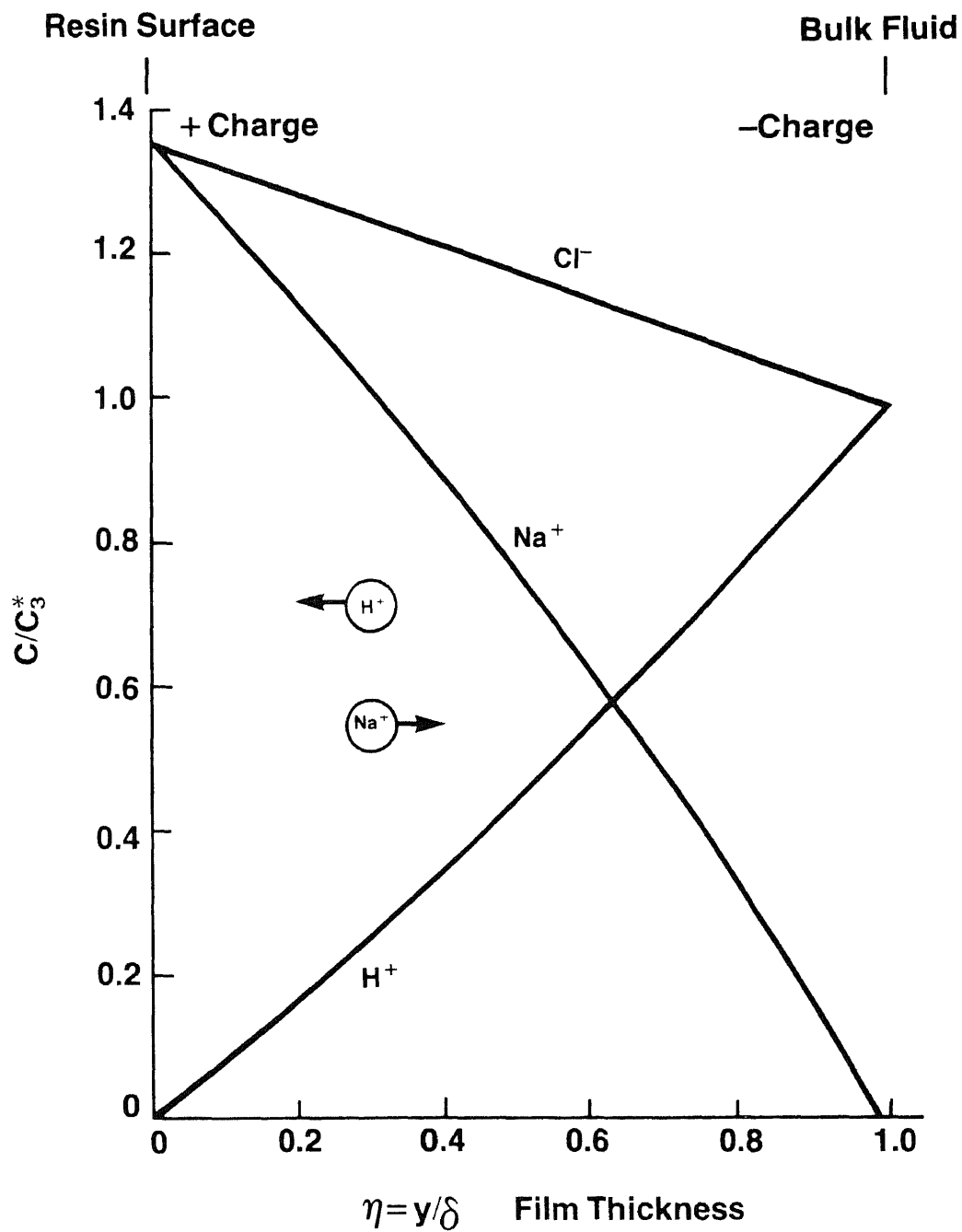
Van Brocklin & David

Their equations were:

$$\circ \quad N_1^* = \left(\frac{D_1^* D_2^* z_1^2 c_1^* + z_2^2 c_2^* + z_a^2 c_a^*}{D_1^* z_1^2 c_1^* + D_2^* \cdot (z_2^2 c_2^* + z_a^2 c_a^*)} \right) \cdot \frac{dc_1^*}{dy} \qquad (4-34)$$

if,

$$x_1^* = \frac{|z_1| c_1^*}{|z_a| c_a^*} \quad \text{and} \quad (x_1^* + x_2^*) = 1 \qquad (4-35)$$

$$\alpha' = \left(\frac{D_1^*}{D_2^*} \right) - 1 \qquad (4-36)$$

then:

$$\circ \hspace{10cm} (2-37)$$

$$N_1^* = - D_1^* \cdot \left(\frac{|z_a|}{|z_1|} \right) \cdot c_a^* \cdot \left[\frac{(|z_2|+|z_a|) + x_1^* \cdot (x_1^* - x_2^*)}{(|z_2|+|z_a|) + x_1^* \cdot \left[(\alpha+1) \cdot (|z_1|+|z_a|) - (|z_2|+|z_a|) \right]} \right]$$

$$\times \frac{dc_1^*}{dy}$$

simplifying for $|z_1| = |z_2| = |z_a| = 1$

$$\circ \qquad c_a^* = c_{a_{bulk}} \cdot \left[\frac{\left(\alpha' \cdot x_{1_{bulk}} + 1 \right)}{\left(\alpha' \cdot x_{1_{bulk}} + 1 \right)} \right]^{\frac{1}{2}} \qquad (4-38)$$

then by substituting (4-38) in (4-37) and integrating:

$$\hspace{10cm} (4-39)$$

$$\circ \quad N_1^* = \frac{D_1^*}{\delta_{eff}} \cdot \left[\frac{2 \cdot c_{a_{bulk}} \cdot (x_{1_{bulk}} - x_{1_{int}}^*)}{(1+\alpha' \cdot x_{1_{int}}^*) + \sqrt{(1+\alpha' \cdot x_{1_{int}}^*) \cdot (1+\alpha' \cdot x_{1_{bulk}})}} \right]$$

so if $\quad N_1^* = k_L \cdot c_{a_{bulk}} \cdot (x_{1_{bulk}} - x_{1_{int}}^*) \qquad (4-40)$

then:

$$(4\text{-}41)$$

$$\circ \quad k_L = \left[\frac{2 \cdot D_1^*}{(1+\alpha' \cdot x_{1_{int}}^*) + \sqrt{(1+\alpha' \cdot x_{1_{int}}^*) \cdot (1+\alpha' \cdot x_{1_{bulk}})}} \right] \cdot \frac{1}{\delta_{eff}}$$

and if $\delta_{eff} \propto \dfrac{D_{eff}^{*\frac{1}{3}}}{b}$, where $\quad (4\text{-}42)$

$$D_{eff}^* = \left[\frac{D_1^*}{(1 + \alpha' \cdot x_{1_{ave}}^*)} \right] \qquad (4\text{-}43)$$

and:

$$x_{1_{ave}}^* = \frac{(x_{1_{bulk}} + x_{1_{int}}^*)}{2} \qquad (4\text{-}44)$$

if b = correlated constant = function Re^n, then: $\quad (4\text{-}45)$

$$\circ \quad k_L = \left[\frac{2 \cdot b \cdot D_1^{*\frac{2}{3}} \cdot (1+\alpha' \cdot x_{1_{ave}}^*)^{\frac{1}{3}}}{(1+\alpha' \cdot x_{1_{int}}^*) + \sqrt{(1+\alpha' \cdot x_{1_{int}}^*) \cdot (1+\alpha' \cdot x_{1_{bulk}})}} \right]$$

Good correlation was shown for the system investigated with the plot on Figure 4-7.

3.5 Summary of Film Models by Previous Investigators

In summary, previous investigators have demonstrated that in highly unfavorable exchange, particular with H^+ because of its relatively high ionic mobility, breakthrough curve computations could be seriously in error if the electric field gradient in the film was not accounted for. They show that integrated solutions of the Nernst-Planck

Figure 4-7

Liquid Film Mass Transfer Coefficients In Ion Exchange
Fluid Bed For H^+-Na^+ System On Zeo-Karb 225
Nernst - Planck Relationship In Resin & Film

$K_L \times 10^3$ cm/sec (y-axis, 0 to 20)

$F_1(y)$ (x-axis, 0.2 to 1.0)

$\triangle$ 0.01N
$\circ$ 0.02N
$\square$ 0.04

$$K_L \alpha \quad D_H^{2/3} F_1(y_H)$$

$$F_1(y_H) = \frac{2(1 + 6\bar{y}_H)^{1/3}}{(1 + 6y_H^*) + \sqrt{(1 + 6y_H^*)(1 + 6y_H^\circ)}}$$

$$y_H = \frac{\bar{y}_H^* + y_H^\circ}{2}$$
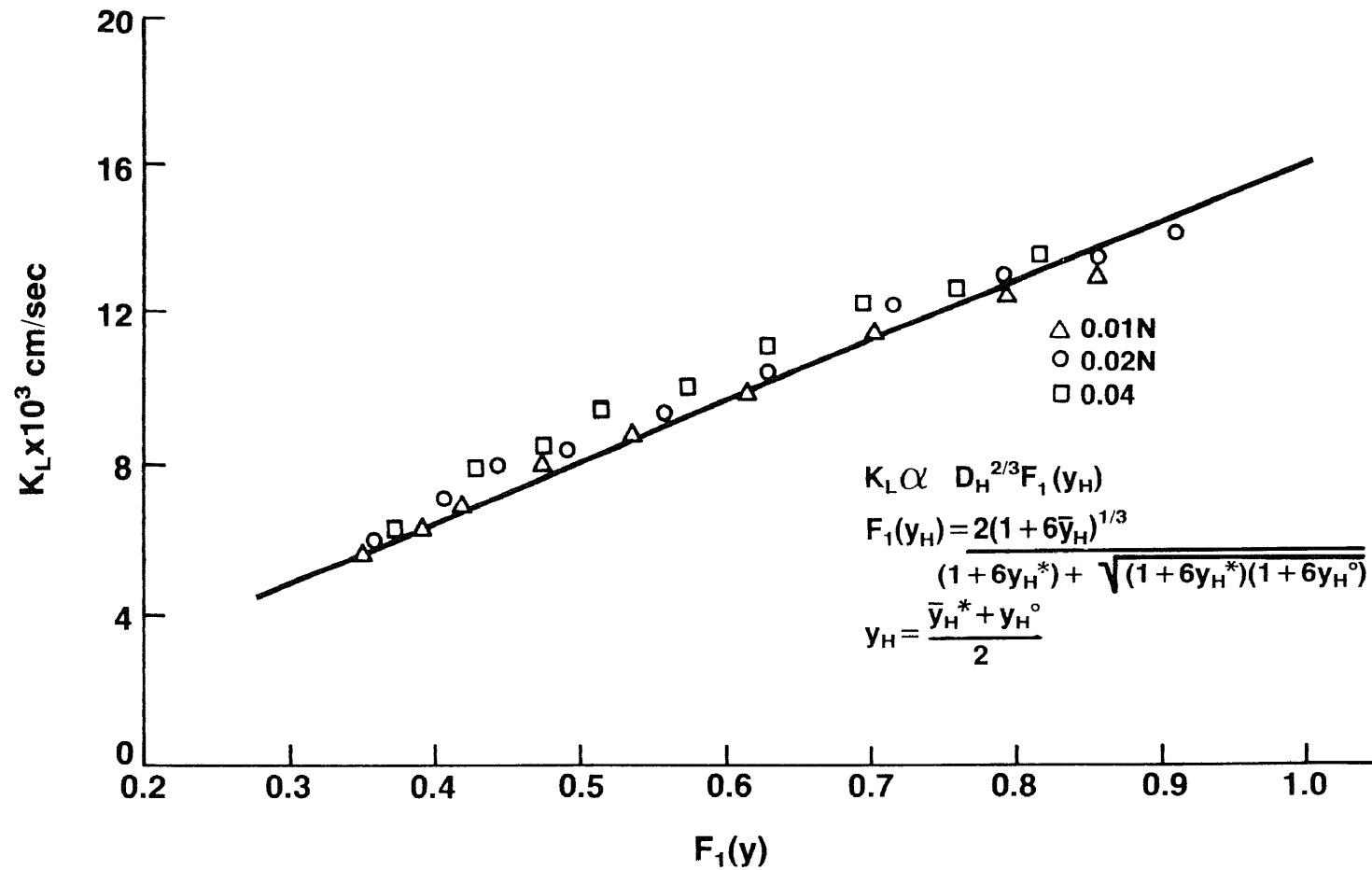
Turner & Snowden

equation for the film can correct film coefficients obtained from published correlations to better simulate "film controlled" ion exchange. The treatments have the following disadvantages:

a. The three investigators cited used ionic diffusivities measured at infinite dilution. This could be corrected using the treatment derived in this work.

b. The treatments are mainly limited to binary ion exchange and in two models the exchanging species have the same valence as the coion.

c. Numerical solution for R_i factor by David and his coworkers (83, 132) has the disadvantage that R_i factors must be generated off line. Modeling of ion exchange processes with this method depends on stored table look up with interpolation at each ΔY and at Δt increment, based on boundary condition concentrations, $x_{i_{bulk}}$ and $x^{*}_{i_{int}}$.

B. Pseudo Treatment for Electric Field Used in This Research Project

1. Assumptions

o Diffusivities of individuals ions are corrected based on bulk solution normality, and as predicted by the integral form of the Nernst-Hartley equation (see Appendix D).

o The normality of the coion remains constant throughout the film; i.e., $\dfrac{\partial c^{*}_i}{\partial y} = 0$ and therefore the charges in the film coion would be analogous to the fixed charges in the resin.

o   All other equations in Nernst-Planck treatment of film remain as previously outlined.

o   The film effective boundary layer "thickness," δ_{eff}, can be predicted from existing film coefficient correlations such as those of Carberry or Koloini and Zumer using an effective diffusivity D^*_{eff} for computing the Schmidt No., Sc.

2.   Binary System - Linear Gradient

Converting the molar flux equation to equivalent flux by:

$$J^*_i = |z_i| \cdot N^*_i \tag{4-46}$$

$$x_i = \frac{c_i \cdot |z_i|}{norm} \quad \text{or} \quad x^*_i = \frac{c^*_i \cdot |z_i|}{norm} \tag{4-49}$$

where norm = normality of coion

$$= \left(c_a \cdot |z_a| \right)_{bulk\ fluid} \tag{4-47}$$

$$= \left(c^*_a \cdot |z_a| \right)_{film\ fluid} \tag{4-48}$$

then:

o
$$N^*_i = - D^*_i \cdot \left[\frac{\partial c^*_i}{\partial y} + c^*_i \cdot z_i \cdot \frac{F}{RT} \cdot \frac{\partial \phi^*}{\partial y} \right] \tag{4-50}$$

$$i = 1,2$$

transforms to:

o
$$\frac{J^*_i}{norm} = - D^*_i \cdot \left[\frac{\partial x^*_i}{\partial y} + x^*_i \cdot z_i \cdot \frac{F}{RT} \cdot \frac{\partial \phi^*}{\partial y} \right] \tag{4-51}$$

$$i = 1,2$$

electroneutrality requires:

$$\sum_{i=1}^{2} x^*_i = 1 \tag{4-52}$$

no electric current plus $J_a^* = 0$, results in:

$$\sum_{i=1}^{2} J_i^* = 0 \tag{4-53}$$

in addition from equation (4-52) :

$$\sum_{i=1}^{2} \frac{\partial x_i^*}{\partial y} = 0 \tag{4-54}$$

and:

$$\frac{\partial x_a^*}{\partial y} = 0 \tag{4-55}$$

Model for film

- linear gradient -

Illustration 4-1
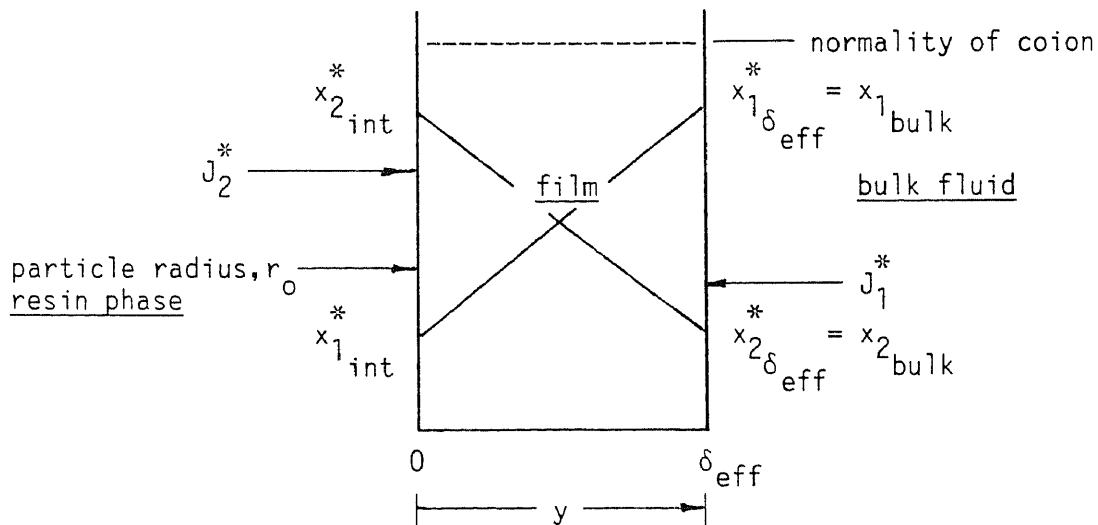
since the concentration gradients are linear:

$$x_{1_{eff}}^* = \left(\frac{(x_{1_{\delta_{eff}}}^* + x_{1_{int}}^*)}{2} \right) \tag{4-56}$$

$$x_{2_{eff}}^* = \left(\frac{(x_{2_{\delta_{eff}}}^* + x_{2_{int}}^*)}{2} \right) \tag{4-57}$$

An effective diffusion coefficient, D_{eff}^* can be derived if the Nernst-Planck equation is utilized and $\frac{\partial \phi^*}{\partial y}$ is eliminated in equation (4-51). This is shown in Chapter V in the derivation of an effective diffusion coefficient for two species exchanging in the resin phase. The "pseudo electric field" then is premised on a level distribution of coion in the film providing "fixed" opposite charges in the film analagous to the resin model.

Then:

$$o \qquad D_{eff}^* = \left[\frac{D_1^* \cdot D_2^* \cdot (x_{1_{eff}}^* \cdot |z_1| + x_{2_{eff}}^* \cdot |z_2|)}{(x_{1_{eff}}^* \cdot |z_1| \cdot D_1^* + x_{2_{eff}}^* \cdot |z_2| \cdot D_2^*)} \right] \qquad (4\text{-}58)$$

and:

$$(4\text{-}59)$$

$$o \qquad \frac{J_1^*}{norm} = + D_{eff}^* \cdot \frac{dx_1^*}{dy} = -D_{eff}^* \cdot \frac{dx_2^*}{dy} = - \frac{J_2^*}{norm}$$

likewise:

$$o \qquad \frac{J_1^*}{norm} = k_{L_{eff}} \cdot (x_{1_{bulk}} - x_{1_{int}}^*) = D_{eff}^* \cdot \frac{dx_1^*}{dy} \qquad (4\text{-}60)$$

Since the concentration gradients were assumed to be linear over the film thickness, δ_{eff}:

$$o \qquad k_{L_{eff}} = \frac{D_{eff}^*}{\delta_{eff}} \qquad (4\text{-}61)$$

if $k_{L_{eff}}$ is defined as

$$\left[\frac{C \cdot \left[\frac{Re'}{\varepsilon}\right]^n \cdot Sc_{eff}^{\frac{1}{3}} \cdot D_{eff}^*}{dp} \right] \qquad (4\text{-}62)$$

then:

$$\circ \qquad \delta_{eff} = \left[\frac{dp}{C \cdot \left[\frac{Re'}{\varepsilon}\right]^n \cdot Sc_{eff}^{\frac{1}{3}}} \right] \qquad (4\text{-}63)$$

"effective boundary layer film thickness"

It is noted that Gopala Rao and his coworkers (92, 93) used a very similar treatment in modeling the ternary batch experiments they performed using radioactive tracer techniques. The major difference is that they calculated a fixed "hydraulic film thickness" which remained constant throughout the simulation. The derivation used in this work utilizes the "effective boundary layer thickness," which is updated for average species concentration in the film at each time step of the simulation. This treatment is closer to the previously discussed rigorous treatments.

In making the computation for $k_{L_{eff}}$, the treatment chosen was to use the concentrations $x_{i_{bulk}}$ and $x_{i_{int}}$ from the preceding or j^{th} time step vs. the $j+\frac{1}{2}th$ time step as prescribed by the Crank-Nicholson procedure. This circumvented the requirement to quasilinearize at the $j+1th$ time step and $k_{L_{eff}}(j)$ was used in place of $k_{L_{eff}}(j+1)$.

On binary runs, with sufficient time increments, i.e., small Δj, systematic bias on $k_{L_{eff}}$ was only in the 0.01% range.

3. Binary System - Non-Linear Gradient

Starting with the equation (4-60):

$$\circ \qquad \frac{J_1^*}{\text{norm}} = D_{eff}^* \cdot \frac{dx_1^*}{dy}$$

this can be put into the form:

$$\frac{J_1^*}{\text{norm}} \cdot \int_{y=0}^{y=\delta_{eff}} dy = \int_{x_{1_{int}}^*}^{x_{1_{bulk}}} D_{eff}^*(x_1^*) \cdot dx_1^* \qquad (4\text{-}64)$$

where equation (4-58) can be shown as:

$$D_{eff}^* = \left(\frac{D_1^* \cdot D_2^* \cdot \left[x_1^* \cdot |z_1| + (1-x_1^*) \cdot |z_2| \right]}{\left[x_1^* \cdot |z_1| \cdot D_1^* + (1-x_1^*) \cdot |z_2| \cdot D_2^* \right]} \right)$$

substitution of the above in equation (4-64), and integrating yields:

$$\circ \qquad \frac{J_1^*}{\text{norm}} \cdot \Delta y = \left(\frac{D_1^* \cdot D_2^*}{\left[|z_1| \cdot D_1^* - |z_2| \cdot D_2^* \right]} \right) \cdot \left\{ \left[|z_2| - \left(\frac{|z_2| \cdot D_2^* \cdot (|z_1| - |z_2|)}{|z_1| \cdot D_1^* - |z_2| \cdot D_2^*} \right) \right] \right.$$

$$\times \ell n \left(\frac{\left[(|z_1| \cdot D_1^* - |z_2| \cdot D_2^*) \cdot x_{1_{bulk}}^* + |z_2| \cdot D_2^* \right]}{\left[(|z_1| \cdot D_1^* - |z_2| \cdot D_2^*) \cdot x_{1_{int}}^* + |z_2| \cdot D_2^* \right]} \right)$$

$$\left. + \ (|z_1| - |z_2|) \cdot (x_{1_{bulk}} - x_{1_{int}}^*) \right\} \qquad (4\text{-}65)$$

since:
$$\frac{J_1^*}{\text{norm}} = k_{L_{eff}} \cdot (x_{1_{bulk}}^* - x_{1_{int}}^*)$$

then: $\quad k_{L_{eff}} = \left[\dfrac{f(x_{1_{bulk}}, x_{1_{int}}^{*})}{\delta_{eff}\,(x_{1_{bulk}} - x_{1_{int}}^{*})} \right]$ (4-66)

and since:

it follows that: $\quad \Delta y = \delta_{eff} = \left[\dfrac{dp}{C \cdot \left[\dfrac{Re}{\epsilon}\right]^{n} \cdot Sc_{eff}^{\frac{1}{3}}} \right]$

(4-67)

$$\circ \quad k_{L_{eff}} = \left[\dfrac{f(x_{1_{bulk}}, x_{1_{int}}^{*})}{(x_{1_{bulk}} - x_{1_{int}}^{*})} \right] \cdot \left[\dfrac{C \cdot \left[\dfrac{Re}{\epsilon}\right]^{n} \cdot Sc_{eff}^{\frac{1}{3}}}{dp} \right]$$

Again this value for $k_{L_{eff}}$ (j) would be calculated at the jth vs. $j^{+\frac{1}{2}th}$ step to avoid quasilinearization complications.

4. Comparison of Binary Models - Linear versus Non-Linear Gradients

Table 4-1 lists data from a comparison of the linear/versus the non-linear model in terms of ion flux (equivalents/cm^2/sec per cm of "film thickness") at various film concentration differences, Δx_1, (driving force). Calculations were performed for the systems Ag^+-H^+, Ag^+-Na^+, and Sr^{++}-Cs^+ in favorable exchange to determine the percent difference between models in predicted flux as the driving force was increased. As could be anticipated in univalent exchange, the Ag^+-H^+ system, with the largest ratio of diffusivities, gave higher differences than the Ag^+-Na^+ system. Multivalent exchange, represented by Sr^{++}-Cs^+, at an even higher ratio of diffusivities gave the largest difference calculation of 30% at $x_{Sr_{int}}^{*} = 0.10$. In an

Table 4-1

Comparison - Linear vs Non-Linear Film Models

System $Ag_1^+ -H_2^+$; $D_1^* = 1 \times 10^{-6}$ cm^2/sec, $D_2^* = 10 \times 10^{-6}$ cm^2/sec

where $z_1 = 1$ and $z_2 = 1$

Film conc. Diff., Δx_1^* equiv. fraction		$J_1^* \cdot \delta_{eff}$ - equiv/cm/sec (flux/cm of film thickness)		%diff.
$x_{1_{bulk}}$	$x_{1_{int}}^*$	linear	non-linear	
0.9	0.8	0.4255	0.4309	1.25
0.9	0.6	0.9195	0.9824	6.4
0.9	0.4	1.205	1.349	10.7
0.9	0.1	1.455	1.740	16.4
0.2	0.1	0.1156	0.1157	nil

System $Ag_1^+ -Na_2^+$; $D_1^* = 1 \times 10^{-6}$ cm^2/sec, $D_2^* = 2.5 \times 10^{-6}$ cm^2/sec

where $z_1 = 1$ and $z_2 = 1$

0.9	0.8	0.2041	0.2043	nil
0.9	0.6	0.5455	0.5504	0.9
0.9	0.4	0.8197	0.8368	2.1
0.9	0.1	1.143	1.191	4.2

System $Sr_1^{++}-Cs_2^+$; $D_i^* = 0.14 \times 10^{-6}$ cm^2/sec $D_2^* = 4.0 \times 10^{-6}$ cm^2/sec

where $z_1 = 2$ and $z_2 = 1$

0.9	0.8	0.1236	0.1260	1.9
0.9	0.6	0.2430	0.2664	10.0
0.9	0.4	0.2920	0.3461	18.5
0.9	0.1	0.3140	0.4157	32
0.0	0.1	-0.01542	-0.01544	nil (1)

(1) In actual simulation of this system at 0.1 n. electrolyte concentration,

the maximum $\Delta x_{Sr}^{++} \cong -0.1$, so error introduced by use of linear

model was nil.

actual "batch mode" simulation of unfavorable exchange between Cs^+ and Sr^{++} in which both models were tested, the maximum % difference in flux between models was nil. This was true because the maximum driving force difference attained in the runs was only $\Delta x_{Sr}^* = 0.1$. This was due to the high selectivity of the resin for Sr^{++} so that $x_{Sr_{int}}^*$, the equilibrium concentration, remained low. Since $x_{Sr_{bulk}}$ was zero, Δx_{Sr}^* could not get very high during the exchange. Non-linearity effects are most pronounced with a high Δx_i^* which occurs in favorable exchange, and this condition tends to be minimized due to the coupling of resin phase resistance to overall diffusion resistance. In many cases the species most favored by an ion exchanger tend to diffuse slower in the resin, so the resin phase resistance is a major factor in favorable exchange. The <u>linear</u> <u>model</u> was utilized in development of the column model since it could be extended readily to the ternary system.

5. Ternary Systems - Linear Gradients

5.1 General Development of Equations

Utilizing the assumptions made for the binary film model, the equations are:

$$0 \quad \frac{J_i^*}{\text{norm}} = -D_i^* \cdot \left(\frac{\partial x_i^*}{\partial y} + |z_i| \cdot x_i^* \cdot \frac{F}{RT} \cdot \frac{\partial \phi^*}{\partial y} \right) \quad i=1,2,3 \qquad (4\text{-}68)$$

electroneutrality conditions require:

$$\sum_{i=1}^{3} x_i^* = 1 \qquad (4\text{-}69)$$

condition of no electric current plus $J_a^* = 0$ (coion flux) requires:

$$\sum_{i=1}^{3} J_i^* = 0 \tag{4-70}$$

and based on equation (4-70):

$$\sum_{i=1}^{3} \frac{\partial x_i^*}{\partial y} = 0 \text{ , with } \frac{\partial x_a^*}{\partial y} = 0 \tag{4-71}$$

If (1) $\frac{\partial \phi^*}{\partial y}$ is eliminated from equation (4-48) as was done in development of the effective diffusion coefficients for the resin phase in Chapter V, (2) component 3 is eliminated in terms of components 1 and 2, and (3) concentration corrected diffusivities of the individual ionic species, D_i^*, i = 1,2,3, are utilized, the following equations result:

$$\circ \quad \frac{J_1^*}{\text{norm}} = \left(D_{11}^* \cdot \frac{\partial x_1^*}{\partial y} + \left(\frac{|z_1|}{|z_2|} \right) \cdot D_{12}^* \cdot \frac{\partial x_2^*}{\partial y} \right) \tag{4-72}$$

$$\circ \quad \frac{J_2^*}{\text{norm}} = \left(D_{22}^* \cdot \frac{\partial x_2^*}{\partial y} + \left(\frac{|z_2|}{|z_1|} \right) \cdot D_{21}^* \cdot \frac{\partial x_1^*}{\partial y} \right) \tag{4-73}$$

5.2 Model with Different Boundary Layer Thickness, Each Ionic Species

The coefficients D_{ij}^* are calculated as with the resin derivation, and are given below in equations (4-96 to 99).

o At this point, assume a linear driving force for each component across the "effective boundary layer" film thickness δ_{eff_i} or Δy_i.

o In order to simplify calculation complexity, it was desirable to generate effective film coefficients for each species, $k_{L_{1_{eff}}}$ and $k_{L_{2_{eff}}}$, since the non-variable (concentration independent) $k_{L_{eff}}$'s had been already incorporated into the first working ternary model developed in this work.

o Writing the equations as follows;

$$\frac{J_1^*}{norm} = D_{11}^* \left[\frac{(x_{1_{bulk}} - x_{1_{int}}^*)}{\Delta y_1} \right] + \left(\frac{|z_1|}{|z_2|} \right) \cdot D_{12}^* \left[\frac{(x_{2_{bulk}} - x_{2_{int}}^*)}{\Delta y_2} \right] \qquad (4\text{-}74)$$

and:

$$\frac{J_2^*}{norm} = D_{22}^* \left[\frac{(x_{2_{bulk}} - x_{2_{int}}^*)}{\Delta y_2} \right] + \left(\frac{|z_2|}{|z_1|} \right) \cdot D_{21}^* \left[\frac{(x_{1_{bulk}} - x_{1_{int}}^*)}{\Delta y_1} \right] \qquad (4\text{-}75)$$

led to equating $\dfrac{J_1^*}{norm}$ to the film coefficient form:

o $$\frac{J_1^*}{norm} = k_{L_{1_{eff}}} \cdot (x_{1_{bulk}} - x_{1_{int}}^*) \qquad (4\text{-}76)$$

and:

o $$\frac{J_2^*}{norm} = k_{L_{2_{eff}}} \cdot (x_{2_{bulk}} - x_{2_{int}}^*) \qquad (4\text{-}77)$$

o With this equality, the film coefficients could be computed:

(4-78)

$$k_{L_{1_{eff}}} = \frac{D^*_{11}}{\Delta y_1} + \left[\frac{|z_1|}{|z_2|}\right] \cdot \frac{D^*_{12}}{\Delta y_2} \cdot \left[\frac{(x_{2_{bulk}} - x^*_{2_{int}})}{(x_{1_{bulk}} - x^*_{1_{int}})}\right]$$

and:

(4-79)

$$k_{L_{2_{eff}}} = \frac{D^*_{22}}{\Delta y_2} + \left[\frac{|z_2|}{|z_1|}\right] \cdot \frac{D^*_{21}}{\Delta y_1} \cdot \left[\frac{(x_{1_{bulk}} - x^*_{1_{int}})}{(x_{2_{bulk}} - x^*_{2_{int}})}\right]$$

Resolution of the value of Δy_i was required at this step. As shown with the binary case, boundary layer theory given in equations (4-62) and (4-61) leads to:

o $$\frac{D^*_{i_{eff}}}{\Delta y_i} = k_{L_{i_{eff}}} = \left[\frac{C \cdot \left(\frac{Re}{\varepsilon}\right)^n \cdot Sc_i^{\frac{1}{3}} \cdot D^*_{i_{eff}}}{dp}\right]$$

(4-80)

for i=1,2,3

or,

o $$\Delta y_i = \left[\frac{dp}{C \cdot \left(\frac{Re}{\varepsilon}\right)^n \cdot Sc_i^{\frac{1}{3}}}\right] = \left[\frac{dp \cdot D^{*\frac{1}{3}}_{i_{eff}}}{C \cdot \left(\frac{Re}{\varepsilon}\right)^n \cdot \left(\frac{\mu}{\rho}\right)^{\frac{1}{3}}}\right]$$

(4-81)

for i=1,2,3

With the binary system,

$$D^*_{1_{eff}} = D^*_{2_{eff}} \quad \text{and} \quad \Delta y_1 = \Delta y_2 = \delta_{eff}$$

In the ternary system case, there are two species moving in one direction, and the other species is moving in the opposite direction at a flux equal to the sum of the first two species:

$$J_3^* = - (J_1^* + J_2^*) \qquad (4\text{-}82)$$

Since

$$\frac{\Delta y_1}{\Delta y_2} = \frac{constant \cdot D_{1_{eff}}^{*\frac{1}{3}}}{constant \cdot D_{2_{eff}}^{*\frac{1}{3}}} = \left(\frac{D_{1_{eff}}^*}{D_{2_{eff}}^*} \right)^{\frac{1}{3}} \qquad (4\text{-}83)$$

where $D_{i_{eff}}^*$ is an effective diffusivity for species i. The values of $D_{1_{eff}}^*$, $D_{2_{eff}}^*$, Δy_1, and Δy_2 can be solved for by solution of a cubic equation which arises due to the 1/3 power in equation 4-80 to 83. The film coefficient for ionic species 3 is:

$$(4\text{-}84)$$

$$k_{L_{3_{eff}}} = - \left[\frac{k_{L_{1_{eff}}} \cdot (x_{1_{bulk}} - x_{1_{int}}^*) + k_{L_{2_{eff}}} \cdot (x_{2_{bulk}} - x_{2_{int}}^*)}{(x_{3_{bulk}} - x_{3_{int}}^*)} \right]$$

This procedure was tried, again making the calculations for $k_{L_{i_{eff}}}$ at the jth time step versus $j^{+\frac{1}{2}th}$ time step to avoid quasilinearization complications, keeping Δt intervals small to avoid large systematic bias. Computational problems occured when the J_3^* flux was the largest flux, since the procedure called for computation of the film coefficients and compositions of the two most favored species. Species 3 film coefficient and composition

were calculated by difference. This difficulty was caused
when one of the preferred two species was at a very low
concentration. Extraction of the cube root of very low
values would result in arithmetic overflows or truncated
computed values. Species 3 flux, calculated by difference,
then gave rise to a poor flux balance thru the film. In
effect three boundary layer film thicknesses were computed
depending on concentration, effective diffusion coefficient
and gradient of each species, and is shown in the following
diagram.

Model for Film - Ternary System

Illustration 4-2
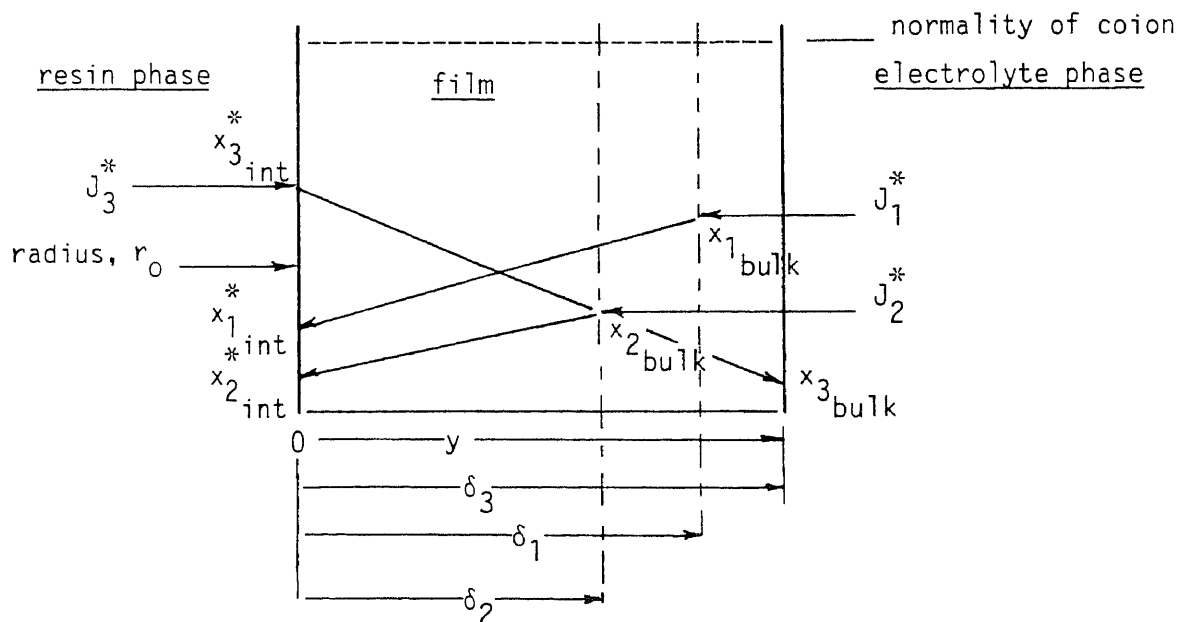
5.3 Use of Single Film Thickness - Maximum Flux

The following procedure was adopted to eliminate the
computational difficulties caused by the procedure described

above. The maximum flux was determined at the jth time step by checking species fluxes at the j^{-1th} time step:

$$\circ \quad \left.\frac{J^*_{i_{max}}}{norm}\right|_j = \left.k_{L_{i_{eff}}}\right|_{j-1} \cdot (x_{i_{bulk}} - x^*_{i_{int}})_j \qquad (4\text{-}85)$$

$$for \ i=1,2,3$$

The species having the maximum flux was chosen to compute the film thickness, $\delta_{eff_{max}}$, at the jth time step by the following derivation:

$$\circ \quad \frac{J^*_{i_{max}}}{norm} = \left(\frac{D^*_{i_{eff_{max}}}}{\delta_{eff_{max}}}\right) \cdot (x_{i_{bulk}} - x^*_{i_{int}}) \qquad (4\text{-}86)$$

where: $\hspace{11cm} (4\text{-}87)$

$$\circ \quad D^*_{i_{eff_{max}}} = D^*_{ii} + \left(\frac{|z_i|}{|z_j|}\right) \cdot D^*_{ij} \cdot \left[\frac{(x_{j_{bulk}} - x^*_{j_{int}})}{(x_{i_{bulk}} - x^*_{i_{int}})}\right]$$

then:

$$\circ \quad \delta_{eff_{max}} = \frac{dp \cdot \left(D^*_{i_{eff_{max}}}\right)^{\frac{1}{3}}}{C \cdot \left(\frac{Re}{\varepsilon}\right)^n \cdot \left(\frac{\mu}{\rho}\right)^{\frac{1}{3}}} = \Delta y_{i_{max}} \qquad (4\text{-}88)$$

and:

$$\circ \quad k_{L_{i_{eff-max}}} = \frac{D^*_{i_{eff_{max}}}}{\delta_{eff_{max}}} \qquad (4\text{-}89)$$

therefore: (4-90)

$$k_{L_j}^{o}{}_{eff-max} = \frac{D_{jj}^*}{\delta_{eff_{max}}} + \left(\frac{|z_j|}{|z_i|}\right) \cdot \frac{D_{jj}^*}{\delta_{eff_{max}}} \cdot \left[\frac{(x_{i_{bulk}} - x_{i_{int}}^*)}{(x_{j_{bulk}} - x_{j_{int}}^*)}\right]$$

and: (4-91)

$$k_{L_k}^{o}{}_{eff-max} = - \left[\frac{k_{L_i}{}_{eff-max} \cdot (x_{i_{bulk}} - x_{i_{int}}^*) + k_{L_j}{}_{eff-max} \cdot (x_{j_{bulk}} - x_{j_{int}}^*)}{(x_{k_{bulk}} - x_{k_{int}}^*)}\right]$$

where i= major flux and, k= smallest flux

The equations used to calculate D_{ii}^* and D_{ij}^* were based on the assumption that since the "film thickness" was fixed at each time step and linear driving forces were assumed, the average film compositions could be calculated for each species as follows:

$$x_{1_{eff}}^* = \frac{(x_{1_{bulk}} + x_{1_{int}}^*)}{2} \qquad (4-92)$$

$$x_{2_{eff}}^* = \frac{(x_{2_{bulk}} + x_{2_{int}}^*)}{2} \qquad (4-93)$$

$$x_{3_{eff}}^* = \frac{(x_{3_{bulk}} + x_{3_{int}}^*)}{2} \qquad (4-94)$$

This procedure also gave rise to physically satisfying the requirement of equation 4-71, since:

$$\sum_{i=1}^{3} \frac{\Delta x_i^*}{\delta_{eff-max}} = 0 , \qquad (4-95)$$

The effective film diffusion coefficients based on species average film concentrations are:

$$\circ \quad D_{ii}^{*} = D_{i}^{*} \cdot \left[1 - \frac{x_{i_{eff}}^{*} \cdot |z_i| \cdot (D_i^{*} - D_k^{*})}{\sum\limits_{i=1}^{3} x_{i_{eff}}^{*} \cdot |z_i| \cdot D_i^{*}} \right] \quad\quad (4\text{-}96)$$

$$\circ \quad D_{jj}^{*} = D_{j}^{*} \cdot \left[1 - \frac{x_{j_{eff}}^{*} \cdot |z_j| \cdot (D_j^{*} - D_k^{*})}{\sum\limits_{i=1}^{3} x_{i_{eff}}^{*} \cdot |z_i| \cdot D_i^{*}} \right] \quad\quad (4\text{-}97)$$

$$\circ \quad D_{ij}^{*} = \frac{D_i^{*} \cdot x_{i_{eff}}^{*} \cdot |z_j| \cdot (D_k^{*} - D_j^{*})}{\sum\limits_{i=1}^{3} x_{i_{eff}}^{*} \cdot |z_i| \cdot D_i^{*}} \quad\quad (4\text{-}98)$$

$$\circ \quad D_{ji}^{*} = \frac{D_j^{*} \cdot x_{j_{eff}}^{*} \cdot |z_i| \cdot (D_k^{*} - D_i^{*})}{\sum\limits_{i=1}^{3} x_{i_{eff}}^{*} \cdot |z_i| \cdot D_i^{*}} \quad\quad (4\text{-}99)$$

where i= major flux and, k= smallest flux

The D_i^{*}, D_j^{*}, D_k^{*} thereby calculated are the diffusion coefficients for each ionic species in the film based on its average concentration, and corrected for electrolyte concentration by the Nernst-Hartley equation. Calculations were all carried out at j^{th} vs. $j^{+1/2th}$ time step with minimum systematic bias as a result of the use of small time increments. Maximum dimensionless time (maximum

dimensionless time is the number of empty column volumes

filled by the column volumetric feed during the run) was

normally divided by 0.01 to 0.05 for computations.

Systematic bias on all $k_{L_{i_{eff}}}$ for all time steps ranged from

0.1 to 0.2% on runs carried out on ternary systems.

6. Pseudo Electric Field Treatment Model Comparison to the Electric Field Gradient Model for Binary Systems

Comparison of results of the "pseudo electric" field

treatment vs. Kataoka & Yoshida (50) rigorous treatment was

performed for the most "difficult" system of Ag^+ & H^+, both

for batch type experiments and column experiments. This is shown

in Table 4-2 which lists the results of unfavorable and favorable

exchange in the batch mode with the system Ag^+/H^+, both at

1.525 normal and 0.05 normal electrolyte concentrations. The

concentration vs. time, film coefficients, as well as equivalent

flux at the resin/electrolyte interface are practically identical

for both models. Unfavorable exchanges at 0.05 normal (film

control) showed the greatest differences between models after 315

sec, but these differences were only 1.5-2%.

Simulations of the favorable exchange of Ag^+ for H^+ in

column experiments performed by Omatete (78) are shown in Figures

7-6 and 7-9 for Cl^- normalities of 0.05 and 1.525. The

simulation was performed using the pseudo electric field

treatment; however, two other "S" curves are shown for which the

rigorous Kataoka et al electric field model was used in the

Table 4-2

DIFFUSION THROUGH FILM - BINARY ION EXCHANGE
BATCH SIMULATION RESULTS

Calculated Comparison of Models - Electric Field Gradient (e.f.g.)
by Kataoka et al, and Pseudo Electric Field Model (p.e.f.), this work

System Ag^+-H^+/NO_3 0.05 normal on Dowex 50W X8 resin
superficial velocity = 0.2 cm/sec
Favorable Exchange $Ag^+ \bar{H}^+$

Time -sec	Normality - interface		$\bar{H}^+$ conc. ave.		Flux at interface equiv/cm/sec		Film coefficient cm/sec	
	e.f.g.	p.e.f.	e.f.g.	p.e.f.	e.f.g.	p.e.f.	e.f.g.	p.e.f.
15	0.05	0.05	0.89	0.89	-0.0158	-0.0158	0.00644	0.00644
45	0.05	0.05	0.69	0.69	-0.0147	-0.0147	0.00682	0.00682
75	0.05	0.05	0.50	0.50	-0.0135	-0.0135	0.00726	0.00726
105	0.05	0.05	0.34	0.34	-0.0114	-0.0114	0.00806	0.00806
135	0.025	0.05	0.20	0.21	-0.0092	-0.0087	0.0104	0.0092
165	0.033	0.05	0.10	0.11	-0.0059	-0.0059	0.0117	0.0105

Unfavorable Exchange $H^+ \bar{Ag}^+$-0.05 normal

			$\bar{Ag}^+$ conc.ave.					
15	0.0636	0.05	0.94	0.934	-0.00735	-0.00769	0.00462	0.00510
75	0.0570	0.05	0.806	0.797	-0.00385	-0.00389	0.00447	0.00469
135	0.055	0.05	0.718	0.709	-0.00291	-0.00293	0.00443	0.00459
195	0.054	0.05	0.648	0.638	-0.0024	-0.00243	0.0044	0.00454
255	0.0537	0.05	0.589	0.0579	-0.00209	-0.00208	0.00439	0.0045
315	0.05325	0.05	0.538	0.528	-0.00181	-0.00179	0.00438	0.00447

Table 4-2 continued

System Ag^+-H^+/NO_3^-

1.525 normal on Dowex 50W X8 resin
superficial velocity = 0.08 cm/sec
Favorable Exchange Ag^+ $\overline{H}^+$

Time -sec	Normality - interface		$\overline{H}^+$ conc. ave.		Flux at interface equiv/cm/sec		Film coefficient cm/sec	
	e.f.g.	p.e.f.	e.f.g.	p.e.f.	e.f.g.	p.e.f.	e.f.g.	p.e.f.
15	1.388	1.525	0.49	0.49	-0.0355	-0.0355	0.007	0.0068
45	1.472	1.525	0.205	0.2056	-0.0135	-0.0135	0.0071	0.00705
75	1.499	1.525	0.077	0.077	-0.0065	-0.00655	0.0072	0.00714
105	1.516	1.525	0.018	0.018	-0.00239	-0.00239	0.0072	0.0072
135	1.523	1.525	0.0024	0.0024	-0.00039	-0.00039	0.0072	0.0072

Unfavorable Exchange H^+ $\overline{Ag}^+$

			$\overline{Ag}^+$ conc. ave.					
15	1.609	1.525	0.719	0.717	-0.0235	-0.0233	0.0023	0.00236
75	1.548	1.525	0.414	0.413	-0.0065	-0.00645	0.0023	0.0023
135	1.537	1.525	0.290	0.290	-0.0034	-0.0034	0.0023	0.00229
195	1.532	1.525	0.219	0.218	-0.00214	-0.00214	0.00227	0.00228
255	1.530	1.525	0.172	0.172	-0.00146	-0.00145	0.00227	0.00228
315	1.529	1.525	0.140	0.139	-0.00104	-0.00104	0.00227	0.00228

simulation. The "S" curves generated for the two models are identical for all practical purposes.

It was concluded that if the <u>pseudo electric field treatment model</u> for worst case conditions, i.e.,

$$\left[\left(\frac{D^*_{Ag^+}}{D^*_{H^+}} \right) \approx 0.09 \text{ and } \overline{K}_{H^+-Ag^+} \approx 0.12 \right],$$

gave results essentially identical to the <u>electric field model</u>, the error in extending its use to other less demanding systems would be minimal--and its simplicity permitted ready extension to ternary systems, as derived above.

CHAPTER V

DIFFUSION IN THE RESIN PHASE

A. Diffusion Resin Phase Coefficients and Electrochemical Potential

1. General Background

This section deals with the effective rate of diffusion
of ionic species within the ion exchanger, and development of
the Nernst-Planck relationship which relates the effects of
field potential within the resin to predict the effective
interdiffusivity of migrating species. Additionally, the
Nernst-Planck relationship will be derived with activities as
potential, as compared to concentrations of the ionic
species. The derivation of the Nernst-Planck model for use
in predicting an effective diffusivity for two species
migrating within an ion exchanger, given the "self" diffusion
coefficients for both species, was first put forth by F.
Helfferich and M. S. Plesset (42). As contrasted to Fick's
first law, several underlying assumptions should be
understood. First, that the electrochemical mobility of a
species, u_i, can be related to the species "self" diffusion
coefficient $\bar{D}_i$ by the Nernst-Einstein relationship (75),

$$\bar{D}_i = R \cdot T \cdot u_i \qquad (5\text{-}1)$$

where:

$\bar{D}_i$ = diffusion coefficient, cm^2/sec

T = temperature, $^\circ K$

R = gas constant (joule/mole/$^\circ K$

u_i = ionic mobility, cm $-$mole/joule/sec

154

J. Newman (75) points out that the equation is strictly

applicable only at infinite dilution. Helfferich (42)

states, however, that experience has shown the applicability

of the Nernst-Einstein equation to ion exchangers as a good

approximation even at higher concentrations.

The second important assumption is that the presence of

coions in the exchanger is neglected. Helfferich (42) points

out that this assumption is valid if the Donnan exclusion of

coions is strong. The Donnan potential, E_{DON} is defined (35) as:

$$\circ \quad E_{DON} = \bar{\phi} - \phi = \frac{1}{z_i \cdot F} \cdot \left[R \cdot T \cdot \ell n \left(\frac{\bar{a}_i}{a_i} \right) - \pi \cdot \nu_i \right] \quad (5\text{-}2)$$

where:

$\bar{\phi} - \phi$ = electric potential difference
between the ion exchanger and
the solution

z_i = valence of species i

F = Faraday's constant

$\bar{a}_i$ = activity of species i in solution

a_i = activity of species i in the resin

π = resin swelling pressure, bar

ν_i = partial molar volume of species i
in the resin, cc/mole

The effect of this potential is to exlude coions from

the exchanger, since migration of just a few ions of the same

charge as the exchanger sites into the ion exchanger will

quickly cause the electric field to build up, thereby

restricting further migration. This assumption tends to be invalid when electrolyte phase concentration is high, or the ion exchanger contains weakly dissociated active sites.

Implicit in almost all treatments of resin phase diffusion is that the resin acts as a solid solution through which the ions migrate.

2. Development of the General Diffusion Equations - Ternary System

In developing the general equations for ternary ion exchange in an ion exchanger, the use of irreversible thermodynamics to formulate the process will be followed, as was carried out by Barrer and Rees (6) in application to Ca^{++} and Sr^{++} exchange in chabazite, and by Rao and his coworkers (94) in their study of ternary ion exchange for the system Ba^{++}, Sr^{++}, Na^{+} on Dowex 50w x8 resin.

The general treatment of ternary systems can readily be reduced to use of concentration driving forces versus activities, and to a binary model if desired. The general equation describing ternary ion exchange in the resin phase is:

$$\overline{N}_k = - \overline{c}_k \cdot \sum_{j=1}^{4} \overline{L}_{kj} \cdot \nabla \overline{\mu}_j \qquad (j=1,2,3,4 \text{ is water}) \qquad (5\text{-}3)$$

where:

$\overline{N}_k$ = molar flux of component k

$\overline{c}_k$ = molar concentration of species k, moles/liter

$\overline{\mu}_j$ = total electrochemical potential of species j

$\overline{L}_k$ = phenomenological coefficients

for k = 1,2,3,4

o $\quad \nabla\bar{\mu}_j = \nabla\bar{\mu}_j^c + |z_j| \cdot F \cdot \nabla\bar{\phi}$ (5-4)

where:

$\bar{\mu}_j^c$ = chemical potential of species j

z_j = valence of species j

F = Faraday's constant

$\bar{\phi}$ = electric potential,volts

J. Newman (76), commenting on ideas put forth by E. A. Guggenheim, states that the splitting of the electrochemical potential into a chemical potential and an electrical potential is purely a mathematical device and is arbitrary, having no physical significance. Newman (76) points out that the treatment will not produce difficulties in application to equilibrium models. In the case of ion exchange with fixed ionic sites, it appears to simplify model development. The Nernst-Planck model for transport of ionic species in dilute electrolytes is given as:

o $\quad \bar{N}_k = -\bar{c}_k \cdot \sum_{j=1}^{4} \bar{L}_{kj} \cdot \nabla\bar{\mu}_j^c -\bar{c}_k \cdot F \cdot \nabla\bar{\phi} \cdot \sum_{j=1}^{4} \bar{L}_{kj} \cdot |z_j|$ (5-5)

for k = 1,2,3,4

The detailed derivation of the equations describing diffusion in the resin phase is given in Appendix G, and leads to the following expression:

o $\quad \bar{N}_k = - \sum_{j=1}^{2} \bar{D}_{kj} \cdot \nabla\bar{c}_j$ (5-6)

for k = 1,2

in which:

o (5-7)

$$\overline{D}'_{kk} = \overline{c}_k \, \overline{D}_k \cdot \left\{ \cdot \left(\frac{1}{\overline{c}_k} + \frac{\partial \ln \overline{\gamma}_k}{\partial \overline{c}_k} \right) - z_k^2 \cdot \left[\frac{\overline{D}_k \cdot \left(1 + \overline{c}_k \cdot \frac{\partial \ln \overline{\gamma}_k}{\partial \overline{c}_k} \right) - \overline{D}_3 \cdot \left(1 + \overline{c}_3 \cdot \frac{\partial \ln \overline{\gamma}_3}{\partial \overline{c}_3} \right)}{\sum\limits_{i=1}^{3} \overline{c}_i \cdot z_i^2 \cdot \overline{D}_i} \right] \right\}$$

for k = 1,2

and:

(5-8)

$$\begin{array}{c} \overline{D}'_{kj} \\ {\scriptstyle j \neq k} \end{array} = \overline{c}_k \cdot \left(|z_k z_j| \right) \cdot \overline{D}_k \cdot \left[\frac{\overline{D}_3 \cdot \left(1 + \overline{c}_3 \cdot \frac{\partial \ln \overline{\gamma}_3}{\partial \overline{c}_3} \right) - \overline{D}_j \cdot \left(1 + \overline{c}_j \cdot \frac{\partial \ln \overline{\gamma}_j}{\partial \overline{c}_j} \right)}{\sum\limits_{i=1}^{3} \overline{c}_i \cdot z_i^2 \cdot \overline{D}_i} \right]$$

for k = 1,2 and j = 1,2

If the system is ideal, then,

o $\quad \overline{c}_k \cdot \dfrac{\partial \ln \overline{\gamma}_k}{\partial \overline{c}_k} = 0 \qquad$ for k = 1,2 (5-9)

so,

o $\quad \overline{D}'_{kk} = \overline{D}_k \cdot \left(1 - \dfrac{\overline{c}_k \cdot z_k^2 \cdot (\overline{D}_k - \overline{D}_3)}{\sum\limits_{i=1}^{3} \overline{c}_i \cdot z_i^2 \cdot \overline{D}_i} \right)$ (5-10)

for k = 1,2

and,

$$\overset{o}{\underset{j \neq k}{\overline{D}'_{kj}}} = \left[\frac{\overline{c}_k \cdot (|z_k z_j|) \cdot \overline{D}_k \cdot (\overline{D}_3 - \overline{D}_j)}{\overset{3}{\underset{i=1}{\sum}} \overline{c}_i \cdot z_i^2 \cdot \overline{D}_i} \right]$$

(5-11)

for $k = 1,2$ and $j = 1,2$

which represent the derivations of Rao and his coworkers (92)

for an ideal ternary system.

If the system is Ideal and Binary, then:

$$\overset{o}{\overline{N}_1} = - \overline{D}'_{11} \cdot \nabla \overline{c}_1$$

(5-12)

and in $\overline{D}'_{kk}$, $\overline{D}_k = \overline{D}_1$ and $\overline{D}_2 = \overline{D}_3$

so by making the appropriate substitutions in equation

(5-10), and clearing fractions the following equation results:

$$\overset{o}{\overline{D}_{12_{eff}}} = \left[\frac{\overline{D}_1 \cdot \overline{D}_2 \cdot (\overline{c}_1 \cdot z_1^2 + \overline{c}_2 \cdot z_2^2)}{(\overline{c}_1 \cdot z_1^2 \cdot \overline{D}_1 + \overline{c}_2 \cdot z_2^2 \cdot \overline{D}_2)} \right]$$

(5-13)

which is the Helfferich, Plesset (42) derivation for an ideal

binary system.

If the System is Binary and Non-ideal, then by making the

appropriate substitutions in equation (5-7) and clearing

fractions there results:

$$\overset{o}{}$$

(5-14)

$$\overline{D}_{12_{eff}} = \left[\frac{\overline{D}_1 \cdot \overline{D}_2 \cdot \left[\overline{c}_1 \cdot z_1^2 + \overline{c}_2 \cdot z_2^2 + z_1^2 \cdot \overline{c}_1 \cdot \dfrac{\partial \ell n(\overline{\gamma}_2 \cdot \overline{c}_2)}{\partial \overline{c}_2} + z_2^2 \cdot \overline{c}_2 \cdot \dfrac{\partial \ell n(\overline{\gamma}_1 \cdot \overline{c}_1)}{\overline{c}_1} \right]}{\overset{2}{\underset{i=1}{\sum}} \overline{c}_i \cdot z_i^2 \cdot \overline{D}_i} \right]$$

where $\overline{\gamma}_1$ and $\overline{\gamma}_2$ have the molar reference state

To simplify, equivalent fractions will be introduced, and total equivalents in the ion exchange resin is given by:

$$\bar{c}_1 \cdot |z_1| + \bar{c}_2 \cdot |z_2| = Q_r \left(\frac{\text{equiv.-monoionic sites}}{\text{liter of resin}}\right) \quad (5\text{-}15)$$

and $\quad \bar{x}_i = \dfrac{|z_i| \cdot \bar{c}_i}{Q_r}$,then $\quad \dfrac{\partial(\ )}{\partial \bar{c}_i} = \dfrac{\partial(\ )}{\partial \bar{x}_i} \cdot \dfrac{|z_i|}{Q_r} \qquad (5\text{-}16,17)$

plus $\quad \bar{x}_1 + \bar{x}_2 = 1 \quad (5\text{-}18),$ and $\dfrac{\partial(\ )}{\partial \bar{x}_1} = -\dfrac{\partial(\ )}{\partial \bar{x}_2} \qquad (5\text{-}19)$

then by converting equation (5-14) to equivalent fraction units the following equation is obtained:

$$\circ \qquad\qquad\qquad\qquad\qquad\qquad\qquad\qquad\qquad (5\text{-}20)$$

$$\bar{D}_{12_{eff}} = \left(\frac{\bar{D}_1 \cdot \bar{D}_2 \cdot \left[\bar{x}_1 \cdot |z_1| + \bar{x}_2 \cdot |z_2| + \bar{x}_1 \cdot \bar{x}_2 \cdot \dfrac{\partial \ln \bar{\gamma}_2^{|z_1|}}{\partial \bar{x}_2} + \bar{x}_1 \cdot \bar{x}_2 \cdot \dfrac{\partial \ln \bar{\gamma}_1^{|z_2|}}{\partial \bar{x}_1} \right]}{\displaystyle\sum_{i=1}^{2} \bar{x}_i \cdot |z_i| \cdot \bar{D}_i} \right)$$

where $\bar{\gamma}_1$ and $\bar{\gamma}_2$ have the molar reference state

By virtue of equation (5-19) and the properties of logarithms, the following arrangements can be made:

$$\circ \qquad\qquad\qquad\qquad\qquad\qquad\qquad\qquad\qquad (5\text{-}21)$$

$$\bar{D}_{12_{eff}} = \left(\frac{\bar{D}_1 \cdot \bar{D}_2 \cdot \left[\bar{x}_1 \cdot |z_1| + \bar{x}_2 \cdot |z_2| + \bar{x}_1 \cdot \bar{x}_2 \cdot \dfrac{\partial \ln \left(\dfrac{\bar{\gamma}_1^{-|z_2|}}{\bar{\gamma}_2^{-|z_1|}} \right)}{\partial \bar{x}_1} \right]}{\displaystyle\sum_{i=1}^{2} \bar{x}_i \cdot |z_i| \cdot \bar{D}_i} \right)$$

where $\bar{\gamma}_1$ and $\bar{\gamma}_2$ have the molar reference state

and this is the Helfferich (45) derivation for the effective
diffusion coefficient in non-ideal binary systems.

However, in using the equation in the convenient form of
equivalent fractions, the flux equation can also be shown as,

$$\circ \quad \bar{J}_i = \bar{N}_i \cdot |z_i| \quad ; \quad \frac{\text{equivalents}}{\text{cm}^2 \text{sec}} \tag{5-22}$$

and

$$\bar{N}_1 \cdot |z_1| = \bar{J}_1 = -\bar{D}_{12_{eff}} \cdot \nabla \bar{x}_1 \cdot Q_r \tag{5-23}$$

$$= -\bar{D}_{12_{eff}} \cdot \nabla \bar{c}_1 \cdot |z_1|$$

or

$$\frac{\bar{J}_1}{Q_r} = -\bar{D}_{12_{eff}} \cdot \nabla \bar{x}_1 = \bar{D}_{12_{eff}} \cdot \nabla \bar{x}_2 \tag{5-24}$$

and

$$\bar{J}_1 = -\bar{J}_2 \quad (5\text{-}25) \text{ , plus, } \quad \nabla \bar{x}_1 = -\nabla \bar{x}_2 \tag{5-26}$$

It is important to note that the activity coefficient, $\bar{\gamma}_i$, is a
molar activity coefficient which is the same as the equivalent
fraction activity coefficient. If the activity coefficient is
based on mole fraction concentration units, a correction factor
must be introduced to be used in the partials taken with respect
to equivalent fraction concentration units. This is covered in
Chapter II, part F.

Converting equations (5-7) and (5-8), which are the activity
driving force effective diffusion coefficients for ternary
systems, to equivalent fraction units results in:

$$\overset{o}{\overline{D}}_{kk}{}' = \overline{D}_k \cdot \left\{ \left[\left(1 + \overline{x}_k \cdot \frac{\partial \ln \overline{\gamma}_k}{\partial \overline{x}_k}\right) - \left(\frac{\overline{x}_k \cdot |z_k|}{\sum\limits_{i=1}^{3} \overline{x}_i \cdot |z_i| \cdot \overline{D}_i}\right) \right. \right.$$

$$\left. \left. \times \left[(\overline{D}_k - \overline{D}_3) + \left[\overline{x}_k \cdot \overline{D}_k \cdot \frac{\partial \ln \overline{\gamma}_k}{\partial \overline{x}_k} - \overline{x}_3 \cdot \overline{D}_3 \cdot \frac{\partial \ln \overline{\gamma}_3}{\partial \overline{x}_3} \right] \right] \right] \right\} \qquad (5\text{-}27)$$

for k of 1,2

where the $\overline{\gamma}_i$'s have the molar reference state

$$\overset{o}{\overline{D}}_{kj}{}' = \overline{x}_k \cdot |z_j| \cdot \overline{D}_k \cdot \left[\frac{(\overline{D}_3 - \overline{D}_j) + \left[\overline{x}_3 \cdot \overline{D}_3 \cdot \frac{\partial \ln \overline{\gamma}_3}{\partial \overline{x}_3} - \overline{x}_j \cdot \overline{D}_j \cdot \frac{\partial \ln \overline{\gamma}_j}{\partial \overline{x}_j} \right]}{\sum\limits_{i=1}^{3} \overline{x}_i \cdot |z_i| \cdot \overline{D}_i} \right] \qquad (5\text{-}28)$$
$$j \neq k$$

for j,k of 1,2 or 2,1

where the $\overline{\gamma}_i$'s have the molar reference state

These equations were derived utilizing the same relationships as were used to derive the equivalent fraction version of the non-ideal binary relationship. Again, $\overline{\gamma}_k$ or $\overline{\gamma}_j$ are <u>molar activity coefficients</u> which are the same as the <u>equivalent fraction activity coefficients</u> by definition of the standard states. Corrections must be applied to partials taken with respect to mole fraction concentration units, if the activity coefficients have been correlated in those units.

The Flux Equations for Ternary Systems are:

$$\circ \quad \bar{J}_k = \bar{N}_k \cdot |z_k| = Q_r \cdot |z_k| \cdot \left(\sum_{j=1}^{2} \bar{D}_{kj} \cdot \left(\frac{\nabla \bar{x}_j}{|z_j|} \right) \right) \qquad (5\text{-}29)$$

$$\text{in } \frac{\text{equivalents}}{\text{cm}^2 \cdot \text{sec}} \quad \text{for } k = 1,2$$

since equivalent fraction is defined as:

$$\bar{x}_k = \frac{|z_k| \cdot \bar{c}_k}{Q_r} \qquad \text{for } k=1,2,3 \qquad (5\text{-}30)$$

then,

$$\nabla \bar{c}_k = \left(\frac{Q_r}{|z_k|} \right) \cdot \nabla \bar{x}_k \qquad \text{for } k = 1,2,3 \qquad (5\text{-}31)$$

$$\text{plus} \quad \bar{x}_1 + \bar{x}_2 + \bar{x}_3 = 1.0 \qquad (5\text{-}32)$$

$$\text{and} \quad \nabla \bar{x}_3 = -\nabla \bar{x}_2 - \nabla \bar{x}_1 \qquad (5\text{-}33)$$

and finally,

$$\circ \quad \frac{\bar{J}_1}{Q_r} = - \left(\bar{D}_{11}' \cdot \nabla \bar{x}_1 + \left(\frac{|z_1|}{|z_2|} \right) \cdot \bar{D}_{12}' \cdot \nabla \bar{x}_2 \right) \qquad (5\text{-}34)$$

$$\circ \quad \frac{\bar{J}_2}{Q_r} = - \left(\bar{D}_{22}' \cdot \nabla \bar{x}_2 + \left(\frac{|z_2|}{|z_1|} \right) \cdot \bar{D}_{21}' \cdot \nabla \bar{x}_1 \right) \qquad (5\text{-}35)$$

The Continuity equations for the resin phase in a ternary system are:

$$\text{o} \quad \frac{\partial \bar{c}_1}{\partial t} = -\frac{1}{r^2} \cdot \frac{\partial (r^2 \cdot \bar{N}_1)}{\partial r} \tag{5-36}$$

$$\text{o} \quad \frac{\partial \bar{c}_2}{\partial t} = -\frac{1}{r^2} \cdot \frac{\partial (r^2 \cdot \bar{N}_2)}{\partial r} \tag{5-37}$$

which in equivalent fraction units are:

$$\text{o} \quad \frac{\partial \bar{x}_1}{\partial t} \cdot Q_r = -\frac{1}{r^2} \cdot \frac{\partial (r^2 \cdot \bar{J}_1)}{\partial r} \tag{5-38}$$

$$\text{o} \quad \frac{\partial \bar{x}_2}{\partial t} \cdot Q_r = -\frac{1}{r^2} \cdot \frac{\partial (r^2 \cdot \bar{J}_2)}{\partial r} \tag{5-39}$$

3. Dimensionless Form and Preparation of Equations for Numerical Solutions

In setting up the diffusion and continuity equations for use in a coupled mode with the fluid phase in a column, it is useful to put the terms in dimensionless form.

Defining:

BL = length of resin bed, cm

l = resin bed length dimension, cm

r_o = particle radius, cm

r = particle radius dimension, cm

v_s = superficial velocity, cm/sec

ε = bed voidage

t = time, sec

E_D = axial dispersion coefficient, cm^2/sec

k_{L_i} = film coefficient, cm/sec

$\bar{D}_{ij_{eff}}$ = resin phase diffusion coefficient, cm^2/sec

$$Y \quad = \frac{1}{BL}$$

$$R \quad = \frac{r}{r_o}$$

$$Pe \quad = \frac{BL \cdot v_s}{E_D \cdot \varepsilon} \ , \ \text{Peclet no.} \qquad (5-40)$$

$$T \quad = \frac{t \cdot v_s}{BL}$$

$$\delta_s \quad = \frac{(1-\varepsilon) \cdot BL}{r_o^2 \cdot v_s} \ , \ \begin{array}{l}\text{dimensionless term} \\ \text{linking resin phase} \\ \text{to electrolyte phase}\end{array} \qquad (5-41)$$

$$Bi_i \quad = \frac{2 \cdot r_o \cdot k_{L_{i_{eff}}}}{\overline{D}_{ij}} \ , \ \begin{array}{l}\text{Biot no. , but} \\ \text{since } \overline{D}_{ij} = f(\overline{x}_i, \overline{x}_j), \\ \text{then form used is:}\end{array} \qquad (5-42)$$

$$Bi_i \quad = 2 \cdot r_o \cdot k_{L_{i_{eff}}} \ , \ \begin{array}{l}\text{since } \overline{D}_{ij} \text{ must remain} \\ \text{in } \frac{\partial(\ )^{ij}}{\partial r}\end{array}$$

Svedberg (125), in his development of a numerical method for simulation of fixed-bed processes has investigated the use of a different grid spacing for intraparticle diffusion. A more accurate approximation of the derivatives would be to have a more dense grid near the particle surface where concentration gradients are greatest. Michelsen (72) and others have used the transformation $\rho = R^2$ to accomplish this alteration of particle grid density. The differential expressions with respect to R become:

$$o \quad \frac{\partial^2(\ )}{\partial R^2} + \frac{2}{R} \cdot \frac{\partial(\ )}{\partial R} = 4 \cdot \rho \cdot \frac{\partial^2(\ )}{\partial \rho^2} + 6 \cdot \frac{\partial(\ )}{\partial \rho} \qquad (5-43)$$

and,

$$o \quad \frac{\partial(\ )}{\partial R} = 2 \cdot \rho^{\frac{1}{2}} \cdot \frac{\partial(\ )}{\partial \rho} \qquad (5-44)$$

Svedberg (125) checked this grid spacing for asymptotic
constant pattern profiles which had previously been solved by
Hall and his coworkers (34) which included both numerical and
analytic solutions for constant pattern, self sharpening
profile, ion exchange problems. Svedberg (125) showed that
the results obtained with the ρ transformation compared more
favorably to the analytical solutions than the R grid
spacings for a variety of Peclet & Biot number variations,
column grid spacings, time increments, and resin grid
increments, particularly for the solid diffusion model as
opposed to a pore diffusion model.

The Continuity Equations Transformed become:

$$\circ \qquad Q_r \cdot \frac{v}{L} \cdot \frac{\partial \bar{x}_1}{\partial T} = - \frac{4}{r_o^2 \cdot \rho^{\frac{1}{2}}} \cdot \frac{\partial (\rho^{\frac{3}{2}} \cdot \bar{J}_1)}{\partial \rho} \qquad\qquad (5\text{-}45)$$

or,

$$\circ \qquad Q_r \cdot \frac{\partial \bar{x}_1}{\partial T} = - \frac{\delta_s \cdot 4}{(1-\varepsilon) \cdot \rho^{\frac{1}{2}}} \cdot \frac{\partial (\rho^{\frac{3}{2}} \cdot \bar{J}_1)}{\partial \rho} \qquad\qquad (5\text{-}46)$$

and,

$$\circ \qquad Q_r \cdot \frac{\partial \bar{x}_2}{\partial T} = - \frac{\delta_s \cdot 4}{(1-\varepsilon) \cdot \rho^{\frac{1}{2}}} \cdot \frac{\partial (\rho^{\frac{3}{2}} \cdot \bar{J}_2)}{\partial \rho} \qquad\qquad (5\text{-}47)$$

substitution of equation (5-34) and (5-35) in equation (5-46)
and (5-47) yields:

$$(5\text{-}48)$$

$$\frac{\partial \overline{x}_1}{\partial T} = \frac{\delta_s}{(1-\varepsilon)} \cdot \left[\overline{D}_{11}' \cdot \left(4 \cdot \rho \cdot \frac{\partial^2 \overline{x}_1}{\partial \rho^2} + 6 \cdot \frac{\partial \overline{x}_1}{\partial \rho} \right) + \overline{D}_{12}' \cdot \left(\frac{|z_1|}{|z_2|} \right) \cdot \left(4 \cdot \rho \cdot \frac{\partial^2 \overline{x}_2}{\partial \rho^2} + 6 \cdot \frac{\partial \overline{x}_2}{\partial \rho} \right) \right.$$

$$+ 4 \cdot \rho \cdot \frac{\partial \overline{D}_{11}'}{\partial \overline{x}_1} \cdot \left(\frac{\partial \overline{x}_1}{\partial \rho} \right)^2 + 4 \cdot \rho \cdot \frac{\partial \overline{D}_{11}'}{\partial \overline{x}_2} \cdot \left(\frac{\partial \overline{x}_1}{\partial \rho} \right) \cdot \left(\frac{\partial \overline{x}_2}{\partial \rho} \right)$$

$$\left. + 4 \cdot \rho \cdot \left(\frac{|z_1|}{|z_2|} \right) \cdot \frac{\partial \overline{D}_{12}'}{\partial \overline{x}_2} \cdot \left(\frac{\partial \overline{x}_2}{\partial \rho} \right)^2 + 4 \cdot \rho \cdot \left(\frac{|z_1|}{|z_2|} \right) \cdot \frac{\partial \overline{D}_{12}'}{\partial \overline{x}_1} \cdot \left(\frac{\partial \overline{x}_1}{\partial \rho} \right) \cdot \left(\frac{\partial \overline{x}_2}{\partial \rho} \right) \right]$$

the last four terms result from:

$$\left(\frac{\partial \overline{D}_{ij}}{\partial \rho} \right) \cdot \left(\frac{\partial \overline{x}_i}{\partial \rho} \right) \qquad \text{where:}$$

$$(5\text{-}49)$$

$$\frac{\partial \overline{D}_{ij}'}{\partial \rho} = \left(\frac{\partial \overline{D}_{ij}'}{\partial \overline{x}_i} \right) \cdot \left(\frac{\partial \overline{x}_i}{\partial \rho} \right) + \left(\frac{\partial \overline{D}_{ij}'}{\partial \overline{x}_j} \right) \cdot \left(\frac{\partial \overline{x}_j}{\partial \rho} \right)$$

and:

$$(5\text{-}50)$$

$$\frac{\partial \overline{x}_2}{\partial T} = \frac{\delta_s}{(1-\varepsilon)} \cdot \left[\overline{D}_{22}' \cdot \left(4 \cdot \rho \cdot \frac{\partial^2 \overline{x}_2}{\partial \rho^2} + 6 \cdot \frac{\partial \overline{x}_2}{\partial \rho} \right) + \overline{D}_{21}' \cdot \left(\frac{|z_2|}{|z_1|} \right) \cdot \left(4 \cdot \rho \cdot \frac{\partial^2 \overline{x}_1}{\partial \rho^2} + 6 \cdot \frac{\partial \overline{x}_1}{\partial \rho} \right) \right.$$

$$+ 4 \cdot \rho \cdot \frac{\partial \overline{D}_{22}'}{\partial \overline{x}_2} \cdot \left(\frac{\partial \overline{x}_2}{\partial \rho} \right)^2 + 4 \cdot \rho \cdot \frac{\partial \overline{D}_{22}'}{\partial \overline{x}_1} \cdot \left(\frac{\partial \overline{x}_1}{\partial \rho} \right) \cdot \left(\frac{\partial \overline{x}_2}{\partial \rho} \right)$$

$$\left. + 4 \cdot \rho \cdot \left(\frac{|z_2|}{|z_1|} \right) \cdot \frac{\partial \overline{D}_{21}'}{\partial \overline{x}_1} \cdot \left(\frac{\partial \overline{x}_1}{\partial \rho} \right)^2 + 4 \cdot \rho \cdot \left(\frac{|z_2|}{|z_1|} \right) \cdot \frac{\partial \overline{D}_{21}'}{\partial \overline{x}_2} \cdot \left(\frac{\partial \overline{x}_1}{\partial \rho} \right) \cdot \left(\frac{\partial \overline{x}_2}{\partial \rho} \right) \right]$$

Boundary Conditions

flux across resin boundary where $\rho = 1$

$$o \qquad \left.\vec{J}_1^*\right|_{r=r_o} = k_{L_1eff} \cdot (x_{1_{bulk}} - x_{1_{int}}^*) \cdot norm$$

$$= \left(\left.\overline{D}_{11}' \cdot \frac{\partial \overline{x}_1}{\partial r}\right|_{r=r_o} + \left(\frac{|z_1|}{|z_2|}\right) \cdot \left.\overline{D}_{12}' \cdot \frac{\partial \overline{x}_2}{\partial r}\right|_{r=r_o}\right) \cdot Q_r$$

transformed to ρ coordinates, (5-51) becomes:

$$o \qquad \frac{2 \cdot \rho^{\frac{1}{2}} \cdot Q_r}{r_o \cdot norm} \cdot \left(\left.\overline{D}_{11}' \cdot \frac{\partial \overline{x}_1}{\partial \rho}\right|_{\rho=1} + \left(\frac{|z_1|}{|z_2|}\right) \cdot \left.\overline{D}_{12}' \cdot \frac{\partial \overline{x}_2}{\partial \rho}\right|_{\rho=1}\right)$$

$$= k_{L_1eff} \cdot (x_{1_{bulk}} - x_{1_{int}}^*)$$

since $Bi_i = 2 \cdot r_o \cdot k_{L_ieff}$, then:

$$o \qquad \frac{4 \cdot Q_r}{Bi_1 \cdot norm} \cdot \left(\left.\overline{D}_{11}' \cdot \frac{\partial \overline{x}_1}{\partial \rho}\right|_{\rho=1} + \left(\frac{|z_1|}{|z_2|}\right) \cdot \left.\overline{D}_{12}' \cdot \frac{\partial \overline{x}_2}{\partial \rho}\right|_{\rho=1}\right)$$

$$= (x_{1_{bulk}} - x_{1_{int}}^*)$$

and for component 2:

$$\frac{4 \cdot Q_r}{Bi_2 \cdot norm} \cdot \left(\left.\overline{D}_{22}' \cdot \frac{\partial \overline{x}_2}{\partial \rho}\right|_{\rho=1} + \left(\frac{|z_2|}{|z_1|}\right) \cdot \left.\overline{D}_{21}' \cdot \frac{\partial \overline{x}_1}{\partial \rho}\right|_{\rho=1}\right)$$

$$= (x_{2_{bulk}} - x_{2_{int}}^*)$$

gradient at resin center:

$$\frac{\partial \bar{x}_1}{\partial \rho} = 0 \ , \ \text{and} \ \frac{\partial \bar{x}_2}{\partial \rho} = 0 \qquad \begin{cases} \rho = 0 \\ 0 \leq Y \leq 1 \\ T \geq 0 \end{cases} \quad (5\text{-}55,56)$$

Initial Conditions

$$\bar{x}_1 , \bar{x}_2 \ (\rho, Y, 0) = \bar{x}_{1_{t_o}} , \bar{x}_{2_{t_o}} \ (\rho, Y) \quad \begin{cases} 0 \leq Y \leq 1 \\ 0 \leq \rho \leq 1 \end{cases} \quad (5\text{-}57,58)$$

Reduction of Ternary System to Binary System

Equation (5-48) is used and terms involving $\bar{D}'_{12}$ and $\bar{x}_2$ are eliminated.

$$(5\text{-}59)$$

$$\text{o} \qquad \frac{\partial \bar{x}_1}{\partial T} = \frac{\delta_s}{(1-\varepsilon)} \cdot \left[\bar{D}'_{11} \cdot \left(4 \cdot \rho \cdot \frac{\partial^2 \bar{x}_1}{\partial \rho^2} + 6 \cdot \frac{\partial \bar{x}_1}{\partial \rho} \right) + 4 \cdot \rho \cdot \frac{\partial \bar{D}'_{11}}{\partial \bar{x}_1} \cdot \left(\frac{\partial \bar{x}_1}{\partial \rho} \right)^2 \right]$$

Boundary Conditions

flux across resin boundary where $\rho = 1$:

$$\text{o} \qquad \frac{4 \cdot \rho^2 \cdot Q_r}{Bi_1 \cdot norm} \cdot \left(\bar{D}'_{11} \cdot \frac{\partial \bar{x}_1}{\partial \rho} \bigg|_{\rho=1} \right) = (x_{1_{bulk}} - x^*_{1_{int}}) \qquad (5\text{-}60)$$

gradient at resin center:

$$\frac{\partial \bar{x}_1}{\partial \rho}(0, Y, T) = 0 \qquad \begin{cases} 0 \leq Y \leq 1 \\ T \geq 0 \end{cases} \qquad (5\text{-}61)$$

Initial Conditions

$$\bar{x}_1(\rho, Y, 0) = \bar{x}_{1_{t_o}} \ (\rho, Y) \quad \begin{cases} 0 \leq Y \leq 1 \\ 0 \leq \rho \leq 1 \end{cases} \qquad (5\text{-}62)$$

B. <u>Solution of the Resin Phase Equations, Numerical Methods</u>

1. <u>General Background</u>

The coupled non-linear parabolic partial differential equations describing intraparticle diffusion of three species have been solved in this work by use of an implicit finite difference method of the Crank-Nicholson type (125). The following discussion will involve the resin phase only, and the solution of the equations described can be used to simulate the type of time varying concentration curves generated by Rao and his coworkers (92, 93) on several binary and ternary systems using the radioactive single particle tracer technique. Later, the two resin phase equations will be coupled with the two parabolic fluid phase equations to simulate fixed bed operations. In treating the "batch" case, it is assumed that bulk fluid phase concentrations of the species do not change (i.e., infinite reservoir); however, the concentration of each ionic species at the resin/fluid interface is in thermodynamic equilibrium. The actual thermodynamic treatment of ternary ion exchange equilibria is discussed in the Chapter II on Equilibrium. The equilibrium relationships can be treated here as:

$$\circ \qquad x^*_{1_{int}} = \phi \; (\bar{x}_{1_{int,}} \; \bar{x}_{2_{int,}} \; x^*_{1_{int,}} \; x^*_{2_{int}}) \qquad (5\text{-}63)$$

$$\text{non-linear implicit functions}$$

$$\circ \qquad x^*_{2_{int}} = \theta \; (\bar{x}_{1_{int,}} \; \bar{x}_{2_{int,}} \; x^*_{1_{int,}} \; x^*_{2_{int}}) \qquad (5\text{-}64)$$

Svedberg (125) linearized non-linear equilibrium

expressions in his work by using a quasilinearization

technique described by Lee (59), but applied it to a binary

system only. The equilibrium functions for a ternary system

would be iteratively solved as follows:

$$
0 \qquad x^*_{1_{int_{n+1}}} = x^*_{1_{int_n}} + (\bar{x}_{1_{int_{n+1}}} - \bar{x}_{1_{int_n}}) \cdot \left(\frac{\partial x^*_{1_{int}}}{\partial \bar{x}_{1_{int}}}\right)_n \qquad (5\text{-}65)
$$

$$
+ (\bar{x}_{2_{int_{n+1}}} - \bar{x}_{2_{int_n}}) \cdot \left(\frac{\partial x^*_{1_{int}}}{\partial \bar{x}_{2_{int}}}\right)_n
$$

$$
0 \qquad x^*_{2_{int_{n+1}}} = x^*_{2_{int_n}} + (\bar{x}_{2_{int_{n+1}}} - \bar{x}_{2_{int_n}}) \cdot \left(\frac{\partial x^*_{2_{int}}}{\partial \bar{x}_{2_{int}}}\right)_n \qquad (5\text{-}66)
$$

$$
+ (\bar{x}_{1_{int_{n+1}}} - \bar{x}_{1_{int_n}}) \cdot \left(\frac{\partial x^*_{2_{int}}}{\partial \bar{x}_{1_{int}}}\right)_n
$$

where n = iteration number

Use of this procedure allows $x^*_{i_{int}}$ to be expressed as

a linear function of $\bar{x}_{i_{int}}$, and the system of linear

algebraic equations is solved iteratively at each time step

until convergence is attained. As Svedberg (125) points out,

quasilinearization is basically a Newton method and has

second order convergence. A serious limitation for Newton

methods is that convergence is guaranteed only if the

starting point lies close to the solution point. In the

technique used here, with sufficiently small time steps, the solution at time step j is an excellent first guess when searching for a solution at time step j+1. Even with the most extreme non-linear conditions experienced in the simulations performed in this research, convergence has normally been reached in 3 to 5 iterations--<u>except</u> at the start of the simulation at j=1. If the concentration distribution and flux balances set up as initial conditions are too far from the j=1 solution points, convergence will not occur.

2. Differentiation of Implicit Functions

The thermodynamic equilibrium functions described above are implicit functions of the type:

$$\circ \quad f(\bar{x}_{1_{int}}, \bar{x}_{2_{int}}, x^*_{1_{int}}, x^*_{2_{int}}) = 0 \qquad (5\text{-}67)$$

$$\circ \quad g(\bar{x}_{1_{int}}, \bar{x}_{2_{int}}, x^*_{1_{int}}, x^*_{2_{int}}) = 0 \qquad (5\text{-}68)$$

where $x^*_{i_{int}}$ are implicit functions of $\bar{x}_{1_{int}}$ and $\bar{x}_{2_{int}}$ and cannot be solved for explicitly. The partials

$$\frac{\partial x^*_{1_{int}}}{\partial \bar{x}_{1_{int}}}, \quad \frac{\partial x^*_{2_{int}}}{\partial \bar{x}_{1_{int}}}, \quad \frac{\partial x^*_{1_{int}}}{\partial \bar{x}_{2_{int}}}, \quad \frac{\partial x^*_{2_{int}}}{\partial \bar{x}_{2_{int}}}$$

are obtained by the procedure described in Mickley, Sherwood & Reed (70) for differentiation of implicit functions.

3. Quasilinearization of Other Non-Linear Terms

Besides the equilibrium relationship, several other

terms in equation (5-48) and equation (5-50) are non linear, since multiplication of the finite difference equations approximating those terms result in algebraic variables which cannot be separated. These are given in Appendix H.

4. Treatment of the Diffusivity Functions

The functions $\bar{D}_{ij}'$, and $\dfrac{\partial \bar{D}_{ij}'}{\partial \bar{x}_i}$, and $\dfrac{\partial \bar{D}_{ij}'}{\partial \bar{x}_j}$ were calculated at time step j for use in time step j+1. Since the Crank-Nicholson method uses values of variables at time step $j^{+1/2}$ by averaging the jth & j^{+1th} values, the computations carried out using this technique were subject to systematic bias. However, the algebraic complications in quasilinearizing the four diffusivities and the eight derivatives, particularly if they involved activity driving force (i.e., $\dfrac{\partial \ln \bar{\gamma}_i}{\partial \bar{x}_i}$), were too great. This treatment was rationalized on the basis that if the time steps were reasonably small, total absolute systematic bias would be small. Table 5-1 gives the results of simulation of the seven binary system "batch" runs made by Rao and his coworkers (92, 93). The results are given in terms of total absolute systematic bias in percent, for all diffusivities grouped together, and all partials of the diffusivities grouped together, summed for all time and resin increments. At the end of the simulation, the sums were then divided by the number of resin and time increments used in the

simulation. Special attention was paid to the outermost resin increment since this increment represents the boundary condition and should have the greatest impact on solution vectors in the electrolyte phase during column simulation. The systematic bias for this increment was calculated separately. Comparison was made for two time increments, ΔT, at values of 0.5 and 0.05. The time increment ΔT in the batch simulation runs is the increment into which actual time, in seconds, is divided. Most simulations were run at $\Delta T=0.01$ to 0.05. Although the systematic bias increased dramatically for $\Delta T=0.5$ in the system Na^+-Mn^{++}, the time varying concentrations for this system simulated at the two ΔTs differed by only 1-1.5% as shown in Table 5-2.

The model versatility in terms of its ability to handle ternary systems concentration dependent diffusivities and film coefficients, as well as use of activity driving forces, would justify the method used in view of the small bias introduced when the number of simulation time increments are 10-20 times the actual experimental time for the "batch" runs of Gopala Rao and his coworkers (92, 93).

C. Solution of System of Linear Equations - Seven Diagonal Array

1. Binary System

1.1 Tridiagonal Systems of Equations

The finite difference equations resulting from use of the Crank Nicholson method are based on breaking the geometry domains into grids to designate values of given

SYSTEMATIC BIAS ON BINARY ION EXCHANGE SIMULATION

Table 5-1

Simulation Runs for experiments of Rao et al

-Activity Driving Force-

$$\Delta T = \frac{\text{total actual time for experimental run}}{\text{no. of time steps used in simulation}}$$

% Systematic Bias

System bar indicates species in resin phase	$\bar{D}'_{ij}$ ΔT		$\bar{D}'_{ij_{max}}$ ΔT		$\partial\bar{D}'_{ij}/\partial\bar{x}_i$ ΔT		$\partial\bar{D}'_{ij}/\partial\bar{x}_j$ ΔT		k_{L_i}-eff ΔT	
	0.50	0.05	0.50	0.05	0.50	0.05	0.50	0.05	0.50	0.05
$\overline{Mn}^{++}Cs^{+}$	0.09	0.009	0.1	0.01	0.134	0.013	0.08	0.008	0.013	0.0013
$\overline{Mn}^{++}Sr^{++}$	0.016	0.0016	0.01	0.001	-0.095	-0.01	-0.006	-0.0006	0.001	0.0001
$\overline{Sr}^{++}Mn^{++}$	0.02	0.002	0.01	0.001	0.05	0.005	0.07	0.007	0.001	0.0001
$\overline{Sr}^{++}Cs^{+}$	0.105	0.0105	0.08	0.008	0.18	0.018	0.11	0.011	0.01	0.001
$\overline{Na}^{+}Cs^{+}$	0.083	0.008	0.08	0.008	0.120	0.046	0.72	0.004	0.02	0.002
$\overline{Mn}^{++}Na^{+}$	0.09	0.009	0.08	0.008	0.88	0.006	0.3	-0.22	0.006	0.0006
$\overline{Na}^{+}Mn^{++}$	0.32	0.020	2.7	0.013	-1.31	-0.04	-1.4	-0.014	0.70	0.003

Table 5-2

SYSTEMATIC BIAS ON BINARY ION EXCHANGE SIMULATION

Comparison of Simulation Results for Rao et al

Experiment on $\overline{Na^+}$-Mn^{++} System

ΔT Effect

Time - sec	$\overline{x}_{Na^+ ave}$ at ΔT = 0.50	$\overline{x}_{Na^+ ave}$ at ΔT = 0.05	% Difference
15	0.802	0.788	1.8
30	0.689	0.681	1.2
45	0.611	0.603	1.3
60	0.550	0.542	1.5
75	0.498	0.492	1.2
90	0.454	0.449	1.1
105	0.415	0.411	1.0
120	0.381	0.377	1.0
135	0.350	0.346	1.1
150	0.322	0.319	1.0
165	0.297	0.294	1.0
180	0.274	0.270	1.5

variables which can then be used to approximate

derivatives at each time step. For example:

If the ρ dimension is broken into M grid points,

then: $\quad \Delta\rho = \dfrac{1}{(M-1)}$, since $\rho = 1$

and,

$$\left[\frac{\partial \bar{x}_1}{\partial \rho}\right]_j = \frac{\left[\bar{x}_1(m+1,j)-\bar{x}_1(m-1,j)\right]}{2\Delta\rho} \qquad (5\text{-}69)$$

plus,

$$(5\text{-}70)$$

$$\left[\frac{\partial^2 \bar{x}_i}{\partial \rho^2}\right]_j = \left(\frac{\left[\dfrac{\bar{x}_1(m+1,j)-\bar{x}_1(m,j)}{\Delta\rho}\right] - \left[\dfrac{\bar{x}_1(m,j)-\bar{x}_1(m-1,j)}{\Delta\rho}\right]}{\Delta\rho}\right)$$

$$= \left(\frac{\left[\bar{x}_1(m+1,j) + \bar{x}_1(m-1,j) - 2\cdot\bar{x}_1(m,j)\right]}{\Delta\rho^2}\right)$$

In the implicit Crank Nicholson method, the time

steps j and j + 1 are averaged, so that j^{+1th}

equivalent versions of the above partials approximations

are averaged with the jth values to represent the

partial derivative approximations as a function of time.

The linear algebraic equations developed, including

terms from the quasilinearization of non-linear

expressions, result in a coefficient matrix for the

variables which is tridiagonal since, as seen, m+1, m ,

and m-1 terms are involved. Representation of the

system of equations which result from the finite difference approximation of the partial differential equation describing <u>binary</u> ion exchange for the resin phase would be:

$$0 \quad A_{i_n} \cdot \bar{x}_{1_{i_{n+1}}} + D_{i_n} + E_{i_n} \cdot x_{1_{bulk}}(i,j+1)_{n+1} \qquad (5\text{-}71)$$

where:

$$A_{i_n} = \begin{bmatrix} a_1 & b_1 & & & \\ c_2 & a_2 & b_2 & & \\ & & & & \\ & & & & \\ & & & c_M & a_M \end{bmatrix}_{i,n} \qquad (5\text{-}72)$$

$$\text{and} \quad \bar{x}_{1_{i_{n+1}}} = \begin{bmatrix} \bar{x}_1(1,i,j+1) \\ \bar{x}_1(2,i,j+1) \\ \bar{x}_1(m,i,j+1) \\ \bar{x}_1(M,i,j+1) \end{bmatrix}_{n+1} \qquad (5\text{-}73)$$

$$D_{i_n} = \begin{bmatrix} d(1,i,j) \\ d(2,i,j) \\ d(m,i,j) \\ \\ d(M,i,j) \end{bmatrix}_n \qquad (5\text{-}74)$$

$$\text{and} \quad E_{i_n} = \begin{bmatrix} 0 \\ 0 \\ 0 \\ \\ e \end{bmatrix}_n \qquad (5\text{-}75)$$

and $x_{1_{bulk}}(i,j+1)_{n+1}$ is the solution phase concentration at column increment i.

This system of resin phase equations would be coupled with a similar system of equations describing

the solution phase concentration at each column length node, i, for i=1 to I. This development is treated in Chapter VII in which the column models are derived. In the "batch" case, $x_{1_{bulk}}$ is a constant and the $E_{i_n} \cdot x_{1_{bulk}} (i,j+1)_{n+1}$ term can be added to the vector D_{i_n}. It is noted that the vector D_{i_n} contains terms from the previous time step, j, as well as the terms resulting from the quasilinearization of non-linear functions at the nth iteration. The Thomas method (13, 125) involves an algorithm for solving systems of equations having tridiagonal coefficient matrices, and is very efficient. It was used by Svedberg (125) with satisfactory results, and is used in this research project to solve the binary systems.

1.2 Treatment of Boundary Conditions by Numerical Approximation

Two resin phase boundary conditions were approximated by finite difference equations and coupled to the general resin phase equation. The first, at the center of the resin particle is the boundary condition that was given in equation (5-61)

$$\frac{\partial \bar{x}_1}{\partial \rho}(0,Y,T) = 0 \qquad \begin{cases} \rho = 0 \\ 0 \leq Y \leq 1 \\ T \geq 0 \end{cases}$$

To solve this B.C., advantage is taken of the general equation (5-59), where ρ is set equal to zero, or:

$$o \qquad \frac{\partial \bar{x}_1}{\partial T} = \frac{\delta_s}{(1-\epsilon)} \cdot \left[6 \cdot \bar{D}_{11} \cdot \frac{\partial \bar{x}_1}{\partial \rho} \right] \qquad (5-76)$$

and in difference terms, using a forward difference for

(5-77)

$$\frac{\partial \bar{x}_i}{\partial \rho} = \left(\frac{\left[\bar{x}_1(2,i,j+1)_{n+1} + \bar{x}_1(2,i,j) - \left[\bar{x}_1(1,i,j+1)_{n+1} + \bar{x}_1(1,i,j) \right] \right]}{2 \cdot \Delta \rho} \right)$$

with

$$\frac{\partial \bar{x}_1}{\partial T} = \left(\frac{\left[\bar{x}_1(1,i,j+1)_{n+1} - \bar{x}_1(1,i,j) \right]}{\Delta T} \right) \qquad (5-78)$$

The finite difference equation can be separated

into $x_1(1,i,j + 1)_{n+1}$ terms to give the coefficients

and solution vector for the resin at node 1 in terms of

node 2. In effect, this treatment is analogous to

treating the spherical volume of radius $r_o \cdot \sqrt{\Delta \rho}$, at the

center of the resin, as a well mixed accumulation

(depletion) volume. Through this defined spherical

surface a diffusion flux passes between node 2 and the

node 1 spherical volume, with the gradient being equal

to:

$$\left(\frac{\left[\text{node 2 conc.} - \text{well mixed node 1 volume conc.} \right]}{\Delta \rho} \right) \qquad (5-79)$$

This treatment was used by Svedberg (125), and no

problems were noted with this treatment either in his

work or in the simulations carried out in this project.

The second boundary condition to be coupled to the

general equation was at the resin film interface. Here,

a derivative at the boundary must be replaced by a

finite difference representation. In at least one reference of many, V. G. Jenson & G. V. Jeffreys (47) suggest using a fictitious point beyond that boundary, which is eliminated by combination with the general equation. Svedberg (125) used this procedure in his work. Boundary condition equation (5-60), in finite difference representation would be:

$$
(5\text{-}80)
$$

$$
\frac{4\ Q_r\ \bar{D}_{11}}{Bi_1\ norm} \cdot \left[\left[\frac{\left[\bar{x}_1(M+1,i,j+1)_{n+1} - \bar{x}_1(M-1,i,j+1)_{n+1} \right]}{4 \cdot \Delta\rho} \right] \right.
$$

$$
\left. + \left[\frac{\left[\bar{x}_1(M+1,i,j) - \bar{x}_1(M-1,i,j) \right]}{4 \cdot \Delta\rho} \right] \right]
$$

$$
= \left[\frac{\left[x_{1_{bulk}}(i,j+1)_{n+1} - x_{1_{bulk}}(i,j) \right]}{2} \right]
$$

$$
- \left[\frac{\left[x_{1_{int}}^{*}(i,j+1)_{n+1} + x_{1_{int}}^{*}(i,j) \right]}{2} \right]
$$

where M = maximum m node, and M+1 is a fictitious point outside the resin boundary

By setting up the general equation in a central difference notation, all M + 1 terms can be eliminated by cross multiplying coefficients and adding the B.C. equation to the general equation. The coefficients for the M and M-1 nodes are then obtained together with the solution vector for the Mth node which contains M and M-1 resin node elements, plus column fluid phase composition elements at the i column node. These resin

phase boundary condition treatments were used with the
Ternary Column Model development as well, though the
derivations were obviously more complicated algebraically
because of equations for two species versus one.

2. <u>Ternary System</u>

When the partial differential equations describing ternary
ion exchange are put into matrix notation, there results:

$$(5-81)$$

$$A_{i_n} \cdot \bar{x}_{1_{i_{n+1}}} = D_{i_n} + R_{i_n} \cdot \bar{x}_{2_{i_{n+1}}} + E1_n \cdot x_{1_{bulk}}(i,j+1)_{n+1} - E2_n \cdot x_{2_{bulk}}(i,j+1)_{n+1}$$

and:

$$(5-82)$$

$$\Lambda_{i_n} \cdot \bar{x}_{2_{i_{n+1}}} = \Pi_{i_n} + \Theta_{i_n} \cdot \bar{x}_{1_{i_{n+1}}} + \Omega2_n \cdot x_{2_{bulk}}(i,j+1)_{n+1} - \Omega1_n \cdot x_{1_{bulk}}(i,j+1)_{n+1}$$

where

$$(5-83) \qquad (5-84)$$

$$A_{i_n} = \begin{pmatrix} a_1 & b_1 & & & \\ c_2 & a_2 & b_2 & & \\ & & \ddots & & \\ & & c_m & a_m & b_m \\ & & & \ddots & \\ & & & c_M & a_M \end{pmatrix}_{i,n} \quad \text{and} \quad \bar{x}_{1_{i_{n+1}}} = \begin{pmatrix} \bar{x}_1(1,i,j+1) \\ \bar{x}_1(2,i,j+1) \\ \\ \bar{x}_1(m,i,j+1) \\ \\ \bar{x}_1(M,i,j+1) \end{pmatrix}_{n+1}$$

$$(5-85) \qquad (5-86)$$

$$R_{i_n} = \begin{pmatrix} r_1 & s_1 & & & \\ t_2 & r_2 & s_2 & & \\ & & \ddots & & \\ & & t_m & r_m & s_m \\ & & & \ddots & \\ & & & t_M & r_M \end{pmatrix}_{i,n} \quad \text{and} \quad \bar{x}_{2_{i_{n+1}}} = \begin{pmatrix} \bar{x}_2(1,i,j+1) \\ \bar{x}_2(2,i,j+1) \\ \\ \bar{x}_2(m,i,j+1) \\ \\ \bar{x}_2(M,i,j+1) \end{pmatrix}_{n+1}$$

$$D_{i_n} = \begin{bmatrix} d(1,i,j) \\ d(2,i,j) \\ \\ d(m,i,j) \\ \\ \\ d(M,i.j) \end{bmatrix}_n \quad (5\text{-}87)$$

$$\text{and } E1_n = \begin{bmatrix} o \\ o \\ \\ o \\ \\ \\ e_1 \end{bmatrix}_n \quad (5\text{-}88)$$

$$E2_n = \begin{bmatrix} o \\ o \\ \\ o \\ \\ \\ e_2 \end{bmatrix}_n \quad (5\text{-}89)$$

It is noted that the vector D_{i_n} contains both $\bar{x}_1$ and $\bar{x}_2$ terms resulting from time step j or iteration n of non-linear term components resulting from quasilinearization.

Similarly

$$\Lambda_{i_n} = \begin{bmatrix} \lambda_1 & \mu_1 & & & \\ k_2 & \lambda_2 & \mu_2 & & \\ & & & & \\ & k_m & \lambda_m & \mu_m & \\ & & & & \\ & & k_M & \lambda_M \end{bmatrix}_{i,n} \quad (5\text{-}90)$$

$$\text{and } \bar{x}_{2_{i_{n+1}}} = \begin{bmatrix} \bar{x}_2(1,i,j+1) \\ \bar{x}_2(2,i,j+1) \\ \\ \bar{x}_2(m,i,j+1) \\ \\ \bar{x}_2(M,i,j+1) \end{bmatrix}_{n+1} \quad (5\text{-}91)$$

$$\Theta_{i_n} = \begin{bmatrix} \theta_1 & \iota_1 & & & \\ \eta_2 & \theta_2 & \iota_2 & & \\ & & & & \\ & \eta_m & \theta_m & \iota_m & \\ & & & & \\ & & \eta_M & \theta_M \end{bmatrix}_{i,n} \quad (5\text{-}92)$$

$$\text{and } \bar{x}_{1_{i_{n+1}}} = \begin{bmatrix} \bar{x}_1(1,i,j+1) \\ \bar{x}_1(2,i,j+1) \\ \\ \bar{x}_1(m,i,j+1) \\ \\ \bar{x}_1(M,i,j+1) \end{bmatrix}_{n+1} \quad (5\text{-}93)$$

$$\Pi_{i_n} = \begin{bmatrix} \pi(1,i,j) \\ \pi(2,i,j) \\ \\ \\ \pi(m,i,j) \\ \\ \\ \pi(M,i,j) \end{bmatrix}_n \quad (5\text{-}94) \qquad \text{and} \quad \Omega2_n = \begin{bmatrix} 0 \\ 0 \\ \\ \\ 0 \\ \\ \\ \omega_2 \end{bmatrix}_n \quad (5\text{-}95) \qquad \Omega1_n = \begin{bmatrix} 0 \\ 0 \\ \\ \\ 0 \\ \\ \\ \omega_1 \end{bmatrix}_n \quad (5\text{-}96)$$

noting here too that the vector Π_{i_n} contains both $\bar{x}_1$ and $\bar{x}_2$ terms resulting from the time step j or iteration n of non-linear term components resulting from quasilinearization.

The system of equations for the ternary case, as was shown in the binary case, is set up for coupling to two systems of equations describing the values of $x_{1_{bulk}}$ $(i,j+1)_{n+1}$ and $x_{2_{bulk}}$ $(i,j+1)_{n+1}$ in the solution phase moving through a column at nodes $i = 1$ to $i = I$. In the "batch" case, $x_{1_{bulk}}$ and $x_{2_{bulk}}$ are constant, so the terms $E1_n \cdot x_{1_{bulk}}$, $E2_n \cdot x_{2_{bulk}}$, $\Omega1_n \cdot x_{1_{bulk}}$, and $\Omega2_n \cdot x_{2_{bulk}}$ can be added to the vectors D_{i_n} and Π_{i_n} respectively--and subscripts i are not used.

When the system of equations described in matrix notation as equation (5-81) and equation (5-82) are combined, a 7 diagonal array results. This is illustrated in Figure 5-1 for a resin phase divided into four ρ segments, or M=5 nodes. An algorithm, analogous to the Thomas method (13, 125) for tri-diagonal arrays, was derived as part of this research to solve systems consisting of 7 diagonal coefficient matrices. The algorithm is given in Appendix E, along with an algorithm derived for a 5 diagonal

Figure 5-1

Seven Diagonal Array for Combined Ternary
Resin Phase Equation Matrices

for ρ divided into 4 segments, or m = 5 nodes

$$
\begin{bmatrix}
a_{1,i} & -r_{1,i} & b_{1,i} & -s_{1,i} & 0 & 0 & 0 & 0 & 0 & 0 \\
-\theta_{1,i} & \lambda_{1,i} & -\int_{1,i} & \mu_{1,i} & 0 & 0 & 0 & 0 & 0 & 0 \\
c_{2,i} & -t_{2,i} & a_{2,1} & -r_{2,i} & b_{2,i} & -s_{2,i} & 0 & 0 & 0 & 0 \\
-\eta_{2,i} & \kappa_{2,i} & -\theta_{2,i} & \lambda_{2,i} & -\int_{2,i} & \mu_{2,i} & 0 & 0 & 0 & 0 \\
0 & 0 & c_{3,i} & -t_{3,i} & a_{3,i} & -r_{3,i} & b_{3,i} & -s_{3,i} & 0 & 0 \\
0 & 0 & -\eta_{3,i} & \kappa_{3,i} & -\theta_{3,i} & \lambda_{3,i} & -\int_{3,i} & \mu_{3,i} & 0 & 0 \\
0 & 0 & 0 & 0 & c_{4,i} & -t_{4,i} & a_{4,i} & -r_{4,i} & b_{4,i} & -s_{4,i} \\
0 & 0 & 0 & 0 & -\eta_{4,i} & \kappa_{4,i} & -\theta_{4,i} & \lambda_{4,i} & -\int_{4,i} & \mu_{4,i} \\
0 & 0 & 0 & 0 & 0 & 0 & c_{5,i} & -t_{5,i} & a_{5,i} & -r_{5,i} \\
0 & 0 & 0 & 0 & 0 & 0 & -\eta_{5,i} & \kappa_{5,i} & -\theta_{5,i} & \lambda_{5,i}
\end{bmatrix}_{n^{th}}
\times
\begin{bmatrix}
\bar{x}_1(1,i,j+1) \\
\bar{x}_2(1,i,j+1) \\
\bar{x}_1(2,i,j+1) \\
\bar{x}_2(2,i,j+1) \\
\bar{x}_1(3,i,j+1) \\
\bar{x}_2(3,i,j+1) \\
\bar{x}_1(4,i,j+1) \\
\bar{x}_2(4,i,j+1) \\
\bar{x}_1(5,i,j+1) \\
\bar{x}_2(5,i,j+1)
\end{bmatrix}_{n+1^{th}}
=
\begin{bmatrix}
d(1,i,j) \\
\pi(1,i,j) \\
d(2,i,j) \\
\pi(2,i,j) \\
d(3,i,j) \\
\pi(3,i,j) \\
d(4,i,j) \\
\pi(4,i,j) \\
d(5,i,j) \\
\pi(5,i,j)
\end{bmatrix}_{n^{th}}
$$

Note that the vectors $d(5,i,j)$ and $\pi(5,i,j)$ represent the resin boundary with the fluid, and contain $x_{1_{bulk}}(i,j)$ and $x_{2_{bulk}}(i,j)$ terms from the fluid phase, as well as n iteration terms from the quasilinearization of equilibrium terms. The vector terms

$e_{1_n} x_{1_{bulk}}(i,j+1)_{n+1}$, $e_{2_n} x_{2_{bulk}}(i,j+1)_{n+1}$ and $\omega_{1_n} x_{1_{bulk}}(i,j+1)_{n+1}$ and $\omega_{2_n} x_{2_{bulk}}(i,j+1)_{n+1}$ are added to $d(5,k,j)$ and $\pi(5,i,j)$ respectively.

coefficient matrix, which is needed to solve the combined fluid phase equation matrices. These algorithms were tested in a program designed in this project to generate a system of equations with coefficients created by a random number generator subroutine. The solution vector terms were calculated for sequences of numbers representing values of the unknown, x_i. Values of x_i calculated by the algorithms, using the predetermined coefficients and calculated solution vectors, were compared to the original values of the variables for matrices up to 500 by 500. Absolute precision of around 1 part in 10^{10} is maintained for the largest matrix; however, most simulations were run with 11 or 21 resin nodes--generating 22 x 22 or 42 x 42 matrices. Absolute precision for a 50 x 50 matrix was about 1 part in 10^{12}. These tests were conducted in double precision on a DEC VAX 11/780 computer.

D. Programs for Simulation of Binary & Ternary Batch Systems

Two simulation programs were developed for so-called batch experiments--one for binary systems called BMAVDM (Batch Mass Action (Equilibrium) Variable Diffusivity Mole Fraction) and one for ternary systems called TRYBCH (Ternary Batch). BMAVDM can be run with mass action equilibrium constants and Redlich-Kister activity coefficient parameters correlated in equivalent fractions or mole fractions--hence the designation mole fraction. It can be run with or without activity driving force, and with fixed film coefficients. It also can be run with the model developed in this work for concentration dependent film coefficients, or with the Kataoka-Yoshida model (50) with electric

field in the film (equal valence exchange only). The program was
designed for use in a diffusion coefficient correlation package and,
therefore, has minimum output options. The initial conditions are set
up by matching the diffusion flux at the resin boundary using equation
(5-60):

$$\frac{4 \cdot Q_r}{Bi_1 \cdot norm} \cdot \frac{\partial \bar{x}_1}{\partial \rho}\bigg|_{\rho=1} \bar{D}_{11}' = (x_{1_{bulk}} - x^*_{1_{int}})$$

The term $\dfrac{\partial \bar{x}_1}{\partial \rho}\bigg|_{\rho=1}$ is calculated using a backward difference numerical
representation between resin layer M and M-1. This "conditions" the
program to begin at the first time step. At each time step, a
subroutine computes the diffusivity, the film coefficient, the
term $\dfrac{\partial \bar{D}_{11}'}{\partial \bar{x}_1}$, and activity effects on the diffusivity coefficient if
that option is chosen, plus other components of the solution vector
D_j, based on concentration values at time step j. Another subroutine
computes the equilibrium quasilinearization derivatives at each
iteration during time step j+1, and yet another subroutine computes the
electrolyte phase equilibrium after convergence criteria have been met
at j+1. The equilibrium subroutines are supported by subroutines which
compute resin and fluid phase activity coefficients. The key
subroutine solves the system of equations representing the resin
concentration profile at time step j+1. It is called by the main
program in successive iterations as the coefficient matrix is updated,
and the solution vector is recomputed for n[th] values of terms
resulting from quasilinearization at each iteration. The Thomas
algorithm (13, 125) for tridiagonal arrays is utilized. The main

program continues to iterate at each time step until convergence criteria are met, then proceeds to the next time step. Criterion for convergence normally employed was:

$$\frac{(x_{1_{n+1}} - x_{1_n})}{x_{1_{n+1}}} < 10^{-4} \text{ to } 10^{-5}$$

Iterations averaged 2-3 per time step.

TRYBCH is obviously more complex, since it deals with components $\bar{x}_1$, $\bar{x}_2$, $x_{1_{bulk}}$, and $x_{2_{bulk}}$, but the solution principles are the same. The major difference is that a "scratch" seven diagonal array subroutine is used into which updated coefficient values are loaded at each time step and iteration; then the variables which have been solved are sorted into $\bar{x}_1(m,j+1)$ & $\bar{x}_2(m,j+1)$ values. Actually two "scratch" arrays are used--one which loads $\bar{x}_1$ as the first variable if $\bar{x}_2(1,j)$ is smaller than $\bar{x}_1(1,j)$ and vice versa, since it was found in the algorithm simulation that precision was improved if this condition was maintained. TRYBCH contains a significant number of output options, including printout of concentrations and flux balances at the resin/fluid interface. In both BMAVDM and TRYBCH average resin concentration is computed at each time step by summing the particle increments, since experimental data would represent particle average concentration.

E. Correlation of Diffusivities for Systems Studies by Rao, and his Coworkers

    1.   Experimental Background

          Rao and his coworkers (92, 93) used single particle

radioactive tracer techniques to study the binary and ternary exchange of cations in Dowex 50w x8 resin, in addition to measuring the binary and ternary equilibrium for those ionic species. The two systems studies were $Sr^{++}-Mn^{++}-Cs^+/Cl^-$ and $Mn^{++}-Cs^+-Na^+/Cl^-$ at 0.1 normal solution concentrations at $28^\circ C$. Several resin beads about 0.1 cm. diameter were put into a column filled with glass beads of about the same diameter. Circulation from a large reservoir through the column at a high superficial velocity of 25 cm/sec insured that the bulk solution concentration was unchanged during the runs, and that film diffusion "control" was minimized. A scintillation detector, with output suitably corrected for background noise, was calibrated to read out the concentration change of the tagged species in the resin beads. Favorable and unfavorable exchanges were studied for binary & ternary compositions of the two cation systems. The equilibrium data were reproducible to ± 2%. In the rate studies, the radioactive ^{137}Cs was evidently of poor purity, and runs in which ^{137}Cs was exchanged were discarded.

2. Model Comparison - Rao and his Coworkers and Those Developed in This Research

Rao and his coworkers (92, 93) used the Nernst-Planck resin diffusion model to simulate the runs, in combination with a film diffusion model somewhat analogous to the model developed for this research project. Major model differences between Rao and his coworkers and this work involve:

o   Film Coefficient

Rao and his coworkers used a fixed "hydrodynamic film thickness" and ionic species diffusivities derived from limiting (infinite dilution) ionic mobilities. This research project used a similar interdiffusivity relationship between ionic species in the film, but corrected the film "thickness" based on boundary layer treatment of the species having the highest flux, and corrected limiting diffusivities for concentration efforts.

o   Equilibrium

Rao and his coworkers (92, 93) used polynomial expressions for the equilibrium distribution coefficients

$$\lambda_1 = \frac{\bar{x}_{1_{int}}}{\bar{x}_{1_{int}}^*} \quad , \text{ of the form } \lambda_1 = a + b\bar{x}_{1_{int}} + c\bar{x}_{1_{int}}^2 \;.$$

For prediction of ternary behavior, the binary coefficients were combined by use of pseudo equivalent fractions obtained by elimination of one or the other of the minor concentration components in the resin. Harned's Rule (Chapter III) was invoked for the solution phase, so activity coefficients were not used in either the resin phase or solution phase in establishing equilibrium constants. The equilibrium treatment utilized by Rao and his coworkers is described in more detail in Chapter II on Equilibrium.

This work used the Bromley equation for liquid phase activity coefficients, and binary and ternary resin phase

activity coefficients were correlated with the Redlich-Kister

relationship (actually the Wilson and NRTL equations were

also used in the thermodynamic correlation but found inferior

to the R-K equations for ion exchange). By being able to

calculate activity coefficients for the resin phase as

functions of composition, activity driving forces could be

tested versus concentration driving forces. As will be

discussed, the use of activities gave some surprisingly

positive results.

o   Method of Solving Partial Differential Equation

Rao and his coworkers used an integro differential

equation in that:

$$\text{o} \qquad \bar{x}_{i_{ave_t}} = \frac{3}{r_o{}^3} \cdot \int_o^{r_o} \bar{x}_i(r,t) \cdot r^2 \cdot dr \qquad (5\text{-}97)$$

$$(i=1,2,3)$$

was used to describe particle concentration history in

combination with the basic partial differential equations

describing fluxes J_1 & J_2, equations (5-34), (5-35),

together with (5-10) and (5-11). A finite difference

approximation with forward differencing was utilized to solve

the equations.

3.   Correlation Model

3.1   General Background

A powerful general purpose non-linear regression program

was developed by Dr. A. K. S. Murthy at Allied Corporation

several years ago.

A general description of the technique is given in Appendix B; however, Dr. Murthy developed the program in two forms. Both versions are variations of the Gauss-Newton method and are identical in all respects except for the sequence in which the elements of the matrices, B^TB and B^Te, defining the normal equation are generated. In both cases, the objective function is e^Te (least square criterion). The method allows weighting of data points or data sets appropriate to the users view of the "goodness" of one set of data versus others being correlated in the same regression analysis (default weight is unity). In the generation of the matrix elements, this weighting factor is appropriately built into the error definition, the e vector. In both versions, each parameter to be fit is perturbed by an appropriate fraction and numerical derivatives of the functions being described are generated with respect to each variable, and other associated calculations are performed. In neither version is the full B matrix ever generated, and this significantly reduces memory requirements. The first version is used to fit parameters in non-linear algebraic equations, such as those describing ion exchanger equilibria in this work, by operating on each point sequentially to generate matrix elements. The second version deals with differential equations such as those describing time varying systems, and in this work were the binary "batch" ion exchange experiments to which diffusion coefficients were fitted. In the latter case it is more efficient to

"simultaneously" generate the elements of the $B^T B$ and $B^T e$

matrices from all of the points varying with time in a given

set, and in this version the sets are then treated

sequentially. In both cases

total sum of squares relative difference $\left(\dfrac{y_{exp} - y_{calc}}{y_{exp}}\right)^2$

for all points (sets) are minimized until convergence

criteria have been met, and best values for the fitted

parameters are obtained. Standard deviations for all

parameters and cross correlation values are printed out at

the end of a run. BMAVDM was appended to this second

non-linear regression program, and the Rao and his coworkers

data sets for seven binary systems were fitted using this

regression program--called DFUSFT (DiFfUSion Coefficient

FiTting Program) to yield diffusion coefficients correlated

for the four species, Sr^{++}, Mn^{++}, Cs^{+}, & Na^{+}.

3.2 Simulations Performed on Rao and his Coworkers' (92, 93)

Experiments

a. Data Sets

Several sets of conditions were used to obtain the

best total fit of the seven binary pairs of ionic

species. The pairs for which data was available were:

$\overline{Sr}^{++}-Mn^{++}$ $\overline{Mn}^{++}-Sr^{++}$

$\overline{Sr}^{++}-Cs^{+}$ $\overline{Mn}^{++}-Cs^{+}$

$\overline{Mn}^{++}-Na^{+}$ $\overline{Na}^{+}-Mn^{++}$

$\overline{Na}^{+}-Cs^{+}$
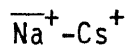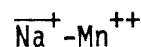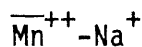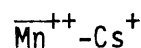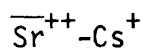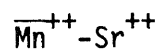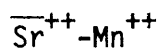
If the ^{137}Cs runs had been useful, 3 more sets would have been available, $\overline{Cs}^+Sr^{++}$, $\overline{Cs}^+Mn^{++}$ & $\overline{Cs}^+Na^+$, but as discussed, Rao et al discarded those runs because of purity problems.

b. Experiments Conducted

The conditions which were tested included:

(i)   Concentration driving force for all seven sets

(ii)   Activity driving force for all seven sets

(iii) Activity driving force for the four diffusion coefficients, and a fifth parameter, FLAMDJ, which fractionally modified the constant in the Carberry film correlation from its stated value of 1.15 (as applied to all sets--not individually adjusted for each set).

(iv)   Fitting of six sets which excluded what appears to be a "maverick" data set, $\overline{Sr}^{++}Mn^{++}$ for both activities and concentration driving force.

(v)   A correlation of just the data sets $\overline{Sr}^{++}Mn^{++}$ and $\overline{Mn}^{++}Sr^{++}$ to get a feel for the magnitude of changes in both $\overline{D}'_{Sr^{++}}$ and $\overline{D}'_{Mn^{++}}$ in order to fit the "maverick" data set.

(vi)   A correlation of seven data sets with the $\overline{D}'_{Sr^{++}}$ and $\overline{D}'_{Mn^{++}}$ fixed at the values obtained above to fit values for $\overline{D}'_{Na^+}$ and $\overline{D}'_{Cs^+}$ under these conditions, and to compare total seven system error with other runs listed above.

(vii) A correlation of five data sets with a "binary"

diffusion model using concentration driving force to compare coefficients and total error with the same five data sets correlated using single diffusion coefficients with activities as the driving force. The "binary" diffusion model introduced the concept of an additional diffusion coefficient pair corrector parameter as an emulation of some recent work by E. E. Graham and J. S. Dranoff (30) on ion exchange in which the Stefan-Maxwell equations were applied to diffusion kinetics in the resin. The five additional pair corrector parameters introduced were $Sr^{++}-Mn^{++}$, $Sr^{++}-Cs^{+}$, $Mn^{++}-Cs^{+}$, $Mn^{++}-Na^{+}$, and $Cs^{+}-Na^{+}$. Five sets were selected to minimize computer time, since the fitting of nine parameters for five data sets containing a total of 136 data points was lengthy (6 hours in CPU time on a DEC VAX 11/780).

4. Discussion of Results

4.1 General Observations

A summary of these results is given in Table 5-3, and sample variance, is given as an indicator of goodness of fit, where

$$(5\text{-}98)$$

$$\text{sample variance} = \frac{\displaystyle\sum_{\text{set}=1}^{n}\ \sum_{\text{point}=1}^{m}\left(\frac{\bar{x}_{1_{\text{ave}_{\text{exp}}}} - \bar{x}_{1_{\text{ave}_{\text{calc}}}}}{\bar{x}_{1_{\text{ave}_{\text{exp}}}}}\right)^{2}}{(\text{total no. of exp. points})}$$

Table 5-3

SUMMARY – FITTED DIFFUSION COEFFICIENTS
EXPERIMENTAL DATA OF G. RAO et al

– Binary Systems of Sr^{++}-Mn^{++}-Cs^{+}-Na^{+}/Cl^{-} on Dowex 50w x8 Resin –

All values of $\bar{D}i'$ x10^6 cm^2/sec

Description of Correlation Experiment	$\bar{D}'_{Mn^{++}}$ Value	STDV	$\bar{D}'_{Sr^{++}}$ Value	STDV	$\bar{D}'_{Cs^{+}}$ Value	STDV	$\bar{D}'_{Na^{+}}$ Value	STDV	Sample Variance s^2
Seven Sets									
• Concentration Driving Force	0.330316±	0.00761	0.148729±	0.0050	10.00	± 0.083	2.07116	± 0.0519	0.0026
• Activity Driving Force	0.322405±	0.00684	0.139227±	0.0038	3.96189	± 0.347	2.74910	± 0.0977	0.00213
• Activity Driving Force with Fit of FLMADJ = 0.8636 ± 0.039	0.33877	± 0.0103	0.142827±	0.00396	4.36702	± 0.475	2.77647	± 0.101	0.00220
• Fit $\bar{S}r^{++}$-Mn^{++}, $\bar{M}n^{++}$-Sr^{++}, Activities	0.88036	± 0.000805	0.084604±	0.0009	----		----		0.00044
• Fit Other Sets, $\bar{D}'_{Sr}$ + $\bar{D}'_{Mn}$+ Fixed	0.88036	± 0.000805	0.08460 ±	0.0009	2.41534	± 0.062	2.0047	± 0.119	0.0269
Six Sets- $\bar{S}r^{++}$-Mn^{++}Excluded									
•Concentration Driving Force	0.32907	± 0.00426	0.184811±	0.0044	9.84776	± 0.134	2.1170	± 0.0308	0.00089
• Activity Driving Force	0.320027±	0.0039	0.172243±	0.0034	3.43355	± 0.155	2.87574	± 0.061	0.00076
Five Sets- $\bar{N}a^{+}Mn^{++}$Excluded									
• Activity Driving Force	0.35592	± 0.00233	0.178738±	0.0017	2.51790	± 0.0525	3.63666	± 0.0575	0.00014
• "Binary" Model[1]	0.149521		0.844332		3.82155		3.21048		0.00011
Pair Corrector									
$Mn^{++}Cs^{+}$	0.25878		---		0.25878		---		
$Mn^{++}Sr^{+}$	0.029884		0.029884		---		---		
$Mn^{++}Na^{+}$	0.072910		---		---		0.072910		
$Sr^{++}Cs^{+}$	---		-0.639182		-0.639182		---		
$Na^{+}Cs^{+}$	---		---		-0.231135		-0.231135		
• Correlated by Rao et al Ref (92,93)	0.22	± N/A	0.195	± N/A	3.0 Estimated		2.05	± N/A	0.0083

(1) Std. dev. not available – these are printed out at end and this set of "correctors" was picked as representing the least total required correction out of several iterations having the same total error.

Figures 5-2 and 5-3 show the best fit of <u>seven</u> sets using <u>activity driving force</u> and the diffusion coefficients derived from that correlation, plotted against lines representing the Rao et al experimental data for the binary systems. The calculated curves in general match the experimental data very well, except for the $\overline{Sr}^{++}$-Mn^{++} and $\overline{Mn}^{++}$-Sr^{++} systems. If the $\overline{Sr}^{++}$-Mn^{++} system is not included in the fit, calculated points for the system $\overline{Mn}^{++}$-Sr^{++} fit the experimental curves very well. The film correlation constant "adjuster," FLMADJ, was kept at 1.0 for the final selected set of parameters utilized in generating the plots. A FLMADJ of 0.86 ± 0.04, derived from the parameter study which included FLMADJ, would indicate the Carberry coefficient of 1.15 is reasonable, and since the Re no. was not varied in the Rao and his coworkers' experiments (92, 93) no other conclusion could be drawn.

4.2 Significance of the Batch Experiment Results

The recent work of E. E. Graham and J. S. Dranoff (30) on application of the Stefan-Maxwell equations to diffusion of ionic species in ion exchange resins was undertaken because previous investigators, using the Nernst-Planck model, were unable to define so-called "self diffusion" coefficients for a given ionic species which would have the same value regardless of the other ionic species present during the exchange. Studies by

Figure 5-2

Binary Exchange for Pairs in System $Sr^{++} - Mn^+ - Cs^+$, Dowex 50W x8, Cl^-

Binary Model – Nernst Planck/Variable Film Coefficient
Activities are Driving Force

0.10 Normal

COMPUTED	ION IN RESIN	ION IN SOLUTION
O	Sr^{++}	Mn^{++}
+	Mn^{++}	Sr^{++}; x Fit w/o Sr Mn System (Top Curve)
□	Mn^{++}	Cs^+
△	Sr^{++}	Cs^+

Experimental Curves – Temp 28°C
R.K. Batjpai, A.K. Gupta, M. Gapola Rao
'AlChE Journal', Sept, 1974 (Vol 20, No 5)

'SELF' DIFFUSION COEFFICIENTS   Std Dev

$D_{SR} = 0.139227 E{-}06$ $\pm 0.0038 E{-}06 \, cm^{-2}/sec$
$D_{MN} = 0.322405 E{-}06$ $\pm 0.0068 E{-}06 \, cm^{-2}/sec$
$D_{CS} = 0.396198 E{-}05$ $\pm 0.0347 E{-}05 \, cm^{-2}/sec$

Y-axis (left): Fractional Conversion EQF. (Time)/EQF. (Initial)

X-axis: Elapsed Time – Sec.

Curve labels: SrMn, MnSr, MnCs, SrCs

Figure 5-3
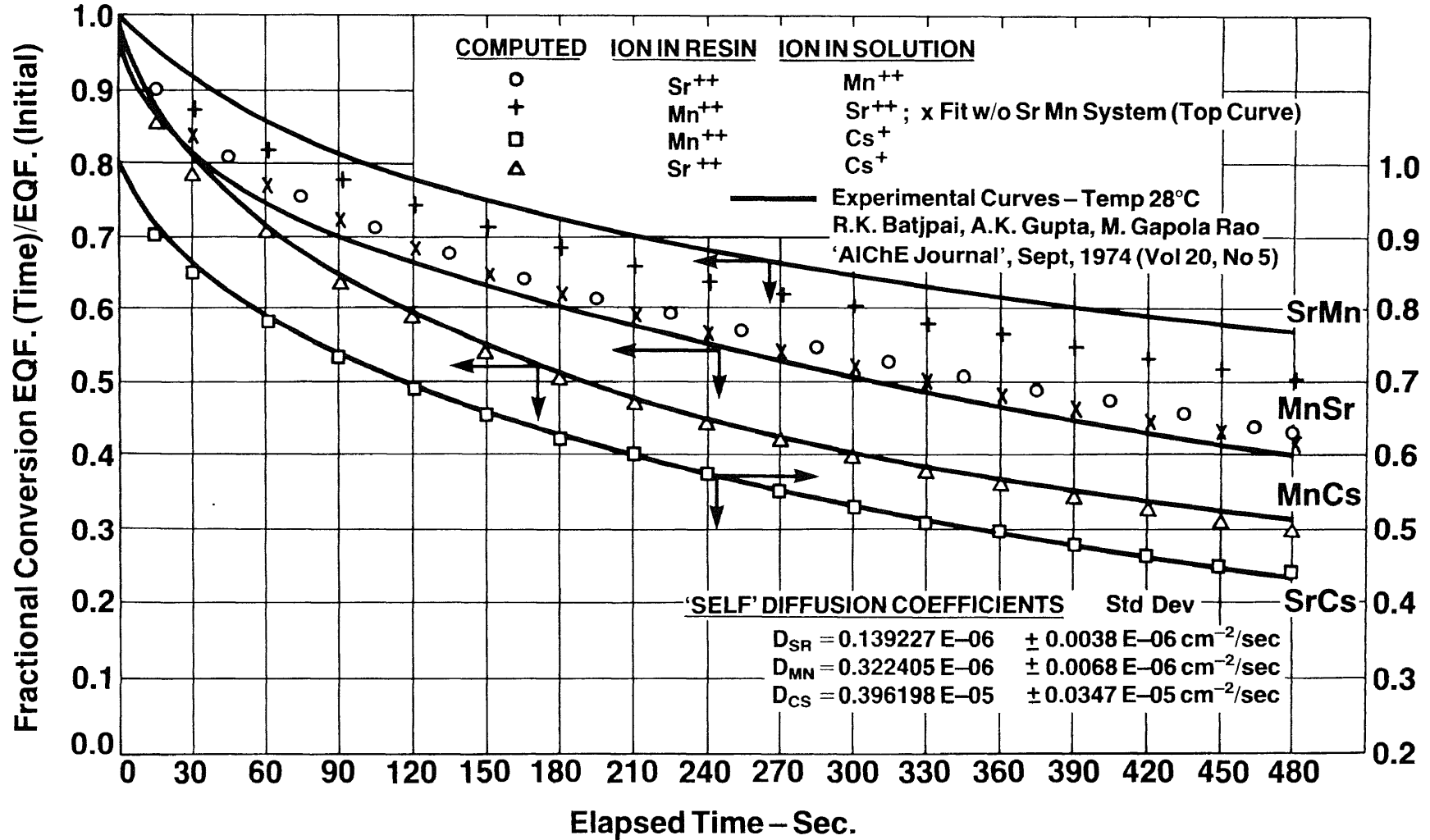
Binary Exchange for Pairs in System $Mn^{++} - Cs^+ - Na^+$, Dowex 50W x8, Cl^-
Binary Model – Nernst Planck/Variable Film Coefficient
Activities are Driving Force
0.10 Normal

COMPUTED	ION IN RESIN	ION IN SOLUTION
○	Mn^{++}	Na^+
+	Mn^{++}	Cs^+
□	Na^+	Mn^{++}
△	Na^+	Cs^+

Experimental Curves – Temp 28°C
R.K. Batjpai, A.K. Gupta, M. Gapola Rao
'AIChE Journal', Sept, 1974 (Vol 20, No 5)

MnNa

MnCs

NaMn

NaCs

'SELF' DIFFUSION COEFFICIENTS	Std Dev
$D_{MN} = 0.322405$ E–06	± 0.0068 E–06 cm^{-2}/sec
$D_{CS} = 0.396189$ E–05	± 0.0347 E–05 cm^{-2}/sec
$D_{NA} = 0.274910$ E–05	± 0.0098 E–05 cm^{-2}/sec

Fractional Conversion EQF. (Time)/EQF. (Initial)

Elapsed Time – Sec.
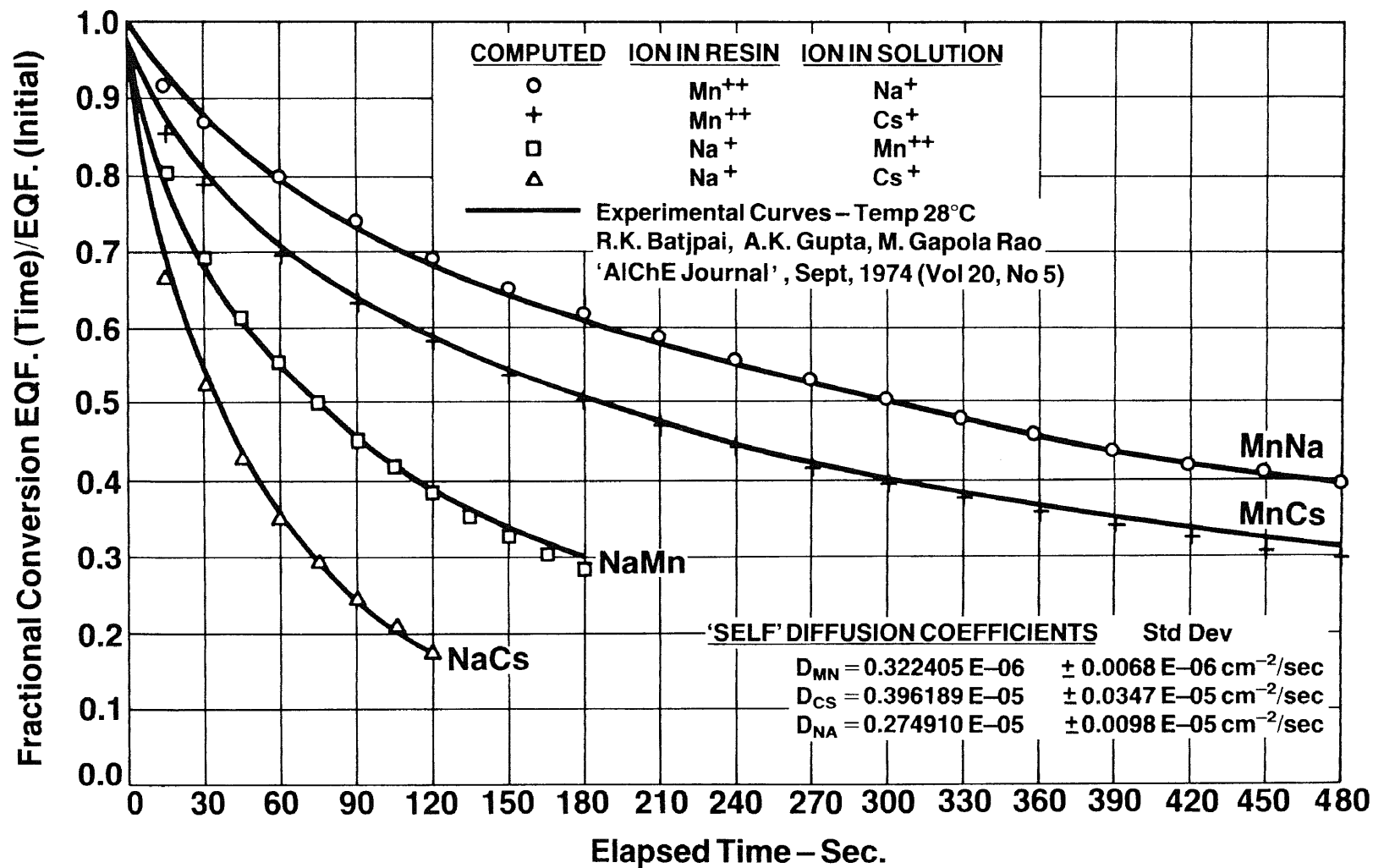
Hering and Bliss (46) on various cation pairs using

Dowex 50w x8 resin at $25^{\circ}C$ for an ion electrolyte

concentration of 1.0 normal showed the following results

(correlated for exchange in both directions):

Diffusion Coefficient x 10^6 cm^2/sec

System	Nernst Planck Model	Fick's Law Model
$Na^+\text{-}Zn^{++}$	$\bar{D}'_{Na} = 2.03$	$\bar{D}'_{Na,Zn} = 0.971$
	$\bar{D}'_{Zn} = 0.231$	$\bar{D}'_{Zn,Na} = 0.395$
$Na^+\text{-}Ag^+$	$\bar{D}'_{Na} = 2.05$	$\bar{D}'_{Na,Ag} = 1.43$
	$\bar{D}'_{Ag} = 0.683$	$\bar{D}'_{Ag,Na} = 0.86$
$Ag^+\text{-}Al^{+++}$	$\bar{D}'_{Ag} = 0.380$	$\bar{D}'_{Ag,Al} = 0.298$
	$\bar{D}'_{Al} = 0.112$	$\bar{D}'_{Al,Ag} = 0.180$
$Cu^{++}\text{-}Zn^{++}$	$\bar{D}'_{Cu} = 0.281$	$\bar{D}'_{Cu,Cn} = 0.230$
	$\bar{D}'_{Zn} = 0.0157$	$\bar{D}'_{Zn,Cu} = 0.181$
$Zn^{++}\text{-}Al^{+++}$	$\bar{D}'_{Zn} = 0.071$	$\bar{D}'_{Zn,Al} = 0.0692$
	$\bar{D}'_{Al} = 0.065$	$\bar{D}'_{Al,Zn} = 0.0648$
$Ce^{+++}\text{-}Al^{+++}$*	$\bar{D}'_{Al} = 0.0455$	$\bar{D}'_{Ce,Al} = 0.0120$
	$\bar{D}'_{Ce} = 0.0091$	

*Available for Ce^{+++} in exchanger only.

As Hering and Bliss (46) point out, the N-P model

is preferable to Fick's Law in that a single "effective"

diffusivity allows prediction of both favorable and

unfavorable exchange; whereas with Fick's Law, the

diffusion coefficients are different depending on

direction of exchange, with the coefficient invariably

higher when the faster ion is in the exchanger. Rao and

his coworkers (92) pointed out in their studies that variation of "self" diffusion coefficients of the ionic species with ionic composition of the resin was not taken into account in their analysis, adding that cross phenomenological coefficients and activity coefficients in the resin phase were neglected in development of their model. Graham and Dranoff (30), although successful in fitting the Na^+-Cs^+ system with their Stefan-Maxwell model, were treating a fairly "ideal" system in terms of limiting activity coefficients determined in this work where $\overline{\gamma}_{Cs}^{-\infty}+ = 0.78$, and $\overline{\gamma}_{Na}^{-\infty}+$ = 1.043. In the case of Sr^{++}-Cs^+ studies in this project, limiting activity coefficients were $\overline{\gamma}_{Sr}^{-\infty}++$ = 0.526, $\overline{\gamma}_{Mn}^{-\infty}++$ = 0.544 (or when correlated with M.F. versus Equiv. Fraction $\overline{\gamma}_{Sr}^{-\infty}++$ = 0.331, $\overline{\gamma}_{Mn}^{-\infty}++$ = 0.464). Graham and Dranoff in their derivation have assumed that Harned's Rule applied in the exchanger phase, i.e.,

$$\left(\frac{\partial \ell n \overline{\gamma}_i}{\partial \overline{x}_i}\right)_{\overline{x}_{active\ sites}} = constant$$

They point out that the Helfferich definition (42) of interdiffusion coefficient for binary exchange (equation 5-13) fits limiting tracer ion data (limiting diffusion values of species 1 migrating in resin essentially loaded with species 2) if the term

$$\frac{\overline{D}_1 \cdot \overline{D}_2}{\sum\limits_{i=1}^{2} \overline{x}_i \cdot \overline{D}_i \cdot |z_i|} \cdot \overline{x}_1 \cdot \overline{x}_2 \cdot \frac{\partial \ell n\left[\frac{\overline{\gamma}_1^{|z_2|}}{\overline{\gamma}_2^{|z_1|}}\right]}{\partial \overline{x}_1}\Bigg|_{molar}$$

is included but treated as a constant, K, as in Harned's
Rule. They suggest that further investigation be made
into the use of Gibbs-Duhem relationship so as to
include the pressure gradient for water flux in the
resin. This is tantamount to saying look at activity
driving forces in the resin, since resin pressure volume
relationships are functions of total system chemical
potential for all species--including water. The final
equation derived by Graham and Dranoff (30) defines
"effective" Nernst-Planck diffusion coefficients as:

$$
\text{o} \qquad d_{1(2)} = \left(\cfrac{1}{\left[\left(\cfrac{\bar{x}_o}{a_{10}} \right) - \left[\left(\cfrac{z_a}{z_2} \right) \cdot \bar{x}_a \cdot \left[\left(\cfrac{1}{a_{12}} \right) - \left(\cfrac{z_2}{z_a} \right) \cdot \cfrac{1}{a_{1a}} \right] \right] \right]} \right) \qquad (5\text{-}99)
$$

$$
\text{o} \qquad d_{2(1)} = \left(\cfrac{1}{\left[\left(\cfrac{\bar{x}_o}{a_{20}} \right) - \left[\left(\cfrac{z_a}{z_1} \right) \cdot \bar{x}_a \cdot \left[\left(\cfrac{1}{a_{21}} \right) - \left(\cfrac{z_1}{z_a} \right) \cdot \cfrac{1}{a_{2a}} \right] \right] \right]} \right) \qquad (5\text{-}100)
$$

where:

$\bar{x}_a$ = mole fraction of active exchanger sites

z_a = valence of active exchanger sites

$\bar{x}_o$ = mole fraction of water in exchanger

a_{i0} = Stefan Maxwell interaction coefficient between ion species i and water

a_{ia} = Stefan Maxwell interaction coefficient between ion species i and active sites

a_{ij} = Stefan Maxwell interaction coefficient between ionic species

This suggested to the investigator in this work that a "simple" version of $d_{1(2)}$ and $d_{2(1)}$ might only require a single pair corrector coefficient for a given ion exchange resin, i.e., $\bar{D}_{12}=\bar{D}_1+\bar{d}_{12}$, and $\bar{D}_{21}=\bar{D}_2+\bar{d}_{12}$ where: $\bar{D}_1$ & $\bar{D}_2$ are the "self" diffusion coefficients and $\bar{d}_{12}$ is the pair "corrector."

This was tried in fitting the set of five ion species exchange curves and was very successful. However, an equally good fit to the set of five was obtained with only four parameters, the "effective self" diffusion coefficient for each species, and correcting for non-ideality by use of the activity driving force. Although the two parameter model effectively fit the data for binaries, it is not obvious how ternary systems could be modeled. Later discussion on the Rao and his coworkers' ternary experiments will include some simulations of ternary systems with the two parameter model in which:

$$\bar{D}'_{12} = \bar{D}'_1 + \left(\frac{\bar{x}_2}{(\bar{x}_2+\bar{x}_3)}\right)\cdot\bar{d}_{12} + \left(\frac{\bar{x}_3}{(\bar{x}_2+\bar{x}_3)}\right)\cdot\bar{d}_{13} \qquad (5\text{-}101)$$

and so forth for $\bar{D}_{21}$ and $\bar{D}_{13}$.

The modeling of all of the ternary data was performed with the activity driving force model since this model is sound theoretically, and the two parameter model discussed above is not. Although Table 5-3 shows that use of concentration driving force gave a fit on the set of seven with only a somewhat increased total

error, the diffusion coefficient for Cs^+ at a value of

10.0E-06 cm^2/sec was unreasonably high in view of

literature values around 2.0E-06 cm^2/sec. This was

true in comparisons made in correlation of the <u>set of</u>

<u>six</u> as well. In the two parameter model, if the pair

correctors are added to the effective diffusion

coefficient, the following values are obtained:

$$\bar{D}_i \times 10^6 \ cm^2/sec$$

Two Parameter Model			Activity Model
Ion	Pair Ion	$\bar{d}_{ij}$ corrector	
$\bar{D}'_{Mn}{}^{++}$	Sr^{++} Cs^+ Na^+	0.1795 0.4083 0.2224	} 0.3559
$\bar{D}'_{Sr}{}^{++}$	Mn^{++} Cs^+	0.8743 0.2051	0.1787
$\bar{D}'_{Cs}{}^+$	Mn^{++} Sr^{++} Na^+	4.080 3.182 3.590	} 2.518
$\bar{D}'_{Na}{}^+$	Mn^{++} Cs^+	3.282 2.980	3.637

The Sr^{++}-Mn^{++} pair shows the greatest

correction requirement, compared to the activity model;

however, most values are not "too different" from the

<u>single coefficient activity model</u> values.

Since the activity model was derived on a

theoretically sound basis and the parameter regressions

yielded diffusion coefficient values not far from

previously observed experimental values, it can be said

that the activity model performed "best" in all

simulations of the Rao and his coworkers' experimental

data.

Finally, Rao and his coworkers simulated their

experimental binary data for the set of five using the

Nernst-Planck model which they derived, and which was

described in previous sections of this chapter. The

sample variance for 48 calculated points was 0.0083

versus 0.00014 on 136 calculated points obtained with

the activity driving force model developed in this work

(standard deviation approximately ± 0.09 vs. ± 0.012

on variable range between 0.2 and 1.0).

F. Simulation of Rao and his Coworkers' Ternary Experimental Data

1. General Discussion

Table 5-4 gives a listing of initial concentration

conditions for 22 ternary rate runs made by Rao and his

coworkers on the systems $Sr^{++}-Mn^{++}-Cs^{+}$ and

$Mn^{++}-Cs^{+}-Na^{+}$, including a subjective quality rating (10

best, 1 worst) for the runs simulated. The quality ratings

are compared for simulation runs made using the activity

driving force model with diffusion coefficients derived from

the set of seven, set of six, plus a few runs based on the

two parameter model (pair correctors). Quality ratings are

given for the simulation results of Rao and his coworkers as

well so that a qualitative comparison of model performance

can be made. Using data from the set of seven fit, an

average quality rating of 7 is somewhat better than the

Table 5-4

BATCH TERNARY ION EXCHANGE EXPERIMENTS
Gopala Rao et al

System $Sr^{++}-Mn^{++}-Cs^+-Na^+$/Dowex 50W x8/Cl$^-$

Run No.	Resin Composition			Solution Composition			Simulation Quality Rating			
							Simulation Data Source			
	Sr^{++}	Mn^{++}	Cs^+	Sr^{++}	Mn^{++}	Cs^+	Rao et al	fit of 6	fit of 7	Pair Corrector Model
33B	0.18	0.82*	---	---	---	1.0	8	8	8	6
43B	0.348	0.652*	---	---	---	1.0	-	5	5	4
44B	1.0*	---	---	---	0.84	0.16	6	7	10	not fit
45B	1.0*	---	---	---	0.40	0.60	7	5	7	not fit
31B	---	0.715*	0.285	1.0	---	---	5	9	6	10
40B	---	0.639*	0.361	1.0	---	---	8	4	7	7
35B	0.745*	---	0.255	---	1.0	---	3	10	8	not fit
41B	0.618*	---	0.382	---	1.0	---	6	5	3	not fit
Run No.	Mn^{++}	Cs^+	Na^+	Mn^{++}	Cs^+	Na^+				
28	---	0.576	0.424*	1.0	---	---	4	not fit	7	not fit
29	---	0.279	0.721*	1.0	---	---	5	not fit	8	not fit
33	0.393	---	0.607*	---	1.0	---	8	9	9	not fit
34	0.486	---	0.514*	---	1.0	---	10	6	6	not fit
30	0.841*	---	0.159	---	1.0	---	4	5	5	not fit
31	0.632*	---	0.368	---	1.0	---	4	not fit	7	not fit
66	0.489*	---	0.511	---	1.0	---	4	4	5	not fit
35	---	---	1.0*	0.40	0.60	---	7	6	6	not fit
36	---	---	1.0*	0.833	0.167	---	6	10	8	not fit
37	0.555*	0.445	---	---	---	1.0	6	6	6	not fit
38	0.804*	0.196	---	---	---	1.0	5	7	7	not fit
49	0.604*	0.396	---	---	---	1.0	5	not fit	not fit	not fit
43	1.0*	---	---	---	0.10	0.90	6	8	8	9
70	1.0*	---	---	---	0.40	0.60	7	10	10	10
Average Quality Rating							5.9	6.9	6.95	

*tagged ion

average rating of 6 for the Rao and his coworkers' simulation results. The results of the simulation runs are shown in Figures 5-4 through 5-8 for diffusion coefficients derived from the fit of seven, since the average quality rating was slightly better than the fit of six.

2. Comparison of Simulated Results with Experimental Data

Rao and his coworkers published the results (94) of simulated "batch" experiments for the system Ba^{++}-Sr^{++}-Na^{+} for a range of initial conditions, but limited to two basic types of exchange: (1) two ions initially in the resin and the third at the surface, (2) one ion in the resin and the other two at the surface. Plots were generated by simulation which showed the depletion rate trends for the "tagged" ion in the resin. Some actual experimental results had been obtained by Rao and his coworkers in earlier work (90) which corroborated the general computed trends. Based on those results, the following observations can be made on the simulation results obtained in this work on the systems Mn^{++}-Cs^{+}-Na^{+} and Sr^{++}-Mn^{++}-Cs^{+}:

a.   For cases such as exp. 35 and 36, where the least favored ion, Na^{+}, is in the resin and has a diffusion coefficient higher than Mn^{++} but lower than Cs^{+}, the expected trend would be for the $\overline{Na}^{*}Mn$ binary to represent the upper boundary, and the $\overline{Na}^{*}Cs$ binary to represent the lower boundary of ternary depletion curves, with the $\overline{Na}^{*}$ depletion curves having greater slopes than the

Figure 5-4

Ternary Exchange in System Mn^{++} $-Cs^+ -Na^+$, Dowex 50W x 8, Cl^-
Ternary Model - Nernst Planck/Variable Film Coefficients
- Activities As Driving Force -

System Calc.	Resin Comp.	Solution Comp.	Experimental**
	$\overline{Mn}^*$	Na Cs	——————— Binaries
o	1.0	0.90 0.10	——— – ——— R-43
×	1.0	0.60 0.40	——— —— —— R-70
	$\overline{Na}^*$	Mn Cs	
△	1.0	0.833 0.167	—— —— —— —— R-36
□	1.0	0.40 0.60	···——···——··· R-35

"Self" Diffusion Coefficients

$D_{Mn} = 0.3224$ E–06 cm^2/sec
$D_{Cs} = 0.3962$ E–05 cm^2/sec
$D_{Na} = 0.2749$ E–05 cm^2/sec
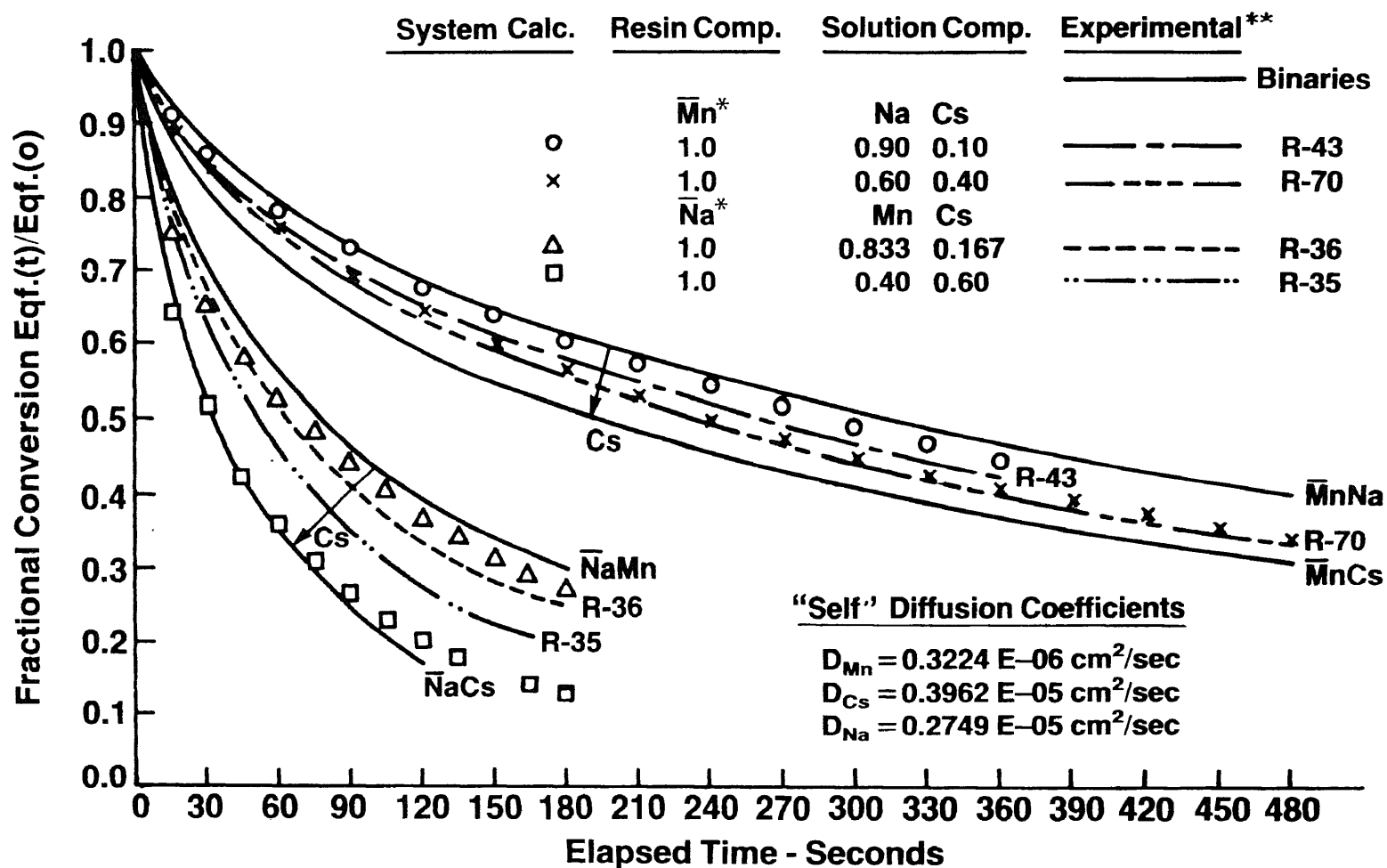
**0.1 Normal, 28°C
R.K. Bajpai, A.K. Gupta, M. Gopala Rao
"AIChE Journal," Sept. 1974 (Volume 20, No. 5)

Figure 5-5

Ternary Exchange in System $Sr^{++} - Mn^{++} - Cs^+$, Dowex 50W x 8, Cl^-
Ternary Model - Nernst Planck/Variable Film Coefficients
- Activities As Driving Force -

"Self" Diffusion Coefficients

$D_{Sr} = 0.1392$ E-06 cm^2/sec

$D_{Mn} = 0.3224$ E-06 cm^2/sec

$D_{Cs} = 0.3962$ E-05 cm^2/sec

R-35B
$\overline{Sr}Mn$
R-41B
R-44B
$\overline{Sr}Cs$

$\overline{Cs}$

R-45B

Fractional Conversion Eqf.(t)/Eqf.(o)

Systems Calc.	Resin Comp.		Solution Comp.		Experimental**	
	$\overline{Sr}^*$	$\overline{Cs}$	Mn		————————	Binaries
o	0.745	0.255	1.0		— — — —	R35-B
+	0.618	0.382	1.0		— — —	R41-B
	$\overline{Sr}^*$		Mn	Cs		
□	1.0		0.84	0.16	—·—·—	R44B
△	1.0		0.40	0.60	—··—··	R45B

Elapsed Time - Seconds
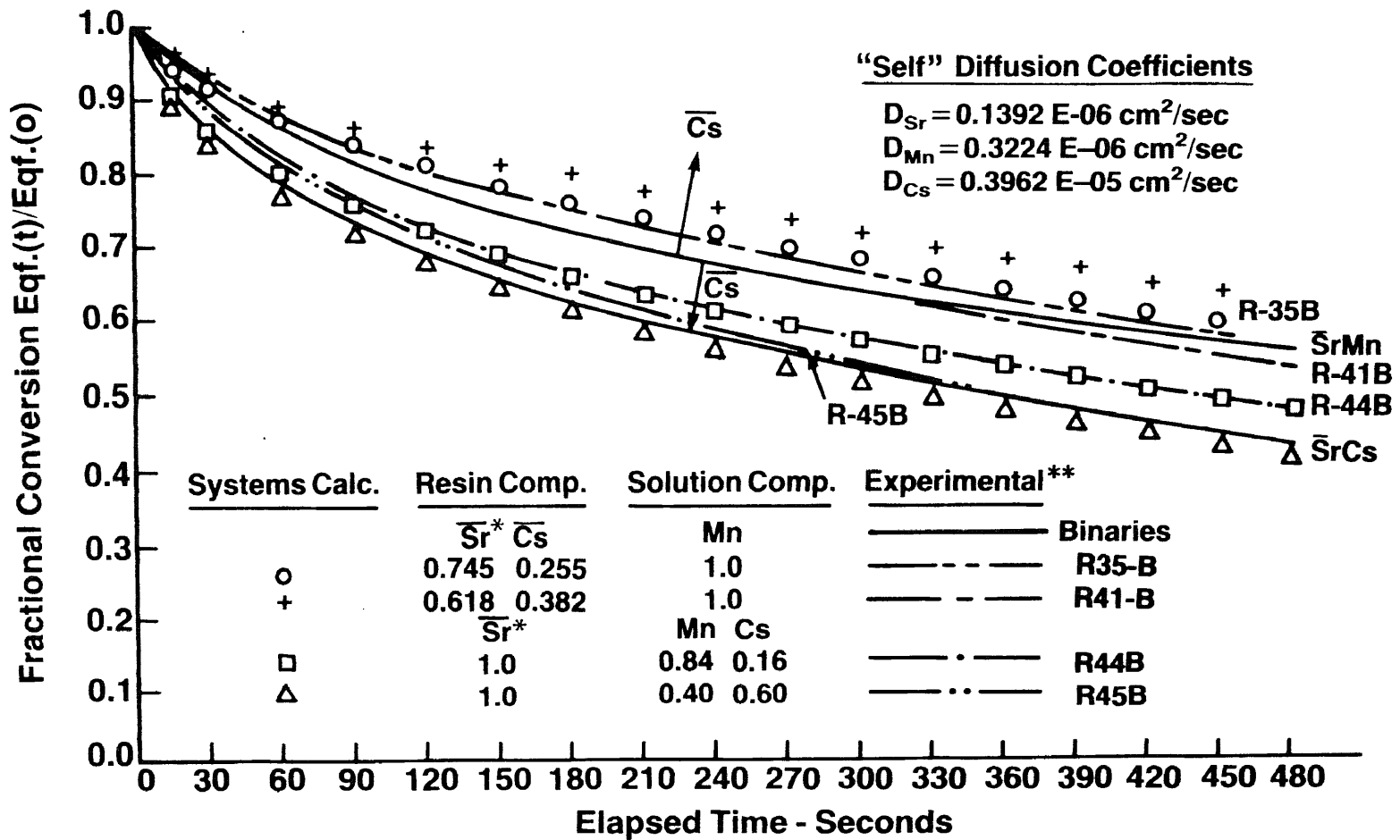
**0.1 Normal, 28°C

R.K. Bajpai, A.K. Gupta, M. Gopala Rao

"AIChE Journal," Sept. 1974 (Volume 20, No. 5)

Figure 5-6

Ternary Exchange in System $Sr^{++}-Mn^{++}-Cs^+$ and $Mn^{++}-Cs^+-Na^+$
on Dowex 50W x 8/Cl⁻
Ternary Model - Nernst Planck/Variable Film Coefficients
- Activities As Driving Force -

Systems Calc.	Resin Comp.		Solution Comp.	Experimental**	
	$\overline{Na}$*	$\overline{Cs}$	Mn	———————	Binaries
o	0.721	0.279	1.0	—— —— ——	R-29
×	0.424	0.576	1.0	—— — — ——	R-28
	$\overline{Mn}$*	$\overline{Cs}$	Sr		
△	0.715	0.285	1.0	—— · ——	R-31B
□	0.639	0.361	1.0	—— ·· ——	R-40B

R-40B

R-31B

$\overline{Mn Sr}$

"Self" Diffusion Coefficients

$D_{Sr} = 0.1392$ E–06 cm²/sec
$D_{Mn} = 0.3224$ E–06 cm²/sec
$D_{Cs} = 0.3962$ E–05 cm²/sec
$D_{Na} = 0.2749$ E–05 cm²/sec

$\overline{Cs}$

$\overline{Na}$
R-28
R-29
$\overline{Na Mn}$
Hypothetical
$\overline{Cs Mn}$

Fractional Conversion Eqf.(t)/Eqf.(o)

1.0
0.9
0.8
0.7
0.6
0.5
0.4
0.3
0.2
0.1
0.0

0 30 60 90 120 150 180 210 240 270 300 330 360 390 420 450 480

Elapsed Time - Seconds
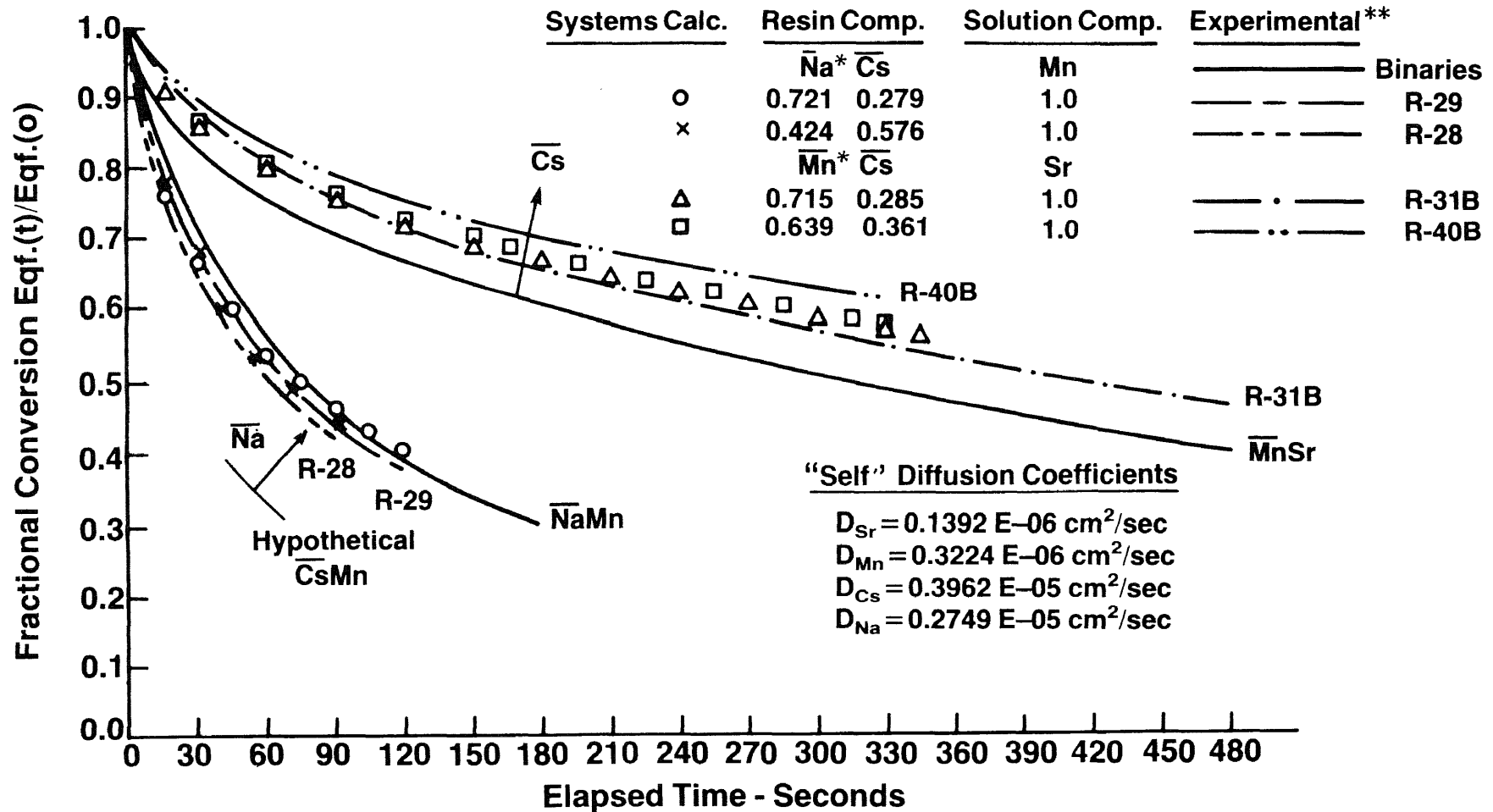
Figure 5-7

Ternary Exchange in System Mn^{++} − Cs$^+$ − Na$^+$, Dowex 50W x 8, Cl$^-$
Ternary Model - Nernst Planck/Variable Film Coefficients
- Activities As Driving Force -

Systems Calc.	Resin Comp.		Solution Comp.	Experimental**	
	$\overline{Mn}^*$	$\overline{Na}$	Cs	———————	Binaries
△	0.841	0.159	1.0	——— . ———	R-30
☐	0.632	0.368	1.0	——— .. ———	R-31
◇	0.489	0.511	1.0	——— . . . ———	R-66
	$\overline{Mn}$	$\overline{Na}^*$	Cs		
o	0.607	0.393	1.0	——— — — ———	R-33
+	0.514	0.486	1.0	——— — — ———	R-34

"Self" Diffusion Coefficients

D_{Mn} = 0.3224 E–06 cm^2/sec
D_{Cs} = 0.3962 E–05 cm^2/sec
D_{Na} = 0.2749 E–05 cm^2/sec
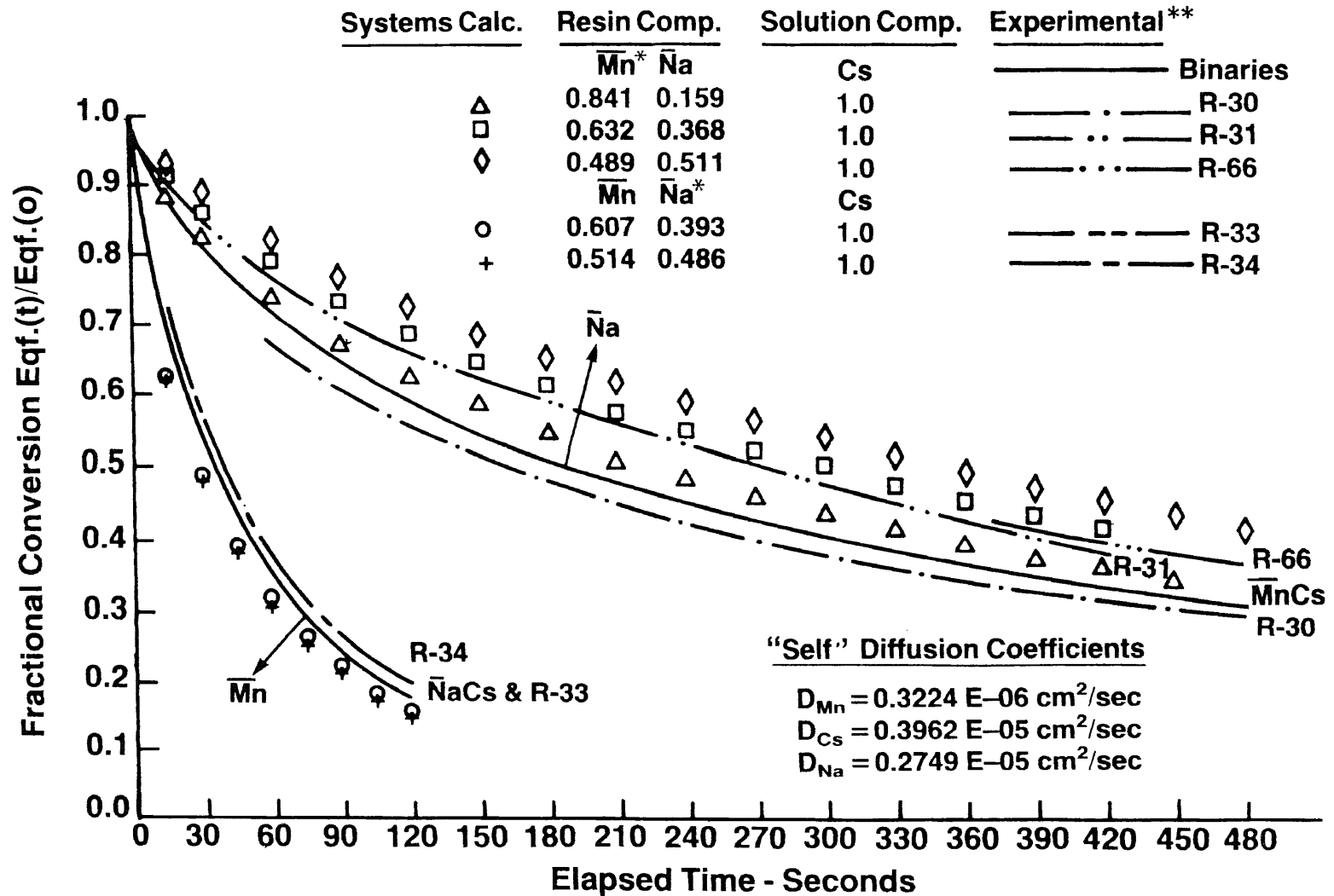
**0.1 Normal, 28°C
R.K. Bajpai, A.K. Gupta, M. Gopala Rao
"AIChE Journal," Sept. 1974 (Volume 20, No. 5)

Figure 5-8

Ternary Exchange in System Sr^{++} –Mn^{++}- Cs$^+$ and Mn^{++} – Cs$^+$ – Na$^+$
on Dowex 50W x 8/Cl$^-$
Ternary Model - Nernst Planck/Variable Film Coefficients
- Activities As Driving Force -

Systems Calc.	Resin Comp.		Solution Comp.	Experimental**	
	Mn*	Cs	Na	———————	Binaries
□	0.804	0.196	1.0	——·——	R-38
◊	0.604	0.396	1.0	————	R-49
△	0.555	0.455	1.0	——·—	R-37
	Mn*	Sr	Cs		
○	0.820	0.180	1.0	——··——	R-33B
+	0.652	0.348	1.0	——·——	R-43B

Cs ↑

Self   Diffusion Coefficients

$D_{Sr} = 0.1392$ E-06 cm^2/sec
$D_{Mn} = 0.3224$ E-06 cm^2/sec
$D_{Cs} = 0.3962$ E-05 cm^2/sec
$D_{Na} = 0.2749$ E-05 cm^2/sec

Sr

R-49 □
R-37

MnNa & R-38
R-43B
MnCs &
R-33B

Fractional Conversion Eqf.(t)/Eqf.(o)

1.0 0.9 0.8 0.7 0.6 0.5 0.4 0.3 0.2 0.1 0.0

0 30 60 90 120 150 180 210 240 270 300 330 360 390 420 450 480

Elapsed Time - Seconds
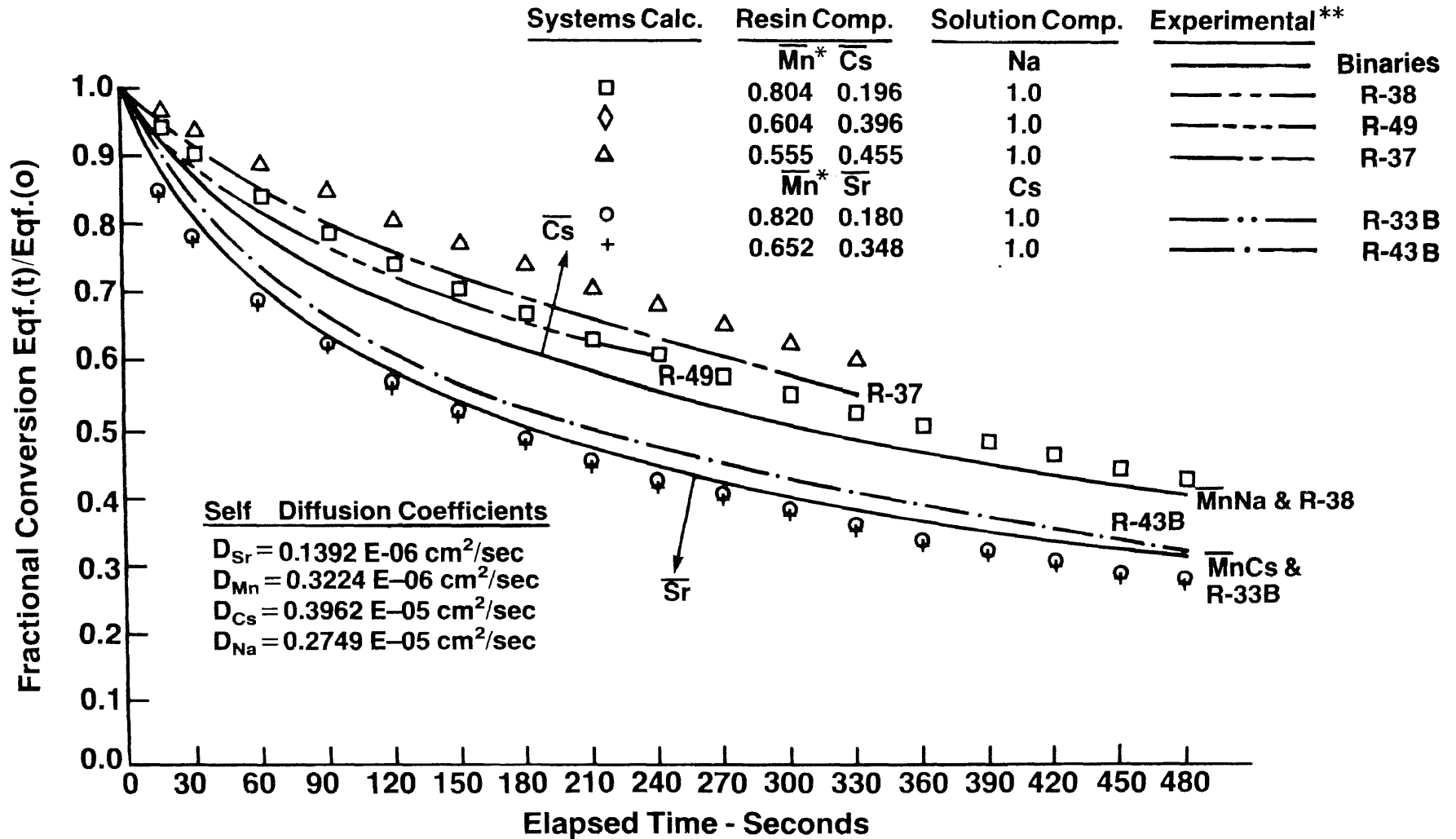
** 0.1 Normal, 28°C
R.K. Bajpai, A.K. Gupta, M. Gopala Rao
"AIChE Journal," Sept. 1974 (Volume 20, No. 5)

upper $\overline{Na}^*Mn$ binary boundary as Cs^+

concentration increases in the electrolyte phase.

This was observed both experimentally and in the

simulation.

b.   For cases such as 44B and 45B, $\overline{Sr}^*MnCs$,

where the most favored ion is in the resin, the

selectivity is Sr>Mn>>Cs and diffusion coefficients

values are Cs>>Mn>Sr, the upper envelope boundary

should be the binary $\overline{Sr}^*Mn$, and the lower

boundary the binary system $\overline{Sr}^*Cs$. The trend in

$\overline{Sr}^*$ depletion curves should be to have greater

slopes as Cs^+ concentration increases in the

electrolyte. This was the case experimentally, and

was the trend in the simulated results; however,

the simulation run with higher Cs^+ (45B) was

slightly under the lower boundary.

The system $\overline{Mn}^*CsNa$, runs 43 and 70, where

selectivity is Mn>>Cs>Na and diffusion coefficients

are Cs>Na>>Mn, should have an upper boundary binary

of $\overline{Mn}^*Na$, with the lower envelope boundary being

$\overline{Mn}^*Cs$. The trend in $\overline{Mn}^*$ depletion curves

should be to have greater slopes as Cs^+

concentration in the electrolyte increases, and

this was the case experimentally and in the

simulated results.

c.   For cases where the most favored ion is in the

electrolyte and the other two in the resin, runs

31B and 40B for $\overline{Mn\overset{*}{}CsSr}$, and runs 28 and 29 for

$\overline{CsNa}^*Mn$ illustrate behavior of this type of

exchange. In the $\overline{Mn\overset{*}{}CsSr}$ system, the upper

boundary should be $\overline{Mn}^*Sr$, and the lower binary

system bounding the envelope, $\overline{Cs}^*Sr$. Due to the

bad batch of Cs^{137}, no experimental curves were

generated by $\overline{Cs}^*$ in the resin. In this system,

as the faster and least selective ion, Cs^+, is

increased in the resin concentration--it exchanges

with the Sr^{++} at a faster rate than the $\overline{Mn}^*$,

and has a retarding effect on the diffusion rate of

the $\overline{Mn}^*$. This behavior was shown experimentally,

and the simulation curves show this trend, although

not laying on the experimental curves. In the case

of $\overline{CsNa}^*Mn$ system, the lower bound should be

$\overline{Cs}^*Mn$ (again no $\overline{Cs}^*$ data) and the upper binary

$\overline{Na}^*Mn$. Increasing amounts of the more preferred

ion, Cs^+, should accelerate the diffusion rate of

$\overline{Na}^*$ ion in the direction of the lower boundary.

This was observed experimentally, although the

simulated runs gave results not much different from

the $\overline{Na}^*Mn$ binary system.

d.   Runs 35B and 41B for $\overline{Sr\overset{*}{}CsMn}$, and runs 30,

31, 33, 34, and 66 for $\overline{Mn\overset{*}{}NaCs}$ and $\overline{MnNa}^*Cs$

illustrated system behavior where the resin

contained both the most preferred and the least

preferred ions, with the other ion consituting the

electrolyte composition. In the $\overline{Sr}^*\overline{Cs}Mn$ system, it would be expected that the displacement of the Cs^+ ion by the slower and more favored Mn^{++} ion would slow the rate of diffusion of $\overline{Sr}^*$ below that observed in the $\overline{Sr}^*Mn$ binary, as Cs^+ concentration is increased. This was not observed experimentally since run 41B, having the larger Cs^+ oncentration, should have had a depletion curve above run 35B. In fact, the simulation of run 35B coincided quite well with the experimental values, and simulation of run 41B gave a depletion curve higher than run 35B, as expected.

The $\overline{Mn}^*\overline{Na}Cs$ and the $\overline{MnNa}^*Cs$ systems should have exhibited a decrease in slope of the depletion curves for $\overline{Mn}^*$ up and away from the $\overline{Mn}^*Cs$ binary as the more preferred ion Cs^+ is exchanged preferentially with Na^+. The Na^* ion should have shown a trend for its depletion curves to decrease in slope down and away from the $\overline{Na}^*Cs$ binary. This was observed experimentally with two exceptions; run 34 was slightly above the $\overline{Na}^*Cs$ binary and run 30 was slightly below the $\overline{Mn}^*Cs$ binary. The simulated runs behaved as expected; however, the cases in which the ion $\overline{Mn}^*$ was diffusing yielded simulation results quite a bit higher than the experimental values.

e. Behavior of systems in which the two most preferred ions were in the exchanger and the least preferred ion constituted the electrolyte phase were exemplified by runs 33B and 43B for the system $\overline{SrMn}^*Cs$ and runs 37, 38 and 49 for the system $\overline{Mn}^*CsNa$. In these cases it would be anticipated that the unfavorable exchange of $\overline{Mn}^*$ for Na^+ ion and $\overline{Sr}$ for Cs^+ ion would result in slower diffusion rates for $\overline{Mn}^*$ and $\overline{Sr}$ as Cs^+ and Mn^{++} ion concentrations increased respectively. It should be easier for the least preferred ion to displace the second most preferred ion than the most preferred ion, resulting in retention of the most preferred species. The diffusion rate for $\overline{Mn}^*$ and $\overline{Sr}$ should be lower than in the respective binary systems $\overline{Mn}^*Na$ and $\overline{Sr}^*Cs$. In the $\overline{SrMn}^*Cs$ system, it was the $\overline{Mn}^*$ which was tagged. In this case, the diffusion rate of $\overline{Mn}^*$ should have been higher than that of $\overline{Mn}^*$ in the binary system $\overline{Mn}^*Cs$. Experiments validated these hypotheses for the $\overline{Mn}^*CsNa$ system, but not for the $\overline{SrMn}^*Cs$ system where run 33B lay on the $\overline{Mn}^*Cs$ binary curve, and run 43B was higher. The simulation of run 33B was good, and the simulation of run 43B gave a depletion curve lower than both the $\overline{Mn}^*Cs$ and the run 33B curve, as hypothesized.

3. Conclusions

The results of the ternary simulation runs were not nearly as good as the binary simulation results, and this was true of the Rao and his coworkers' (92, 93) ternary simulation studies as well. One problem which is quite obvious is that in a ternary rate run, two compositions should be followed experimentally in order to define the total system dynamics. Using radioactive tracer techniques, this would be difficult to carry out experimentally within any single run; however, replicate runs in which first one ion in the exchanger is tagged, then the other, would be one way to accomplish this requirement. In fact runs 34 and 66, $\overline{Mn}^*NaCs$ and $\overline{MnNa}^*Cs$, at $\overline{Mn}$ of 0.488 and $\overline{Na}$ of 0.512 equivalent fraction, were carried out in this way. Based on the regression results from the fit of six and the fit of seven, the diffusion coefficient for $\overline{Cs}^+$ was determined as 0.34 $\times 10^{-5}$ and 0.396 $\times 10^{-5}$ cm^2/sec respectively; whereas, the $\overline{Mn}^{++}$ and $\overline{Na}^+$ values did not change appreciably. Run 34 was reasonably well simulated at both $\overline{Cs}^+$ diffusion coefficient values; however, the depletion curve for run 66 was simulated above the experimental curve, and was worse with the lower $\overline{Cs}^+$ diffusion coefficient value (higher curve). The $\overline{Cs}^+$ ion concentration in the resin has been calculated by material balance and is compared below for the experimental and the simulated data points.

$\overline{Cs}^+$ Concentration Calculated

Time (Sec.)	Experimental	Simulated
0	0	0
15	0.2336	0.2024
30	0.3202	0.3162
60	0.4390	0.4450
90	0.5216	0.5204
120	0.5694	0.5806

This shows reasonable agreement. There is no $\overline{Cs}^*Na$ curve to compare it to, as discussed before.

One problem encountered with the ternary program TRYBCH when running with activity driving force was that the flux balances, i.e., transfer across the film flux and resin accumulation (loss) flux, often did not balance well. This was not observed with the binary model BMAVD or RFMAVD, nor was it observed with TRYBCH when running with concentration driving force. In some cases, better flux balance could be obtained by juxtaposition of species, i.e., Sr^{++}-Cs^+-Mn^{++} versus Sr^{++}-Mn^{++}-Cs^+ in terms of the species 1 and 2 for which the calculations are performed. In simulations of $\overline{SrCsMn}$ type systems this was helpful; however the equilibrium constants, Redlich-Kister constants, and diffusion coefficients have to be readjusted accordingly, and read in correctly.

Basically, it is believed that the calculation of $\overline{D}'_{ij}$ and $\overline{D}'_{ii}$, at the jth versus $j^{+1/2th}$ step caused the flux imbalance at time step $j^{1/2}$ as a result of adding the extremely non-linear activity terms,

$$\bar{x}_i \cdot \bar{x}_j \cdot \frac{\partial \ell n \left[\frac{\bar{\gamma}_i^{|z_j|}}{\bar{\gamma}_j^{|z_i|}} \right]_{molar}}{\partial \bar{x}_i} \qquad (5\text{-}102)$$

for $i=1,2$; $j=1,2$; $i \neq j$

to the diffusion coefficient expressions. Quasilinearization of all of these terms would solve the problem, since at each time step the iterative process would be carried out until convergence was attained, and the fluxes would balance. The difficulty in the derivation of matrix coefficients and solution vectors resulting from the additional terms would make this an unwarranted approach. Some other solution methods might be examined, but only if additional reliable ternary data, for which two concentrations are measured, are made available to test a revised model. In any event, the applicability of activity driving force in ion exchange should be tested further on binary systems before applying the model to additional ternary systems.

CHAPTER VI

AXIAL DIFFUSION IN PACKED BEDS

A. General Background

Axial diffusion or longitudinal dispersion of a species dissolved in a flowing fluid, or one gas mixed with another, is an important fluid mixing effect which must be accounted for in packed bed operations involving catalytic reactions or ion exchange processes, since it adversely affects concentration driving forces in the bed. In a streaming fluid, the following partial differential equation is commonly used to describe this phenomenon:

$$\circ \qquad E_d \cdot \frac{\partial^2 c}{\partial z^2} - U \cdot \frac{\partial c}{\partial z} = \frac{\partial c}{\partial t} \qquad\qquad (6\text{-}1)$$

where:

c = concentration of species in bed

z = bed length dimension

U = interstitial velocity

t = time

E_d = axial dispersion coefficient or axial eddy diffusivity

Correlation of the axial dispersion coefficient are usually displayed as Reynold No. vs. Peclet No. where:

$$Re = \frac{dp \cdot U' \cdot \rho}{\mu} \qquad\qquad (6\text{-}2)$$

$$Pe = \frac{U \cdot dp}{E_d} \qquad \frac{U' \cdot dp}{\varepsilon \cdot E_d} \qquad\qquad (6\text{-}3)$$

where:

dp = particle diameter

ε = bed voidage

U' = superficial velocity

U = interstitial velocity = $\dfrac{U'}{\varepsilon}$ (6-4)

Figure 6-1 is a graph on which the work of various investigators has been plotted (12, 23, 26, 27, 32, 61, 78, 115, 124), including coefficients developed in this research effort. The various investigators have used either concentration pulse analysis or frequency response analysis to characterize the axial eddy diffusivity in a variety of liquids and gases, over a range of flow rates and particle sizes. The two experimental points by Farkas & Byleveld (27) were carried out at low flow rates on Amberlite IR-120-plus ion exchange resin which was being eluted by a pulse of deionized water injected behind a flow of "city water." Conductivity measurements were used to characterize the effluent pulse dispersion.

B. Correlation of Axial Dispersion Coefficients - This Research

1. Experiments of Omatete and his Coworkers

The results obtained in this research project during the fitting of the resin loading curves for Omatete's data (78) on Ag^+, Na^+, H^+ are in the generally expected "range." This was not fortuitous, since values were chosen from this "range" when the resin phase ion diffusion coefficients were fit. It was found that the use of these eddy diffusion coefficients taken from the generalized plot, coupled with literature values for film coefficient parameters, resulted in close matching of the

Figure 6-1

Axial Dispersion in Packed Beds - Peclet No. vs. Reynolds No.
- Approximate Representation of Published Data -

Ion Exchange Experimental Data
- ① K.L Erickson, NH_3-ETDA
- ② Omatete, Ag-Na-H
- □ Farkas & Byleveld
- – – "Mass Transfer"
  Sherwood, Pigford, Wilke
  p. 136

———— Carberry & Bretton   •••••• Liles & Geankoplis
——·—— Ebach & White   — ··—— Strang & Geankoplis
— – —— Gunn & England

y-axis: $Pe = Udp/E_D = U_{ave} \, dp/(\epsilon E_D)$

x-axis: $Re = dp \, U_{ave}/\nu$
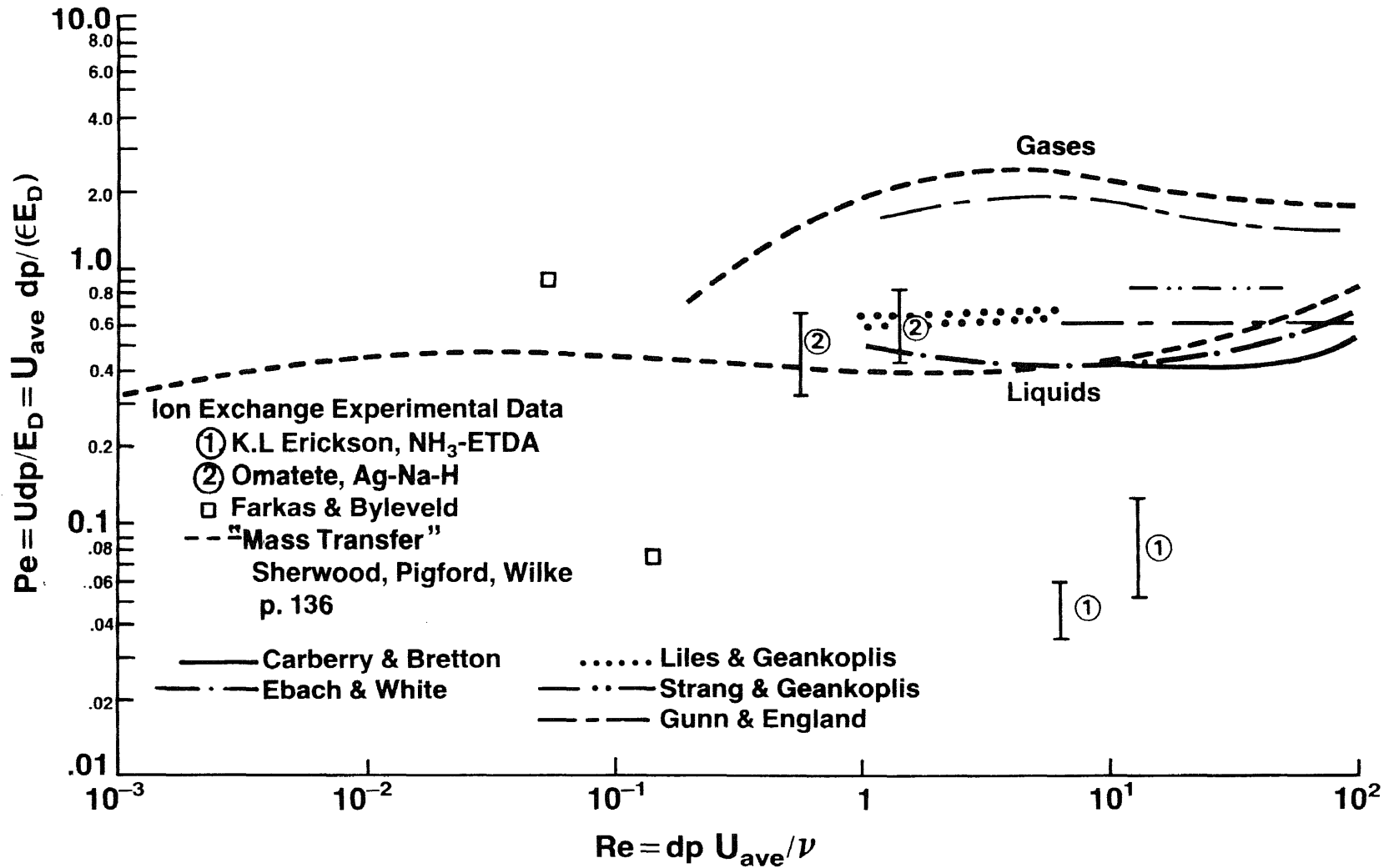
experimental data solely by adjustment of resin phase diffusion coefficients. The fact that the values of the fitted resin phase diffusion coefficients were close to literature values, and that this single set of fitted diffusion coefficients for $\bar{D}_{Ag}$, $\bar{D}_{Na}$, & $\bar{D}_H$ gave excellent simulations for 6 runs on binary systems and 3 runs on ternary systems--at minimum, suggested that the eddy diffusion coefficients taken from the generalized plot were "correct."

2. Erickson Experiments

2.1 Experimental Results

Erickson (26), on the other hand, actually ran dispersion tests in his experimental column by immersing the resin bed in 0.05 normal NH_4^+ solution, then followed with a step introduction of 0.1 normal NH_4^+ at two flow rates--and traced the effluent concentration by measuring conductivity. Plots of data at these two flow rates are given in Figures 6-2 and 6-3. The curves for various eddy diffusion coefficients are the result of an axial dispersion model derived in this research project. Erickson fitted the experimental data by solving equation 6-1 given above numerically; however, dispersion curves generated by Erickson could not account for the "tailing off" effect after the plug flow time (defined as total column voidage/volumetric flow rate). Erickson ascribed this tailing effect to holdup of 0.05 normal solution in the boundary layer around the resin beads, and chose "best"

modeled "S" curves at E_d=0.75 and E_d-1.2cm/sec for the two flow rates.

2.2 Simulation of Erickson Data - This Research

The following model was developed in this work to test Erickson's boundary layer hypothesis.

Column c_{in} , flow = v • column area

Illustration 6-1

Axial Dispersion Model Schematic

Resin Particle

Assumptions:

- o No radial gradients in column

- o Uniform spherical particles, r_o

- o Uniform bed void space,

- o Existence of a stagnant film around each particle with thickness, δ_f, constant down column
- o Resin at r_o is saturated with preferred ion and is impenetrable to further ionic migration
- o Diffusion coefficient in the stagnant film is D_i^*, constant through film and constant down column
- o Axial dispersion coefficient, E_d, is constant down the column

Fluid equation

$$(6-5)$$

$$\circ \quad \frac{\varepsilon' \cdot \partial c_{1_{bulk}}}{\partial t} + \left[\frac{vol_f \cdot 3 \cdot (r_o + \delta_f)^2}{\left[(r_o + \delta_f)^3 - r_o^3 \right]} \right] \cdot N_1^* \bigg|_{r = r_o + \delta_f} = \frac{\varepsilon' \cdot \partial^2 c_{1_{bulk}}}{\partial z^2}$$

$$- \frac{v \cdot \partial c_{1_{bulk}}}{\partial z}$$

Film Equation

$$\circ \quad \frac{\partial c_1^*}{\partial t} = D_1^* \cdot \left[\frac{\partial^2 c_1^*}{\partial y^2} + \frac{2}{(r_o + y)} \cdot \frac{\partial c_1^*}{\partial y} \right] \qquad (6-6)$$

Since:

$$(6-7,8,9)$$

$$r = r_o + y \; ; \; \frac{\partial(\ )}{\partial r} = \frac{\partial(\ )}{\partial y} \bigg|_{r > r_o} \; ; \; and \; \frac{\partial^2(\ )}{\partial r^2} = \frac{\partial^2(\ )}{\partial y^2} \bigg|_{r > r_o}$$

where:

$$vol_f = \frac{Volume\ Film}{Volume\ Column} = (1-\varepsilon) \cdot \left[\frac{\left[(r_o + \delta_f)^3 - r_o^3 \right]}{r_o^3} \right], \ cm^3$$

ε' = column voidage for flowing fluid

$= (\varepsilon - vol_f)$, cm^3

$c_{1_{bulk}}$ = concentration of species 1 in flowing fluid, $moles/cm^3$

c_1^* = concentration of species 1 in film, $moles/cm^3$

N_1^* = molar flux into or out of film, $moles/cm^2/sec$

r_o = particle radius, cm

δ_f = film thickness, cm

L = column length, cm

y = film dimension, cm

z = column length dimension, cm

D_1^* = species 1 diffusivity in film, cm^2/sec

E_d = species 1 axial diffusion coefficient, cm^2/sec

v = superficial velocity in the column, cm/sec

norm = normality of coion, milliequiv./cm^3 solution

z_1 = valence of species 1

Putting the terms into dimensionless form;

o $\quad Pe = \dfrac{L \cdot v}{E_d \cdot \varepsilon}$ $\quad$ (6-10), $\quad x_{1_{bulk}} = \dfrac{c_{1_{bulk}} \cdot z_1}{norm}$ $\quad$ (6-11)

o $\quad x_1^* = \dfrac{c_1^* \cdot z_1}{norm}$ $\quad$ (6-12), $\quad Z = \dfrac{z}{L}$ (6-13), $\quad Y = \dfrac{y}{\delta_f}$ (6-14)

o $\quad T = \dfrac{t \cdot v}{L}$ $\quad$ (6-15), $\quad J_1^* = \dfrac{N_1^* \cdot z_1}{norm}$ $\quad$ (6-16)

o $\quad \lambda = \dfrac{3 \cdot \text{vol}_f \cdot (r_o + \delta_f)^2 \cdot L}{\left[(r_o + \delta_f)^3 - r_o{}^3 \right] \cdot v}$ (6-17), $\quad \eta = \dfrac{D_1^* \cdot L}{\delta_f{}^2 \cdot v}$ (6-18)

(6-19)

o $\quad \dfrac{\varepsilon' \cdot \partial x_{1_{bulk}}}{\partial T} + \lambda \cdot J_1^* \bigg|_{Y=1} = \dfrac{1}{Pe} \cdot \dfrac{\partial^2 x_{1_{bulk}}}{\partial Z^2} - \dfrac{\partial x_{1_{bulk}}}{\partial Z}$

and:

o $\quad \dfrac{\partial x_1^*}{\partial T} = \eta \cdot \left[\left(\dfrac{\partial^2 x_1^*}{\partial Y^2} \right) + \left(\dfrac{2 \cdot \delta_f}{(r_o + \delta_f \cdot Y)} \right) \cdot \dfrac{\partial x_1^*}{\partial Y} \right]$ (6-20)

Initial Conditions:

o $\quad x_{1_{bulk}} - in(T)$ $\qquad\qquad\qquad$ $T \geq 0$ $\qquad$ (6-21)

o $\quad x_{1_{bulk}}(Z,0) = x_{1_{bulk_{T_o}}}(Z)$ $\qquad$ $0 \leq Z \leq 1$ $\qquad$ (6-22)

o $\quad x_1^*(Y,Z,0) = x_{1_{T_o}}^*(Y,Z)$ $\qquad$ $\begin{cases} 0 \leq Z \leq 1 \\ 0 \leq Y \leq 1 \\ T = 0 \end{cases}$ (6-23)

Boundary Conditions-Column Exit

o $\quad \dfrac{\partial x_{1_{bulk}}(1,T)}{\partial Z} = 0$ $\qquad\qquad\qquad$ $T \geq 0$ $\qquad$ (6-24)

Boundary Conditions-Column Inlet

o $\quad x_{1_{bulk}}(0,T) - \dfrac{1}{Pe} \cdot \dfrac{\partial x_{1_{bulk}}(0,T)}{\partial Z} = x_{1_{bulk}} - in(T), T \geq 0$ (6-25)

Gradient at Resin-Film Interface

$$\text{o} \qquad \frac{\partial x_1^*}{\partial Y}(0,Z,T) \; = \; 0 \qquad\qquad \begin{cases} Y = 0 \\ 0 \le Z \le 1 \\ T \ge 0 \end{cases} \qquad (6\text{-}26)$$

Boundary Condition at Film-Fluid Interface

$$\text{o} \qquad x_{1_{bulk}}(Z,T) \; = \; x_1^*(1,Z,T) \qquad\qquad \begin{cases} Y = 1 \\ 0 \le Z \le 1 \\ T \ge 0 \end{cases} \qquad (6\text{-}27)$$

so;

$$\text{o} \qquad \frac{\partial x_{1_{bulk}}(Z,T)}{\partial Y} \; = \; \frac{\partial x_1^*(1,Z,T)}{\partial Y} \qquad\qquad \begin{cases} Y = 1 \\ 0 \le Z \le 1 \\ T \ge 0 \end{cases} \qquad (6\text{-}28)$$

and;

$$\text{o} \qquad J_1^*(1,Z,T) \; = \; \frac{D_1^* \cdot \partial x_1^*(1,Z,T)}{\delta_f \cdot \partial Y} \qquad\qquad \begin{cases} Y = 1 \\ 0 \le Z \le 1 \\ T \ge 0 \end{cases} \qquad (6\text{-}29)$$

The equations were solved based on the implicit Crank-Nicholson finite difference technique. Since there are no non-linear terms, quasilinearization is not required, and solution of the coupled matrices for the fluid phase and the stagnant film phase is performed readily through use of the tridiagonal array algorithm developed by Thomas (13, 125). The simulation program developed in this work is called DISPRS, and was used to compute the concentration of

species 1 ($0.1NH_4^+$) exiting the column vs. time for

various axial diffusion coefficients and "film thicknesses,"

as shown on Figures 6-2 & 6-3. Since the "film thickness"

based on calculation of k_L by Carberry's correlation

(arrived at by equating k_L to $\frac{D_1}{\delta_f}$) was in the range of

0.001 to 0.002 cm, the stagnant boundary layer could not

account for more than 2.5-5% of the void volume. The model

results showed this in that the calculated curves showed

almost negligible differences with "film thickness"

variations of from 0.001-0.004 cm. It becomes obvious in

looking at the experimental points with reference to the

plug flow time that the material balance on input vs. output

did not reconcile.

The area under the "S" curve on the left side of the

plug flow time should equal the area above the curve on the

right side for proper reconciliation of material in versus

out. The obvious answer was that the resin beads can absorb

more 0.1 normal NH_4^+ ion than 0.05 normal NH_4^+ ion,

and the assumption of impenetrable resin was incorrect

(i.e., $\frac{\partial x_1^*}{\partial Y}(0,Z) \neq 0$).

In choosing an axial diffusion coefficient to best fit

the experimental data it was therefore more important to

match the concentration profile on the left side of plug

flow time, representing first appearance due to dispersive

effects. Axial dispersion coefficients of 3 to 7 cm^2/sec

gave rise to Peclet No.s about an order of magnitude lower

Figure 6-2

Residence Time Distribution - Axial Dispersion
System NH$_4$Cl and Dowex 50W x 8 Resin
- Stagnant Film, Impenetrable Sphere Model -

o Experimental Data - Ave. Runs 5 & 6*
Temp. 26°C
Column Normality = 0.0519
Feed Normality = 0.1038
Superficial Velocity = 0.820 cm/sec
Resin Bed Depth = 55.6 cm
Column Dia. = 3.98 cm
Particle Radius = 0.039 cm
Plug Flow Residence Time = 23.9 sec
———— Calculated E$_D$ = 5.0 cm^2/sec
— — — Calculated E$_D$ = 3.0 cm^2/sec
- - - - - Calculated E$_D$ = 1.2 cm^2/sec
D$_{NH_4}^+$ = 1.994x10^{-5} cm^2/sec
K$_f$ = 0.011 cm/sec
δ = 0.0019 cm (film"thickness")

Plug flow time

*K.L. Erickson, "Fixed Bed Ion Exchange with Differing Ionic
Mobilities & Non-linear Equilibria" U. Texas 1977

230

Figure 6-3

Residence Time Distribution - Axial Dispersion
System NH$_4$Cl and Dowex 50W x 8 Resin
- Stagnant Film, Impenetrable Sphere Model -

o Experimental Data - Ave. Runs 1, 2, 7 & 8*
Temp. 26°C
Column Normality = 0.0519
Feed Normality = 0.1038
Superficial Velocity = 1.682 cm/sec
Resin Bed Depth = 55.6 cm
Column Dia. = 3.98 cm
Particle Radius = 0.039 cm
Plug Flow Residence Time = 11.7 sec
———— Calculated E$_D$ = 3.0 cm^2/sec
– – – – Calculated E$_D$ = 5.0 cm^2/sec
— –– — Calculated E$_D$ = 7.0 cm^2/sec

$D_{NH_3}^+$ = 1.994x10^{-5} cm^2/sec
K$_f$ = 0.015 cm/sec
δ = 0.00133 cm (Film "Thickness")
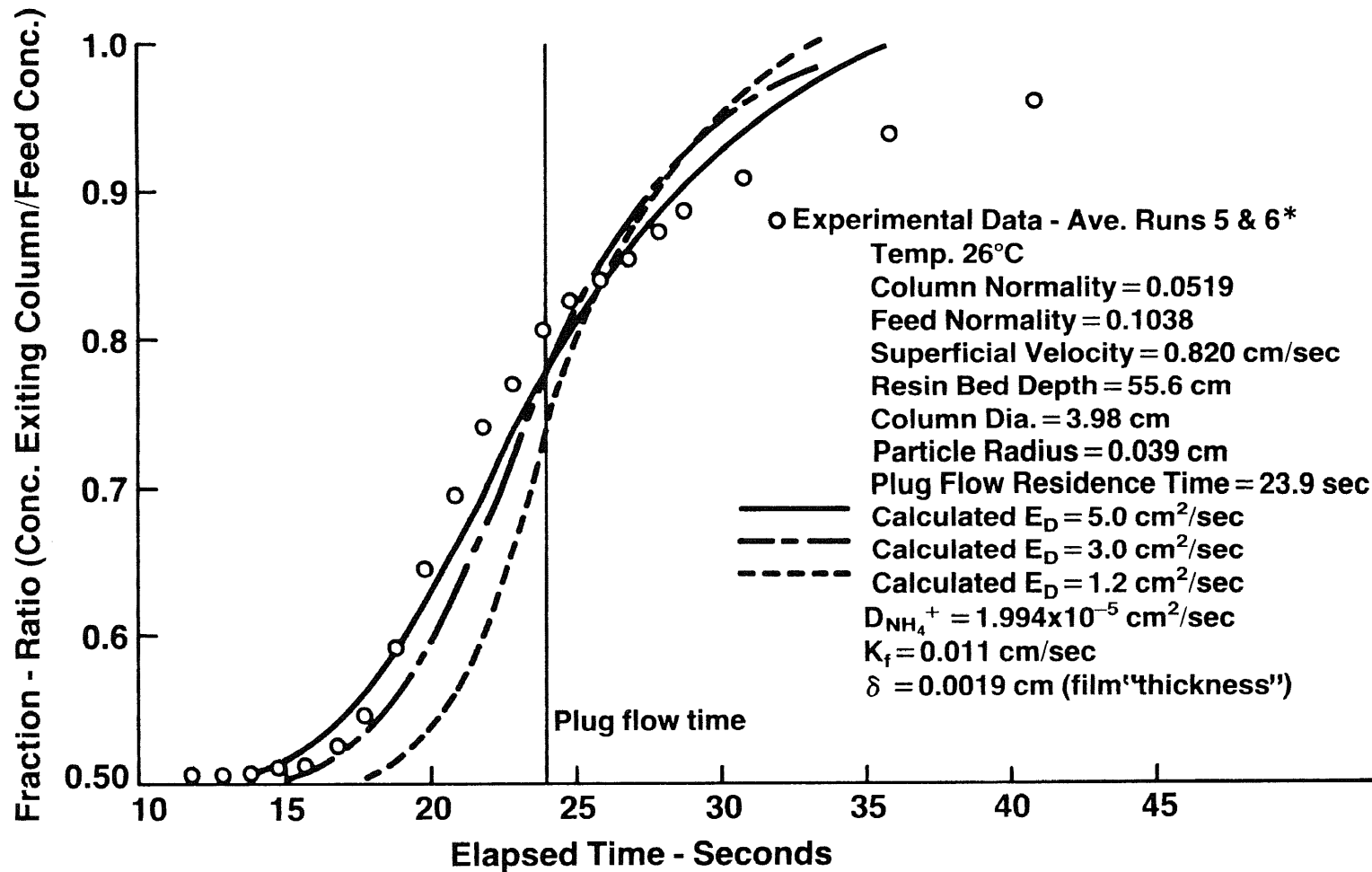
* K.L. Erickson, "Fixed Bed Ion Exchange with Differing Ionic
Mobilities & Non-linear Equilibria" U. Texas 1977

than other correlations on the generalized plot (Figure 6-1). A value of E_d=4.0 cm^2/sec was used in subsequent ion exchange simulations with the Erickson experimental exchange data (26). Values in the range of previous correlations shown on the generalized plot were used in the Omatete simulations, as stated above.

CHAPTER VII

DEVELOPMENT OF TERNARY ION EXCHANGE MODEL FOR COLUMN OPERATION

A. Development of General Ternary Model

The development of a ternary diffusion model for the resin phase was described in Chapter V; moreover, the treatment was general so that activity driving force could be used as opposed to concentration driving force. A program, TRYBCH, was developed to simulate radioactive tracer "batch" experiments on ternary systems. Likewise a binary version, BMAVDM, was developed to be used in conjunction with a general purpose non-linear regression program, DFUSFT, which was used to correlate diffusion coefficients and film coefficients utilizing "batch" data obtained from radioactive tracer experiments. Chapter IV on treatment of diffusion of ionic species through the boundary layer film for binary and ternary exchange included the development of a "pseudo electric field" model for use in the TRYBCH and BMAVDM simulation programs.

Additionally, development of a general purpose non-linear regression program, RIONFT, was described in the chapter on Equilibrium. This program was utilized to correlate the equilibrium constants relating the mass action between ionic species in electrolytes in equilibrium with ion exchangers, and the activity coefficient parameters for ionic species in the resin phase for both binary and ternary systems. Based on correlation of data on four ternary systems, the Redlich-Kister equation was chosen versus the Wilson and NRTL equations as having greater

233

ability to portray resin phase activity coefficient relationships in ion exchange systems, and yielded better predictions of equilibrium data on ternary systems based on equilibrium constants derived from binary systems and activity coefficient parameters.

All of these previous chapters have dealt with the data gathering phase which precedes any modeling effort. As was discussed in the preceding chapters, some of the data can be obtained from existing correlations, such as those describing film coefficients, electrolyte ionic species activity and diffusion coefficients, with appropriate correction for effects of electrolyte concentration. Correlations for axial dispersive effects are less well developed, and the treatment in this work compares the existing correlations, along with results derived from a simulation program, DISPRS, which can be used to simulate suitably designed experiments in columns. The results from two such axial diffusion simulations were discussed in Chapter VI.

Experimental data are required to correlate resin phase equilibrium parameters for the 3 binary pairs in a ternary system since literature background is sparse in this area. It has been shown in this work that binary correlation parameters can be combined to estimate ternary equilibrium data with fair reliability, although it is desirable to have experimental data points on ternary systems in the region of interest so that material balance requirements of column operation can be satisfied.

Similarly, shallow bed experiments using radioactive tracers are desirable to establish the effective diffusion coefficients

for ionic species in the particular resin grade which will be utilized in column operation. As demonstrated in this work, it is possible to correlate single value effective diffusivities for multicomponent systems by using activity driving forces. As will be shown subsequently in this chapter, the effective diffusion coefficients can be derived from column effluent concentration histories (ECH), but the fitting of diffusion parameters involves a trial and error procedure through simulation of column experiments. A starting point is to use best available literature values of the resin phase diffusion coefficients for the species involved, and then "tuning" the values to get a best fit.

The development of the general "batch" equations for both ternary and binary ion exchange in the resin phase included a column dimension, i, which implied varying bulk fluid ion species concentration as a function of time and column position. The i dimension was dropped out for the less complicated case developed for "infinite reservoir" type batch simulations. The fluid phase equations describing column operation will be developed in this chapter, and then coupled to the resin phase equations developed in Chapter V to yield two simulation models. RFMAVD (Revised Final Mass Action (Equilibrium) Variable (Solid Phase) Diffusivity) is the model for binary ion exchange column simulation, and is utilized to fit diffusion coefficients from the experimental column effluent concentration history (ECH). These coefficients can be used in the ternary simulation model. TERNEX (Ternary Ion Exchange) is the ternary column simulation model for ternary ion exchange. Both

have extensive diagnostics and write out options which will be described later.

B. Fluid Phase - Ternary Ion Exchange, Column Operation

    1. Development of Fluid Phase Equations

The general ternary ion exchange model for column operation will be developed first, since the binary ion exchange model for column operation is a simplified subset of the ternary equations.

Volumetric Flow = v(velocity)x empty column area

Illustration 7-1

Model for Ternary Ion Exchange, Column Operation
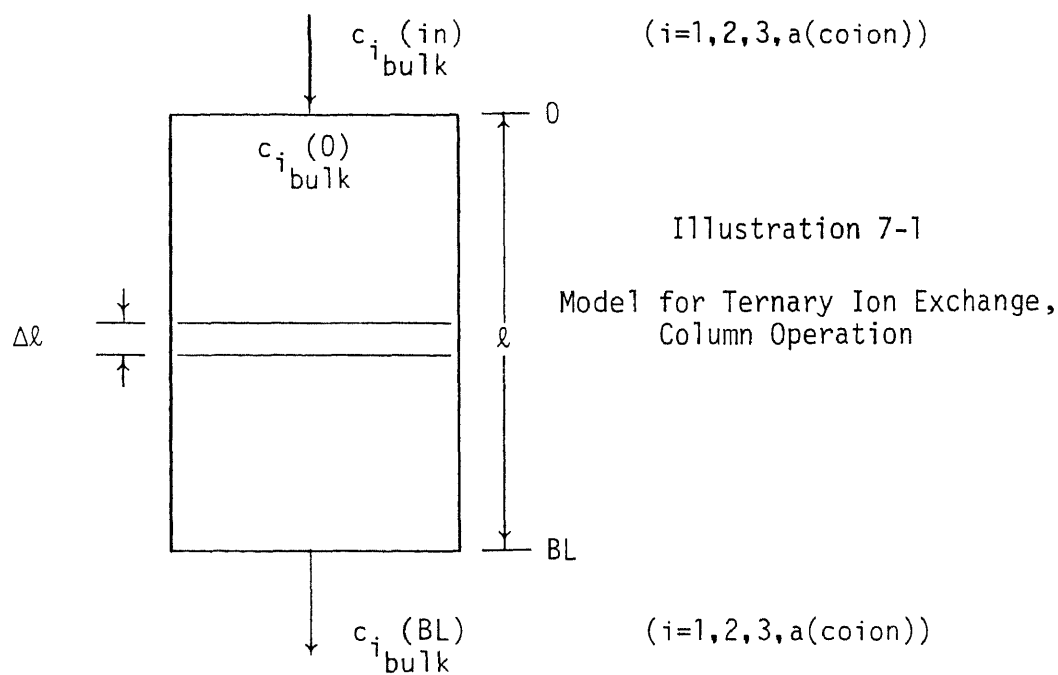
Assumptions:

o   No radial concentration gradients in column

o   Uniform spherical resin particles

o   Uniform bed voidage

o   No swelling of resin, i.e., no bed volume change with time

o Isothermal behavior throughout column

o Stoichiometric exchange, i.e., no adsorption of undissociated salts

o No electric field gradients in column streaming fluid

o Axial dispersion coefficient, E_d, is constant down the column

Fluid Equations

$$(7-1)$$

$$\frac{\partial c_{i_{bulk}}}{\partial t} + \frac{(1-\varepsilon)}{\varepsilon} \cdot \frac{3}{r_o} \cdot k_{L_{i_{eff}}} \cdot (c_{i_{bulk}} - c^*_{i_{int}}) = E_D \cdot \frac{\partial^2 c_{i_{bulk}}}{\partial \ell^2} - \frac{v}{\varepsilon} \cdot \frac{\partial c_{i_{bulk}}}{\partial \ell}$$

for (i=1,2,3)

where from Chapter IV, Treatment of Electrolyte Phase Film Coefficients, equation (4-90) is given in molar units as:

$$o \qquad k_{L_{i_{eff}}} = \frac{D^*_{ii}}{\delta_{eff_{max}}} + \frac{D^*_{ij}}{\delta_{eff_{max}}} \cdot \left[\frac{(c_{j_{bulk}} - c^*_{j_{int}})}{(c_{i_{bulk}} - c^*_{i_{int}})} \right]$$

c_i = concentration of species i in flowing fluid, moles/cc

c^*_i = concentration of species i in film at interface with resin, and in equilibrium, moles/cc

above for (i = 1,2,3)

ε = column voidage for flowing fluid, <u>cc void</u>

ℓ = resin bed length dimension, cm

BL = resin bed length, cm

r_o = resin particle radius, cm

E_D = axial diffusion coefficient (all species) - cm^2/sec

v = superficial velocity of fluid in column, cm/sec

norm = normality of coion, equiv/cc

z_i = valence of species i (i = 1,2,3,Y; where Y = coion)

t = time, sec

$3/r_o$ = area/volume ratio for a sphere

Q_r = equivalents of active sites in resin/cc resin

D_{ii}^* & D_{ij}^* = effective diffusion coefficients in the film as defined by equations (4-96), (4-97), (4-98), and (4-99)

$\delta_{eff_{max}}$ = "effective boundary layer thickness" as defined by equation (4-88)

Putting the terms into dimensionless form.

o $Y = \dfrac{\ell}{BL}$, $R = \dfrac{r}{r_o}$, $T = \dfrac{t \cdot v}{BL}$ (7-2,3,4)

                                                                    (7-5,6)

o $Pe = \dfrac{BL \cdot v}{E_D \cdot \varepsilon}$, $\delta_s = \dfrac{BL \cdot (1-\varepsilon)}{r_o^2 \cdot v}$, bed length parameter

o $x_{i_{bulk}} = \dfrac{c_{i_{bulk}} \cdot (|z_i|)}{norm}$, $x_{i_{bulk}}^* = \dfrac{c_{i_{bulk}}^* \cdot (|z_i|)}{norm}$ (7-7,8)

o $Bi_i = 2 \cdot k_L \cdot r_o$; Biot no.   (7-9)

where (i = 1,2,3) for above equations

In Fick's Law treatment where $\bar{D}_i$ = constant (i = 1,2,3)

$$(7\text{-}10,11)$$

o $\quad Bi_i = \dfrac{2 \cdot r_o \cdot k_{L_{i_{eff}}}}{\bar{D}_i}$, and $\quad \delta_s = \dfrac{BL \cdot (1-\varepsilon) \cdot \bar{D}_i}{r_o^2 \cdot v}$

so

o $\quad Bi_i \cdot \delta_s = \left[\dfrac{2 \cdot k_{L_{i_{eff}}} \cdot BL \cdot (1-\varepsilon)}{r_o \cdot v} \right]$ $\qquad(7\text{-}12)$

however $\bar{D}_i = f(\bar{x}_i)$, and must be kept inside the partials

$$\dfrac{\partial(\;)}{\partial \bar{x}_i} \qquad \text{and} \qquad \dfrac{\partial^2(\;)}{\partial \bar{x}_i^2}$$

Using the transformation $\rho = R^2$ as discussed in Chapter V,

Diffusion in the Resin Phase, the column equations are

derived below.

Setting up the equations for the two most favored species, 1

and 2:

$$(7\text{-}13)$$

o $\quad \dfrac{\varepsilon \cdot \partial x_{1_{bulk}}}{\partial T} + \dfrac{3}{2} \cdot \delta_s \cdot Bi_1 \cdot (x_{1_{bulk}} - x_{1_{int}}^*) = \dfrac{1}{Pe} \cdot \dfrac{\partial^2 x_{1_{bulk}}}{\partial Y^2} - \dfrac{\partial x_{1_{bulk}}}{\partial Y}$

$$(7\text{-}14)$$

o $\quad \dfrac{\varepsilon \cdot \partial x_{2_{bulk}}}{\partial T} + \dfrac{3}{2} \cdot \delta_s \cdot Bi_2 \cdot (x_{2_{bulk}} - x_{2_{int}}^*) = \dfrac{1}{Pe} \cdot \dfrac{\partial^2 x_{2_{bulk}}}{\partial Y^2} - \dfrac{\partial x_{2_{bulk}}}{\partial Y}$

Initial Conditions

o $\quad x_{1_{bulk}} -\text{in} \;(T) \qquad\qquad T \geq 0 \qquad (7\text{-}15)$

o $\quad x_{2_{bulk}} -\text{in} \;(T) \qquad\qquad T \geq 0 \qquad (7\text{-}16)$

$$\circ \quad x_{1_{bulk}}(Y,0) = x_{1_{bulk_{T_o}}}(Y) \qquad 0 \le Y \le 1 \qquad (7\text{-}17)$$

$$\circ \quad x_{2_{bulk}}(Y,0) = x_{2_{bulk_{T_o}}}(Y) \qquad 0 \le Y \le 1 \qquad (7\text{-}18)$$

Boundary Conditions

$$\circ \quad \frac{\partial x_{1_{bulk}}(1,T)}{\partial Y} = 0 \qquad\qquad T \ge 0 \qquad (7\text{-}19)$$

$$\circ \quad \frac{\partial x_{2_{bulk}}(1,T)}{\partial Y} = 0 \qquad\qquad T \ge 0 \qquad (7\text{-}20)$$

note: this B.C. gave rise to instability and will be

discussed in a subsequent section of this Chapter.

$$(7\text{-}21)$$

$$\circ \quad x_{1_{bulk}}(0,T) - \frac{1}{Pe}\cdot\frac{\partial x_{1_{bulk}}(0,T)}{\partial Y} = x_{1_{bulk}}^{-in}(T) \qquad \begin{cases} 0 \le Y \le 1 \\ T \ge 0 \end{cases}$$

$$(7\text{-}22)$$

$$\circ \quad x_{2_{bulk}}(0,T) - \frac{1}{Pe}\cdot\frac{\partial x_{2_{bulk}}(0,T)}{\partial Y} = x_{2_{bulk}}^{-in}(T) \qquad \begin{cases} 0 \le Y \le 1 \\ T \ge 0 \end{cases}$$

Resin – Film Interface where $\rho = 1$ at conditions of $\begin{cases} 0 \le Y \le 1 \\ T \ge 0 \end{cases}$

$$(7\text{-}23)$$

$$\circ \quad \frac{Q_r}{norm}\cdot\frac{4}{Bi_1}\cdot\left[\bar{D}_{11}'\cdot\frac{\partial \bar{x}_1}{\partial \rho}\bigg|_{\rho=1} + \left(\frac{|z_1|}{|z_2|}\right)\cdot\bar{D}_{12}'\cdot\frac{\partial \bar{x}_2}{\partial \rho}\bigg|_{\rho=1}\right] = (x_{1_{bulk}} - x_{1_{int}}^{*})$$

$$(7\text{-}24)$$

$$\circ \quad \frac{Q_r}{norm}\cdot\frac{4}{Bi_2}\cdot\left[\bar{D}_{22}'\cdot\frac{\partial \bar{x}_2}{\partial \rho}\bigg|_{\rho=1} + \left(\frac{|z_2|}{|z_1|}\right)\cdot\bar{D}_{21}'\cdot\frac{\partial \bar{x}_1}{\partial \rho}\bigg|_{\rho=1}\right] = (x_{2_{bulk}} - x_{2_{int}}^{*})$$

Equilibrium is maintained between $x_{i_{int}}^{*}$ and $\bar{x}_{i_{int}}$

Chapter V, Diffusion in the Resin Phase, contains
equations (5-65) and (5-66) which deal with the
quasilinearization of $x^*_{i_{int}}$ as an implicit function of
$(x^*_{i_{int}}, \bar{x}_{i_{int}})$, and differentiation of implicit
functions is discussed as a method to obtain the partial
derivatives required for quasilinearization.

As with the treatment of the non-linear parabolic
partial differential equations describing diffusion of ionic
species in the resin phase, the non-linear parabolic partial
differential equations describing the fluid phase in column
operation were solved using the Crank-Nicholson implicit
method (125) with quasilinearization of non-linear terms
(59). It is the addition of the axial dispersion terms to
the hyperbolic equations describing the concentration changes
in the fluid phase which convert them to parabolic partial
differential equations. As such, they cannot be decoupled
from the resin phase equations in a straightforward
manner--since finite difference representations in both
phases involve nodes n, n+1, & n-1. The solution of the
system of finite difference equations, including the resin
phase equations, will be covered below.

Matrix Equations - Fluid Phase

The setting up of finite difference equations for the
two ionic species, where column length Y (=1) is divided into
I nodes, or I-1 increments ($\Delta Y=1/(I-1)$), involves a matrix
representation, since the terms in the partial differential
equations are approximated as:

$$\circ \quad \left(\frac{\partial x_{i_{bulk}}}{\partial Y}\right)_j \approx \frac{\left[x_{i_{bulk}}(i+1,j) - x_{i_{bulk}}(i-1,j)\right]}{2 \cdot \Delta Y} \qquad (7\text{-}25)$$

$$(7\text{-}26)$$

$$\circ \quad \left(\frac{\partial^2 x_{i_{bulk}}}{\partial Y^2}\right)_j \approx \frac{\left[x_{i_{bulk}}(i+1,j) + x_{i_{bulk}}(i-1,j) - 2 \cdot x_{i_{bulk}}(i,j)\right]}{\Delta Y^2}$$

In the Crank-Nicholson method, the time steps j and j+1 are averaged so that the j+1th equivalent versions of the above partials are averaged with the jth versions to give the partial derivative approximations as a function of time.

Matrix equations to be solved at iteration n+1 and time step j+1 are:

$$(7\text{-}27)$$

$$\circ$$

$$B1_i \cdot x_{1_{bulk_{n+1}}} = U1_{i_n} + V1_i \cdot \left[\frac{dx_1^*}{d\bar{x}_1}\bigg|_{int}(i,j+1)\right]_n \cdot \bar{x}_1(M,i,j+1)_{n+1}$$

$$+ \ V1_i \cdot \left[\frac{dx_1^*}{d\bar{x}_2}\bigg|_{int}(i,j+1)\right]_n \cdot \bar{x}_2(M,i,j+1)_{n+1}$$

$$\circ \qquad\qquad\qquad\qquad\qquad\qquad\qquad (7\text{-}28)$$

$$B2_i \cdot x_{2_{bulk_{n+1}}} = U2_{i_n} + V2_i \cdot \left[\frac{dx_2^*}{d\bar{x}_2}\bigg|_{int}(i,j+1)\right]_n \cdot \bar{x}_2(M,i,j+1)_{n+1}$$

$$+ \ V2_i \cdot \left[\frac{dx_2^*}{d\bar{x}_1}\bigg|_{int}(i,j+1)\right]_n \cdot \bar{x}_1(M,i,j+1)_{n+1}$$

where equation solution vectors $U1_n$ and $U2_n$ contain terms from time step j, as well as the values of resulting terms qualilinearization of non-linear terms at the previous iteration, n.

When the matrices and vectors are expanded:

$$B1_{i_n} = \begin{bmatrix} \alpha1_1 & \beta1_1 & & & \\ \gamma1_2 & \alpha1_2 & \beta1_2 & & \\ & \gamma1_i & \alpha1_i & \beta1_i & \\ & & & \gamma1_I & \alpha1_I \end{bmatrix}_n \quad (7\text{-}29)$$

$$\text{and} \quad x1_{bulk} = \begin{bmatrix} x1_{bulk}(i,j+1) \\ x1_{bulk}(2,j+1) \\ x1_{bulk}(i,j+1) \\ x1_{bulk}(I,j+1) \end{bmatrix}_{n+1} \quad (7\text{-}30)$$

$$V1_{i_n} = \begin{bmatrix} v1_1 & & \\ & v1_i & \\ & & v1_I \end{bmatrix}_n \quad (7\text{-}31)$$

$$\text{and} \quad U1_{i_n} = \begin{bmatrix} u1(1,d) \\ u1(i,j) \\ u1(I,j) \end{bmatrix}_n \quad (7\text{-}32)$$

and

$$B2_{i_n} = \begin{bmatrix} \alpha2_1 & \beta2_1 & & & \\ \gamma2_2 & \alpha2_2 & \beta2_2 & & \\ & \gamma2_i & \alpha2_i & \beta2_i & \\ & & & \gamma2_I & \alpha2_I \end{bmatrix}_n \quad (7\text{-}33)$$

$$\text{and} \quad x2_{bulk} = \begin{bmatrix} x2_{bulk}(1,j+1) \\ x2_{bulk}(2,j+1) \\ x2_{bulk}(i,j+1) \\ x2_{bulk}(I,j+1) \end{bmatrix}_{n+1} \quad (7\text{-}34)$$

$$V2_{i_n} = \begin{bmatrix} v2_1 & & \\ & v2_i & \\ & & v2_I \end{bmatrix}_n \quad (7\text{-}35)$$

$$\text{and} \quad U2_{i_n} = \begin{bmatrix} u2(1,j) \\ u2(i,j) \\ u2(I,j) \end{bmatrix}_n \quad (7\text{-}36)$$

2. <u>Coupling of Resin Phase Equations to Fluid Phase Equations</u>

The coupled set of two resin phase matrix equations
(equations (5-81) and (5-82)) with the two fluid phase matrix
equations can be solved through use of algorithms developed
in this project for inverting seven diagonal and five
diagonal arrays (Appendices E&F) following the Thomas method
(13, 125) for tridiagonal arrays. In order to solve the
fluid phase matrix equations, values of $\bar{x}_1(M,i,j+1)_{n+1}$
and $\bar{x}_2(M,i,j+1)_{n+1}$ derived from the solution of the resin
phase algorithm are expressed as functions of $x_{1_{bulk}}(i,j+1)_{n+1}$
and $x_{2_{bulk}}(i,j+1)_{n+1}$, since the fluid phase concentrations of
species 1 and 2 appear in the resin phase equations (5-81)
and (5-82) at the resin-fluid interface.

Equations (7-27) and (7-28) then have the following
matrix notation when the substitution is made:

$$(7\text{-}37)$$

$$\overset{\circ}{B1}_i \cdot x_{1_{bulk_{n+1}}} = U1_i + V1_i \cdot \left[\left. \frac{dx_1^*}{d\bar{x}_1} \right|_{int} (i,j+1) \right]_n \cdot g1(i,j+1)_n \cdot x_{1_{bulk}}(i,j+1)_{n+1}$$

$$+ V1_i \cdot \left[\left. \frac{dx_1^*}{d\bar{x}_2} \right|_{int} (i,j+1) \right]_n \cdot g2(i,j+1)_n \cdot x_{2_{bulk}}(i,j+1)_{n+1}$$

where

$$\overset{\circ}{\bar{x}}_1(M,i,j+1)_{n+1} = g1(i,j+1)_n \cdot x_{1_{bulk}}(i,j+1)_{n+1} \qquad (7\text{-}38)$$

$$\overset{\circ}{\bar{x}}_2(M,i,j+1)_{n+1} = g2(i,j+1)_n \cdot x_{2_{bulk}}(i,j+1)_{n+1} \qquad (7\text{-}39)$$

○   (7-40)

$$B2_{i_n} \cdot x2_{bulk_{n+1}} = U2_{i_n} + V2_i \cdot \left[\frac{dx_2^*}{d\bar{x}_2} \bigg|_{int} (i,j+1) \right]_n \cdot h2(i,j+1)_n \cdot x_{2_{bulk}}(i,j+1)_{n+1}$$

$$+ V2_i \cdot \left[\frac{dx_2^*}{d\bar{x}_1} \bigg|_{int} (i,j+1) \right]_n \cdot h(i,j+1)_n \cdot x_{1_{bulk}}(i,j+1)_{n+1}$$

where:

○   (7-41)

$$\bar{x}_2(M,i,j+1)_{n+1} = h2(i,j+1)_n \cdot x_{2_{bulk}}(i,j+1)_{n+1}$$

○   (7-42)

$$\bar{x}_1(M,i,j+1)_{n+1} = h1(i,j+1)_n \cdot x_{1_{bulk}}(i,j+1)_{n+1}$$

or to simplify:

○   (7-43)

$$B1_{i_n} \cdot x_{1_{bulk_{n+1}}} = U1'_{i_n} + g1'(i,j+1)_n \cdot x_{1_{bulk_{n+1}}}(i,j+1)_{n+1} + g2'(i,j+1)_n \cdot x_{2_{bulk}}(i,j+1)_{n+1}$$

○   (7-44)

$$B2_{i_n} \cdot x_{2_{bulk_{n+1}}} = U2'_{i_n} + h2'(i,j+1)_n \cdot x_{2_{bulk_{n+1}}}(i,j+1)_{n+1} + h1'(i,j+1)_n \cdot x_{1_{bulk}}(i,j+1)_{n+1}$$

The equations can then be depicted in terms of a five diagonal array as shown in Figure 7-1, for a simple five node example. The values of $x_{1_{bulk}}(i,j+1)_{n+1}$ and $x_{2_{bulk}}(i,j+1)_{n+1}$ are calculated through use of the five diagonal array algorithm, then these values are used to compute values of $\bar{x}_1(M,i,j+1)_{n+1}$ and $\bar{x}_2(M,i,j+1)_{n+1}$ which represent the concentration of $\bar{x}_1$

Figure 7-1

Five Diagonal Array – Fluid Phase Equations

Matrix combining 2 fluid equations
to be solved for $x_{1_{bulk}}$ and $x_{2_{bulk}}$ at I column nodes

$$
\begin{bmatrix}
\alpha 1_1' & -g2_1' & \beta 1_1 & 0 & 0 & 0 & 0 & 0 & 0 & 0 \\
-h1_1' & \alpha 2_1' & 0 & \beta 2_1 & 0 & 0 & 0 & 0 & 0 & 0 \\
\gamma & 0 & \alpha 1_2' & -g2_2' & \beta & 0 & 0 & 0 & 0 & 0 \\
0 & \gamma & -h1_2' & \alpha 2_2' & 0 & \beta & 0 & 0 & 0 & 0 \\
0 & 0 & \gamma & 0 & \alpha 1_3' & -g2_3' & \beta & 0 & 0 & 0 \\
0 & 0 & 0 & \gamma & -h1_3' & \alpha 2_3' & 0 & \beta & 0 & 0 \\
0 & 0 & 0 & 0 & \gamma & 0 & \alpha 1_4' & -g2_4' & \beta & 0 \\
0 & 0 & 0 & 0 & 0 & \gamma & -h1_4' & \alpha 2_4' & 0 & \beta \\
0 & 0 & 0 & 0 & 0 & 0 & \gamma_{I=5} & 0 & \alpha 1_5' & -g2_5' \\
0 & 0 & 0 & 0 & 0 & 0 & 0 & \gamma_{I=5} & -h1_5' & \alpha 2_5'
\end{bmatrix}_n
\times
\begin{bmatrix}
x1\,(1,j+1)_{bulk} \\
x2\,(1,j+1)_{bulk} \\
x1\,(2,j+1)_{bulk} \\
x\,(2,j+1)_{bulk} \\
x1\,(3,j+1)_{bulk} \\
x2\,(3,j+1)_{bulk} \\
x1\,(4,j+1)_{bulk} \\
x2\,(4,j+1)_{bulk} \\
x1\,(5,j+1)_{bulk} \\
x2\,(5,j+1)_{bulk}
\end{bmatrix}_{n+1}
=
\begin{bmatrix}
U1'(1,j) \\
U2'(1,j) \\
U1'(2,j) \\
U2'(2,j) \\
U1'(3,j) \\
U2'(3,j) \\
U1'(4,j) \\
U2'(4,j) \\
U1'(5,j) \\
U2'(5,j)
\end{bmatrix}_n
$$

where $\quad \alpha 1_i' = \alpha 1_i - g1_i'$

$\qquad\quad \alpha 2_i' = \alpha 2_i - h2_i'$

and $\bar{x}_2$ at the resin-film interface at each column length node. The remaining values of $\bar{x}_1(m,i,j+1)_{n+1}$ and $\bar{x}_2(m,i,j+1)_{n+1}$, m=1 to M-1, are solved with the seven diagonal array algorithm, and the process continues at each time step j+1 until the iterative process brings all values of $\bar{x}_i$ and $x_{i\ bulk}$ to within the solution tolerance limits--then proceeds to the next time step. As with the seven diagonal array, a scratch five diagonal array is used to load n^{th} iteration values of coefficients and solution vectors for both $x_{1\ bulk}$ and $x_{2\ bulk}$ at each time step j+1, solves for values of x, and sorts them alternately into $x_{1\ bulk}$ and $x_{2\ bulk}$ values for the $n+1^{th}$ iteration. Appendix I covers the detailed development of the coupling of the resin phase matrix equations with those of the fluid phase for the Ternary Model.

C. <u>Solution for Column Ion Exchange Operation - Binary Systems</u>

1. <u>Finite Difference Equations and General Solution</u>

Treatment of the development of the binary column model are covered in some detail in Appendix J, since it is quite easy to see how the solution of the resin phase equation is coupled to the fluid phase equation, in that both result in tridiagonal arrays. The ternary column model, although more complex, is solved using the same general procedure. In addition, treatment of the boundary conditions by finite difference equations in both the resin phase and fluid phase are also discussed in Appendix J.

2. Initialization Procedures

The proper "conditioning" of the column is essentially the same as described by eq 5-60 in the chapter V, Diffusion in the Resin Phase. That is, the initial conditions in the resin are set up by matching the diffusion flux at the resin boundary: (7-45)

$$
o \quad \frac{4 \cdot Q_r}{Bi_1(i,0) \cdot norm} \cdot \bar{D}_{11}'(i,0) \cdot \frac{\partial \bar{x}_1}{\partial \rho}\bigg|_{\rho=1} (i,0) = (x_{1_{bulk}}(i,0) - x_{i_{int}}^*(i,0))
$$

where $\dfrac{\partial \bar{x}_1}{\partial \rho}\bigg|_{\rho=1}(i,0)$ is calculated using a backward difference

numerical representation between resin node M and M-1. In the "batch case," a trial and error procedure (false positioning) is used to solve the flux balance equations, since the equilibrium expression relating the resin surface concentration $\bar{x}_{1_{int}}$, and the fluid phase concentration, $x_{1_{int}}^*$, is non-linear. However, the relationship is monotonic and this procedure works very quickly. In the column model, some distribution of the bulk fluid concentration down the column is required at time equal 0 (j = 0), since a step input at j = 1 generally will not result in convergence for the solution to the coupled resin and fluid phase equations. Svedberg (125) suggested an exponential decay type of relationship of the form:

$$
o \quad x_{1_{bulk}}(i,0) = x_{1_{bulk}} - in(i,0) \cdot exp\left[-(i-1)\right] \cdot disfac \quad (7-46)
$$

$$
(i = 1 \text{ to } I)
$$

where:

$$\text{disfac} = 3 \cdot \Delta Y \cdot k_{L_{eff}}(1,0) \cdot (1-\varepsilon) \cdot \frac{BL}{v \cdot r_o} \qquad (7\text{-}47)$$

In this work, three revisions were made to the Svedberg approach:

o   A constant, <u>diskon</u>, was multiplied times <u>disfac</u> to allow a read-in input adjustment to the initial distribution. This was required, since under certain combinations of the elements of <u>disfac</u> the column, including the resin phase, could be "preloaded" up to 8% by the initialization procedure. In almost all runs made in this work, a <u>diskon</u> factor could be used such that only 0.1 to 0.5% column "preloading" occurred, consistent with a smooth start. The amount of "preloading" is calculated and printed out by RFMAVD before starting the simulation so that without much difficulty the appropriate <u>diskon</u> factor can be used for each case.

o   Since most of the column capacity is in the resin phase, it required fewer adjustments to minimize column "preloading" if the resin phase was treated according to:

$$(7\text{-}48)$$

$$\bar{x}_1(M,i,0) = \bar{x}_{1_{initial}}(M,1,0) \cdot \exp\left[-(i-1)\right] \cdot \text{disfac}$$

$$(i = 1 \text{ to } I)$$

The flux balance then determined the appropriate

$$x_{1_{bulk}}(i,0) \quad \text{for } i=1 \text{ to } I$$

o   As a further refinement for column operation, $\bar{x}_1$ (M,1,0)

was defined as the composition of resin surface in

equilibrium with $x_{1_{bulk}}$ (1,0), node 1 or Y = 0. As noted

by B.C. eq 21, $x_{1_{bulk}}$ (1,0) is not $x_{1_{bulk}}$ (feed) but the

resultant of the amount of species 1 moving into the

column by convection minus the amount moving away due to

the axial dispersion flux.

These refinements are included in RFMAVD, and invariably lead

to a smooth start with minimum column "preloading" due to

initiation. The trial and error procedure (false positioning) is

used to solve for $\bar{x}_1$ (M,1,0), from which all other column

compositions at $\bar{x}_1$(M,i,0) are calculated, (i=2 to I) by equation

(7-48). Finally, $x_1^*(i,0)$ values are computed, (i=1 to I), and

$x_{1_{bulk}}^{int}$ (i,0) values are given by equation (7-45), (i=1 to I).

3. Treatment of Boundary Conditions by Numerical Approximation

Two fluid phase boundary conditions were approximated by finite

difference equations, and coupled to the general fluid phase

equation. The first, at the column inlet, transforms eq 7-21 into a

central difference approximation using a "fictitious" point outside

the column inlet.

(7-49)

o $\frac{1}{2} \cdot \left[x_{1_{bulk}}(1,j+1)_{n+1} + x_{1_{bulk}}(1,j) \right] - \frac{1}{4 \cdot Pe \cdot \Delta Y} \cdot \left[x_{1_{bulk}}(2,j+1)_{n+1} \right.$

$\left. - x_{1_{bulk}}(0,j+1)_{n+1} + x_{1_{bulk}}(2,j) - x_{1_{bulk}}(0,j) \right] = x_{1_{bulk}}^{-in}$

The numerical approximation of the general equation for the fluid

phase is also set up around i nodes 0, 1, 2, and through cross

multiplication of coefficients, $x_1(0,j+1)_{bulk}\,_{n+1}$ and $x_1(0,j)_{bulk}$ are eliminated. This gives the coefficients and solution vector for node i = 1 in terms of column nodes i = 1 and 2.

This representation of the column inlet boundary condition presented no problems in the binary model for the simulations performed in conjunction with this research. Svedberg notes (125) however that in his studies of the numerical simulation of fixed bed processes that if the concentration profile is too steep as caused by a low Peclet No. (high axial dispersion), and the column length grid is too "coarse," the composition at the bed inlet will oscillate. He found that the oscillations are local and not transferred into the bed. This problem was not observed with RFMAVD on binary simulations; however in the ternary model, TERNEX, this problem was severe and was corrected with an initializing procedure to be discussed later.

The second boundary condition, at the column outlet, was represented initially in this work as the method Svedberg (125) had used, i.e.:

$$\frac{\partial x_1 \,_{bulk}(I,j)}{\partial Y} = 0 \text{ , where at node I, Y=1} \qquad (7\text{-}50)$$

Svedberg represented this with a forward difference approximation instead of a central difference, since he found the latter approximation gave incorrect solutions for high Peclet Numbers. He stated that the central difference gave

too much weight to the concentration value at the boundary.
The forward difference, using a "fictitious" point outside of
the column could represent equation (7-50) as:

$$(7-51)$$

$$x_{1_{bulk}}(I,j+1)_{n+1} + x_{1_{bulk}}(I,j) = x_{1_{bulk}}(I+1,j+1) + x_{1_{bulk}}(I+1,j)$$

The "fictitious" point, I+1, is eliminated in the usual
way by combination with a central differenced general
equation for node i = I. The coefficients and solution
vector for this node are then obtained. Even so, Svedberg
noted that for high Peclet no. values, oscillations in
concentration occurred at the column exit as the mass
transfer zone passed through this boundary. He noted that
this was probably due to the "stiff" component introduced
into the solution by the boundary condition, and that more
column length nodes (smaller increments) decreased the
oscillations. In this work, these oscillations were not
observed, probably because (1) liquid Peclet numbers are an
order of magnitude lower than Peclet Nos. for gases, and
Svedberg was investigating both gas adsorption as well as
liquid ion exchange type processes; and (2) dimensionless bed
length increments were small (0.01). Use of RFMAVD for
simulation of binary ion exchange gave no problem in this
regard; however TERNEX, in ternary ion exchange modeling gave
rise to a "piling up" of concentration at the column exit.
The following treatment was used to minimize this effect in
TERNEX, and was therefore adopted for RFMAVD, and will be

discussed for the binary system since it is easy to draw comparisons.

Assume the bottom column increment, ΔY, is a CFSTR, then a material balance on that section gives:

$$(7\text{-}52)$$

$$0 \quad -x_{1_{bulk}}(I-1) + x_{1_{bulk}}(I) + \frac{3}{2}\cdot\delta_s\cdot Bi_1(I)\cdot\left[x_{1_{bulk}}(I) - x^*_{1_{int}}(I)\right]\cdot\Delta Y$$

$$+ \frac{1}{Pe}\cdot\frac{\partial x_{1_{bulk}}(I-1)}{\partial Y} = -\varepsilon\cdot\Delta Y\cdot\frac{\partial x_{1_{bulk}}(I)}{\partial T}$$

that is,

$$(7\text{-}53)$$

convection (out-in) + transfer to resin + in

from diffusion = accumulation

in finite difference terms:

$$(7\text{-}54)$$

$$0 \quad \frac{1}{2}\cdot\left[x_{1_{bulk}}(I,j+1)_{n+1} + x_{1_{bulk}}(I,j)\right] - \frac{1}{2}\cdot\left[x_{1_{bulk}}(I-1,j+1) - x_{1_{bulk}}(I-1,j)\right]$$

$$+ \frac{3}{4}\cdot\delta_s\cdot Bi_1(I)\cdot\Delta Y\cdot\left[x_{1_{bulk}}(I,j+1)_{n+1} + x_{1_{bulk}}(I,j) - x^*_{1_{int}}(I,j+1)_{n+1}\right.$$

$$\left.-x^*_{1_{int}}(I,j)\right] + \frac{1}{2\cdot Pe\cdot\Delta Y}\cdot\left[x_{1_{bulk}}(I,j+1)_{n+1} - x_{1_{bulk}}(I-1,j+1)_{n+1}\right.$$

$$\left.+ x_{1_{bulk}}(I,j) - x_{1_{bulk}}(I-1,j)\right] = -\varepsilon\cdot\frac{\Delta Y}{\Delta T}\cdot\left[x_{1_{bulk}}(I,j+1)_{n+1} - x_{1_{bulk}}(I,j)\right]$$

This leads to coefficients and solution vector for the Ith node, where α_I is the $x_{1_{bulk}}(I)$ coefficient and γ_I is the $x_{1_{bulk}}(I-1)$ coefficient. Comparison of these coefficients for the various methods are:

o   Forward difference

$$\alpha_I = 1 + \frac{3}{4} \cdot \frac{\delta_s \cdot Bi_1(I) \cdot \Delta T}{\varepsilon} + \frac{\Delta T}{4 \cdot \varepsilon \cdot \Delta Y} + \frac{1}{2} \cdot \frac{\Delta T}{\varepsilon \cdot Pe \cdot \Delta Y^2} \qquad (7\text{-}55)$$

$$\gamma_I = - \frac{\Delta T}{4 \cdot \varepsilon \cdot \Delta Y} - \frac{\Delta T}{2 \cdot \varepsilon \cdot Pe \cdot \Delta Y^2} \qquad (7\text{-}56)$$

o   CFSTR

$$\alpha_I = 1 + \frac{3}{4} \cdot \frac{\delta_s \cdot Bi_1(I) \cdot \Delta T}{\varepsilon} + \frac{\Delta T}{2 \cdot \varepsilon \cdot \Delta Y} + \frac{1}{2} \cdot \frac{\Delta T}{\varepsilon \cdot Pe \cdot \Delta Y^2} \qquad (7\text{-}57)$$

$$\gamma_I = - \frac{\Delta T}{2 \cdot \varepsilon \cdot \Delta Y} - \frac{\Delta T}{2 \cdot \varepsilon \cdot Pe \cdot \Delta Y^2} \qquad (7\text{-}58)$$

o   Central Difference

$$\alpha_I = 1 + \frac{3}{4} \cdot \frac{\delta_s \cdot Bi_1(I) \cdot \Delta T}{\varepsilon} \qquad (7\text{-}59)$$

$$\gamma_I = - \frac{\Delta T}{\varepsilon \cdot Pe \cdot \Delta Y^2} \qquad (7\text{-}60)$$

Inspection would suggest that increase in the Pe no. term is moderated in the CSFTR case by giving more weight to the convective term. It also suggests why the central difference at this B.C. gave trouble, since neither coefficient, α_I or γ_I, contained a convective term. A high Pe no. would reduce the coefficients in this case, which for a given value of $x_{1_{bulk}}(I\text{-}1)$, would tend to have a pronounced upward leveraging effect on the value of $x_{1_{bulk}}(I)$. In any event, the CSFTR model applied to TERNEX ameliorated the concentration "pile up" for particular species at the column exit. The CSFTR model also is, in effect, the treatment for the center spherical node of the resin, as discussed before.

4. <u>Convergence and Stability of the Simulation Model</u>

It would be useful at this point to discuss the convergence and stability performance of the implicit Crank-Nicholson method for approximating solutions to parabolic partial differential equations. Sherwood, Mickley & Reed (71) indicate that the accuracy of the results obtained by numerical solution methods is difficult to estimate; however, it is known that if the method used is both "convergent" and "stable" for the equations being solved then the accuracy is determined by the number of increments used in the grids. Estimate of accuracy for a given solution can be tested by rerunning solutions with finer grid spacings until the difference between results is within limits tolerable to the user. The <u>convergence</u> criterion deals with the approach of the approximation solution to the exact solution in the limit as number of grid nodes approaches infinity. <u>Stability</u> deals with the growth of error in the numerical approximation as the solution proceeds. Error is due to the fact that numerical representation is an approximation and, in a practical sense, a finite number of increments must be used, and in any arithmetic computation roundoff error is present. If the errors do not increase in magnitude as the solution proceeds, the method is said to be stable. Jenson and Jeffreys, (48) in discussing stability and convergence criteria recommend the Crank-Nicholson methods for solution of initial value equations such as the

linear parabolic heat conduction equation: $\frac{\partial T}{\partial t} = \alpha \cdot \frac{\partial^2 T}{\partial x^2}$

for which a finite difference equation modulus $M = \alpha \cdot \frac{\Delta t}{(\Delta x)^2}$

They state the Crank-Nicholson method for this type of equation is stable for all values of M, and recommend it for initial value problems with a modulus M <1. R. E. Carlile and B. E. Gillett, (14) in discussing numerical methods for solution of both initial value and boundary value (hyperbolic equations) problems, recommend implicit methods such as Crank-Nicholson because of their stability and improved accuracy over explicit methods.

Choi, Fan, and Hsu (16), in developing a simulation model for a diabatic absorbtion, used the Crank-Nicolson implicit finite difference method to solve their system of parabolic partial differential equations. They had chosen this method after reviewing the collocation method and the method of characteristics. Specifically, Choi, Fan, and Hsu cite the less stringent stability and convergence restrictions offered by the Crank-Nicolson method than the explicit methods, and less computing time than the method of characteristics, and particular applicability of the method to solution of parabolic partial differential equations.

In a study of fixed bed adsorption modeling with non-linear equilibria, Brown, Mullins and Melsheimer (10) investigated solution of equations identical to those describing the fluid phase in this research. In their investigation the equation was:

$$o \quad D \cdot \frac{\partial^2 c}{\partial z^2} - v \cdot \frac{\partial c}{\partial z} = \frac{\partial c}{\partial t} + k \cdot (c - c^*) \qquad (7\text{-}61)$$

They noted that second order parabolic equations of this type are commonly solved by the Crank-Nicholson method. However, as Svedberg noted (125), if the $D \cdot \frac{\partial^2 c}{\partial z^2}$ dispersive term is deleted, the equation is of hyperbolic form, and they cite commentary by Von Rosenberg (137) on the nonapplicability of the Crank-Nicholson method to solution of hyperbolic forms of partial differential equations. Brown and his coworkers state that when the dispersive term is small relative to the convection term, $v \cdot \frac{\partial c}{\partial z}$, the equation takes on many of the characteristics of hyperbolic systems, and difficulty may be encountered in applying the Crank-Nicholson method.
McCracken and his coworkers (65) in one paper; and Meyer and Weber (69) in another study, indicate that in these cases, rather stringent restrictions on size of grid increments must be observed to avoid instability and to obtain convergence with the exact solution. Brown and his coworkers compared results of simulation of adsorption experiments they performed using the Crank-Nicholson methods with various Δt and Δz increments, to results obtained by using the State Variable method of McCrackin et al (65). In the State Variable method, $X \equiv \frac{\partial c}{\partial z}$, and equation (7-61) becomes:

$$o \quad D \cdot \frac{\partial X}{\partial z} - v \cdot X = \frac{\partial c}{\partial t} + k \cdot (c - c^*) \qquad (7\text{-}62)$$

thereby reducing a second order equation to a pair of first order equations. The result of the study by Brown and his

coworkers indicated that at the same Δz and Δt, if the increments were sufficiently small, both models converged to the same numerical solution. However, as the grid increments were "coarsened," the Crank-Nicholson method did not converge and the ECH curves smeared" out around the experimental curves in a lazy "S", whereas the State Variable method continued to converge and simulate the experimental points. Obtaining convergent solutions with a coarser grid spacing using the State Variable method used 67.5% less computation time than that required by the Crank-Nicholson method when utilizing "finer" convergent grid increments.

Future work on ternary ion exchange modeling should examine the State Variable method as an alternate solution method--mainly to shorten computation time, since in all of the simulations performed in this research the grid spacing and time intervals were decreased until the calculated values were essentially identical, as suggested in Sherwood, Mickley & Reed (71). Examples of this can be seen in the ECH curve for Ag^+ exchange for H^+ at 1.5 normal solution concentration, Figure 7-10, where the number of column and resin increments were systematically increased. As the number of column nodes were increased from 101 to 201, no further change in ECH was observed and, indeed, this curve closely fits the experimental data utilizing the resin phase diffusion coefficients fitted in runs on other Ag^+-Na^+-H^+ systems. The effect on the general shape of the ECH curves in the ternary run P-15, is

shown in Figure 7-13, as the column nodes are increased from 51 to 101 and the number of time steps is increased from 800 to 2100. The initial simulated ECH curve showing appearance of H^+ and disappearance of Na^+ versus the experimental data is definitely improved by finer grid spacings, although the appearance of Ag^+ is 250 sec late. However this difference represents less than a 1% effect on the total material balance for the run.

5. Activity Effects - Resin Phase

A few column runs were made using activity driving force to simulate the ECH curves of Erickson (26) and Omatete (78) experiments. As discussed in Chapter V on Diffusion in the Resin Phase, using activity driving force vs. concentration driving force is more elegant because a single value of an ionic specie's diffusion coefficient can be used in describing interchange with many other ionic species. This precludes the need for multi-parameter or multi-value methods such as the Stefan-Maxwell model or ion-species "pair corrector" coefficients. It was observed in making these runs that use of activity driving force did not alter the shape of the ECH curves appreciably in column operation unless the system was highly non-ideal, and even then the effect was not dramatic. The "batch" type of experiment is clearly best able to discriminate between activity and concentration models. The starting points for ECH fitting in this research were literature values for resin phase diffusion coefficients, when

available, which had been derived by the various investigators using concentration driving force analysis. It was decided, therefore, to perform all column simulations in this research project using concentration driving force--and to test a few extreme cases for effect of activity driving force.

It is interesting to analyze how the activity correction would alter the ECH curve. As discussed, the activity correction for effective diffusion coefficient, $\bar{D}_i$ involves the addition of the following term to the equation for calculating the effective diffusion coefficient for an ideal binary pair (equation 5-13):

$$\text{o} \quad \frac{\bar{D}_1 \cdot \bar{D}_2}{\sum\limits_{i=1}^{2} \bar{D}_i \cdot |z_i| \cdot \bar{x}_i} \cdot \bar{x}_1 \cdot \bar{x}_2 \cdot \frac{\partial \ell n \left[\frac{\bar{\gamma}_1^{-|z_2|}}{\diagup} \Bigg/ \frac{\diagup}{\bar{\gamma}_2^{-|z_1|}} \right]_{molar}}{\partial \bar{x}_1} \qquad (7\text{-}63)$$

where $\bar{\gamma}_1$ and $\bar{\gamma}_2$ have the molar reference state

For a positive deviation system, as $\bar{x}_1$ increases from zero concentration, the following term is negative:

$$\frac{\partial \ell n \left[\dfrac{\bar{\gamma}_1^{|z_2|}}{\bar{\gamma}_2^{|z_1|}} \right]_{molar}}{\partial \bar{x}_1}$$

and the effective diffusion coefficient is decreased. Therefore as $x_{1_{bulk}}$ displaces $x_{2_{bulk}}$, the ECH curve will show appearance of $x_{1_{bulk}}$ earlier than the concentration model since it cannot penetrate the resin as quickly, and this was observed with the

positive deviation system NH_4^+-$ETDA^{++}$, and is shown in

Figure 7-3. With negative deviation systems such as

Ag^+-Na^+ the reverse is true, and the effective diffusivity

is increased, leading to a delayed appearance of Ag^+ in the

ECH compared with the concentration model. This was observed,

as is shown in Figure 7-9.

One other way of examining this effect is to look at a

limiting case where $\bar{x}_1$ is departing from zero concentration

to higher values. The equivalent fluxes can be shown as:

$$\circ \quad \bar{J}_1 = - \bar{D}_{eff} \cdot \frac{\partial \bar{a}_1}{\partial \rho} = - \bar{J}_2 = \bar{D}_{eff} \cdot \frac{\partial \bar{a}_2}{\partial \rho} \tag{7-64}$$

However, as $\bar{x}_2$ approaches 1.0, the activity, $\bar{a}_2$, approaches

$\bar{x}_2$, and the following relationship obtains:

$$\tag{7-65}$$

$$\circ \quad \bar{J}_1 = -\bar{D}_{eff} \cdot \frac{\partial(\bar{\gamma}_1 \cdot \bar{x}_1)}{\partial \rho} = - \bar{J}_2 = \bar{D}_{eff}' \cdot \frac{\partial \bar{x}_2}{\partial \rho} = - \bar{D}_{eff}' \cdot \frac{\partial \bar{x}_1}{\partial \rho}$$

Electroneutrality in the resin requires that $\frac{\partial \bar{x}_2}{\partial \rho} = - \frac{\partial \bar{x}_1}{\partial \rho}$

so that the following relationship results from expansion of

equation (7-65):

$$\circ \quad \bar{J}_1 = -\bar{D}_{eff} \cdot \left[\frac{\partial \bar{\gamma}_1}{\partial \bar{x}_1} \cdot \frac{\partial \bar{x}_1}{\partial \rho} \cdot \bar{x}_1 + \bar{\gamma}_1 \cdot \frac{\partial \bar{x}_1}{\partial \rho} \right] = - \bar{D}_{eff}' \cdot \frac{\partial \bar{x}_1}{\partial \rho} \tag{7-66}$$

The following equality can be derived from equation (7-66):

$$\tag{7-67}$$

$$\circ \quad - \bar{D}_{eff} \cdot \left[\frac{\partial \bar{\gamma}_1}{\partial \bar{x}_1} \cdot \bar{x}_1 + \bar{\gamma}_1 \right] \cdot \frac{\partial \bar{x}_1}{\partial \rho} = - \bar{D}_{eff}' \cdot \frac{\partial \bar{x}_1}{\partial \rho} \text{, as } \bar{x}_2 \to 1.0$$

The relationship defining the effective diffusion coefficient as $\bar{x}_2$ approaches 1, or as $\bar{x}_1$ is departing from zero concentration is:

$$o \quad \bar{D}'_{eff} = \bar{D}_{eff} \cdot \left[\frac{\partial \bar{\gamma}_1}{\partial \bar{x}_1} \cdot \bar{x}_1 + \bar{\gamma}_1 \right] \qquad (7\text{-}68)$$

If the system is ideal $\bar{D}'_{eff}$ is equal to $\bar{D}_{eff}$ since $\dfrac{\partial \bar{\gamma}_1}{\partial \bar{x}_1}$ is equal to zero and $\bar{\gamma}_1$ has a value of one. If the system has a positive deviation, then the effective diffusion coefficient, $\bar{D}'_{eff}$ used in conjunction with the concentration gradient $\dfrac{\partial \bar{x}_1}{\partial \rho}$, is smaller than the effective diffusion coefficient $\bar{D}_{eff}$ defined for use in ideal systems. This is derived from equation (7-68) where as $\bar{x}_1$ approaches zero, the term $\left[\dfrac{\partial \bar{\gamma}_1}{\partial \bar{x}_1} \right] \cdot \bar{x}_1$ approaches zero, and the term $\bar{\gamma}_1$ is greater than one and increasing. Exactly the opposite occurs with negative deviation systems. In these systems, the term $\bar{D}'_{eff}$ is greater than the ideal effective diffusion coefficient, $\bar{D}_{eff}$, since the expression $\left[\dfrac{\partial \bar{\gamma}_1}{\partial \bar{x}_1} \right] \cdot \bar{x}_1$ is approaching zero and the activity coefficient, $\bar{\gamma}_1$, is less than one and decreasing.

6. RFMAVD-A Modeling Program for Binary Ion Exchange in Fixed Beds, Including Activity Driving Force

The discussion above led to development of a model which utilizes the implicit Crank-Nicholson method to approximate the coupled equations describing the operation of a fixed bed binary ion exchange process. Chapter V on Diffusion in the

Resin Phase dealt with development of the Nernst-Planck (N.P.) diffusion model including use of activity driving force, and Chapter IV on Diffusion Through the Film treated the development of a pseudo electric field model which provided film coefficients based on N.P. type interdiffusivity relationships between migrating ionic species. This chapter has provided the development of the features of coupling the resin phase equations to those describing the fluid phase, with quasilinearization of non-linear terms using the quasilinearization technique developed by Lee (59). The reduction of the ternary general case to the simpler binary case illustrated the use of the Thomas algorithm (13, 125) to invert tridiagonal matrices, and showed how the two matrix equations were coupled at the resin-fluid interface. An iterative process at each time step resolved non-linear terms. The treatment of boundary conditions was discussed, as well as the initialization procedure. The details of other features built into program RFMAVD are given in Appendix K, Features of RFMAVD.

D. Binary Simulation of Column Operation

1. General

Nine binary simulations were performed using experimental effluent concentration histories (ECH) from the work of K. L. Erickson (26) on NH_4^+-Ethylene Diamine^{++}(ETDA^{++}) and O. O. Omatete (78) on the systems comprised by Ag^+-Na^+-H^+. The equilibrium constants and

Redlich-Kister activity coefficient parameters for these systems were correlated with RIONFT, and this is covered in Chapter II on equilibrium. In general, the binary model was able to provide a close match to the experimental ECH curves by making only modest adjustments to previously observed resin phase ionic diffusion coefficients. The modeling effort was based on (a) previously fitted equilibrium parameters, (b) the pseudo electric field film coefficients based on the Carberry (11) and the Koloini et al (54, 55) film coefficient correlations for packed beds, (c) electrolyte phase activity coefficients based on the Bromley equation (9), and (d) the use of generalized correlations for axial diffusion coefficients (Fig. 6-1). Normally, 10 increments or 11 nodes were used for resin grid spacing, and 100 increments or 101 nodes were used for column gridspacing--although the program is dimensioned for a 21 x 301 grid spacing. Maximum dimensionless time is defined as the number of empty column displacements (based on superficial velocity) to completion of the run. Normally, this maximum dimensionless time was divided into 100 to 500 increments to establish j-max, or the total number of time steps increments used in the computation. The number of increments used was based on the shape of the ECH curve, and for a very steep curve, such as that of Ag^+-H^+ in favorable exchange, more time increments were required to provide adequate solution stability. This was tested by

trying a series of different time increments until no change was observed (figure 7-10).

2. <u>Research of K. L. Erickson</u> (26) System NH_4^+ - $ETDA^{++}/Cl$ on DOWEX 50Wx8 Resin

   2.1 <u>Discussion - Erickson Experiments</u>

   Erickson conducted two batch experiments by very quickly dropping a 1 normal solution of ETDA (500 cc) into a well stirred flask of resin (33 cc) suspended in 1 normal NH_4^+ solution (20 cc), then quickly withdrawing samples at timed intervals. Total solution volume due to sampling dropped to 70% of the initial volume, and the total resin capacity in equivalents was about 25% of the total initial solution equivalents. Erickson set up material balance equations, including the following equation for the resin, to fit the $\overline{D}_{NH_4^+}$ and $\overline{D}_{ETDA^{++}}$ values which best represented the data:

$$o \quad \overline{W}_1(t) = \frac{3 \cdot Q \cdot Vol}{r_o^3} \cdot \int_o^{r_o} r^2 \cdot \overline{x}_1(r,t) \cdot dr \qquad (7\text{-}69)$$

where:

$\overline{W}_1(t)$ = total equivalents of species 1 in the resin utilized in the batch experiment at time-t

Q = equivalents of active sites in resin/cc resin

Vol = total volume of resin utilized in batch experiments

This equation was integrated by utilizing Simpson's Rule.

In order to define $\bar{x}_1(r,t)$ in the above equation, the following expression was solved:

$$\circ \quad \frac{\partial \bar{x}_1(r,t)}{\partial t} = \frac{1}{r^2} \cdot \left[\frac{\partial(r^2 \cdot \bar{J}_1)}{\partial r}\right] \qquad (7\text{-}70)$$

where $\bar{J}_1$ is defined by the Nernst-Planck model described in Chapter V, equations 5-24 and 5-13.

Erickson used the Crank-Nicholson method to solve for the resin phase concentration profile, then used that profile in conjunction with equation (7-69). The batch material balance equation was given as:

$$(7\text{-}71)$$
$$\circ \quad x_{1_{bulk}}(t+\Delta t) = \frac{V(t)}{V(t+\Delta t)} \cdot x_{1_{bulk}}(t) - \frac{1}{N_t \cdot V(t+\Delta T)} \cdot \left[\bar{W}_1(t+\Delta t) - \bar{W}_1(t)\right]$$

where $V(t)$ = total solution volume at time t

N_t = normality of solution

It was assumed because of high agitation speed that the film resistance was low, so the B.C. utilized was:

$$\circ \quad \bar{x}_1(t) = g(\bar{x}_1(1,t)) \qquad (7\text{-}72)$$

relating equilibrium between the bulk solution and the outer surface of the resin.

Erickson felt the data from one experiment was somewhat more reliable than the other, and the following pairs of coefficients were found to fit the 6 data

points with excellent accuracy for the experimental run:

$\bar{D}'_{ETDA^{++}}$	$\bar{D}'_{NH_4^+}$	Sample variance $-s^2$
cm^2/sec	cm^2/sec	
1.2×10^{-6}	4.0×10^{-6}	0.00016
1.3×10^{-6}	3.9×10^{-6}	0.00018
2.0×10^{-6}	2.9×10^{-6}	0.00023
1.8×10^{-6}	2.9×10^{-6}	0.00045

Erickson, in simulating the ECH of his column experiments found little difference in goodness of fit using diffusion coefficient ratios, $\bar{D}'_{ETDA^{++}}/\bar{D}'_{NH_4^+}$ of 1.2/4.0 versus 2.0/2.9.

In order to define the equilibrium relationship between the resin and the electrolyte, Erickson derived the following empirical expression for the 1 normal system (he did not attempt to fit the 0.1 normal data):

for $\quad 0.012 \leq x^*_{eq} \leq 1.0$ $\qquad\qquad$ (7-73)

o $\quad \bar{x}^*_{eq} = x^{*\,0.33}_{eq} - (1-x^{*\,0.1}_{eq}) \cdot x^{*\,0.1}_{eq} + 0.17 \cdot (1-x^{*\,2}_{eq}) \cdot x^{*\,0.17}_{eq}$

$\qquad\qquad - 0.034 \cdot (x^*_{eq} - x^{*\,6}_{eq}) + 0.03 \cdot (1-x^{*\,0.25}_{eq}) \cdot (|\sin(2\pi \cdot x^*_{eq})|)$

for $\quad 0.0 \leq x^*_{eq} \leq 0.012$ $\qquad\qquad$ (7-74)

o $\quad \bar{x}^*_{eq} = 8.333 \cdot x^*_{eq}$

where:

$\bar{x}^*_{eq}$ = ETDA^{++} cocentration in resin in equilibrium with electrolyte in equiv. fraction

x^*_{eq} = ETDA^{++} concentration in electrolyte in equilibrium with resin, equv. fraction

Whereas the expression represented the experimental data extremely well, the relationship has no theoretical merit, and cannot be extended to other concentrations such as the 0.1 normal data for same system. Other parameters measured by Erickson included the axial dispersion effects, and these experimental results were discussed in Chapter VI. Additionally, Erickson found the uptake of coion Cl^- by the resin to be only 0.023 mequiv/mequiv of total capacity. This indicated that the Donnan potential was strong enough to minimize coion intrusion for this system. Resin volume change in the transition from the NH_4^+ form to the ETDA $^{++}$ form was minus 8%. The average bed void volume, ε, was measured as 0.352.

The column effluent histories (ECH) for six runs were included in Erickson's report. These were:

Runs 13 and 15   for favorable exchange of $ETDA^{++}$ for NH_4^+ at 0.94 cm/sec superficial velocity

Runs 17 and 18   for favorable exchange of $ETDA^{++}$ of NH_4^+ at 1.85 cm/sec superficial velocity

Runs 14 and 16   for unfavorable exchange of NH_4^+ for $ETDA^{++}$ at 1.85 cm/sec superficial velocity

The ECH data points for experiments 17-18 (1.85 cm/sec, favorable) were so close at each time interval so that they

are represented together in Figure 7-2 of this report as averaged data points. The ECH data points for experiments 13 and 15 were sufficiently different that they are both plotted in Figure 7-3. The two unfavorable exchanges, experiments 14 and 16, had somewhat different velocities, 1.75 cm/sec and 1.85 cm/sec and could not be combined. Consequently only experiment 16 was used in this current work, primarily because it had Reynolds no. criteria (41.0) identical to favorable exchange experiments 13 and 15, and could be compared directly with those runs.

2.2   Erickson Simulation Model Development & Simulation Results

Erickson's Column Model was premised on the equations for the resin phase given above. The diffusion across the stagnant layer from the bulk fluid to the resin was modeled by using the conventional equation:

$$o \qquad \overline{J}_i^* = k_f \cdot (x_{i_{bulk}} - x_{i_{int}}^*) \qquad (7\text{-}75)$$

$$\text{where} \qquad k_f = \frac{D_{eff}^*}{\delta} \qquad (7\text{-}76)$$

D_{eff}^* = average diffusion coefficient of two ionic species at infinite dilution

δ = "film thickness"

The film thickness, δ, was a parameter modeled by Erickson to fit the initial portion of the ECH curve. He found $\delta = 0.0065$ cm for Re = 41, and $\delta = 0.0035$ cm for Re = 20, gave the best fit to his data.

The Column equations utilized were:

$$o \qquad \frac{\partial x_{i_{bulk}}}{\partial t} + \frac{(1-\varepsilon)}{\varepsilon} \cdot \frac{\partial \bar{W}}{\partial t} = - \frac{v}{\varepsilon} \cdot \frac{\partial x_{i_{bulk}}}{\partial \ell} + E_D \cdot \frac{\partial^2 x_{i_{bulk}}}{\partial \ell^2} \qquad (7\text{-}77)$$

However, the finite difference method employed was explicit in character, since the partials were expressed as forward differences in both the time and column dimension domain. The method by which the difference equations were solved was to guess forward values at $t+\Delta t$ and $\ell+\Delta\ell$, then use those values to resolve the equations at length step $\ell+\Delta\ell$ and time step $t+\Delta t$ until a reasonable tolerance criterion was met. The process then proceeded to the next time increment. Quasilinearization of non-linear terms was not performed, and as discussed earlier, explicit methods tend to instability if the moduli are not carefully chosen. Indeed, in order to fit the experimental data, Erickson had to include Δt, the finite difference time increment, as one of the "variables." Higher or lower values of time increment would not fit the experimental ECH curves. With this stipulation, and the film "thickness" values previously cited, Erickson obtained reasonable fits to the experimental data.

Erickson's experimental work was carefully performed, and the batch experimental technique he utilized to measure resin phase diffusion coefficients is an alternative to radioactive tracer experiments. The latter tend to be more costly in terms of equipment and materials and require higher experimental skill levels. The experimental work on axial diffusion gave rise to values an order of magnitude higher

than general correlations (figure 6-1) would predict for Re numbers between 20-40. One observation by the researcher on this current work is that within the time constraints of a doctoral research program for a process of this kind, it is difficult to be thorough on both the experimental side as well as the modeling component of the work.

2.3 Simulation of Erickson Experiments - This Research Project

The results of simulation of Erickson's column experiments are shown in Figures 7-2, 7-3, & 7-4. Two favorable exchange runs in which $ETDA^{++}$ displaced NH_4^+ at two flow rates--1.85 cm/sec and 0.94 cm/sec, and one unfavorable exchange in which NH_4^+ displaced $ETDA^{++}$ at a velocity of 1.85 cm/sec, have been simulated and the results closely match the experimental data. The parameters used in the simulation were (1) equilibrium constant and Redlich-Kister parameters for resin phase activity coefficients correlated with RIONFT, plus the Bromley equation for electrolyte species activity coefficients to predict equilibrium between the resin surface and the fluid film, (2) film coefficients based on the Carberry correlation--using the pseudo electric field model with electrolyte species diffusivity corrected for concentration, (3) axial diffusion coefficients obtained by simulating Erickson's axial dispersion experiments, and (4) resin phase diffusion coefficient values of:

$$\bar{D}'_{EDTA^{++}} = 2.0 \cdot 10^{-6} \text{ cm}^2/\text{sec}$$

$$\bar{D}'_{NH_4^+} = 2.9 \cdot 10^{-6} \text{ cm}^2/\text{sec}$$

Ethylene Diamine Exchange with NH_3 on Dowex 50W x 8 - Cl^-

Figure 7-2

Binary Model - Nernst Planck Relationship
For Resin Diffusivities
- Favorable Equilibrium -

Equilibrium Data

$K_{ETDA^{++}NH_4^+} = 16.1206$

Redlich - Kister Constants

$B = 0.34626$

$C = -0.02223$

Bromley Constants

$B_{ETDACl_2} \cong 0.09$

$B_{NH_4Cl} = 0.02$

Experiments 17 & 18[*]

o Data at 28°C

$v = 0.94$ cm/sec (superficial)

$L = 53.5$ cm (effective bed length)

Normalilty = 1.019 (pH = 3.5)

Equivalents in Resin = 3.0 eq./liter

Void Fraction = 0.352 (ϵ)

——— Calculated N.P. Model

$D_{ETDA}^{++} = 2.0 \times 10^{-6}$ cm^2/sec

$D_{NH_4}^+ = 2.9 \times 10^{-6}$ cm^2/sec

$E_D = 4.0$ cm^2/sec (experimental fit)

K_f varies with soln. conc.[1]

$\quad$ 0.004 − 0.009 cm/sec

Re= 20.5 (Based on V/ϵ)

[1] J.J. Carberry, Re >1.0 $K_f = 1.15 \, Re^{1/2}Sc^{1/3} \, D_{eff}/dp$

X-axis: **Elapsed Time - Seconds**

Y-axis: **X_A - Equiv. Fraction ETDA Exiting Column**

[*]K.L. Erickson "Fixed bed ion exchange with differing ionic mobilities and non-linear equilibrium." U. Texas 1977.

Figure 7-3

Ethylene Diamine Exchange with NH_3 on Dowex 50W x 8 - Cl^-
Binary Model - Nernst Planck Relationship
For Resin Diffusivities
- Favorable Equilibrium -

Y-axis: X_A - Equiv. Fraction ETDA Exiting Column (1.00, 0.90, 0.80, 0.70, 0.60, 0.50, 0.40, 0.30, 0.20, 0.10, 0.0)

X-axis: Elapsed Time - Seconds (0, 10, 20, 30, 40, 50, 60, 70, 80, 90, 100, 110, 120, 130, 140, 150, 160, 170)

Equilibrium Data

$K_{ETDA^{++}NH_4^+} = 16.1206$

Redlich-Kister Constants

$B = 0.34626$

$C = -0.02223$

Bromley Constants

$B_{ETDACl_2} \cong 0.09$

$B_{NH_4Cl} = 0.02$

driving force conc. activities

Experiments 13 & 15*

○ △ Data at 28°C

$V = 1.85$ cm/sec (superficial)

$L = 52.7$ cm (effective bed length)

Normalilty $= 1.025$ (pH $= 3.5$)

Equivalents in Resin $= 3.08$ eq/liter

Void Fraction $= 0.352$ (ϵ)

– – – – Calculated N.P. Model

$D_{ETDA^{++}} = 2.0 \times 10^{-6}$ cm^2/sec

$D_{NH_4^+} = 2.9 \times 10^{-6}$ cm^2/sec

$E_D = 4.0$ cm^2/sec (experimental fit)

K_f varies with soln. conc.[1]

0.006 – 0.013 cm/sec

Re $= 41.0$ (V/ϵ as velocity)

[1] J.J. Carberry, Re > 1.0 $K_f = 1.15$ Re$^{1/2}$Sc$^{1/3}$ D_{eff}/dp

*K.L. Erickson "Fixed bed ion exchange with differing ionic mobilities and non-linear equilibrium." U. Texas 1977.

Ethylene Diamine Exchange with NH_3 on Dowex 50W x 8 - Cl^-

Figure 7-4

Binary Model - Nernst Planck Relationship
For Resin Diffusivities
- Unfavorable Equilibrium -

X_B - Equiv. Fraction NH_3 Exiting Column (y-axis: 0.0, 0.10, 0.20, 0.30, 0.40, 0.50, 0.60, 0.70, 0.80, 0.90, 1.00)

Elapsed Time - Seconds (x-axis: 0, 10, 20, 30, 40, 50, 60, 70, 80, 90, 100, 110, 120, 130, 140, 150, 160)

Experiment 16 *

o Data at 28°C
v = 1.85 cm/sec (superficial)
L = 51.3 cm (effective bed depth)
Normalilty = 1.022 (pH = 3.5)
Equivalents in Resin = 3.55 eq./liter
Void Fraction = 0.352 (ϵ)

—— Calculated N.P. Model
$D_{ETDA}^{++} = 2.0 \times 10^{-6}$ cm^2/sec
$D_{NH_4}^{+} = 2.9 \times 10^{-6}$ cm^2/sec
$E_D = 4.0$ cm^2/sec (experimental fit)
K_f varies with soln. conc.[1]
   0.006 − 0.014 cm/sec
$R_e = 41.0$ (based on V/ϵ)

Equilibrium Data

$K_{ETDA^{++} NH_4^+} = 16.1206$
Redlich Kister Constants
   B = 0.34626
   C = −0.02223
Bromley Constants
   $B_{ETDACl_2} \cong 0.09$
   $B_{NH_4Cl} = 0.02$

[1] J.J. Carberry, Re > 1.0 $K_f = 1.15 \, Re^{1/2} Sc^{1/3} \, D_{eff}/dp$

*K.L. Erickson "Fixed bed ion exchange
with differing ionic mobilities and non-linear
equilibria." U. Texas 1977.

274

Other diffusion coefficients were tried in trial and error parameter searches but they did not give as satisfactory a total fit to the effluent concentration histories (ECH) of the three experimental runs. Admittedly, this was an "eyeball" judgment; however the diffusion pair selected was one of the pairs which Erickson had fitted in his batch experiments.

In fitting the predicted ECH curve to the experimental curve, the experimentally determined resin capacity of 3.24 milliequiv./cc of resin had to be adjusted downward by 5 to 8% to "center" the plug flow time for the favorable exchange runs, and upward by 9% for the unfavorable exchange run. This "centering" made the area under the ECH curve before plug flow time equal to that above the ECH curve after plug flow time, thereby insuring reconciliation of the material balance. Of all of the quantities measured in ion exchange experiments, the least reliable is resin capacity/volume of resin "in use"--since the capacity will be somewhat different for each of the species involved. The resin swells to different degrees depending on the various ion species concentrations in the resin, and the resin volume changes during the course of a run. Flow rate, time, and electrolyte phase ionic species concentration measurements are normally quite accurate. It is not unreasonable,

therefore, to adjust the resin capacity within reasonable limits from that measured to insure reconciliation of the material balance. This was done in the other systems simulated as well.

The Carberry film coefficient correlation for packed beds has the form,

$$\text{o} \qquad k_L = b \cdot \frac{Re^{\frac{1}{2}} \cdot Sc^{\frac{1}{3}} \cdot D^*_{eff}}{\epsilon^{\frac{1}{2}} \cdot dp} \qquad \text{for } Re > 1 \qquad (7\text{-}78)$$

so the film coefficient values should differ by about 40% if the Re numbers differ by a factor of two. Reynolds' numbers differed by a factor of two in Erickson's favorable exchange experiments, run at velocities of 0.94 and 1.85 cm/sec. If the value of "b" were chosen to obtain a good simulation of the experimental ECH at one velocity, the fit was poor at the other velocity. Two values of "b", different from Carberry's recommended value of 1.15, were used in early simulations to obtain satisfactory mataching of the experimental results at the two velocities. Use of the pseudo electric field model brought the simulated ECH curves for both velocities into remarkable agreement with the experimental data, using the Carberry film correlation (b=1.15) to estimate "boundary layer effective film thickness" as a function of the average concentration of ionic species in the film. At the lower velocity, gradients are steeper, and the effect is to increase the average concentration of the slower ion,

ETDA^{++}, in the film--thereby reducing flux. The "apparent" film coefficient is lower than would be predicted by Re$^{1/2}$ adjustment alone, since now the effective diffusion coefficient is also lower.

In the unfavorable exchange, the initial appearance and early steep slope of the ECH was "insensitive" to all parametric variations, with the initial appearance time being equal to the column length divided by the interstitial velocity, or 9 seconds, i.e., the inlet concentration of the least favored species runs at convection velocity directly to the column bottom without interchange with the resin. The fit from two "column displacement times" (18 sec) onward was good using the same parameters used to fit the experimental data for the two favorable exchange systems.
The simulation model allows fractional adjustment (FLMADJ) of the constant "b" in either the Carberry (11) or the Koloini et al (54, 55) correlations to test the effect on simulated ECH profile (Appendix K). As discussed in Chapter V, Diffusion in the Resin Phase, the Rao and coworkers' binary batch run results (92, 93) were regressed in one set with FLMADJ as a parameter, yielding a value of 0.86 ±0.04. The parametric study of FLMADJ was made in all of the nine sets of binary ECH curves fit (Erickson and Omatete), using values used of 0.7, 1.0 and 1.2. Overall, the most consistent results were obtained when FLMADJ was unity, as portrayed in the original correlations.

The Erickson equilibrium data were regressed with the Redlich-Kister activity coefficient correlation using both mole fraction and equivalent fraction concentration units, with equally good results (discussed in Chapter II on equilibrium). Experiments 13 and 15 were simulated with RFMAVD utilizing equilibrium constants and activity coefficient parameters both derived for mole fraction and equivalent fraction concentration units, and the results were identical to within ±0.5%.

3. Research of O. O. Omatete - Ag^+-Na^+-H^+ (78)

3.1 Discussion - Omatete Experiments

Omatete carried out favorable exchange experiments for the system Ag^+,Na^+,H^+/NO_3^- on Dowex 50W x8 resin having an average particle diameter of 0.71 mm. The columns used were 1" l.d. glass with lengths ranging from one to four feet. Ag^+ and H^+ concentrations were determined by titration to ± 0.2% accuracy and Na^+ concentration was determined by material balance, with check by flame spectroscopy (±7%). Flow rates varied from 3 to 60 ml/min, and equal effluent volumes were collected with an automatic fraction collector. Feed rate and column length were selected to insure that the concentration profiles in the favorable exchange runs had reached a stable configuration, or constant pattern breakthrough ECHs. A total of eighteen runs were made to determine the binary equilibrium relationships for the three binary pairs at 0.1 normal

concentration, with ten runs out of the eighteen for the Na^+-H^+ system alone. Six additional points were measured at 1.5 normal concentrations, one each for the Ag^+-Na^+ and Ag^+-H^+ systems, and four for the Na^+-H^+ system. Only two ternary equilibrium points were measured. In order to simulate the three ternary column experiments, the closing of a satisfactory material balance in this research effort resulted in the addition of three additional ternary equilibrium points which were consistent with the equilibrium parameters correlated from the experimental data. Needless to say, this represented far too few data points since, as will be shown, the equilibrium relationships in "azeotrope" type (selectivity reversal) systems, such as that of Na^+-H^+, largely determine the shape of the ECH curves. Indeed, additional literature data had to be utilized in the Na^+-H^+ system to better define the "azeotrope" cross over point versus concentration, since at 0.1 normal the upper region "pinches" in a "pseudo azeotrope" manner and at 1.5 normal the system "azeotropes." In addition, the lower part of the "x-y" curve for the Na^+-H^+ system tends to a lower "pinch" region.

Experimental rate runs were made for favorable exchange of each binary system at normalities of 0.05 and 1.5 to demonstrate film diffusion control at the low

normality, and resin phase diffusion control at the higher concentration. Actually, this was done since Omatete's model was a <u>single</u> resistance model (it could simulate film or resin phase transport resistance, but not both). In addition, two favorable ternary runs were made, one at each normality (0.05 and 1.5), and one unfavorable ternary run was made at 1.5 normal solution concentration. In a paper presenting Omatete's work by Omatete, Clazie and Vermeulen (79, 80), only one ternary (0.05 normal) was presented--stating that the "other" rate run did not have fully developed concentration plateaus. Omatete's dissertation work performed six years earlier contained three ternary system runs as described above. All three were simulated in this research project with good results by TERNEX program, utilizing equilibrium parameters correlated from the experimental data with RIONFT for the binary and ternary systems.

3.2 Omatete Simulation Model Development

The Omatete model of fixed bed ion exchange involving binary and ternary systems had the following features which, in effect, represent considerable simplification and "bending" of theory.

a. Equilibrium

    (i) Binary equilibrium was based on a separation factor which is similar to the K value in distillation,

$$\circ \qquad \alpha_{ij} = \frac{1}{\alpha_{ji}} = \frac{\left(\dfrac{\overline{x}_i}{x^*_{i_{int}}}\right)}{\left(\dfrac{\overline{x}_j}{x^*_{j_{int}}}\right)} \qquad (7\text{-}79)$$

, where bar indicates the resin phase, 'int' the resin-fluid interface, and the star depicts an equilibrium condition

As with non-ideal vapor-liquid system equilibrium, α_{ij} (equivalent to K_{ij}) values are not constant over the composition range.

(ii) Ternary equilibrium was represented by the following general multicomponent relationship;

$$\circ \qquad x^*_{j_{int}} = \frac{\alpha_j^{ref} \cdot \overline{x}_j}{\sum\limits_{k=1}^{n} \alpha_k^{ref} \cdot \overline{x}_k} \qquad (7\text{-}80)$$

for $j = 1, 2, \text{---} n$

b. Dynamics - Binary and Ternary Systems

(i) Diffusion between the bulk fluid and the resin was based on a "film" in one phase or the other.

○ <u>fluid phase control</u>

$$\frac{norm}{Q_r} \cdot \left(\frac{\partial \overline{x}_i}{\partial t}_{ave}\right)_v = \sum\limits_{\substack{j=1 \\ j \neq i}}^{n} k'_{L_{ij}} \cdot (x^*_{j_{bulk_{ave}}} - x_{j_{bulk_{ave}}}) \qquad (7\text{-}81)$$

where

$$k'_{L_{ij}} = \frac{a_p}{\delta_F} \cdot D^*_{ij} \quad ; \quad \delta_F \text{ is film 'thickness'} \qquad (7\text{-}82)$$

o   <u>resin phase control</u>

    assumes an "effective constant solid

    phase film", $\overline{\delta}_F$, in the resin phase:

o $\qquad \left(\dfrac{\partial \overline{x}_{i_{ave}}}{\partial t} \right)_v = \sum\limits_{\substack{j=1 \\ j \ne i}}^{n} \overline{k}'_{ij} \cdot (\overline{x}_{j_{ave}} - x^{*}_{j_{ave}})$ (7-83)

    where i = 1,2,------n

and:

$$\overline{k}'_{ij} = \frac{a_p}{(1-\varepsilon)\cdot\overline{\delta}_F} \cdot \overline{D}_{ij} \qquad (7\text{-}84)$$

(ii) <u>Film Coefficient Representation</u> - <u>Fick's</u>

    <u>Law Solution Phase</u>

o   <u>Simple Fick's Law</u>

(7-85)

$$k'_{L_{ij}} = \frac{k_{L_{ij}} \cdot \left[(x_{j_{bulk}} + x_{k_{bulk}}) \cdot k_{L_{ik}} + x_{i_{bulk}} \cdot k_{L_{jk}} \right]}{\left(x_{i_{bulk}} \cdot k_{L_{jk}} + x_{j_{bulk}} \cdot k_{L_{ik}} + x_{k_{bulk}} \cdot k_{L_{ij}} \right)}$$

    where $k_{L_{ij}}$'s(unprimed) are binary Fick's Law
    rate coefficients.

o   <u>An improved Fick's Law</u> was also evaluated

    in which:

(7-86)

$$k_{L_{ij}} = (b_0)_{ij} + (b_1)_{ij} \cdot x_{i_{bulk}} + (b_2)_{ij} \cdot x^2_{i_{bulk}}$$

i.e., the Fick's Law rate coefficients are fit

to a polynomial expression.

(iii)Film Coefficient Representation -Fick's Law

<u>Resin Phase</u>

o   <u>Fick's Law applied to the resin phase</u>

"film"

The equations describing diffusion in the
resin phase "film" are similar to (7-85)
and (7-86), except that $\bar{k}_{ij}$ is a
function of:

(7-87)

$\bar{x}_{i_{ave}}$, $\bar{x}_{j_{ave}}$, $\bar{x}_{k_{ave}}$ and the individual $\bar{k}_{L_{ij}}$'s.

(iv) <u>Film Coefficient Representation-Nernst-Planck,</u>

<u>Solution Phase</u>

o   <u>Simple Nernst Planck representation</u>

$$k_{L_{ij}}' = k_i' \cdot \left[1 + \frac{z_i \cdot x_{i_{bulk}} \cdot (k_j' - k_i')}{\sum\limits_{i=1}^{n} z_i \cdot x_{i_{bulk}} \cdot k_i} \right] \qquad (7-88)$$

for i=1,2,---n and j=1,2,---n

o   <u>Improved Nernst-Planck representation</u>

$$k_i' = \sum\limits_{j=1}^{n} x_{j_{bulk}} \cdot (k_i')_j \qquad (7-89)$$

for i=1,2,---n

$(k_i')_j$ is the rate coefficient
for species i in "pure" component j

(v) Film Coefficient Representation - Nernst Planck,

Resin Phase

o k_{ij}' has the same functional representation

as (7-88) and (7-89) but is a function of the

variables.

(7-90)

$\bar{x}_{i_{ave}}$, $\bar{x}_{j_{ave}}$, $\bar{x}_{k_{ave}}$ plus the individual $\bar{k}_i'$'s

c. Material Balance equations

Using a dimensionless throughput parameter, $\bar{\tau}$

where: $\bar{\tau} = T \cdot v - \bar{T} \cdot v$ (7-91)

and $\bar{T}$ is the reciprocal of the dimensionless velocity

at which the center of the "S" curve moves, the

following can be shown:

$$o \quad R_i = - \left(\frac{\partial x_{i_{bulk_{ave}}}}{\partial v} \right)_{\bar{T} \cdot v} = \left(\frac{\partial \bar{x}_{i_{ave}}}{\partial (\bar{T} \cdot v)} \right)_v \quad (7-92)$$

Since a constant concentration profile was assumed to

be traveling through the column, all concentrations

travel together and are time independent functions of

the column volume coordinate. This leads to:

$$o \quad \left(\frac{dx_{i_{bulk_{ave}}}}{d\bar{\tau}} \right) = \bar{T} \cdot \left(\frac{d\bar{x}_{i_{ave}}}{d\bar{\tau}} \right) \quad (7-93)$$

For a binary system with column presaturation entirely by

one component, and feed containing only the more favored

component, $\bar{T} = 1$. Integration of equation (7-93) yields,

$$x_{i_{bulk_{ave}}} = \bar{x}_{i_{ave}} \quad (7-94)$$

Using the method of characteristics, equation (7-92)

is uncoupled into two independent variables yielding

ordinary differential equations in each variable i.e.,

$$
\text{o} \qquad \left(\frac{dx_{i_{bulk_{ave}}}}{dv} \right)_{\bar{T} \cdot v} = -R_i \ , \ i=1,2,\text{---}n-1 \qquad (7\text{-}95)
$$

$$
\text{o} \qquad \left(\frac{d\bar{x}_{i_{ave}}}{d(\bar{T} \cdot v)} \right)_v = R_i \ , \ i=1,2,\text{---}n-1 \qquad (7\text{-}96)
$$

also the continuity equations become:

$$
\text{o} \qquad \frac{d\bar{x}_{i_{ave}}}{d\bar{\tau}} = \frac{k_{L_{ij}}'}{F} \cdot (x_{i_{bulk_{ave}}} - x_{i_{bulk_{ave}}}^*) \qquad (7\text{-}97)
$$

$$
i=1,2,\text{-----}n-1
$$

Following a constant characteristic, Ri, the

equations are numerically integrated to solve for

species concentration profiles versus dimensionless

time, $\bar{\tau}$.

d. __Determining rate constants from experimental data.__

For a binary system which meets the criteria that

allows $\bar{T} = 1$, equation (7-94) can be approximated as:

$$
\text{o} \qquad k_{L_{ij}}' = \left[\frac{F \cdot \bar{T} \cdot \Delta x_{i_{bulk_{ave}}}}{\Delta\bar{\tau} \cdot (x_{i_{bulk_{ave}}} - x_{i_{bulk_{ave}}}^*)} \right] \qquad (7\text{-}98)
$$

$$
i=1,2,\text{----}n-1
$$

so by selecting points on the "S" curve $k'_{L_{ij}}$ can be approximated as a function of $x_{i_{bulk_{ave}}}$ (or $\overline{k}_{ij}$ as a function of $\overline{x}_{i_{ave}}$), and fit to a polynomial for Fick's Law. The same procedure is used to obtain $k'_{L_{ij}}$ or $\overline{k}'_{ij}$ for N.P. treatment.

3.3 Simulation Results - Omatete

In general, the six binary column effluent concentration histories (ECHs) were fitted well with the polynomial version of Fick's Law, using a common set of nine parameters $((b_0)_{ij}, (b_1)_{ij}, (b_2)_{ij})$, for $i,j,k = 1,2,3,.$ Unfortunately, correlated values of neither these nor the twelve N.P. parameters $((k_i)_i, (k_i)_j, (k_j)_i, (k_j)_j)$, for $i,j,k = 1,2,3,$bear any relationship to the film coefficients or diffusion coefficients measured by other investigators. The model should be considered semi-empirical due to the simplifications made in both the equilibrium relationship and the diffusion mechanism. The "transportability"of the parameters to other ion exchange systems should be regarded as low.

In the three binary cases in which fluid film control was assumed, the fits using the Improved Fick's Law were by far the best--and this should be no surprise since a polynomial fit was specific to the ECH curves. In general, all models gave reasonable representation in the 0.05 normal runs, except Simple Fick's Law in the Ag^+-Na^+ run, and Simple Nernst Planck in the Na^+-H^+ run.

The three resin "film" control runs were more
difficult to simulate, with only the polynomial version
of Fick's Law fitting all three runs well, as could be
anticipated. The Simple Nernst Planck Model, followed
by the Improved Nernst Planck Model, gave the poorest
fits to the "resin film" controlled binary rate run ECH
curves. This was due to the attempt to represent the
complex dynamics of resin diffusion, having space and
time varying compositions, with a simple film
representation. Ternary simulation of the two favorable
exchanges was good, but the ternary simulation of the
unfavorable exchange was only fair, and will be
discussed below.

One complication which has to be taken into account in
any simulation of the Ag^+ systems is the high degree of
association of Ag^+ to form $AgNO_3$, particularly at high
normalities. The resin then adsorbs the $AgNO_3$, taking up
NO_3^-, which makes the exchange non-stoichiometric
during the uptake period. This effect can be offset to a
large degree by adjusting the resin equivalent ion exchange
site concentration upward to include the adsorbed $AgNO_3$
as Ag^+ equivalents as well as the ion exchanged Ag^+ in
any exchange process involving Ag^+. Omatete's throughput
parameter $\overline{T}$, at a value of one, is essentially the plug
flow time used in this research. That is, all of the
equivalents of counterion in the solution fed into the
column up to the plug flow time $(t_{p.f.})$, displaces

all of the equivalents of the other counterions in the column resin plus solution in the voids. Omatete adjusted his throughput parameter upward by including the adsorbed Ag^+ in the column equivalent capacity. This approach works provided the adsorption process is faster than the ion exchange process, and all of the material balance transactions occur before the ECH curve leaves the column, with its pattern established primarily due to the ion exchange process.

3.4 Simulation of Omatete's Binary Experiments - This Research Project

a. General

The results of the simulation of the six favorable binary exchanges are shown in Figures 7-5 through 7-10. These runs are in contrast to the Erickson experiments in that the superficial velocities were much lower, with Re numbers of 2 to 4 compared to values of 20 to 40 in Erickson's work. This is an important distinction in that the axial diffusion flux in the region of maximum mass transfer for Omatete's work was about 1-2 orders of magnitude lower than that observed in simulating Erickson's experiments (values of 0.5×10^{-4} equiv/cm^2/sec versus 0.1×10^{-2} equiv/cm^2/sec). In the very favorable exchange of Ag^+ for H^+, gradients were steep and, as discussed earlier, if the grid increments chosen were too "coarse," the Crank-Nicholson method would not converge to the exact solutions. As discussed, Figure 7-10 for the depicts 1.5 normal

Figure 7-5

Na^+ Exchange with H^+ on Dowex 50W x 8 Resin - NO_3^-
Binary Model - Nernst Planck
- Favorable Equilibrium -
0.055 Normal

Equilibrium Data

$K_{Na^+ H^+} = 1.49827$
Redlich-Kister Constants
B = -0.15021
C = -0.15682
D = -0.08917
Bromley Constants
$B_{NaNO_3} = -0.0128$
$B_{HNO_3} = 0.0776$

Run S - 2*

○ Experimental Data at $23 \pm 2°C$
r = 0.036 cm (ave. particle radius)
v = 0.1885 cm/sec (superficial)
L = 60.32 cm (effective bed depth)
Equivalents in Resin = 2.19 eq./liter
Void Fraction = 0.324 (ϵ)
—— Calculated N.P. Model
$D_{Na^+} = 2.5 \times 10^{-6}$ cm²/sec
$D_H^+ = 10.0 \times 10^{-6}$ cm²/sec
K_f varies with soln. conc.
    0.0038-0.014 cm/sec
$E_D = 0.05$ cm²/sec
Re = 4.2 (based on V/ϵ)

Y-axis: X_{Na}^+ Equivalent Fraction Na^+ Exiting Column (0.0 to 1.0)

X-axis: Elapsed Time - Seconds (7200, 7600, 8000, 8400, 8800, 9200, 9600, 10,000, 10,400)

*Omatete, "Column Dynamics of Ternary
Ion Exchange" U. CA. 1971

Figure 7-6

Ag⁺ Exchange with Na⁺ on Dowex 50W x 8 Resin - NO₃⁻
Binary Model - Nernst Planck
- Favorable Equilibrium -
0.053 Normal

Equilibrium Data
$K_{AG^+NA^+} = 5.924$
Redlich - Kister Constants
$B = -1.000$
$C = 1.2472$
$D = -0.8957$
Bromley Constants
$B_{AGNO_3} = -0.0828$
$B_{NANO_3} = -0.0128$

Run S - 3*
o Experimental Data at $23 \pm 2°C$
  r = 0.036 (ave. particle radius)
  v = 0.183 cm/sec (superficial)
  L = 60.32 cm (effective bed depth)
  Equivalents in Resin = 2.12 eq./liter
  Void Fraction = 0.324 (ϵ)
  ——— Calculated N.P. Model
  $D_{AG}^+ = 0.9 \times 10^{-6}$ cm²/sec
  $D_{NA}^+ = 2.5 \times 10^{-6}$ cm²/sec
  K_f varies with soln. conc.
      0.0037–0.0043 cm/sec
  $E_D = 0.05$ cm²/sec
  Re = 4.07 (based on V/ϵ)

Elapsed Time - Seconds

*Omatete "Column Dynamics of Ternary
Ion Exchange" U. CA. 1971

290

Ag$^+$ Exchange with H$^+$ on Dowex 50W x 8 Resin - NO$_3^-$

Figure 7-7

Binary Model - Nernst Planck
- Favorable Equilibrium -
0.05 Normal

Equilibrium Data

$K_{Ag^+ H^+} = 8.8761$
Redlich-Kister Constants
B = –0.7257
C = 0.8988
D = –0.9350
Bromley Constants
$B_{AgNO_3} = -0.0828$
$B_{HNO_3} = 0.0776$

Run S - 5*

o Experimental Data at 23 ± 2°C
r = 0.036 cm (ave. particle radius)
v = 0.198 cm/sec (superficial)
L = 60.32 cm (effective bed depth)
Equivalents in Resin = 1.97 eq./liter
Void Fraction = 0.324 (ϵ)

———— Calculated N.P. Model
$D_{Ag}^+ = 0.9 \times 10^{-6}$ cm^2/sec
$D_H^+ = 10.0 \times 10^{-6}$ cm^2/sec
K_f varies with soln. conc.
    0.0045–0.014 cm/sec
$E_D = 0.05$ cm^2/sec

x Calculated using Kataoka, Yoshida
  Relationship for Electric Field in Film.
  Re = 4.4 (based on V/ϵ)

X-axis: **Elapsed Time - Seconds** (7500, 7700, 7900, 8100, 8300, 8500, 8700)

Y-axis: **X$_{Ag}^+$ Equivalent Fraction Ag$^+$ Exiting Column** (0.0 to 1.0)

*Omatete, "Column Dynamics of Ternary Ion Exchange" U. CA. 1971

291

Na$^+$ Exchange with H$^+$ on Dowex 50W x 8 Resin - NO$_3^-$

Figure 7-8

Binary Model - Nernst Planck Relationship
- Favorable Equilibrium -
1.54 Normal

Equilibrium Data

$K_{Na^+ H^+} = 1.4983$

Redlich-Kister Constants

B = −0.15021

C = −0.15682

D = −0.08917

Bromley Constants

$B_{NaNO_3} = -0.0128$

$B_{HNO_3} = 0.0776$

Run P - 11*

o Experimental Data at 23$\pm$2°C

r = 0.036 cm (ave. particle radius)

v = 0.079 cm/sec (superficial)

L = 121.65 cm (effective bed depth)

Equivalents in Resin =3.92 eq./liter

Void Fraction = 0.324 (ϵ)

───── Calculated N.P. Model

$D_{Na^+} = 2.5 \times 10^{-6}$ cm^2/sec

$D_{H^+} = 10.0 \times 10^{-6}$ cm^2/sec

K$_f$ varies with soln. conc.

0.0023–0.0094 cm/sec

$E_D = 0.025$ cm^2/sec

Re = 1.89 (based on V/ϵ)

Y-axis: X$_{Na}^+$ Equivalent Fraction Na$^+$ Exiting Column

X-axis: Elapsed Time - Seconds

2200 2600 3000 3400 3800 4200 4600

*Omatete, "Column Dynamics of Ternary Ion Exchange" U. CA. 1971

292

Figure 7-9

Ag^+ Exchange with Na^+ on Dowex 50W x 8 Resin - NO_3^-
Binary Model - Nernst Planck
- Favorable Equilibrium -
1.5 Normal

Equilibrium Data

$K_{AG^+NA^+} = 5.924$

Redlich - Kister Constants

$B = -1.000$
$C = 1.2472$
$D = -0.8957$

Bromley Constants

$B_{AGNO_3} = -0.0828$
$B_{NaNO_3} = -0.0128$

Run P - 12*

○ Experimental Data at $23 \pm 2°C$
r = 0.036 (ave. particle radius)
v = 0.079 cm/sec (superficial)
L = 121.65 cm (effective bed length)
Equivalents in Resin = 4.37 eq./liter
Void Fraction = 0.301 (ϵ)

—— Calculated N.P. Model

$D_{AG}^+ = 0.9 \times 10^{-6}$ cm²/sec
$D_{NA}^+ = 2.5 \times 10^{-6}$ cm²/sec
K_F varies with soln. conc.
    0.00235–0.00245 cm/sec
$E_D = 0.025$ cm²/sec
Re = 1.9 (based on V/ϵ)

– – – – activity driving force

X axis: Elapsed Time - Seconds (3400, 3500, 3600, 3700, 3800, 3900, 4000, 4100)
Y axis: X_{Ag}^+ Equivalent Fraction Ag^+ Exiting Column (0.0 – 1.0)

Omatete "Column Dynamics of Ternary
Ion Exchange" U. CA. 1971

293

Figure 7-10

Ag^+ Exchange with H^+ on Dowex 50W x 8 Resin - NO_3^-
Binary Model - Nernst Planck
- Favorable Equilibrium -
1.525 Normal

Equilibrium Data

$K_{Ag^+H^+} = 8.8761$

Redlich-Kister Constants

$B = -0.7257$
$C = 0.8998$
$D = -0.9350$

Bromley Constants

$B_{AgNO_3} = -0.0828$
$B_{HNO_3} = 0.0776$

Key

I = Column Slices (Nodes)
M = Resin Slices (Nodes)

——— I = 101 & 201, M = 11
—·—· I = 51, M = 11
— — — I = 31, M = 7

Run P - 4*

o **Experimental Data at $23 \pm 2°C$**
r = 0.036 cm (ave. particle radius)
v = 0.079 cm/sec (superficial)
L = 121.65 cm (effective bed length)
Equivalents in Resin = 4.67 eq./liter
Void Fraction = 0.324 (ϵ)

——— Calculated N.P. Model

$D_{Ag^+} = 0.9 \times 10^{-6}$ cm^2/sec
$D_{H^+} = 10.0 \times 10^{-6}$ cm^2/sec
K_f varies with soln. conc.
    0.0024–0.0094 cm/sec
$E_D = 0.025$ cm^2/sec
Re = 1.42 (based on V/ϵ)

x Film Coefficient Calculated Using
Kataoka-Yoshida Relationship for
Electric Field in Film (I = 101, M = 11)

Axis labels:

Y-axis: X_{Ag^+} Equivalent Fraction Ag^+ Exiting Column

X-axis: Elapsed Time - Seconds

*Omatete, "Column Dynamics of Ternary
Ion Exchange" U. CA. 1971

294

exchange of Ag^+ for H^+ and shows the effect of decreasing resin and column grid spacing on solution convergence. Utilizing 11 resin nodes and 101 column nodes provided a convergent solution, since no further improvement was made by increasing column nodes to 201. In general, increasing resin nodes from 11 to 21 had little effect on improvement in convergence. This intuitively makes sense since the ratio of actual column dimension to resin dimension was 500-1500 to 1.

b.   Literature Values of Diffusion Coefficient -

   Resin Phase

The simulation program RFMAVD was used with (1) equilibrium parameters derived from the program RIONFT, (2) the pseudo electric field film coefficient derived using the Carberry correlation for "effective boundary layer film thickness," (3) axial diffusion coefficients derived from Figure 6-1, and (4) starting values of resin phase diffusion coefficients derived from literature sources. These literature sources gave the following experimental values:

Hering & Bliss, (46) using Dowex 50w x8 resin found the N.P. effective resin diffusion coefficients for Na^+-Ag^+ to be

$$\bar{D}_{Na}{}^+ = 2.05 \times 10^{-6} \ cm^2/sec$$

$$\bar{D}_{Ag}{}^+ = 0.68 \times 10^{-6} \ cm^2/sec$$

Graham & Dranoff (30) in studying the exchange of Na^+-Cs^+ on Dowex 50w x8 found the effective diffusion coefficient of Na^+ to be $\bar{D}_{Na}$ = 2.04 x 10^{-6} cm^2/sec

Boyd & Soldano (7) studied isotopic exchange of ions to obtain self diffusion coefficients, and for Dowex 50w x8 resin obtained:

$$\bar{D}_{Na^+} = 0.944 \times 10^{-6} \ cm^2/sec$$

$$\bar{D}_{Ag^+} = 0.642 \times 10^{-6} \ cm^2/sec$$

Reichenberg, (97) using Dowex 50w x5, found the effective Fick's Law diffusion coefficient for Na^+ displacing H^+ to be

$$\bar{D}_{Na^+H^+} = 7.3 \times 10^{-6}$$

Although the value of $\bar{D}_{H^+}$ is "buried" in the effective overall coefficient, a value of 10.0 x 10^{-6} cm^2/sec for $\bar{D}_{H^+}$ relative to $\bar{D}_{Na^+}$ of 2.0-2.5 cm^2/sec would not seem unreasonable. No other value for $\bar{D}_{H^+}$ was found in the literature for the Dowex 50w X8 resin system. In electrolytes at infinite dilution, the diffusion coefficient ratio, $\bar{D}_{H^+}/\bar{D}_{Na^+}$ is about 7.

Gopala Rao and his coworkers (92, 93) measured $\bar{D}_{Na^+}$ to be 2.04 x 10^{-6} cm^2/sec in their tracer experiments on Dowex 50w x8 resin. The research in this work on Rao et al data yielded a correlated value of $\bar{D}_{Na^+}$ to be 2.11 x $10^{-6}cm^2$/sec

using concentration driving force, and 2.88×10^{-6} cm^2/sec using activity driving force.

c. Diffusion Coefficients - Resin Phase

Diffusion coefficient values were obtained through repeated simulation of the experimental ECH curves in order to obtain a single set of values for $\bar{D}_{Ag}+$, $\bar{D}_{Na}+$, & $\bar{D}_{H}+$. This single set of values had to reproduce the three binary systems at two concentration levels, and give good representation of the three ternary systems as well.

The following ranges of diffusion coefficients were investigated:

	cm^2/sec $\times 10^6$
$\bar{D}_{ag}+$	0.7 - 1.1
$\bar{D}_{Na}+$	1.0 - 3.5
$\bar{D}_{H}+$	5.0 - 15.0

The set of values finally selected to fit the 9 systems were

$$\bar{D}_{Ag}+ = 0.9 \times 10^{-6} \text{ cm}^2/\text{sec}$$
$$\bar{D}_{Na}+ = 2.5 \times 10^{-6} \text{ cm}^2/\text{sec}$$
$$\bar{D}_{H}+ = 10.0 \times 10^{-6} \text{ cm}^2/\text{sec}$$

As can be noted, the value for $\bar{D}_{Ag}+$ was not greatly different from the Hering & Bliss value of 0.68×10^{-6} cm^2/sec or the Boyd & Soldano value of 0.64×10^{-6} cm^2/sec. The value of $\bar{D}_{Na}+$ at 2.5 cm^2/sec was higher than the measurements of

most investigators who found $\overline{D}_{Na}+$ to be about

2.05 x 10^{-6} cm^2/sec. Dranoff & Graham found $\overline{D}_{Na}+$

to be 2.4 x 10^{-6} cm^2/sec with the Stefan-Maxwell

model, and this current work found a value of $\overline{D}_{Na}+$ to

be 2.87 x 10^{-6} cm^2/sec using activity driving

force. No comment can be made on the value of

10.0 x 10^{-6} cm^2/sec for $\overline{D}_{H}+$, since no literature

values were found for exchange in Dowex 50w X8 ion

exchange resin. Turner and his coworkers (129) found

the effective diffusion coefficient for $\overline{D}_{H}+$ to be

5.7 x $10^{-6}cm^2$ in Zeokarb 225-x8 resin based on the

Nernst Planck Model. The other ion exchanged was Na^+

in a 0.1N Cl^- solution and the value obtained for

$\overline{D}_{Na}+$ was 1.21 x $10^{-6}cm^2$/sec. On a straight ratio

basis, using $\overline{D}_{Na}+$ as the key, $\overline{D}_{H}+$ would be about

11.4 x 10^{-6} cm^2/sec.

d. Axial Dispersion Coefficients

Although the values of axial diffusion

coefficients were taken from Figure 6-1, several

runs were made in which axial diffusion coefficient

values ten times larger than those given in Figure

6-1 were tried. Considerable "slewing" of the

simulated ECHs resulted, with obviously poorer

fit. The effective resin diffusion coefficients

would have had to be adjusted upward considerably

to match the ECH curves in the Ag^+-H^+ and

Ag^+-Na^+ systems, utilizing the exaggerated axial diffusion coefficients. This was particularly true at a normality of 1.5 where resin phase flux rate tends to control the overall transport of ions. The effect in the more dilute systems, where the film tends to control the diffusion rate, is that smaller film "thicknesses", $\delta_{F_{eff}}$, would have had to be employed. These film coefficients would have been higher than and outside of the range of coefficients predicted by the Carberry correlation. It was for this reason that the values of E_D (axial diffusion coefficients) from Figure 6-1 were judged to be about the correct order of magnitude.

e. Equilibrium Effects

   Considerable effort was expended in attempting to fit the Na^+-H^+ binary systems by utilizing various combinations of diffusion coefficients with little initial success. While a given $\bar{D}_{Na^+}/\bar{D}_{H^+}$ ratio might provide a better fit, the ratio selected invariably "ruined" the fit on the other four binary systems. Examination of Figure 7-5 showing the ECH curve for Na^+-H^+ exchange at 0.05 normality shows a "lazy S" shape. Using equilibrium parameters correlated from the experimental data developed by Omatete, fits of this system tended to be late in first appearance

of the Na^+ ion, and would tend to undershoot the experimental points at the end of the run. This suggested that the driving force was too high at low values of Na^+ ion, and too low at the high concentration end. This same problem was encountered with the 1.5 normal Na^+-H^+ run as well, shown on Figure 7-8. Indeed, the equilibrium data of Omatete gave correlation parameters which, when used to predict the full binary equilibrium curves, showed upper "azeotropes" for both normalities, and no "pinch point" at the lower Na^+ concentrations. Turner and his coworkers (129) had developed Na^+-H^+ system data at 0.1 normality in their work on ion exchange mass transfer mechanisms. Use of eleven additional points from their work, particularly in the upper and lower regions, allowed refitting of the Na^+-H equilibrium data. The equilibrium curves calculated from the new correlation parameters showed pronounced "pinching" in the region of 0 to 0.1 equivalent fraction Na^+ for both normalities. The 0.1 normal curve now "pinched" at the 0.9 to 1.0 region but did not show a reversal of selectivity. The "azeotrope" point for the 1.5 normal system was pushed up from around 0.7 to 0.82 Na^+ equivalent fraction, with the selectivity reversal being not so pronounced.

Upon resimulating the ion exchange dynamics

for the Na-H systems, satisfactory fits could now

be obtained using reasonable values (by literature

standards) of $\bar{D}_{Na}{}^+$ and $\bar{D}_H{}^+$ without disturbing

the fits on the other four systems. The lower

"pinch" point reduced driving force in the transfer

region where Na^+ concentration was low, so the

Na^+ ion appeared early, matching the experimental

points. The driving force at both normalities was

increased in the region where Na^+ predominated,

and the previously observed undershoot of the

experimental ECH curves by the simulation model was

no longer evident, since the driving forces had

been increased.

This merely illustrates the obvious point that

before dynamic processes can be modeled, the

equilibrium values representing driving force

potential should be experimentally measured and

correlated or estimated as precisely as possible,

particularly when any physical-chemical process

exhibits dramatic selectivity changes as a function

of composition.

4. Conclusions - Binary Ion Exchange Simulation - Column Operation

The binary model developed based on the features discussed

in this chapter gave excellent simulated representation of the

experimental effluent concentration histories for nine systems,

with literature correlations for all important parameters except

for resin phase diffusion coefficients and equilibrium data. The equilibrium parameters used to provide equilibrium driving force potential were obtained by correlating the experimental data of Erickson and Omatete using the program RIONFT, except as supplemented from other literature sources as cited above. The values of the fitted resin phase diffusion coefficients were close to previously cited values where such information was available in the literature.

D. Ternary Solution for Column Ion Exchange Operation

1. General

Section B of this chapter covered the development of the fluid phase equations describing the diffusional processes and material balance for ternary ion exchange. The two resulting fluid phase non-linear partial differential equations were approximated by finite difference equations using the Crank-Nicholson approach, and these finite difference equations were expressed in matrix notation in eq (7-27) & (7-28). Section B also described how the two fluid phase matrix equations were coupled to the two resin phase matrix equations which were developed in Chapter V, Section C, describing the diffusional processes and material balance for ternary ion exchange.

The detailed development of the solution of the four coupled matrix equations is given in Appendix G, and involves the use of seven and five diagonal array algorithms developed in this research to solve the coupled sets of equations. The resulting solution of the finite difference equations at each time step, with resolution of non-linear terms through the

quasilinearization procedure, leads to an approximation of the concentration profiles in both the resin phase and the fluid phase, along with diffusional fluxes if desired. Appropriate adjustment of standard parameters such as film coefficients, axial diffusion coefficients, and resin phase diffusion coefficients should result in profiles which match the experimental effluent concentration histories (ECH) for column operation.

The binary solution for column ion exchange operations was covered in Section C of this chapter, since it provided a simpler treatment of initialization procedures and approximation by finite difference equations of the relevant boundary conditions, along with attendant model operating problems and their solutions. The performance of the binary model in simulating nine experimental column ion exchange effluent concentration histories, under widely varying conditions, was judged to be good. This section will deal with the same initialization procedures and representation of boundary conditions as they apply to the ternary exchange. The essential features of the ternary simulation program, TERNEX, will be described in this section, as well as the results of simulation of the three Omatete experimental ternary runs using TERNEX.

2.   Initialization Procedures

The initialization procedure for the binary model was described in Section C, para. 2. In the ternary model, a similar "conditioning" of the column is essential to obtain a smooth start to the solution of the finite difference equations. In the

ternary model, the procedure is also based on balancing the ionic

species flux at the fluid/resin interface, using a backward

difference numerical representation of

$$\left.\frac{\partial \bar{x}_i}{\partial \rho}\right|_{\rho=1}(i,0) \tag{7-99}$$

The equations describing flux at the interface where $\rho = 1$ are:

$$\frac{2 \cdot Q_r}{k_{f_{eff}} \cdot r_o \cdot norm} \cdot \left[\bar{D}_{ii}' \cdot \left.\frac{\partial \bar{x}_i}{\partial \rho}\right|_{\rho=1} + \left(\frac{|z_i|}{|z_j|}\right) \cdot \bar{D}_{ij} \cdot \left.\frac{\partial \bar{x}_j}{\partial \rho}\right|_{\rho=1} \right] \tag{7-100}$$

$$= (x_{i_{bulk}} - x^*_{i_{int}})$$

for i= 1 , j= 2 , and i= 2 , j= 1

and $x^*_{i_{int}}$ is an implicit fuction of $(\bar{x}_i, x^*_{i_{int}})$

The equations are approximated in finite difference terms for

column length node 1 (column inlet) as:

$$\frac{2 \cdot Q_r}{k_{f_{eff}}(1) \cdot r_o \cdot norm \cdot \Delta\rho} \cdot \left[\bar{D}_{ii}'(M,1) \cdot \left[\bar{x}_i(M,1) - \bar{x}_i(M-1,1) \right] \right. \tag{7-101}$$

$$\left. + \left(\frac{|z_i|}{|z_j|}\right) \cdot \bar{D}_{ij}'(M,1) \cdot \left[\bar{x}_j(M,1) - \bar{x}_j(M-1,1) \right] \right]$$

$$= \left[x_{i_{bulk}}(1) - x^*_{i_{int}}(1) \right]$$

for i= 1 , j= 2 , and i= 2 , j= 1

Note $\bar{x}_i(M-1,1)$ and $\bar{x}_j(M-1,1)$ equal $\bar{x}_i(initial)$ and $\bar{x}_j(initial)$

respectively.

Since the equations are non-linear, i.e., equilibrium relationship and diffusion coefficients are functions of $\bar{x}_i(M,1)$ and $\bar{x}_j(M,1)$, the Newton-Raphson procedure is used to solve for $\bar{x}_i(M,1)$ and $\bar{x}_j(M,1)$.

Having determined $\bar{x}_i(M,1)$ and $\bar{x}_j(M,1)$, the distribution of concentrations of $\bar{x}_i(M,\ell)$ and $\bar{x}_j(M,\ell)$ are determined using the exponential decay function described in Section C, para. 2. In the ternary case, however, there are four potential starting distributions:

1. $\bar{x}_1(M,1)$ and $\bar{x}_2(M,1)$ are $> \bar{x}_1(initial)$ and $\bar{x}_2(initial)$

2. $\bar{x}_1(M,1)$ and $\bar{x}_2(M,1)$ are $< \bar{x}_1(initial)$ and $\bar{x}_2(initial)$

3. $\bar{x}_1(M,1) > \bar{x}_1(initial)$ and $\bar{x}_2(M,1) < \bar{x}_2(initial)$

4. $\bar{x}_1(M,1) < \bar{x}_1(initial)$ and $\bar{x}_2(M,1) > \bar{x}_2(initial)$

The initial value of ionic species concentration in the bed is model input data, selected by the user to represent the case to be simulated. In the three Omatete experiments, two were based on the resin bed completely in the H^+ form, or case 1, and one was based on the resin bed completely in the Na^+ form, or case 3 (since $Ag^+ = 1$, $Na^+ = 2$, $H^+ = 3$ in order of selectivity). Once the program tests for type of distribution, the appropriate exponential decrease or increase is made for each component, starting with $\bar{x}_i(M,1)$ and $\bar{x}_j(M,1)$, down the length of the column at each column node.

The concentration of electrolyte ionic species in equilibrium with $\bar{x}_i$ or $_j(M,\ell)$, $(\ell=1,I)$ or $x^*_{i_{int}}(\ell)$, $(\ell=1,I)$, is calculated next. Then, using the flux balance equations

described above, equation (7-101), the fluid phase

concentrations are calculated for $x_{iorj_{bulk}}(\ell)$, ($\ell = 1,I$).

This technique was used to provide starting compositions

prior to time step $j = 1$, which would "condition" the column

for a smooth start with minimum "presaturation" due to

initialization, and indeed only 0.5-1.0% initial preloading

was experienced.

In discussing the finite difference representation of

the Boundary condition at the column inlet for the binary

case, Section C, para. 3, it was noted that the

representation given in equation (7-49) worked well for the

binary model RFMAVD. It was further noted that Svedberg

(125) had found in cases where the concentration gradients

were too steep that the composition at the bed inlet tended

to oscillate, but that the oscillations were not transferred

into the bed. In simulating ternary ion exchange under the

experimental conditions used by Omatete, i.e., very low electrolyte

convection flux relative to resin takeup flux, it was found that

the concentration gradients were steep   Even using a fine grid

spacing ($\Delta Y = 0.01$), in the simulation, oscillations in electrolyte

concentration, $x_{i_{bulk}}(\ell)$, and $x_{j_{bulk}}(\ell)$ would pass down the column in a

"ripple" effect. A revised initialization procedure corrected this

problem, so it will be described here under Initialization rather

than under the section on Boundary Conditions.

The revised procedure was to allow the solution to the

equations describing the ternary ion exchange to proceed

through the first ten dimensionless time steps, but at each step

$$(7-102)$$

$$\circ \quad \bar{x}_{i \atop or_j}(m,1)_{t+1} = \bar{x}_{i \atop or_j}(m,1)_{t+1} \cdot (wgt) + \bar{x}_{i \atop or_j}(m,i)_{t} \cdot (1-wgt)$$

for m = 1,M and 1 = 1,I

It was found that a "wgt" (weight) of about 0.50 minimized the perturbations after running the calculations through j = 10. The "clock" is then set back to j = 1, and the solution restarted using the distribution of concentrations in the resin and solution phases resulting from the solution at j = 10 (start). After the new start, the weighting relationship described above is "turned off" for the remainder of the computation. Invariably this procedure led to a smooth initial second start, and although some bed "presaturation" was a natural consequence of the procedure, the "preloading" rarely exceeded 2-3%. This initialization procedure is used in TERNEX, the ternary ion exchange simulation program.

3. <u>Treatment of Boundary Conditions by Numerical Approximation</u>

The numerical approximation of Boundary Condition (B.C.) at the column inlet was described in Section C, para. 3, for the binary model, along with a discussion of potential instability problems. The revised initialization procedure ameliorated the problem of composition oscillation at this B.C. for the ternary model.

The approximation of the second boundary condition, at

the column exit, was described in Section C, para 3, for the binary model. As discussed, the column increment between column nodes i = I-1, and I was approximated by a CFSTR model, and this was based on experience gained from results of early simulation trials with the ternary model. Use of the CFSTR model reduced the "stiff" condition at the column exit, and allowed the "S" curve to pass through in a normal manner. Prior to the new initialization procedure described above, the ripple caused by the inlet oscillation would reach the column exit and the concentration "pile up" was even more severe. The combination of smoothing the initial operation enhanced the effect of using the CFSTR model at the column exit in terms of producing reasonable ECHs for the three ternary cases simulated.

4.   Features of Ternary Modeling Program - TERNEX

4.1   The ternary model is based on the coupled matrix equations describing the Nernst-Planck diffusion model for three ionic species in the resin phase, along with the coupling of the ternary fluid phase matrix equations to the resin phase matrix equations to describe the effluent concentration history of fixed bed ion exchange operation. Diffusion through the "film," or stagnant layer separating the resin phase from the fluid phase, is based on a pseudo electric field model, which again utilizes the Nernst-Planck relationship describing interdiffusivity under the influence of an electric

field--in this case assumed constant through the "film,"
as is coion concentration. Axial dispersion for all
species is accounted for by a single value for the axial
diffusion coefficient, and the ternary equilibrium is
described by mass action type of relationships, using
the Redlich-Kister activity coefficient model to predict
resin phase activity coefficients for each ionic species.

Discussion in Sections A and B of this chapter
described the use of the quasilinearization technique to
"linearize" non-linear terms and, through use of seven
and five diagonal algorithms, the four coupled matrix
equations are solved at each time step.

4.2   The ternary model, TERNEX, unlike the two binary
models, BMAVD AND RFMAVD, or the batch ternary model,
TRYBCH, does not have an option to use activity driving
force instead of concentration driving force. The case
for use of activities versus concentrations in ion
exchange processes is best tested by simulating batch
type experiments based on, for example, radioactive
tracer techniques. Unless the deviation from ideality
is large, the activity effect on column effluent history
is difficult to discriminate. As was shown in the
discussion of the simulation of Erickson's experiments
on the system ETDA-NH$_3$, use of equilibrium parameters
correlated in terms of either mole fraction or
equivalent fraction give identical results for all

practical purposes. Consequently the ternary model,
TERNEX, utilizes equilibrium parameters correlated in
equivalent fraction only.

4.3   The detailed features of TERNEX are given in
Appendix L.

E. Ternary Simulation of Column Operations

1. Discussion - Omatete Experiments and Simulation Results

1.1 Experimental Results and Model Development

The experimental technique used by Omatete in both
the binary and ternary runs is described in Section D,
para. 3.1 of this chapter. In developing experimental
ECH data on the film controlled ternary systems (0.05
normal), Omatete performed two runs, S-17 and S-18, but
only S-17 was used. The plateau concentration in run
S-18 was not fully developed due either to a flow rate
which was too high, or the column (2 ft.) was too short
for the conditions imposed (feed x_{Ag} = 0.75, x_{Na} = 0.25;
column preloading $\bar{x}_{Ag}$ = 0.250, $\bar{x}_{Na}$ = 0.240, $\bar{x}_{H}$ - 0.510).

Experiments in the region where resin diffusion rates
were controlling (1.5 normal) were performed using four
different combinations of feed and column conditions, labeled
runs P-7, P-8, P-15 and P-16. Of these, only runs P-8 and
P-15 had fully developed concentration plateaus and so were
simulated. The two runs not used were for conditions in which
the column was presaturated with all three species, rather
than a single species as in runs P-8 and P-15. No explanation

was given for the lack of development of the concentration plateaus in the two rejected experiments; however, in retrospect, the rejected experiments may have been more useful if only one species, say H^+, was in the elution feed thereby simulating column regeneration (unfavorable exchange).

Omatete's model development is covered in detail in Section D, para. 3.2 and, as discussed, was based on constant separation factors to describe equilibrium, and rate laws in which either a fluid interface film controlled at low normalities, or a pseudo resin "film" controlled at high concentrations of electrolyte. Four models were described: (1) Simple Fick's Law, (2) Improved Fick's Law, (3) Nernst Planck, and (4) Improved Nernst Planck. The Improved Fick's Law, with polynomial fitted constants, gave the best all around representation of the six binary runs. The same binary models were extended to the ternary case by use of the combinatorial rules given in Section D, para. 3.2.

1.2   The ternary ECH curves were fit equally well by all four models. Two ECH curves, S-17 (0.05 normal) and P-8 (1.5 normal), were fit quite well, and P-15 (1.5 normal - unfavorable) would have been reasonably good if an adjustment had been made in the thruput parameter (resin equivalents) to account for less adsorption of $AgNO_3$ than had been allowed for by Omatete in this run. As will be discussed below, equilibrium considerations and material balance are extremely important in ternary ion exchange in defining the height and

length of plateaus, so even if the dynamic considerations are not correctly predicted, the general shape of the ternary ECH curves will appear to be satisfactory. It is likely that these considerations made model discrimination difficult in the ternary cases, and therefore the binary rate runs are more useful in determining ion exchange parameters from simulation of experimental data.

2.0 Simulation of Omatete's Ternary Experiments - This Research Project

2.1 General

The results of simulation of the three ternary runs, S-17, P-8, and P-15, are shown on Figures 7-11, 7-12, and 7-13. TERNEX was used to perform the computations leading to the simulated ECH curves for the ternary cases. In all cases, the ternary equilibrium concentrations were calculated from the fitted equilibrium constants, and resin phase activity coefficients derived from the correlated experimental binary data including the two ternary data points. The electrolyte phase activity coefficients were calculated from the Bromley Equation. The film coefficients were derived based on corrected single ion diffusion coefficients plus the Carberry film coefficient correlation using the pseudo electric field film model. The axial diffusion coefficients were obtained from the generalized correlations, Figure 6-1. The resin phase "self" diffusion coefficients were derived from "best" fits of the six binary rate runs, and used in program TERNEX with concentration driving forces (vs. activities). The literature values of the "self" diffusion coefficients were

Figure 7-11

Ag^+ and Na^+ Displacing H^+ on Dowex 50W x 8 Resin - NO_3^-
Ternary Model - Nernst Planck
- Favorable Equilibrium -
0.0533 Normal

Run S - 17*
O Experimental Data at $23 \pm 2°C$
r = 0.036 cm (ave. particle radius)
v = 0.0967 cm/sec (superficial)
L = 60.365 cm (effective bed length)
Equivalents in Resin = 2.38 eq./liter
Void Fraction = 0.356 (ϵ)
—— Calculated N.P. Model

$D_{Ag}^+ = 0.9 \times 10^{-6}$ cm²/sec
$D_{Na}^+ = 2.5 \times 10^{-6}$ cm²/sec
$D_H^+ = 10.0 \times 10^{-6}$ cm²/sec

H^+

Na^+

Ag^+

X_i Equivalent Fraction of Species Exiting Column

Elapsed Time - Seconds
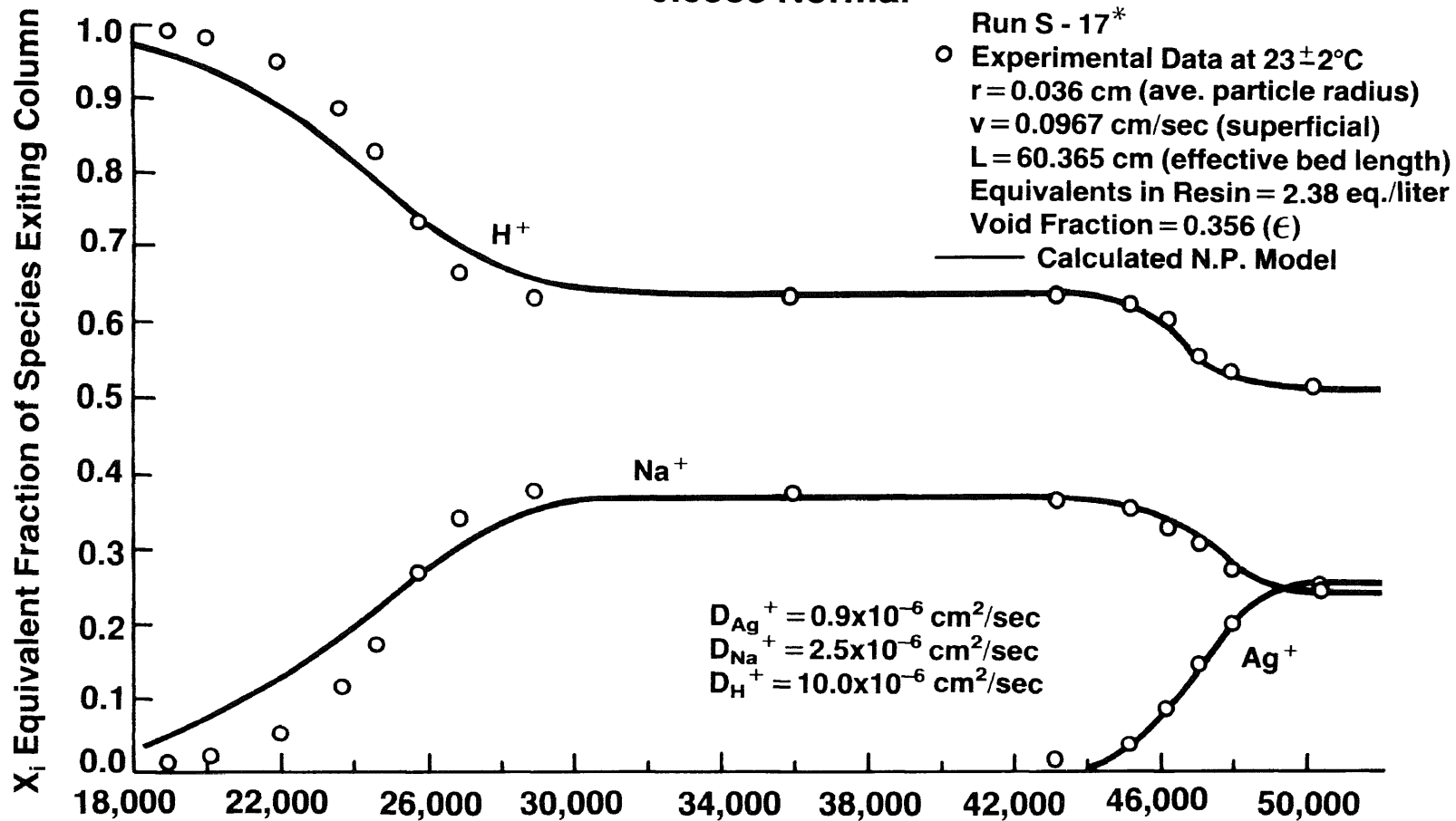
*Omatete "Column Dynamics of Ternary
Ion Exchange" U. CA. 1971

Figure 7-12

Ag^+ and Na^+ Displacing H^+ on Dowex 50W x 8 Resin - NO_3^-
Ternary Model - Nernst Planck
- Favorable Equilibrium -
1.51 Normal

Run R - P8*
O Experimental Data at $23 \pm 2°C$
  r = 0.036 cm (ave. particle radius)
  v = 0.03455 cm/sec (superficial)
  L = 121.28 cm (effective bed length)
  Equivalents in Resin = 3.7 eq./liter
  Void Fraction = 0.356 (ϵ)
  ———— Calculated N.P. Model

$D_{Ag}^+ = 0.9 \times 10^{-6} \, cm^2/sec$
$D_{Na}^+ = 2.5 \times 10^{-6} \, cm^2/sec$
$D_H^+ = 10.0 \times 10^{-6} \, cm^2/sec$

X-axis: Elapsed Time - Seconds
Y-axis: X_i Equivalent Fraction of Species Exiting Column
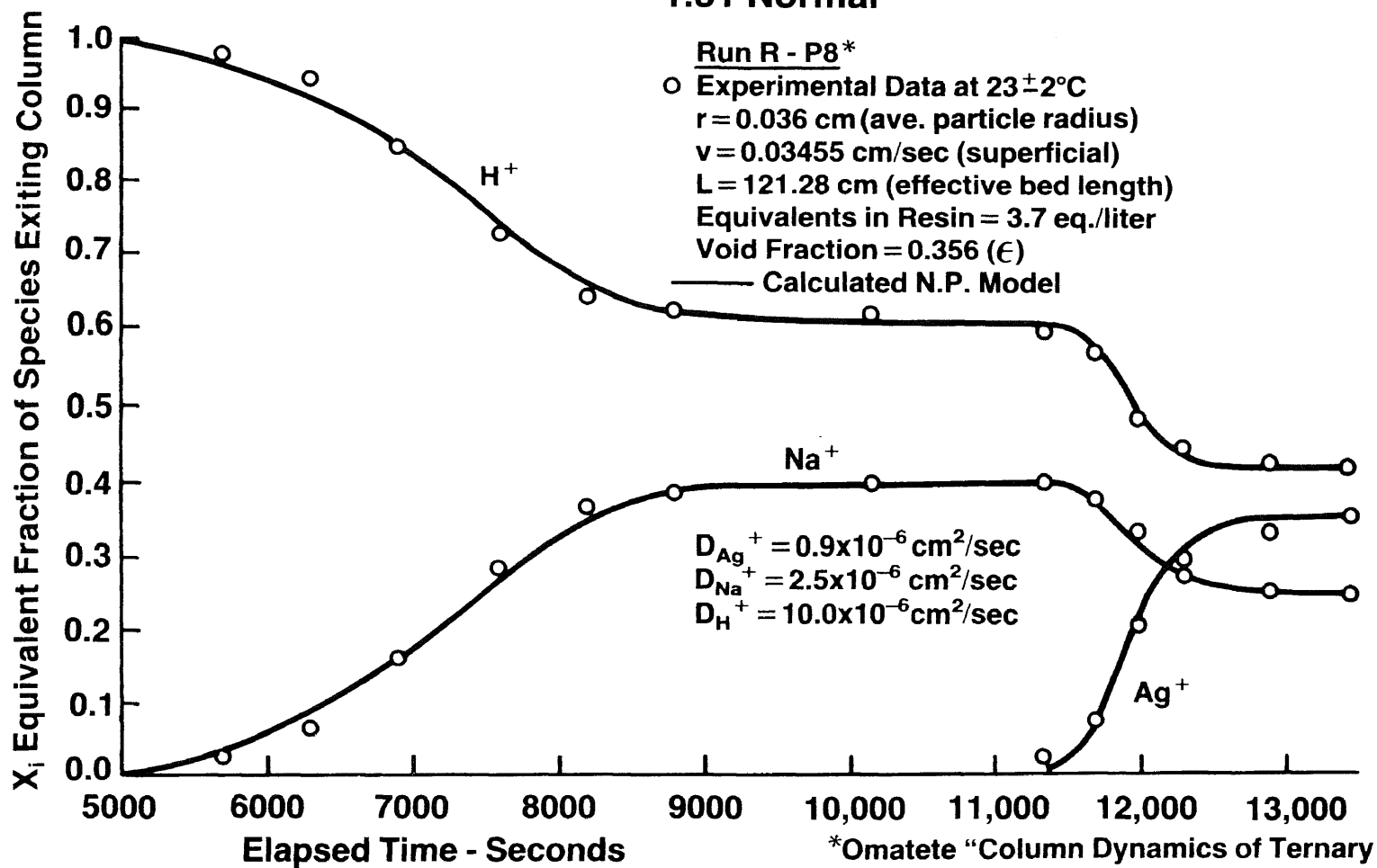
*Omatete "Column Dynamics of Ternary
Ion Exchange" U. CA. 1971

Figure 7-13

Ag$^+$ and H$^+$ Displacing Na$^+$ on Dowex 50W x 8 Resin - NO$_3^-$
Ternary Model - Nernst Planck
- Unfavorable Equilibrium -
1.5 Normal

Key
I = Column Nodes, M = Resin Nodes
J = Dimensionless Time Steps
——— I = 101, M = 11, J = 2100
– – – – I = 51, M = 11, J = 800

H$^+$

Run R - P15 *
o Experimental Data at 23±2°C
r = 0.036 cm (ave. particle radius)
v = 0.0461 cm/sec (superficial)
L = 121.28 cm (effective bed length)
Equivalents in Resin = 3.15 eq./liter
Void Fraction = 0.356 (ϵ)
——— Calculated N.P. Model
$D_{Ag}^+ = 0.9 \times 10^{-6}$ cm^2/sec
$D_{Na}^+ = 2.5 \times 10^{-6}$ cm^2/sec
$D_{H}^+ = 10.0 \times 10^{-6}$ cm^2/sec

Ag$^+$

Na$^+$

X$_i$ Equivalent Fraction of Species Exiting Column

Elapsed Time - Seconds
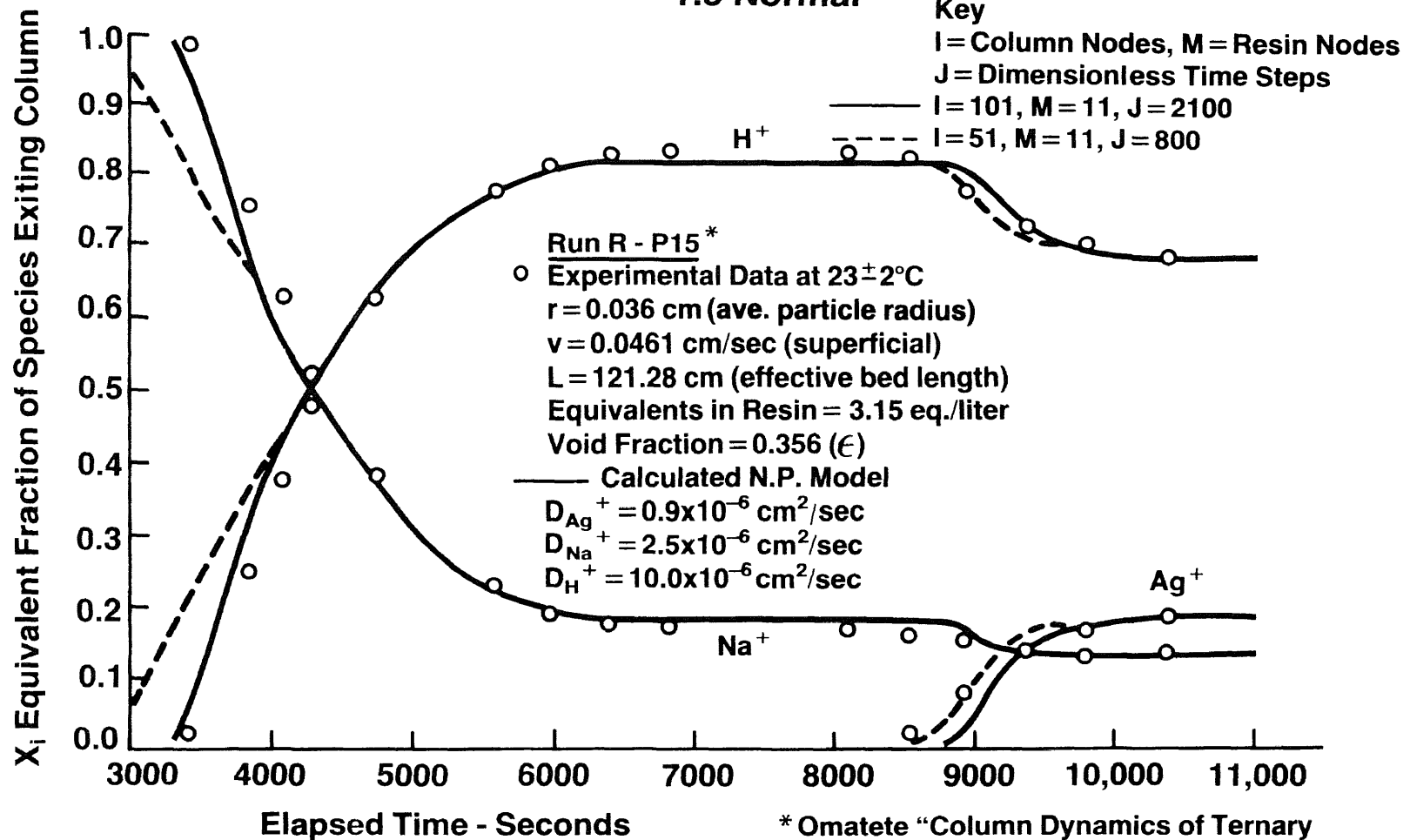
* Omatete "Column Dynamics of Ternary
Ion Exchange" U. CA. 1971

cited in Section D, para. 3.0, subsection 3.4, and the values utilized in the simulation of 6 binary systems and 3 ternary systems were not far different from those values. The results, as seen in the plots, are reasonably good, particularly since all of the information used provided good simulations of the six binary cases as well.

2.2 Equilibrium and Material Balance Considerations

This section will deal with the problems encountered in representing the period of "dwell" for plateaus in the ternary simulations. As can be seen, in a favorable exchange of a feed consisting of Ag^+ and Na^+ with a column containing resin presaturated with the least favored species, H^+, the first breakthru is Na^+ ion at a concentration level which exceeds the Na^+ ion inlet concentration. H^+ ion level decreases, but to a plateau level higher than its feed concentration. The total exchange is completed when the Ag^+ breakthru is observed, and all concentrations reach their feed values.

This phenomena can be best visualized by assuming instantaneous ion exchange of Ag^+ for H^+, allowing Na^+ and H^+ released by the ion exchanger to proceed ahead in a "binary" mode. The resin ahead of the Ag^+ front soaks up Na^+ ion, in effect storing it, until the Ag^+ ion rich feed front gets to that point. The excess Na^+ is then "chased" and lends its concentration to the forward front—thereby building Na^+ concentration to a higher level than the Na^+ concentration in the feed. The Na^+ in the fluid phase has

concentration gradients allowing it to attempt to diffuse up and down the column away from the plateau. In the down column direction, the gradient is gradual as some Na^+ is ion exchanged with H^+ in the resin. Up column, the gradient is steep, since there is no place for Na^+ to go except to satisfy the ternary equilibrium requirements of the feed with the resin. Keep in mind, when looking at an ECH curve, that as an observer in the column you would view the concentration history as occuring in the reverse direction from the time plot. First Na^+ arrives displacing H^+, then the Na^+ concentration drops as it is exchanged to satisfy the feed equilibrium, and Ag^+ ion appears in the electrolyte phase for the first time as the resin is saturated.

The concentration height of the Na^+ ion above inlet value can be approximated simply by material balance as follows:

assume:

o   wave fronts are square

o   the most preferred ion displaces all species 2 and 3 ions ahead of it

o   the concentration of species 2 and 3 ions represents a pseudo binary in equilibrium with the resin in their end of the column

o   in the diagram below, excess species 2 in area B = deficit of species 3 in area A.

Illustration 7-2
Material Balance Schematic
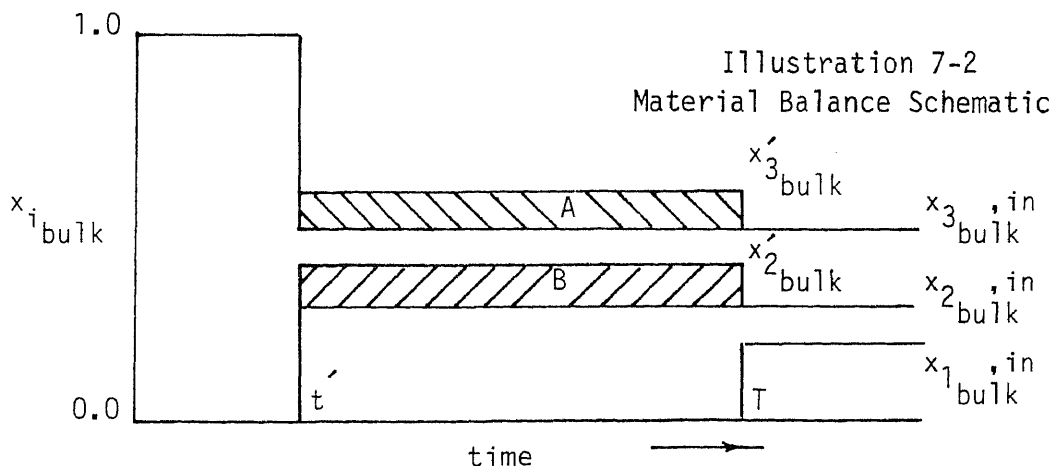
Material Balance (7-103)

$$(T-t')\cdot(x_{3_{bulk}}' - x_{3_{bulk}},in) \simeq (T-t')\cdot(x_{2_{bulk}}' - x_{2_{bulk}},in)$$

or
$$x_{2_{bulk}}' \simeq (1 - x_{3_{bulk}},in + x_{2_{bulk}},in)/2$$

Checking this approximate method

bulk concentrations

	$x_{1_{in}}$	$x_{2_{in}}$	$x_{3_{in}}$	calc. x_2'	obs. x_2'	calc. x_3'	obs. x_3'
S-17	0.25	0.24	0.51	0.365	0.365	0.635	0.635
P-8	0.350	0.24	0.41	0.415	0.39	0.585	0.61
P-15*	0.187	0.133	0.680	0.22	0.175	0.78	0.83

*unfavorable non-sharpening "S" curve so area A = area B

The next question is, what determines the approximate "dwell" for the species 2 and 3 plateaus? Again, a material balance gives the approximation, but this time it involves the ternary resin composition in equilibrium with the feed composition. Time T depicted in Figure 7-14 can be computed based on favored species 1 by balancing equivalents into the column against the holdup of species 1 in the column up to time T, i.e.:

(7-104)

$$T = \frac{\left[(\text{equiv.-resin})\cdot \overline{x}_1^* + (\text{equiv.-col. voids})\cdot x_{1_{bulk}},\text{in}\right]}{\left[(\text{total equiv. into column})\cdot x_{1_{bulk}},\text{in}\right]}$$

where:
$\overline{x}_1^*$ = resin concentration of species 1 in equilibrium with the ternary system feed composition

In the case of run S-17 time T works out to 46,700 seconds versus about 46,600 seconds observed. It is by this mechanism that the resin equivalents were adjusted in this work to account for adsorption of complexed $AgNO_3$ (Omatete adjusted his Thruput Parameter in an analogous manner). Time T is thereby anchored to the observed value by material balance. In the case of the two Ag^+ binary systems, this correction was about 15%. In the case of the ternary systems, the $AgNO_3$ adjustments would be less because the Ag^+ feed compositions were lower (between 0.187-0.350 equivalent ionic fraction), and the adjustment represented approximately 7% for the worst case, P-8 (100 milliequiv/1500 milliequiv).

Similarly, the initial plateau time for Na^+, or species 2, can be approximated by a material balance on species 2 and knowledge of the ternary phase equilibrium diagram.

(7-105)

Species 2 balance

$$(\text{total equiv. flow in})\cdot\left[t\cdot x_{2_{bulk}},\text{in} - (T-t')\cdot(x_{2_{bulk}} - x_{2_{bulk}},\text{in})\right]$$

$$= \left[(\text{equiv.-resin})\cdot \overline{x}_2^* + (\text{equiv.-col. voids})\cdot x_{2_{bulk}},\text{in}\right]$$

where:
$\overline{x}_2^*$ = resin concentration of species 2 in equilibrium with the ternary system feed composition

This simple approach, using values from S-17, gave a t' from Figure 7-14 equal to 23,860 seconds vs. 24,000 observed. In this case, the equilibrium concentration value of Na^+ taken from Figure 2-5 was 0.16, and represented one of the ternary data points resulting from closing the material balance on the three ternary runs. The initial correlation of Omatete equilibrium data using program RIONFT, not including the material balance points, gave $x_{Na}^{*}+$ for S-17 as 0.185--resulting in a simulation result with $t' = 25,100$ seconds, or 5% less dwell time. Run P-15 would have had an 8% shorter dwell for the H^+ plateau based on correlation of the Omatete initial equilibrium data. The ternary equilibrium point correlated for P-8 conditions was close to the material balance requirement for that run, and no change was observed during recorrelation with the material balance points.

The previous discussion was detailed, not so much to provide a simple method of predicting ternary ECH curves, but to show the rationale for engaging in the somewhat time consuming procedure required to reconcile material balance and equilibrium data by a procedure consisting of:

(a) approximating the ternary equilibrium points from the correlation of the original data without the material balance points

(b) simulating the ternary runs and observing from material balance considerations, based on the plateau dwell, what the ternary equilibria concentrations should be to give a better fit

(c) refitting the binary and ternary equilibrium data with program RIONFT, using the new material balance equilibrium points in addition to the original data

(d) resimulating the six binary rate runs to make sure that the influence of the new material balance points on total data regression to obtain new equilibrium parameters did not alter those ECH curves significantly

(e) resimulating the three ternary systems to check out the effect of the new equilibrium parameters on the general material balances and Na^+ and H^+ plateau "dwells"

(f) repeating above, to "fine tune" the equilibrium correlation. This procedure was time consuming, and future investigators are encouraged to add a few more measured equilibrium data points in order to reduce correlation effort. The first ternary phase diagrams generated with the ternary phase diagram regression program, RIONFT, would have provided an excellent first "map" to select regions for additional experimental equilibrium data points.

2.3 Stability and Convergence of TERNEX

The general considerations of convergence and stability of the Crank-Nicholson method were discussed in Section C, para. 4, for binary model simulation results. The solution time for TERNEX, with resin mode grid spacings of 11, and column nodes of 50, with maximum dimensionless time (number of empty columns full displaced by the feed

solution during the run) divided by 800 required about 2.5-3.0 CPU hours. Therefore the number of tests at varying increment spacings during the ternary modeling was limited, in view of the iterations required to resolve the equilibrium and material balance tolerance as described above. In the case of experiment S-17, runs of M = 7, I = 51, T = 1200 were identical with M = 11, I = 101, T = 1200 (resin nodes = M, column nodes = I, time increments = T) and convergence and stability were assumed. In experiment P-8, runs of M = 7, I = 51, T =1850 were identical to M = 11, I = 101, T = 1850, and convergence and stability were assumed.

Run P-15, Figure 7-13, an unfavorable exchange was fitted at M = 11, I = 51, and T = 800 with good results except for the initial appearance of Na^+ and H^+ ions. A final check at M = 11, I = 101, and T = 2100 (7 CPU hours on a DEC VAX 11/780) showed some tightening up of ECH profile for this unfavorable (nonsharpening "S" curve profile) exchange. However, the final appearance of the Ag^+ ion in the electrolyte phase was delayed by 250 seconds (less than 1% of the total material balance), and it was deemed proper not to "retune" the H^+ equilibrium point to compensate for this difference. It would suggest that in ever spreading elution ECH curves, where unfavorable exchange exists, that a "fine" grid should be utilized with the Crank-Nicholson method to maintain

stability and convergence. Whether the State Variable
method (65) or Collocation method (29) would be better
(less computer time) than Crank-Nicholson remains to be
tested.

3. Conclusions

The ability of the binary model, RFMAVD, and its ternary
version, program TERNEX, to simulate ion exchange in columns
under wide ranging conditions has been demonstrated, as verified
against experimental data on actual column runs. The use of
literature information on all input parameters, except
equilibrium data and ionic species "self" diffusion coefficients
makes the models "powerful." The non-linear regression packages
accompanying the dynamic models has improved the overall model
capability, since with minimum experimental data if necessary,
thermodynamically sound equilibrium parameters can be
determined. Additionally, "self" diffusion coefficients found
in literature sources for ubiquitous ions in the more common ion
exchange resins (Dowex 50w) can provide a starting point for
diffusion coefficient parameter estimation utilizing
experimental ECH curves. Future studies should be concentrated
on use of activity driving force versus concentration driving
force, but this can best be explored with "batch" type
experimentation on a variety of ion pair combinations. Finally,
other numerical methods should be investigated for inherent
convergence, stability and potential for reduction in
computation time. Industrially, CPU solution times of 6 hours

are acceptable given the fact that the numbers of VAX 11/780 type systems are growing in industry at an accelerated pace. Even with existing installations, CPU utilization is normally limited to 6 out of 21 shifts/week, so access for longer running programs is not a problem. The major advantage of faster running methods which are both convergent and stable would be to couple the binary column ion exchange model based on those methods to a non-linear regression package. This was done with program BMAVD, the batch binary model, to develop program DFUSFT, the non-linear regression model designed to fit diffusion coefficients based on data generated in batch type ion exchange experiments. It should be possible to use experimental ECH data for a variety of binary ionic pairs as input to a regression routine from which diffusion and film coefficients could be derived. Using program RFMAVD as a subroutine, solution times of 20 minutes/ECH curve would be needed to yield a practical regression model of this type. This would require a 4-5 fold reduction from current solution times on a DEC VAX 11/780. This next step is a logical refinement of the currently described ion exchange modeling package.

CHAPTER VIII

SUMMARY

A. Background

The development of a model to simulate the exchange of two or three counterions in an ion exchange resin selective for a desired ionic species has wide application in hydrometallurgical processes, waste treatment operations, winning of precious metals, and by analogous mechanism, to future biotechnology applications. Past treatments of ion exchange models have been concerned primarily with binary systems. These models represent phase equilibria with simple linear isotherms and the dynamics have been simulated using dominant film theory. The dominant film models are based on treatment of ionic diffusion in the resin phase as through a fictitious solid "film" surrounding the resin particle.

In all cases, in order to arrive at analytical solutions to the system of equations describing binary ion exchange in a fixed bed, the axial diffusion term has been neglected, linear equilibrium isotherms have been assumed, and diffusion parameters have been assumed to be constant. Numerical methods treating binary ion exchange kinetics have been a natural evolution in ion exchange theory over the past ten years. It was recognized that the axial dispersive effects cannot be ignored and that the equilibrium relationships are non-linear, so that numerical methods must be employed in order to obtain solutions.

The Nernst-Planck model has been shown to be effective in describing interdiffusivity of ions within the resin phase and also

325

in the film surrounding the resin particle, and these additional nonlinear effects mandate numerical solution methods. Investigators have examined separately the application of the Nernst-Planck model to the resin phase and to the film around the resin in order to determine the applicability of the model in each domain. Models of ion exchange dynamics in binary systems inclusive of both effects have been investigated by Turner and Snowdon in shallow fluidized beds (131) and Rao and his coworkers (92, 93) in batch type single particle experiments. Pan and David (83) developed a model inclusive of both effects for moving beds, but without axial diffusion terms.

Ternary ion exchange systems are more important in industrial applications than binary systems. For example, in selectively separating one cation from another, the mixed cations may be dissolved in dilute acid, or the selectively recovered cation may be eluted with strong acid, so H^+ ion normally is involved with the two cations being separated. Two recent models were developed for simulating ternary ion exchange systems. Rao and his coworkers (92, 93) incorporated the Nernst-Planck diffusion model in the resin phase together with a pseudo Nernst-Planck treatment in the film to simulate batch experiments, and Omatete (78) developed a single film kinetic approach to fixed bed simulation. Neither model utilized thermodynamic equilibrium relationships to describe the distribution of ionic species between the electrolyte phase and the resin phase, and consequently neither characterizes phase equilibria adequately.

The present status of ion exchange in industrial process applications is similar to that of distillation technology twenty years ago. Distillation theory then treated the equilibrium stages

required, with dynamics of tray efficiency left to experiments in standard laboratory devices such as Oldershaw columns, plus generalized correlations which could be used to estimate the tray efficiencies as first approximations. Predictive methods for phase equilibria have advanced enormously during the period including the development of the NRTL and UNIFAC equations for prediction and/or correlation of liquid phase activity coefficients. Through the efforts of Fractionation Research Institute (FRI) and other similar agencies, tray efficiencies now can be predicted with good confidence. Systems for component separation by distillation can now be designed reliably without resort to experimental confirmation in many instances.

B. Objective

The objective of this research work was to likewise advance the engineering of ion exchange systems. Specifically, the objective was to develop a simulation model for ion exchange in ternary systems which would embody all of the currently proven factors applying to prediction of phase equilibria and the dynamics of ion exchange in fixed beds. A further objective was to develop a model requiring a minimum of experimentation for parameter estimation. A ternary system simulation model has been developed and, together with parameter estimation support programs, computer based optimization of the design and scale up of ion exchange systems can be carried out with reasonable confidence. The time and cost required to optimize and develop scale-up parameters through laboratory and pilot plant investigations should be reduced considerably.

C. General Approach to Development of Model and Parameter Estimation
   Programs

   1. Overview

      Figure 8-1 provides a "road map" of the development of the
   general purpose Ion Exchange Model for binary and ternary
   systems, along with the support regression analysis programs for
   parameter estimation. Along with Figure 1-1, which depicts the
   summary approach to model development and application discussed
   in the introduction, Figure 8-1 can be utilized to describe the
   necessary steps required to develop a model of any physical
   process. The discussion to follow will highlight only those
   activities considered to be the key advancements or improvements
   in the present work over other ion exchange models. The general
   approach utilized in the model development was to treat (1) the
   Fluid Phase Material Balance, (2) the Phase Equilibrium
   connecting the electrolyte phase to the ion exchange phase, and
   (3) Transport Resistance to ionic diffusion through the film and
   within the resin phase, all as separate phenomena to be
   researched and developed before combining them into the
   framework of an overall ion exchange model. The Figure 8-1
   "roadmap" should be referred to as each major model element is
   discussed in the subsequent Part C paragraphs.

   2. Fluid Phase Material Balance

      The major consideration in the development of the
   electrolyte phase material balance equations was the addition of
   an axial dispersion term to the basic equations describing the
   concentration dependence of each ionic species as it moves

FIG. 8-1

DEVELOPMENT OF ION EXCHANGE MODEL
- BINARY AND TERNARY SYSTEMS
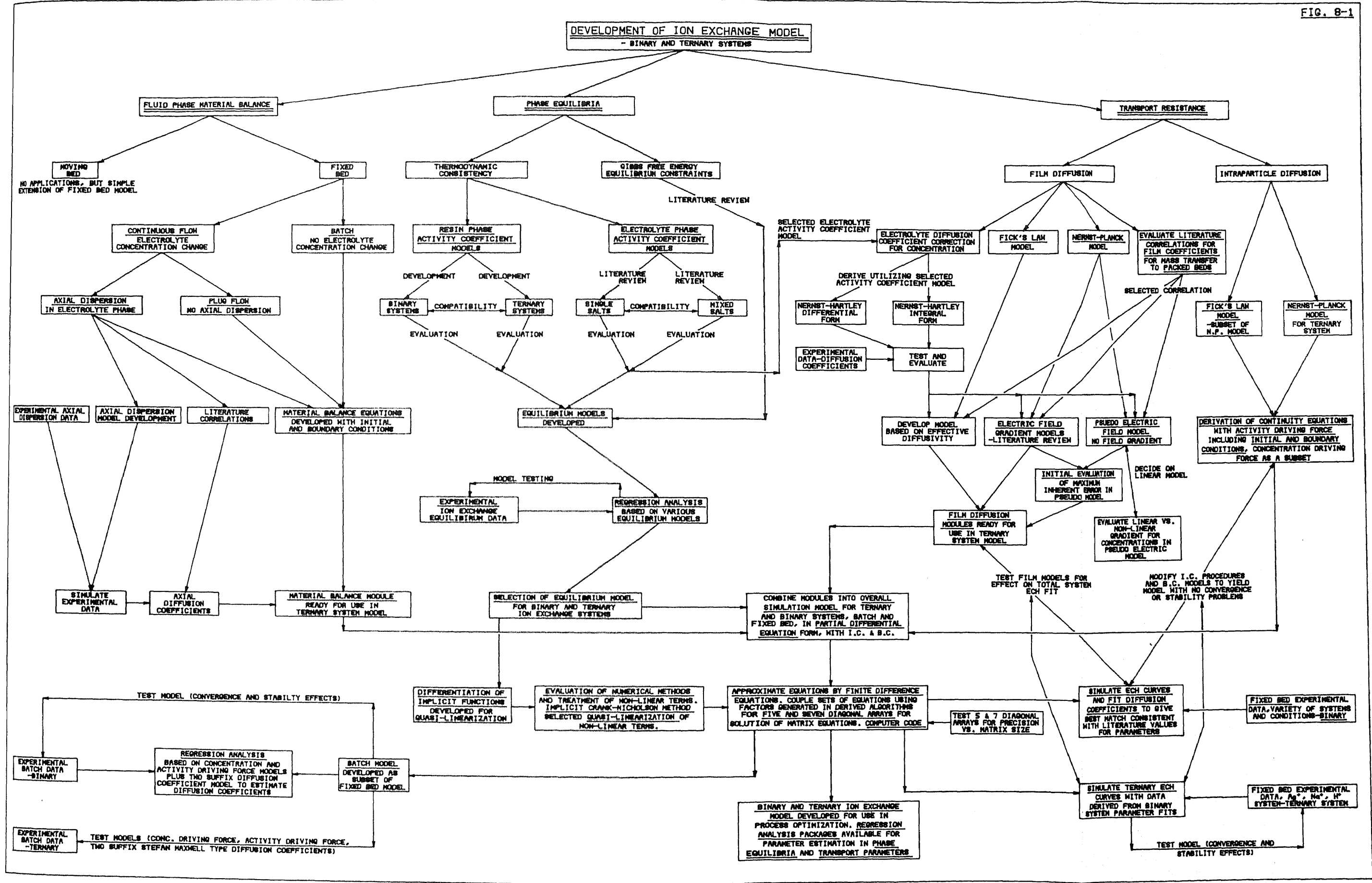
through a fixed ion exchange bed. This feature is obviously not a new concept and has been examined by most investigators of fixed bed operation involving adsorption or ion exchange. Due to the mathematical complications involved, it has been assumed to be negligible in most analytical solutions. Binary system models based on numerical solution methods which have been developed by other investigators normally have included the axial diffusion term for simulation of adsorption or ion exchange in fixed beds. These investigators found through simulation of experimental results that the axial dispersive effects were significant and could not be neglected. The fixed bed ion exchange model for ternary systems developed and tested by Omatete (78) did not include axial dispersive effects in order to simplify his numerical method solution procedure. An alternative material balance case shown on Figure 8-1 is that for the moving bed. The moving bed has not had wide industrial application due to practical problems involved with the handling of fragile resin beads without damage. In any event it represents a simple revision to the fixed bed model, since the fluid phase material balance reflects a steady state relationship to the resin phase at all points in the column. The "batch" model listed on Figure 8-1 requires no fluid phase material balance, since its use in this work assumed no change in electrolyte composition during the exchange of ionic species within the resin.

A search of the literature for correlations of axial diffusion coefficients in packed beds led to development of

Figure 6-1 (12, 23, 27, 32, 61, 78, 115, 124). A model for

simulating axial dispersion in packed beds was developed in this

research. This model was used to determine the axial dispersion

coefficients at two Reynolds numbers from the experimental data

developed by K. L. Erickson (26). These points were added to

Figure 6-1.

The material balance module for the electrolyte phase was

prepared in the form of partial differential equations,

including appropriate Initial and Boundary Conditions, to be

included in the overall model.

3. Phase Equilibria

The phase equilibria relationships describing the distribution

of three counterions between the electrolyte phase and the ion

exchange resin phase had to be developed in order to obtain reliable

predictable driving force potentials for the dynamic model.

Utilization of a standard format known as the rational thermodynamic

equilibrium constant satisfied the Gibbs free energy equilibrium

constraints in that the activity relationship of each species, in

both the resin and electrolyte phases were related by a constant at

a given temperature. The equilibrium constants in a ternary system

are therefore related by the chain rule (equation (2-19)),

$$\overline{K}_{ij} = \frac{\overline{K}_{ik}^{(|z_j|/|z_k|)}}{\overline{K}_{jk}^{(|z_i|/|z_k|)}} \quad \text{for species i,j, and k}$$

This relationship is useful in the estimation of ternary ion exchange

system equilibrium parameters since the degree to which it is

satisfied is a measure of the consistency of the experimental data.

A survey of literature on correlation of activity coefficients of single ionic species in single salt and mixed salt electrolyte solutions led to selection of the Bromley version (9) of the extended Debye-Huckel equation (equation (3-4)). The Bromley equation was tested in this research against experimental values given by Robinson and Stokes (106) for activity coefficients on 17 salts at concentrations up to 5-6 molal, and was found to yield satisfactory predictions. Bromley parameters (9) which extend the predictive concentration range to the 5-6 molal region are available for a large number of salts, and the Bromley equation format has been arranged to allow prediction of single ion activity coefficients in mixed salt electrolyte solutions.

The equilibrium model could not be completed until a satisfactory model was found to describe the activity coefficient relationship of three ionic species within an ion exchange resin as a function of concentration. Three models were selected based on a review of the literature, including the work of Smith and Woodburn (116) on the $NO_3^- - Cl^- - SO_4^=$ system. These models were the three suffix Redlich-Kister, the Wilson, and the NRTL equations.

The _rational thermodynamic equilibrium_ relationship, including the Bromley equation to describe electrolyte phase activity coefficients, was tested with each of the resin phase activity coefficient models described above. The models were also tested with regard to improved predictive capability depending on whether mole fraction or equivalent fraction

concentration units were used in the resin phase. Use of

A. K. S. Murthy's non-linear regression program to estimate

unknown parameters in explicit algebraic equations allowed

testing of the models against experimental data available in the

literature for four ternary ion exchange systems. These were

(1) Mn^{++}, Cs^{+}, Na^{+}, (2) Sr^{++}, Mn^{++}, Cs^{+}, (3) NH_4^{+}, Na^{+}, H^{+},

and (4) NO_3^{-}, Cl^{-}, $SO_4^{=}$.

The selected equilibrium model included the three suffix

Redlich-Kister equation utilizing equivalent fraction

concentration units to describe activity coefficient

relationships in the resin phase. The selection was based on

overall ability of that model to correlate binary systems and to

predict ternary data points from the binary system parameters.

4. Transport Resistance

All models of diffusion processes must deal with the

phenomena related to movement of physical entities through a

medium, whether the entities are electrons, ions, or molecules.

The rate of movement or diffusion can be characterized by

(1) driving forces and (2) parameters related to the ease of

movement of the entities, the diffusion coefficients. Movement

of ions within an ion exchange resin, or intraparticle

diffusion, has been characterized successfully with the

Nernst-Planck model (equation (5-5)). The general equation has

been derived for ternary systems in terms of chemical potential

(equations (5-6), (5-7), and (5-8), and has been reduced to the

ideal case (equations (5-10) and (5-11)) and to the binary

non-ideal and ideal cases (equations (5-21) and (5-13)). The

inclusion of the Nernst-Planck model in the continuity equations for the resin phase is shown in equations (5-48) and (5-50). These equations, including appropriate initial and boundary conditions, constituted formulation of the resin phase diffusion model.

Many correlations for prediction of resistance to diffusion of molecular species through a film have been produced over the years, premised for the most part on boundary layer theory (equation (4-1)). Carberry's correlation (11) for fixed beds has been found satisfactory by many investigators and was adopted in this research (equation (4-2)). Defining the effective diffusion coefficient for use in such film resistance correlations as applied to ion exchange has attracted the interest of many investigators (26, 50, 78, 83, 131, 132), who variously recommend use of the value for the slowest ion, the average value, or the harmonic mean value. In most cases, the limiting value (infinite dilution) diffusion coefficients of single ions have been used regardless of the convention used in the choice of diffusion coefficient. By combining the Nernst-Hartley (104) equation, which relates the effect of the activity of an ionic species on its diffusion coefficient (equation (3-11)), with the Bromley equation which predicts the effect of solution Ionic Strength on ionic species activity, a relationship was derived between ionic diffusion coefficients and electrolyte concentration. Both an integrated and a differential form of that relationship was derived in this research. The two forms were tested against experimental

diffusion coefficient values given by Robinson and Stokes (106) on 17 salts involving concentrations up to 4 molal, and the integrated form was found to yield reasonable results. This correction was applied to all electrolyte phase diffusion coefficients in this work.

Migration of ions through the film surrounding each resin particle was recognized in previous work as being subject to an interdiffusivity dependency based on the Nernst-Planck model, the coions in the film electrolyte being analogous to the fixed charges in the resin. In this instance, however, the coions are free to move and do so in such a way that the concentration gradient of the coions in the film are counterbalanced by the electric charge gradient in the film. This phenomenon is interrelated with the relative diffusion coefficients of the counterions diffusing through the film.

The effect of an electric field in the film for binary systems had been treated rigorously by several investigators (43, 50, 131, 132); however the complexity in applying these rigorous derivations to ternary systems led this investigator to adopt a model somewhat similar to that adopted by Rao and his coworkers (92, 93). If the coion gradient in the film is assumed to be small, i.e., $\frac{\partial c_i^*}{\partial y} = 0$, then the coion charges of sign opposite to those of the counterions are distributed uniformly thru the film, in a manner analogous to the fixed charges in the resin. The Nernst-Planck equations derived for the resin phase system can then be applied to the film phase to interrelate the diffusivities of the exchanging ions. Assuming

the concentration gradients of all species to be linear across the film, average electrolyte phase ionic concentrations can be used in the model to yield concentration corrected diffusion coefficients for each species. The Nernst-Planck equations then are used to predict the flux of each species through the film. The film "thickness," δ_{eff}, is computed for the major flux based on the following equation:

$$k_{L_{i_{eff-max}}} = \frac{D^*_{i_{eff-max}}}{\delta_{eff_{max}}} \qquad \text{as taken from equation}$$

$$(4-89)$$

The effective diffusion coefficient $D^*_{i_{eff-max}}$ is derived from the Nernst-Planck relationship and the film coefficient, $k_{L_{i_{eff-max}}}$, is calculated from the Carberry film coefficient correlation using $D^*_{i_{eff-max}}$ for the major flux species. This film "thickness" is utilized to compute the film coefficients of the other ionic species using equation (4-90) and (4-91). The pseudo electric field model was tested against the rigorously derived Kataoka and Yoshida correlation (50) for homovalent exchange and found to yield comparable results in subsequent simulations. The pseudo electric field film model was judged adequate for incorporation into the overall simulation models for both batch and fixed bed cases.

5. Overall Simulation Model - Partial Differential Equations

    The general ternary system equations were developed for the resin phase (equations (5-48) and (5-50)) and the electrolyte

phase (equations (7-13) and (7-14)), along with the appropriate boundary conditions described in Chapters V and VII. The equations describing flux of species through the film linked the two non-linear parabolic equations describing the electrolyte phase with the two non-linear parabolic equations describing the resin phase through the phase equilibria relationships at the resin-film interface. The models could then be reduced to numerical difference equations and subsequently solved.

6. Numerical Methods and Reduction of Equations to Finite Difference Format

6.1 General Background

Svedberg (125), in his doctoral disseration involving numerical methods for simulation of fixed bed processes, found that the implicit Crank-Nicholson finite difference method, combined with Lee's quasilinearization technique (59) for resolution of non-linear terms, simulated fixed bed operations successfully for a wide variety of conditions. Svedberg used the Thomas algorithm (13, 125) for solution of algebraic equations having tridiagonal matrices, since the quasilinearization technique reduced the system to a set of linear algebraic equations. Solutions were found to be convergent and stable, providing that grid increments were made fine enough. This method was adopted for this research project.

6.2 Binary and Ternary System Batch Model

The batch model involved solving the resin phase

equations only, and in ternary systems, the combining of the continuity equations for two species resulted in algebraic coefficient matrices having 7-diagonal regularity. An algorithm was derived and tested to invert the seven-diagonal matrix in order to obtain solutions for the unknown resin phase concentration values. The two equations describing the ternary system phase equilibrium involved an implicit relationship between the electrolyte phase concentrations and the resin surface concentrations. Since the particular derivatives were required for quasilinearization of terms nonlinear in concentration, the use of techniques for differentiation of implicit functions (70) was required.

To reduce the quasilinearization complexity, values for $\bar{D}_{ii}$ and $\bar{D}_{ij}$ and their eight partial derivatives with respect to species 1 and 2 concentrations were performed at time step j versus $j^{+1/2}$. It was subsequently shown that systematic bias introduced by the simplification was very small (0.01%). The binary system batch model developed in this work was used as a subroutine of Dr. A. K. S. Murthy's non-linear regression program for time varying system parameter estimation. Several resin phase models, (1) concentration driving force, (2) activity driving force, and (3) multi-suffix diffusion coefficients (Stefan-Maxwell model), were used to simulate experimental batch data of Rao and his coworkers (92, 93), with ionic species diffusion coefficients estimated for a variety of

cases. The model utilizing the activity driving force expressions performed best in these verification trials.

Subsequent verification of the resin phase batch models against prediction of data generated by Rao and his coworkers on ternary system ion exchange gave qualitative indication that the activity driving force model performed best.

6.3 Binary and Ternary System Fixed Bed Model

The equations describing the fluid phase concentration change in ternary systems could be reduced to finite difference equations which, when combined, resulted in matrix equations yielding a regular 5-diagonal coefficient matrix. An algorithm for inversion of this type of matrix equation was derived and tested. Coupling of the resin phase matrix equations to the fluid phase matrix equations was performed through the film boundary condition representing equilibrium with the resin surface. The 7-diagonal algorithm factors containing fluid phase concentration vectors in terms of resin surface concentration vectors could be carried over into the 5-diagonal algorithm containing resin surface concentration vectors, and substituted to eliminate resin phase concentrations at each column node. The fluid phase equations could now be solved for fluid phase concentrations at each node down the packed bed. These fluid phase concentrations could then be used back in the 7-diagonal algorithm to solve for the resin phase

concentrations at each column node and at each resin node. This mode of coupling permitted solution for all concentrations at each iteration, and was repeated after updates on derivatives for non-linear expressions until convergence of non-linear terms had been achieved at each time step.

At this stage, complete fixed bed <u>effluent</u> <u>concentration</u> <u>histories</u> (ECH) could be simulated, and this was performed for the Erickson (26) experimental work on the system NH_4^+-ETDA^{++}, Dowex 50W X8/Cl$^-$ in order to verify the binary system fixed bed model. In addition, comparison of the rigorous derivation of film field effects by Kataoka and Yoshida (50) against the <u>pseudo electric</u> <u>field</u> model was performed to confirm the efficacy of the latter model.

The diffusion coefficient parameters for the system Ag^+-Na^+-H^+/Dowex 50W X8 researched by Omatete (78) were determined by matching the ECH curves on the six binary system runs. These diffusion coefficients were utilized to simulate the three ternary system runs. Representation of the column exit boundary condition (B.C.) as $\frac{dx_i}{d\ell} = 0$ gave rise to oscillation in concentration of the column exit. Representation of this B.C. as a CFSTR at the last column increment ameliorated the problem. The CFSTR representation was added to the binary model as well, and all binary simulations were rerun to confirm that no unforeseen problems occurred. The three Omatete ternary

systems were successfully simulated.

Other studies of Crank-Nicholson method stability as a function of time and geometry increment size were performed to provide guidelines in the use of the model.

The fixed bed model for ternary ion exchange and the regression analysis support programs had now been proven and tested against a wide variety of experiment conditions and systems.

D. Results

1. Fluid Phase Material Balance

The generation of the fluid phase material balance equations for ion exchange in ternary systems was straightforward. Addition of axial dispersive terms required information on values of Axial Diffusion Coefficients versus Reynolds number. A number of correlations are plotted on Figure 6-1. However, Erickson (26) had obtained data on dispersion of NH_4^+ ion in aqueous solutions in fixed beds by pulsing conentration, and a model was developed in this work to fit the Erickson experimental dispersion curves. Values of axial dispersion coefficients of 3-7 cm^2/sec obtained from the parameter fitting process were plotted on Figure 6-1 and are an order of magnitude higher than values derived from other correlations. A value of 4 cm^2/sec was used in simulating the Erickson binary system fixed bed experimental ion exchange ECH curves with good results.

Use of the axial dispersion coefficient values within the range indicated on Figure 6-1 for the Omatete (78) experimental

runs gave satisfactory fits to the 9 ECH curves which he
generated experimentally. Resin phase diffusion coefficients
which were close to literature values for Ag^+, Na^+, and H^+
were used in the simulations. Use of higher values for axial
dispersion coefficients than those derived from Figure 6-1
resulted in poor simulations of the effluent concentration
histories. Consequently, this investigator recommends that
Figure 6-1 correlations be used when actual data are not
available for simulation with the dispersion model developed in
this work.

2. Phase Equilibria

2.1 Gibbs Free Energy Equilibrium Constraints

There are many equilibrium conventions which have been
used in defining ion exchange equilibrium. The rational
thermodynamic equilibrium constant was selected for this
work. The resin phase concentrations can be represented as
mole fraction or equivalent fraction concentration units
and, in this form, most of the ion exchanger selectivity is
vested in the equilibrium constant since the standard
states for the resin and electrolyte phases are different.
The activity coefficients for species in the resin phase
"trim up" the equilibrium correlations. In systems for
which the total number of moles is a constant, the
Gibb-Duhem relationship is given for constant temperature
and pressure as:

$$\bar{c}_1 \cdot d\ell n\bar{\gamma}_1 + \bar{c}_2 \cdot d\ell n\bar{\gamma}_2 + \text{----} \ \bar{c}_n \cdot d\ell n\bar{\gamma}_n + d\frac{G^o}{T} = 0$$

In heterovalent ion exchange, $\bar{dc}_T \neq 0$, and the activity coefficients estimated for such systems must "absorb" this effect, since all of the equilibrium models for ion exchange assume $\bar{dc}_T$ to be zero. The activity relationships resulting from Gibbs free energy constraints in a ternary system provide that one of the equilibrium constants is derivable from the other two. In correlation of ternary system data, this relationship (chain rule given by equation (2-19)) was used to provide an indication of the data consistency.

2.2 Electrolyte Phase Activity Coefficient Model

The Bromley equation (9) for the extended Debye-Huckel equation for prediction of activity coefficients of ionic species in aqueous solutions of salts was selected. It was tested in this work against literature values given by Robinson and Stokes (106) for activity coefficients on 17 salts at concentrations up to 5-6 molal. The averaged root mean square of % relative difference, actual to predicted, was 2.7% for the combined total of all 17 salts. In addition, parameters to extend the concentration range have been estimated by Bromley (9) for a wide variety of salts, and can be utilized to predict single ion activities in mixed salts, obviating the need to use Harned's Rule (105) as an approximation in this research.

2.3 Resin Phase Activity Coefficient Models

Three models were tested for ability to model the resin phase activity coefficient as a function of

composition. These were the three suffix Redlich-Kister, the Wilson, and the NRTL equations. Each model has the ability to predict ternary system data from the binary system parameters.

2.4 Development of Equilibrium Models and Model Evaluation

The three models described above were incorporated into the rational thermodynamic equilibrium constant along with the Bromley equation (9) for the electrolyte phase activity coefficients. A non-linear regression program created by Dr. A. K. S. Murthy allowed parameters to be estimated for explicit algebraic relationships utilizing as the objective function the global minimum of the sum of squares of normalized difference between experimental and observed data points. Experimental data on thirteen binary systems (26, 91, 116, 121) and four ternary systems (91, 116, 121) were regressed to yield equilibrium parameter estimates. The three suffix Redlich-Kister equation, using equivalent fraction concentration units, was selected as the most accurate model based on its ability to predict ternary data points using binary system parameters. In some regression runs using the Wilson equation the molar volume ratio (ρ_{ij}) was included as a parameter to be estimated. In the case of regression runs using the NRTL equation, the constant α_{ij} was included as an estimated parameter. Fixed values of $\rho_{ij} = 1.0$ and $\alpha_{ij} = 0.3$ gave overall better results for those two models than were obtained when these constants were included as estimated

parameters. The results for the Erickson experiments (26) are shown in Figure 2-7. Table 2-2 compiles the summary information relevant to the experiments performed to obtain equilibrium data on ternary ion exchange systems, and the associated binary systems. Omatete's data (78) was not used in the equilibrium model selection process, so the experimental data used for model validation involved 4 ternary systems and 12 associated binary systems. Table 2-3 gives the comparative results of the equilibrium model simulations performed in this work using the three suffix Redlich-Kister, the Wilson, and the NRTL equations. Standard deviations based on % normalized difference between the experimental and calculated values are tabulated for each case.

2.5   Preparation of Equilibrium Model for Use in Overall Ion Exchange Model

The expressions representing equilibria in ternary systems are implicit in nature, and particular derivatives are required in the quasilinearization of these expressions, so methods (70) for differentiation of implicit functions were employed to meet this requirement.

Additionally, a Newton-Raphson method was developed to solve simultaneously the two implicit non-linear equilibrium expressions to yield the composition of each ionic species in the electrolyte phase in equilibrium with the composition of species at the resin surface, based on the fitted parameters.

3. Transport Resistance

3.1 Film Diffusion

Most investigators (26, 50, 78, 83, 131, 132) utilize the infinite dilution values of diffusion coefficients of single ions in electrolyte solutions. Using the Nernst-Hartley expression (equation (3-11)) in both an integral and differential form, and utilizing the Bromley equation to predict activity coefficient behavior as a function of concentration, diffusion coefficient values at concentration levels up to 3-4 molal were predicted and compared to experimental data given by Robinson and Stokes (106) for 17 salts. The integral version was found to be best, yielding a root mean square of % normalized difference of 13.2%, averaged for all 17 salts, as compared to 26.6% for the differential version. The integral version was even better in the range up to 1.5 molal which was the upper limit for ion exchange simulations performed in this work. The integrated version of the Nernst-Hartley equation was used in the dynamic models to correct individual ionic species diffusion coefficients for concentration effects.

As described in Section C, part 4, of this chapter, a *pseudo* *electric* *field* model was adopted for both the binary and ternary system models based on Carberry's correlation (11) for film coefficient in packed beds above Reynold's number equal to 1. Integration of the ionic flux equation across a film of "thickness", δ_{eff}, yields concentration

gradients in the film which are nonlinear, as was derived for the case of binary systems in Chapter IV (equation (4-65)). Table 4-1 indicates maximum possible error in using the linear gradient model versus the more rigorous nonlinear case. These errors could approach 30% in heterovalent exchange if the concentration difference across the film was very high. In actual simulation of ion exchange in heterovalent binary systems, the film concentration difference values across the film were so low as to yield negligible error in applying the simpler linear driving force model. The pseudo electric field model based on linear driving force was tested against the rigorous electric field model derived by Kataoka and Yoshida (50) for homovalent exchange and was found to give comparable results. This is shown in Table 4-2 and Figures 7-7 and 7-10 for the Ag^+-H^+ system. The calculated data given in Table 4-2 for concentration profiles and mass flux values, compared over time, show little difference between the two models.

The effectiveness of the pseudo electric field model was demonstrated further in the two Erickson (26) experiments involving the favorable exchange of $ETDA^{++}$ for NH_4^+ on Dowex 50W X8 resin. Figures 7-2 and 7-3 show that the simulated ECH (effluent concentration history) curves fit the experimental data very well, although the two runs had Reynolds numbers differing by a ratio of two (20 and 40). Prior to use of the pseudo

electric <u>field</u> model, film coefficients derived from all cited literature correlations had failed to allow successful simulation of the two ECH curves with any given film coefficient relationship. This was true whether the diffusion coefficient used in any of the film correlations was based on the slowest ion, the average, the harmonic mean, or the fastest diffusing ion. The <u>pseudo electric</u> <u>field</u> model using Carberry's (11) film coefficient correlation for packed beds resulted in the successful simulations shown in Figures 7-2 and 7-3, all parameters being the same except for the Reynolds numbers.

3.2 Intraparticle Diffusion

The inclusion of activity driving force was a key feature of the development of the Nernst-Planck model for binary and ternary exchange systems in this research. The results are described below. The ionic flux equations describing the transport of ions in the resin phase were derived in molar concentration units, then transformed to equivalent fraction concentration units for ease of mathematical manipulation through the relationship

$$\bar{x}_i = \frac{\bar{c}_i \cdot |z_i|}{Q_r} \quad ,$$ where $\bar{x}_i$ for species i is in

equivalent fraction units, $\bar{c}_i$ is the molar concentration of species i, $|z_i|$ represents the species valence, and Q_r is the equivalent concentration of fixed charge moities in the resin/liter. If the chemical potential, $\bar{\mu}_i^c$, is used as driving force instead of concentration then, in non-ideal systems, the effective diffusion

coefficient which describes ion exchange in binary systems contains the additional term

$$\frac{\overline{D}_1 \cdot \overline{D}_2}{\sum\limits_{i=1}^{2} \overline{x}_i \cdot \overline{D}_i \cdot |z_i|} \cdot \overline{x}_1 \cdot \overline{x}_2 \cdot \frac{\partial \ell n \left[\dfrac{\overline{\gamma}_1^{\;|z_2|}}{\overline{\gamma}_2^{\;|z_1|}}\right]_{molar}}{\partial \overline{x}_1}$$

Since all of the equilibrium parameter correlations were performed using activity coefficient models in which the concentration units were either mole fractions or equivalent fractions, activity coefficient corrections are required for mole fraction concentration units to reflect the change in standard state to the molar basis as given in the expression above. These transformations are discussed in Chapter II, section F.

4. <u>Numerical Representation of the Ternary System Ion Exchange Model</u>

The selection of the Implicit Crank-Nicholson Finite Difference method, along with quasilinearization of non-linear terms, is discussed in section C, part 6, of this chapter. As described, use of a non-linear regression program developed by Dr. A. K. S. Murthy for time varying relationships allowed regression estimation of diffusion coefficients for Sr^{++}, Mn^{++}, Cs^+ and Na^+, utilizing the data of Rao and his coworkers (92, 93). Table 5-3 compares the normalized sample variance, s^2, for models involving (1) concentration or (2) activity driving force and (3) a two suffix diffusion coefficient similar to the Stefan-Maxwell model (30). These

regressions were performed for data sets consisting of 5, 6, and 7 binary systems, and the fitted values of diffusion coefficients with their standard deviations are listed. The activity driving force model is elegant in its ability to use single values for so called "self diffusion" coefficients and yet yield the best overall results. Heretofore, investigators (46, 89) have found that the "self diffusion" coefficient for a given counterion species has a different value depending on the nature of the other counterion being exchanged. Figures 5-2 and 5-3 show the plots of experimental data versus the predicted values, using the activity driving force model.

5. Ternary Model - Batch System

The ternary ion exchange data for tagged single particle experiments conducted by Rao and his coworkers (92, 93) were simulated with the Ternary Batch Model using activity driving force, concentration driving force, and some limited work with the two suffix diffusion coefficient. Table 5-4 gives a subjective quality rating to the observed results, and the activity driving force model was rated somewhat better than the others. The plots of experimental versus simulated time varying concentration curves are shown in Figures 5-4 to 5-8. This is the first ternary ion exchange model in which activity driving forces have been utilized, and the results are gratifying.

6. Binary and Ternary Fixed Bed Models

The results of simulating nine binary ion exchange experiments conducted in fixed beds are shown on Figures 7-2 to 7-4 and Figures 7-5 to 7-10. The runs were made utilizing

concentration driving force, since the ternary system batch model which included activity driving force has not been extended to the fixed bed model. The activity driving force was used in the model for a fixed bed in binary systems, and Figure 7-3 shows the effect of use of activities in a positive deviation system (NH_4^+-ETDA^{++}), while Figure 7-9 shows the effect in a negative deviation system (Ag^+-Na^+). Generally the fixed bed simulation results are quite good, given the use of literature correlations for all parameters except for resin phase diffusion coefficients. The "ground rule," with respect to the fit of the latter parameter, was that the values must be not far different than reported literature values, and that the same values for each species be used in all simulations involving that species.

The simulation results of three ternary system experimental runs by Omatete (78) are shown in Figures 7-11, 7-12, and 7-13. The equilibrium data and diffusion coefficient values derived from the work on the binary systems were used unchanged in simulating the ternary experiments. Values for diffusion coefficients which yielded best ECH curve fits during simulations performed on this system were $\bar{D}_{Ag}$=0.9x10^{-6} cm^2/sec, $\bar{D}_{Na}$=2.5x10^{-6} cm^2/sec, and $\bar{D}_{H}$=10x10^{-6} cm^2/sec. The coefficients for Ag^+ and Na^+ are close to literature values of 0.68x10^{-6} and 2.05x10^{-6} respectively on Dowex 50W X8, as reported by Hering and Bliss (46).

CHAPTER IX

CONCLUSIONS AND RECOMMENDATIONS

A. Conclusions

1. Phase Equilibria

It has been shown in this research that ion exchange equilibria can be correlated very well in homovalent or heterovalent binary systems using the rational thermodynamic equilibrium constant in combination with the following activity coefficient models. Electrolyte phase molal activity coefficients can be estimated adequately for most salts in aqueous solution by the Bromley (9) version of the extended Debye-Huckel equation. Bromley (9) has published values of his short range interaction parameter, B, for 175 salts. In tests performed in this work the model proved to provide accurate estimates of electrolyte phase activity coefficients for salts in concentrations up to 6 molal. The Bromley equation (9) is available in a form which permits estimation of the molal activity coefficients of single ionic species in mixed electrolytes. The incorporation of the Bromley equation into the phase equilibria models, developed and tested in this work, precluded any need to include electrolyte phase activity coefficient parameters in the correlation of ion exchange equilibrium data.

Three models were used to represent the relationship of activity coefficient of each ionic species in an ion exchange

resin as a function of its concentration: the three suffix Redlich-Kister, the Wilson, and the NRTL equations. All three models can give adequate representation of a single binary system. However, in a ternary system, the Gibbs free energy constraints require that one of the three rational thermodynamic equilibrium constants be predictable from the other two. With this restriction, the three suffix Redlich-Kister equation was clearly superior to the others, as shown in Table 2-3.

The ability of the three models to predict equilibrium compositions for ternary systems based on parameters derived from the binary systems was good in the one cationic homovalent ternary system used in this work, and only fair in the two cationic heterovalent ternary systems. This is indicated by the standard deviations of % relative difference shown in Table 2-3 for these systems and models. Correlation results were also good with the one heterovalent anionic ternary system tested, as shown in Table 2-3. The three suffix Redlich-Kister model, utilizing equivalent fraction concentration units, yielded overall best results in predicting ternary system equilibria from binary system parameters. The poorer results with heterovalent systems are believed to be caused by a non-zero $d\bar{c}_{total}$ ($\bar{c}_{total}$=total moles of ionic species per unit volume of ion exchange resin) term in the Gibbs-Duhem expression. This residual would then be "absorbed" into the equilibrium constant and activity

coefficient parameters during regression analysis. Recombination of these binary system parameters to predict ternary equilibria in heterovalent systems will lead to poorer estimations in areas of the phase diagram close to the homovalent ionic pair (where the "absorbed factors" are not needed to describe the system).

Equivalent fraction concentration units gave better results than mole fraction units in the prediction of ternary system equilibria, as is shown in Table 2-4. The number of equivalents in an ion exchange resin is constant, and the rational equilibrium constant based on equivalent fractions reflects a linear concentration pattern history during heterovalent exchange. The mole fraction of a species in a heterovalent exchange is not a linear function of the number of moles of that species exchanged during the process. A rational equilibrium constant based on mole fraction units would represent a system having a greater degree of non-linearity when contrasted to equivalent fraction representation. This non-linearity effect must be compensated for in the resin phase activity coefficient parameters. Recombination of such parameters would give poorer predictions of ternary system equilibria, as was indicated in Table 2-4.

2. Fluid Phase Material Balance

It is concluded from the research performed in this work that the axial dispersive term should be included in

equations describing the electrolyte phase in order to adequately represent the unsteady state concentration profiles in fixed beds. The generalized correlations of axial diffusion coefficients, as depicted in Figure 6-1, should yield reasonable predictions of ECH (effluent concentration history) curves over a wide range of Reynolds number for liquid systems. If experimental axial dispersion data is available for the ion exchange system under investigation, the axial dispersion model developed in this research should be used to obtain values of axial dispersion coefficient for use in overall system modeling.

3. Diffusion in the Film

The pseudo electric field model based on the Nernst-Planck equation, as derived in this work compares favorably with the rigorously derived electric field model. This was the case even when the ratio of diffusion coefficients for exchanging species was large, and under conditions of unfavorable exchange. As Pan and David (83) point out, the conditions described above should produce a high electric field gradient, a commensurate high coion gradient in the film, and a large deviation from film mass transfer coefficients calculated without consideration of electric field effects. Kataoka and Yoshida (50) indicate that errors of up to 30% can occur in prediction of breakthrough curve (ECH) and column utilization efficiency if a film coefficient model is used which does not account for

electric field effects.

Although unfavorable heterovalent exchanges, such as those involving H^+, are unlikely to occur in industrial practice, simulations of the types of exchange which would give rise to these deviations were performed in this work. Diffusion in the resin phase controls the magnitude of ionic species flux throughout most ion exchange processes (except for very dilute electrolyte concentrations). The ionic species which diffuses most slowly through the resin phase is normally the species most preferred by the ion exchanger. Therefore in unfavorable exchange in a heterovalent system, the resin phase flux is influenced by the slower more favored ion, and its interfacial equilibrium concentration in the electrolyte film would be low due to the favorable selectivity the ion exchanger has for it. Since the film flux must equal the resin phase flux, the concentration gradients across the film are low along with commensurately lower coion and electric field gradients.

Simulations carried out in this work showed that film concentration gradients were low in systems such as the exchange of Sr^{++} for Cs^+ as shown in Table 4-2. If the counterion gradients are small, the coion gradient is low, and the pseudo electric field model yields results equivalent to rigorous models such as developed by Kataoka and Yoshida (50) for homovalent exchange. This result can be seen in Figures 7-7 and 7-10. The pseudo electric field model can be

extended readily to mulicomponent systems, whereas the
rigorous models cannot.

4. Diffusion in the Resin Phase

The use of the Nernst-Planck model to predict
interdiffusivity of species within the ion exchange resin is
now well established. Investigators have performed
experiments designed to isolate this effect from coupled film
diffusion. Two mechanisms are normally beneficial: (1) use
of concentrated solutions to increase gradients, and (2) high
electrolyte phase velocities to minimize film "thickness."
The experiments have generally been run in "batch" type
apparatus, i.e., where the change in electrolyte phase
concentration remains "unchanged" during the exchange.
Studies performed in fixed beds do not adequately
discriminate between the Fick's law models and the
Nernst-Planck model since ECH or "S" curves can be
represented readily by many mathematical models.

The clear advantage which the Nernst-Planck model has
over Fick's Law is that a single pair of "self" diffusion
coefficients can be used to predict both favorable and
unfavorable exchange (whereas with Fick's law a different
diffusion coefficient pair is required to model each exchange
direction).

The use of activity driving force in conjunction with
the Nernst-Planck model gave the best representation of the
ion exchange results obtained by Rao and his coworkers, as

given in Table 5-3 and shown in Figures 5-2 and 5-3.
Activity driving force, used with the Nernst-Planck model,
may be shown to be a unifying ion exchange theorem. Single
and unique "self" diffusion coefficients for ionic species
could be used to characterize ion exchange in a given resin
without need for ion pair specific values or ion pair
corrector models, such as the Stefan-Maxwell model (30).

5. Overall Ternary Ion Exchange Model

This research project has shown that a practical model
has been developed for simulation of ternary ion exchange in
fixed beds which can be used to optimize process design
applications. The model utilizes recognized published
correlations for estimation of all parameters required,
except those specific to the ion exchange system being
investigated. Parameters which must be determined by
experimental measurement include the equilibrium parameters
and the resin phase "self" diffusion coefficients for each
species being exchanged.

Simple laboratory experiments utilizing tagged particle
techniques or other experimental methods as outlined in
Helfferich's publication, "Ion Exchange," (44) can yield data
for use in the regression analysis programs developed in this
research project. These regression programs can yield
parameter estimates for design, to map areas for further
experimentation to fill in gaps, or to resolve questionable
experimental results.

The use of the Implicit Crank-Nicholson finite difference method, using Lee's quasilinearization technique (59) for resolving non-linear terms, is a robust solution technique in terms of convergence and stability. Faster solution times may be desirable in order to tie the ion exchange model into a larger optimization model for process plant design, such as ASPEN, or use it as a subroutine in regression analysis for parameter estimation based on ECH curve experimental data, and recommendations will be made below to address this issue.

The model as now constituted is for stoichiometric exchange. However it was shown in this work that non-stoichiometric exchange resulting from complex formation can be simulated. In the systems involving Ag^+-NO_3^-, the stable complex $AgNO_3$ is formed and adsorbs into the resin phase. Assuming that the physical adsorption of $AgNO_3$ takes place as fast as the ion exchange process, satisfactory system simulations can be realized by adjusting the equivalent capacity of the ion exchange resin upward to account for the additional Ag^+ uptake as $AgNO_3$.

The ion exchange dynamic model could be modified to include physical adsorption of complexed species, but the quasilinearization algebra, size of matrices, and computational time presently would limit this to a single complex for practical purposes. The same conclusion could be drawn with regard to addition of a reaction term to the resin

phase material balance, or enthalpy terms to handle adiabatic ion exchange processes for which there is a significant heat of reaction. The latter case would occur when the ion exchanged reacts with coion in the electrolyte phase accompanied by a substantial heat of reaction (ex., H^+ and OH^-), particularly when there has been significant coion intrusion into the resin. The model could be readily modified to a pore diffusion model if that feature were desirable to model ion exchange in macroreticular resins (relatively large pore openings).

B. Recommendations

1. Phase Equilbria

Although the phase equilibria model used in correlating binary and ternary ion exchange system data was satisfactory for binary systems, the ability of the model to predict ternary equilibria from binary parameters was only fair in heterovalent systems. As pointed out by Soldatov (119), the Gibbs-Duhem expression leading to thermodynamic consistency in models of excess free energy must take into account the net change of moles in heterovalent exchange. This should be examined in future work.

Other excess free energy models for equilibrium relationships in ion exchange resins should be proposed and examined, including a Debye-Huckel type model with terms to extend its applicability to higher concentrations. At higher concentrations of electrolyte in a resin, more resin swelling occurs and the resin osmotic pressure changes are greater

during the ion exchange. Most investigators have assumed that the resin volume and pressure changes are small during ion exchange and is neglected by setting the Gibbs-Duhem equation equal to zero ($\partial(\pi v)_T = 0$). In fact, significant resin volume changes occur and the osmotic pressure build up can be quite large. Although satisfactory correlation of binary system phase equilibria was possible with the above stated assumption, this assumption may be in part responsible for the poorer ability of the equilibria models to predict ternary equilibria. The impact of the constant pressure volume assumption should be assessed.

The phase equilibrium correlation package used in this work allowed for one charged ionic complex to exist in the electrolyte phase. However, the exchange selectivity of the charged complexed species was assumed to be zero since the existence in the resin of alternate complex forms of an ionic species is not distinguished readily by experimental procedures. Models which would correlate the activities of three ionic species plus a charged complex form of one of the species would be a quaternary model. It would be valuable to know whether any of the models reviewed and tested in this research would provide adequate prediction of quaternary systems. This should be examined in future phase equilibria model development for ion exchange systems.

Finally, resins are available with varying degrees of cross linking, and this effect has a pronounced influence on ionic species selectivity. It would be important to see if

predictive trends can be established in the parameters which characterize equilibrium ion exchange, i.e., K_{ij} and the activity coefficient parameters, which would portray them as functions of the degree of crosslinking in the resin.

2. Dynamics of Ion Exchange

One key observation which requires follow-on verification is that, by use of activity driving force, single "self" diffusion coefficients can characterize ion exchange in binary systems without recourse to multisuffix diffusion coefficients or use of different values for various ionic pair combinations. If activity "corrects" for hydration shells around specific ions and other charge potential effects, the verification of this observation on a wider spectrum of ionic systems is required. As discussed above in connection with equilibria, it would be valuable to determine if the same "self" diffusion coefficient could be used for resins with increasing degrees of crosslinking, providing that the activity differences were known for each ionic species within the various resins having different degrees of crosslinking. Based on concentration driving force models, the measured diffusion coefficients decrease dramatically as crosslinking is increased, and perhaps this primarily is an activity related effect.

The model developed in this work utilized the Implicit rank-Nicholson numerical method. The State Variable (65) and Collocation (29) methods should be evaluated for potential improvement in computation speed commensurate with equivalent

convergence and stability performance. The method of Characteristics (2, 22, 58) is an attractive alternative, but its use limits the user to asymptotic solutions which infer stable self-sharpening elution or loading patterns (not both) which have existed within the column long enough to have reached a stable configuration. Effects of uneven bed presaturation which exist in many practical applications could not be evaluated with the above method, nor could unfavorable exchange processes.

Finally, the model developed in this research simulated fixed bed operations successfully based on data derived from 1" diameter glass columns. Obviously, scale-up effectiveness has yet to be proven in an industrial application. This will most likely not be within the purview of future academic investigators, but result from actual industrial applications.

3. Other Potential Applications

With modification, the model could be utilized to simulate isothermal adsorption processes. The required changes would include a pore diffusion model to describe diffusion in the particle, and equilibrium relationships such as the Langmuir or Freundlich models. Substantial changes would be required, but the basic partial differential equations and numerical solution techniques should be reviewed for applicability to biotechnology operations involving reactions induced by immobilized enzymes or bacterial cultures within porous beads or gels.

EFFECT OF CONCENTRATION UNITS ON ACTIVITY COEFFICIENT

RELATIONSHIPS IN AN ION EXCHANGER

A. Molar versus Equivalent Fraction Concentration Units

The free energy relationship for the exchange of ionic species in an ion exchange resin are as follows for the concentration units of molar versus equivalent fraction:

$$\overline{G}_1^0 = \overline{G}_1'{}_{molar} + RT\ln(\overline{c}_1 \cdot {}^n\overline{\gamma}_1{}_{molar}) \tag{A-1}$$

$$\overline{G}_1^0 = \overline{G}_1'{}_{eqf} + RT\ln(\overline{x}_1 \cdot {}^n\overline{\gamma}_1) \tag{A-2}$$

Setting (A-1) and (A-2) equal to each other results in:

$$\ln\left(\frac{\overline{c}_1}{\overline{x}_1}\right) + \frac{\left(\overline{G}_1'{}_{molar} - \overline{G}_1'{}_{eqf}\right)}{RT} = \ln\left(\frac{{}^n\overline{\gamma}_1}{{}^n\overline{\gamma}_1{}_{molar}}\right) \tag{A-3}$$

From equation (2-14), the following limits are observed:

$$\text{as } \overline{x}_1 \longrightarrow 1.0 \text{ , } {}^n\overline{\gamma}_1 \longrightarrow 1.0 \text{ , and } {}^n\overline{a}_1 \longrightarrow 1.0 \tag{A-4}$$

$$\text{Likewise, as } \overline{c}_1 \longrightarrow \frac{Q_r}{|z_1|} = \overline{c}_T \text{ , } {}^n\overline{\gamma}_1{}_{molar} \longrightarrow 1.0 \text{ , and } {}^n\overline{a}_1{}_{molar} \longrightarrow \frac{Q_r}{|z_1|}$$

Solving equation (A-3) at the limits gives the free energy difference due to concentration units.

$$\ln\left(\frac{\left(\frac{Q_r}{|z_1|}\right)}{1}\right) = -\frac{\left(\overline{G}_1'{}_{molar} - \overline{G}_1'{}_{eqf}\right)}{RT} + \ln\left(\frac{1}{1}\right)$$

and,

$$\ln\left(\frac{Q_r}{|z_1|}\right) = -\frac{\left(\overline{G}_1{}_{molar} - \overline{G}_1{}_{eqf}\right)}{RT} \tag{A-5}$$

substituting (A-5) into (A-3) yields:

$$\ln\left(\frac{\bar{c}_1}{\bar{x}_1}\right) - \ln\left(\frac{Q_r}{|z_1|}\right) = \ln\left(\frac{{}^n\bar{\gamma}_1}{{}^n\bar{\gamma}_{1_{molar}}}\right) \qquad (A-6)$$

$$\text{but } \bar{x}_1 = \frac{\bar{c}_1 \cdot |z_1|}{Q_r}$$

so, it is obvious from (A-6) that:

$$\left(\frac{{}^n\bar{\gamma}_1}{{}^n\bar{\gamma}_{1_{molar}}}\right) = 1 \qquad (A-7)$$

This relationship applies at all concentrations. This can be proven at the other concentration extreme where $\bar{x}_1$ and $\bar{c}_1$ approach zero. Looking at Figure 2-2, and equations (2-15) and (2-16), the following construct is possible:
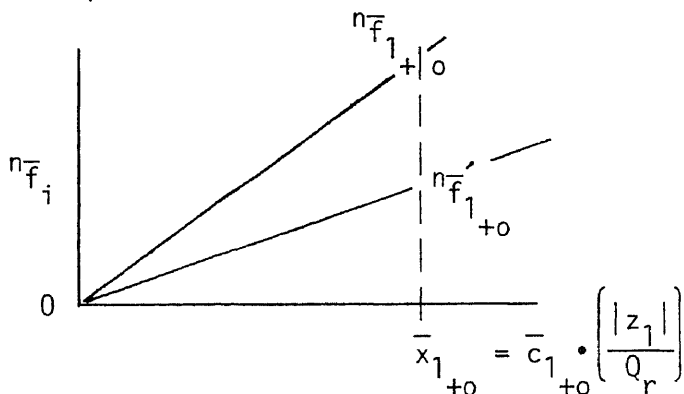
Then for $\bar{x}_1$, as in (2-15) and (2-16),

$${}^n\bar{\gamma}_{1_{+o}} = {}^n\bar{\gamma}_1 = \frac{K}{{}^n\bar{f}_1^0}$$

Using the same treatment for molar units at the identical ${}^n\bar{f}_{1_{+o}}$ point,

$$K = \frac{\left({}^n\bar{f}_{1_{+o}} - 0\right)}{\left(\bar{c}_{1_{+o}}\left(\frac{|z_1|}{Q_r}\right) - 0\right)} = \frac{{}^n\bar{f}_{1_{+o}}}{\bar{c}_{1_{+o}}} \cdot \frac{Q_r}{|z_1|} \qquad (A-8)$$

and,

$$n\overline{f}_1'{}_{+o} = n\overline{f}_1^0 \cdot \left(\frac{\overline{c}_1{}_{+o}}{\overline{c}_1{}_{total}} \right) = n\overline{f}_1^0 \cdot \left(\frac{\overline{c}_1{}_{+o}}{\left(\frac{Q_r}{|z_1|} \right)} \right) \tag{A-9}$$

so,

$$n\overline{\gamma}_1{}_{molar} = \frac{K \cdot \overline{c}_1{}_{+o} \cdot \left(\frac{|z_1|}{Q_r} \right)}{n\overline{f}_1^0 \cdot \overline{c}_1{}_{+o} \cdot \left(\frac{|z_1|}{Q_r} \right)} = \frac{K}{n\overline{f}_1^0} \tag{A-10}$$

Substitution of $n\overline{\gamma}_1$ and $n\overline{\gamma}_1{}_{molar}$ in equation (A-3) leads to equation (A-5) since:

$$\ell n \left(\frac{n\overline{\gamma}_1}{n\overline{\gamma}_1{}_{molar}} \right) = \ell n \left(\frac{\left(\frac{K}{n\overline{f}_1^0} \right)}{\left(\frac{K}{n\overline{f}_1^0} \right)} \right) = 0 \text{ , and the proof of } n\overline{\gamma}_1 = n\overline{\gamma}_1{}_{molar} \text{ is made at the other concentration extreme.}$$

B. Molar versus Mole Fraction Concentration Units

The relationship between molar units and mole fraction units is given as:

$$\overline{x}_1{}_{mf} = \frac{\overline{c}_1}{\left(\left(\frac{Q_r}{|z_2|} \right) + (1-VR) \cdot \overline{c}_1 \right)} \tag{A-11}$$

$$\text{where } VR = \left(\frac{|z_1|}{|z_2|} \right)$$

Using the free energy relationship given by equation (A-1) in conjunction with:

$$\overline{G}_1^0 = \overline{G}_1'{}_{mf} + RT\ell n(\overline{x}_1{}_{mf} \cdot n\overline{\gamma}_1{}_{mf}) \tag{A-12}$$

then,

$$\ln\left(\frac{\bar{c}_1}{\bar{x}_{1_{mf}}}\right) = -\frac{\left[\bar{G}'_{1_{molar}} - \bar{G}'_{1_{mf}}\right]}{RT} + \ln\left(\frac{{}^n\bar{\gamma}_{1_{mf}}}{{}^n\bar{\gamma}_{1_{molar}}}\right) \qquad (A-13)$$

Defining the limits as was done in equation (A-4),

$$\text{as } \bar{x}_{1_{mf}} \longrightarrow 1.0 \; , \; {}^n\bar{\gamma}_{1_{mf}} \longrightarrow 1.0 \; , \text{ and } {}^n\bar{a}_{1_{mf}} \longrightarrow 1.0 \quad (A-14)$$

and equation (A-4) gives the limits in molar units. Substitution in equation (A-13) gives:

$$\ln\left(\frac{Q_r}{|z_1|}\right) = -\frac{\left[\bar{G}'_{1_{molar}} - \bar{G}'_{1_{mf}}\right]}{RT} \qquad (A-15)$$

Substitution of equation (A-15) in equation (A-13) yields:

$$\ln\left(\frac{\bar{c}_1}{\bar{x}_{1_{mf}}}\right) - \ln\left(\frac{Q_r}{|z_1|}\right) = \ln\left(\frac{{}^n\bar{\gamma}_{1_{mf}}}{{}^n\bar{\gamma}_{1_{molar}}}\right) \qquad (A-16)$$

but,

$$\bar{x}_{1_{mf}} = \frac{\bar{c}_1}{\left(\left|\frac{Q_r}{|z_2|}\right| + (1-VR)\cdot\bar{c}_1\right)}$$

so,

$$\left(\frac{\bar{c}_1}{\bar{c}_1}\right)\cdot\left(\left[\left|\frac{Q_r}{|z_2|}\right| + (1-VR)\cdot\bar{c}_1\right]\cdot\left(\frac{|z_1|}{Q_r}\right)\right) = \left(\frac{{}^n\bar{\gamma}_{1_{mf}}}{{}^n\bar{\gamma}_{1_{molar}}}\right) \quad (A-17)$$

therefore,

$${}^n\bar{\gamma}_{1_{molar}} = {}^n\bar{\gamma}_{1_{mf}} \cdot \left(\frac{1}{\left[VR + (1-VR)\cdot\bar{x}_1\right]}\right) \qquad (A-18)$$

noting that $\bar{x}_1$ is equivalent fraction since

$$\bar{x}_1 = \frac{\bar{c}_1\cdot|z_1|}{Q_r}$$

A like derivation can be made for ${}^{n}\overline{\gamma}_{2_{molar}}$ versus ${}^{n}\overline{\gamma}_{2_{mf}}$ in that:

$$\overline{x}_{2_{mf}} = \frac{\overline{c}_2}{\left[\left(\dfrac{Q_r}{|z_1|}\right) + (1- \dfrac{1}{VR})\cdot\overline{c}_2\right]} \qquad (A-19)$$

so,

$$\ln\left(\frac{\overline{c}_2}{\overline{x}_{2_{mf}}}\right) - \ln\left(\frac{Q_r}{|z_2|}\right) = \ln\left(\frac{{}^{n}\overline{\gamma}_{2_{mf}}}{{}^{n}\overline{\gamma}_{2_{molar}}}\right) \qquad (A-20)$$

Substituting equation (A-19) in (A-20) gives:

$$\left[\left(\frac{Q_r}{|z_1|}\right) + (1- \frac{1}{VR})\cdot\overline{c}_2\right]\cdot\left[\frac{|z_2|}{Q_r}\right] = \left(\frac{{}^{n}\overline{\gamma}_{2_{mf}}}{{}^{n}\overline{\gamma}_{2_{molar}}}\right) \qquad (A-21)$$

which leads to:

$$ {}^{n}\overline{\gamma}_{2_{molar}} = {}^{n}\overline{\gamma}_{2_{mf}}\cdot\frac{1}{\left[\dfrac{1}{VR} + (1- \dfrac{1}{VR})\cdot\overline{x}_2\right]} \qquad (A-22)$$

Checking the relationship at the limit where $\overline{x}_{1_{mf}} \longrightarrow 0$

$$\overline{c}_{1_{+o}} = \frac{\overline{x}_{1_{mf_{+o}}}\cdot Q_r}{(|z_2|)\cdot\left[1 + \overline{x}_{1_{mf_{+o}}}\cdot(VR-1)\right]}$$
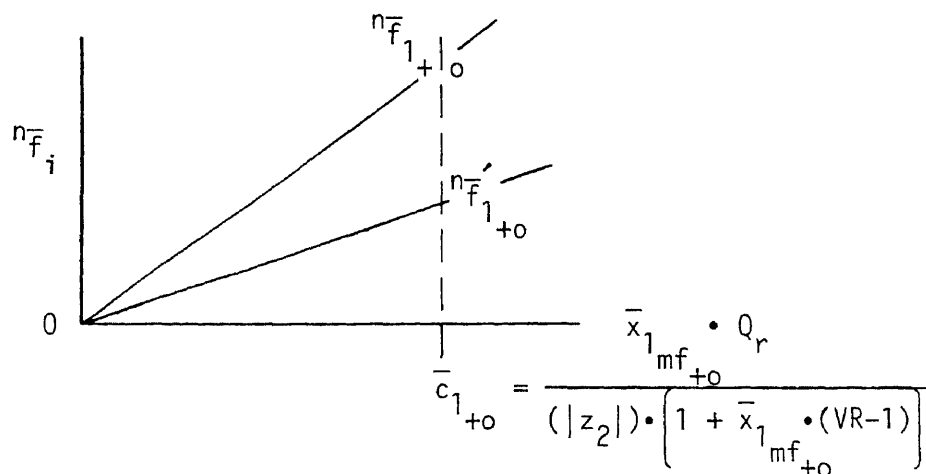
The lower limits are then defined as:

$$ {}^{n}\overline{\gamma}_{1_{molar_{+o}}} = {}^{n}\overline{\gamma}_{1_{molar}} = \frac{K'}{{}^{n}\overline{f}_1^0}\cdot\left(\frac{|z_1|}{Q_r}\right) \qquad (A-23)$$

since,

$$K' = \frac{{}^n\bar{f}_{1_{+o}}}{\bar{c}_{1_{+o}}} \quad, \quad \text{and} \quad {}^n\bar{f}'_{1_{+o}} = \left(\frac{\bar{c}_{1_{+o}}}{\left(\dfrac{Q_r}{|z_1|}\right)}\right) \cdot {}^n\bar{f}_1^0$$

it follows that:

$$^n\bar{\gamma}_{1_{molar}} = \left(\frac{K' \cdot \bar{c}_{1_{+o}}}{{}^n\bar{f}_1^0 \cdot \bar{c}_{1_{+o}}}\right) \cdot \left(\frac{Q_r}{|z_1|}\right) = \frac{K'}{{}^n\bar{f}_1^0} \cdot \left(\frac{Q_r}{|z_1|}\right) \qquad (A-24)$$

Performing the same procedure in mole fraction units,

$$K'_{mf} = {}^n\bar{f}_{1_{+o}} \cdot \left[\frac{(|z_2|) \cdot \left(1 + \bar{x}_{1_{mf_{+o}}}^o \cdot (VR-1)\right)}{\bar{x}_{1_{mf_{+o}}} \cdot Q_r}\right] = \frac{{}^n\bar{f}_{1_{+o}}}{\bar{x}_{1_{mf_{+o}}}} \cdot \left(\frac{|z_2|}{Q_r}\right)$$

since $\bar{x}_{1_{mf_{+o}}} = 0$ as it approaches 0

and,

$$^n\bar{f}'_{1_{+o}} = {}^n\bar{f}_1^0 \cdot \bar{x}_{1_{mf_{+o}}}$$

it similarly follows that:

$$^n\bar{\gamma}_{1_{mf}} = \frac{{}^n\bar{f}_{1_{+o}}}{{}^n\bar{f}'_{1_{+o}}} = \frac{K'_{mf}}{{}^n\bar{f}_1^0} \cdot \left(\frac{Q_r}{|z_2|}\right) \qquad (A-25)$$

Substitution of equation (A-24) and (A-25) in equation (A-13) leads to:

$$\ell n\left[\frac{\left(\dfrac{\bar{x}_{1_{mf_{+o}}} \cdot Q_r}{(|z_2|) \cdot \left(1 + \bar{x}_{1_{mf_{+o}}} \cdot (VR-1)\right)}\right)}{\bar{x}_{1_{mf_{+o}}}}\right] = -\frac{\left[\bar{G}_{1_{molar}} - \bar{G}'_{1_{mf}}\right]}{RT}$$

$$+ \ell n\left\{\frac{\dfrac{K'_{mf}}{{}^n\bar{f}_1^0} \cdot \left(\dfrac{Q_r}{|z_2|}\right)}{\dfrac{K'}{{}^n\bar{f}_1^0} \cdot \left(\dfrac{Q_r}{|z_1|}\right)}\right\}$$

Since $\bar{x}_{1_{mf_{+o}}} = 0$, and $K_{mf}' = K'$ as the concentration of species 1 approaches zero, then the following expression is derived:

$$-\frac{\left[\bar{G}_{1_{molar}} - \bar{G}_{1_{mf}}\right]}{RT} = \ell n\left[\frac{Q_r}{|z_2|}\right] - \ell n\left[\frac{|z_1|}{|z_2|}\right] \qquad (A-26)$$

Substitution of equation (A-26) in (A-13) leads to,

$$\ell n\left[\frac{\bar{c}_1}{\bar{x}_{1_{mf}}}\right] - \ell n\left[\frac{Q_r}{|z_1|}\right] = \ell n\left[\frac{{}^n\bar{\gamma}_{1_{mf}}}{{}^n\bar{\gamma}_{1_{molar}}}\right]$$

or,

$$ {}^n\bar{\gamma}_{1_{molar}} = {}^n\bar{\gamma}_{1_{mf}} \cdot \left[\frac{\bar{c}_1 \cdot |z_1|}{\bar{x}_{1_{mf}} \cdot Q_r}\right] \qquad (A-27)$$

The expression for $\bar{x}_{1_{mf}}$ in terms of $\bar{c}_1$ is,

$$\bar{x}_{1_{mf}} = \frac{\bar{c}_1}{\left[\left[\frac{Q_r}{|z_2|}\right] + (1-VR)\cdot\bar{c}_1\right]}$$

Substitution for $\bar{x}_{1_{mf}}$ leads to:

$$ {}^n\bar{\gamma}_{1_{molar}} = {}^n\bar{\gamma}_{1_{mf}} \cdot \left[\frac{1}{\left[VR + (1-VR)\cdot\bar{x}_1\right]}\right] \qquad (A-28)$$

where $\bar{x}_1$ is the equivalent fraction unit

This expression is identical to equation (A-18).

NON-LINEAR PARAMETER ESTIMATION

A. K. S. Murthy

A. Introduction

The problem of establishing mathematical relationships between a set of dependent variables and a set of independent variables using experimental data is frequently encountered in applied science. For example, it may be necessary to obtain expressions for the exit composition of a chemical reactor in terms of the inlet composition. The functional form of the mathematical relationships, whether they are derived based on fundamental physical and chemical principles or simply selected to give sufficient mathematical flexibility, may be written as:

$$y_i = f_i(b_k; x_j) \qquad (B-1)$$

where, x_j are the independent variables, y_i the dependent variables, and b_k are parameters. The functional relationships, although shown above as explicit algebraic expressions, can also be implicity defined in the form of algebraic, differential or integral equations, or even a complex series of calculations performed by computer simulation programs. Parameters are constants whose numerical values change from system to system and are usually not directly measurable. The mathematical process of determining the values of the parameters using experimental x-y data is known as regression analysis. When the functions f_i are such that the partial derivatives $(\partial f_i / \partial b_k)$ are independent of b_k, linear regression techniques can be used to obtain the values of the parameters. However, many chemical engineering models (mathematical relationships)

371

are nonlinear with respect to the parameters and require iterative techniques for parameter estimation. The purpose of this report is to describe an algorithm (mathematical recipe) for nonlinear regression and to provide instructions for using three general purpose computer programs based on that algorithm. One program handles explicit algebraic models and the other two differential equation models. In the latter case, one version has built-in integration procedures for ordinary differential equations with initial conditions. The other version requires the user to provide an integration routine for the partial or ordinary differential equations.

B. The Weighted Least Squares Procedure

If $y_{j\ell}^{*}$ are experimentally observed values corresponding to a set of independent variables $x_{j\ell}$ in the ℓ-th observation, the object of regression analysis is to determine the values of the parameters such that the difference between $y_{i\ell}^{*}$ and the values of y_i calculated using $x_{j\ell}$ in equation (B-1) is a minimum according to some statistically valid criterion. The use of a statistically valid criterion is important since, due to random errors, the exact x-y relationship cannot be experimentally observed. Consequently, the parameter values obtained from such measurements are subject to uncertainty. A statistical procedure for obtaining the best estimates of the parameters is the method of maximum likelihood (Draper and Smith 1966). The least squares procedure developed by Gauss is the most frequently used for parameter estimation and is the maximum likelihood procedure when the following assumptions are satisfied. Only the dependent variable measurements are subject to error. The

errors are purely random and obey Gaussian statistics with zero mean
and known variance.

The least squares method calls for the minimization of the
following objective function.

$$S(b) = \sum_{i=1}^{m} \left\{ \sum_{\ell=1}^{L} (y_{i\ell}^{*} - y_{i\ell})^2 \right\} /s_i^2 \qquad (B-2)$$

$$= \sum_{i=1}^{m} \left\{ \sum_{\ell=1}^{L} [y_{i\ell}^{*} - f_i(b;x_{j\ell})]^2 \right\} /s_i^2$$

where s_i is the variance associated with the measurement of y_i,
L is the total number of data points, and m is the number of
dependent variables measured experimentally, or derived from those
measurements.

C. The Gauss-Newton Method

An efficient method for finding the minimum of a multidimensional
function is due to Newton. His method consists of guessing the
location of the minimum, approximating the function by the first
three terms of the Taylor series expansion about the guess point,
finding the minimum of the approximation and using that minimum point
as the next guess. This procedure is repeated until the true minimum
is found. If b_o is the guess point, the quadratic approximation is

$$S = S(b_o) + \sum_{k=1}^{P} \frac{\partial S}{\partial b_k} \Delta b_k + 1/2 \sum_{i=1}^{P} \sum_{j=1}^{P} \frac{\partial^2 S}{\partial b_i \partial b_j} \Delta b_i \Delta b_j \qquad (B-3)$$

where, the function and the derivatives are evaluated at $b=b_o$. A
set of corrections, Δb, which should be added to b_o to obtain the
minimum of the above approximation is given by

$$\sum_{j=1}^{P} \frac{\partial^2 S}{\partial b_i \partial b_j} \Delta b_j = -\frac{\partial S}{\partial b_i} \qquad i = 1,P \qquad (B-4)$$

where, P is the number of parameters in the model. It can be shown that,

$$\frac{\partial S}{\partial b_k} = -2 \sum_{i=1}^{m} \frac{1}{s_i^2} \sum_{\ell=1}^{L} [y_{i\ell}^* - f(x_\ell)] \frac{\partial f_i}{\partial b_k} \quad ; k=1,P \qquad (B-5)$$

and
$$(B-6)$$

$$\frac{\partial^2 S}{\partial b_k \partial b_n} = -2 \left[\sum_{i=1}^{m} \frac{1}{s_i^2} \sum_{\ell=1}^{L} \left([y_{i\ell}^* - f_i(x_\ell)] \frac{\partial^2 f_i}{\partial b_k \partial b_n} - \frac{\partial f_i}{\partial b_k} \frac{\partial f_i}{\partial b_n} \right) \right]$$
$$k=1,P$$

If the guess values are good, $(y_{i\ell} - f_i)$ should be small and hence

$$\frac{\partial^2 S}{\partial b_k \partial b_n} \simeq 2 \sum_{i=1}^{m} \frac{1}{s_i^2} \sum_{\ell=1}^{L} \frac{\partial f_i}{\partial b_k} \frac{\partial f_i}{\partial b_n} \quad ; k=1,P \qquad (B-7)$$

Equation (B-7) is the approximation by Gauss leading to the Gauss-Newton method. When the guess value is near the minimum, this method gives quadratic convergence like Newton's method, but does not require the evaluation of the second derivatives. Gauss-Newton corrections are given by
$$(B-8)$$

$$\sum_{n=1}^{P} \sum_{i=1}^{m} \frac{1}{s_i^2} \sum_{\ell=1}^{L} \frac{\partial f_i}{\partial b_k} \frac{\partial f_i}{\partial b_n} \Delta b_n = \sum_{i=1}^{m} \frac{1}{s_i^2} \sum_{\ell=1}^{L} (y_{i\ell}^* - f_i) \frac{\partial f_i}{\partial b_k}$$
$$k=1,P$$

If B_i is an (LxP) matrix who ℓj-th element is $(\partial f_i/\partial b_j)$ for the ℓ-th data point, the above equation may be written as

$$\left[\sum_{i=1}^{m} (B_i^T B_i)/s_i^2 \right] \Delta b = \sum_{i=1}^{m} B_i^T e_i/s_i^2 \qquad (B-9)$$

m = number of dependent variables measured or derived from those measurements,

where, e_i is a vector whose ℓ-th element is $(y_{i\ell}^* - f_i)$. Let

$$G = \sum_{i=1}^{m} B_i/s_i \qquad \text{and} \qquad r = \sum_{i=1}^{m} e_i/s_i$$

Then equation (B-9) may be written as

$$G^T G \, \Delta b = G^T r \qquad \qquad (B-10)$$

Sometimes it is necessary to analyze several sets of data, obeying different functional relationships but having a common set of parameters. For example, one may attempt to estimate the parameters in a liquid phase excess free energy model using vapor-liquid as well as liquid-liquid equilibrium data. In such cases equation (B-10) becomes

$$(\sum_{i=1}^{N} W_i G_i^T G_i) \Delta b - \sum_{i=1}^{N} W_i G_i^T r_i \qquad \qquad (B-11)$$

where W_i is the weighting factor for the i-th set and G_i and r_i are the G and r matrices associated with that set. As defined in the computer program, weight $= W_i / s_i^2$.

Both the Newton's method and the Gauss-Newton method are known to be the most efficient algorithms when good guesses at the minimum can be made. They are unreliable if good guesses cannot be made. The author's experience is that this unreliability is due to a few poorly determined directions in applying the Newton's method, and can be rectified by a quadratic surface analysis of the Gauss-Newton matrix $(G^T G)$ as shown in the next section.

D. A Modified Gauss-Newton Method

The Gauss-Newton method uses the following quadratic approximation of the objective function about the guess point to obtain the corrections to be added to the guess values.

$$S = S(b_o) - 2(G^T r)^T \Delta b = \Delta b^T (G^T G) \, \Delta b \qquad \qquad (B-12)$$

The nature of the quadratic surface given by equation (B-12) can be determined by the eigenvalues and the eigenvectors of the G^TG matrix. It can be shown that G^TG is a positive definite matrix (all positive eigenvalues) and hence equation (B-12) represents a hyperellipsoid. The eigenvectors give the directions of the axes of the ellipsoid. The lengths of the axes are proportional to the reciprocals of the eigenvalues. Directions corresponding to very small eigenvalues are directions in which the function does not change very rapidly [according to the local approximation given by (B-12)] and hence large changes would be recommended by the Gauss-Newton method. Large corrections given by any local approximation method are likely to be unreliable. The modification of the Gauss-Newton algorithm presented in this report is based on this heuristic argument. The Gauss-Newton corrections are given by

$$\Delta b = (G^TG)^{-1}G^Tr \qquad (B-13)$$

If Q is a matrix whose columns are eigenvectors of G^TG, then Q is an orthonormal matrix and

$$Q^T(G^TG)Q = L \qquad (B-14)$$

where L is a diagonal matrix containing the eigenvalues of G^TG. Readers not famikliar with these properties should refer to any textbook on matrix theory covering quadratic forms and unitary transformation. From equations (B-13) and (B-14) it can be seen that

$$\Delta b = (QL^{-1}Q^T)G^Tr$$

or

$$\Delta b = \left[\sum_{i=1}^{n} (1/\ell_i) V_i V_i^T \right] G^Tr \qquad (B-15)$$

where, V_i is the i-th eigenvector and ℓ_i the i-th eigenvalue. The above equation gives the total Gauss—Newton correction as a sum of corrections along the eigenvector.

The modified method consists of summing the terms of equation (B-15) in the order of decreasing eigenvalues and, after the addition of each term, checking the cumulative corrections to determine if any of the corrections exceed the allowable step size. When the step size is exceeded, no additional terms are included in the summation. Only a fraction of the last term is used so that no correction exceeds the allowable step size. User supplied scale factors are used to scale the parameters and the corrections to comparable magnitude so that the same step size can be used for all the variables. The step size starts with a user specified value and increases by 10% for every successful step (steps leading to decrease in the objective function) and is cut to half for every unsuccessful step. It is possible to conceive of several other alternate strategies similar to the strategy outlined in this section. A systematic study to determine the best strategy has not been carried out, primarily because the present method has been very satisfactory in a number of practical problems.

RESIN PHASE ION EXCHANGE FITTING PROGRAM

RIONFT (AKM 62)

RIONFT (AKM 62) is a non-linear regression program for estimation of the equilibrium parameters in binary and ternary ion exchange systems, and has the following features:

A. Input module - subroutine M62A

1.0   Input 1 - title

2.0   Input 2 gives the following information in free format:

    2.1   the total number of data sets

    2.2   the total number of parameters involved

    2.3   debug options selected

    2.4   non-default values, if desired, for parameter search step size, numerical Jacobian perturbation values, and run time limit

    2.5   print control on a variety of computed values giving full, partial, or minimum information

    2.6   switching options on selection of $\overline{K}_{ij}$ to be computed by the chain rule from $\overline{K}_{ik}$ and $\overline{K}_{jk}$ values

    2.7   choice of resin phase activity coefficient correlation method (i.e., Redlich-Kister, Wilson, or NRTL)

3.0   Input 3

A fit string which allows selection, 0 or 1, of those parameters which are to be fit in a given run. Those parameters not fit can be either zero, or be used in the regression analysis with a preset estimate value

4.0   Inputs 4 and 5

     Involve scale factors and initial estimates for parameters

5.0   Input 6

     Allows individual parameters to be bounded by upper and

     lower values if known

6.0   The data sets are then read in giving, for each set,

     6.1   Input 1 gives no. of data points, no. of constants,

          no. of variables (y and x), no. of dependent

          variables (y)

     6.2   Input 2 - labels for constants

     6.3   Input 3 gives the relative weight to be given to each

          dependent variable (default = 1), and constants

     6.4   Input 4 - labels for the variables

     6.5   Input 5 - data points (y and x)

B.   The <u>subroutine CONTROL</u> performs the sequencing of regression runs

1 through 26 as outlined in Chapter II, para. D, section 2.

C.   The <u>evaluation subroutine, M62G,</u> is specifically designed by the

user of <u>program AKM62</u> to compute the dependent and independent

variables for user specific equations in response to calls from

<u>AKM62</u> subroutines. The independent variables are computed for

each data point utilizing the constants, and the dependent

variables are computed for the latest values of the fitted

parameters. Equations (2-73) and (2-75) given in Chapter II

represent the dependent and independent variables computed at

each call. If the data set being regressed is a ternary system,

the <u>M62G,</u> as designed for RIONFT, will switch to another part

of the subroutine where the $Y(1)_{exp}$, $Y(2)_{exp}$, and $Y(3)_{exp}$ independent variables and the $Y(1)_{calc}$, $Y(2)_{calc}$, and $Y(3)_{calc}$ dependent variables are calculated, the latter representing the dependent portions of the three binary pair equilibrium relationships.

D. Subroutines supporting M62G are the resin phase activity coefficient generators, REDKIS, WILSON, and NRTL, and the electrolyte phase activity coefficient gen rator, LIQION. LIQION also computes the equilibrium composition of a stable complex, if there is one, along with its effect on ionic strength including the activity coefficient for the complex species and the coion.

E. When the regression has met convergence criteria on all fitted parameters for all sets within one of the 26 controlled runs, subroutine M62C is called, which provides optional printout of the best value of parameters along with standard deviation and correlation coefficients between parameters. M62C stores the best parameter values fitted, to be used by CONTROL in setting the initial estimates for the next run, or in subsequent runs where these values are required. It optionally will print out a variety of information related to that run, including the activity coefficients for each species in the resin and electrolyte phase, ionic strength, and fraction of complex present if any, for each data point.

F. Two major subroutines, called by the main program after each of the 26 controlled runs, are TERION and BINION. These subroutines, TERION for ternary systems, and BINION for binary

systems, compute the equilibrium resin phase composition for each experimental electrolyte composition data point for all sets within a run, on a set-by-set basis. They compute the standard sample deviation of the calculated equilibrium composition from the experimental values for each set within a run, on a % difference and a % relative difference basis. These routines print out the standard deviation information along with optional information including actual data points alongside the calculated points for all species. The resin and electrolyte phase activity coefficients are printed out, along with ionic strength.

The equations describing either binary or ternary equilibria are non-linear because of the relationships describing the activity coefficient correlations. In BINION, a false positioning method is utilized to solve the single equilibrium relationship describing a binary pair, since the function is monotonic. With TERION, a simultaneous solution of two of the equilibrium relationships is required to define the equilibrium concentrations of x_i and x_j, with $x_k = 1-x_i-x_j$. The Newton-Raphson method is used in that subroutine to provide solution to the coupled non-linear algebraic equations.

CONCENTRATION EFFECTS ON DIFFUSION COEFFICIENTS OF IONIC SPECIES

IN AQUEOUS SOLUTIONS

A. **Diffusion Coefficients of Salts in Aqueous Solution-Infinite Dilution**

$$D_{\pm}^{0} = 8.931 \cdot 10^{-10} \cdot T \cdot \left[\frac{L_{+}^{0} L_{-}^{0}}{\Lambda^{0}} \right] \cdot \left[\frac{|z_{+}| + |z_{-}|}{|z_{+} \cdot z_{-}|} \right] \qquad (D-1)$$

where:

$D_{\pm}^{0}$ = diffusion coefficient of salt as concentration $\rightarrow 0$, cm^2/sec

L_{+}^{0} = conductance of cation, mhos/equiv.

L_{-}^{0} = conductance of anion, mhos/equiv.

Λ^{0} = $L_{+} + L_{-}$, salt conductance, mhos/equiv.

T = ^{0}K

z_{+}, z_{-} = charge on ion

$\dfrac{R}{F^2}$ = $8.931 \; 10^{-6}$, gas constant/Faraday constant^2 ,joule/^{0}K/mole/Coulomb/equiv.

B. **Diffusion Coefficients of Ions in Aqueous Solution-Infinite Dilution**

$$D_{+}^{0} = 8.931 \cdot 10^{-10} \cdot T \cdot \left[\frac{L_{+}^{0}}{|z_{+}|} \right] \qquad (D-2)$$

$$D_{-}^{0} = 8.931 \cdot 10^{-10} \cdot T \cdot \left[\frac{L_{-}^{0}}{|z_{-}|} \right] \qquad (D-3)$$

combining (D-2) and (D-3) into (D-1) yields:

$$D_{\pm}^{0} = D_{+}^{0} \cdot D_{-}^{0} \cdot \left[\frac{(|z_{+} \cdot z_{-}|)}{(|z_{+}| \cdot D_{+}^{0} + |z_{-}| \cdot D_{-}^{0})} \right] \qquad (D-4)$$

C. <u>Diffusion Coefficient Variation with Electrolyte Concentration</u>

Nernst-Hartley Equation for Dilute Solutions:

$$D_\pm = D_\pm^0 \cdot \left[1 + c_\pm \cdot \frac{d\ell n \eta_\pm}{dc_\pm} \right] \qquad \text{(D-5)}$$

where:

$c_\pm$ = molality (assume equal to molarity at specific gravity of one)

$\eta_\pm$ = molar activity coefficient of salt

If molality is equal to molarity, then

$$D_\pm = D_\pm^0 \cdot \left[1 + c_\pm \cdot \frac{d\ell n \gamma_\pm}{dc_\pm} \right] \qquad \text{(D-6)}$$

where:

$\gamma_\pm$ = molal activity coefficient as given by the Bromley equation.

D. <u>Differential Form of Correction to Diffusion Coefficient</u>

<u>for Concentration</u>

If the viscous drag effects on hydrated ions which occur at high electrolyte concentration are ignored, the following treatment can be used to correct $D_\pm^0$ for the effect of electrolyte concentration. Using the Bromley equation to relate $\gamma_\pm(c_\pm)$ to concentration, $c_\pm$, the Bromley equation can be differentiated with respect to $c_\pm$, molarity (molality).

1.0 <u>Single Salt in Aqueous Solution</u>

Substitution of Ionic Strength, I , in the Bromley and Nernst-Hartley equations leads to:

$$I = \frac{1}{2} \cdot \left(c_+ \cdot z_+^2 + c_- \cdot z_-^2 \right) \tag{D-7}$$

If norm = electrolyte normality

$$= c_- \cdot (|z_-|) \tag{D-8}$$

And,

$$c_+ = \left(\frac{c_- \cdot (|z_-|)}{z_+} \right) = \frac{norm}{z_+} \tag{D-9}$$

The molarity of the salt is given by:

$$c_\pm = \frac{norm}{(|z_+ \cdot z_-|)} \tag{D-10}$$

Differentiating (D-10) with respect to $c_\pm$ and

substituting in equation (D-6) leads to:

$$D_\pm = D_\pm^0 \cdot \left(1 + norm \cdot \frac{d\ln\gamma_\pm}{d(norm)} \right) \tag{D-11}$$

By differentiating the Bromley equation, the following

expression is obtained:

$$\tag{D-12}$$

$$
\frac{d\ln\gamma_\pm}{d(norm)} = 2.303 \cdot \left[\frac{-0.511 \cdot (|z_+ \cdot z_-|) \cdot \left[\frac{(|z_+|+|z_-|)}{2} \right]^{\frac{1}{2}}}{2 \cdot norm^{\frac{1}{2}} \cdot \left[1 + \left(\frac{1}{2} \cdot norm \cdot (|z_+|+|z_-|) \right)^{\frac{1}{2}} \right]^2} \right.
$$

$$
+ \frac{(0.06 + 0.6 \cdot Bia) \cdot (|z_+ \cdot z_-|) \cdot \left[1 - \left[\frac{\frac{3}{4} \cdot (|z_+|+|z_-|) \cdot norm}{(|z_+ \cdot z_-|)} \right] \right] \cdot \left[\frac{(|z_+|+|z_-|)}{2} \right]}{\left[1 + \left[\frac{\frac{3}{4} \cdot norm \cdot (|z_+|+|z_-|)}{(|z_+ \cdot z_-|)} \right] \right]^3}
$$

$$
\left. + \left[\frac{(|z_+|+|z_-|)}{2} \right] \cdot Bia \right]
$$

This relationship can be substituted into equation (D-11)

to correct the Diffusion Coefficient of a salt for

electrolyte concentration.

2.0 Cation Relationship with a Single Salt in Aqueous Solution

$$(D-13)$$

$$\frac{d\ell n\gamma_+}{d(norm)} = 2.303 \cdot \left[\frac{-0.511 \cdot z_+^2 \cdot \left[\frac{(|z_+|+|z_-|)}{2} \right]^{\frac{1}{2}}}{2 \cdot norm^{\frac{1}{2}} \cdot \left[1 + \left(\frac{1}{2} \cdot norm \cdot (|z_+|+|z_-|) \right)^{\frac{1}{2}} \right]^2} \right.$$

$$+ \frac{(0.06+0.6 \cdot Bia) \cdot (|z_+ \cdot z_-|) \cdot \left[1 - \left[\frac{\frac{3}{4} \cdot (|z_+|+|z_-|) \cdot norm}{(|z_+ \cdot z_-|)} \right] \right] \cdot \left[\frac{(|z_+|+|z_-|)}{2} \right]^2 \cdot \left(\frac{1}{|z_-|} \right)}{\left[1 + \left[\frac{\frac{3}{4} \cdot norm \cdot (|z_+|+|z_-|)}{(|z_+ \cdot z_-|)} \right] \right]^3}$$

$$\left. + Bia \cdot \left[\frac{(|z_+|+|z_-|)}{2} \right]^2 \cdot \left(\frac{1}{|z_-|} \right) \right]$$

The Nernst-Hartley equation for a single cation is,

$$D_+ = D_+^0 \cdot \left(1 + c_+ \cdot \frac{d\ell n\gamma_+}{dc_+} \right) \tag{D-14}$$

where:

$$c_+ = \frac{norm}{z_+} \quad (D-15), \text{ and } \quad \frac{d(norm)}{dc_+} = z_+ \quad (D-16)$$

The substitution of equations (D-15) and (D-16) in equation (D-14) yields:

$$D_+ = D_+^0 \cdot \left(1 + norm \cdot \frac{d\ell n\gamma_+}{d(norm)} \right) \tag{D-17}$$

Substitution of equation (D-13) in (D-17) gives the relationship for dependency of a single cation diffusion coefficient on electrolyte normality.

Analagous treatment can be used for the anion diffusion coefficient.

3.0 Three Cations in Aqueous Solution with a Single Anion

3.1 The ionic strength is given as,

$$I = \frac{1}{2} \cdot \left[\left(\sum_{i=1}^{3} c_{+_i} \cdot z_{+_i}^2 \right) + c_{-_A} \cdot z_{-_A}^2 \right] \qquad (D-18)$$

or in equivalent fractions,   (D-19)

$$x_i = \left[\frac{c_{+_i} \cdot z_{+_i}}{\sum_{j=1}^{3} c_{+_j} \cdot z_{+_j}} \right] = \left(\frac{c_{+_i} \cdot z_{+_i}}{c_{-_A} \cdot (|z_{-_A}|)} \right) = \left(\frac{c_{+_i} \cdot z_{+_i}}{norm} \right)$$

$$\text{for } i = 1,2,3$$

and equation (D-18) becomes:

$$I = \frac{1}{2} \cdot norm \cdot \left[\left(\sum_{i=1}^{3} x_{+_i} \cdot |z_{+_i}| \right) + (|z_{-_A}|) \right] \qquad (D-20)$$

$$\text{for } i = 1,2,3$$

3.2 Differentiating equation (D-19) yields:

$$\frac{dx_{+_i}}{dc_{+_i}} = \left(\frac{|z_{+_i}|}{norm} \right) \qquad (D-21)$$

$$\text{for } i = 1,2,3$$

and the Nernst-Hartley equation becomes,

$$D_{+_i} = D_{+_i}^0 \cdot \left(1 + x_{+_i} \cdot \frac{d\ln\gamma_{+_i}}{dx_{+_i}} \right) \qquad (D-22)$$

$$\text{for } i = 1,2,3$$

3.3 The Bromley Equation in terms of Equivalent Fraction versus Ionic Strength becomes upon substitution of equation (D-20) in equation (3-4):

$$\ell n\gamma_{+_i} = 2.303 \cdot \left[\frac{-0.511 \cdot z_{+_i}^2 \cdot \left[\frac{1}{2} \cdot \left(\left[\sum_{j=1}^{3} x_{+_j} \cdot |z_{+_j}| \right] + |z_{-_A}| \right) \right]^{\frac{1}{2}} \cdot norm^{\frac{1}{2}}}{\left[1 + \left[\frac{norm}{2} \cdot \left(\left[\sum_{j=1}^{3} x_{+_j} \cdot |z_{+_j}| \right] + |z_{-_A}| \right) \right]^{\frac{1}{2}} \right]} \right.$$

$$+ \frac{(0.06+0.6 \cdot Bia) \cdot (|z_{+_i} \cdot z_{-_A}|) \cdot \left[\frac{(|z_{+_i}| + |z_{-_A}|)}{2} \right]^2 \cdot \left[\frac{norm}{|z_{-_A}|} \right]}{\left[1 + \frac{\frac{3}{4} \cdot \left[norm \cdot \left(\left[\sum_{j=1}^{3} x_{+_j} \cdot |z_{+_j}| \right] + |z_{-_A}| \right) \right]^2}{(|z_{+_i} \cdot z_{-_A}|)} \right]}$$

$$\left. + Bia \cdot \left[\frac{(|z_{+_i}| + |z_{-_A}|)}{2} \right]^2 \cdot \left[\frac{norm}{|z_{-_A}|} \right] \right]$$

for $i = 1,2,3$

It is noted that the major variable in computing γ_{+_i} is I, the ionic strength, so even if a cation species equivalent fraction approaches zero, its activity coefficient will remain relatively constant in mixed cation solutions. For example, if a system has $z_{+_1} = z_{+_2} = z_{+_3}$, I is constant, and γ_{+_1} is a function of _norm_ only. In another example, if a system has $z_{+_1} = z_{+_2} = 2$ and $z_{+_3} = 1$, then relative values of I will vary only between 1 and 1.5 as x_{+_3} goes from a concentration value of one to zero.

$$(D-23)$$

$$\ln\gamma_{+_i} = 2.303 \cdot \left[\frac{-0.511 \cdot z_{+_i}^2 \cdot \left[\frac{1}{2} \cdot \left[\left(\sum_{j=1}^{3} x_{+_j} \cdot |z_{+_j}| \right) + |z_{-_A}| \right] \right]^{\frac{1}{2}} \cdot norm^{\frac{1}{2}}}{\left[1 + \left[\frac{norm}{2} \cdot \left[\left(\sum_{j=1}^{3} x_{+_j} \cdot |z_{+_j}| \right) + |z_{-_A}| \right] \right]^{\frac{1}{2}} \right]} \right.$$

$$+ \frac{(0.06 + 0.6 \cdot Bia) \cdot (|z_{+_i} \cdot z_{-_A}|) \cdot \left(\frac{(|z_{+_i}| + |z_{-_A}|)}{2} \right)^2 \cdot \left(\frac{norm}{|z_{-_A}|} \right)}{\left[1 + \frac{\frac{3}{4} \cdot \left[norm \cdot \left[\left(\sum_{j=1}^{3} x_{+_j} \cdot |z_{+_j}| \right) + |z_{-_A}| \right] \right]^2}{(|z_{+_i} \cdot z_{-_A}|)} \right]}$$

$$\left. + Bia \cdot \left(\frac{(|z_{+_i}| + |z_{-_A}|)}{2} \right)^2 \cdot \left(\frac{norm}{|z_{-_A}|} \right) \right]$$

for $i = 1,2,3$

It is noted that the major variable in computing γ_{+_i} is I, the ionic strength, so even if a cation species equivalent fraction approaches zero, its activity coefficient will remain relatively constant in mixed cation solutions. For example, if a system has $z_{+_1} = z_{+_2} = z_{+_3}$, I is constant, and γ_{+_1} is a function of _norm_ only. In another example, if a system has $z_{+_1} = z_{+_2} = 2$ and $z_{+_3} = 1$, then relative values of I will vary only between 1 and 1.5 as x_{+_3} goes from a concentration value of one to zero.

3.4 Equation (D-23) must be differentiated in order

to use the relationship in the Nernst-Hartley equation.

This expression is:

$$(D-24)$$

$$\frac{d\ln\gamma_{+_i}}{d(norm)} = 2.303 \cdot \left[\frac{-0.511 \cdot z_{+_i}^2 \cdot \left[\frac{1}{2} \cdot \left[\left(\sum_{j=1}^{3} x_{+_j} \cdot |z_{+_j}| \right) + |z_{-_A}| \right] \right]^{\frac{1}{2}}}{2 \cdot norm^{\frac{1}{2}} \cdot \left[1 + \left[\frac{norm}{2} \cdot \left(\left(\sum_{j=1}^{3} x_{+_j} \cdot |z_{+_j}| \right) + |z_{-_A}| \right) \right]^{\frac{1}{2}} \right]^2} \right]$$

$$+ \left[\frac{(0.06+0.6 \cdot Bia) \cdot (|z_{+_i} \cdot z_{-_A}|) \cdot \left[1 - \frac{\left[\frac{3}{4} \cdot norm \cdot \left(\left(\sum_{j=1}^{3} x_{+_j} \cdot |z_{+_j}| \right) + |z_{-_A}| \right) \right]}{(|z_{+_i} \cdot z_{-_A}|)} \right]}{\left[1 + \frac{\frac{3}{4} \cdot \left[norm \cdot \left(\left(\sum_{j=1}^{3} x_{+_j} \cdot |z_{+_j}| \right) + |z_{-_A}| \right) \right]}{(|z_{+_i} \cdot z_{-_A}|)} \right]^3} + Bia \right.$$

$$\left. \cdot \left[\frac{(|z_{+_i}| + |z_{-_A}|)}{2} \right]^2 \cdot \left[\frac{1}{|z_{-_A}|} \right] \right]$$

for i = 1,2,3

3.5 Equation (D-19) can be differentiated to give:

$$\frac{d(norm)}{dc_{+_i}} = \frac{|z_{+_i}|}{x_{+_i}} \qquad (D-25)$$

Then the Nernst-Hartley equation becomes:

$$D_{+_i} = D_{+_i}^0 \cdot \left[1 + norm \cdot \frac{d\gamma_{+_i}}{d(norm)} \right] \qquad (D-26)$$

for i = 1,2,3

E. <u>Integral Form of Correction to Diffusion Coefficients</u>

   <u>for Concentration</u>

   Most salts show the following variation of mean activity

   coefficient $\gamma_\pm$, with $c_\pm$(molarity $\simeq$ molality):
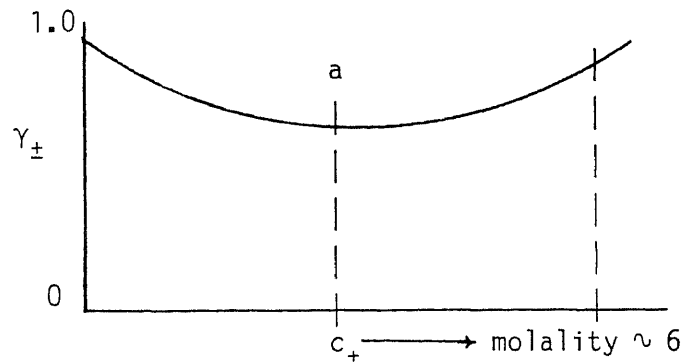
   The differential form of the Nernst-Hartley equation would

   hold up to point a, but not at higher concentrations.

1.0 <u>Single Salt in Aqueous Solution</u>   (D-27)

$$D_\pm = D_\pm^0 \cdot \left[1 + \ell n \gamma_\pm - \left(\frac{2 \cdot B \cdot (|z_+ \cdot z_-|)}{A^2 \cdot c_\pm} \right) \cdot \left\{ \frac{1}{2} \cdot \left(1 + A \cdot c^{\frac{1}{2}} \right)^2 \right. \right.$$

$$\left. - 2 \cdot \left(1 + A \cdot c_\pm^{\frac{1}{2}} \right) + \ell n \left(1 + A \cdot c_\pm^{\frac{1}{2}} \right) + 1.5 \right\}$$

$$\left. - \left(\frac{F}{G^2 \cdot c_\pm} \right) \cdot \left[\frac{1}{(1 + G \cdot c_\pm)} + \ell n \left(1 + G \cdot c_\pm \right) - 1 \right] - \frac{E \cdot c_\pm}{2} \right]$$

where:

$$c_\pm = \text{molality} \simeq \text{molarity of salt}$$

$$A = \left[\frac{1}{2} \cdot (|z_+ \cdot z_-|) \cdot (|z_+| + |z_-|) \right]^{\frac{1}{2}}$$

$$B = -2.303 \cdot 0.511 = -1.1768$$

$$F = 2.303 \cdot \left[\left[\frac{(0.06+0.6 \cdot Bia)}{2} \right] \cdot (|z_+ \cdot z_-|)^2 \cdot (|z_+| + |z_-|) \right]$$

$$= (0.06909 + 0.6909 \cdot Bia) \cdot (|z_+ \cdot z_-|)^2 \cdot (|z_+| + |z_-|)$$

$$G = 0.75 \cdot (|z_+| + |z_-|)$$

$$E = 2.303 \cdot Bia \cdot A^2$$

2.0 Three Cations in Aqueous Solution with a Single Anion

$$(D-28)$$

$$
\begin{aligned}
D_{+_i} = D^0_{+_i} \cdot \Bigg[1 + \ell n \gamma_{+_i} \quad - \left[\frac{2 \cdot B \cdot z^2_{+_i}}{A^2 \cdot norm} \right] \cdot \left[\frac{1}{2} \cdot \left(1 + A \cdot norm^{\frac{1}{2}} \right)^2 \right. \\
\left. - 2 \cdot \left(1 + A \cdot norm^{\frac{1}{2}} \right) + \ell n \left(1 + A \cdot norm^{\frac{1}{2}} \right) + 1.5 \right] \\
- \left[\frac{F}{G^2 \cdot norm} \right] \cdot \left[\frac{1}{(1+G \cdot norm)} + \ell n \left(1+G \cdot norm \right) - 1 \right] \\
- \frac{E \cdot norm}{2} \Bigg]
\end{aligned}
$$

for $i = 1,2,3$

where:

$$norm = c_{-_A} \cdot (|z_{-_A}|)$$

$$A = \left[\frac{1}{2} \cdot \left[\left(\sum_{j=1}^{3} x_{+_j} \cdot |z_{+_j}| \right) + |z_{-_A}| \right] \right]^{\frac{1}{2}}$$

$$B = -1.1768$$

$$F = (0.034 + 0.34 \cdot Bia) \cdot (|z_{+_i} \cdot z_{-_A}|) \cdot (|z_{+_i}| + |z_{-_A}|)^2 \cdot \frac{1}{(|z_{-_A}|)}$$

$$G = 0.75 \cdot \left[\frac{\left[\left[\left(\sum_{i=1}^{3} x_{+_j} \cdot |z_{+_j}| \right) + |z_{-_A}| \right] \right]}{\left(|z_{+_i} \cdot z_{-_A}| \right)} \right]$$

$$E = 0.5758 \cdot Bia \cdot \left(|z_{+_i}| + |z_{-_A}| \right)^2 \cdot \frac{1}{\left(|z_{-_A}| \right)}$$

Equation (D-28) can be used for three anions with a single cation by obvious juxtaposition of the terms.

F. Summary of Results

Calculations were performed to predict the activity coefficients and the diffusion coefficients for 17 salts, and the results were compared to experimental data given by Robinson and Stokes(106). The molalities of the solutions ranged from 0 to 6.0, and the resulting output from the computations is shown in the following pages. However, a summary of results is as follows:

	Root Mean Square of % Relative Difference
Activity Coefficients, Bromley Equation	2.7 %
Diffusion Coefficients, Nernst-Hartley	
- differential form	26.6 %
- integral form	13.2 %

COMPOUND NACL

THIS PROGRAM EVALUATES THE EFFECT OF CONCENTRATION ON THE ACTIVITY AND DIFFUSION COEFFICIENTS
OF SALTS USING THE BROMLEY EQUATION AND THE Nernst-Hartley EQUATION FOR DIFFUSIVITY
$D(c)=D(0)*(1+c*d(ln(GAMA))/dc)$; DILUTE SOLUTIONS

VALENCE OF COMP.A	1
VALENCE OF ANION	1
CATION A CONDUCTANCE-MHOS/EQIV.-298 K,INFINITE DILUTION	50.1000
ANION CONDUCTANCE-MHOS/EQIV.-298 K,INFINITE DILUTION	76.3500
BROMLEY EQ. SALT PARAMETER -CATION A,COMMON ANION	0.057400
Nernst LIMITING DIFFUSIVITY-CM**2/SEC	0.16100E-04
DIFFUSIVITY CALCULATED FROM CONDUCTANCES-CM**2/SEC	0.16159E-04
NUMBER OF DEPENDENT VARIABLES	3
NUMBER OF DATA POINTS	11

CONCENTRATION	ACTIVITY COEFF.	DIFFUSION COEFF.
0.100000	0.778000	0.148300E-04
0.200000	0.735000	0.147500E-04
0.300000	0.710000	0.147500E-04
0.500000	0.681000	0.147400E-04
0.700000	0.667000	0.147500E-04
1.000000	0.657000	0.148400E-04
1.500000	0.656000	0.149500E-04
2.000000	0.668000	0.151600E-04
3.000000	0.714000	0.156500E-04
4.000000	0.783000	0.159400E-04
5.000000	0.875000	0.159000E-04

AQUEOUS SOLUTION OF COMPOUND NACL

COMPARISON OF ACTIVITY COEFFICIENTS-ACTUAL VS. PREDICTED BY BROMLEY EQUATION

CONCENTRATION	ACTUAL	PREDICTED	DIFFERENCE-%
0.100000	0.778000	0.776447	0.199641
0.200000	0.735000	0.732401	0.353670
0.300000	0.710000	0.707714	0.321941
0.500000	0.681000	0.679917	0.159089
0.700000	0.667000	0.665477	0.228334
1.000000	0.657000	0.656161	0.127705
1.500000	0.656000	0.657962	0.299096
2.000000	0.668000	0.671844	0.575377
3.000000	0.714000	0.720452	0.903614
4.000000	0.783000	0.788211	0.665570
5.000000	0.875000	0.871853	0.359644

AVERAGE DIFFERENCE= 0.0028   AVERAGE PERCENT DIFFERENCE= 0.3812
ROOT MEAN SQUARE-DIFFERENCE= 0.0032   ROOT MEAN SQUARE-PERCENT DIFFERENCE= 0.4443

COMPARISON OF DIFFUSION COEFFICIENTS-ACTUAL VS. PREDICTED BY INTEGRAL VERSION OF Nernst-Hartley EQUATION

CONCENTRATION	ACTUAL	PREDICTED	DIFFERENCE-%
0.100000	0.148300E-04	0.150116E-04	1.224846
0.200000	0.147500E-04	0.148765E-04	0.857423
0.300000	0.147500E-04	0.148312E-04	0.550607
0.500000	0.147400E-04	0.148371E-04	0.658847
0.700000	0.147500E-04	0.149070E-04	1.064588
1.000000	0.148400E-04	0.150790E-04	1.610595
1.500000	0.149500E-04	0.154674E-04	3.460655
2.000000	0.151600E-04	0.159244E-04	5.042277
3.000000	0.156500E-04	0.169329E-04	8.197252
4.000000	0.159400E-04	0.179959E-04	12.897660
5.000000	0.159000E-04	0.190805E-04	20.002844

AVERAGE DIFFERENCE= 0.78941E-06   AVERAGE PERCENT DIFFERENCE= 5.0516
ROOTMEAN SQUARE-DIFFERENCE= 0.12427E-05   ROOTMEAN SQUARE-PERCENT DIFFERENCE= 7.8495

COMPARISON OF DIFFUSION COEFFICIENTS-ACTUAL VS. PREDICTED BY DIFFERENTIAL VERSION OF Nernst-Hartley EQUATION

CONCENTRATION	ACTUAL	PREDICTED	DIFFERENCE-%
0.100000	0.148300E-04	0.147793E-04	0.341746
0.200000	0.147500E-04	0.147260E-04	0.162981
0.300000	0.147500E-04	0.147619E-04	0.080500
0.500000	0.147400E-04	0.149472E-04	1.405421
0.700000	0.147500E-04	0.152259E-04	3.226667
1.000000	0.148400E-04	0.157479E-04	6.117671
1.500000	0.149500E-04	0.167570E-04	12.086767
2.000000	0.151600E-04	0.178391E-04	17.671994
3.000000	0.156500E-04	0.200656E-04	28.214406
4.000000	0.159400E-04	0.223038E-04	39.923294
5.000000	0.159000E-04	0.245333E-04	54.297635

AVERAGE DIFFERENCE= 0.23251E-05   AVERAGE PERCENT DIFFERENCE= 14.8663
ROOTMEAN SQUARE-DIFFERENCE= 0.36440E-05   ROOTMEAN SQUARE-PERCENT DIFFERENCE= 23.0543

COMPOUND NABR

THIS PROGRAM EVALUATES THE EFFECT OF CONCENTRATION ON THE ACTIVITY AND DIFFUSION COEFFICIENTS
OF SALTS USING THE BROMLEY EQUATION AND THE Nernst-Hartley EQUATION FOR DIFFUSIVITY
D(c)=D(0)*(1+c*d(ln(GAMA))/dc); DILUTE SOLUTIONS

VALENCE OF COMP.A	1
VALENCE OF ANION	1
CATION A CONDUCTANCE-MHOS/EQIV.-298 K,INFINITE DILUTION	50.1000
ANION CONDUCTANCE-MHOS/EQIV.-298 K,INFINITE DILUTION	78.1400
BROMLEY EQ. SALT PARAMETER -CATION A,COMMON ANION	0.074900
Nernst LIMITING DIFFUSIVITY-CM**2/SEC	0.16250E-04
DIFFUSIVITY CALCULATED FROM CONDUCTANCES-CM**2/SEC	0.16280E-04
NUMBER OF DEPENDENT VARIABLES	3
NUMBER OF DATA POINTS	9

CONCENTRATION	ACTIVITY COEFF.	DIFFUSION COEFF.
0.100000	0.782000	0.151700E-04
0.200000	0.741000	0.150700E-04
0.300000	0.719000	0.151500E-04
0.500000	0.697000	0.154200E-04
0.700000	0.689000	0.156900E-04
1.000000	0.687000	0.159600E-04
1.500000	0.703000	0.162900E-04
2.000000	0.731000	0.166800E-04
2.500000	0.768000	0.170200E-04

AQUEOUS SOLUTION OF COMPOUND NABR

COMPARISON OF ACTIVITY COEFFICIENTS-ACTUAL VS. PREDICTED BY BROMLEY EQUATION

CONCENTRATION	ACTUAL	PREDICTED	DIFFERENCE-%
0.100000	0.782000	0.781008	0.126815
0.200000	0.741000	0.740442	0.075256
0.300000	0.719000	0.718797	0.028261
0.500000	0.697000	0.696498	0.072010
0.700000	0.689000	0.687277	0.250025
1.000000	0.687000	0.685789	0.176300
1.500000	0.703000	0.701362	0.233059
2.000000	0.731000	0.730433	0.077509
2.500000	0.768000	0.768869	0.113146

AVERAGE DIFFERENCE= 0.0009   AVERAGE PERCENT DIFFERENCE= 0.1280
ROOT MEAN SQUARE-DIFFERENCE= 0.0010 ROOT MEAN SQUARE-PERCENT DIFFERENCE= 0.1470

COMPARISON OF DIFFUSION COEFFICIENTS-ACTUAL VS. PREDICTED BY INTEGRAL VERSION OF Nernst-Hartley EQUATION

CONCENTRATION	ACTUAL	PREDICTED	DIFFERENCE-%
0.100000	0.151700E-04	0.151977E-04	0.182312
0.200000	0.150700E-04	0.150994E-04	0.195378
0.300000	0.151500E-04	0.150880E-04	0.409135
0.500000	0.154200E-04	0.151574E-04	1.703054
0.700000	0.156900E-04	0.152892E-04	2.554594
1.000000	0.159600E-04	0.155545E-04	2.540965
1.500000	0.162900E-04	0.161017E-04	1.156220
2.000000	0.166800E-04	0.167210E-04	0.245804
2.500000	0.170200E-04	0.173793E-04	2.110761

AVERAGE DIFFERENCE= 0.19741E-06   AVERAGE PERCENT DIFFERENCE= 1.2331
ROOTMEAN SQUARE-DIFFERENCE= 0.25073E-06   ROOTMEAN SQUARE-PERCENT DIFFERENCE= 1.5626

COMPARISON OF DIFFUSION COEFFICIENTS-ACTUAL VS. PREDICTED BY DIFFERENTIAL VERSION OF Nernst-Hartley EQUATION

CONCENTRATION	ACTUAL	PREDICTED	DIFFERENCE-%
0.100000	0.151700E-04	0.150045E-04	1.091182
0.200000	0.150700E-04	0.150192E-04	0.337214
0.300000	0.151500E-04	0.151171E-04	0.216839
0.500000	0.154200E-04	0.154230E-04	0.019722
0.700000	0.156900E-04	0.158246E-04	0.858091
1.000000	0.159600E-04	0.165369E-04	3.614805
1.500000	0.162900E-04	0.178740E-04	9.723775
2.000000	0.166800E-04	0.192905E-04	15.650772
2.500000	0.170200E-04	0.207364E-04	21.835480

AVERAGE DIFFERENCE= 0.98608E-06   AVERAGE PERCENT DIFFERENCE= 5.9275
ROOTMEAN SQUARE-DIFFERENCE= 0.16165E-05   ROOTMEAN SQUARE-PERCENT DIFFERENCE= 9.6116

COMPOUND NAI

THIS PROGRAM EVALUATES THE EFFECT OF CONCENTRATION ON THE ACTIVITY AND DIFFUSION COEFFICIENTS
OF SALTS USING THE BROMLEY EQUATION AND THE Nernst-Hartley EQUATION FOR DIFFUSIVITY
$D(c)=D(0)*(1+c*d(\ln(GAMA))/dc)$; DILUTE SOLUTIONS

VALENCE OF COMP.A	1
VALENCE OF ANION	1
CATION A CONDUCTANCE-MHOS/EQIV.-298 K,INFINITE DILUTION	50.1000
ANION CONDUCTANCE-MHOS/EQIV.-298 K,INFINITE DILUTION	76.8000
BROMLEY EQ. SALT PARAMETER -CATION A,COMMON ANION	0.099400
Nernst LIMITING DIFFUSIVITY-CM**2/SEC	0.16140E-04
DIFFUSIVITY CALCULATED FROM CONDUCTANCES-CM**2/SEC	0.16255E-04
NUMBER OF DEPENDENT VARIABLES	3
NUMBER OF DATA POINTS	10

CONCENTRATION	ACTIVITY COEFF.	DIFFUSION COEFF.
0.100000	0.787000	0.152000E-04
0.200000	0.751000	0.153200E-04
0.300000	0.735000	0.154700E-04
0.500000	0.723000	0.158000E-04
0.700000	0.724000	0.161200E-04
1.000000	0.736000	0.166200E-04
1.500000	0.771000	0.175100E-04
2.000000	0.820000	0.184600E-04
2.500000	0.883000	0.192500E-04
3.000000	0.963000	0.199200E-04

AQUEOUS SOLUTION OF COMPOUND NAI

COMPARISON OF ACTIVITY COEFFICIENTS-ACTUAL VS. PREDICTED BY BROMLEY EQUATION

CONCENTRATION	ACTUAL	PREDICTED	DIFFERENCE-%
0.100000	0.787000	0.787439	0.055842
0.200000	0.751000	0.751849	0.113111
0.300000	0.735000	0.734605	0.053797
0.500000	0.723000	0.720394	0.360478
0.700000	0.724000	0.719003	0.690226
1.000000	0.736000	0.729529	0.879249
1.500000	0.771000	0.766972	0.522428
2.000000	0.820000	0.821142	0.139237
2.500000	0.883000	0.888651	0.639955
3.000000	0.963000	0.968510	0.572169

AVERAGE DIFFERENCE= 0.0032   AVERAGE PERCENT DIFFERENCE= 0.4026
ROOT MEAN SQUARE-DIFFERENCE= 0.0039   ROOT MEAN SQUARE-PERCENT DIFFERENCE= 0.4927

COMPARISON OF DIFFUSION COEFFICIENTS-ACTUAL VS. PREDICTED BY INTEGRAL VERSION OF Nernst-Hartley EQUATION

CONCENTRATION	ACTUAL	PREDICTED	DIFFERENCE-%
0.100000	0.152000E-04	0.151590E-04	0.270029
0.200000	0.153200E-04	0.151146E-04	1.341028
0.300000	0.154700E-04	0.151508E-04	2.063161
0.500000	0.158000E-04	0.153079E-04	3.114446
0.700000	0.161200E-04	0.155240E-04	3.697497
1.000000	0.166200E-04	0.159149E-04	4.242222
1.500000	0.175100E-04	0.166743E-04	4.772931
2.000000	0.184600E-04	0.175092E-04	5.150670
2.500000	0.192500E-04	0.183854E-04	4.491396
3.000000	0.199200E-04	0.192857E-04	3.184327

AVERAGE DIFFERENCE= 0.56443E-06   AVERAGE PERCENT DIFFERENCE= 3.2328
ROOTMEAN SQUARE-DIFFERENCE= 0.63188E-06   ROOTMEAN SQUARE-PERCENT DIFFERENCE= 3.5654

COMPARISON OF DIFFUSION COEFFICIENTS-ACTUAL VS. PREDICTED BY DIFFERENTIAL VERSION OF Nernst-Hartley EQUATION

CONCENTRATION	ACTUAL	PREDICTED	DIFFERENCE-%
0.100000	0.152000E-04	0.150245E-04	1.154576
0.200000	0.153200E-04	0.151345E-04	1.211049
0.300000	0.154700E-04	0.153176E-04	0.985178
0.500000	0.158000E-04	0.157867E-04	0.084046
0.700000	0.161200E-04	0.163528E-04	1.443963
1.000000	0.166200E-04	0.173182E-04	4.200788
1.500000	0.175100E-04	0.190892E-04	9.018721
2.000000	0.184600E-04	0.209472E-04	13.473277
2.500000	0.192500E-04	0.228377E-04	18.637225
3.000000	0.199200E-04	0.247398E-04	24.195605

AVERAGE DIFFERENCE= 0.13931E-05   AVERAGE PERCENT DIFFERENCE= 7.4404
ROOTMEAN SQUARE-DIFFERENCE= 0.21310E-05   ROOTMEAN SQUARE-PERCENT DIFFERENCE= 11.0415

THIS PROGRAM EVALUATES THE EFFECT OF CONCENTRATION ON THE ACTIVITY AND DIFFUSION COEFFICIENTS
OF SALTS USING THE BROMLEY EQUATION AND THE Nernst-Hartley EQUATION FOR DIFFUSIVITY
$D(c)=D(0)*(1+c*d(\ln(GAMA))/dc)$; DILUTE SOLUTIONS

VALENCE OF COMP.A	1
VALENCE OF ANION	1
CATION A CONDUCTANCE-MHOS/EQIV.-298 K,INFINITE DILUTION	73.5000
ANION CONDUCTANCE-MHOS/EQIV.-298 K,INFINITE DILUTION	76.3500
BROMLEY EQ. SALT PARAMETER -CATION A,COMMON ANION	0.024000
Nernst LIMITING DIFFUSIVITY-CM**2/SEC	0.19930E-04
DIFFUSIVITY CALCULATED FROM CONDUCTANCES-CM**2/SEC	0.20047E-04
NUMBER OF DEPENDENT VARIABLES	3
NUMBER OF DATA POINTS	12

CONCENTRATION	ACTIVITY COEFF.	DIFFUSION COEFF.
0.100000	0.770000	0.184400E-04
0.200000	0.718000	0.183800E-04
0.300000	0.688000	0.183800E-04
0.500000	0.649000	0.185000E-04
0.700000	0.626000	0.186600E-04
1.000000	0.604000	0.189200E-04
1.500000	0.583000	0.194300E-04
2.000000	0.573000	0.199900E-04
2.500000	0.569000	0.205700E-04
3.000000	0.569000	0.211200E-04
3.500000	0.572000	0.216000E-04
4.000000	0.577000	0.219600E-04

AQUEOUS SOLUTION OF COMPOUND KCL

COMPARISON OF ACTIVITY COEFFICIENTS-ACTUAL VS. PREDICTED BY BROMLEY EQUATION

CONCENTRATION	ACTUAL	PREDICTED	DIFFERENCE-%
0.100000	0.770000	0.767815	0.283813
0.200000	0.718000	0.717294	0.098363
0.300000	0.688000	0.687034	0.140353
0.500000	0.649000	0.649357	0.055073
0.700000	0.626000	0.625770	0.036671
1.000000	0.604000	0.603120	0.145633
1.500000	0.583000	0.582445	0.095193
2.000000	0.573000	0.572747	0.044083
2.500000	0.569000	0.569139	0.024440
3.000000	0.569000	0.569400	0.070306
3.500000	0.572000	0.572353	0.061635
4.000000	0.577000	0.577307	0.053201

AVERAGE DIFFERENCE= 0.0006   AVERAGE PERCENT DIFFERENCE= 0.0924
ROOT MEAN SQUARE-DIFFERENCE= 0.0008   ROOT MEAN SQUARE-PERCENT DIFFERENCE= 0.1150

COMPARISON OF DIFFUSION COEFFICIENTS-ACTUAL VS. PREDICTED BY INTEGRAL VERSION OF Nernst-Hartley EQUATION

CONCENTRATION	ACTUAL	PREDICTED	DIFFERENCE-%
0.100000	0.184400E-04	0.184747E-04	0.188210
0.200000	0.183800E-04	0.182179E-04	0.881899
0.300000	0.183800E-04	0.180817E-04	1.622876
0.500000	0.185000E-04	0.179406E-04	3.023954
0.700000	0.186600E-04	0.178838E-04	4.159787
1.000000	0.189200E-04	0.178821E-04	5.485964
1.500000	0.194300E-04	0.179995E-04	7.362488
2.000000	0.199900E-04	0.181953E-04	8.978112
2.500000	0.205700E-04	0.184320E-04	10.393838
3.000000	0.211200E-04	0.186919E-04	11.496660
3.500000	0.216000E-04	0.189657E-04	12.195736
4.000000	0.219600E-04	0.192482E-04	12.348989

AVERAGE DIFFERENCE= 0.13338E-05   AVERAGE PERCENT DIFFERENCE= 6.5115
ROOTMEAN SQUARE-DIFFERENCE= 0.16365E-05   ROOTMEAN SQUARE-PERCENT DIFFERENCE= 7.8328

COMPARISON OF DIFFUSION COEFFICIENTS-ACTUAL VS. PREDICTED BY DIFFERENTIAL VERSION OF Nernst-Hartley EQUATION

CONCENTRATION	ACTUAL	PREDICTED	DIFFERENCE-%
0.100000	0.184400E-04	0.180904E-04	1.895686
0.200000	0.183800E-04	0.178639E-04	2.808078
0.300000	0.183800E-04	0.177639E-04	3.352227
0.500000	0.185000E-04	0.177149E-04	4.243521
0.700000	0.186600E-04	0.177786E-04	4.723331
1.000000	0.189200E-04	0.179905E-04	4.912751
1.500000	0.194300E-04	0.184940E-04	4.817457
2.000000	0.199900E-04	0.190742E-04	4.581147
2.500000	0.205700E-04	0.196817E-04	4.318446
3.000000	0.211200E-04	0.202979E-04	3.892499
3.500000	0.216000E-04	0.209154E-04	3.169384
4.000000	0.219600E-04	0.215311E-04	1.952948

AVERAGE DIFFERENCE= 0.72945E-06   AVERAGE PERCENT DIFFERENCE= 3.7223
ROOTMEAN SQUARE-DIFFERENCE= 0.75595E-06   ROOTMEAN SQUARE-PERCENT DIFFERENCE= 3.8625

THIS PROGRAM EVALUATES THE EFFECT OF CONCENTRATION ON THE ACTIVITY AND DIFFUSION COEFFICIENTS
OF SALTS USING THE BROMLEY EQUATION AND THE Nernst-Hartley EQUATION FOR DIFFUSIVITY
$D(c)=D(0)*(1+c*d(\ln(GAMA))/dc)$; DILUTE SOLUTIONS

VALENCE OF COMP.A	1
VALENCE OF ANION	1
CATION A CONDUCTANCE-MHOS/EQIV.-298 K,INFINITE DILUTION	73.5000
ANION CONDUCTANCE-MHOS/EQIV.-298 K,INFINITE DILUTION	78.1400
BROMLEY EQ. SALT PARAMETER -CATION A,COMMON ANION	0.029600
Nernst LIMITING DIFFUSIVITY-CM**2/SEC	0.20160E-04
DIFFUSIVITY CALCULATED FROM CONDUCTANCES-CM**2/SEC	0.20246E-04
NUMBER OF DEPENDENT VARIABLES	3
NUMBER OF DATA POINTS	12

CONCENTRATION	ACTIVITY COEFF.	DIFFUSION COEFF.
0.100000	0.772000	0.187400E-04
0.200000	0.722000	0.187000E-04
0.300000	0.693000	0.187200E-04
0.500000	0.657000	0.188500E-04
0.700000	0.636000	0.191700E-04
1.000000	0.617000	0.197500E-04
1.500000	0.600000	0.206200E-04
2.000000	0.593000	0.213200E-04
2.500000	0.593000	0.219900E-04
3.000000	0.595000	0.228000E-04
3.500000	0.600000	0.235400E-04
4.000000	0.608000	0.243000E-04

AQUEOUS SOLUTION OF COMPOUND KBR

COMPARISON OF ACTIVITY COEFFICIENTS-ACTUAL VS. PREDICTED BY BROMLEY EQUATION

CONCENTRATION	ACTUAL	PREDICTED	DIFFERENCE-%
0.100000	0.772000	0.769255	0.355541
0.200000	0.722000	0.719805	0.304057
0.300000	0.693000	0.690459	0.366666
0.500000	0.657000	0.654384	0.398241
0.700000	0.636000	0.632259	0.588278
1.000000	0.617000	0.611704	0.858283
1.500000	0.600000	0.594473	0.921175
2.000000	0.593000	0.588279	0.796171
2.500000	0.593000	0.588289	0.794443
3.000000	0.595000	0.592312	0.451722
3.500000	0.600000	0.599190	0.134971
4.000000	0.608000	0.608249	0.040881

AVERAGE DIFFERENCE= 0.0032   AVERAGE PERCENT DIFFERENCE= 0.5009
ROOT MEAN SQUARE-DIFFERENCE= 0.0035   ROOT MEAN SQUARE-PERCENT DIFFERENCE= 0.5724

COMPARISON OF DIFFUSION COEFFICIENTS-ACTUAL VS. PREDICTED BY INTEGRAL VERSION OF Nernst-Hartley EQUATION

CONCENTRATION	ACTUAL	PREDICTED	DIFFERENCE-%
0.100000	0.187400E-04	0.187062E-04	0.180184
0.200000	0.187000E-04	0.184616E-04	1.274628
0.300000	0.187200E-04	0.183375E-04	2.043386
0.500000	0.188500E-04	0.182199E-04	3.342815
0.700000	0.191700E-04	0.181867E-04	5.129119
1.000000	0.197500E-04	0.182214E-04	7.739744
1.500000	0.206200E-04	0.184018E-04	10.757572
2.000000	0.213200E-04	0.186626E-04	12.464352
2.500000	0.219900E-04	0.189655E-04	13.753768
3.000000	0.228000E-04	0.192925E-04	15.383970
3.500000	0.235400E-04	0.196337E-04	16.594136
4.000000	0.243000E-04	0.199840E-04	17.761459

AVERAGE DIFFERENCE= 0.19522E-05   AVERAGE PERCENT DIFFERENCE= 8.8688
ROOTMEAN SQUARE-DIFFERENCE= 0.24363E-05   ROOTMEAN SQUARE-PERCENT DIFFERENCE= 10.7663

COMPARISON OF DIFFUSION COEFFICIENTS-ACTUAL VS. PREDICTED BY DIFFERENTIAL VERSION OF Nernst-Hartley EQUATION

CONCENTRATION	ACTUAL	PREDICTED	DIFFERENCE-%
0.100000	0.187400E-04	0.183339E-04	2.166890
0.200000	0.187000E-04	0.181320E-04	3.037583
0.300000	0.187200E-04	0.180553E-04	3.550718
0.500000	0.188500E-04	0.180530E-04	4.227988
0.700000	0.191700E-04	0.181652E-04	5.241708
1.000000	0.197500E-04	0.184531E-04	6.566418
1.500000	0.206200E-04	0.190889E-04	7.425440
2.000000	0.213200E-04	0.198046E-04	7.107872
2.500000	0.219900E-04	0.205488E-04	6.553790
3.000000	0.228000E-04	0.213023E-04	6.568846
3.500000	0.235400E-04	0.220573E-04	6.298731
4.000000	0.243000E-04	0.228105E-04	6.129580

AVERAGE DIFFERENCE= 0.11413E-05   AVERAGE PERCENT DIFFERENCE= 5.4063
ROOTMEAN SQUARE-DIFFERENCE= 0.12122E-05   ROOTMEAN SQUARE-PERCENT DIFFERENCE= 5.6569

COMPOUND KI

THIS PROGRAM EVALUATES THE EFFECT OF CONCENTRATION ON THE ACTIVITY AND DIFFUSION COEFFICIENTS
OF SALTS USING THE BROMLEY EQUATION AND THE Nernst-Hartley EQUATION FOR DIFFUSIVITY
D(c)=D(0)*(1+c*d(ln(GAMA))/dc); DILUTE SOLUTIONS

VALENCE OF COMP.A	1
VALENCE OF ANION	1
CATION A CONDUCTANCE-MHOS/EQIV.-298 K,INFINITE DILUTION	73.5000
ANION CONDUCTANCE-MHOS/EQIV.-298 K,INFINITE DILUTION	76.8000
BROMLEY EQ. SALT PARAMETER -CATION A,COMMON ANION	0.042800
Nernst LIMITING DIFFUSIVITY-CM**2/SEC	0.19990E-04
DIFFUSIVITY CALCULATED FROM CONDUCTANCES-CM**2/SEC	0.20031E-04
NUMBER OF DEPENDENT VARIABLES	3
NUMBER OF DATA POINTS	11

CONCENTRATION	ACTIVITY COEFF.	DIFFUSION COEFF.
0.100000	0.778000	0.186500E-04
0.200000	0.733000	0.185900E-04
0.300000	0.707000	0.188400E-04
0.500000	0.676000	0.195500E-04
0.700000	0.660000	0.200100E-04
1.000000	0.645000	0.206500E-04
1.500000	0.636500	0.216600E-04
2.000000	0.637000	0.225400E-04
2.500000	0.644000	0.234700E-04
3.000000	0.652000	0.244000E-04
3.500000	0.662000	0.253300E-04

AQUEOUS SOLUTION OF COMPOUND KI

COMPARISON OF ACTIVITY COEFFICIENTS-ACTUAL VS. PREDICTED BY BROMLEY EQUATION

CONCENTRATION	ACTUAL	PREDICTED	DIFFERENCE-%
0.100000	0.778000	0.772662	0.686172
0.200000	0.733000	0.725758	0.987965
0.300000	0.707000	0.698599	1.188256
0.500000	0.676000	0.666385	1.422285
0.700000	0.660000	0.647819	1.845551
1.000000	0.645000	0.632425	1.949664
1.500000	0.636500	0.623816	1.992700
2.000000	0.637000	0.626575	1.636562
2.500000	0.644000	0.636016	1.239702
3.000000	0.652000	0.650034	0.301511
3.500000	0.662000	0.667535	0.836166

AVERAGE DIFFERENCE= 0.0085   AVERAGE PERCENT DIFFERENCE= 1.2806
ROOT MEAN SQUARE-DIFFERENCE= 0.0091   ROOT MEAN SQUARE-PERCENT DIFFERENCE= 1.3838

COMPARISON OF DIFFUSION COEFFICIENTS-ACTUAL VS. PREDICTED BY INTEGRAL VERSION OF Nernst-Hartley EQUATION

CONCENTRATION	ACTUAL	PREDICTED	DIFFERENCE-%
0.100000	0.186500E-04	0.185913E-04	0.314659
0.200000	0.185900E-04	0.183843E-04	1.106753
0.300000	0.188400E-04	0.182929E-04	2.903848
0.500000	0.195500E-04	0.182352E-04	6.725559
0.700000	0.200100E-04	0.182591E-04	8.750042
1.000000	0.206500E-04	0.183786E-04	10.999734
1.500000	0.216600E-04	0.187014E-04	13.659072
2.000000	0.225400E-04	0.191067E-04	15.231993
2.500000	0.234700E-04	0.195555E-04	16.678642
3.000000	0.244000E-04	0.200292E-04	17.912959
3.500000	0.253300E-04	0.205180E-04	18.997411

AVERAGE DIFFERENCE= 0.23307E-05   AVERAGE PERCENT DIFFERENCE= 10.2982
ROOTMEAN SQUARE-DIFFERENCE= 0.28352E-05   ROOTMEAN SQUARE-PERCENT DIFFERENCE= 12.1770

COMPARISON OF DIFFUSION COEFFICIENTS-ACTUAL VS. PREDICTED BY DIFFERENTIAL VERSION OF Nernst-Hartley EQUATION

CONCENTRATION	ACTUAL	PREDICTED	DIFFERENCE-%
0.100000	0.186500E-04	0.182605E-04	2.088633
0.200000	0.185900E-04	0.181238E-04	2.507556
0.300000	0.188400E-04	0.181051E-04	3.900776
0.500000	0.195500E-04	0.182131E-04	6.838161
0.700000	0.200100E-04	0.184359E-04	7.866634
1.000000	0.206500E-04	0.188935E-04	8.505830
1.500000	0.216600E-04	0.198195E-04	8.497122
2.000000	0.225400E-04	0.208302E-04	7.585686
2.500000	0.234700E-04	0.218714E-04	6.811363
3.000000	0.244000E-04	0.229227E-04	6.054411
3.500000	0.253300E-04	0.239760E-04	5.345548

AVERAGE DIFFERENCE= 0.12944E-05   AVERAGE PERCENT DIFFERENCE= 6.0002
ROOTMEAN SQUARE-DIFFERENCE= 0.13863E-05   ROOTMEAN SQUARE-PERCENT DIFFERENCE= 6.3834

COMPOUND LICL

THIS PROGRAM EVALUATES THE EFFECT OF CONCENTRATION ON THE ACTIVITY AND DIFFUSION COEFFICIENTS
OF SALTS USING THE BROMLEY EQUATION AND THE Nernst-Hartley EQUATION FOR DIFFUSIVITY
D(c)=D(0)*(1+c*d(ln(GAMA))/dc); DILUTE SOLUTIONS

VALENCE OF COMP.A	1
VALENCE OF ANION	1
CATION A CONDUCTANCE-MHOS/EQIV.-298 K,INFINITE DILUTION	38.6800
ANION CONDUCTANCE-MHOS/EQIV.-298 K,INFINITE DILUTION	76.3500
BROMLEY EQ. SALT PARAMETER -CATION A,COMMON ANION	0.128300
Nernst LIMITING DIFFUSIVITY-CM**2/SEC	0.13660E-04
DIFFUSIVITY CALCULATED FROM CONDUCTANCES-CM**2/SEC	0.13669E-04
NUMBER OF DEPENDENT VARIABLES	3
NUMBER OF DATA POINTS	11

CONCENTRATION	ACTIVITY COEFF.	DIFFUSION COEFF.
0.100000	0.790000	0.126900E-04
0.200000	0.757000	0.126700E-04
0.300000	0.744000	0.126900E-04
0.500000	0.739000	0.127800E-04
0.700000	0.748000	0.128800E-04
1.000000	0.774000	0.130200E-04
1.500000	0.838000	0.133100E-04
2.000000	0.921000	0.136300E-04
2.500000	1.026000	0.139700E-04
3.000000	1.156000	0.143000E-04
3.500000	1.317000	0.146400E-04

AQUEOUS SOLUTION OF COMPOUND LICL

COMPARISON OF ACTIVITY COEFFICIENTS-ACTUAL VS. PREDICTED BY BROMLEY EQUATION

CONCENTRATION	ACTUAL	PREDICTED	DIFFERENCE-%
0.100000	0.790000	0.795094	0.644778
0.200000	0.757000	0.765531	1.126991
0.300000	0.744000	0.753699	1.303605
0.500000	0.739000	0.749637	1.439363
0.700000	0.748000	0.758314	1.378822
1.000000	0.774000	0.784724	1.385498
1.500000	0.838000	0.852299	1.706339
2.000000	0.921000	0.942726	2.358992
2.500000	1.026000	1.054150	2.743678
3.000000	1.156000	1.187200	2.698935
3.500000	1.317000	1.343757	2.031675

AVERAGE DIFFERENCE= 0.0161   AVERAGE PERCENT DIFFERENCE= 1.7108
ROOT MEAN SQUARE-DIFFERENCE= 0.0183   ROOT MEAN SQUARE-PERCENT DIFFERENCE= 1.8264

COMPARISON OF DIFFUSION COEFFICIENTS-ACTUAL VS. PREDICTED BY INTEGRAL VERSION OF Nernst-Hartley EQUATION

CONCENTRATION	ACTUAL	PREDICTED	DIFFERENCE-%
0.100000	0.126900E-04	0.128938E-04	1.605731
0.200000	0.126700E-04	0.129092E-04	1.888302
0.300000	0.126900E-04	0.129875E-04	2.344319
0.500000	0.127800E-04	0.132085E-04	3.352770
0.700000	0.128800E-04	0.134763E-04	4.629931
1.000000	0.130200E-04	0.139345E-04	7.023993
1.500000	0.133100E-04	0.147926E-04	11.139300
2.000000	0.136300E-04	0.157187E-04	15.324156
2.500000	0.139700E-04	0.166823E-04	19.415331
3.000000	0.143000E-04	0.176680E-04	23.552642
3.500000	0.146400E-04	0.186673E-04	27.508812

AVERAGE DIFFERENCE= 0.14872E-05   AVERAGE PERCENT DIFFERENCE= 10.7078
ROOTMEAN SQUARE-DIFFERENCE= 0.19781E-05   ROOTMEAN SQUARE-PERCENT DIFFERENCE= 13.9512

COMPARISON OF DIFFUSION COEFFICIENTS-ACTUAL VS. PREDICTED BY DIFFERENTIAL VERSION OF Nernst-Hartley EQUATION

CONCENTRATION	ACTUAL	PREDICTED	DIFFERENCE-%
0.100000	0.126900E-04	0.128373E-04	1.160838
0.200000	0.126700E-04	0.130256E-04	2.806368
0.300000	0.126900E-04	0.132662E-04	4.540848
0.500000	0.127800E-04	0.138283E-04	8.202733
0.700000	0.128800E-04	0.144743E-04	12.377896
1.000000	0.130200E-04	0.155488E-04	19.422788
1.500000	0.133100E-04	0.174900E-04	31.404751
2.000000	0.136300E-04	0.195128E-04	43.160341
2.500000	0.139700E-04	0.215665E-04	54.376883
3.000000	0.143000E-04	0.236314E-04	65.254757
3.500000	0.146400E-04	0.256996E-04	75.543392

AVERAGE DIFFERENCE= 0.40273E-05   AVERAGE PERCENT DIFFERENCE= 28.9320
ROOTMEAN SQUARE-DIFFERENCE= 0.54747E-05   ROOTMEAN SQUARE-PERCENT DIFFERENCE= 38.6105

COMPOUND LIBR

THIS PROGRAM EVALUATES THE EFFECT OF CONCENTRATION ON THE ACTIVITY AND DIFFUSION COEFFICIENTS
OF SALTS USING THE BROMLEY EQUATION AND THE Nernst-Hartley EQUATION FOR DIFFUSIVITY
D(c)=D(0)*(1+c*d(ln(GAMA))/dc); DILUTE SOLUTIONS

VALENCE OF COMP.A	1
VALENCE OF ANION	1
CATION A CONDUCTANCE-MHOS/EQIV.-298 K,INFINITE DILUTION	38.6800
ANION CONDUCTANCE-MHOS/EQIV.-298 K,INFINITE DILUTION	78.1400
BROMLEY EQ. SALT PARAMETER -CATION A,COMMON ANION	0.152700
Nernst LIMITING DIFFUSIVITY-CM**2/SEC	0.13770E-04
DIFFUSIVITY CALCULATED FROM CONDUCTANCES-CM**2/SEC	0.13869E-04
NUMBER OF DEPENDENT VARIABLES	3
NUMBER OF DATA POINTS	11

CONCENTRATION	ACTIVITY COEFF.	DIFFUSION COEFF.
0.100000	0.796000	0.127900E-04
0.200000	0.766000	0.128500E-04
0.300000	0.756000	0.129600E-04
0.500000	0.753000	0.132800E-04
0.700000	0.767000	0.136000E-04
1.000000	0.803000	0.140400E-04
1.500000	0.895000	0.147300E-04
2.000000	1.015000	0.154200E-04
2.500000	1.161000	0.159700E-04
3.000000	1.341000	0.165000E-04
3.500000	1.584000	0.169300E-04

AQUEOUS SOLUTION OF COMPOUND LIBR

COMPARISON OF ACTIVITY COEFFICIENTS-ACTUAL VS. PREDICTED BY BROMLEY EQUATION

CONCENTRATION	ACTUAL	PREDICTED	DIFFERENCE-%
0.100000	0.796000	0.801614	0.705285
0.200000	0.766000	0.777276	1.472122
0.300000	0.756000	0.770206	1.879072
0.500000	0.753000	0.775249	2.954700
0.700000	0.767000	0.793172	3.412259
1.000000	0.803000	0.834563	3.930653
1.500000	0.895000	0.931689	4.099360
2.000000	1.015000	1.059292	4.363729
2.500000	1.161000	1.217656	4.879935
3.000000	1.341000	1.409859	5.134898
3.500000	1.584000	1.640713	3.580347

AVERAGE DIFFERENCE= 0.0340   AVERAGE PERCENT DIFFERENCE= 3.3102
ROOT MEAN SQUARE-DIFFERENCE= 0.0393   ROOT MEAN SQUARE-PERCENT DIFFERENCE= 3.5785

COMPARISON OF DIFFUSION COEFFICIENTS-ACTUAL VS. PREDICTED BY INTEGRAL VERSION OF Nernst-Hartley EQUATION

CONCENTRATION	ACTUAL	PREDICTED	DIFFERENCE-%
0.100000	0.127900E-04	0.130521E-04	2.049455
0.200000	0.128500E-04	0.131129E-04	2.045827
0.300000	0.129600E-04	0.132322E-04	2.100544
0.500000	0.132800E-04	0.135299E-04	1.881995
0.700000	0.136000E-04	0.138723E-04	2.002067
1.000000	0.140400E-04	0.144425E-04	2.866745
1.500000	0.147300E-04	0.154909E-04	5.165684
2.000000	0.154200E-04	0.166111E-04	7.724631
2.500000	0.159700E-04	0.177715E-04	11.280690
3.000000	0.165000E-04	0.189556E-04	14.882497
3.500000	0.169300E-04	0.201543E-04	19.044972

AVERAGE DIFFERENCE= 0.10141E-05   AVERAGE PERCENT DIFFERENCE= 6.4586
ROOTMEAN SQUARE-DIFFERENCE= 0.14200E-05 ROOTMEAN SQUARE-PERCENT DIFFERENCE= 8.6675

COMPARISON OF DIFFUSION COEFFICIENTS-ACTUAL VS. PREDICTED BY DIFFERENTIAL VERSION OF Nernst-Hartley EQUATION

CONCENTRATION	ACTUAL	PREDICTED	DIFFERENCE-%
0.100000	0.127900E-04	0.130440E-04	1.986012
0.200000	0.128500E-04	0.133148E-04	3.617110
0.300000	0.129600E-04	0.136303E-04	5.172256
0.500000	0.132800E-04	0.143374E-04	7.962223
0.700000	0.136000E-04	0.151306E-04	11.254340
1.000000	0.140400E-04	0.164330E-04	17.044025
1.500000	0.147300E-04	0.187661E-04	27.400721
2.000000	0.154200E-04	0.211884E-04	37.408749
2.500000	0.159700E-04	0.236448E-04	48.057529
3.000000	0.165000E-04	0.261138E-04	58.265261
3.500000	0.169300E-04	0.285864E-04	68.850844

AVERAGE DIFFERENCE= 0.41018E-05   AVERAGE PERCENT DIFFERENCE= 26.0926
ROOTMEAN SQUARE-DIFFERENCE= 0.56140E-05 ROOTMEAN SQUARE-PERCENT DIFFERENCE= 34.5350

COMPOUND LINO3

THIS PROGRAM EVALUATES THE EFFECT OF CONCENTRATION ON THE ACTIVITY AND DIFFUSION COEFFICIENTS
OF SALTS USING THE BROMLEY EQUATION AND THE Nernst-Hartley EQUATION FOR DIFFUSIVITY
$D(c)=D(0)*(1+c*d(ln(GAMA))/dc)$; DILUTE SOLUTIONS

VALENCE OF COMP.A	1
VALENCE OF ANION	1
CATION A CONDUCTANCE-MHOS/EQIV.-298 K,INFINITE DILUTION	38.6800
ANION CONDUCTANCE-MHOS/EQIV.-298 K,INFINITE DILUTION	71.4600
BROMLEY EQ. SALT PARAMETER -CATION A,COMMON ANION	0.093800
Nernst LIMITING DIFFUSIVITY-CM**2/SEC	0.13360E-04
DIFFUSIVITY CALCULATED FROM CONDUCTANCES-CM**2/SEC	0.13375E-04
NUMBER OF DEPENDENT VARIABLES	3
NUMBER OF DATA POINTS	13

CONCENTRATION	ACTIVITY COEFF.	DIFFUSION COEFF.
0.100000	0.788000	0.124000E-04
0.200000	0.752000	0.124300E-04
0.300000	0.736000	0.124800E-04
0.500000	0.726000	0.126000E-04
0.700000	0.729000	0.127400E-04
1.000000	0.743000	0.129300E-04
1.500000	0.783000	0.131700E-04
2.000000	0.835000	0.133200E-04
2.500000	0.896000	0.133600E-04
3.000000	0.966000	0.133200E-04
4.000000	1.125000	0.129200E-04
5.000000	1.310000	0.123800E-04
6.000000	1.506000	0.115700E-04

AQUEOUS SOLUTION OF COMPOUND LINO3
COMPARISON OF ACTIVITY COEFFICIENTS-ACTUAL VS. PREDICTED BY BROMLEY EQUATION

CONCENTRATION	ACTUAL	PREDICTED	DIFFERENCE-%
0.100000	0.788000	0.785965	0.258269
0.200000	0.752000	0.749227	0.368786
0.300000	0.736000	0.730961	0.684646
0.500000	0.726000	0.714861	1.534353
0.700000	0.729000	0.711625	2.383470
1.000000	0.743000	0.719291	3.190944
1.500000	0.783000	0.751454	4.028865
2.000000	0.835000	0.799463	4.255981
2.500000	0.896000	0.859724	4.048708
3.000000	0.966000	0.931045	3.618483
4.000000	1.125000	1.106689	1.627648
5.000000	1.310000	1.330316	1.550823
6.000000	1.506000	1.610329	6.927566

AVERAGE DIFFERENCE= 0.0264   AVERAGE PERCENT DIFFERENCE= 2.6522
ROOT MEAN SQUARE-DIFFERENCE= 0.0366   ROOT MEAN SQUARE-PERCENT DIFFERENCE= 3.2316

COMPARISON OF DIFFUSION COEFFICIENTS-ACTUAL VS. PREDICTED BY INTEGRAL VERSION OF Nernst-Hartley EQUATION

CONCENTRATION	ACTUAL	PREDICTED	DIFFERENCE-%
0.100000	0.124000E-04	0.125358E-04	1.095092
0.200000	0.124300E-04	0.124890E-04	0.474518
0.300000	0.124800E-04	0.125100E-04	0.240371
0.500000	0.126000E-04	0.126233E-04	0.185276
0.700000	0.127400E-04	0.127861E-04	0.361610
1.000000	0.129300E-04	0.130856E-04	1.203267
1.500000	0.131700E-04	0.136733E-04	3.821388
2.000000	0.133200E-04	0.143228E-04	7.528621
2.500000	0.133600E-04	0.150060E-04	12.320557
3.000000	0.133200E-04	0.157088E-04	17.934155
4.000000	0.129200E-04	0.171459E-04	32.708171
5.000000	0.123800E-04	0.186035E-04	50.270411
6.000000	0.115700E-04	0.200698E-04	73.464463

AVERAGE DIFFERENCE= 0.19185E-05   AVERAGE PERCENT DIFFERENCE= 15.5083
ROOTMEAN SQUARE-DIFFERENCE= 0.32647E-05   ROOTMEAN SQUARE-PERCENT DIFFERENCE= 27.0921

COMPARISON OF DIFFUSION COEFFICIENTS-ACTUAL VS. PREDICTED BY DIFFERENTIAL VERSION OF Nernst-Hartley EQUATION

CONCENTRATION	ACTUAL	PREDICTED	DIFFERENCE-%
0.100000	0.124000E-04	0.124136E-04	0.109941
0.200000	0.124300E-04	0.124866E-04	0.455472
0.300000	0.124800E-04	0.126220E-04	1.137509
0.500000	0.126000E-04	0.129790E-04	3.008006
0.700000	0.127400E-04	0.134159E-04	5.305560
1.000000	0.129300E-04	0.141662E-04	9.561070
1.500000	0.131700E-04	0.155484E-04	18.059210
2.000000	0.133200E-04	0.170010E-04	27.635326
2.500000	0.133600E-04	0.184799E-04	38.322750
3.000000	0.133200E-04	0.199681E-04	49.910939
4.000000	0.129200E-04	0.229486E-04	77.620944
5.000000	0.123800E-04	0.259223E-04	109.388663
6.000000	0.115700E-04	0.288863E-04	149.665088

AVERAGE DIFFERENCE= 0.47091E-05   AVERAGE PERCENT DIFFERENCE= 37.7062
ROOTMEAN SQUARE-DIFFERENCE= 0.72089E-05   ROOTMEAN SQUARE-PERCENT DIFFERENCE= 59.2064

COMPOUND CSCL

THIS PROGRAM EVALUATES THE EFFECT OF CONCENTRATION ON THE ACTIVITY AND DIFFUSION COEFFICIENTS
OF SALTS USING THE BROMLEY EQUATION AND THE Nernst-Hartley EQUATION FOR DIFFUSIVITY
D(c)=D(0)*(1+c*d(ln(GAMA))/dc); DILUTE SOLUTIONS

VALENCE OF COMP.A   1
VALENCE OF ANION   1
CATION A CONDUCTANCE-MHOS/EQIV.-298 K,INFINITE DILUTION   77.2000
ANION CONDUCTANCE-MHOS/EQIV.-298 K,INFINITE DILUTION   76.3500
BROMLEY EQ. SALT PARAMETER -CATION A,COMMON ANION   0.002500
Nernst LIMITING DIFFUSIVITY-CM**2/SEC   0.20440E-04
DIFFUSIVITY CALCULATED FROM CONDUCTANCES-CM**2/SEC   0.20506E-04
NUMBER OF DEPENDENT VARIABLES   3
NUMBER OF DATA POINTS   11

CONCENTRATION	ACTIVITY COEFF.	DIFFUSION COEFF.
0.100000	0.756000	0.181700E-04
0.200000	0.694000	0.185700E-04
0.300000	0.656000	0.185500E-04
0.500000	0.606000	0.186000E-04
0.700000	0.575000	0.187100E-04
1.000000	0.544000	0.190200E-04
2.000000	0.496000	0.202900E-04
3.000000	0.479000	0.217500E-04
4.000000	0.474000	0.229100E-04
5.000000	0.475000	0.236400E-04
6.000000	0.480000	0.233500E-04

AQUEOUS SOLUTION OF COMPOUND CSCL

COMPARISON OF ACTIVITY COEFFICIENTS-ACTUAL VS. PREDICTED BY BROMLEY EQUATION

CONCENTRATION	ACTUAL	PREDICTED	DIFFERENCE-%
0.100000	0.756000	0.762309	0.834504
0.200000	0.694000	0.707735	1.979048
0.300000	0.656000	0.674043	2.750504
0.500000	0.606000	0.630417	4.029153
0.700000	0.575000	0.601473	4.604045
1.000000	0.544000	0.571268	5.012525
2.000000	0.496000	0.516833	4.200296
3.000000	0.479000	0.489371	2.165118
4.000000	0.474000	0.472448	0.327489
5.000000	0.475000	0.460961	2.955678
6.000000	0.480000	0.452718	5.683731

AVERAGE DIFFERENCE= 0.0173   AVERAGE PERCENT DIFFERENCE= 3.1402
ROOT MEAN SQUARE-DIFFERENCE= 0.0193   ROOT MEAN SQUARE-PERCENT DIFFERENCE= 3.5447

COMPARISON OF DIFFUSION COEFFICIENTS-ACTUAL VS. PREDICTED BY INTEGRAL VERSION OF Nernst-Hartley EQUATION

CONCENTRATION	ACTUAL	PREDICTED	DIFFERENCE-%
0.100000	0.181700E-04	0.188761E-04	3.886321
0.200000	0.185700E-04	0.185537E-04	0.087727
0.300000	0.185500E-04	0.183611E-04	1.018302
0.500000	0.186000E-04	0.181183E-04	2.589559
0.700000	0.187100E-04	0.179655E-04	3.979259
1.000000	0.190200E-04	0.178220E-04	6.298555
2.000000	0.202900E-04	0.176591E-04	12.966266
3.000000	0.217500E-04	0.176722E-04	18.748500
4.000000	0.229100E-04	0.177412E-04	22.561372
5.000000	0.236400E-04	0.178315E-04	24.570827
6.000000	0.233500E-04	0.179301E-04	23.211419

AVERAGE DIFFERENCE= 0.24038E-05   AVERAGE PERCENT DIFFERENCE= 10.9016
ROOTMEAN SQUARE-DIFFERENCE= 0.32493E-05   ROOTMEAN SQUARE-PERCENT DIFFERENCE= 14.3004

COMPARISON OF DIFFUSION COEFFICIENTS-ACTUAL VS. PREDICTED BY DIFFERENTIAL VERSION OF Nernst-Hartley EQUATION

CONCENTRATION	ACTUAL	PREDICTED	DIFFERENCE-%
0.100000	0.181700E-04	0.184182E-04	1.366076
0.200000	0.185700E-04	0.180799E-04	2.639241
0.300000	0.185500E-04	0.178819E-04	3.601394
0.500000	0.186000E-04	0.176481E-04	5.117930
0.700000	0.187100E-04	0.175276E-04	6.319683
1.000000	0.190200E-04	0.174582E-04	8.211188
2.000000	0.202900E-04	0.175761E-04	13.375407
3.000000	0.217500E-04	0.178194E-04	18.071664
4.000000	0.229100E-04	0.180692E-04	21.129606
5.000000	0.236400E-04	0.183071E-04	22.558853
6.000000	0.233500E-04	0.185312E-04	20.637064

AVERAGE DIFFERENCE= 0.24309E-05   AVERAGE PERCENT DIFFERENCE= 11.1844
ROOTMEAN SQUARE-DIFFERENCE= 0.30659E-05   ROOTMEAN SQUARE-PERCENT DIFFERENCE= 13.6252

COMPOUND NH4CL

THIS PROGRAM EVALUATES THE EFFECT OF CONCENTRATION ON THE ACTIVITY AND DIFFUSION COEFFICIENTS
OF SALTS USING THE BROMLEY EQUATION AND THE Nernst-Hartley EQUATION FOR DIFFUSIVITY
D(c)=D(0)*(1+c*d(ln(GAMA))/dc); DILUTE SOLUTIONS

VALENCE OF COMP.A	1
VALENCE OF ANION	1
CATION A CONDUCTANCE-MHOS/EQIV.-298 K,INFINITE DILUTION	73.5000
ANION CONDUCTANCE-MHOS/EQIV.-298 K,INFINITE DILUTION	76.3500
BROMLEY EQ. SALT PARAMETER -CATION A,COMMON ANION	0.020000
Nernst LIMITING DIFFUSIVITY-CM**2/SEC	0.19940E-04
DIFFUSIVITY CALCULATED FROM CONDUCTANCES-CM**2/SEC	0.20047E-04
NUMBER OF DEPENDENT VARIABLES	3
NUMBER OF DATA POINTS	14

CONCENTRATION	ACTIVITY COEFF.	DIFFUSION COEFF.
0.100000	0.770000	0.183800E-04
0.200000	0.718000	0.183600E-04
0.300000	0.687000	0.184100E-04
0.500000	0.649000	0.186100E-04
0.700000	0.625000	0.188300E-04
1.000000	0.603000	0.192100E-04
1.500000	0.581000	0.198600E-04
2.000000	0.570000	0.205100E-04
2.500000	0.564000	0.211300E-04
3.000000	0.561000	0.216400E-04
3.500000	0.560000	0.220300E-04
4.000000	0.560000	0.223500E-04
4.500000	0.561000	0.225700E-04
5.000000	0.562000	0.226400E-04

AQUEOUS SOLUTION OF COMPOUND NH4CL
COMPARISON OF ACTIVITY COEFFICIENTS-ACTUAL VS. PREDICTED BY BROMLEY EQUATION

CONCENTRATION	ACTUAL	PREDICTED	DIFFERENCE-%
0.100000	0.770000	0.766787	0.417233
0.200000	0.718000	0.715506	0.347412
0.300000	0.687000	0.684599	0.349546
0.500000	0.649000	0.645791	0.494457
0.700000	0.625000	0.621177	0.611699
1.000000	0.603000	0.597063	0.984613
1.500000	0.581000	0.574003	1.204315
2.000000	0.570000	0.561905	1.420122
2.500000	0.564000	0.555843	1.446202
3.000000	0.561000	0.553579	1.322846
3.500000	0.560000	0.553922	1.085364
4.000000	0.560000	0.556174	0.683168
4.500000	0.561000	0.559896	0.196841
5.000000	0.562000	0.564794	0.497224

AVERAGE DIFFERENCE= 0.0047   AVERAGE PERCENT DIFFERENCE= 0.7901
ROOT MEAN SQUARE-DIFFERENCE= 0.0052   ROOT MEAN SQUARE-PERCENT DIFFERENCE= 0.8962

COMPARISON OF DIFFUSION COEFFICIENTS-ACTUAL VS. PREDICTED BY INTEGRAL VERSION OF Nernst-Hartley EQUATION

CONCENTRATION	ACTUAL	PREDICTED	DIFFERENCE-%
0.100000	0.183800E-04	0.184710E-04	0.495274
0.200000	0.183600E-04	0.182034E-04	0.853032
0.300000	0.184100E-04	0.180575E-04	1.914625
0.500000	0.186100E-04	0.178985E-04	3.823147
0.700000	0.188300E-04	0.178245E-04	5.339748
1.000000	0.192100E-04	0.177971E-04	7.355129
1.500000	0.198600E-04	0.178710E-04	10.015018
2.000000	0.205100E-04	0.180226E-04	12.127773
2.500000	0.211300E-04	0.182146E-04	13.797631
3.000000	0.216400E-04	0.184294E-04	14.836414
3.500000	0.220300E-04	0.186579E-04	15.306771
4.000000	0.223500E-04	0.188949E-04	15.458992
4.500000	0.225700E-04	0.191373E-04	15.209208
5.000000	0.226400E-04	0.193831E-04	14.385695

AVERAGE DIFFERENCE= 0.19892E-05   AVERAGE PERCENT DIFFERENCE= 9.3513
ROOTMEAN SQUARE-DIFFERENCE= 0.23652E-05   ROOTMEAN SQUARE-PERCENT DIFFERENCE= 10.9260

COMPARISON OF DIFFUSION COEFFICIENTS-ACTUAL VS. PREDICTED BY DIFFERENTIAL VERSION OF Nernst-Hartley EQUATION

CONCENTRATION	ACTUAL	PREDICTED	DIFFERENCE-%
0.100000	0.183800E-04	0.180750E-04	1.659499
0.200000	0.183600E-04	0.178291E-04	2.891732
0.300000	0.184100E-04	0.177117E-04	3.793033
0.500000	0.186100E-04	0.176294E-04	5.269086
0.700000	0.188300E-04	0.176594E-04	6.216603
1.000000	0.192100E-04	0.178194E-04	7.239075
1.500000	0.198600E-04	0.182337E-04	8.188638
2.000000	0.205100E-04	0.187233E-04	8.711297
2.500000	0.211300E-04	0.192394E-04	8.947360
3.000000	0.216400E-04	0.197640E-04	8.669212
3.500000	0.220300E-04	0.202897E-04	7.899605
4.000000	0.223500E-04	0.208136E-04	6.874214
4.500000	0.225700E-04	0.213345E-04	5.474207
5.000000	0.226400E-04	0.218519E-04	3.480989

AVERAGE DIFFERENCE= 0.12540E-05   AVERAGE PERCENT DIFFERENCE= 6.0939

COMPOUND AMNO3

THIS PROGRAM EVALUATES THE EFFECT OF CONCENTRATION ON THE ACTIVITY AND DIFFUSION COEFFICIENTS
OF SALTS USING THE BROMLEY EQUATION AND THE Nernst-Hartley EQUATION FOR DIFFUSIVITY
D(c)=D(0)*(1+c*d(ln(GAMA))/dc); DILUTE SOLUTIONS

VALENCE OF COMP.A	1
VALENCE OF ANION	1
CATION A CONDUCTANCE-MHOS/EQIV.-298 K,INFINITE DILUTION	73.5000
ANION CONDUCTANCE-MHOS/EQIV.-298 K,INFINITE DILUTION	71.4600
BROMLEY EQ. SALT PARAMETER -CATION A,COMMON ANION	-0.035800
Nernst LIMITING DIFFUSIVITY-CM**2/SEC	0.19290E-04
DIFFUSIVITY CALCULATED FROM CONDUCTANCES-CM**2/SEC	0.19415E-04
NUMBER OF DEPENDENT VARIABLES	3
NUMBER OF DATA POINTS	13

CONCENTRATION	ACTIVITY COEFF.	DIFFUSION COEFF.
0.100000	0.740000	0.176900E-04
0.200000	0.677000	0.174900E-04
0.300000	0.636000	0.173900E-04
0.500000	0.582000	0.172400E-04
0.700000	0.545000	0.170900E-04
1.000000	0.504000	0.169000E-04
1.500000	0.456000	0.166100E-04
2.000000	0.419000	0.163300E-04
2.500000	0.391000	0.160500E-04
3.000000	0.368000	0.157800E-04
4.000000	0.331000	0.152400E-04
5.000000	0.302000	0.147200E-04
6.000000	0.279000	0.142100E-04

AQUEOUS SOLUTION OF COMPOUND AMNO3
COMPARISON OF ACTIVITY COEFFICIENTS-ACTUAL VS. PREDICTED BY BROMLEY EQUATION

CONCENTRATION	ACTUAL	PREDICTED	DIFFERENCE-%
0.100000	0.740000	0.752598	1.702499
0.200000	0.677000	0.691020	2.070966
0.300000	0.636000	0.651507	2.438151
0.500000	0.582000	0.598034	2.754977
0.700000	0.545000	0.560504	2.844744
1.000000	0.504000	0.518637	2.904096
1.500000	0.456000	0.468230	2.682093
2.000000	0.419000	0.430406	2.722152
2.500000	0.391000	0.399708	2.227094
3.000000	0.368000	0.373645	1.533961
4.000000	0.331000	0.330581	0.126601
5.000000	0.302000	0.295511	2.148726
6.000000	0.279000	0.265858	4.710544

AVERAGE DIFFERENCE= 0.0113   AVERAGE PERCENT DIFFERENCE= 2.3744
ROOT MEAN SQUARE-DIFFERENCE= 0.0121   ROOT MEAN SQUARE-PERCENT DIFFERENCE= 2.5718

COMPARISON OF DIFFUSION COEFFICIENTS-ACTUAL VS. PREDICTED BY INTEGRAL VERSION OF Nernst-Hartley EQUATION

CONCENTRATION	ACTUAL	PREDICTED	DIFFERENCE-%
0.100000	0.176900E-04	0.176942E-04	0.023899
0.200000	0.174900E-04	0.172906E-04	1.139882
0.300000	0.173900E-04	0.170199E-04	2.128310
0.500000	0.172400E-04	0.166260E-04	3.561367
0.700000	0.170900E-04	0.163227E-04	4.489870
1.000000	0.169000E-04	0.159491E-04	5.626768
1.500000	0.166100E-04	0.154331E-04	7.085497
2.000000	0.163300E-04	0.149815E-04	8.257768
2.500000	0.160500E-04	0.145618E-04	9.272496
3.000000	0.157800E-04	0.141595E-04	10.269365
4.000000	0.152400E-04	0.133815E-04	12.194948
5.000000	0.147200E-04	0.126196E-04	14.269259
6.000000	0.142100E-04	0.118636E-04	16.512393

AVERAGE DIFFERENCE= 0.11420E-05
ROOTMEAN SQUARE-DIFFERENCE= 0.13434E-05

AVERAGE PERCENT DIFFERENCE= 7.2948
ROOTMEAN SQUARE-PERCENT DIFFERENCE= 8.7932

COMPARISON OF DIFFUSION COEFFICIENTS-ACTUAL VS. PREDICTED BY DIFFERENTIAL VERSION OF Nernst-Hartley EQUATION

CONCENTRATION	ACTUAL	PREDICTED	DIFFERENCE-%
0.100000	0.176900E-04	0.171548E-04	3.025649
0.200000	0.174900E-04	0.166573E-04	4.760838
0.300000	0.173900E-04	0.163102E-04	6.209496
0.500000	0.172400E-04	0.157806E-04	8.465205
0.700000	0.170900E-04	0.153546E-04	10.154694
1.000000	0.169000E-04	0.148072E-04	12.383498
1.500000	0.166100E-04	0.140022E-04	15.699977
2.000000	0.163300E-04	0.132481E-04	18.872518
2.500000	0.160500E-04	0.125104E-04	22.053565
3.000000	0.157800E-04	0.117769E-04	25.368416
4.000000	0.152400E-04	0.103062E-04	32.373819
5.000000	0.147200E-04	0.882375E-05	40.056026
6.000000	0.142100E-04	0.732880E-05	48.425027

AVERAGE DIFFERENCE= 0.29753E-05
ROOTMEAN SQUARE-DIFFERENCE= 0.35407E-05

AVERAGE PERCENT DIFFERENCE= 19.0653
ROOTMEAN SQUARE-PERCENT DIFFERENCE= 23.4170

COMPOUND HCL

THIS PROGRAM EVALUATES THE EFFECT OF CONCENTRATION ON THE ACTIVITY AND DIFFUSION COEFFICIENTS
OF SALTS USING THE BROMLEY EQUATION AND THE Nernst-Hartley EQUATION FOR DIFFUSIVITY
D(c)=D(0)*(1+c*d(ln(GAMA))/dc); DILUTE SOLUTIONS

VALENCE OF COMP.A	1
VALENCE OF ANION	1
CATION A CONDUCTANCE-MHOS/EQIV.-298 K,INFINITE DILUTION	349.8000
ANION CONDUCTANCE-MHOS/EQIV.-298 K,INFINITE DILUTION	76.3500
BROMLEY EQ. SALT PARAMETER -CATION A,COMMON ANION	0.143300
Nernst LIMITING DIFFUSIVITY-CM**2/SEC	0.33360E-04
DIFFUSIVITY CALCULATED FROM CONDUCTANCES-CM**2/SEC	0.33371E-04
NUMBER OF DEPENDENT VARIABLES	3
NUMBER OF DATA POINTS	12

CONCENTRATION	ACTIVITY COEFF.	DIFFUSION COEFF.
0.100000	0.796000	0.305000E-04
0.200000	0.767000	0.306400E-04
0.300000	0.756000	0.309300E-04
0.500000	0.757000	0.318400E-04
0.700000	0.772000	0.328600E-04
1.000000	0.809000	0.343600E-04
1.500000	0.896000	0.374300E-04
2.000000	1.009000	0.404600E-04
2.500000	1.147000	0.433700E-04
3.000000	1.316000	0.465800E-04
3.500000	1.518000	0.492000E-04
4.000000	1.762000	0.517000E-04

AQUEOUS SOLUTION OF COMPOUND HCL

COMPARISON OF ACTIVITY COEFFICIENTS-ACTUAL VS. PREDICTED BY BROMLEY EQUATION

CONCENTRATION	ACTUAL	PREDICTED	DIFFERENCE-%
0.100000	0.796000	0.799096	0.388923
0.200000	0.767000	0.772731	0.747132
0.300000	0.756000	0.763804	1.032297
0.500000	0.757000	0.765280	1.093786
0.700000	0.772000	0.779557	0.978903
1.000000	0.809000	0.814998	0.741469
1.500000	0.896000	0.900265	0.475954
2.000000	1.009000	1.012770	0.373592
2.500000	1.147000	1.151860	0.423714
3.000000	1.316000	1.319521	0.267560
3.500000	1.518000	1.519243	0.081872
4.000000	1.762000	1.755699	0.357604

AVERAGE DIFFERENCE= 0.0052   AVERAGE PERCENT DIFFERENCE= 0.5802
ROOT MEAN SQUARE-DIFFERENCE= 0.0056   ROOT MEAN SQUARE-PERCENT DIFFERENCE= 0.6603

COMPARISON OF DIFFUSION COEFFICIENTS-ACTUAL VS. PREDICTED BY INTEGRAL VERSION OF Nernst-Hartley EQUATION

CONCENTRATION	ACTUAL	PREDICTED	DIFFERENCE-%
0.100000	0.305000E-04	0.315699E-04	3.508009
0.200000	0.306400E-04	0.316750E-04	3.377953
0.300000	0.309300E-04	0.319264E-04	3.221345
0.500000	0.318400E-04	0.325777E-04	2.316743
0.700000	0.328600E-04	0.333395E-04	1.459321
1.000000	0.343600E-04	0.346198E-04	0.756253
1.500000	0.374300E-04	0.369886E-04	1.179164
2.000000	0.404600E-04	0.395283E-04	2.302774
2.500000	0.433700E-04	0.421631E-04	2.782721
3.000000	0.465800E-04	0.448540E-04	3.705398
3.500000	0.492000E-04	0.475794E-04	3.293822
4.000000	0.517000E-04	0.503268E-04	2.656014

AVERAGE DIFFERENCE= 0.98983E-06   AVERAGE PERCENT DIFFERENCE= 2.5466
ROOTMEAN SQUARE-DIFFERENCE= 0.10825E-05   ROOTMEAN SQUARE-PERCENT DIFFERENCE= 2.7116

COMPARISON OF DIFFUSION COEFFICIENTS-ACTUAL VS. PREDICTED BY DIFFERENTIAL VERSION OF Nernst-Hartley EQUATION

CONCENTRATION	ACTUAL	PREDICTED	DIFFERENCE-%
0.100000	0.305000E-04	0.315047E-04	3.294233
0.200000	0.306400E-04	0.320852E-04	4.716561
0.300000	0.309300E-04	0.327815E-04	5.986119
0.500000	0.318400E-04	0.343634E-04	7.925180
0.700000	0.328600E-04	0.361525E-04	10.019709
1.000000	0.343600E-04	0.391032E-04	13.804349
1.500000	0.374300E-04	0.444043E-04	18.632905
2.000000	0.404600E-04	0.499150E-04	23.368834
2.500000	0.433700E-04	0.555056E-04	27.981482
3.000000	0.465800E-04	0.611255E-04	31.226970
3.500000	0.492000E-04	0.667539E-04	35.678744
4.000000	0.517000E-04	0.723818E-04	40.003418

AVERAGE DIFFERENCE= 0.80172E-05   AVERAGE PERCENT DIFFERENCE= 18.5532
ROOTMEAN SQUARE-DIFFERENCE= 0.10324E-04   ROOTMEAN SQUARE-PERCENT DIFFERENCE= 22.2623

COMPOUND HBR

THIS PROGRAM EVALUATES THE EFFECT OF CONCENTRATION ON THE ACTIVITY AND DIFFUSION COEFFICIENTS
OF SALTS USING THE BROMLEY EQUATION AND THE Nernst-Hartley EQUATION FOR DIFFUSIVITY
D(c)=D(0)*(1+c*d(ln(GAMA))/dc); DILUTE SOLUTIONS

VALENCE OF COMP.A	1
VALENCE OF ANION	1
CATION A CONDUCTANCE-MHOS/EQIV.-298 K,INFINITE DILUTION	349.8000
ANION CONDUCTANCE-MHOS/EQIV.-298 K,INFINITE DILUTION	78.1400
BROMLEY EQ. SALT PARAMETER -CATION A,COMMON ANION	0.173400
Nernst LIMITING DIFFUSIVITY-CM**2/SEC	0.34000E-04
DIFFUSIVITY CALCULATED FROM CONDUCTANCES-CM**2/SEC	0.34073E-04
NUMBER OF DEPENDENT VARIABLES	3
NUMBER OF DATA POINTS	6

CONCENTRATION	ACTIVITY COEFF.	DIFFUSION COEFF.
0.100000	0.805000	0.314000E-04
0.200000	0.782000	0.319000E-04
0.300000	0.777000	0.324900E-04
0.500000	0.789000	0.338800E-04
0.700000	0.815000	0.355200E-04
1.000000	0.871000	0.387000E-04

AQUEOUS SOLUTION OF COMPOUND HBR

COMPARISON OF ACTIVITY COEFFICIENTS-ACTUAL VS. PREDICTED BY BROMLEY EQUATION

CONCENTRATION	ACTUAL	PREDICTED	DIFFERENCE-%
0.100000	0.805000	0.807188	0.271747
0.200000	0.782000	0.787382	0.688201
0.300000	0.777000	0.784493	0.964322
0.500000	0.789000	0.797662	1.097847
0.700000	0.815000	0.823998	1.104049
1.000000	0.871000	0.879319	0.955096

AVERAGE DIFFERENCE= 0.0068   AVERAGE PERCENT DIFFERENCE= 0.8469
ROOT MEAN SQUARE-DIFFERENCE= 0.0072   ROOT MEAN SQUARE-PERCENT DIFFERENCE= 0.8957

COMPARISON OF DIFFUSION COEFFICIENTS-ACTUAL VS. PREDICTED BY INTEGRAL VERSION OF Nernst-Hartley EQUATION

CONCENTRATION	ACTUAL	PREDICTED	DIFFERENCE-%
0.100000	0.314000E-04	0.323417E-04	2.999017
0.200000	0.319000E-04	0.325863E-04	2.151467
0.300000	0.324900E-04	0.329658E-04	1.464306
0.500000	0.338800E-04	0.338578E-04	0.065627
0.700000	0.355200E-04	0.348546E-04	1.873253
1.000000	0.387000E-04	0.364895E-04	5.711965

AVERAGE DIFFERENCE= 0.83365E-06   AVERAGE PERCENT DIFFERENCE= 2.3776
ROOTMEAN SQUARE-DIFFERENCE= 0.10735E-05   ROOTMEAN SQUARE-PERCENT DIFFERENCE= 2.9413

COMPARISON OF DIFFUSION COEFFICIENTS-ACTUAL VS. PREDICTED BY DIFFERENTIAL VERSION OF Nernst-Hartley EQUATION

CONCENTRATION	ACTUAL	PREDICTED	DIFFERENCE-%
0.100000	0.314000E-04	0.324239E-04	3.260739
0.200000	0.319000E-04	0.332622E-04	4.270182
0.300000	0.324900E-04	0.341940E-04	5.244728
0.500000	0.338800E-04	0.362341E-04	6.948213
0.700000	0.355200E-04	0.384901E-04	8.361844
1.000000	0.387000E-04	0.421650E-04	8.953471

AVERAGE DIFFERENCE= 0.21465E-05   AVERAGE PERCENT DIFFERENCE= 6.1732
ROOTMEAN SQUARE-DIFFERENCE= 0.23158E-05   ROOTMEAN SQUARE-PERCENT DIFFERENCE= 6.5158

COMPOUND CACL2

THIS PROGRAM EVALUATES THE EFFECT OF CONCENTRATION ON THE ACTIVITY AND DIFFUSION COEFFICIENTS
OF SALTS USING THE BROMLEY EQUATION AND THE Nernst-Hartley EQUATION FOR DIFFUSIVITY
D(c)=D(O)*(1+c*d(ln(GAMA))/dc); DILUTE SOLUTIONS

VALENCE OF COMP.A	2
VALENCE OF ANION	1
CATION A CONDUCTANCE-MHOS/EQIV.-298 K,INFINITE DILUTION	59.5000
ANION CONDUCTANCE-MHOS/EQIV.-298 K,INFINITE DILUTION	76.3500
BROMLEY EQ. SALT PARAMETER -CATION A,COMMON ANION	0.094800
Nernst LIMITING DIFFUSIVITY-CM**2/SEC	0.13350E-04
DIFFUSIVITY CALCULATED FROM CONDUCTANCES-CM**2/SEC	0.13434E-04
NUMBER OF DEPENDENT VARIABLES	3
NUMBER OF DATA POINTS	11

CONCENTRATION	ACTIVITY COEFF.	DIFFUSION COEFF.
0.100000	0.518000	0.111000E-04
0.200000	0.472000	0.110700E-04
0.300000	0.455000	0.111600E-04
0.500000	0.448000	0.114000E-04
0.700000	0.460000	0.116800E-04
1.000000	0.500000	0.120300E-04
1.500000	0.616000	0.126300E-04
2.000000	0.792000	0.130700E-04
2.500000	1.063000	0.130600E-04
3.000000	1.483000	0.126500E-04
3.500000	2.080000	0.119500E-04

AQUEOUS SOLUTION OF COMPOUND CACL2

COMPARISON OF ACTIVITY COEFFICIENTS-ACTUAL VS. PREDICTED BY BROMLEY EQUATION

CONCENTRATION	ACTUAL	PREDICTED	DIFFERENCE-%
0.100000	0.518000	0.517008	0.191430
0.200000	0.472000	0.475877	0.821387
0.300000	0.455000	0.460006	1.100149
0.500000	0.448000	0.454181	1.379672
0.700000	0.460000	0.466020	1.308655
1.000000	0.500000	0.504512	0.902362
1.500000	0.616000	0.612326	0.596362
2.000000	0.792000	0.775249	2.115001
2.500000	1.063000	1.005329	5.425313
3.000000	1.483000	1.323511	10.754493
3.500000	2.080000	1.760267	15.371788

AVERAGE DIFFERENCE= 0.0531   AVERAGE PERCENT DIFFERENCE= 3.6333
ROOT MEAN SQUARE-DIFFERENCE= 0.1093   ROOT MEAN SQUARE-PERCENT DIFFERENCE= 5.9739

COMPARISON OF DIFFUSION COEFFICIENTS-ACTUAL VS. PREDICTED BY INTEGRAL VERSION OF Nernst-Hartley EQUATION

CONCENTRATION	ACTUAL	PREDICTED	DIFFERENCE-%
0.100000	0.111000E-04	0.114678E-04	3.313806
0.200000	0.110700E-04	0.116249E-04	5.012953
0.300000	0.111600E-04	0.118337E-04	6.036678
0.500000	0.114000E-04	0.123280E-04	8.140323
0.700000	0.116800E-04	0.129240E-04	10.650781
1.000000	0.120300E-04	0.139657E-04	16.090539
1.500000	0.126300E-04	0.159367E-04	26.181217
2.000000	0.130700E-04	0.180546E-04	38.137453
2.500000	0.130600E-04	0.202404E-04	54.979737
3.000000	0.126500E-04	0.224591E-04	77.542645
3.500000	0.119500E-04	0.246942E-04	106.646225

AVERAGE DIFFERENCE= 0.39754E-05   AVERAGE PERCENT DIFFERENCE= 32.0666
ROOTMEAN SQUARE-DIFFERENCE= 0.56651E-05   ROOTMEAN SQUARE-PERCENT DIFFERENCE= 45.7862

COMPARISON OF DIFFUSION COEFFICIENTS-ACTUAL VS. PREDICTED BY DIFFERENTIAL VERSION OF Nernst-Hartley EQUATION

CONCENTRATION	ACTUAL	PREDICTED	DIFFERENCE-%
0.100000	0.111000E-04	0.115411E-04	3.973834
0.200000	0.110700E-04	0.120124E-04	8.513259
0.300000	0.111600E-04	0.124955E-04	11.967175
0.500000	0.114000E-04	0.136939E-04	20.122035
0.700000	0.116800E-04	0.151669E-04	29.853197
1.000000	0.120300E-04	0.176631E-04	46.825443
1.500000	0.126300E-04	0.221278E-04	75.200333
2.000000	0.130700E-04	0.266965E-04	104.257636
2.500000	0.130600E-04	0.312741E-04	139.464851
3.000000	0.126500E-04	0.358369E-04	183.295707
3.500000	0.119500E-04	0.403802E-04	237.909372

AVERAGE DIFFERENCE= 0.97353E-05   AVERAGE PERCENT DIFFERENCE= 78.3075
ROOTMEAN SQUARE-DIFFERENCE= 0.13503E-04   ROOTMEAN SQUARE-PERCENT DIFFERENCE=108.6670

COMPOUND BACL2

THIS PROGRAM EVALUATES THE EFFECT OF CONCENTRATION ON THE ACTIVITY AND DIFFUSION COEFFICIENTS
OF SALTS USING THE BROMLEY EQUATION AND THE Nernst-Hartley EQUATION FOR DIFFUSIVITY
D(c)=D(0)*(1+c*d(ln(GAMA))/dc); DILUTE SOLUTIONS

VALENCE OF COMP.A	2
VALENCE OF ANION	1
CATION A CONDUCTANCE-MHOS/EQIV.-298 K,INFINITE DILUTION	63.6300
ANION CONDUCTANCE-MHOS/EQIV.-298 K,INFINITE DILUTION	76.3500
BROMLEY EQ. SALT PARAMETER -CATION A,COMMON ANION	0.063800
Nernst LIMITING DIFFUSIVITY-CM**2/SEC	0.13850E-04
DIFFUSIVITY CALCULATED FROM CONDUCTANCES-CM**2/SEC	0.13953E-04
NUMBER OF DEPENDENT VARIABLES	3
NUMBER OF DATA POINTS	7

CONCENTRATION	ACTIVITY COEFF.	DIFFUSION COEFF.
0.100000	0.508000	0.115900E-04
0.200000	0.450000	0.115000E-04
0.300000	0.425000	0.115100E-04
0.500000	0.403000	0.116000E-04
0.700000	0.397000	0.116800E-04
1.000000	0.401000	0.117900E-04
1.500000	0.431000	0.118000E-04

AQUEOUS SOLUTION OF COMPOUND BACL2

COMPARISON OF ACTIVITY COEFFICIENTS-ACTUAL VS. PREDICTED BY BROMLEY EQUATION

CONCENTRATION	ACTUAL	PREDICTED	DIFFERENCE-%
0.100000	0.508000	0.497463	2.074233
0.200000	0.450000	0.444917	1.129617
0.300000	0.425000	0.419691	1.249093
0.500000	0.403000	0.396617	1.583762
0.700000	0.397000	0.390412	1.659553
1.000000	0.401000	0.397471	0.880003
1.500000	0.431000	0.435248	0.985711

AVERAGE DIFFERENCE= 0.0060   AVERAGE PERCENT DIFFERENCE= 1.3660
ROOT MEAN SQUARE-DIFFERENCE= 0.0063   ROOT MEAN SQUARE-PERCENT DIFFERENCE= 1.4216

COMPARISON OF DIFFUSION COEFFICIENTS-ACTUAL VS. PREDICTED BY INTEGRAL VERSION OF Nernst-Hartley EQUATION

CONCENTRATION	ACTUAL	PREDICTED	DIFFERENCE-%
0.100000	0.115900E-04	0.116474E-04	0.495099
0.200000	0.115000E-04	0.116405E-04	1.221480
0.300000	0.115100E-04	0.117160E-04	1.789704
0.500000	0.116000E-04	0.119698E-04	3.188173
0.700000	0.116800E-04	0.123302E-04	5.566518
1.000000	0.117900E-04	0.130111E-04	10.357246
1.500000	0.118000E-04	0.143609E-04	21.702594

AVERAGE DIFFERENCE= 0.74370E-06   AVERAGE PERCENT DIFFERENCE= 6.3315
ROOTMEAN SQUARE-DIFFERENCE= 0.11132E-05   ROOTMEAN SQUARE-PERCENT DIFFERENCE= 9.4443

COMPARISON OF DIFFUSION COEFFICIENTS-ACTUAL VS. PREDICTED BY DIFFERENTIAL VERSION OF Nernst-Hartley EQUATION

CONCENTRATION	ACTUAL	PREDICTED	DIFFERENCE-%
0.100000	0.115900E-04	0.115266E-04	0.546714
0.200000	0.115000E-04	0.117406E-04	2.092229
0.300000	0.115100E-04	0.119998E-04	4.255149
0.500000	0.116000E-04	0.127468E-04	9.886105
0.700000	0.116800E-04	0.137424E-04	17.657109
1.000000	0.117900E-04	0.154879E-04	31.364544
1.500000	0.118000E-04	0.186584E-04	58.122252

AVERAGE DIFFERENCE= 0.20799E-05   AVERAGE PERCENT DIFFERENCE= 17.7034
ROOTMEAN SQUARE-DIFFERENCE= 0.30841E-05   ROOTMEAN SQUARE-PERCENT DIFFERENCE= 26.1704

COMPOUND AM2SO4

THIS PROGRAM EVALUATES THE EFFECT OF CONCENTRATION ON THE ACTIVITY AND DIFFUSION COEFFICIENTS
OF SALTS USING THE BROMLEY EQUATION AND THE Nernst-Hartley EQUATION FOR DIFFUSIVITY
$$D(c)=D(0)*(1+c*d(\ln(GAMA))/dc); \text{ DILUTE SOLUTIONS}$$

VALENCE OF COMP.A	1
VALENCE OF ANION	2
CATION A CONDUCTANCE-MHOS/EQIV.-298 K,INFINITE DILUTION	73.5000
ANION CONDUCTANCE-MHOS/EQIV.-298 K,INFINITE DILUTION	80.0200
BROMLEY EQ. SALT PARAMETER -CATION A,COMMON ANION	-0.028700
Nernst LIMITING DIFFUSIVITY-CM**2/SEC	0.15300E-04
DIFFUSIVITY CALCULATED FROM CONDUCTANCES-CM**2/SEC	0.15346E-04
NUMBER OF DEPENDENT VARIABLES	3
NUMBER OF DATA POINTS	12

CONCENTRATION	ACTIVITY COEFF.	DIFFUSION COEFF.
0.100000	0.423000	0.825000E-05
0.200000	0.343000	0.867000E-05
0.300000	0.300000	0.897000E-05
0.500000	0.248000	0.938000E-05
0.700000	0.218000	0.972000E-05
1.000000	0.189000	0.101100E-04
1.500000	0.160000	0.104700E-04
2.000000	0.144000	0.106900E-04
2.500000	0.132000	0.108800E-04
3.000000	0.125000	0.110600E-04
3.500000	0.119000	0.112200E-04
4.000000	0.116000	0.113500E-04

AQUEOUS SOLUTION OF COMPOUND AM2SO4
COMPARISON OF ACTIVITY COEFFICIENTS-ACTUAL VS. PREDICTED BY BROMLEY EQUATION

CONCENTRATION	ACTUAL	PREDICTED	DIFFERENCE-%
0.100000	0.423000	0.443425	4.828548
0.200000	0.343000	0.364001	6.122638
0.300000	0.300000	0.319207	6.402475
0.500000	0.248000	0.264697	6.732861
0.700000	0.218000	0.230207	5.599323
1.000000	0.189000	0.195110	3.232685
1.500000	0.160000	0.157178	1.763951
2.000000	0.144000	0.131537	8.655208
2.500000	0.132000	0.112392	14.854847
3.000000	0.125000	0.097279	22.176523
3.500000	0.119000	0.084932	28.628396
4.000000	0.116000	0.074611	35.679909

AVERAGE DIFFERENCE= 0.0195   AVERAGE PERCENT DIFFERENCE= 12.0564
ROOT MEAN SQUARE-DIFFERENCE= 0.0221   ROOT MEAN SQUARE-PERCENT DIFFERENCE= 16.0001

COMPARISON OF DIFFUSION COEFFICIENTS-ACTUAL VS. PREDICTED BY INTEGRAL VERSION OF Nernst-Hartley EQUATION

CONCENTRATION	ACTUAL	PREDICTED	DIFFERENCE-%
0.100000	0.825000E-05	0.120429E-04	45.974038
0.200000	0.867000E-05	0.114752E-04	32.355218
0.300000	0.897000E-05	0.110937E-04	23.675366
0.500000	0.938000E-05	0.105204E-04	12.157892
0.700000	0.972000E-05	0.100681E-04	3.580809
1.000000	0.101100E-04	0.950263E-05	6.007596
1.500000	0.104700E-04	0.870273E-05	16.879332
2.000000	0.106900E-04	0.797772E-05	25.372170
2.500000	0.108800E-04	0.728143E-05	33.075096
3.000000	0.110600E-04	0.659585E-05	40.363018
3.500000	0.112200E-04	0.591317E-05	47.297911
4.000000	0.113500E-04	0.522984E-05	53.922097

AVERAGE DIFFERENCE= 0.28989E-05   AVERAGE PERCENT DIFFERENCE= 28.3884
ROOTMEAN SQUARE-DIFFERENCE= 0.33854E-05   ROOTMEAN SQUARE-PERCENT DIFFERENCE= 32.5502

COMPARISON OF DIFFUSION COEFFICIENTS-ACTUAL VS. PREDICTED BY DIFFERENTIAL VERSION OF Nernst-Hartley EQUATION

CONCENTRATION	ACTUAL	PREDICTED	DIFFERENCE-%
0.100000	0.825000E-05	0.112609E-04	36.496010
0.200000	0.867000E-05	0.105908E-04	22.154631
0.300000	0.897000E-05	0.100792E-04	12.366037
0.500000	0.938000E-05	0.926873E-05	1.186216
0.700000	0.972000E-05	0.861311E-05	11.387716
1.000000	0.101100E-04	0.775865E-05	23.257669
1.500000	0.104700E-04	0.644406E-05	38.452114
2.000000	0.106900E-04	0.514528E-05	51.868321
2.500000	0.108800E-04	0.382793E-05	64.816826
3.000000	0.110600E-04	0.248736E-05	77.510331
3.500000	0.112200E-04	0.112549E-05	89.968859
4.000000	0.113500E-04	-0.254553E-06	102.242762

AVERAGE DIFFERENCE= 0.47087E-05   AVERAGE PERCENT DIFFERENCE= 44.3090
ROOTMEAN SQUARE-DIFFERENCE= 0.59686E-05   ROOTMEAN SQUARE-PERCENT DIFFERENCE= 54.4470

Appendix E

SOLUTION ALGORITHM - 7 DIAGONAL ARRAY

The following matrix equation is to be solved for X_i:

$$A_i^7 X_i = bb7_i \tag{E-1}$$

$$
A_i^7 = \begin{bmatrix}
A_1^7 & B_1^7 & C_1^7 & D_1^7 & 0 & 0 & 0 & 0 & 0 & 0 \\
E_2^7 & A_2^7 & B_2^7 & C_2^7 & D_2^7 & 0 & 0 & 0 & 0 & 0 \\
F_3^7 & E_3^7 & A_3^7 & B_3^7 & C_3^7 & D_3^7 & 0 & 0 & 0 & 0 \\
G_4^7 & F_4^7 & E_4^7 & A_4^7 & B_4^7 & C_4^7 & D_4^7 & 0 & 0 & 0 \\
0 & G_5^7 & F_5^7 & E_5^7 & A_5^7 & B_5^7 & C_5^7 & D_5^7 & 0 & 0 \\
0 & 0 & G_6^7 & F_6^7 & E_6^7 & A_6^7 & B_6^7 & C_6^7 & D_6^7 & 0 \\
0 & 0 & 0 & G_7^7 & F_7^7 & E_7^7 & A_7^7 & B_7^7 & C_7^7 & D_7^7 \\
0 & 0 & 0 & 0 & G_8^7 & F_8^7 & E_8^7 & A_8^7 & B_8^7 & C_8^7 \\
0 & 0 & 0 & 0 & 0 & G_9^7 & F_9^7 & E_9^7 & A_9^7 & B_9^7 \\
0 & 0 & 0 & 0 & 0 & 0 & G_{10}^7 & F_{10}^7 & E_{10}^7 & A_{10}^7
\end{bmatrix}
\times
\begin{bmatrix}
X_1 \\ X_2 \\ X_3 \\ X_4 \\ X_5 \\ X_6 \\ X_7 \\ X_8 \\ X_9 \\ X_{10}
\end{bmatrix}
=
\begin{bmatrix}
bb7_1 \\ bb7_2 \\ bb7_3 \\ bb7_4 \\ bb7_5 \\ bb7_6 \\ bb7_7 \\ bb7_8 \\ bb7_9 \\ bb7_{10}
\end{bmatrix}
\tag{E-2}
$$

A_i^7 can be specified as:

$$A_i^7 = L_i^7 U_i^7 \qquad \text{(E-3)}$$

where

$$\text{(E-4)} \\ \&\ \text{(E-5)}$$

$$L_i^7 = \begin{bmatrix}
\omega_1^7 & 0 & 0 & 0 & 0 & 0 & 0 & 0 & 0 & 0 \\
\beta_2^7 & \omega_2^7 & 0 & 0 & 0 & 0 & 0 & 0 & 0 & 0 \\
\alpha_3^7 & \beta_3^7 & \omega_3^7 & 0 & 0 & 0 & 0 & 0 & 0 & 0 \\
\theta_4^7 & \alpha_4^7 & \beta_4^7 & \omega_4^7 & 0 & 0 & 0 & 0 & 0 & 0 \\
0 & \theta_5^7 & \alpha_5^7 & \beta_5^7 & \omega_5^7 & 0 & 0 & 0 & 0 & 0 \\
0 & 0 & \theta_6^7 & \alpha_6^7 & \beta_6^7 & \omega_6^7 & 0 & 0 & 0 & 0 \\
0 & 0 & 0 & \theta_7^7 & \alpha_7^7 & \beta_7^7 & \omega_8^7 & 0 & 0 & 0 \\
0 & 0 & 0 & 0 & \theta_8^7 & \alpha_8^7 & \beta_8^7 & \omega_8^7 & 0 & 0 \\
0 & 0 & 0 & 0 & 0 & \theta_9^7 & \alpha_9^7 & \beta_9^7 & \omega_9^7 & 0 \\
0 & 0 & 0 & 0 & 0 & 0 & \theta_{10}^7 & \alpha_{10}^7 & \beta_{10}^7 & \omega_{10}^7
\end{bmatrix}$$

$$U_i^7 = \begin{bmatrix}
1 & \gamma_1^7 & \delta_1^7 & \phi_1^7 & 0 & 0 & 0 & 0 & 0 & 0 \\
0 & 1 & \gamma_2^7 & \delta_2^7 & \phi_2^7 & 0 & 0 & 0 & 0 & 0 \\
0 & 0 & 1 & \gamma_3^7 & \delta_3^7 & \phi_3^7 & 0 & 0 & 0 & 0 \\
0 & 0 & 0 & 1 & \gamma_4^7 & \delta_4^7 & \phi_4^7 & 0 & 0 & 0 \\
0 & 0 & 0 & 0 & 1 & \gamma_5^7 & \delta_5^7 & \phi_5^7 & 0 & 0 \\
0 & 0 & 0 & 0 & 0 & 1 & \gamma_6^7 & \delta_6^7 & \phi_6^7 & 0 \\
0 & 0 & 0 & 0 & 0 & 0 & 1 & \gamma_7^7 & \delta_7^7 & \phi_7^7 \\
0 & 0 & 0 & 0 & 0 & 0 & 0 & 1 & \gamma_8^7 & \delta_8^7 \\
0 & 0 & 0 & 0 & 0 & 0 & 0 & 0 & 1 & \gamma_9^7 \\
0 & 0 & 0 & 0 & 0 & 0 & 0 & 0 & 0 & 1
\end{bmatrix}$$

matrix multiplication of (E-4) and E-5), setting the coefficients
equal to those in (E-1), yields:

$$\theta_i^7 = G_i^7 \quad \text{for } i = 4 \text{ --- } N \tag{E-6}$$

$$\phi_1^7 = D_1^7/\omega_1^7 = D_1^7/A_1^7 \tag{E-7}$$

$$\phi_i^7 = D_i^7/\omega_1^7 \quad \text{for } i = 2 \text{ --- } N-3 \tag{E-8}$$

$$\delta_1^7 = C_1^7/\omega_1^7 = C_1^7/A_1^7 \tag{E-9}$$

$$\delta_i^7 = \frac{C_i^7 - \beta_i^7 \phi_{i-1}}{\omega_i^7} \quad \text{for } i = 2 \text{ --- } N-2 \tag{E-10}$$

$$\gamma_1^7 = B_1^7/\omega_1^7 = B_1^7/A_1^7 \tag{E-11}$$

$$\gamma_2^7 = \frac{B_2^7 - \beta_2^7 \delta_1^7}{\omega_2^7} \tag{E-12}$$

$$\gamma_i^7 = \frac{B_i^7 - \alpha_i^7 \phi_{i-2}^7 - \beta_i^7 \delta_{i-1}^7}{\omega_i^7} \quad \text{for } i = 3 \text{ --- } N-1 \tag{E-13}$$

$$\beta_2^7 = E_2^7 \tag{E-14}$$

$$\beta_3^7 = E_3^7 - \alpha_3^7 \gamma_1^7 \tag{E-15}$$

$$\beta_i^7 = E_i^7 - \theta_i^7 \delta_{i-3}^7 - \alpha_i^7 \gamma_{i-2}^7 \quad \text{for } i = 4 \text{ --- } N \tag{E-16}$$

$$\alpha_3^7 = F_3^7 \tag{E-17}$$

$$\alpha_i^7 = F_i^7 - \theta_i^7 \gamma_{i-3}^7 \quad \text{for } i = 4 \text{ --- } N \tag{E-18}$$

$$\omega_1^7 = A_1^7 \tag{E-19}$$

$$\omega_2^7 = A_2^7 - \beta_2^7 \gamma_1^7 \tag{E-20}$$

$$\omega_3^7 = A_3^7 - \beta_3^7 \gamma_2^7 - \alpha_3^7 \delta_1^7 \tag{E-21}$$

$$\omega_i^7 = A_i^7 - \beta_i^7 \gamma_{i-1}^7 - \alpha_i^7 \delta_{i-2}^7 - \theta_i^7 \phi_{i-3}^7 \quad \text{for } i = 4 \text{ --- } N \tag{E-22}$$

defining $FF_i^7 \equiv U_i^7 X_i$ (E-23)

then $L_i^7 FF_i^7 = bb_i^7$ (E-24)

where (E-25)

$$L_i^7 = \begin{vmatrix} \omega_1^7 & & & & & \\ \beta_2^7 & & & & & \\ \alpha_3^7 & & & & & \\ \theta_4^7 & & & & & \\ & \theta_N^7 & \alpha_N^7 & \beta_N^7 & & \omega_N^7 \end{vmatrix} \quad \times \quad \begin{vmatrix} FF_1^7 \\ \\ \\ \\ FF_N^7 \end{vmatrix} \quad = \quad \begin{vmatrix} bb_1^7 \\ \\ \\ \\ bb_N^7 \end{vmatrix}$$

solution to the sets of equations defined by (E-25)

$$FF_1^7 = bb_1^7 / \omega_1^7 \qquad (E-26)$$

$$FF_1^7 \beta_2^7 + FF_2^7 \omega_2^7 = bb_2^7$$

$$\text{or } FF_2^7 = \frac{bb_2 - FF_1^7 \beta_2^7}{\omega_2^7} \qquad (E-27)$$

$$FF_3^7 = \frac{bb_3^7 - FF_1^7 \alpha_3^7 - FF_2^7 \beta_3^7}{\omega_3^7} \qquad (E-28)$$

$$FF_4^7 = \frac{bb_4^7 - FF_1^7 \theta_4^7 - FF_2^7 \alpha_4^7 - FF_3^7 \beta_4^7}{\omega_4^7} \qquad (E-29)$$

$$FF_i^7 = \frac{bb_i^7 - FF_{i-3}^7 \theta_i^7 - FF_{i-2}^7 \alpha_i^7 - FF_{i-1}^7 \beta_i^7}{\omega_i^7} \quad \text{for } i = 4 \text{ --- } N \qquad (E-30)$$

Returning to $U_i^7 X_i \equiv FF_i^7$ (E-23)

$$\begin{vmatrix} 1 & \gamma_1^7 & \delta_1^7 & \phi_1^7 & & & \\ & 1 & \gamma_{N-3}^7 & \delta_{N-3}^7 & \phi_{N-3}^7 & & \\ & & 1 & \gamma_{N-2}^7 & \delta_{N-2}^7 & \\ & & & 1 & \gamma_{N-1}^7 & \\ & & & & 1 \end{vmatrix} \times \begin{vmatrix} X_1 \\ X_{N-3} \\ X_{N-2} \\ X_{N-1} \\ X_N \end{vmatrix} = \begin{vmatrix} FF_1^7 \\ FF_{N-3}^7 \\ FF_{N-2}^7 \\ FF_{N-1}^7 \\ FF_N^7 \end{vmatrix} \qquad (E-31)$$

solution to equations defined by (E-31) in terms of (E-30)

$$X_N = FF_N^7 = \frac{bb_N^7 - FF_{N-3}^7 \theta_N^7 - FF_{N-2}^7 \alpha_N^7 - FF_{N-1}^7 \beta_N^7}{\omega_N^7}$$ (E-32)

and

$$FF_{N-1}^7 = X_{N-1} + \gamma_{N-1}^7 X_N$$ (E-33)

$$FF_{N-2}^7 = X_{N-2} + \gamma_{N-2}^7 X_{N-1} + \delta_{N-2}^7 X_N$$ (E-34)

$$FF_{N-3}^7 = X_{N-3} + \gamma_{N-3}^7 X_{N-2} + \delta_{N-3}^7 X_{N-1} + \phi_{N-3}^7 X_N$$ (E-35)

$$FF_i^7 = X_i + \gamma_i^7 X_{i+1} + \delta_i^7 X_{i+2} + \phi_i^7 X_{i+3} \quad \text{for } i = N-3 \text{ --- } 1$$ (E-36)

so $$FF_1^7 = X_1 + \gamma_1^7 X_2 + \delta_1^7 X_3 + \phi_1^7 X_4$$ (E-37)

Rearranging in terms of X_i

$$X_{N-1} = FF_{N-1}^7 - \gamma_{N-1}^7 X_N$$ (E-38)

$$X_{N-2} = FF_{N-2}^7 - \gamma_{N-2}^7 X_{N-1} - \delta_{N-2}^7 X_N$$ (E-39)

$$X_{N-3} = FF_{N-3}^7 - \gamma_{N-3}^7 X_{N-2} - \delta_{N-3}^7 X_{N-1} - \phi_{N-3}^7 X_N$$ (E-40)

$$X_i = FF_i^7 - \gamma_i^7 X_{i+1} - \delta_i^7 X_{i+2} - \phi_i^7 X_{i+3} \quad \text{for } i = N-3 \text{ --- } 1$$ (E-41)

so $$X_1 = FF_1^7 - \gamma_1^7 X_2 - \delta_1^7 X_3 - \phi_1^7 X_4$$ (E-42)

from equation (E-30)

$$FF_{N-i}^7 = \frac{bb_{N-i}^7 - FF_{N-3-i}^7 \theta_{N-i}^7 - FF_{N-2-i}^7 \alpha_{N-i}^7 - FF_{N-1-i}^7 \beta_{N-i}^7}{\omega_{N-i}^7}$$ (E-43)

$$\text{for } i = 1 \text{ --- } N-4$$

with FF_1^7, FF_2^7, FF_3^7 given in equations (E-26) through (E-28).

The 7 diagonal algorithm then consists of separating the coefficient matrix A_i^7 into an upper and lower diagonal matrix, which when multiplied and set equal to the terms in A_i^7, allows values to be computed for the factors:

$$\omega_i^7, \ \beta_i^7, \ \alpha_i^7, \text{ and } \theta_i^7$$

By defining a vector $FF_i^7 \equiv U_i^7 X_i$, advantage is taken of the upper diagonal U_i^7 in which all diagonal elements are unity to solve for X_i in terms of vectors bb_i^7 and vector FF_i^7, which is known in terms of the lower diagonal factors. X_i is then solved for starting with X_N and proceeding to X_1. Thus in effect inverting the matrix A_i^7 and solving for X_i.

SOLUTION ALGORITHM - 5 DIAGONAL ARRAY

The following matrix equation is to be solved for X_i:

$$A_i^5 X_i = bb5_i \tag{F-1}$$

$$A_i^5 = \begin{bmatrix}
A_1^5 & B_1^5 & C_1^5 & 0 & 0 & 0 & 0 & 0 & 0 & 0 \\
E_2^5 & A_2^5 & B_2^5 & C_2^5 & 0 & 0 & 0 & 0 & 0 & 0 \\
F_3^5 & E_3^5 & A_3^5 & B_3^5 & C_3^5 & 0 & 0 & 0 & 0 & 0 \\
0 & F_4^5 & E_4^5 & A_4^5 & B_4^5 & C_4^5 & 0 & 0 & 0 & 0 \\
0 & 0 & F_5^5 & E_5^5 & A_5^5 & B_5^5 & C_5^5 & 0 & 0 & 0 \\
0 & 0 & 0 & F_6^5 & E_6^5 & A_6^5 & B_6^5 & C_6^5 & 0 & 0 \\
0 & 0 & 0 & 0 & F_7^5 & E_7^5 & A_7^5 & B_7^5 & C_7^5 & 0 \\
0 & 0 & 0 & 0 & 0 & F_8^5 & E_8^5 & A_8^5 & B_8^5 & C_8^5 \\
0 & 0 & 0 & 0 & 0 & 0 & F_9^5 & E_9^5 & A_9^5 & B_9^5 \\
0 & 0 & 0 & 0 & 0 & 0 & 0 & F_{10}^5 & E_{10}^5 & A_{10}^5
\end{bmatrix} \times \begin{bmatrix} X_1 \\ X_2 \\ X_3 \\ X_4 \\ X_5 \\ X_6 \\ X_7 \\ X_8 \\ X_9 \\ X_{10} \end{bmatrix} = \begin{bmatrix} bb5_1 \\ bb5_2 \\ bb5_3 \\ bb5_4 \\ bb5_5 \\ bb5_6 \\ bb5_7 \\ bb5_8 \\ bb5_9 \\ bb5_{10} \end{bmatrix}$$

$$\tag{F-2}$$

A_i^5 can be specified as:

$$A_i^5 = L_i^5 U_i^5 \qquad \text{(F-3)}$$

where

$$
L_i^5 = \begin{bmatrix}
\omega_1^5 & 0 & 0 & 0 & 0 & 0 & 0 & 0 & 0 & 0 \\
\beta_2^5 & \delta_2^5 & 0 & 0 & 0 & 0 & 0 & 0 & 0 & 0 \\
\alpha_3^5 & \beta_3^5 & \omega_3^5 & 0 & 0 & 0 & 0 & 0 & 0 & 0 \\
0 & \alpha_4^5 & \beta_4^5 & \omega_4^5 & 0 & 0 & 0 & 0 & 0 & 0 \\
0 & 0 & \alpha_5^5 & \beta_5^5 & \omega_5^5 & 0 & 0 & 0 & 0 & 0 \\
0 & 0 & 0 & \alpha_6^5 & \beta_6^5 & \omega_6^5 & 0 & 0 & 0 & 0 \\
0 & 0 & 0 & 0 & \alpha_7^5 & \beta_7^5 & \omega_7^5 & 0 & 0 & 0 \\
0 & 0 & 0 & 0 & 0 & \alpha_8^5 & \beta_8^5 & \omega_8^5 & 0 & 0 \\
0 & 0 & 0 & 0 & 0 & 0 & \alpha_9^5 & \beta_9^5 & \omega_9^5 & 0 \\
0 & 0 & 0 & 0 & 0 & 0 & 0 & \alpha_{10}^5 & \beta_{10}^5 & \omega_{10}^5
\end{bmatrix}
$$

$$
U_i^5 = \begin{bmatrix}
1 & \gamma_1^5 & \delta_1^5 & 0 & 0 & 0 & 0 & 0 & 0 & 0 \\
0 & 1 & \gamma_2^5 & \delta_2^5 & 0 & 0 & 0 & 0 & 0 & 0 \\
0 & 0 & 1 & \gamma_3^5 & \delta_3^5 & 0 & 0 & 0 & 0 & 0 \\
0 & 0 & 0 & 1 & \gamma_4^5 & \delta_4^5 & 0 & 0 & 0 & 0 \\
0 & 0 & 0 & 0 & 1 & \gamma_5^5 & \delta_5^5 & 0 & 0 & 0 \\
0 & 0 & 0 & 0 & 0 & 1 & \gamma_6^5 & \delta_6^5 & 0 & 0 \\
0 & 0 & 0 & 0 & 0 & 0 & 1 & \gamma_7^5 & \delta_7^5 & 0 \\
0 & 0 & 0 & 0 & 0 & 0 & 0 & 1 & \gamma_8^5 & \delta_8^5 \\
0 & 0 & 0 & 0 & 0 & 0 & 0 & 0 & 1 & \gamma_9^5 \\
0 & 0 & 0 & 0 & 0 & 0 & 0 & 0 & 0 & 1
\end{bmatrix}
$$

matrix multiplication of (F-4) and (F-5), setting the coefficients equal to those in (F-1), yields:

$$\alpha_i^5 = F_i^5 \quad \text{for } i - 3 \text{ --- } N \tag{F-6}$$

$$\delta_i^5 = C_i^5/\omega_i^5 \quad \text{for } i - 1 \text{ --- } N-2 \tag{F-7}$$

$$\delta_1^5 = C_1^5/\omega_1^5 = C_1^5/A_1^5 \tag{F-8}$$

$$\omega_1^5 = A_1^5 \tag{F-9}$$

$$\gamma_1^5 = B_1^5/\omega_1^5 = B_1^5/A_1^5 \tag{F-10}$$

$$\gamma_i^5 = \frac{B_i^5 - \beta_i^5 \delta_{i-1}^5}{\omega_i^5} \quad \text{for } i = 2 \text{ --- } N-1 \tag{F-11}$$

$$\beta_2^5 = E_2^5 \tag{F-12}$$

$$\beta_i^5 = E_i^5 - \alpha_i^5 \gamma_{i-2}^5 \quad \text{for } i - 3 \text{ --- } N \tag{F-13}$$

$$\omega_2^5 = A_2^5 - \beta_2^5 \gamma_1^5 \tag{F-14}$$

$$\omega_i^5 = A_i^5 - \alpha_i^5 \delta_{i-2}^5 - \beta_i^5 \gamma_{i-1}^5 \quad \text{for } i = 3 \text{ --- } N \tag{F-15}$$

defining $FF_i^5 \equiv U_i^5 X_i$ (F-16)

then $L_i^5 FF_i^5 = bb_i^5$ (F-17)

where (F-18)

solution to the sets of equations defined by (F-18)

$$FF_1^5 = bb_1^5/\omega_1^5 \tag{F-19}$$

$$FF_1^5 \beta_2^5 + FF_2^5 \omega_2^5 = bb_2^5 \tag{F-20}$$

or $$FF_2^5 = \frac{bb_2^5 - FF_1^5 \beta_2^5}{\omega_2^5} \tag{F-21}$$

$$FF_3^5 = \frac{bb_3^5 - FF_1^5 \alpha_3^5 - FF_2^5 \beta_3^5}{\omega_3^5} \tag{F-22}$$

$$FF_i^5 = \frac{bb_i^5 - FF_{i-2}^5 \alpha_i^5 - FF_{i-1}^5 \beta_i^5}{\omega_i^5} \quad \text{for } i = 3 \text{ --- } N \tag{F-23}$$

returning to $U_i^5 X_i \equiv FF_i^5$ $\qquad$ (F-16)

$$
\begin{vmatrix}
1 & \gamma_1^5 & \delta_1^5 & & & \\
 & 1 & & & & \\
 & & & & & \\
 & & 1 & \gamma_{N-2}^5 & \delta_{N-2}^5 \\
 & & & 1 & \gamma_{N-1}^5 \\
 & & & & 1
\end{vmatrix}
\times
\begin{vmatrix}
X_1 \\
\\
\\
X_{N-2} \\
X_{N-1} \\
X_N
\end{vmatrix}
=
\begin{vmatrix}
FF_1^5 \\
\\
\\
FF_{N-2}^5 \\
FF_{N-1}^5 \\
FF_N^5
\end{vmatrix}
$$

$\qquad$ (F-24)

solution to equations defined by (F-24) in terms of (F-23)

$$X_N = FF_N^5 = \frac{bb_N^5 - FF_{N-2}^5 \alpha_N^5 - FF_{N-1}^5 \beta_N^5}{\omega_N^5} \qquad \text{(F-25)}$$

and

$$FF_{N-1}^5 = X_{N-1} + \gamma_{N-1}^5 X_N \qquad \text{(F-26)}$$

$$FF_{N-2}^5 = X_{N-2} + \gamma_{N-2}^5 X_{N-1} + \delta_{N-2}^5 X_N \qquad \text{(F-27)}$$

$$FF_i^5 = X_i + \gamma_i^5 X_{i+1} + \delta_i^5 X_{i+2} \qquad \text{(F-28)}$$

so $\quad FF_1^5 = X_1 + \gamma_1^5 X_2 + \delta_1^5 X3 \qquad$ (F-29)

rearranging in terms of X_i

$$X_{N-1} = FF_{N-1}^5 - \gamma_{N-1}^5 X_N \qquad \text{(F-30)}$$

$$X_{N-2} = FF_{N-2}^5 - \gamma_{N-2}^5 X_{N-1} - \delta_{N-2}^5 X_N \qquad \text{(F-31)}$$

$$X_i = FF_i^5 - \gamma_i^5 X_{i+1} - \delta_i^5 X_{i+2} \qquad \text{for } i = N-2 \text{ --- } 1 \qquad \text{(F-32)}$$

so $\quad X_1 = FF_1^5 - \gamma_1^5 X_2 - \delta_1^5 X_3 \qquad$ (F-33)

from equation (F-23)

$$FF_{N-i}^5 = \frac{bb_{N-i}^5 - FF_{N-2-i}^5 \alpha_{N-i}^5 - FF_{N-1-i}^5 \beta_{N-i}^5}{\omega_{N-i}^7} \qquad \text{for } i = 1 \text{ --- } N-3 \qquad \text{(F-34)}$$

with FF_1^5 and FF_2^5 given in equations (F-20) and (F-21).

Use of the above algorithm inverts the A_i^5 matrix and solves for X_i.

DERIVATION OF THE GENERAL EQUATION FOR DIFFUSION OF IONIC

SPECIES IN THE RESIN PHASE — TERNARY SYSTEMS

A. Derivation using irreversible thermodynamics treatment

The Nernst-Planck equation for transport of ionic species in dilute electrolytes is given as:

$$\overline{N}_k = - \overline{c}_k \cdot \sum_{j=1}^{4} \overline{L}_{kj} \cdot \nabla \overline{\mu}_j^c - \overline{c}_k \cdot F \cdot \nabla \overline{\phi} \cdot \sum_{j=1}^{4} \overline{L}_{kj} \cdot |z_j| \qquad (G-1)$$

for $k = 1, 2, 3, 4$

where:

$\overline{N}_k$ = molar flux of component k

$\overline{c}_k$ = molar concentration of species k (moles/liter)

$\overline{\mu}_j^c$ = chemical potential of species j

z_j = charge on species j

$\overline{L}_{kj}$ = phenomenological coefficients

F = Faraday constant

$\overline{\phi}$ = electric potential, volts

For electroneutrality in the resin, the following relationship holds:

$$\sum_{i=1}^{4} |z_i| \cdot \overline{c}_i = \text{constant}^{(1)}; \qquad \text{charge of water,} |z_4| = 0 \qquad (G-2)$$

$$(1) \text{ constant} = \left(|z|_{sites} \right) \cdot \overline{c}_{sites}$$

Then the gradient is given by:

$$\sum_{i=1}^{4} |z_i| \cdot \nabla \overline{c}_i = 0 \quad , \qquad (G-3)$$

and since no electric current flows,

$$\sum_{i=1}^{4} |z_i| \cdot \overline{N}_i = 0. \tag{G-4}$$

Substituting (G-1) in (G-4),

$$\nabla \overline{\phi} = \left\{ \frac{\sum_{i=1}^{4} \left[|z_i| c_i \cdot \left(\sum_{j=1}^{4} \overline{L}_{ij} \cdot \nabla \overline{\mu}_j^c \right) \right]}{F \cdot \sum_{i=1}^{4} \left[|z_i| \cdot \overline{c}_i \cdot \left(\sum_{j=1}^{4} \overline{L}_{ij} \cdot |z_j| \right) \right]} \right\} \tag{G-5}$$

Putting $\nabla \overline{\phi}$ from equation (G-5) into equation (G-1)

yields:

$$\overline{N}_k = - \overline{c}_k \cdot \sum_{j=1}^{4} \overline{L}_{kj} \cdot \nabla \overline{\mu}_j^c + \left\{ \left(\overline{c}_k \cdot \sum_{i=1}^{4} \overline{L}_{ki} \cdot |z_i| \right) \right.$$

$$\left. \cdot \left[\frac{\sum_{j=1}^{4} \left[\overline{c}_j \cdot |z_j| \cdot \left(\sum_{i=1}^{4} \overline{L}_{ij} \cdot \nabla \overline{\mu}_j^c \right) \right]}{\sum_{i=1}^{4} \overline{c}_i \cdot z_i^2 \cdot \overline{L}_{ij}} \right] \right\} \tag{G-6}$$

for $k = 1,2,3,4$

From the chain rule,

$$\nabla \overline{\mu}_j^c = \nabla \overline{c}_j \cdot \frac{\partial \overline{\mu}_j^c}{\partial \overline{c}_j} \tag{G-7}$$

and substituting (G-7) in (G-6) gives,

$$(G-8)$$

$$\overline{N}_k = \left\{ -\overline{c}_k \cdot \sum_{j=1}^{4} \overline{L}_{kj} \cdot \frac{\partial \overline{\mu}_j^c}{\partial \overline{c}_j} + \left\{ \left(\overline{c}_k \cdot \sum_{i=1}^{4} \overline{L}_{ki} \cdot |z_i| \right) \cdot \left(\frac{\sum_{j=1}^{4} \left[\overline{c}_j \cdot |z_j| \cdot \left(\sum_{i=1}^{4} \overline{L}_{ij} \cdot \frac{\partial \overline{\mu}_i^c}{\partial \overline{c}_j} \right) \right]}{\sum_{i=1}^{4} \overline{c}_i \cdot z_i^2 \cdot \overline{L}_{ij}} \right) \right\} \right\}$$

for k = 1,2,3,4

This can be expressed as:

$$\overline{N}_k = - \sum_{j=1}^{4} \overline{D}_{kj} \cdot \nabla \overline{c}_j \qquad (G-9)$$

where:

$$(G-10)$$

$$\overline{D}_{kj} = \overline{c}_k \cdot \left\{ \overline{L}_{kj} \cdot \frac{\partial \mu_j^c}{\partial \overline{c}_j} - \left\{ \left(\sum_{i=1}^{4} \overline{L}_{ki} \cdot |z_i| \right) \cdot \left(\frac{\sum_{i=1}^{4} \overline{c}_i \cdot |z_i| \cdot \overline{L}_{ij} \cdot \frac{\partial \overline{\mu}_i^c}{\partial \overline{c}_j}}{\sum_{i=1}^{4} \overline{c}_i \cdot z_i^2 \cdot \overline{L}_{ij}} \right) \right\} \right\}$$

for k = 1,2,3,4 and j = 1,2,3,4

B. Simplifying Assumptions

1.0 Elimination of Cross Phenomenological Coefficients

If we assume that cross phenomenological coefficients are zero,

$$\bar{L}_{1k} = \bar{L}_{k1} = \bar{L}_{2k} = \bar{L}_{k2} = \bar{L}_{3k} = \bar{L}_{k3} = \bar{L}_{4k} = \bar{L}_{k4} = 0 \quad \text{(G-11)}$$

and,

$$\sum_{i=1}^{4} \bar{L}_{ki} \cdot |z_i| = \bar{L}_{kk} \cdot |z_k| \quad \text{(G-12)}$$

resulting in:

$$\sum_{i=1}^{4} \bar{c}_i \cdot z_i^2 \cdot \bar{L}_{ij} = \sum_{i=1}^{4} \bar{c}_i \cdot z_i^2 \cdot \bar{L}_{ii} \quad \text{(G-13)}$$

The following diffusion coefficients result from substitution

of (G-12) and (G-13) in equation (G-10): (G-14)

$$\bar{D}_{kj} = \bar{c}_k \cdot \left\{ \bar{L}_{kj} \cdot \frac{\partial \bar{\mu}_j^c}{\partial \bar{c}_j} - \left[\frac{\bar{L}_{kk} \cdot (|z_k|) \cdot \bar{c}_j \cdot (|z_j|) \cdot \bar{L}_{jj} \cdot \dfrac{\partial \bar{\mu}_j^c}{\partial \bar{c}_j}}{\sum_{i=1}^{4} z_i^2 \cdot \bar{c}_i \bar{L}_{ii}} \right] \right\}$$

$$= - \left[\frac{\bar{c}_k \cdot \bar{c}_j \cdot \bar{L}_{kk} \cdot \bar{L}_{jj} \cdot (|z_k \cdot z_j|)}{\sum_{i=1}^{4} z_i^2 \cdot \bar{c}_i \cdot \bar{L}_{ii}} \right] \cdot \frac{\partial \bar{\mu}_j^c}{\partial \bar{c}_j}$$

for k = 1,2,3,4 and j = 1,2,3,4

and, (G-15)

$$\bar{D}_{kk} = \bar{c}_k \cdot \left[\bar{L}_{kk} - \frac{\bar{L}_{kk}^2 \cdot z_k^2 \cdot \bar{c}_k}{\sum_{i=1}^{4} z_i^2 \cdot \bar{c}_i \cdot \bar{L}_{ii}} \right] \cdot \frac{\partial \bar{\mu}_k^c}{\partial \bar{c}_k}$$

for k = 1,2,3,4

2.0 Pressure-Volume Effects

If pressure in the resin and the volume of the resin are

assumed to be constant, i.e.,

$$\left[\frac{\partial(\pi\upsilon)}{\partial\bar{c}_i}\right]_T = 0 \qquad\qquad (G-16)$$

then water diffusion is negligible, and,

$$\bar{D}_{k_4}\cdot\nabla\bar{c}_4 = 0 \qquad\qquad (G-17)$$

therefore,

$$\bar{N}_k = -\sum_{j=1}^{3}\bar{D}_{kj}\cdot\nabla\bar{c}_j \qquad\qquad (G-18)$$

and

$$\left[\sum_{j=1}^{3}|z_j|\cdot\nabla\bar{c}_j\right] = 0, \text{ since } z_4 = 0 \qquad\qquad (G-19)$$

C. Elimination of species 3 in sets of equations

By expanding equation (G-18), there results

$$\bar{N}_k = -\bar{D}_{k_1}\cdot\nabla\bar{c}_1 - \bar{D}_{k_2}\cdot\nabla\bar{c}_2 - \bar{D}_{k_3}\cdot\nabla\bar{c}_3 \qquad\qquad (G-20)$$

and in view of (G-19) which yields,

$$-\nabla\bar{c}_3 = \left(\frac{|z_2|}{|z_3|}\right)\cdot\nabla\bar{c}_2 + \left(\frac{|z_1|}{|z_3|}\right)\cdot\nabla\bar{c}_1 \qquad\qquad (G-21)$$

so ,   (G-22)

$$\bar{N}_k = -\left[\bar{D}_{k_1} - \left(\frac{|z_1|}{|z_3|}\right)\cdot\bar{D}_{k_3}\right]\cdot\nabla\bar{c}_1 - \left[\bar{D}_{k_2} - \left(\frac{|z_2|}{|z_3|}\right)\cdot\bar{D}_{k_3}\right]\cdot\nabla\bar{c}_2$$

This can be shown as,

$$\bar{N}_k = -\sum_{j=1}^{2}\left[\bar{D}_{kj} - \left(\frac{|z_j|}{|z_3|}\right)\cdot\bar{D}_{k3}\right]\cdot\nabla\bar{c}_j \qquad\qquad (G-23)$$
$$\text{for } k = 1,2$$

or,

$$\bar{N}_k = -\sum_{j=1}^{2}\bar{D}'_{kj}\cdot\nabla\bar{c}_j \quad , \text{ for } k = 1,2 \qquad\qquad (G-24)$$

D. Effective Diffusion Coefficients – chemical potential

By combining equations (G-15) and (G-16) to satisfy (G-23) and (G-24), there results,

$$(G-25)$$

$$\overline{D}'_{kj} = \overline{c}_k \cdot (|z_j \cdot z_k|) \cdot \overline{L}_{kk} \cdot \left[\frac{\left(\overline{L}_{33} \cdot \overline{c}_3 \cdot \dfrac{\partial \overline{\mu}_3^c}{\partial \overline{c}_3} - \overline{L}_{jj} \cdot \overline{c}_j \cdot \dfrac{\partial \overline{\mu}_j^c}{\partial \overline{c}_j} \right)}{\displaystyle\sum_{i=1}^{3} \overline{c}_i \cdot z_i^2 \cdot \overline{L}_{ii}} \right]$$

$$k \neq j$$

for $k = 1,2$ and $j = 1,2$

Assuming the "self" diffusion coefficient of species k is:

$$\overline{D}_k = R \cdot T \cdot \overline{L}_{kk} \qquad (G-26)$$

The chemical potential is defined as:

$$\overline{\mu}_k^c \equiv R \cdot T \cdot \ell n(\overline{a}_k) \qquad (G-27)$$

then:

$$\frac{\partial \overline{\mu}_k^c}{\partial \overline{c}_k} = R \cdot T \cdot \left(\frac{\partial \ell n(\overline{a}_k)}{\partial \overline{c}_k} \right) \qquad (G-28)$$

Substituting equations (G-26) and (G-27) in equation (G-24) yields,

$$(G-29)$$

$$\overline{D}'_{kj} = \overline{c}_k \cdot (|z_k \cdot z_j|) \cdot \overline{D}_k \cdot \left[\frac{\left(\overline{D}_3 \cdot \overline{c}_3 \cdot \dfrac{\partial \ell n(\overline{a}_3)}{\partial \overline{c}_3} - \overline{D}_j \cdot \overline{c}_j \cdot \dfrac{\partial \ell n(\overline{a}_j)}{\partial \overline{c}_j} \right)}{\displaystyle\sum_{i=1}^{3} \overline{c}_i \cdot z_i^2 \cdot \overline{D}_i} \right]$$

$$k \neq j$$

for $k = 1,2$ and $j = 1,2$

likewise (G-30)

$$
\overline{D}_{kk}' = \overline{c}_k \cdot \overline{D}_k \cdot \left\{ \frac{\partial \ell n(\overline{a}_k)}{\partial \overline{c}_k} - z_k^2 \cdot \left[\frac{\left(\overline{D}_k \cdot \overline{c}_k \cdot \dfrac{\partial \ell n(\overline{a}_k)}{\partial \overline{c}_k} - \overline{D}_3 \cdot \overline{c}_3 \cdot \dfrac{\partial \ell n(\overline{a}_3)}{\partial \overline{c}_3} \right)}{\displaystyle\sum_{i=1}^{3} \overline{c}_i \cdot z_i^2 \cdot \overline{D}_i} \right] \right\}
$$

for $k = 1,2$

The activity of species k is given as,

$$
\overline{a}_k = \overline{\gamma}_k \cdot \overline{c}_k \tag{G-31}
$$

where $\overline{\gamma}_k$ is the molar activity coefficient

and therefore,

$$
\frac{\partial \ell n(\overline{a}_k)}{\partial \overline{c}_k} = \frac{1}{\overline{c}_k} + \frac{\partial \ell n(\overline{\gamma}_k)}{\partial \overline{c}_k} \tag{G-32}
$$

Substituting for $\dfrac{\partial \ell n(\overline{a}_k)}{\partial \overline{c}_k}$ in equations (G-29) and (G-30)

yields, (G-33)

$$
\overline{D}_{kk}' = \overline{c}_k \cdot \overline{D}_k \cdot \left\{ \left[\frac{1}{\overline{c}_k} + \frac{\partial \ell n(\overline{\gamma}_k)}{\partial \overline{c}_k} \right] \right.
$$

$$
\left. - z_k^2 \cdot \left[\frac{\left(\overline{D}_k \cdot \left[1 + \overline{c}_k \cdot \dfrac{\partial \ell n(\overline{\gamma}_k)}{\partial \overline{c}_k} \right] - \overline{D}_3 \cdot \left[1 + \overline{c}_3 \cdot \dfrac{\partial \ell n(\overline{\gamma}_3)}{\partial \overline{c}_3} \right] \right)}{\displaystyle\sum_{i=1}^{3} \overline{c}_i \cdot z_i^2 \cdot \overline{D}_i} \right] \right\}
$$

for $k = 1,2$

and ,

$$(G-34)$$

$$\overline{D}'_{kj} = \overline{c}_k \cdot (|z_k \cdot z_j|) \cdot \overline{D}_k \cdot \left[\frac{\left[\overline{D}_3 \cdot \left(1 + \overline{c}_3 \cdot \frac{\partial \ell n(\overline{\gamma}_3)}{\partial \overline{c}_3} \right) \right] - \overline{D}_j \cdot \left(1 + \overline{c}_j \cdot \frac{\partial \ell n(\overline{\gamma}_j)}{\partial \overline{c}_j} \right)}{\sum\limits_{i=1}^{3} \overline{c}_i \cdot z_i^2 \cdot \overline{D}_i} \right]$$

$$j \neq k$$

for $k = 1,2$ and $j = 1,2$

Quasilinearization of Non-linear Terms

Numerical Approximation of Resin Phase Continuity Equations

- Ternary System -

Several terms appear in the resin phase continuity equations
for the ternary system which are non linear, in addition to the
equilibrium relationship. Multiplication of finite difference
equations approximating those terms result in algebraic variables
which cannot be separated, and the quasilinearization approach
is used to resolve those terms. The following terms are treated
accordingly.

o $\quad \left(\dfrac{\partial \bar{x}_i}{\partial \rho}\right)^2 \quad$ at j^{+1th} time step

---

quasilinearization, where n+1 is the n+1th iteration

leads to: $\hfill$ (H-1)

$$\left(\frac{\partial \bar{x}_i}{\partial \rho}\right)^2_{n+1} = \left(\frac{\partial \bar{x}_i}{\partial \rho}\right)^2_n + \left(\left(\frac{\partial \bar{x}_i}{\partial \rho}\right)_{n+1} - \left(\frac{\partial \bar{x}_i}{\partial \rho}\right)_n\right) \cdot \left(\frac{\partial \left(\frac{\partial \bar{x}_i}{\partial \rho}\right)^2}{\partial \left(\frac{\partial \bar{x}_i}{\partial \rho}\right)}\right)_n$$

$$= 2 \cdot \left(\frac{\partial \bar{x}_i}{\partial \rho}\right)_n \cdot \left(\frac{\partial \bar{x}_i}{\partial \rho}\right)_{n+1} - \left(\frac{\partial \bar{x}_i}{\partial \rho}\right)^2_n$$

o $\quad \left(\dfrac{\partial \bar{x}_i}{\partial \rho}\right) \cdot \left(\dfrac{\partial \bar{x}_j}{\partial \rho}\right) \quad$ at j^{+1th} time step

---

quasilinearization leads to: $\hfill$ (H-2)

$$\left(\left(\frac{\partial \bar{x}_i}{\partial \rho}\right) \cdot \left(\frac{\partial \bar{x}_j}{\partial \rho}\right)\right)_{n+1} = \left(\left(\frac{\partial \bar{x}_i}{\partial \rho}\right) \cdot \left(\frac{\partial \bar{x}_j}{\partial \rho}\right)\right)_n + \left(\left(\frac{\partial \bar{x}_i}{\partial \rho}\right)_{n+1} - \left(\frac{\partial \bar{x}_i}{\partial \rho}\right)_n\right) \cdot \left(\frac{\partial \bar{x}_j}{\partial \rho}\right)_n$$

(H-2) continued

$$+ \left[\left[\frac{\partial \overline{x}_i}{\partial \rho} \right]_{n+1} - \left[\frac{\partial \overline{x}_i}{\partial \rho} \right]_n \right] \cdot \left[\frac{\partial \overline{x}_i}{\partial \rho} \right]_n$$

since:

$$\frac{\partial \left[\left[\frac{\partial \overline{x}_i}{\partial \rho} \right] \cdot \left[\frac{\partial \overline{x}_i}{\partial \rho} \right] \right]}{\partial \left[\frac{\partial \overline{x}_i}{\partial \rho} \right]} = \left[\frac{\partial \overline{x}_i}{\partial \rho} \right] \tag{H-3}$$

and:

$$\frac{\partial \left[\left[\frac{\partial \overline{x}_i}{\partial \rho} \right] \cdot \left[\frac{\partial \overline{x}_i}{\partial \rho} \right] \right]}{\partial \left[\frac{\partial \overline{x}_i}{\partial \rho} \right]} = \left[\frac{\partial \overline{x}_i}{\partial \rho} \right] \tag{H-4}$$

clearing terms in (H-2) leads to:

$$\text{o} \quad \left[\left[\frac{\partial \overline{x}_i}{\partial \rho} \right] \cdot \left[\frac{\partial \overline{x}_i}{\partial \rho} \right] \right]_{n+1} = \left[\frac{\partial \overline{x}_i}{\partial \rho} \right]_{n+1} \cdot \left[\frac{\partial \overline{x}_i}{\partial \rho} \right]_n + \left[\frac{\partial \overline{x}_i}{\partial \rho} \right]_{n+1} \cdot \left[\frac{\partial \overline{x}_i}{\partial \rho} \right]_n \tag{H-5}$$

$$- \left[\left[\frac{\partial \overline{x}_i}{\partial \rho} \right] \cdot \left[\frac{\partial \overline{x}_i}{\partial \rho} \right] \right]_n$$

Since the concentration values from the nth iteration are known, they are treated as constants in the $n+1^{th}$ iteration, and the iterations are repeated until convergence criteria are met at each time step. Satisfactory solution tolerances were met in 3 to 5 iterations in most cases studied.

COUPLING OF RESIN PHASE MATRIX EQUATIONS TO THE
FLUID PHASE MATRIX EQUATIONS – TERNARY FIXED BED MODEL

A. General

The seven diagonal array solution algorithm allows the solution of the coupled resin phase diffusion equations. The boundary conditions at the resin–electrolyte phase interface allow carrying the resin phase compositions into the solution of the coupled electrolyte phase equations, which equations are solved by the five diagonal array algorithm. This section deals with the coupling of the matrices and vectors describing the equations for both phases, through that boundary condition relationship.

B. Resin Phase Equations – Matrix Notation

In matrix notation, the coupled resin phase equations (5-81) and (5-82) are: (I-1)

$$A_{i_n} \cdot \bar{x}1_{i_{n+1}} = D_{i_n} + R_{i_n} \cdot \bar{x}2_{i_{n+1}} + E1_n \cdot x1_{bulk}(i,j+1)_{n+1} - E2_n \cdot x2_{bulk}(i,j+1)_{n+1}$$

and (I-2)

$$\Lambda_{i_n} \cdot \bar{x}2_{i_{n+1}} = \Pi_{i_n} + \Theta_{i_n} \cdot \bar{x}1_{i_{n+1}} + \Omega2_n \cdot x2_{bulk}(i,j+1)_{n+1} - \Omega1_n \cdot x1_{bulk}(i,j+1)_{n+1}$$

C. Seven Diagonal Array Algorithm and Resolving of Resin Surface Concentration in terms of the Bulk Electrolyte Concentrations

The coefficients and vectors are loaded into a scratch 7 diagonal array (fig. 5-1) and (fig. E-2) in which the vectors bb_N^7 and bb_{N-1}^7 are the solution vectors for equations (I-2) and (I-1) respectively. These two vectors also contain the

boundary conditions:

$$\Omega2_n \bullet x_{2_{bulk}}(i,j+1)_{n+1} \qquad (I-3)$$

$$\Omega1_n \bullet x_{1_{bulk}}(i,j+1)_{n+1} \qquad (I-4)$$

and:

$$E1_n \bullet x_{1_{bulk}}(i,j+1)_{n+1} \qquad (I-5)$$

$$E2_n \bullet x_{2_{bulk}}(i,j+1)_{n+1} \qquad (I-6)$$

respectively.

Taking advantage of the solution algorithms given by

equation (E-32),

$$\bar{x}_2(M,i,j+1)_{n+1} = FF_N^7 = \overbrace{\left[\frac{bb_N^7 - FF_{N-3}^7 \bullet \theta_N^7 - FF_{N-2}^7 \bullet \alpha_N^7}{\omega_N^7}\right]}^{\varepsilon} - \left[\frac{FF_{N-1}^7 \bullet \beta_N^7}{\omega_N^7}\right] \qquad (I-7)$$

$$\text{where } bb_N^7 = \pi_n(M,i,j) \qquad (I-8)$$

but bb_N^7 includes the term $\left[\Omega2_n \bullet x_{2_{bulk}}(i,j+1)_{n+1} - \Omega1_n \bullet x_{1_{bulk}}(i,j+1)\right]$

so

$$\bar{x}_2(M,i,j+1)_{n+1} = \varepsilon - \left[\frac{FF_{N-1}^7 \bullet \beta_N^7}{\omega_N^7}\right] \qquad (I-9)$$

$$+ \left[\frac{\left[\Omega2_n \bullet x_{2_{bulk}}(i,j+1)_{n+1} - \Omega1_n \bullet x_{1_{bulk}}(i,j+1)_{n+1}\right]}{\omega_N^7}\right]$$

and therefore by equations (E-43) and (I-1):

$$FF_{N-1}^7 = \overbrace{\left[\frac{\left[bb_{N-1}^7 - FF_{N-4}^7 \bullet \theta_{N-1}^7 - FF_{N-3}^7 \bullet \alpha_{N-1}^7 - FF_{N-2}^7 \bullet \beta_{N-1}^7\right]}{\omega_{N-1}^7}\right]}^{\varepsilon\varepsilon} \qquad (I-10)$$

$$+ \left[\frac{\left[E1_n \bullet x_{1_{bulk}}(i,j+1)_{n+1} - E2_n \bullet x_{2_{bulk}}(i,j+1)_{n+1}\right]}{\omega_{N-1}^7}\right]$$

$$= \varepsilon\varepsilon + \left[\frac{\left[E1_n \bullet x_{1_{bulk}}(i,j+1)_{n+1} - E2_n \bullet x_{2_{bulk}}(i,j+1)_{n+1}\right]}{\omega_{N-1}^7}\right]$$

where:

$$bb^7_{N-1} = d_n(M,i,j) \tag{I-11}$$

so from equation (E-38) the following expression results:

$$\bar{x}_1(M,i,j+1)_{n+1} = FF^7_{N-1} - \gamma^7_{N-1} \cdot \bar{x}_2(M,i,j+1)_{n+1} \tag{I-12}$$

Combining equation (I-10) with (I-12) yields: (I-13)

$$\bar{x}_1(M,i,j+1)_{n+1} = \varepsilon\varepsilon + \left[\frac{\left[E1_n \cdot x_{1_{bulk}}(i,j+1)_{n+1} - E2_n \cdot x_{2_{bulk}}(i,j+1)_{n+1} \right]}{\omega^7_{N-1}} \right]$$

$$- \gamma^7_{N-1} \cdot \bar{x}_2(M,i,j+1)_{n+1}$$

and in terms of $\bar{x}_2$, using equations (I-10) and (I-9): (I-14)

$$\bar{x}_2(M,i,j+1)_{n+1} = \varepsilon + \left[\frac{\left[\Omega2_n \cdot x_{2_{bulk}}(i,j+1)_{n+1} - \Omega1_n \cdot x_{1_{bulk}}(i,j+1)_{n+1} \right]}{\omega^7_N} \right]$$

$$- \left[\frac{\varepsilon\varepsilon \cdot \beta^7_N}{\omega^7_N} \right] - \left[\frac{\left[E1_n \cdot x_{1_{bulk}}(i,j+1)_{n+1} - E2_n \cdot x_{2_{bulk}}(i,j+1)_{n+1} \right]}{\omega^7_{N-1} \cdot \omega^7_N} \right] \cdot \beta^7_N$$

$$= \varepsilon - \left[\frac{\varepsilon\varepsilon \cdot \beta^7_N}{\omega^7_N} \right] + \overbrace{\left[\frac{\Omega2_n}{\omega^7_N} + \frac{E2_n \cdot \beta^7_N}{\omega^7_{N-1} \cdot \omega^7_N} \right]}^{\psi_2} \cdot x_{2_{bulk}}(i,j+1)_{n+1}$$

$$- \overbrace{\left[\frac{\Omega1_n}{\omega^7_N} + \frac{E1_n \cdot \beta^7_N}{\omega^7_{N-1} \cdot \omega^7_N} \right]}^{\psi_1} \cdot x_{1_{bulk}}(i,j+1)_{n+1}$$

$$= \varepsilon - \left[\frac{\varepsilon\varepsilon \cdot \beta^7_N}{\omega^7_N} \right] + \psi_2 \cdot x_{2_{bulk}}(i,j+1)_{n+1} - \psi_1 \cdot x_{1_{bulk}}(i,j+1)_{n+1}$$

In view of (I-13) and (I-14), the following can be shown:

$$(I-15)$$

$$\overline{x}_1(M,i,j+1)_{n+1} = \varepsilon\varepsilon + \left[\frac{\left(E1_n \cdot x_{1_{bulk}}(i,j+1)_{n+1} - E2_n \cdot x_{2_{bulk}}(i,j+1)_{n+1}\right)}{\omega_{N-1}^7}\right]$$

$$- \gamma_{N-1}^7 \cdot \varepsilon + \left(\frac{\gamma_{N-1}^7 \cdot \beta_N^7}{\omega_N^7}\right) \cdot \varepsilon\varepsilon - \gamma_{N-1}^7 \cdot \psi_2 \cdot x_{2_{bulk}}(i,j+1)_{n+1}$$

$$+ \gamma_{N-1}^7 \cdot \psi_1 \cdot x_{1_{bulk}}(i,j+1)_{n+1}$$

$$= \varepsilon\varepsilon \cdot \overbrace{\left[1 + \left(\frac{\beta_N^7 \cdot \gamma_{N-1}^7}{\omega_N^7}\right)\right]}^{\tau_2} + \overbrace{\left[\frac{E1_n}{\omega_{N-1}^7} + \psi_1 \cdot \gamma_{N-1}^7\right]}^{\rho_1} \cdot x_{1_{bulk}}(i,j+1)_{n+1}$$

$$- \overbrace{\left[\frac{E2_n}{\omega_{N-1}^7} + \psi_2 \cdot \gamma_{N-1}^7\right]}^{\rho_2} \cdot x_{2_{bulk}}(i,j+1)_{n+1} - \varepsilon \cdot \gamma_{N-1}^7$$

So,

$$(I-16)$$

$$\overline{x}_1(M,i,j+1)_{n+1} = \tau_2 + \rho_1 \cdot x_{1_{bulk}}(i,j+1)_{n+1} - \rho_2 \cdot x_{2_{bulk}}(i,j+1)_{n+1} - \varepsilon \cdot \gamma_{N-1}^7$$

The resin phase concentrations at the boundary condition have now been described in terms of the bulk electrolyte phase concentrations at every column node, $i = 1$ to I.

D. Resolution of the Electrolyte Phase Concentrations – Five Diagonal Array

In matrix notation, the coupled electrolyte phase equations, (7-27) and (7-28), are:

$$(I-17)$$

$$B1_{i_n} \cdot x_{1_{bulk}}(i,j+1)_{n+1} = U1_{i_n} + V1_i \cdot \left\{ \left. \left(\frac{dx_1^*}{d\bar{x}_1} \right) \right|_{int} (i,j+1) \right\}_n \cdot \bar{x}_1(M,i,j+1)_{n+1}$$

$$+ V1_i \cdot \left\{ \left. \left(\frac{dx_1^*}{d\bar{x}_2} \right) \right|_{int} (i,j+1) \right\}_n \cdot \bar{x}_2(M,i,j+1)_{n+1}$$

$$B2_{i_n} \cdot x_{2_{bulk}}(i,j+1)_{n+1} = U2_{i_n} + V2_i \cdot \left\{ \left. \left(\frac{dx_2^*}{d\bar{x}_2} \right) \right|_{int} (i,j+1) \right\}_n \cdot \bar{x}_2(M,i,j+1)_{n+1}$$

$$+ V2_i \cdot \left\{ \left. \left(\frac{dx_2^*}{d\bar{x}_1} \right) \right|_{int} (i,j+1) \right\}_n \cdot \bar{x}_1(M,i,j+1)_{n+1}$$

Substituting (I-16) and (I-14) into (I-17) and (I-18) results in:

$$B1_{i_n} \cdot x_{1_{bulk}}(i,j+1)_{n+1} = U1_{i_n} + \left\{ \left[V1_i \cdot \left. \left(\frac{dx_1^*}{d\bar{x}_1} \right) \right|_{int} (i,j+1) \right]_n \cdot \left[\tau_2 + \rho_1 \cdot x_{1_{bulk}}(i,j+1)_{n+1} \right. \right.$$

$$\left. \left. - \rho_2 \cdot x_{2_{bulk}}(i,j+1)_{n+1} - \varepsilon \cdot \gamma_{N-1}^7 \right] + \left[V1_i \cdot \left. \left(\frac{dx_1^*}{d\bar{x}_2} \right) \right|_{int} (i,j+1) \right]_n \right.$$

$$\left. \cdot \left[\varepsilon - \left(\frac{\varepsilon\varepsilon \cdot \beta_N^7}{\omega_N^7} \right) + \psi_2 \cdot x_{2_{bulk}}(i,j+1)_{n+1} - \psi_1 \cdot x_{1_{bulk}}(i,j+1)_{n+1} \right] \right\}$$

and, (I-20)

$$B2_{i_n} \cdot x_{2_{bulk}}(i,j+1)_{n+1} = U2_{i_n} + \left\{ \left[V2_i \cdot \left| \frac{dx_2^*}{d\overline{x}_2} \right|_{int} (i,j+1) \right]_n \cdot \left[\varepsilon - \left(\frac{\varepsilon\varepsilon \cdot \beta_N^7}{\omega_N^7} \right) \right] \right.$$

$$+ \psi_2 \cdot x_{2_{bulk}}(i,j+1)_{n+1} - \psi_1 \cdot x_{1_{bulk}}(i,j+1)_{n+1} \Bigg] \Bigg]$$

$$+ \left[V2_i \cdot \left| \frac{dx_2^*}{d\overline{x}_1} \right|_{int} (i,j+1) \right]_n \cdot \left[\tau_2 + \rho_1 \cdot x_{1_{bulk}}(i,j+1)_{n+1} - \rho_2 \cdot x_{2_{bulk}}(i,j+1)_{n+1} \right] \Bigg\}$$

Collecting terms, the following expressions result:

(I-21)

$$\overbrace{}^{VV1(i,j+1)_n}$$

$$B1_{i_n} \cdot x_{1_{bulk}}(i,j+1)_{n+1} = U1_{i_n} + \left\{ \left[V1_i \cdot \left| \frac{dx_1^*}{d\overline{x}_1} \right|_{int} (i,j+1) \right]_n \cdot \left[\tau_2 - \varepsilon \cdot \gamma_{N-1}^7 \right] \right.$$

$$\overbrace{}^{VV1(i,j+1)_n,\ continued}$$

$$+ V1_i \cdot \left| \frac{dx_1^*}{d\overline{x}_2} \right|_{int} (i,j+1) \Bigg]_n \cdot \left[\varepsilon - \left(\frac{\varepsilon\varepsilon \cdot \beta_N^7}{\omega_N^7} \right) \right] \Bigg\}$$

$$\overbrace{}^{g1(i,j+1)_n}$$

$$+ \left[\left[V1_i \cdot \left| \frac{dx_1^*}{d\overline{x}_1} \right|_{int} (i,j+1) \right]_n \cdot \rho_1 - \left[V1_i \cdot \left| \frac{dx_1^*}{d\overline{x}_2} \right|_{int} (i,j+1) \right]_n \cdot \psi_1 \right] \cdot x_{1_{bulk}}(i,j+1)_{n+1}$$

$$\overbrace{}^{g2(i,j+1)_n}$$

$$+ \left[\left[V1_i \cdot \left| \frac{dx_1^*}{d\overline{x}_2} \right|_{int} (i,j+1) \right]_n \cdot \psi_2 - \left[V1_i \cdot \left| \frac{dx_1^*}{d\overline{x}_1} \right|_{int} (i,j+1) \right]_n \cdot \rho_2 \right] \cdot x_{2_{bulk}}(i,j+1)_{n+1}$$

Final condensation of terms results in: (I-22)

$$B1_{i_n} \cdot x_{1_{bulk}}(i,j+1)_{n+1} = U1_{i_n} + VV1(i,j+1)_n + g1(i,j+1)_n \cdot x_{1_{bulk}}(i,j+1)_{n+1}$$

$$+ g2(i,j+1)_n \cdot x_{2_{bulk}}(i,j+1)_{n+1}$$

where from Figure (7-1),

$$\alpha 1_i{}' = \alpha 1_i - g1(i,j+1)_n \qquad (I-23)$$

Likewise, (I-24)

$$B2_{i_n} \cdot x_{2_{bulk}}(i,j+1)_{n+1} = U2_{i_n} + \overbrace{\left[V2_i \cdot \left(\left.\frac{dx_2^*}{d\bar{x}_2}\right|_{int}(i,j+1) \right)_n \cdot \left(\varepsilon - \left[\frac{\varepsilon\varepsilon \cdot \beta_N^7}{\omega_N^7} \right] \right) \right.}^{VV2(i,j+1)_n}$$

$$\overbrace{\left. + V2_i \cdot \left(\left.\frac{dx_2^*}{d\bar{x}_1}\right|_{int}(i,j+1) \right)_n \cdot \left(\tau_2 - \varepsilon \cdot \gamma_{N-1}^7 \right) \right]}^{VV2(i,j+1)_n \ , \ continued}$$

$$+ \overbrace{\left[\left(V2_i \cdot \left(\left.\frac{dx_2^*}{d\bar{x}_2}\right|_{int}(i,j+1) \right)_n \cdot \psi_2 - V2_i \cdot \left(\left.\frac{dx_2^*}{d\bar{x}_1}\right|_{int}(i,j+1) \right)_n \cdot \rho_2 \right) \cdot x_{2_{bulk}}(i,j+1)_{n+1} \right]}^{h2(i,j+1)_n}$$

$$+ \overbrace{\left[\left(V2_i \cdot \left(\left.\frac{dx_2^*}{d\bar{x}_1}\right|_{int}(i,j+1) \right)_n \cdot \rho_1 - V2_i \cdot \left(\left.\frac{dx_2^*}{d\bar{x}_2}\right|_{int}(i,j+1) \right)_n \cdot \psi_1 \right) \cdot x_{1_{bulk}}(i,j+1)_{n+1} \right]}^{h1(i,j+1)_n}$$

(I-25)

$$B2_{i_n} \cdot x_{2_{bulk}}(i,j+1)_{n+1} = U2_{i_n} + VV2(i,j+1)_n + h2(i,j+1)_n \cdot x_{2_{bulk}}(i,j+1)_{n+1}$$

$$+ h1(i,j+1)_n \cdot x_{1_{bulk}}(i,j+1)_{n+1}$$

where from Figure (7-1),

$$\alpha 2_i' = \alpha 2_i - h2(i,j+1)_n \qquad (I-26)$$

The five diagonal algorithm, called ZSOLVE, solves for values

of $x_{1_{bulk}}(i,j+1)_{n+1}$ and $x_{2_{bulk}}(i,j+1)_{n+1}$ as illustrated in Fig. (7-1),

and as outlined in Appendix F.

E. <u>Resolution of Resin Phase Concentrations – Seven Diagonal Array</u>

In order to compute the values for $\bar{x}_1(M,i,j+1)_{n+1}$ and

$\bar{x}_2(M,i,j+1)_{n+1}$ we note that from Appendix E and Fig. (5-1),

$\bar{x}_2(M,i,j+1)_{n+1} = FF_N^7$ as defined by equation (I-9), for which

the $n+1^{th}$ values of $x_{i_{bulk}}(i,j+1)_{n+1}$ are now known, and:

$$\bar{x}_1(M,i,j+1)_{n+1} = FF_{N-1}^7 - \gamma_{N-1}^7 \cdot \bar{x}_2(M,i,j+1)_{n+1} \qquad (I-12)$$

The FF_{N-1}^7 term can be computed from (I-10) since the

$x_{i_{bulk}}(i,j+1)_{n+1}$ values are known, and $\bar{x}_1(M,i,j+1)_{n+1}$ values

can be computed from (I-12) since $\bar{x}_2(M,i,j+1)_{n+1}$ values are

known. Using the algorithm described in Appendix E for the

remaining sequence of $\bar{x}_i$ values, and keeping in mind that the

$\bar{x}_1$ and $\bar{x}_2$ values alternate in the scratch array XSOLVE, the

remaining resin phase concentrations are calculated.

The sequence is repeated, updating quasilinearized

expressions at each iteration, until convergence is attained

for the given time step.

NUMERICAL SOLUTION DEVELOPMENT

MODEL FOR ION EXCHANGE IN FIXED BEDS

BINARY SYSTEMS

A. Resin and Fluid Phase Matrix Equations

The resin phase equations in matrix notation are given in

equation (5-71) as:

$$
A_{i_n} \cdot \bar{x}_{1_{i_{n+1}}} = D_{i_n} + E_{i_n} \cdot x_{1_{bulk}} (i,j+1)_{n+1} \tag{J-1}
$$

The fluid phase equations in matrix notation are given as an

adaptation of equation (7-27):

$$
B_{i_n} \cdot x_{1_{bulk}} (i,j+1)_{n+1} = U_{i_n} + V_i \cdot \left[\frac{dx_1^*}{d\bar{x}_1} \bigg|_{int} (i,j+1) \right]_n \cdot \bar{x}_1 (M,i,j+1)_{n+1} \tag{J-2}
$$

B. Tridiagonal Treatment, Resin Phase

Recognizing that $E_{i_n} \cdot x_{1_{bulk}} (i,j+1)_{n+1}$ applies only at $m = M$, the

resin-film interface, then:

A_{i_n} can be divided into two matrices, L_{i_n} and Q_{i_n},

such that:

$$
A_{i_n} = L_{i_n} \cdot Q_{i_n} \tag{J-3}
$$

where:

$$ \tag{J-4} $$

$$
L_{i_n} = \begin{bmatrix} w_{1,i} & & & & \\ c_{2,i} & w_{2,i} & & & \\ & & c_{m,i} & w_{m,i} & \\ & & & c_{M,i} & w_{M,i} \end{bmatrix}_n
$$

lower diagonal

matrix

and,

$$Q_{i_n} = \begin{bmatrix} 1 & & & q_{1,i} & & \\ & 1 & & & q_{2,i} & \\ & & 1 & & & q_{m,i} \\ & & & & 1 & \end{bmatrix}_n \quad \text{upper diagonal matrix} \tag{J-5}$$

and since, from equation (5-72)

$$A_{i_n} = \begin{bmatrix} a_{1,i} & b_{1,i} & & & \\ c_{2,i} & a_{2,i} & b_{2,i} & & \\ & c_{m,i} & a_{m,i} & b_{m,i} & \\ & & c_{M,i} & a_{M,i} & \end{bmatrix}_n \tag{J-6}$$

If matrix L_{i_n} is multiplied by matrix Q_{i_n}, and the result is set equal to matrix A_{i_n}, there results the following algorithm:

$$w_{1,i} = a_{1,i} \tag{J-7}$$

$$q_{1,i} = \frac{b_{1,i}}{w_{1,i}} \tag{J-8}$$

$$w_{m,i} = a_{m,i} - c_{m,i} \cdot q_{m-1,i} \tag{J-9}$$

$$q_{m,i} = \frac{b_{m,i}}{w_{m,i}} \tag{J-10}$$

for m = 2 to M-1 and i = 1 to I, for the nth iteration

Define vector $F_{i_{n+1}} \equiv Q_{i_n} \cdot x_{1_{i_{n+1}}}$ \hfill (J-11)

where:

$$F_{i_{n+1}} = \begin{bmatrix} f_{1,i} \\ f_{m,i} \\ f_{M,i} \end{bmatrix}_{n+1} \tag{J-12}$$

and ,

$$L_{i_n} \cdot F_{i_{n+1}} = D_{i_n} + E_{i_n} \cdot x_{1_{bulk}} (i,j+1)_{n+1} \tag{J-13}$$

then ,

$$f_{1,i_{n+1}} = \left[\frac{d_{1,i}}{w_{1,i}} \right]_n \tag{J-14}$$

resulting in:

$$f_{m,i_{n+1}} = \left[\frac{\left[d_{m,i} - c_{m,i} \cdot f_{m-1,i} \right]_n}{w_{m,i_n}} \right] \tag{J-15}$$

for $m = 2$ to $M-1$

At the resin surface, the relationship becomes:

$$f_{M,i} = \left[\frac{\left[d_{M,i} - c_{M,i} \cdot f_{M-1,i} \right]_n + e_i \cdot x_{1_{bulk}} (i,j+1)_{n+1}}{w_{M,i_n}} \right] \tag{J-16}$$

In addition, since Q_{i_n} is upper triangular with all diagonal elements equal to unity, then:

$$\tag{J-17}$$

$$\bar{x}_1 (M,i,j+1)_{n+1} = f_{M,i_{n+1}} = \left[\frac{\left[d_{M,i} - c_{M,i} \cdot f_{M-1,i} \right]_n + e_i \cdot x_{1_{bulk}} (i,j+1)_{n+1}}{w_{M,i_n}} \right]$$

and $\bar{x}_1 (M,i,j+1)_{n+1}$ is now expressed as a function of $x_{1_{bulk}} (i,j+1)_{n+1}$.

C. Tridiagonal Treatment, Fluid Phase Resolution of Concentrations

Referring to the fluid phase coefficient matrix, $B1_{i_n}$ (equation (7-29)), and vector $V1_i$ (equation (7-31)), and using the revised notation for binary systems, i.e. $B1_{i_n} = B_{i_n}$, and $V1_i = V_i$, then:

$$B_{i_n} = \begin{bmatrix} \alpha_1 & \beta_1 & & & \\ \gamma_2 & \alpha_2 & \beta_2 & & \\ & \gamma_i & \alpha_i & \beta_i & \\ & & & & \\ & & & \gamma_I & \alpha_I \end{bmatrix}_n \quad \text{(J-18)} \qquad \text{and } V_i = \begin{bmatrix} v_1 \\ \vdots \\ v_i \\ \vdots \\ v_I \end{bmatrix}_n \qquad \text{(J-19)}$$

but since $\bar{x}_1(M,i,j+1)_{n+1}$ is now known in terms of $x_{1_{bulk}}(i,j+1)_{n+1}$,

a revised coefficient matrix and solution vector can be derived

for the fluid phase,

$$B'_{i_n} = \begin{bmatrix} \alpha'_1 & \beta_1 & & & \\ \gamma_2 & \alpha'_2 & \beta_2 & & \\ & \gamma_i & \alpha'_i & \beta_i & \\ & & & & \\ & & & \gamma_I & \alpha'_I \end{bmatrix}_n \qquad \text{(J-20)}$$

where: $\qquad$ (J-20)

$$\alpha'_i = \alpha_i - \left(\frac{e_i \bullet v_i \bullet \left[\frac{dx_1^*}{d\bar{x}_1} \bigg|_{int} (i,j+1) \right]_n}{w_{M,i}} \right)$$

Also, substitution of (J-17) in equation (J-2) results in:

$$\qquad \text{(J-22)}$$

$$V'_i \qquad \begin{bmatrix} v'_1 \\ \vdots \\ v'_i \\ \vdots \\ v'_I \end{bmatrix}_n \qquad \text{where:} \qquad v'_i = v_i \bullet \left(\frac{\left[d_{M,i} - c_{M,i} \bullet f_{M-1,i} \right]_n}{w_{M,i_n}} \right)$$

for i=1 to I

The matrix equation then becomes:

$$B'_{i_n} \cdot x_{1_{bulk}}(i,j+1)_{n+1} = U_{i_n} + V'_{i_n} \qquad (J-23)$$

D. Resin Phase - Resolution of Concentrations

The values of $x_{1_{bulk}}(i,j+1)_{n+1}$ are found with the tridiagonal

algorithm derived above for the fluid phase. These values are

substituted in equation (J-17) for $f_{M,i_{n+1}}$ to obtain the values

for the resin phase compositions at the surface, $\bar{x}_1(M,i,j+1)_{n+1}$,

at each i node. In view of the definition of $F_{i_{n+1}}$, equation (J-11):

$$\bar{x}_1(m,i,j+1)_{n+1} = f_{m,i_{n+1}} - q_{m,i_n} \cdot \bar{x}_1(m+1,i,j+1)_{n+1} \qquad (J-24)$$

$$\text{for } i = 1 \text{ to } I \text{ and } m = 1 \text{ to } M-1$$

E. Convergence

The remaining values of resin compositions at each node m can

be calculated for each column node i at the n+1th iteration

during time step j+1. The iterative process is continued at

time step j+1 until convergence criteria have been met for all

values of $\bar{x}_1(m,i,j+1)$ and $x_{1_{bulk}}(i,j+1)$. The criterion for convergence

normally was:

$$\frac{(value_{n+1} - value_n)}{value_{n+1}} < 10^{-5} \qquad (J-25)$$

F. Summary

In summary, the defined resin solution vectors, $f_{m,i}$, made up of

the lower diagonal coefficients and solution vectors from the

resin phase matrix equation are calculated from the resin center

to the resin surface-fluid interface. The defined vectors, $f_{M,i}$,

are then carried into the solution phase to obtain the column

compositions through the equilibrium relationship. This

relationship, as result of the quasilinearization procedure,

expresses $x_1(i)\Big|_{bulk}\Big|_{int}$ as a linear function of $\bar{x}_1(M,i)\Big|_{int}$.

The column matrix equations are then solved for $x_1(i)\Big|_{bulk}$

The values of the vector $f_{M,i}$ are then calculated, and since

$f(M,i) = \bar{x}_1(M,i)$ the values of $\bar{x}_1(M,i)$ are now known. Through use

of the calculated resin phase matrix equation upper diagonal

coefficients and the defined factors, $f_{m,i}$, the remaining

compositions in the resin phase are calculated from the surface

to the center dimension. Equilibrium estimates are refined at

each iteration through the quasilinearization procedure and the

process is repeated until convergence is attained. Normally, with

proper "conditioning" of the column prior to the time step j=1,

5 iterations per time step were required to meet the convergence

criteria at the beginning, dropping quickly to 3 and continuing to

the end of the run. This was true of both the concentration and

the activity models.

RFMAVD – FEATURES OF SIMULATION PROGRAM

FOR ION EXCHANGE IN FIXED BEDS

– BINARY SYSTEMS –

A. Main Program

1. Input and Display Options

RFMAVD, (Revised Final Mass Action (equilibrium)
Variable (solid phase) Diffusivity), the binary
model program, calls required input data, then
displays the read in information plus key calculated
parameters such as:

o diffusion coefficients of ions in electrolyte phase
at infinite dilution

o diffusion coefficients of salts in electrolyte phase
at infinite dilution

o diffusion coefficients of salts in electrolyte phase
corrected to feed normality

o activity coefficients of salts at feed normality

o Reynolds number

o Peclet number

o initial column concentration values, $\bar{x}_1(m,i)$,
$x_1{}_{bulk}(i)$, $x_1^*{}_{int}(i)$

o initial values of film coefficients, $k_L{}_{eff}(i)$

o initial average Biot number

o percent bed capacity available after initialization
procedure

    o   plug flow time to completely utilize available

          capacity in solution and resin

    o   debug options selected

2. Run Options available include:

    a. Operation in a "batch" mode.

    b. Operation with resin phase equilibrium parameters
        correlated in equivalent fraction or mole fraction
        for the resin phase.

    c. Operation with activity driving force vs.
        concentration driving force.

    d. Operation with Kataoka et al (50) electric field
        model for equal valence exchange.

    e. Selection of a particle form factor, $\alpha = 0, 1, 2$,
        for slab, cylinder, or sphere.

    f. Fractional adjustment of the constants in the
        Carberry (11) or Koloini et al (54) film
        coefficient correlation to observe effect on fit
        of ECH curves.

    g. Selection of a bypass option in which a fraction of
        the feed is assumed to bypass directly from the
        feed inlet to mix with the effluent stream.

    h. Option of no printout until $x_{1_{bulk}}$ (column outlet)
        reaches a preselected value, i.e., first appearance
        of "S" curve at column exit. Key column variables
        are written out to a separate file during that "blind
        period" for every 10 dimensionless time steps, with

every third file being replaced by the current data update. This allows examination and early "killing" of runs which appear to be of no interest to the user.

i. Since on some runs where, because of use of small grid spacing, column length spacing, and many time steps, CPU time can be up to 1-2 hours -- all required data is read out into a file every 50 minutes, which can be used to restart the program at that point if the computer is inadvertently shut down, or if the system has a batch queue time limit. In the latter case, an option is provided to shut the program down prior to the time limit for resubmission to the queue.

3. <u>Output Options</u>

o At selected times and intervals:

- Profiles at 0.1 column lengths for species 1 for:

• fluid phase composition

• interface (equilibrium) composition of fluid

• interface (equilibrium) composition of resin surface

• film coefficient

o and at a second selected interval

- either

all profiles for j and j+1 time steps for

$$\bar{x}_1(m,i), \quad x_{1_{bulk}}(i), \quad x_{1_{int}}^{*}(i), \quad \bar{D}_1(m,i), \quad \frac{\partial \bar{D}_1'(m,i)}{\partial \bar{x}_1(m,i)}$$

and $\quad \dfrac{\partial x_{1_{int}}^{*}(i)}{\partial \bar{x}_1(M,i)}$

\- or

Complete flux balance for species 1 in <u>both</u> <u>phases,</u> showing convection flux, axial dispersion flux, holdup flux, film diffusion flux, and resin accumulation flux. In addition, an approximation of the B.C. flux is computed by a backward difference approximation for comparison to the resin accumulation flux. Species 1 film diffusion flux is also calculated by the net difference resulting from the fluid phase fluxes for comparison to the resin accumulation flux. All printed at column intervals preselected.

B. <u>RFMAVD Subroutines</u>

1. <u>Input</u>

Reads in data, performs computations to obtain key program control parameters and constants, and writes out prerun information described above.

2. <u>INISHL</u>

Computes the initial distribution for column nodes 2 to IMAX, of $\bar{x}_1(MMAX,i)$, $x_{1_{bulk}}(i)$, and $x_{1_{int}}^{*}(i)$, by a procedure described in Chapter VII, Section C, paragraph 2. This procedure is based on a flux balance in which diffusion flux into the top resin layer is set equal to the flux across the film. The equilibrium values, $x_{1_{int}}^{*}(i)$, calculated by subroutine ISOTEM from the $\bar{x}_1(MMAX,i)$ values, and the film coefficients $k_{L_{eff}}(i)$ calculated by subroutine KONST, are used to obtain

the $x_{1_{bulk}}(i)$ values which permit the flux balance to close at each column node. This subroutine is used in conjunction with an initializing procedure in the Main Program in which the flux at column node 1 is balanced, based on the Boundary Condition described by equation (7-21) in Chapter VII, Section B. If the first column increment is treated as a CSFTR, then

$$x_{1_{bulk}}(1) = \frac{\left[x_{1_{bulk}}(2) + x_{1_{bulk}}(in) \cdot Pe \cdot \Delta \text{ column} \right]}{(1 + Pe \cdot \Delta \text{ column})}$$

The procedure in the Main Program solves the monotonic non-linear relationship with a false positioning procedure (secant method) embodied in subroutine AKM33.

3. <u>KONST</u>

Computes $k_{L_{eff}}(i)$ and the Biot numbers (i), at every j+1 time step using time step j values of (1) average film concentrations if the <u>pseudo electric field</u> method is utilized, or (2) calculated values of film concentrations $x_{1_{int}}^{*}(i)$ and $x_{1_{bulk}}(i)$ and $k_{L_{eff}}(i)$ if the Kataoka et al (50) electric field model is selected (applies to homovalent exchange only).

Additionally calculates the $j+1^{th}$ and n^{th} iteration values of both the resin phase and the electrolyte phase matrix coefficients and solution vectors.

4. <u>ISOTEM</u>

Computes the values of electrolyte phase concentrations $x_{1_{int}}^{*}(i)$ in equilibrium with the resin

surface compositions $\bar{x}_1$(MMAX,i). This subroutine

utilizes Lee's quasilinearization procedure to solve

the non-linear equilibrium relationship. Since this

procedure is a variant of the Newton-Raphson method,

if a guess value close to the solution is utilized,

rapid convergence is obtained. Since the concentrations

do not change rapidly between time steps, use of the

value of $x_{1_{int}}^*$ (i) from time step j as a first guess makes
this procedure work rapidly.

5. LEECAL

Calculates the derivatives required for the

quasilinearization procedure which allows expression of

$x_{1_{int}}^*$ (i) as a linear function of $\bar{x}_1$(MMAX,i). This
procedure is:

$$
\begin{aligned}
x_{1_{int}}^*(i)_{n+1} &= x_{1_{int}}^*(i)_n + \Bigg\{ \left[\frac{d\left[f\{x_{1_{int}}^*(i),\bar{x}_1(MMAX,i)\} \right]}{d\{\bar{x}_1(MMAX,i)\}} \right]_n \\
&\qquad \bullet \left[\bar{x}_1(MMAX,i)_{n+1} - \bar{x}_1(MMAX,i)_n \right] \Bigg\} \\
&\quad + \Bigg\{ \left[\frac{d\left[f\{x_{1_{int}}^*(i),\bar{x}_1(MMAX,i)\} \right]}{d\{x_{1_{int}}^*(i)\}} \right]_n \\
&\qquad \bullet \left[x_{1_{int_{n+1}}}^*(i) - x_{1_{int_n}}^*(i) \right] \Bigg\}
\end{aligned}
$$

Therefore the derivatives given in the expression
must be updated at each iteration, n + 1, with nth
values of the concentrations. The subroutine computes
the derivatives by numerical perturbation, and calls
the subroutines GAMCAL and GAMRCL to obtain the
activity coefficients.

6. GAMCAL

Computes solution ionic strength, I, and the
electrolyte phase ionic species molal activity
coefficients, γ_1 and γ_2, which are derived from the
Bromley equation. In addition, the derivatives,
$d\gamma_i/dI$ are calculated for use in the quasilinearization
procedure used to compute the equilibrium
concentrations in ISOTEM.

7. GAMRCL

Computes resin phase ion species activity
coefficients based on the Redlich-Kister equation for
binary systems, with parameters correlated in either
mole or equivalent fraction concentration units, based
on concentration arguments from the various calling
subroutines.

8. LEEKON

Performs the solution to the coupled resin and
electrolyte matrices at each time step, j+1, and
iteration, n, as described in Appendix J. Portions of
the solution vector and coefficient matrices involving
the boundary condition at the resin-film interface

are updated at the beginning of this subroutine using n^{th} iteration values of compositions. The $n+1^{th}$ values of $\bar{x}_1(m, i)$ and x_1 (i) are computed, and ISOTEM
$_{bulk}$
is called to calculate values of x_1^* (i) from the
$_{int}$
latest values of $\bar{x}_1(m, i)$.

9. DFDVNU

If the activity driving force model is used then in arriving at the term $\dfrac{\partial \bar{D}_1(m, i)}{\partial \bar{x}_1(m, i)}$, which is needed in the resin phase continuity equation, the following expression must be evaluated and added to the simpler partial derived for the concentration driving force model:

$$\frac{\partial \left[\dfrac{\left[\bar{D}_1 \cdot \bar{D}_2 \cdot \bar{x}_1 \cdot \bar{x}_2 \cdot \dfrac{\partial \ln \left[\dfrac{\gamma_1^{-|z_2|}}{\gamma_2^{-|z_1|}} \right]}{\partial \bar{x}_1} \right]}{\sum\limits_{i=1}^{2} \bar{x}_i \cdot |z_i| \cdot \bar{D}_i} \right]}{\partial \bar{x}_1}$$

The expression is separated into parts u and v, and the relationship $d(uv) = u \cdot dv + v \cdot du$ is used in the solution. The derivative of part u is taken analytically, and dv is solved by numerical perturbation.

10. AKM33

This subroutine, developed by Dr. A.K.S. Murthy, involves the secant method false positioning technique to solve non-linear relationships which are monotonic with respect to the variable whose value is required.

C. Main Program Function Details

Performs the following functions:

o   calls Input

o   performs the initialization procedure involving
    calling the subroutine INISHL. Prints out initial
    concentrations and other parameters resulting from
    the initialization procedure

o   performs the calculation procedure for dimensionless
    time, $j = 1$ to $j_{max} - 1$, by performing the following
    functions:

o   at iteration $n = 1$, sets all concentrations to
    values from the last time step j as a first
    approximation

o   at iterations $n = 2$ to n(convergence), resets all
    $j+1^{th}$ concentration approximations calculated at the
    $n-1^{th}$ iteration to those calculated at the nth
    iteration. These values are used to compute the
    derivatives required in the quasilinearization
    procedure.

o   computes the effective diffusion coefficients, $\overline{D}_{eff}(m,i)$,
    based on the jth concentration values. The effective
    diffusion coefficients can be (1) based on the harmonic
    mean of the individual species diffusion coefficients
    (Fick's Law), (2) based on the concentration model of
    Nernst-Planck, or (3) include activity effects so that
    the activity driving force is utilized instead of
    concentration.

o computes the partial derivatives of $\bar{D}_{eff}(m,i)$ with respect to $\bar{x}_1(m,i)$ when using the N-P model. When the activity driving force model is used, calls subroutine DFDVNU to obtain the second derivative terms.

o calls LEEKON for each iteration, which in turn calls KONST and LEECAL to obtain the nth values of $\bar{x}_1(m,i)$ and $x_{1_{bulk}}(i)$ at time step $j+1$. Also, LEEKON calls ISOTEM to obtain the nth values of $x_{1_{int}}^*(i)$.

o checks the indicator, ICOUNT, which represents the number of variables not meeting convergence criteria, and if>0, recycles through another iteration. The user inputs the maximum number of iterations desired before moving on, from j to $j + 1$. Since this override represents moving on without total convergence, a warning message is written out giving the count of variables not meeting convergence criteria. Iterations normally ranged between 3-5 for convergence. If the system was ill conditioned due to poor initialization, or if one species reached a very low value (binary), increasing the maximum number of iterations above, say, 20 did not provide convergent solutions. Simulations containing non-convergent sections were discarded as suspect.

o controls all output options.

TERNEX – FEATURES OF SIMULATION PROGRAM

FOR ION EXCHANGE IN FIXED BEDS

– TERNARY SYSTEMS –

A. Main Program

1. Input and Display Options

TERNEX, (TERNary Ion EXchange), the ternary model

program, calls required input data, then displays the

read in information plus key calculated parameters

such as:

o diffusion coefficients of ions in electrolyte phase

at infinite dilution

o diffusion coefficients of salts in electrolyte phase

at infinite dilution

o diffusion coefficients of salts in electrolyte phase

corrected to feed normality

o activity coefficients of salts at feed normality

o Reynolds number

o Peclet number

and displays the initial values of $\bar{x}_{j_{max}}(i)$, $x_{j_{bulk}}(i)$, $x^*_{j_{int}}(i)$,

and $k_{L_{eff}}(i)$ for the three species.

Additionally, the column average concentration for each

species is shown for each phase after initialization to

give an indication of column "preloading". Debugging options

are shown as selected by the user, if required. Unlike the

binary model, RFMAVD, only a few run options are available.

2. <u>Run Options</u>:

    a. Option of no printout until $x_{1_{bulk}}$ (column outlet) reaches a preselected value, i.e., first appearance of "S" curve at column exit. Key column variables are written out to a separate file during that "blind period", for every 10 dimensionless time steps, with every third file being replaced by the current data update. This allows examination and early "killing" of runs which appear to be of no interest to the user.

    b. Since on some runs where, because of use of small grid spacing, column length spacing, and many time steps, CPU time can be up to 1-2 hours, all required data is read out into a file every 50 minutes which can be used to restart the program at that point if the computer is inadvertently shut down, or if the system has a batch queue time limit. In the latter case, an option is provided to shut the program down prior to the time limit for resubmission to the queue.

3. <u>Output Options</u>:

    o At selected times

        −   Column average concentration for each species, both phases.

        −   Profiles @ 0.1 column lengths

               fluid phase − each component

               film coefficients − each component.

    o At other selected times

- Either

  Complete flux balance for <u>each species</u> in <u>both phases</u>, showing convection flux, dispersion flux, holdup flux, film diffusion flux, matching resin boundary condition flux, resin boundary condition flux, and resin accumulation flux. In addition, an approximation of the B.C. flux is computed by a backward difference approximation, and species 3 fluxes are computed and also arrived at by difference from species 1 and 2 fluxes for comparison.

  All printed at column intervals preselected.

- Or

  Complete composition printout of $\bar{x}_i$, $x_{i_{bulk}}$, and $x^*_{i_{int}}$ for i = 1,2,3 at both j and j+1 time steps at all column and resin nodes.

B. <u>TERNEX Subroutines</u>

  1. <u>INPUT</u>

    Reads in data, performs computations to obtain key program control parameters and constants, and writes out prerun information described above.

  2. <u>ENISHL</u>

    Supported by subroutines INSHDV and FLXCAL, performs the flux balance solution to obtain initial compositions of $\bar{x}_i(M,1)$, $x_{i_{bulk}}(i)$, and $x^*_{i_{int}}(i)$, using the Newton-Raphson method, for solution of non-linear equations.

3. <u>KFCALC</u>

Calculates $k_{L_{k_{eff}}}(i)$ and $Bi_{k_{eff}}(i)$ (Biot no.), for

$k = 1,2,3$ at every $j + 1$ calculation using j^{th}

values of fluid phase compositions. Also computes

these values as called by ENISHL for initialization.

4. <u>DRVCAL</u>

Calculates the derivatives:

$$\left[\frac{d\left(x_{k_{int}}^{*}(i,j+1)\right)}{d\left(\overline{x}_{k}(M,i,j+1)\right)}\right]_{n} \quad and, \quad \left[\frac{d\left(f\{x_{k_{int}}^{*}(i,j+1)\}\right)}{d\left(x_{k_{int}}^{*}(i,j+1)\right)}\right]_{n}$$

for $k = 1,2,3$ and $i = 1$ to I

This is performed at each time step, $j+1$, and at each

iteration,n. The method (70) for differentiation of

implicit functions is utilized (uses Cramer's Rule).

5. <u>GAMRCL</u>

Computes resin phase ionic species activity

coefficients based on the Redlich-Kister equation for

ternary systems, with parameters correlated in equivalent

fractions, based on concentration arguments from the

various calling subroutines.

6. <u>GAMCAL</u>

Computes electrolyte phase ionic species molal activity

coefficients,γ_k(where $k = 1,2,3$),based on the Bromley equation

plus the derivatives, $d\gamma_k/dI$ (where I = ionic strength),

based on concentration arguments from the various calling

subroutines.

7. <u>EQUILB</u>

Computes, with its support subroutine, EQICAL,

the values of $x_{k_{int}}^*(i,j+1)_n$ from input values of

$\bar{x}_k(M,i,j+1)_n$ for $k = 1,2,3$ at $i=1$ to I based on the

Newton-Raphson method for solution of non-linear

equations. EQICAL computes the numerical derivatives

of the functions with respect to $x_{1_{int}}^*(i,j+1)_n$ and

$x_{2_{int}}^*(i,j+1)_n$ for use in the Newton-Raphson method

for solving non-linear equations.

8. <u>DFTYCL</u>

Computes:

$$\bar{D}_{kk}'(m,i,j), \quad \bar{D}_{k\ell}'(m,i,j), \quad \frac{\partial \bar{D}_{kk}'(m,i,j)}{\partial \bar{x}_k(m,i,j)}, \quad \frac{\partial \bar{D}_{k\ell}'(m,i,j)}{\partial \bar{x}_k(m,i,j)}$$

for $k = 1,2,3$ and $\ell = 1,2,3$

at $m = 1$ to M and $i = 1$ to I utilizing concentrations

calculated at time step j versus $j+1$.

9. <u>CONCAL</u>

Computes the $j+1^{th}$ and n^{th} iteration values of

resin phase matrix coefficients and solution vectors.

10. <u>ZCONCL</u>

Computes the $j+1^{th}$ and n^{th} iteration values of

electrolyte phase matrix coefficients and solution

vectors.

11. <u>ZSOLVE</u>

Scratch 5-diagonal array algorithm which solves for

electrolyte phase concentrations $x_{k_{bulk}}(i.j+1)_n$ $(k = 1,2)$

for $i = 1$ to I at each time step, $j+1$, and each iteration, n,

based on coefficients and vectors computed by ZCONCL.

12. **X1SOLVE and X2SOLVE**

Scratch 7-diagonal array algorithm which solves for resin phase concentrations $\bar{x}_k(m,i,j+1)_n$ ($k = 1,2$) for $m = 1$ to M and $i = 1$ to I, at each iteration, n, and time step, $j+1$, with coefficients and vectors computed by CONCAL. Calls ZCONCL and ZSOLVE to get latest values of $x_{k_{bulk}}(i,j+1)_n$, since these are part of the solution vector for $\bar{x}_k(M,i,j+1)_n$ ($k = 1,2$) for $i = 1$ to I. As discussed in Chapter V, Section D, the algorithms give better precision if the larger of $\bar{x}_1(1,i,j+1)_{n+1}$ or $\bar{x}_2(1,i,j+1)_{n+1}$ is in the first position in the scratch array, the decision being based on their respective values at the nth iteration.

C. **Main Program Function Details**

Performs following functions:

o   calls INPUT

o   calls ENISHL

o   performs the calculation procedure from dimensionless time, $j = 1$ to $j_{max} - 1$, by performing the following functions:

o   calls EQUILB, KFCALC, and DFTYCL to get j^{th} values of variables

o   at $n = 1$, sets all concentrations to values at last time step j as a first approximation, where n is iteration number

o   at n_2 to $n_{convergence}$, resets all $j+1^{th}$ concentration approximations calculated at the $n-1^{th}$ iteration to those calculated at the nth iteration. These values are used to compute the derivatives required in the quasilinearization procedure.

o   calls X1SOLVE or X2SOLVE

o   checks the indicator, ICOUNT, which represents the number of variables not meeting convergence criteria, and if>0, recycles through another iteration. The user inputs the maximum number of iterations desired before moving on, from j to j + 1. Since this override represents moving on without total convergence, a warning message is written out giving the count of variables not meeting convergence criteria. Iterations normally ranged between 3-5 for convergence. If the system was ill conditioned due to poor initialization, or if one species reached a very low value (binary), increasing the maximum number of iterations above say 20 did not provide convergent solutions. Simulations containing non-convergent sections were discarded as suspect.

o   controls all output options.

LISTING OF PROGRAMS DEVELOPED IN THIS RESEARCH

The following listing gives a brief description of programs developed in the course of this research project. All programs are written in Fortran and are compatible with the Fortran 77 standards as compilable on the DEC VAX 11/780 SYSTEM. Since the eight basic programs comprise over 12,000 lines of source code, the source code listings are not included in this dissertation. The source code listings are given in a supplement which is available in the New Jersey Institute of Technology library. In addition, source codes may be obtained on magnetic tapes for a nominal fee either from the NJIT Chemical Engineering and Chemistry Computational Center or from the author at the following address: D. W. H. Roth, Jr., Allied Corporation, P.O. Box 1021R, Morristown, NJ 07960. The following is a list of programs in the shapter order in which they were utilized.

1. Chapter 2 - RIONFT

    This program is used to regress non-linear ion exchange equilibrium data to obtain equilibrium constants and resin phase activity coefficient parameters for binary and ternary systems. The main features are covered in Appendix C. Including diagnostics and commentary statements, the program has about 2600 lines of coding.

2. Chapter 3 - DIFACT

    This program utilizes the Bromley equation to compute activity coefficients of salts in aqueous solution. In addition, the Nernst-Hartley equation is used to predict the values of

diffusion coefficients for salts at concentrations up to 6 molal.
Both an integral and a differential form of the equation are used
for comparison. The program has about 160 lines of coding.

3. Chapter 5 - BMAVDM

This program is based on the batch binary ion exchange dynamic
model, i.e., the electrolyte concentration does not change during
the exchange. It can handle equilibrium correlated in either mole
or equivalent fraction concentration units, and the driving force
can be defined either as a concentration or an activity difference.
About 880 lines of coding.

4. Chapter 5 - DFUSFT

This program is designed to fit ion exchange "self" diffusion
coefficients by modeling experimental batch ion exchange curves.
It consists of BMAVDM appended to A. K. S. Murthy's non-linear
regression program discussed in Appendix B. It can fit parameters
using either the concentration or activity driving force models,
plus a two parameter diffusion model involving an ion pair
interaction factor. There are about 1420 lines of coding.

5. Chapter 5 - TRYBCH

This program is based on the batch ternary ion exchange dynamic
model, i.e., the electrolyte concentration does not change during
the exchange. It runs with either concentration or activity driving
force. It is used to test the ability of "self" diffusion
coefficients correlated with DFUSFT to predict ternary system
behavior. About 2700 lines of coding.

6. Chapter 6 - DISPRS

    This program models dispersive diffusion experiments to correlate axial dispersion coefficients in packed columns based on step change in inlet concentration. The resulting effluent concentration histories (ECH) or "S" curves are matched by adjusting the axial dispersion coefficient and are discussed in Chapter 6. About 400 lines of coding.

7. Chapter 7 - RFMAVD

    This is the dynamic ion exchange column modeling program for binary systems as described in Appendix K. There are about 1920 lines.

8. Chapter 7 - TERNEX

    This is the dynamic ion exchange column modeling program for ternary systems as described in Appendix L. About 2380 lines.

BIBLIOGRAPHY

1. Acrivos, Andreas, "On the Combined Effect of Longitudinal
      Diffusion and External Mass Transfer in Fixed-Bed
      Operations," Chem. Eng. Science, Vol. 13, no. 1, 1960, pp.
      1-6.

2. Acrivos, Andreas, "Method of Characteristics Technique," Eng.
      Des. and Process Devel., Ind. & Eng. Chem., Vol. 48, no. 4,
      Apr. 1956, pp. 703-710.

3. Amundson, N. R., "Mathematics of Adsorption in Beds," Journal of
      Physical Chemistry, Vol. 54, 1950, pp. 812-820.

4. Babcock, R. E., D. W. Green, and R. H. Perry, "Longitudinal
      Dispersion Mechanisms in Packed Beds," AIChE Jr, Sept. 1966,
      pp. 22-26.

5. Barrer, R.M., Colloque international sur les reactions clans
      l'etat solide, Paris, 1948.

6. Barrer, R. M., and L. V. C. Rees, "Self- and Exchange Diffusion
      Coefficients," Jr Phys. Chem. Solids, Vol. 25, pp.
      1035-1038, Pergamon Pr., 1964.

7. Boyd, G. E., and B. A. Soldano, "Self-diffusion of Cations in and
      through Sulfonated Polystyrene Cation-exchange Polymers," Jr
      Amer. Chem. Soc., Vol. 75, no. 24, Jan. 14, 1954, pp.
      6091-6099.

8. Bradley, W. G., and N. H. Sweed, "Rate Controlled Constant Pattern
      Fixed bed Sorption with Axial Dispersion and Nonlinear
      Multicomponent Equilibria," AIChE Symp. Series, 1975, Vol.
      71, no. 152, pp. 59-68.

9. Bromley, L. A., "Thermodynamic Properties of Strong Electrolytes
      in Aqueous Solutions," AIChE Jr, Vol. 19, no. 2, Mar. 1973,
      pp. 313-320.

10. Brown, N. L., J. C. Mullins, and S. S. Melsheimer, "A Nonlinear
      Equilibrium, Isothermal Fixed-bed Adsorption Model Using
      Pulse Chromatographic Rate Parameters," AIChE Symp. Series,
      1978, pp. 9-18.

11. Carberry, James J., "A Boundary-Layer Model of Fluid-Particle
      Mass Transfer in Fixed Beds," AIChE Jr, Vol. 6, no. 3,
      Sept. 1964, pp. 460-463.

12. Carberry, A. A., and R. H. Bretton, "Axial Dispersion of Mass in
      Flow through Fixed Beds," AIChE Jr, Vol. 4, no. 3,
      Sept. 1958, pp. 367-375.

13. Carlile, R. E., and B. E. Gillett, Fortran and Computer Mathematics for the Engineer and Scientist, Petroleum Publ. Co., Tulsa, 1973, pp. 352-358.

14. Carlile, R. E., and B. E. Gillett, Fortran and Computer Mathematics for the Engineer and Scientist, Petroleum Publ. Co., Tulsa, 1973, p. 383.

15. Chmutov, K. V., A. I. Kalinichev, and T. D. Semenovskaya, "Approximate Solution of the Equations of the Kinetic of Ion Exchange on Complexing Ion Exchangers," Institute of Physical Chemistry. Academy of Sciences of the USSR, Moscow. Translation from Doklady Akademii Nauk SSSR, Vol. 239, No. 3, March 1978, pp. 650-653.

16. Choi, P. S. K., L. T. Fan, H. H. Hsu, "Modeling and Simulation of an Adiabatic Adsorber," Separation Science 10(6), 1975, p. 706.

17. Cooney, D. O., and R. A. Marra, "The Effects of Sorbent Shrinking and Swelling on Fixed-Bed Sorption Operations," AIChE Symposium Series, No. 152, Vol. 71, pp. 148-156.

18. Cooney, David O., and E. N. Lightfoot, "Existence of Asymptotic Solutions to Fixed-bed Separations and Exchange Equations," I & E C Fund, Vol. 4, no. 2, May 1965, pp. 233-236.

19. Danes, S. and F. Danes, "Ion Exchange Equilibrium in Polyionic Systems,"Chimie et Industrie, Genie Chimique, 105, No. 15, June-July (1972).

20. Davidson, A. W. and W. J. Argersinger, Jr., "Equilibrium Constants of Cation Exchange Processes," Annals New York Academy of Sciences, Vol. 57, 1953/1954, p. 111.

21. Dranoff, Joshua, and L. Lapidus, "Equilibrium in Ternary Ion Exchange Systems," I & E Chem., Vol. 48, no. 8, Aug. 1957, pp. 1297-1302.

22. Dranoff, Joshua, and L. Lapidus, "Multicomponent Ion Exchange Column Calculations," I&E Chem, Vol. 50, 1958, pp. 1648-1653.

23. Ebach, E. A., and R. R. White, AIChE Journal, 4, 1958, p. 161.

24. Edwards, T. J., J. Newman, and J. M. Prausnitz, "Thermodynamics of Aqueous Solutions Containing Volatile Weak Electrolytes," AIChE Jr, Vol. 21, no. 2, Mar. 1975, pp. 248-251.

25. Electrolyte Phase Equilibria Project, Design Institute for Physical Property Data (DIPPR), Project 811, AIChE, 1982. Principal investigator Dr. J. F. Zemaitis.

26. Erickson, Kenneth L., "Fixed-bed Ion Exchange with Differing Ionic Mobilities and Nonlinear Equilibria," Dissertation; pres. to Univ. of Texas at Austin, May 1977, Prod. Univ. Microfilms Intern'l., Ann Arbor, Mich.

27. Farkas, E. J., and E. Byleveld, "Longitudinal Dispersion at Low Liquid Flow Rates in Fixed beds with Application to Elution in Demineralization by Ion Exchange," Can. Jr Chem Eng, Ser. 57, iss. 4, Aug. 1979, pp. 527-531.

28. Fleck, Jr., Robert D., D. J. Kirwan, and K. R. Hall, "Mixed-Resistance Diffusion Kinetics in Fixed-bed Adsorption under Constant Pattern Conditions," Ind Eng Chem Fund, Vol. 12, no. 1, 1973, pp. 95-99.

29. Finlayson, Bruce A., "Orthogonal Collocation in Chemical Reaction Engineering," Cat. Rev.-Sci. Eng., 10(1), 1974, pp. 69-138.

30. Graham, E. Earl, and J. S. Dranoff, "Application of the Stefan-Maxwell Equations to Diffusion in Ion Exchangers. 1. Theory," and "2. Experimental," Ind Eng Chem Fund, Vol. 21, No. 4, 1982, pp. 360-369.

31. Guggenheim, E. A., and J. C. Turgeon, "Specific Interaction of Ions," Trans Faraday Soc., 1955, Vol. 51, pp. 747-761.

32. Gunn, D. J., and R. England, "Dispersion and Diffusion in Beds of Porous Particles," Chem Eng Sci, Vol. 26, 1971, pp. 1413-1423.

33. Harned, H. S., and B. B. Owen, "The Physical Chemistry of Electrolyte Solutions," Reinhold Publishing Company, New York, 1956.

34. Hall, Kenneth R., L. C. Eagleton, A. Acrivos, and T. Vermeulen, "Pore- and Solid-diffusion Kinetics in Fixed-bed Adsorption under Constant Pattern Conditions," I & E C Fund, Vol. 5, no. 2, May 1966, pp. 212-223.

35. Helfferich, Friedrich, Ion Exchange. McGraw-Hill, New York, 1962, pp. 141.

36. Helfferich, Friedrich, Ion Exchange. McGraw-Hill, New York, 1962, pp. 152-156.

37. Helfferich, Friedrich, Ion Exchange. McGraw-Hill, New York, 1962, pp. 166.

38. Helfferich, Friedrich, Ion Exchange. McGraw-Hill, New York, 1962, pp. 169-170.

39. Helfferich, Friedrich, <u>Ion Exchange</u>. McGraw-Hill, New York, 1962, pp. 176.

40. Helfferich, Friedrich, <u>Ion Exchange</u>. McGraw-Hill, New York, 1962, pp. 177-182.

41. Helfferich, Friedrich, <u>Ion Exchange</u>. McGraw-Hill, New York, 1962, pp. 193-195.

42. Helfferich, Friedrich, <u>Ion Exchange</u>. McGraw-Hill, New York, 1962, pp. 268-273.

43. Helfferich, Friedrich, <u>Ion Exchange</u>. McGraw-Hill, New York, 1962, pp. 273-278.

44. Helfferich, Friedrich, <u>Ion Exchange</u>. McGraw-Hill, New York, 1962, pp. 229-239 and pp. 309-317.

45. Helfferich, Friedrich, <u>Ion Exchange</u>. McGraw-Hill, New York, 1962, pp. 358.

46. Hering, Burton, and H. Bliss, "Diffusion in Ion Exchange Resins," <u>AIChE Jr</u>,Vol. 9, no. 4, July 1963, pp. 495-503.

47. Jenson, V. G., and G. V. Jeffreys, <u>Mathematical Methods in Chemical Engineering</u>, 2nd Edit., Academic Press, New York, London, San Francisco, 1977, p. 260 and pp. 423-431.

48. Jenson, V. G., and G. V. Jeffreys, <u>Mathematical Methods in Chemical Engineering</u>, 2nd Edit., Academic Press, New York, London, San Francisco, 1977, p. 260 and pp. 416-421.

49. Kataoka, T. and H. Yoshida, "Resin Phase Mass Transfer in Ion Exchange Between Different Ions Accompanied by Resin Volume Change," <u>Journal of Chemical Engineering</u>, Japan, Vol. 8, no. 6, 1975, pp. 451-455.

50. Kataoka, T., and H. Yoshida, "Breakthrough Curve in Equal Valence Ion Exchange-Liquid Phase Diffusion Control," <u>Journal of Engineering Science</u>, Vol. 9, no. 5, 1976, pp. 383-387.

51. Kataoka, Takeshi, H. Yoshida, and Y. Ozasa, "Intraparticle Ion Exchange Mass Transfer Accompanied by Instantaneous Irreversible Reaction," <u>Chemical Engineering Science</u>, Vol. 32, 1977, pp. 1237-1240.

52. Kataoka, Takeshi, H. Yoshida, and Y. Ozasa, "Breakthrough Curve in Ion Exchange Column - Particle Diffusion Control," <u>Jr Chem Eng of Japan</u>, Vol. 10, no. 5, 1977, pp. 385-390.

53. Kielland, J., <u>Jr. Soc. Chem. Ind.</u>, (London) 54, 232 T (1935).

54. Koloini, T., M. Sopcic, and M. Zumer, "Mass Transfer in Liquid-FluidizedBeds at Low Reynolds Numbers," Chem Eng Sci, 1975, Vol. 32, pp. 637-641.

55. Koloini, T., M. Zumer, S. Mlinar, and M. Novak, "Mass Transfer in Liquid Fluidized Beds at Low Reynolds Numbers," Chem Eng Commun., Vol. 5, 1980, pp. 233-244.

56. Kuo, James C. W., and M. M. David, "Single Particle Studies of Cation-Exchange Rates in Packed Beds: Barium Ion- Sodium Ion System," AIChE Jr, Vol. 9, no. 3, May 1963, pp. 365-370.

57. Kurotaki, Katsumi, and S. Kawamura, "Thermodynamics of Ion Exchange of Trivalent Co^{+++} or Cr^{+++} Complex with Cerium (III) Ions on Cation Exchange Resin," Jr Chem Soc, Faraday Trans. 1, Ser. 75, iss. 4, 1979, pp. 925-934.

58. Lapidus, L., "Digital Computation for Chemical Engineers," McGraw-Hill, NY 1962.

59. Lee, E. S., "Quasi-linearization, Non-linear Boundary Value Problems and Optimization," Chem Eng Sci, 1966, Vol. 21, pp. 183-194.

60. Levenspiel, O., "Chemical Reaction Engineering," John Wiley & Sons, 1972, pp. 361-366.

61. Liles, A. W., and C. J. Geankoplis, "Axial Diffusion of Liquids in Packed Beds and End Effects," AIChE Jr, Vol. 6, no. 4, Dec. 1960, pp. 591-595.

62. Lightfoot, E., C. Massot, F. Ivoni, Chemical Eng. Progress Symposia Series 61, No. 58, 28, 1966.

63. Masamune, Shinobu, and J. M. Smith, "Transient Mass Transfer in a Fixed Bed," I & E C Fund, Vol. 3, no. 2, May 1964, pp. 179-181.

64. Masamune, Shinobu, and J. M. Smith, "Adsorption Rate Studies - Interaction of Diffusion and Surface Processes," AIChE Jr, Jan. 1965, pp. 34-40.

65. McCracken, E. A., G. L. Leefe, and R. E. C. Weaver, "Transient Numerical Solutions for two Phase Fluid-Bed Models," Chem. Eng. Progr. Symposium Ser. No. 101, 1970, pp. 66, 37-46.

66. Meissner, H. P., and C. L. Kusik, "Aqueous Solutions of Two or More Strong Electrolytes-Vapor Pressures and Solubilities," I & E C Proc. Des.Devel., 1973, Vol. 12, no. 2, pp. 205-208.

67. Meissner, H. P., and C. L. Kusik, "Activity Coefficients of Strong Electrolytes in Multicomponent Aqueous Solutions," AIChE Jr, Vol. 18, no. 2, Mar. 1972, pp. 294-298.

68. Meissner, H. P., and C. L. Kusik, "Calculating Activity Coefficients in Hydrometallurgy - a Review," International Journal of Mineral Processing, 2, 1975, pp. 105-155.

69. Meyer, O. A., and T. W. Weber, "Nonisothermal Adsorption in Fixed-Beds," AIChE Jr., 13, 1967, p. 457.

70. Mickley, H. S., T. K. Sherwood, and C. E. Reed, "Applied Mathematics in Chemical Engineering," 2nd Edition, McGraw-Hill Book Company, 1957, pp. 215-217.

71. Mickley, H. S., T. K. Sherwood, and C. E. Reed, "Applied Mathematics in Chemical Engineering," 2nd Edition, McGraw-Hill Book Company, 1957, pp. 358.

72. Michelsen, M. L., "Algorithms for Collocation Solution of Ordinary and Partial Differential Equations," Instituttet for Kemiteknik, Technical University of Denmark, 1973.

73. Nelson, Paul A., and T. R. Galloway, "Particle-to-fluid heat and Mass Transfer in Dense Systems of Fine Particles," Chem Eng Sci, 1975, Vol. 30, pp 1-6.

74. Newman, John, "Engineering Design of Electrochemical Systems," I & E Chem, Vol. 60, no. 4, Apr. 1968, pp. 12-27.

75. Newman, John, "Transport Processes in Electrolytic Solutions," Advances in Electrochemistry and Electrochemical Engineering, Volume 5, Interscience Publishers, New York, 1967, p. 95.

76. Newman, John, "Transport Processes in Electrolytic Solutions," Advances in Electrochemistry and Electrochemical Engineering, Volume 5, Interscience Publishers, New York, 1967, pp. 130-131.

77. Novosad, J., and A. L. Meyers, "Thermodynamics of Ion Exchange as an Adsorption Process," Can Jr of Chem Eng, Vol. 60, Aug. 1982, pp. 500-503.

78. Omatete, Ogbemi O., Column Dynamics of Ternary Ion Exchange, Dissertation pres. to University of California, Berkeley, June 1971.

79. Omatete, O. O., Ron N. Clazie, and T. Vermeulen, "Column Dynamics of Ternary Ion Exchange, Part I: Diffusional and Mass Transfer Relations," Chem Eng Jr, Vol. 19, 1980, pp. 229-240. Netherlands.

80. Omatete, O. O., R. N. Clazie, and T. Vermeulen, "Column Dynamics of Ternary Ion Exchange Part II: Solution Mass Transfer Controlling," Chem Eng Jr, Vol. 19, 1980, pp. 241-250. Netherlands.

81. Pal, G. C., A. K. Chakravarti, and M. Sengupta, "Studies in Ion Exchange Equilibria, II: Some Cation and Anion Exchange Selectivities in Amberlite Resins," Ion Exch and Membranes, Vol. 2, 1974, pp. 21-27.

82. Pal, G. C., M. Sengupta, A. K. Chakravarti, and P. Mukherjee, "Ionic Interaction Coefficients: Activity Calculations in Mixed Electrolyte Solutions in Ion Exchange Studies," Jr. Indian Chem. Soc., Vol. LII, Aug. 1975, pp. 675-678.

83. Pan, Shih-Hsie, and M. M. David, "Design Effect of Liquid Phase Ionic Migration on a Moving Packed-bed Ion Exchange Process," AIChE Symp Series, Vol. 74, no. 179, 1978, pp. 74-82.

84. Pan, Shih-Hsie, "Model Identification for and Design Effects of Liquid-Phase Mass-Transfer Rates in Packed-Bed Ion Exchange," Dissertation pres. to Univ. of Washington, 1976, produced by Xerox University Microfilms, Ann Arbor, Mich.

85. Pieroni, L. F., and J. S. Dranoff, "Ion Exchange Equilibria in a Ternary System," AIChE Jr, Vol. 9, no. 1, 1963, pp. 42-45.

86. Pitzer, K. S., "Thermodynamics of Electrolyte I: Theoretical Basis and General Equations, Jr Phys Chem, Vol. 77, no. 2, 1973, pp. 268-277.

87. Rao, H. C. Subba, and M. M. David, "Equilibrium in the System $Cu^{++}-Na^{+}-Dowex-50$:, AIChE Jr, Vol. 3, no. 2, 1957, pp. 187-190.

88. Rao, M. Gopala, and M. M. David, "Single-particle Studies of Ion Exchange in Packed Beds: Cupric Ion-Sodium Ion System," AIChE Jr, Vol. 10, no. 2, March 1964, pp. 213-219.

89. Rao, M. Gopala, and C. R. Morig, "Diffusion in Ion Exchange Resins: Sodium Ion-Strontium Ion System," Chem Eng Sci, Vol. 20, 1965, pp. 889-893. Gt. Britain.

90. Rao, M. Gopala, S. Viswanathan, D. P. Rao, and S. Y. Kekre, "Ternary Ionic Diffusion in Ion Exchange Resins," paper presented at Int. Conference on Ion Exchange in Process Industries, (Soc. Chem. Ind.) London, July 1969.

91. Rao, M. G., A. K. Gupta, and R. K. Bajpai, "Binary and Ternary Ion-exchange Equilibria, Sodium-Cesium-Manganese-Dowex 50W-X8 and Cesium-Manganese-Strontium-Dowex 50W-X8 Systems," Jr Phys Chem, Vol. 77, no. 10, 1973, reprint.

92. Rao, M. Gopala, R. K. Bajpai, and A. K. Gupta, "Single Particle Studies of Binary and Ternary Cation Exchange Kinetics," AIChE Jr, Vol. 20, no. 5, Sept. 1974, pp. 989-995.

93. Rao, M. Gopala, R. K. Bajpai, and A. K. Gupta, "Single Particle Studies of Binary and Ternary Cation Exchange Kinetics," Supplementary Material, rev., Dept. of Chem. Eng., Indian Inst. Tech., Kanpur, 17 pp.

94. Rao, M. Gopala, A. K. Gupta, S. Y. Kekre, "Ion Exchange Rates in Ternary Systems," Indian Jr. of Tech., Vol. 12, Sept. 1974, pp. 395-402.

95. Rao, M. Gopala, A. K. Gupta, "Isotopic Ion Exchange in Heteroionic Systems," Chemical Engineering Science, Vol. 34, 1979, pp. 279-283.

96. Rao, M. Gopala, A. K. Gupta, E. S. Williams, and A. A. Aguwa, "Sorption of Heavy Metal Ions on Chelex 100 Resin," (paper presented at AIChE national meeting, (Nov. 1983). Study made under NSF grant RIM 78-13307 and American Can-Howard U. Research grant.

97. Reichenberg, D., "Properties of Ion-exchange Resins in Relation to their Structure, III: Kinetics of Exchange," Jr of Amer Chem Soc, Vol 75, Feb. 5, 1953, pp. 589-597.

98. Renon, Henri, and J. M. Prausnitz, "Local Compositions in Thermodynamic Excess Functions for Liquid Mixtures," AIChE Jr, Vol. 14, no. 1, Jan. 1968, pp. 135-144.

99. Rhee, Hyun-Ku, and N. R. Amundson, "An Analysis of an Adiabatic Adsorption Column: Part I, Theoretical Development," Chem Eng Jr, Vol. 1, 1970, Gt. Britain, pp. 241-254.

100. Rhee, Hyun-Ku, R. Aris, and N. R. Amundson, "On the Theory of Multicomponent Chromatography," Royal Soc of London, Phil. Trans., Vol. 267, Oct. 1970, pp. 419-455.

101. Rhee, Hyun-Ku, and N. R. Amundson, "A Study of the Shock Layer in Non Equilibrium Exchange Systems," Chemical Engineering Science, Vol. 27, 1972, pp. 199-211.

102. Rhee, Hyun-Ku, E. D. Heerdt, and N. R. Amundson, "An Analysis of an Adiabatic Adsorption Column: Part II, Adiabatic Adsorption of a Single Solute," Chem Eng Jr, Vol. 1, 1970, Gt. Britain, pp. 279-290.

103. Robinson, R. A., and R. H. Stokes, Electrolyte Solutions, 2nd Edition, New York: Academic Press, Inc. London: Butterworth's Scientific Publ. 1959, p. 231.

104. Robinson, R. A., and R. H. Stokes, Electrolyte Solutions, 2nd Edition, New York: Academic Press, Inc. London: Butterworth's Scientific Publ. 1959, p. 288.

105. Robinson, R. A., and R. H. Stokes, Electrolyte Solutions, 2nd Edition, New York: Academic Press, Inc. London: Butterworth's Scientific Publ. 1959, pp. 438-439.

106. Robinson, R. A., and R. H. Stokes, Electrolyte Solutions, 2nd Edition, New York: Academic Press, Inc. London: Butterworth's Scientific Publ. 1959, pp. 463-515.

107. Rosen, J. B., "Kinetics of a Fixed Bed System for Solid Diffusion into Spherical Particles," Jr Chem Physics, Vol. 20, no. 3, March 1952, pp. 387-394.

108. Rosen, J. B., "General Numerical Solution for Solid Diffusion in Fixed Beds," Eng Des and Proc Devel , Vol. 46, no. 8, 1954, pp. 1590-1594.

109. Rowe, P. N., "Particle-to-liquid Mass Transfer in Fluidized Beds," Chem Eng Sci, 1975, Vol. 30, pp. 7-9.

110. Salmon, J. E., "Thermodynamic Studies of Some Anion-Exchange Equilibria, 2,"Trans. Faraday Soc, Vol. 65, no. 563, Nov. 1969, pp. 2879-2885.

111. Sangster, J., and F. Lenzi, "On the Choice of Methods for the Predictions of the Water-activity and Activity Coefficients for Multicomponent Aqueous Solutions," Can Jr of Chem Eng, Vol. 52, June 1974, pp. 392-396.

112. Selim, M. Sami, and R. C. Seagrave, "Solution of Moving-Boundary Transport Problems in Finite Media by Integral Transforms," Ind Eng Chem Fund, Vol. 12, no. 1, 1973, pp. 14-17.

113. Selke, W. A., and H. Bliss, "Copper- Amberlite IRK-120 in Fixed Beds," Chem Eng Progr, Vol. 46, no. 10, Oct. 1950, pp. 509-516.

114. Selke, W. A., Y. Bard, A. D. Pasternak, and S. K. Aditya, "Mass Transfer Rates in Ion Exchange," AIChE Jr, Vol. 2, no. 4, pp. 468-470.

115. Sherwood, T. K., R. L. Pigford, and C. R. Wilke, "Mass Transfer," McGraw Hill, NY, 1975, p. 130.

116. Smith, Robert P. and E. T. Woodburn, "Prediction of Multi-Component Ion Exchange Equilibria for the Ternary System SO_4, NO_3, Cl^- from Data of Binary Systems," AIChE Jr, Vol. 24, no. 4, July 1978, pp. 577-586.

117. Smith, Buford D., "Design of Equilibrium Stage Processes," McGraw-Hill Book Co. Inc., 1963, P. 58

118. Snowdon, C. B. and J. C. R. Turner, "Mass Transfer in Liquid-Fluidized Beds of Ion Exchange Resin Beads," Proc Int Symp on Fluidization, 1967, Netherlands University Press, pp. 599-609.

119. Soldatov, V. S., "Thermodynamics of Ion-exchange Equilibria, Russ. Jr Phys Chem, Vol. 46, no. 2, 1972, pp. 250-252.

120. Soldatov, V. S., and V. A. Bychkova, "Calculation of Activity Coefficients of Components of the Ion Exchanger Phase in Multicomponent Systems," Russ Jr Phys Chem, Vol. 45, no. 5, 1971, pp. 707-709.

121. Soldatov, V. S., and V. A. Bychkova, "Experimental Investigation of Ammonium-Sodium-Hydrogen Ion-exchange Equilibrium on a Sulphonated Styrene Exchanger," Russ Jr Phys Chem, Vol. 45, no. 5, 1971, pp. 700-702.

122. Soldatov, V. S., and V. A. Bychkova, "Ion Exchange in Multicomponent Systems; Calculation of Ion-exchange Equilibrium in the Ternary System K^+,NH_4^+,H^+ from Data for Binary Systems," Russ Jr Phys Chem, Vol. 44, no. 9, 1970, pp. 1297-1300.

123. Soldatov, V. S., and V. A. Bychkova, "Ternary Ion-exchange Equilibria," Separation Sci & Tech, Vol. 15, no. 2, 1980, pp. 89-110.

124. Strang, D. A., and C. J. Geankoplis, Ind. Eng. Chem., 50, 1958, p. 1305

125. Svedberg, Gunnar, "A Numerical Method for the Simulation of Fixed-Bed Processes," Doctoral dissertation, Sept. 1975, Dept. of Chem. Eng., Royal Institute of Technology, Stockholm, Sweden.

126. Thodos, George, and Chi Tien, "Ion Exchange Kinetics for Systems of Non-Linear Equilibrium Relationships," AIChE Jr, Vol. 5, no. 3, Sept. 1959, pp. 373-78.

127. Thomas, H. C., "Heterogeneous Ion Exchange in a Flowing System," Journal of American Chemical Society, Vol. 66, 1944, pp. 1664-1666.

128. Truesdell, A. H., and B. F. Jones, "Wateq - A Computer Programme for Calculating Chemical Equilibria of Natural Water," U.S. Geological Survey, Washington, DC Rept. no. PB 220646 (1973).

129. Turner, J. C. R., M. R. Church, A. S. W. Johnson, and C. B. Snowdon, "An Experimental Verification of the Nernst-Planck Model for Diffusion in an Ion-Exchange Resin," Chemical Engineering Science, Vol. 21, 1966, pp. 317-325.

130. Turner, J. C. R., T. K. Murphy, "A CSTR Method for Determining Ion-Exchange Equilibria," Chemical Engineering Science, Vol. 38, no. 1, 1983, pp. 147-153.

131. Turner, J. C. R., and C. B. Snowdon, "Liquid-side Mass-transfer Coefficients in Ion Exchange: An Examination of the Nernst-Planck Model," Chem Eng Sci, Vol. 23, 1968, pp. 221-230.

132. Van Brocklin, Lester P., and M. M. David, "Coupled Ionic Migration and Diffusion During Liquid-phase Controlled Ion Exchange," Ind Eng Chem Fund, Vol. 11, no. 1, 1972, pp. 91-99.

133. Van Brocklin, L. P., and M. M. David, "Ionic Migration Effects During Liquid Phase Controlled Ion Exchange," AIChE Symp Series, Vol. 71, no. 152, 1975, pp. 191-201.

134. Vermeulen, T., and N. K. Hiester, "Ion-exchange Chromatography of Trace Components," I & E Chem, Vol. 44, no. 3, March 1952, pp. 636-651.

135. Vermeulen, Theodore, "Theory for Irreversible and Constant-pattern Solid Diffusion," I & E Chem, Vol. 45, no. 8, Aug. 1953, pp. 1664-1670.

136. Vermeulen T., and N. K. Hiester, "Ion-exchange and Adsorption Column Kinetics with Uniform Partial Presaturation," Jr Chem Phys, Vol. 22, no. 1, Jan. 1954, pp. 96-101.

137. Von Rosenberg, D. U., Methods for the Solution of Partial Differential Equations, Elsevier, New York (1969).

138. Wilson, E. J., and G. J. Geankoplis, "Liquid Mass Transfer at Very Low Reynolds Numbers in Packed Beds," I&E Chem. Fundamentals, Vol. 5, Feb.1966, pp. 9-14.

139. Zemaitis, Jos. F., Jr., "Predicting Vapor-Liquid-Solid Equilibria in Multicomponent Aqueous Solutions of Electrolytes," Paper pres. at Symp on Thermodynamics of Aqueous Systems with Ind. Applications, co-spons. AIChE, NBS, and NSF, Oct. 22-25, 1979, Wash., DC